The hydrogeological and geotechnical properties of household waste in relation to sustainable landfilling.

Beaven, Richard P

The hydrogeological and geotechnical properties of household waste in relation to sustainable landfilling

by

Richard P Beaven

A dissertation submitted for the
degree of Doctor of Philosophy
at
the University of London

Department of Civil Engineering[RIP]
Queen Mary and Westfield College

May 1999

Published January 2000

Abstract

This thesis reports an investigation into the hydrogeological and geotechnical properties of household wastes within the context of sustainable landfilling and, particularly, the development of a high rate flushing bioreactor.

The design and construction of a large-scale (2-metre diameter) purpose built compression cell used in the research are described. Tests on a number of different household waste materials (including pulverised and aged wastes) were undertaken at varying applied loads up to 600 kPa, equivalent to a 60 metre depth of landfill. Results of variations in refuse density, stiffness, absorptive capacity, effective porosity and hydraulic conductivity are reported against average effective stress in the waste. It was concluded that the hydrogeological properties of household waste vary considerably with effective stress and, hence, with depth in landfills. For example, the hydraulic conductivity of crude household waste could reduce by over three orders of magnitude from approximately $1x10^{-5}$ m/s to $1x10^{-8}$ m/s between placement (with minimal compaction) and burial to a depth of 60 metres.

The principles of sustainable development are considered and applied to landfilling. The view that the polluting potential of landfills should be reduced to acceptable levels within a generation is supported. In most cases this will require that contaminants in the landfill are removed by introducing water into the site and recirculating and flushing leachate from it. The feasibility of achieving this with a variety of different leachate recirculation systems is examined in the light of the findings of the research. A new module has been written for MODFLOW, the USGS's groundwater flow model, to allow hydraulic conductivity to vary throughout simulations with effective stress. The altered code is used to model a grid of leachate abstraction and injection wells to illustrate the potential for flushing.

It is concluded that changes are needed to current landfill design and operational practices to enable wastes to be flushed efficiently within landfills. It is argued, in particular, that there are significant benefits of operating landfills with large saturated zones.

Acknowledgements

This thesis was only possible with the backing of a number of organisations and individuals. Firstly, I recognise that without the support of Cleanaway Ltd, and in particular the encouragement of Nick Walker, I would not have started the research. Funding for the project was jointly provided by the Waste Technical Division of the Department of the Environment and Cleanaway Ltd, who also provided facilities at their Pitsea landfill site to locate the compression cell. I would like to thank Karl Shek, Ifti Ahmed, Ben McCarthy, and Lewis Parker for their help in the running of the experiments.

My thanks also go to my supervisor William Powrie for his advice, comments and attention to detail throughout the project, and to Angela Cole who proof read the thesis, rearranged a random spatter, of commas, and generally helped make the thesis more readable than what it otherwise might have been.

To the many others who have given me help, support and encouragement throughout, I offer my sincerest thanks.

Table of Contents

Abstract 3

Acknowledgements 4

Table of contents 5

List of Figures 12

List of Tables 18

1. Introduction 21

1.1 Summary 21

1.2 Introduction 21

1.3 Sustainable development 22

1.3.1 The need for sustainable development 23

1.3.2 The Brundtland Report 23

1.3.3 Sustainable development in practice 24

1.3.4 Waste management in relation to sustainable development 25

1.3.5 Sustainable landfills - The UK's position 27

1.4 Historical perspective - evolution of landfill design in the UK 28

1.4.1 Why are landfills not already more sustainable? 29

1.4.2 The early years 30

1.4.3 Development of Waste Management Practices 31

1.4.4 Controlled tipping - State of the art landfilling for 50 years 33

1.4.5 The start of 'dilute and attenuate' and 'containment' philosophies 36

1.4.6 The mid 1980s to 1990s - a decade of change 39

1.4.7 Risk assessment approach/ controlled release philosophy 41

1.5 Rationale for research 41

1.6 Structure of thesis 42

2. Literature review and definition of terms 44

2.1 Summary 44

2.2 Introduction 44

2.2.1 Sustainable landfill 44

2.2.2 Nature of pollutants within a landfill 45

2.2.3 Accelerated degradation techniques 46

2.2.4 The role of liquid recirculation and flushing in sustainable landfill 46

2.2.5 Overview of chapter 47

2.3 Composition of refuse 48

2.3.1 Waste characterisation 49

2.3.2 Material classification, water content and particle size distribution (PSD) 51

2.4 Refuse density 53
2.4.1 Definition of terms 53
2.4.2 Literature review 54
2.5 Water content, absorptive capacity and porosity 58
2.5.1 Definition of terms 58
2.5.2 Literature review 63
2.6 Hydraulic conductivity 70
2.6.1 Definition of terms 70
2.6.2 Literature review 72
2.6.3 Summary of data relating to hydraulic conductivity 77
2.7 Stress and stiffness 79
2.7.1 Total and effective stress 79
2.7.2 Stiffness 80

3. Equipment design and construction 81
3.1 Summary 81
3.2 Introduction 81
3.2.1 Need for purpose built equipment 82
3.3 Design Requirements 83
3.3.1 Diameter of cell 83
3.3.2 Height 84
3.3.3 Applied load to simulate required depth of landfill 92
3.3.4 Monitoring requirements 92
3.4 Design Elements 93
3.4.1 Introduction 93
3.4.2 Steelwork 94
3.4.3 Hydraulics 97
3.4.4 Ancillaries - Water flow systems 101
3.4.5 Operation of the Cell 102
3.5 Construction 104
3.5.1 Introduction 104
3.6 Monitoring systems 105
3.6.1 Reference systems 105
3.6.2 Load cells 106
3.6.3 Total earth pressure cells 108
3.6.4 Differential compression 108
3.6.5 Water flow rates and quantities 109
3.6.6 Piezometric heads 110
3.7 Calibration techniques 111
3.7.1 Load cells 111
3.7.2 Earth pressure cells 112
3.7.3 Flow meters 116

4. Testing Methodology 117
4.1 Summary 117
4.2 Introduction 117
4.3 Testing Methodology 118
4.3.1 Sample selection 118
4.3.2 Waste characterisation 118
4.3.3 Loading of waste into compression cell 118
4.3.4 General testing methodology 120
4.3.5 Compression tests 121
4.3.6 Absorptive capacity and water content at field capacity 122
4.3.7 Effective porosity 123
4.3.8 Constant head hydraulic conductivity tests 124
4.3.9 Falling head hydraulic conductivity test 128

5. Results 129
5.1 Summary 129
5.2 Introduction 129
5.3 Crude household waste (Test series DM1) 131
5.3.1 Waste source 131
5.3.2 Waste characterisation 131
5.3.3 Loading of waste into compression cell 131
5.3.4 Changes in average waste density in response to changes in applied stress 132
5.4 Crude household waste (Test series DM2) 134
5.4.1 Waste source 134
5.4.2 Waste characterisation 134
5.4.3 Loading of waste into the compression cell 135
5.4.4 Absorptive capacity 135
5.4.5 Changes in average waste density in response to changes in applied stress 136
5.4.6 Water content at field capacity 136
5.4.7 Differential compression (String data) 138
5.4.8 Earth pressure cell data 140
5.4.9 Effective porosity 141
5.4.10 Hydraulic conductivity 143
5.5 Crude household waste (Test series DM3) 144
5.5.1 Waste source 144
5.5.2 Waste characterisation 144
5.5.3 Loading of waste into the compression cell 145
5.5.4 Absorptive capacity 145
5.5.5 Changes in average waste density in response to changes in applied stress 146
5.5.6 Water content at field capacity 147
5.5.7 Differential compression (String data) 147
5.5.8 Total stress cell data 150
5.5.9 Effective porosity 150
5.5.10 Hydraulic conductivity 155

5.6 Pulverised waste (Test series PV1) 158
5.6.1 Waste Source 158
5.6.2 Waste characterisation 159
5.6.3 Loading of waste into compression cell 159
5.6.4 Absorptive capacity 160
5.6.5 Changes in average waste density in response to changes in applied stress 161
5.6.6 Water content at field capacity 161
5.6.7 Differential compression (String data) 162
5.6.8 Total stress cell data 164
5.6.9 Effective porosity 164
5.6.10 Hydraulic conductivity 168
5.7 Pulverised waste (Test series PV2) 172
5.7.1 Waste Source 172
5.7.2 Waste characterisation 172
5.7.3 Loading of waste into compression cell 172
5.7.4 Absorptive capacity 173
5.7.5 Changes in average waste density in response to changes in applied stress 173
5.7.6 Water content at field capacity 173
5.7.7 Differential compression (String data) 173
5.7.8 Total stress cell data 175
5.7.9 Effective porosity 176
5.7.10 Hydraulic conductivity 176
5.8 Aged waste (Test series AG1) 178
5.8.1 Waste Source 178
5.8.2 Waste characterisation 178
5.8.3 Loading of waste into compression cell 179
5.8.4 Absorptive capacity 179
5.8.5 Changes in average waste density in response to changes in applied stress 179
5.8.6 Water content at field capacity 180
5.8.7 Differential compression (String data) 180
5.8.8 Total stress cell data 182
5.8.9 Effective porosity 183
5.8.10 Hydraulic conductivity 188
5.9 Summary of experimental results 191

6. Data interpretation and analysis 192
6.1 Summary 192
6.2 Introduction 193
6.3 Analysis of differential compression data. 193
6.4 Analysis of total earth pressure cell data 196
6.4.1 Comparison of stress readings from earth pressure cells located in waste 196
6.4.2 Stress readings from earth pressure cell in lower gravel 199
6.4.3 Correlation of stress readings with theoretical model 199
6.4.4 Average vertical stress in waste at different applied loads 201

6.4.5 Waste density in relation to effective stress 202
6.4.6 Effective porosity and water contents in relation to effective stress 206
6.4.7 Relationship between hydraulic conductivity and effective stress 211
6.5 Relationship between depth of burial and stress 216
6.6 Waste stiffness 218
6.7 Specific volume and dry particle density 220

7. A stress dependent hydraulic conductivity flow model 223
7.1 Summary 223
7.2 Introduction 223
7.3 MODFLOW and Groundwater Vistas 224
7.4 Structure of MODFLOW 225
7.5 Conceptual design of a stress dependent hydraulic conductivity (SDK) package 226
7.6 Programming 229
7.6.1 Revision of programme module MAIN 229
7.6.2 Module SDK1AL 229
7.6.3 Module SDK1RP 229
7.6.4 Module SDK1FM 231
7.7 Verification of model 235
7.7.1 Vertical flow 236
7.7.2 Flow to a confined well 241
7.8 Limitations of model 247

8. Discussion and application of results to sustainable landfilling 249
8.1 Summary 249
8.2 Introduction 250
8.3 General considerations 250
8.3.1 Relationship between the hydrogeological properties and density of household waste 250
8.3.2 Relationship between density of household waste and compactive effort 252
8.3.3 Relationship between density of household waste and effective stress 252
8.4 Application of results to leachate control in existing landfills 255
8.4.1 Estimation of leachate volumes 255
8.4.2 Leachate control in existing sites using wells 257
8.5 Application of results to the flushing of wastes in a sustainable landfill 260
8.5.1 Raising the water content of wastes to field capacity 261
8.5.2 Estimation of the bed volume of a landfill 263
8.5.3 Estimation of flushing volumes and flushing rates 264
8.5.4 Estimation of hydraulic conductivity 271
8.5.5 Leachate recirculation - collection systems 272
8.5.6 Leachate recirculation - injection systems 277
8.5.7 Vertical flushing - downward unsaturated flow 279
8.5.8 Vertical flushing - benefit of operating with a saturated zone 280
8.5.9 Vertical flushing - upward flow 285

8.5.10 Vertical flushing - combined upward and unsaturated downward flow 288
8.5.11 Vertical flushing - impact of barriers and routes of preferential flow 294
8.5.12 Horizontal flushing - injection and abstraction wells 298
8.5.13 Impact of waste pre-compaction on flushing 315
8.5.14 Impact of waste type on flushing 318
8.6 Technical constraints and possible solutions to the operation of a high rate flushing sustainable landfill 320
8.6.1 Saturation of wastes 320
8.6.2 Maximum depth of landfill and density of waste 321
8.6.3 Pre-treatment of wastes 322
8.6.4 Low permeability barriers and preferential flow routes 322
8.6.5 Source of flushing fluid 323
8.6.6 Design and operation of leachate collection and distribution system 325
8.6.7 Regulation of leachate quality to accelerate refuse degradation 327
8.6.8 Accelerated waste degradation and effect of gas production on flushing 327
8.6.9 Restoration, settlement and planning issues 327
8.6.10 Site location 328
8.6.11 Summary of overall design concept 328

9. Summary, conclusions and recommendations 330
9.1 Research methodology 331
9.1.1 The compression cell 331
9.1.2 Testing methods 332
9.1.3 Future research developments 333
9.1.4 Timescale of testing 334
9.2 The geotechnical and hydrogeological properties of waste 334
9.3 Leachate control systems 337
9.4 Modelling of fluid flow in landfills 337
9.5 Sustainable flushing of wastes 338
9.5.1 Flushing volume 338
9.5.2 Flushing rates 339
9.5.3 Flushing scenarios 339
9.6 Implications for sustainable landfilling practice 342
9.6.1 Depth of landfill 342
9.6.2 Saturation of waste 342
9.6.3 Liners 342
9.6.4 Pre-processing of waste 342
9.6.5 Waste placement densities 343
9.6.6 Removing barriers to flow 343
9.6.7 Leachate recirculation infrastructure 343
9.6.8 Source of new water 343
9.6.9 Siting of a high rate flushing bioreactor 344
9.7 Concluding remarks 344

Bibliography 345
Papers based on the findings of this thesis 357

Appendix A - Specifications 359
Fabrication of compression cell 359
Hydraulic and electrical circuit diagrams 359
Water recirculation pump 359
Hydraulic pumps 363
Electrical motors 363
Hydraulic pump units 363
Load cells 364
Electromagnetic flow recorders 364

Appendix B - Analysis of differential compression data 365

Appendix C - MODFLOW program listings 371
Source code for MAIN.for 371
Source code for new SDK module 378

Appendix D - Flushing volumes 386

List of Figures

2. Literature review and definition of terms 44

Figure 2.1 Section through a double porosity medium 49
Figure 2.2 Refuse as a three-phase material 54
Figure 2.3 Compressibility tests on refuse 56
Figure 2.4 Illustrative relationship between density and water content at field capacity 62
Figure 2.5 Original water content and water content at field capacity of household waste 66
Figure 2.6 Water capacity (Water content at field capacity) vs density 67
Figure 2.7 Water content of shredded MSW at field capacity 68
Figure 2.8 Hydraulic conductivity vs depth - Fresh Kills Landfill New York 77

3. Equipment design and construction 81

Figure 3.1 Conceptual model of stresses acting on a layer of thickness z at depth z within the compression cell 86
Figure 3.2 Forces acting on layer of thickness z at depth z within the cell 87
Figure 3.3 Schematic section through compression cell 95
Figure 3.4 Compression cell as built 96
Figure 3.5 Compression cell showing operation of "jack up" cylinders prior to rotation of testing cylinder 97
Figure 3.6 Schematic diagram of part of the hydraulic circuit used to control the operation of the compression cell 100
Figure 3.7 Schematic representation of flow system through cell 102
Figure 3.8 Control Panel Schematic 103
Figure 3.9 Insertion of strings into refuse through piezometer ports to measure differential compression 109
Figure 3.10 The effect of the elevation of the upper platen depth on load cell readout 112
Figure 3.11 Variation of cell error with flexibility factor 114
Figure 3.12 Calibration of total pressure cells in gravel 115
Figure 3.13 Calibration results of earth pressure cell installed in gravel 115

4. Testing Methodology 117

Figure 4.1 Extrusion of waste DM3 from the compression cell 126
Figure 4.2 Schematic representation of falling head hydraulic conductivity test 128

5. Results 129

Figure 5.1 The loading of waste DM2 into the compression cell 136
Figure 5.2 Average dry and wet densities of DM2 at varying applied stresses 137
Figure 5.3 Differential compression of waste DM2 at applied stress of 87 kPa 139
Figure 5.4 Differential compression of waste DM2 at applied stress of 165 kPa 139
Figure 5.5 Differential compression of waste DM2 at applied stress of 322 kPa 139
Figure 5.6 Differential compression of waste DM2 at applied stress of 603 kPa 140
Figure 5.7 Uncorrected pressure cell data during compression of DM2 at an applied stress of 87 kPa 140

Results (cont'd)

Figure 5.8 Maximum total stress recorded during each compression stage of DM2 141
Figure 5.9 Effective porosity determination of DM2 prior to compression 142
Figure 5.10 Effective porosity determination of DM2 at an applied stress of 40 kPa 142
Figure 5.11 Constant head hydraulic conductivity test on DM2 prior to compression 143
Figure 5.12 Constant head hydraulic conductivity test on DM2 at an applied stress of 40 kPa. 143
Figure 5.13 The loading of waste DM3 into the compression cell 145
Figure 5.14 Average dry and wet densities of DM3 at varying applied stresses 147
Figure 5.15 Differential compression of waste DM3 at applied stress of 40 kPa 148
Figure 5.16 Differential compression of waste DM3 at applied stress of 87 kPa 148
Figure 5.17 Differential compression of waste DM3 at applied stress of 165 kPa 148
Figure 5.18 Differential compression of waste DM3 at applied stresses of 244 kPa 149
Figure 5.19 Differential compression of waste DM3 at applied stress of 322 kPa 149
Figure 5.20 Differential compression of waste DM3 at applied stress of 603 kPa 149
Figure 5.21 Maximum total stresses recorded during each compression stage of DM3 150
Figure 5.22 Total storage capacity of waste DM3 with no confining stress 151
Figure 5.23 Effective porosity determination of DM3 at an applied stress of 40 kPa 152
Figure 5.24 Effective porosity determination of DM3 at an applied stress of 87 kPa 152
Figure 5.25 Effective porosity determination of DM3 at an applied stress of 165 kPa 153
Figure 5.26 Effective porosity determination of DM3 at an applied stress of 322 kPa 153
Figure 5.27 Effective porosity determination of DM3 at an applied stress of 603 kPa 154
Figure 5.28 Constant head hydraulic conductivity test on DM3 at an applied stress of 40 kPa 155
Figure 5.29 Constant head hydraulic conductivity test on DM3 at an applied stress of 87 kPa 156
Figure 5.30 Constant head hydraulic conductivity test on DM3 at an applied stress of 165 kPa 156
Figure 5.31 Constant head hydraulic conductivity test on DM3 at an applied stress of 322 kPa 157
Figure 5.32 Constant head hydraulic conductivity test on DM3 at an applied stress of 603 kPa 157
Figure 5.33 Differential compression of waste PV1 at applied stress of 40 kPa 162
Figure 5.34 Differential compression of waste PV1 at applied stress of 87 kPa 162
Figure 5.35 Differential compression of waste PV1 at applied stress of 165 kPa 163
Figure 5.36 Differential compression of waste PV1 at applied stress of 322 kPa 163
Figure 5.37 Differential compression of waste PV1 at applied stress of 603 kPa 163
Figure 5.38 Maximum total stress recorded during each compression stage of PV1 164
Figure 5.39 Effective porosity determination of PV1 with no confining stress 165
Figure 5.40 Effective porosity determination of PV1 at an applied stress of 40 kPa 165
Figure 5.41 Effective porosity determination of PV1 at an applied stress of 87 kPa 166
Figure 5.42 Effective porosity determination of PV1 at an applied stress of 165 kPa 166
Figure 5.43 Effective porosity determination of PV1 at an applied stress of 322 kPa 167
Figure 5.44 Constant head hydraulic conductivity test on PV1 with no confining stress 169

Results (cont'd)

Figure 5.45 Constant head hydraulic conductivity test on PV1 at an applied stress of 40 kPa 169
Figure 5.46 Constant head hydraulic conductivity test on PV1 at an applied stress of 87 kPa 170
Figure 5.47 Constant head hydraulic conductivity test on PV1 at an applied stress of 165 kPa 170
Figure 5.48 Constant head hydraulic conductivity test on PV1 at an applied stress of 322 kPa 171
Figure 5.49 Constant head hydraulic conductivity test on PV1 at an applied stress of 603 kPa 171
Figure 5.50 The loading of waste PV2 into the compression cell 172
Figure 5.51 Differential compression of waste PV2 at applied stress of 40 kPa 174
Figure 5.52 Differential compression of waste PV2 at applied stress of 87 kPa 174
Figure 5.53 Differential compression of waste PV2 at applied stress of 165 kPa 174
Figure 5.54 Differential compression of waste PV2 at applied stress of 322 kPa 175
Figure 5.55 Differential compression of waste PV2 at applied stress of 603 kPa 175
Figure 5.56 Maximum total stress recorded during each compression stage of PV2 176
Figure 5.57 Total Storage capacity of waste PV2 determined at an applied stress of 603 kPa 177
Figure 5.58 Falling head hydraulic conductivity test for waste PV2 at an applied stress of 603 kPa 177
Figure 5.59 The loading of waste AG1 into the compression cell 179
Figure 5.60 Differential compression of waste AG1 at applied stress of 40 kPa 181
Figure 5.61 Differential compression of waste AG1 at applied stress of 87 kPa 181
Figure 5.62 Differential compression of waste AG1 at applied stress of 165 kPa 181
Figure 5.63 Differential compression of waste AG1 at applied stress of 322 kPa 182
Figure 5.64 Differential compression of waste AG1 at applied stress of 603 kPa 182
Figure 5.65 Maximum total stress recorded during each compression stage of AG1 183
Figure 5.66 Total Storage capacity of waste AG1 at an applied stress of 40 kPa 183
Figure 5.67 Effective porosity determination of AG1 at an applied stress of 40 kPa 184
Figure 5.68 Effective porosity determination (by saturation) of AG1 at an applied stress of 87 kPa 184
Figure 5.69 Effective porosity determination (by draining) of AG1 at an applied stress of 87 kPa 185
Figure 5.70 Effective porosity determination (by saturation) of AG1 at an applied stress of 165 kPa 185
Figure 5.71 Effective porosity determination (by draining) of AG1 at an applied stress of 165 kPa 186
Figure 5.72 Effective porosity determination of AG1 at an applied stress of 322 kPa 186
Figure 5.73 Effective porosity determination of AG1 at an applied stress of 603 kPa 187
Figure 5.74 Constant head hydraulic conductivity test on AG1 at an applied stress of 40 kPa 188
Figure 5.75 Constant head hydraulic conductivity test on AG1 at an applied stress of 87 kPa 189
Figure 5.76 Constant head hydraulic conductivity test on AG1 at an applied stress of 165 kPa 189
Figure 5.77 Constant head hydraulic conductivity test on AG1 at an applied stress of 322 kPa 190

Results (cont'd)

Figure 5.78 Constant head hydraulic conductivity test on AG1 at an applied stress of 603 kPa 190

6. Data interpretation and analysis 192

Figure 6.1 Calculated dry density profile of DM2 at varying applied stresses 195
Figure 6.2 Calculated dry density profile of DM3 at varying applied stresses 195
Figure 6.3 Calculated dry density profile of AG1 at varying applied stresses 195
Figure 6.4 Transmission of stress between upper and middle (waste) earth pressure cells 199
Figure 6.5 Corrected vertical stress in basal gravel with depth for all wastes 200
Figure 6.6 Ratio of transmitted stress vs depth in cell 200
Figure 6.7 Average density of DM3 vs effective stress 204
Figure 6.8 Average density of PV1 vs effective stress 205
Figure 6.9 Average density of AG1 vs effective stress 205
Figure 6.10 Volumetric water contents vs effective stress for DM3 208
Figure 6.11 Volumetric water contents vs effective stress for PV1 208
Figure 6.12 Volumetric water contents vs effective stress for AG1 209
Figure 6.13 Water content at field capacity of DM3 vs effective stress 209
Figure 6.14 Water content at field capacity of PV1 vs effective stress 210
Figure 6.15 Water content at field capacity of AG1 vs effective stress 210
Figure 6.16 Hydraulic conductivity of DM3 vs effective stress 214
Figure 6.17 Hydraulic conductivity of PV1 vs effective stress 214
Figure 6.18 Hydraulic conductivity of AG1 vs effective stress 215
Figure 6.19 Hydraulic conductivity of all wastes vs effective stress 215
Figure 6.20 Constrained modulus vs vertical effective stress for all wastes 220

7. A stress dependent hydraulic conductivity flow model 223

Figure 7.1 Relationship and dependency of model variables 227
Figure 7.2 Existing and revised program structure 228
Figure 7.3 Consideration of a small volume of waste at depth z in a landfill 232
Figure 7.4 Analysis of vertical infiltration through a landfill 236
Figure 7.5 Example of vertical flow spreadsheet analysis for a 10m deep landfill 238
Figure 7.6 Comparison of infiltration rates between models 240
Figure 7.7 Comparison of pore water pressures and effective stresses between models: drainage blanket completely dewatered (PWP=0) 240
Figure 7.8 Confined well analysis 241
Figure 7.9 MODFLOW grid design to simulate flow to a well 243
Figure 7.10 Comparison of calculated flow rates for confined well 246

8. Discussion and application of results to sustainable landfilling 249

Figure 8.1 Hydrogeological properties of waste DM3 in relation to dry density 251
Figure 8.2 Changes in effective stress and waste density in a 30m deep landfill 253
Figure 8.3 Volume of water required to bring waste DM3 to field capacity 262

Discussion (cont'd)

Figure 8.4 Flushing volumes to reduce the ammoniacal nitrogen concentration in a unit volume of waste to < 10 mg/l 267

Figure 8.5 Flushing volumes to reduce NH_3-N concentrations in a unit volume of waste at various dry densities to <10 mg/l 269

Figure 8.6 Maximum yield, expressed as a recharge rate, of a pumped well located in a 20 metre grid of wells in a 40m deep landfill 276

Figure 8.7 Flushing rates through various depths of unsaturated landfill 280

Figure 8.8 Comparison of maximum flushing rates through saturated and unsaturated landfills. 282

Figure 8.9 Variation in vertical effective stress, pore water pressure and hydraulic conductivity with depth in a 30 m deep landfill with saturated downward flow 282

Figure 8.10 Maximum flushing rates through saturated and unsaturated landfills:- hydraulic conductivity based on unsaturated stress distribution. 283

Figure 8.11 Variation in vertical effective stress and pore water pressure with depth in a 30 m deep landfill with saturated downward flow:- hydraulic conductivity based on unsaturated stress distribution 284

Figure 8.12 Infiltration rate through a 30 m deep landfill for various heads in a basal drainage layer: hydraulic conductivity varies with effective stress 286

Figure 8.13 Infiltration rate through a 30 m deep landfill for various heads in a basal drainage layer: hydraulic conductivity based on effective stress distribution with zero head in drainage layer 287

Figure 8.14 Infiltration rate through a 30 m deep landfill for various heads in a basal drainage layer: hydraulic conductivity based on unsaturated stress distribution 288

Figure 8.15 Specific flushing rates according to the depth of an upper collector drain in a 30m deep landfill: hydraulic conductivity varies with effective stress 289

Figure 8.16 Variation in vertical effective stress, pore water pressure and hydraulic conductivity with depth in a 30 m deep landfill with saturated upward flow to a drain located at a depth of 10 m 291

Figure 8.17 Variation in vertical effective stress, pore water pressure and hydraulic conductivity with depth in a 30 m deep landfill with saturated upward flow to a drain located at a depth of 20 m 291

Figure 8.18 Specific flushing rates according to the depth of an upper collector drain in a 30m deep landfill: hydraulic conductivity based on effective stress under hydrostatic conditions 293

Figure 8.19 Specific flushing rates according to the depth of an upper collector drain in a 30m deep landfill: hydraulic conductivity based on unsaturated effective stress 293

Figure 8.20 Variation in specific flushing rate through a landfill with a low permeability layer 294

Figure 8.21 Downward flow through a 30 m deep landfill with a low permeability layer at a depth of 15m 295

Figure 8.22 Upward flow through a 30 m deep landfill with a low permeability layer at a depth of 15m 296

Figure 8.23 Variation in specific flushing rate through a landfill with a low permeability layer where the hydraulic conductivity and density of the waste are related to the stress under unsaturated conditions 297

Figure 8.24 Different pumping configurations from a block centred grid of wells 299

Discussion (cont'd)

Figure 8.25 MODFLOW grid design to simulate operation of injection and abstraction wells 299

Figure 8.26 Variation in hydraulic conductivity with depth, based on unsaturated stress distribution 302

Figure 8.27 Head distribution for injection wells and abstraction wells on parallel grid, with hydraulic conductivity based on unsaturated stress distribution 303

Figure 8.28 Head distribution for injection wells and abstraction wells on parallel grid with hydraulic conductivity varying with effective stress 303

Figure 8.29 Head distribution along column 2 between injection and abstraction well 304

Figure 8.30 Variation of flow rate with depth into pumped / injection well: hydraulic conductivity based on unsaturated stress distribution 306

Figure 8.31 Variation of flow rate with depth into pumped/ injection well: hydraulic conductivity varies with effective stress 306

Figure 8.32 Variation of specific flushing rate with depth at various localities in fixed hydraulic conductivity model 308

Figure 8.33 Variation of specific flushing rate with depth at various localities in variable hydraulic conductivity model 308

Figure 8.34 Head distribution for diagonally oriented abstraction and injection wells: hydraulic conductivity based on unsaturated stress distribution 310

Figure 8.35 Head distribution for diagonally oriented abstraction and injection wells: hydraulic conductivity varies with effective stress 310

Figure 8.36 Variation of flow rate with depth for diagonally oriented abstraction and injection wells: hydraulic conductivity based on unsaturated stress distribution 311

Figure 8.37 Variation of flow rate with depth for diagonally oriented abstraction and injection wells: hydraulic conductivity varies with effective stress 311

Figure 8.38 Variation in specific flushing rate with depth for diagonally oriented abstraction and injection wells: hydraulic conductivity based on unsaturated stress distribution 312

Figure 8.39 Variation in specific flushing rate with depth for diagonally oriented abstraction and injection wells: hydraulic conductivity varies with effective stress 312

Figure 8.40 Variation of specific flushing rate with depth in a landfill with an area of high permeability at a depth of 20.5 metres 313

Figure 8.41 Relationship between density of waste DM3 and hydraulic conductivity 316

Figure 8.42 Infiltration rate for a) $K=2.1(s')^{-2.71}$ and b) $K=17(s')^{-3.26}$ against landfill depth for various pre-compacted waste densities 317

Figure 8.43 Design of a double composite liner to mitigate the effects of high leachate heads 321

Figure 8.44 Proposed high rate flushing bioreactor design 329

Appendix A - Specifications 359

Figure A1 Hydraulic control circuit 360

Figure A2 Master electrical circuit 361

Figure A3 Power circuits 362

List of Tables

2. Literature review and definition of terms 44

Table 2.1 Releasable nitrogen content of refuse determined in laboratory scale experiments 46

Table 2.2 Composition of waste arisings from the City of Philadelphia in the early 1900s 50

Table 2.3 Breakdown of waste composition over a 30 year period in the UK 50

Table 2.4 Water contents of individual components of household wastes 51

Table 2.5 Composition and water contents of an 'average' UK household waste 52

Table 2.6 Reported values of absorptive capacity for household wastes (MSW) 65

Table 2.7 Summary of reported values for hydraulic conductivity of household wastes 78

3. Equipment design and construction 81

Table 3.1 Calculated reduction in vertical effective stress with depth for varying values of ϕ' and δ 90

Table 3.2 Monitoring requirements of compression cell 93

Table 3.3 Hydraulic cylinder summary 99

Table 3.4 Use of hydraulic cylinders with different pumps 100

Table 3.5 Reference levels of various points on the compression cell 106

4. Testing Methodology 117

Table 4.1 Increments of applied load used in compression tests 120

5. Results 129

Table 5.1 Summary of materials tested and test codes 130

Table 5.2 Size and category analysis of waste used in tests DM1 and DM2 132

Table 5.3 Detailed compositional analysis of waste used in tests DM1 and DM2 133

Table 5.4 Summary of the loading of waste into compression cell for Test DM1 133

Table 5.5 Compression of waste DM1 at varying applied stresses 134

Table 5.6 Water contents at field capacity of DM2 138

Table 5.7 Effective porosity of DM2 at varying applied stresses 141

Table 5.8 Size and category analysis of waste DM3 144

Table 5.9 Changes in dry density and water content at field capacity of DM3 146

Table 5.10 Effective porosity of DM3 at varying applied stresses 154

Table 5.11 Hydraulic conductivity of DM3 at varying applied stresses 158

Table 5.12 Size and category analysis of waste used in tests PV1 and PV2 160

Table 5.13 Changes in dry density and water content at field capacity of PV1 161

Table 5.14 Effective porosity of PV1 at varying applied stresses 167

Table 5.15 Hydraulic conductivity of PV1 at varying applied stresses 168

Table 5.16 Changes in dry density of waste PV2 at different applied stresses 173

Table 5.17 Size and category analysis of waste used in tests AG1 178

Table 5.18 Changes in dry density and water content at field capacity of AG1 180

Table 5.19 Effective porosity of AG1 at varying applied stresses 187

Table 5.20 Hydraulic conductivity of AG1 at varying applied stresses 188
Table 5.21 Summary of results 191

6. Data interpretation and analysis 192
Table 6.1 Separation distances and stresses recorded by total earth pressure cells in waste DM2 197
Table 6.2 Separation distances and stresses recorded by total earth pressure cells in waste DM3 197
Table 6.3 Separation distances and stresses recorded by total earth pressure cells in waste PV2 198
Table 6.4 Separation distances and stresses recorded by total earth pressure cells in waste AG1 198
Table 6.5 Estimated average vertical effective stress in wastes at varying applied loads 201
Table 6.6 Effective porosity and density of waste DM2 at different average stresses 203
Table 6.7 Effective porosity and density of waste DM3 at different average stresses 203
Table 6.8 Effective porosity and density of waste PV1 at different average stresses 203
Table 6.9 Effective porosity and density of waste PV2 at different average stresses 204
Table 6.10 Effective porosity and density of waste AG1 at different average stresses 204
Table 6.11 Effective porosity and volumetric water contents of waste DM3 at different average stresses 207
Table 6.12 Effective porosity and volumetric water contents of waste PV1 at different average stresses 207
Table 6.13 Effective porosity and volumetric water contents of waste AG1 at different average stresses 207
Table 6.14 Average stress and hydraulic conductivity for DM3 213
Table 6.15 Average stress and hydraulic conductivity for PV1 213
Table 6.16 Average stress and hydraulic conductivity for AG1 213
Table 6.17 The constrained modulus of waste DM1 218
Table 6.18 The constrained modulus of waste DM2 218
Table 6.19 The constrained modulus of waste DM3 218
Table 6.20 The constrained modulus of waste PV1 219
Table 6.21 The constrained modulus of waste PV2 219
Table 6.22 The constrained modulus of waste AG1 219
Table 6.23 Specific volume and average particle density of waste DM3 221
Table 6.24 Specific volume and average particle density of waste PV1 222
Table 6.25 Specific volume and average particle density of waste AG1 222

7. A stress dependent hydraulic conductivity flow model 223
Table 7.1 Format of data input files to SDK module 230
Table 7.2 List of variables relating to Figure 7.3 232
Table 7.3 SDK MODFLOW data file for vertical flow problem 239
Table 7.4 Design of finite difference grid 244
Table 7.5 SDK MODFLOW data file for confined well analysis 246
Table 7.6 Analytical model data input for confined well 246

8. Discussion and application of results to sustainable landfilling 249

Table 8.1 Variables used to calculate average effective stress in Table 8.2 256

Table 8.2 Maximum average effective porosity in various depths of landfill 256

Table 8.3 Well spacings required to control leachate heads in various depths of landfill 259

Table 8.4 Number of wells per hectare for various grid spacings 260

Table 8.5 Flushing volumes to reduce the NH_3-N concentration in a unit volume of waste to < 10 mg/l 266

Table 8.6 Flushing volumes to reduce NH_3-N concentrations in a unit volume of waste at various dry densities to <10 mg/l 268

Table 8.7 Specific flushing rates required to flush various volumes of leachate through a unit volume of waste over different time-spans 270

Table 8.8 Maximum possible effective stress that maintains various hydraulic conductivities 272

Table 8.9 Drain spacings for various depths of landfill and infiltration rates 274

Table 8.10 Maximum well yields, expressed as a recharge rate, for varying saturated depths in a 40 metre deep landfill 276

Table 8.11 Available methods for introducing leachate into landfills 278

Table 8.12 Variables used in saturated downward flow analysis 281

Table 8.13 Variables used in upward and downward flow analysis 285

Table 8.14 Maximum infiltration and specific flushing rates through a 30m deep landfill with a 0.5m thick low permeability layer at various depths 294

Table 8.15 Design of finite difference model grid for four wells 300

Table 8.16 SDK MODFLOW data input file: injection and abstraction wells 301

Table 8.17 Location of model cells where specific flushing rate is calculated 307

Table 8.18 Relationship between tipping densities and saturated densities for DM3 316

Chapter 1

Introduction

1.1 Summary

The core concepts of sustainable development are outlined and then applied in general terms to waste management. The European Commission and the UK Government's interpretations of sustainable development as applied to waste management are reviewed. It is concluded that current day landfills do not meet the criteria of sustainable development. The reasons for this are considered within a historical review of the evolution of landfill design and operations. For a landfill to be sustainable it must be brought to a stable non-polluting state within a timescale that does not pass pollution problems on to future generations. This requires that methods have to be adopted to remove the pollution load of the waste which, if undertaken within the landfill, will require an element of accelerated flushing. The ability to flush a waste is dependent on its hydrogeological properties. The need for research into the geotechnical and hydrogeological properties of wastes for the purpose of understanding flushing and the movement and control of leachate in landfills is also described.

1.2 Introduction

Sustainable development has become a cornerstone of many areas of national and local policy making in the UK (HMSO, 1994). It is reflected in numerous government guidance notes, and is being incorporated into many policies on the environment and transport (e.g. DETR, 1998). The principal aim of the Environment Agency, as defined by section 4 of the Environment Act 1995 (DoE, 1995), is to contribute towards

achieving sustainable development, whilst discharging its duties to protect or enhance the environment (e.g. DoE, 1996). Many Local and Unitary Authorities are already implementing Local Agenda 21 initiatives, which aim to foster the principles of sustainable development at a local level (e.g. Chelmsford Borough Council, c.1998).

Sustainable development is about change; change to present day practices and attitudes which, if left unchecked, will cause lasting and potentially irreparable damage to global infrastructures to the detriment of future generations. Change is required to many areas of life: to activities that produce large quantities of greenhouse gasses that threaten global weather systems; to operations that cause pollution and wastefully deplete the world's ecological capital and resources; and to global economics and markets that result in an inequitable distribution of those resources over the world.

When viewed in the light of these global issues, the disposal of household waste to landfill may seem relatively insignificant. However, for sustainable development to work, it has to be universally applied to all manners of activities at a local, national and international level. Landfilling is not exempt from this process. This thesis is based on an investigation of the hydrogeological and geotechnical properties of household waste. The findings of the research are applied to the development of more sustainable landfilling practices.

This chapter reviews the general topic of sustainable development (Section 1.3) before considering how waste management fits into this overall framework (Section 1.3.4). The UK government's position on the meaning of sustainable landfill is detailed and interpreted further (Section 1.3.5). The reasons why existing landfill sites of today are not sustainable are considered alongside a review of the evolution of landfill designs (Section 1.4). Finally the rationale for the research is explained, in particular the link between the hydrogeological properties of waste and the development of sustainable landfilling practices (Section 1.5).

1.3 Sustainable development

"Sustainable development is a very simple idea. ***It is about ensuring a better quality of life for everyone, now and for generations to come"*** (DETR, 1998).

Alternatively, sustainable development can be considered as *"development that meets the needs of the present without compromising the ability of future generations to meet their own needs"* (World Commission on Environment and Development, 1987).

1.3.1 The need for sustainable development

Approximately two hundred and fifty years ago, the beginning of the Industrial Revolution in the UK heralded in a period of unprecedented growth in the use and exploitation of natural resources, that shows no signs of abating to this day. The process of industrialisation led to a further deterioration in (already poor) standards of public health associated with overcrowding and environmental pollution in urban conurbations. In the middle of the nineteenth century, the first concerted steps were taken to remedy the situation with general improvements in sanitation, water supply and treatment and the construction of sewerage systems. These improvements continued into the twentieth century with the progressive implementation of more stringent controls over air and water pollution.

The extent of world-wide industrialisation in recent times, however, means that what would have been considered local or, at worst, national problems a century ago have now taken on a global context. For example, concerns over localised smogs in central London in the 1950's, successfully dealt with by the Clean Air Act 1956 (HMSO, 1956), have now been replaced by anxieties over the emissions of greenhouse gasses (including those from landfills) widely considered to be responsible for global warming and problems associated with acidification.

Global problems related to water include increasing levels of micro-pollutants in the world's rivers and oceans and world-wide shortages of drinking water, made worse by more erratic weather patterns, a rapidly increasing population and increasing demand. In the mid 1980's, the World Health Organisation estimated that there were 1.7 billion people who did not have an adequate supply of drinking water.

Per capita production of waste is increasing. Between the mid 1970's and late 1980's, there was a 26% increase in the arisings of municipal waste within countries covered by the Organisation for Economic Co-operation and Development (OECD) (HMSO, 1994).

1.3.2 The Brundtland Report

The nature, extent and speed of various detrimental and global environmental changes were brought to the World's attention in 1987 with the publication of the Brundtland Report entitled 'Our Common Future' (World Commission on Environment and Development, 1987; summary by Hinrichsen, 1989). It was the final report of the World Commission on Environment and Development, set up by the United Nations in 1983. The report summarised a century of unprecedented growth: in human population; in technology and the use and misuse of natural resources; and, perhaps most importantly, in the ability of man's actions to alter the ecosystems of the world. The report

extrapolates existing trends to describe an impoverished future given continued unchecked 'development' and growth.

Brundtland argued that humanity should proceed in a way which will sustain activity and progress for the entire planet into the distant future. This will require a transformation from a world economy which relies on the exploitation of the earth's ecological capital to an economy and way of life based on sustainable husbandry of the earth's resources.

Sustainable development entails preserving the overall balance and value of the earth's natural capital stock. It requires that cost benefit criteria (short, medium and long term) are redefined to reflect real socio-economic effects and costs of consumption, exploitation and conservation. It also requires a more equitable distribution of resources over the world (e.g. EC, 1993). The following characteristics of sustainable development were defined:-

a) maintenance of an overall quality of life;

b) maintenance of continuing access to natural resources; and

c) avoidance of lasting environmental damage.

1.3.3 Sustainable development in practice

The Brundtland report led to the Rio de Janeiro Earth Summit in 1992 and the drawing up of a multi-point action plan called Agenda 21 (e.g. Quarrie, 1992 - abridged version). Many countries, including the UK, recognised the need for change and signed up to Agenda 21, thereby committing themselves to making their future activities and developments more sustainable.

There are many activities where it is relatively easy to understand what sustainable development means. For example, the exploitation of replaceable natural resources, such as timber and fish, would require that felling is balanced by replanting schemes and that fish stocks are not depleted to an extent that regeneration no longer becomes possible. In both cases there is also the requirement to preserve the quality of the environment, e.g. the nature and structure of the soil in the case of forestry and the quality and biodiversity of the oceans in the case of fishing. The application of the principal of sustainable development to activities such as power generation, exploitation of non replenishable mineral resources and waste management is, however, more difficult.

Brundtland's vision was for a low energy future grounded in energy efficiency, conservation and the aggressive development of new and renewable resources, such as hydroelectric power, wind and solar energy. Less reliance is therefore placed on the current use of carbon based energy sources, which are both finite and contribute to greenhouse gas emissions of CO_2, and on nuclear power with its unsolved problem of radioactive waste disposal.

Industrial manufacturing will always require raw materials, which are often not replenishable; therefore, their exploitation is perhaps not sustainable in the conventional sense of the word. However, where minerals or resources can be won without causing lasting environmental damage there is little reason for society not to benefit from their use at some point in the future. Therefore, a sustainable development of non-replenishable resources encourages production systems that prolong the benefit of the resource, by using it efficiently, reducing the amount of waste produced and reusing or using recycled materials as much as possible. This is the starting point for sustainable waste management - systems to prevent the generation of wastes. However, on the basis that it does not seem feasible (certainly at the present) to have a zero waste society, a slightly wider definition of sustainable development is required to help formulate policy on the disposal of wastes.

1.3.4 Waste management in relation to sustainable development

In 1993 the European Commission published their fifth Programme of Policy and Action in Relation to the Environment and Sustainable Development which included a hierarchy of waste management options (EC, 1993). The primary emphasis of the hierarchy is the prevention or reduction of wastes, followed by promotion of recycling and reuse, and then the optimization of final disposal methods for waste that is not reused. Any waste that cannot be recycled or reused is to be disposed of safely in an order of preference, starting with combustion with energy recovery, landfilling with energy recovering, and lastly incineration or landfilling without any energy recovery (HMSO, 1994).

The placement of landfills at the very bottom of the waste management hierarchy perhaps reflects the legacy of many decades of relatively uncontrolled landfilling (see Section 1.4). Modern 'state of the art' landfill designs in Europe and the USA are not generally considered sustainable. This may, at first sight, seem slightly surprising as landfills can be, and increasingly are, operated so that there are no adverse environmental impacts.

Standards in the UK for new landfill design, engineering and operation are high (e.g. DoE, 1995a). Modern landfills are lined to protect groundwater from contamination.

Leachate production is discouraged by cellular landfilling, capping and surface water drainage. Any leachate that is produced is removed to limit the build up of head on the base of the site. Landfill gas extraction systems are included to prevent gas migration and to facilitate energy recovery. Furthermore, there is legislation (Water Resources Act, 1991) to restore the environment should pollution occur with, for example, provisions for groundwater to be cleaned up at the operator's expense (DoE, 1991). It is reasonable to assume that modern day landfills will not be allowed to cause environmental pollution, which certainly corresponds with characteristic c) of sustainable development defined in Section 1.3.2 above. However, to understand why landfills are not sustainable, reference needs to made to the underlying concept of sustainable development.

The definition of sustainable development in the Brundtland report appears useful: a "development that meets the need of the present without compromising the ability of future generations to meet their own needs", or in other words, one that should not pass problems onto future generations. The polluting potential of wastes deposited in highly engineered 'dry tomb' landfills of today will exist for many centuries (e.g. Harris *et al*, 1994) as degradation processes are inhibited and there are no mechanisms to remove the pollution load. Even if it were possible that the integrity of today's landfills could be engineered to last that long (Hall, 1997), such sites would require the input of resources, in terms of monitoring and maintenance, over these protracted timescales and, therefore, cannot be considered sustainable.

There is an argument that as long as adequate financial provision for the long term maintenance and aftercare of sites is made during the landfill's operational life, then this will not carry a burden forward to future generations (e.g. Frost, 1997). In the UK, landfill operators already have to demonstrate that they are financially fit and proper to operate. For example, they have to make adequate financial provisions to discharge all their future responsibilities (Environmental Protection Act, 1990 (DoE, 1990)). However, it is difficult to envisage how these guarantees will last over a length of time that is measured in centuries rather than decades. Furthermore, do we really want to pass on a pollution liability of such scale, with or without a guarantee from the bank? Within the UK, approximately 137 million tonnes of controlled wastes are landfilled each year (DoE, 1992). This excludes arisings from agriculture, mining and quarrying and dredged spoils. If all of these wastes were sent to dry tomb landfills where their polluting potential still existed in 500 years time, society in the UK in the middle of the next millennium would have stewardship over a backlog of some 68.5 billion tonnes of waste (again using current day figures). What type of financial provision can adequately safeguard against such risks?

Whilst there is a broad framework of European policy promoting sustainable development (EC, 1993), European legislation on waste management does not specifically promote it as an over-riding objective. For example, sustainability is not explicitly mentioned in the June 1998 proposal for a council directive on the landfill of waste (EC, 1998). The emphasis of the proposal is on the reduction of the pollution load of wastes prior to their disposal, but not necessarily to levels where the pre-treated waste can be safely landfilled in non-contained and non monitored sites. Although this could be considered to be more sustainable than direct landfilling of crude wastes, the core principle of sustainable development is not achieved, especially when the pre-treated wastes are placed in a 'dry tomb' landfill. It should be noted that many existing waste pre-treatment processes do not adequately remove the polluting potential of the residues which are ultimately landfilled. For instance, wastes which have been pre-treated to final storage quality in Germany would still need to be flushed, possibly within the landfill environment, to meet the criteria for sustainable landfill. As an example, the assignment value for ammonium within Class II (non-inert) landfills in Germany is 200 mg/l, and it is recognised (e.g. Stegmann 1997) that these sites require high standards of engineering and long term aftercare. The requirement for flushing would also apply to the concentrated inorganic pollutants contained in the ash from MSW incinerators.

1.3.5 Sustainable landfills - The UK's position

The UK government has recently stated that landfill will remain a fundamental component of its waste management strategy for the foreseeable future (DoE, 1995b). This is not surprising as it is inconceivable that any solid waste management policy in an industrial nation could avoid the final disposal to land of some solid fraction, no matter how much pre-treatment, reuse and recycling it incorporates. The UK has also defined a sustainable landfill as one which is brought to a stable non- polluting state 30 to 50 years after the cessation of landfilling activities (DoE, 1995a). Gronow (1996) interpreted this to mean that a sustainable landfill would be in equilibrium with its surrounding environment and there could be confidence that no future maintenance or monitoring of the wastes would be required. This does not mean that the wastes would need to be 100% degraded or that any leachate released would have to be at drinking water quality. However, it does mean that the majority of the waste's pollution load would need to be removed within the timescale. There appear to be two possible strategies for achieving this:

1) pre-treatment of the waste to remove the majority of the pollution load prior to landfill; or

2) *in situ* treatment of the wastes to remove the pollution load to acceptable levels by operating the landfill as a bioreactor with a high rate of flushing.

This thesis is concerned with the second of these two options. The principle of a high rate flushing bioreactor, as outlined in WMP26B (DoE, 1995a), is to transfer the pollution load of the solid waste into landfill gas or leachate to enable the load to be removed within a period of approximately one generation. The ease with which landfills can be operated as high rate flushing bioreactors will depend to a large extent on the hydrogeological properties of the landfill. The key features of a high rate flushing bioreactor are:-

1) the acceleration of the rates of waste degradation and gas production by a variety of methods, including the introduction and circulation of fluids in the landfill; and

2) the introduction and circulation of large volumes of liquid within the landfill to flush out and remove soluble degradation products in the leachate.

These features are almost diametrically opposed to the design principles being recommended by the Government less than a decade previously (DoE, 1986). It is little wonder that the landfill industry has been less than enthusiastic about embracing such a concept. There remains considerable debate over what constitutes a sustainable landfill (e.g. IWM, 1999), with many in the industry fundamentally disagreeing with the above approach and rationale (e.g. Jones, 1997); there is concern that the necessary technology is not proven, (e.g. Savory, 1998) and there is considerable scepticism about the justification for the additional costs that would be entailed.

1.4 Historical perspective - evolution of landfill design in the UK

The rapid changes in landfill engineering and practices that have occurred over the last decade could be taken as evidence of an ill-considered or inadequately researched waste disposal policy. Whilst there may be some merit to this argument, the evolution of landfill design and operation has followed a fairly logical path bearing in mind the state of (perhaps incomplete) knowledge at any particular time. However, a review of this evolutionary process indicates that there have been past opportunities to take a different, and perhaps more sustainable, approach to landfilling.

1.4.1 Why are landfills not already more sustainable?

Concerns about public health since Victorian times have led to the development of modern day waste disposal and sewage treatment techniques (see Section 1.4.2). Waste collection and disposal together with sewage treatment are essential pre-requisites to maintain the public health of any industrial or consumer based society. However, sewage treatment methods have developed to progressively higher standards of treatment of effluents returned to the environment, whilst landfills have progressed towards zero treatment and full containment. On this basis, sewage treatment is considered to be a far more sustainable process than the disposal of waste to landfills.

The initial priority of both sewage and waste management systems is the removal of the offending matter from the communities they serve. This need originally lead to the building of sewers (when sewage was eventually separated from surface water drainage) and the adoption of waste collection systems. Polluting matter was thus divided into material that could satisfactorily be removed by running water and solid wastes that needed to be carried away.

Volumes of sewage and other industrial effluents are immense and long term storage is clearly not possible, as is the case for solid waste: it has to be returned to the general water cycle. When this was done without any treatment (as was accepted practice in this country before the late nineteenth century) the detrimental impact on rivers and even coastal sea water was all too apparent. The effect of the pollution was clearly recognisable, and the need to develop systems to treat the effluent was readily apparent. Consequently, it has since been the aim of the waste water industry to treat waste waters to a standard compatible with the receiving environment. Over the years the understanding of what is compatible with the environment has evolved, treatment systems have improved and more stringent regulatory controls have been progressively applied. Very large sums of capital have been invested in the relevant infrastructure and in the development of more advanced and efficient treatment technologies. It is accepted that there will be ongoing running costs for which charges are levied directly on the general public by water utility companies.

In comparison, it is not generally accepted that there is a need to treat solid wastes to a standard compatible with the environment. This is partly because, historically, attention was given to aspects that had an immediate impact on the environment; water pollution in the case of sewage, public health nuisances (smells, vermin etc.) in the case of deposits of waste to land. As the composition of wastes changed (from predominantly ash - e.g. Parsons, 1906) it became clearer (principally because of discharges of leachate to rivers and streams) that wastes did have a large capacity to pollute water. At this stage efforts were directed to the containment of the problem

rather than treatment of the wastes. More recently attention has been turned to the treatment of solid wastes (e.g. Heerenklage and Stegmann, 1995; von Felde and Doedens, 1997), but in comparison with waste water treatment these techniques are still in their infancy. A further problem is the greater difficulty in defining how much treatment a waste needs to make it compatible with the environment. It will depend heavily on site location and on natural attenuation mechanisms, not currently understood in enough detail to be relied on.

The evolution of landfilling philosophy and practice is examined in more detail below.

1.4.2 The early years

Stephen (1951) summarised the early history of waste disposal up until the beginning of the 20th century, and this Section is based primarily on his review. Waste management involving the disposal of wastes to land has been practised by humanity from an early time. Perhaps the earliest records of organised landfilling come from the Neolithic, or late Stone Age, where mounds or middens of kitchen debris and food wastes were created. Some middens were of a considerable size, with examples 100 metres long, 50 metres wide and 1 metre high in Denmark, and up to 350 metres long, 70 metres wide and 3 metres high in Scandinavia.

The Romans operated a cleansing service, partly based on a system of sewers. Much of their rubbish and filth was discharged into the sewers which, not surprisingly, would periodically require digging out - a job reserved for slaves and convicts.

The Middle Ages in the UK, as in the rest of Europe, was a period of gross neglect. There were no organised waste collection or disposal systems and virtually any unwanted item was thrown into the streets. It was not until passage along the streets became impaired that a corporation would be forced to hire carts to remove the material, presumably to the nearest convenient place beyond the confines of the town or city. Attempts to prevent the deposit of material were relatively sporadic and ineffectual. The Berwick Lawes of the Guild in 1294 included provision that any person "*depositing filth, dust or ashes on the street, market place or banks of the River*" would be fined ninety six silver pennies. In 1357 King Edward III exhorted the Mayor and Sheriffs of London to "*enact a remedy against the fumes and other abominable stenches arising from dung, laystalls, and other filth accumulated on the Banks of the Thames.*". Whatever action was taken was either ineffectual or short lived as in 1751 a report entitled 'Observations on the past growth and present state of the City of London' (Morris, 1752) proposed that "*the cleansing of the entire Metropolitan area of London should be put under one uniform public management and all the filth be carted into lighters and conveyed by*

Thames to proper distances in the country", but these recommendations were also not acted on. It would take another 100 years before concerted steps were taken to improve the insanitary conditions in society.

1.4.3 Development of Waste Management Practices

In 1842 the Poor Law Commission produced the General Report on the Sanitary Condition of the Labouring Population of Great Britain (ENGLAND, 1842). The report linked the presence of decomposing remains and filth to various forms of epidemic, endemic or other diseases. The report echoed the widely held view that the main cause of the transmission of the ailments was through atmospheric or miasmic conditions. It was concluded that the frequency and intensity of disease could be reduced by removal of any material giving cause to stenches, by drainage, proper cleansing, better ventilation and other means of diminishing atmospheric impurity. The report recommended that the primary and most important measures to be taken were drainage, the removal of all refuse from habitations, streets and roads, and improvements to the water supplies. As a result there were great improvements to the supply of water to houses between 1840 and 1870 (Hassan, 1998).

Many Local Authorities rapidly accepted the need for organised public cleansing and adopted measures through Local Police Acts. Glasgow, in 1843, appointed an Inspector of Cleansing to make regulations for the watering, sweeping and cleansing of closes, thoroughfares and areas.

In London improved cleansing was to lead to the disposal or washing of wastes into the storm water system, resulting in increased levels of water pollution. This eventually led to the construction of the London Sewerage system by Sir Joseph Bazalgette between 1859 and 1875.

The Public Health Act of 1848 (ENGLAND, 1848) gave weight to the various local initiatives and Acts, by establishing a General Board of Health to provide guidance and aid to Local Authorities in matters of sanitation. However, the actions of Local Authorities to improve sanitary conditions were not always greeted with universal approval. For some the accumulations of filth, dung and human excreta provided an opportunity to make a living by selling the 'end-product' for agricultural purposes. Attempts to remove this source of income were met with (sometimes violent) opposition.

The early findings of the Poor Law Commission were soon backed up by more scientifically based work. In 1854 John Snow linked the occurrence of cholera with the

Broad Street Pump and hence established that the disease was carried through water, not the atmosphere. This led to rapid improvements in water supply and treatment systems with the initial introduction of filtration plants, followed soon after by chlorination. The work of Pasteur in the 1860's and 70's provided a scientific basis to disease prevention and helped place the presence of filth, decomposing and malodorous materials correctly in the chain of infectious transmission.

Modern day waste disposal was therefore borne out of public health concerns to remove refuse from the presence of human habitations. Little regard was given to where the material should be taken, although a primary requirement would have been to a location in close proximity to the area of production. The lack of tipping sites in close proximity to towns led to attempts being made in about 1870 to incinerate refuse in closed furnaces, and to the successful commissioning of "The Destructor" in Manchester in 1878 (Stephen, 1951).

At the beginning of this century H. de B. Parsons published his book "The Disposal of Municipal Refuse" (Parsons, 1906) based on work undertaken on the eastern seaboard of the United States. This was the first comprehensive treatise on waste disposal and provides a valuable insight into the activities and attitudes of the day. A classification of general refuse included categories for ashes, garbage, rubbish and street sweepings.

Garbage was defined as animal or vegetable wastes from kitchens, markets and slaughter houses. After ashes it was the largest component (by weight) of the general refuse. Rubbish included a variety of miscellaneous materials consisting of paper, wood, rags, metals and glass. Already in 1906 there were differences in attitude between the US and England with respect to separation of wastes at source. To ask householders in the United States at this time to separate garbage, ash and rubbish into separate containers was seen as no great problem, compared with England where, historically, the whole of the household refuse was thrown into a receptacle known as an ash-bin or ash pit.

Separation of the wastes at source in the US provided commercial opportunities for recycling and 'material' recovery. A considerable portion of the contents of rubbish could be sorted out and sold at a profit (a job generally done by Italians). In 1903 the privilege for picking rubbish in the Borough of Manhatten and the Bronx brought in US $71,000 (which is equivalent to approximately US $1.3 million at 1998 prices). In large towns or cities, where the high capital cost could be borne, rendering of garbage in digesters would produce a solid material suitable for fertiliser and a liquid 'tankage' from which oils and greases could be extracted. The grease had a number of uses including as a base for the manufacture of cheaper grades of perfume, hair dressings (pomades) and grease for wagon wheels (Parson, 1906)

Methods for disposing of wastes were listed as: dumping on land, dumping in water, ploughing into the soil, feeding to swine, reduction and incineration. The main requirement for selecting a site for the final deposition of refuse was that it should involve the shortest haulage possible. It is of note that H. de B. Parsons was generally against the dumping of refuse and garbage on land for the very reasons encompassed by the concept of sustainable development today. Apart from the most untidy and unsightly result of such dumps, "*covered garbage remains in a putrefactive condition for long periods ... Land thus filled is not safe for improvement until many years have passed. Such a method is not suitable for large communities as the spreading of this material in thin layers would require too large a land area.*" The implication of this statement is that waste should be placed in thin uncovered layers to allow rapid (presumably aerobic) degradation to occur. The use of ashes to fill land was considered acceptable and indeed desirable, as too was the periodic burning of the combustible part of a landfill.

The above guidance indicates a philosophy that wastes should be made inert, either before or soon after placement in the ground, to prevent the occurrence of future problems. Admittedly, the full extent of the problems would not have been appreciated at the time, especially with regard to environmental pollution. However, if this philosophy had been carried forward from the start of the twentieth century, with more attention being given to how to make wastes 'inert', in addition to how to control and reducing the impact of their undesirable nature, it is certain that waste disposal methods would have been very different to today.

1.4.4 Controlled tipping - State of the art landfilling for 50 years

Improvements to the method used to deposit refuse on land were pioneered in Bradford during the early 1920's, and became known as 'controlled tipping'. The system was adopted by the Ministry of Health in guidance from 1929 to 1932 (example reproduced by Bevan, 1967), the principles of which were to influence landfilling for the next 50 years. The method involved depositing and compacting refuse on land in shallow layers and covering the exposed surfaces with soil or other suitable material to form a seal. One specified purpose was to secure controlled biological decomposition by the retention of heat gases and moisture. The method resulted in significant savings compared with incineration and was accomplished without fire, fermentation or vermin problems. Tipping into water was to be avoided, mainly due to the creation of atmospheric nuisances (smells).

Jones & Owen (1934) published a report entitled "Some notes on the Scientific Aspects of Controlled Tipping" based on a series of experiments undertaken at Wythenshawe

landfill, (Manchester) and in the laboratory. The main purpose of this research was to provide scientific data to answer the question "is controlled tipping safe?". The emphasis on 'safe' was, at the time, related to public health rather than the protection of the environment.

The report is important for a number of reasons:-

1) it gave credibility to the practice of controlled tipping as an effective and safe method for waste disposal; and

2) it established a scientific basis for understanding landfilling processes.

In many ways the authors clearly understood and supported many of the principles of sustainable development being discussed today. The work identified the various aerobic and anaerobic processes that would cause the organic material in landfills to decompose over (a short period of) time to a state of 'final inertia' and stabilisation, rendering the landfill completely 'dead'. A landfill in this state "*would create no further problems to human health by being a source for smells or a breeding ground for flies and vermin*". There would also be no problems associated with settlement. In laboratory experiments it was demonstrated that cellulose and other organic materials could be completely broken down in 100 days. It was recognised that the microbiological conditions in a landfill were not ideal for rapid degradation and no attempt was made to estimate how long it would take for a landfill to stabilise. However, the advantages of pulverising or shredding wastes to create a homogeneous waste mass, and of adding water to speed up the degradation processes, were recognised.

The report also identified the various by-products of degradation and assessed their dangers to human health. The production of ammoniacal nitrogen was seen as a potential benefit, because it could be used as an agricultural fertiliser. Although various gaseous by-products were identified as being either poisonous or explosive, it was felt that the operation of controlled tipping would include sufficient safeguards to prevent any problems.

Ironically it was possibly this latter finding - that landfills were safe - that removed the need for the development of strategies to bring landfills to a state of inertia as quickly as possible. If it had been concluded that landfills were not safe until a state of inertia had been achieved, more attention might have been given to making sure inertia was reached.

By the early 1950's landfilling was still considered to be a "*legitimate, sound and economic disposal method, and if suitable sites exist for its adoption then a scheme for*

its successful application must be devised and costed against other possible schemes" (Stephen, 1951). By this time, the importance of suitable geology to site location was recognised, as were the existence of sites considered to be totally unsuitable for landfilling under any circumstances due to the risks of water pollution. An unsuitable location was cited as one on water bearing strata used for domestic drinking water.

Although the general scientific consensus was that controlled tipping of waste was both a safe and an acceptable form of disposal, arguments were being put for a different, and what has turned out to be a more sustainable, approach to landfilling. The following extract (Civic Trust, c.1968) was quoted in 'Notes on the Science and Practice of the Controlled Tipping of Refuse' (Bevan, 1967).

Extract from "Derelict Land" - Civic Trust (1963 - 1967)

"Britain's wealth and power were built, and to a large extent still rest, on the exploitation and industrial use of her mineral resources. This is a process which invariably makes a mess of the land. Our forebears, for the most part, left the mess as it was: either they did not mind, or they found the task of cleaning it up too difficult or too costly. The legacy of their neglect is that today, in England and Wales alone, more than 150,000 acres lie derelict .... each succeeding year sees a larger addition to the total acreage of land that has been worked out and left unproductive. The spread of dereliction has now reached at least 3,500 acres a year.

The area blighted by this creeping canker is, of course, much more extensive still. Our derelict acreage is made up of tens of thousands of separate patches. In some parts of the country these patches are sparsely scattered, but in the older industrial regions (where most of them lie) they are often close together. Where one acre in ten is laid waste, the whole landscape is disfigured; and such areas between them cover something like 2,000 square miles. Throughout much of South Lancashire and South Wales, Tyneside and Coalbrookdale, South-West Yorkshire and the black Country, the face of the earth is riddled with abandoned mineral workings, pocked with subsidence, gashed with quarries, littered with disused plant and piled high with stark and sterile banks of dross and debris, spoil and slag.

These deformities of nature do more than mar the view. Their grim desolation dulls the spirit - as their dust and fumes defile the fabric of the human settlements that straggle among them. Smouldering pit heaps foul the air, poisonous chemicals pollute the waterways and treacherous pits endanger the lives of adventurous children. Neglected wastes breed vermin and disease. Their very existence fosters slovenliness and vandalism, invites the squatter's shack and engenders a 'derelict land mentality' that can never be eradicated until the mess itself has been cleared up. Dereliction indeed, breeds a brutish insensibility, bordering on positive antagonism, to the life and loveliness of the natural landscape it has supplanted. It debases as well as disgraces our civilisation.

'Where there's muck there's money' was the big cliché that comforted our forebears' conscience. Today we are beginning to see that dirt, dereliction and decay are major obstacles to the future prosperity of our older industrial centres. We have undertaken to abate the pollution of the atmosphere in these 'black' areas. We have made up our minds progressively to purify their streams and rivers. But as yet we have made no systematic effort to tackle the mess that sullies the earth. If clean air and (eventually) clean waters, why not clean land too? Is the job too big for us? Would it cost too much? Is it not technically feasible? Or is a comprehensive programme of land renewal prevented by nothing more than 'administrative difficulties'?"

The inherent message in this extract, that the polluting potential of derelict land or landfills must be reduced, was to be ignored for the next 30 years.

1.4.5 The start of 'dilute and attenuate' and 'containment' philosophies

The terms 'dilute and attenuate' and 'containment' have often been used to describe two types of landfills. A stereotypical dilute and attenuate site would be one where any leachate produced would migrate through the base of the site and diffuse into the underlying geological formations and eventually into groundwater. A typical site might be an infill of an old chalk, or sand and gravel quarry which may have been excavated down to the water table. The 'containment' site would be one where any leachate produced would be largely contained within the site. A typical site might be a clay pit. In reality most landfills were not totally 'dilute and attenuate' or 'containment' in nature and fell in a continuum between these two extremes.

By the mid 1950's, a shortage of suitable sites meant that the general recommendations (not to tip into water or onto land overlying groundwater) stemming from the 1930's Ministry of Health guidance, were not always being adhered to. There were plenty of voids that did not match the criteria: worked out chalk pits in Hertfordshire, Kent and Surrey; gravel pits (usually water logged) in the Thames Valley, Hertfordshire and Essex and numerous other excavations. Experiments involving the tipping of wastes into water had already started at Egham, Surrey with the aim of establishing methods to control aerial pollution (i.e. smells).

As a result of this drive for new sites the Minister of Housing and Local Government (having taken over responsibility for waste disposal from the Ministry of Health) set up a Technical committee to report on the risks of polluting groundwater by tipping refuse either directly into groundwater or onto ground overlying groundwater. The report, 'Pollution of Water by Tipped Refuse' was published in 1961 and was based on a series of bench scale and larger scale experiments located at a disused sewage treatment works at Bushey in Hertfordshire (Ministry of Housing and Local Government, 1961).

The experiments established the quantity, rate of release and composition of polluting liquids resulting from the passage of rainfall through refuse tipped dry, and from refuse tipped into water. The research also investigated and demonstrated that the leachate would undergo purification, or attenuation, when passed through a filter of sand and gravel. The research indicated that the polluting load released from landfills was quite considerable, but that it also reduced quite rapidly.

This research made no attempt to investigate ways in which the degradation of the waste could be accelerated - the term 'final inertia' does not appear in the report. The emphasis had switched from trying to stabilise waste to developing an understanding of the effects of the pollution load on the environment and ways to control them.

Although it was demonstrated that polluting matter was removed from solid waste by 'flushing' at both wet and dry sites, dry tipping was recommended in favour of wet tipping because:-

a) the quantity of polluting matter extracted from refuse tipped dry was smaller than refuse tipped wet (it is probable that the refuse tipped dry became methanogenic, liberating a large proportion of the organic carbon load as landfill gas);

b) there was a delay in the release of the polluting matter; and

c) there was the opportunity for any polluting matter to be attenuated in the unsaturated zone.

It was concluded that dry sites could be safely located on fissured water bearing rocks if any of the following applied:-

a) material which had previously been deposited on safe sites and whose polluting potential had been removed was excavated and re-deposited;

b) the base of the site was lined to prevent leakage;

c) the top of the site was capped to reduce the amount of water entering the landfill. Leachate generation could further be limited by utilising the absorptive capacity of the waste; and

d) an aerobic saturated zone was maintained beneath the base of the site which would attenuate and treat any migrating leachate.

These conclusions helped crystallise thinking regarding containment and dilute and attenuate sites (although these terms were only applied retrospectively) and were used to justify the siting of many landfills in or on aquifers. However, the conclusion that the pollution load diminished rapidly (due to the high flushing rates that were utilised), probably provided a false sense of security about the actual long term polluting potential of wastes. There was little acknowledgement that the measures to limit the production of leachate outlined above, would mean that the pollution potential would diminish only very slowly.

It was clear that when Bevan (1967) published 'Notes on the Science and Practice of Controlled Tipping of Refuse', some of the conclusions of the 1961 report had been

adopted. Bevan reports one of the first engineered containment scheme - using puddled chalk and leachate drains in a chalk pit in Croydon.

In the early 1970's there were two significant Government commissioned reports published on waste disposal: on the Disposal of Solid Toxic Waste (Ministry of Housing and Local Government, 1970), and on Refuse Disposal (DoE, 1971). Both reports concluded that there were insufficient controls over the disposal of both hazardous and household wastes and contributed to the implementation of the Deposit of Poisonous Wastes Act 1972 and the Control of Pollution Act 1974 (HMSO, 1972 & 1974). These Acts introduced stricter controls over the operation of landfill sites in general, and the disposal of hazardous wastes in particular.

The reports reflect the fact that there was still relatively little concern over so called 'dilute and disperse' sites. The 1971 report highlighted that the experience of practitioners was more of problems with surface water contamination than with groundwater contamination. This was often related to an inadequate or incorrect site location. Problems relating to controlled tipping were blamed mainly on the failure of operators to adequately follow the 1930's Ministry of Health guidance. It was suggested that large sites were preferable to smaller sites as it would be easier to enforce the necessary controls. Pulverisation of wastes was also favoured as a means to accelerate biological breakdown and reduce the long term problems of settlement. It was recommended that wet pits should only be filled with inert wastes.

One conclusion of the 1970 report was that insufficient scientific research had been carried out on the methods of solid toxic waste disposal and on any resulting water pollution. This led to the establishment of a major co-operative research programme which investigated twenty existing landfills located in different geological settings and containing a variety of different waste types (DoE, 1978). Although the investigations showed that the polluting potential of the majority of the landfills was high even after a considerable period of time, the impact on surrounding groundwaters was generally of limited extent. It concluded that attenuation mechanisms (although not properly understood) both within the body of the landfill and within any unsaturated zone were extremely beneficial resulting in recommendations for at least 2 metres of unsaturated material beneath the base of sites. It was finally concluded that there could be no objection to "sensible" landfilling and that an ultra-cautious approach to landfill of hazardous and other types of waste was unjustified.

To summarise, the report strongly supported the principle of dilute and attenuate sites.

The implementation of the Control of Pollution Act 1974 (HMSO, 1974) put statutory duties on local authorities to licence and control the activities of waste disposal sites. This meant there was a need for comprehensive advice and guidance on all aspects of disposal. This was achieved through the publication of a series of Waste Management Papers by the Department of Environment.

Waste Management Paper 26 on "Landfilling Wastes" was published in 1986 and provided guidance on Planning and Site licensing, landfill site selection, design and engineering, landfill operations and site restoration (DoE, 1986). The use of both containment type sites and dilute and attenuate sites was supported subject to stringent site investigation and design to prevent water pollution. Techniques to minimise leachate production were adopted for all sites. It was also acknowledged that containment sites would require maintenance of active leachate collection systems for long periods of time after restoration.

1.4.6 The mid 1980s to 1990s - a decade of change

The decade following the publication of WMP 26 saw very rapid changes in the design philosophy of landfills, with dilute and attenuate sites outlawed virtually overnight. Walker (1994) identified a number of reasons for this:-

1) although the principle of attenuation had been demonstrated, there was an insufficient research base to allow the fundamental mechanisms to be properly understood. Hence, it was impossible to justify, on a rigorous and scientific basis, a landfill design which was relying on these principles. Justification of landfill designs became mandatory following the requirement to submit an Environmental Statement with any new Planning applications for major landfill developments. This requirement was in response to an EC directive (EC, 1985) and was enacted by regulation (DoE, 1988);

2) the landfill gas explosion at Loscoe in March 1986, resulting in a Public inquiry (Ryan, 1986) and guidance in the form of Waste Management Paper 27 on how to prevent landfill gas migration (DoE, 1991a), strengthened the case for containment site;

3) European legislation: the EC directives on waste (EC, 1991) and groundwater (EC, 1980) require the implementation of controls on landfilling operations to prevent groundwater pollution. The directive on wastes requires member states to take necessary measures to ensure that waste is disposed of without endangering human health or using methods which could harm the environment and, in particular,

without risk to water. The groundwater directive required member states (by the end of 1981) to prevent or limit the discharge into groundwater of a number of substances on two lists, List I and List II. Bearing in mind that ammoniacal nitrogen was included in List II (containing substances whose discharge to groundwater was to be limited) it is surprising that WMP 26, published in 1986, had not taken a more cautious approach to accepting dilute and attenuate sites. Transposition of this directive into UK law was not achieved until 1994 with the implementation of Regulation 15 of the Waste Management Licensing Regulations (DoE, 1994);

4) guidelines on the use of landfill liners were produced by the North West Waste Disposal Officers' Group in 1988 (NWWDO, 1988). Although the group had no jurisdiction outside its regional area, the standards were widely adopted nationally, especially after the formation of the National Rivers Authority (NRA) in 1989. The requirement for liners to be at least 1 metre thick and to meet a specification of a maximum hydraulic conductivity of $1x10^{-9}$ m/s was established;

5) major advances in lining technology and quality control in America and Europe meant it became possible to engineer high quality containment systems on sites where it had hitherto been impossible. The standards of the North West Waste Disposal Officers' Group soon became accepted as the minimum. Adoption of high lining standards at one site meant it became progressively more difficult to justify not using them on another;

6) the formation of the National Rivers Authority in 1989, with a remit to protect and preserve groundwater resources led to the development of a unified approach with the publication, for the first time, in 1992 a national policy on groundwater protection (NRA, 1992). The policy adopted a risk assessment approach, with risk being defined as a combination of the hazard, i.e. polluting potential, the vulnerability of the location to cause pollution, and the preventative measures taken. The Policy opposed landfilling in areas close to an abstraction source and called for high standards of engineering for any sites accepting biodegradable waste located on major or minor aquifers, whether they were being exploited or not;

7) increased public awareness of environmental issues was driving up environmental standards.

1.4.7 Risk assessment approach/ controlled release philosophy

In 1995 the DoE published revised guidance on the design and operation of landfill sites in the form of Waste Management Paper 26B (DoE, 1995a). The guidance takes an overall approach based on risk assessment rather than prescription. The principles of sustainable development are adopted, such that the requirement to return products of waste stabilisation to the environment must be carried out in a manner that minimises pollution control burdens on future generations. Three ways to achieve this objective are suggested:

1) selection of inert wastes for landfill disposal;
2) pre-treatment to a quality which will not cause unacceptable harm; and
3) management of bioreactive waste in such a way that the system degrades to approach a stable non-polluting state.

This thesis is primarily concerned with the last of these options as it is recognised that, in general, contaminants will need to be flushed from untreated or partially treated landfilled wastes before a stable non-polluting state is achieved.

1.5 Rationale for research

The need for further research into the hydrogeological and geotechnical properties of refuse was recognised in the late 1980's. At that time it was not, however, related to the need for sustainable development or the operation of high rate flushing bioreactor landfills but, rather, to practical problems that were being experienced in the operation of leachate management systems on landfill sites. It was clear that not only was there no specific hydrogeological data on which to base dewatering designs, but there was evidence that the hydrogeological properties of waste changed within the landfill environment. Beaven (1996) detailed case studies that illustrated this latter point: firstly, it was shown how changes in leachate levels in a landfill over time had to result from reductions in either the drainable porosity or the storativity of the waste; secondly, repeat pumping tests at the same location in a landfill after a period of nine years demonstrated that the hydraulic conductivity of the waste had reduced by almost an order of magnitude. In both cases the changes appeared to result from an increase in the depth of the site from continued landfilling, rather than from the passage of time itself.

A more detailed understanding of the hydrogeological properties of refuse was thus needed:

1) to help understand and predict changes in leachate levels within sites;

2) to provide hydrogeological data for use in the design of leachate dewatering or control systems, with two parameters of particular interest:
   a) the storativity, or drainable porosity, gives an indication of how much leachate needs to be removed to lower leachate heads by a given amount; and
   b) the hydraulic conductivity, in conjunction with the effective porosity, is required to allow leachate dewatering systems to be designed;

3) to understand how the properties of refuse may change over time, particularly as a result of increasing the depth of landfill. Changes in the properties of refuse as a result of degradation are also important but outside the scope of this research.

Although leachate control issues originally prompted the commissioning of the research reported here, its main value now lies in the application of the results to the development of sustainable landfilling. For landfills to be brought to a stable non polluting state then some contaminants will inevitably need to be flushed from the waste. Consequently, an understanding of the hydrogeological properties of the waste is of paramount importance. This research makes a significant contribution to that understanding.

1.6 Structure of thesis

Chapter 2 of this thesis reviews the available literature on the hydrogeological and geotechnical properties of waste and defines terms subsequently used.

Undertaking tests on the hydrogeological properties of wastes is not an easy task. Field tests are not suitable for developing a fundamental understanding of wastes because of the general lack of control, the difficulties in monitoring and the probable lack of information relating to the physical characteristics and distribution of the material being tested. Laboratory style tests can provide the necessary controls over variables, but standard Soil Mechanics testing equipment is not large enough to accommodate household wastes. There was, therefore, a need for specialised testing equipment to be used in this research. The design and construction of a large-scale compression cell is described in Chapter 3.

Chapter 4 describes the testing methodologies that were adopted.

Chapter 5 presents the results of tests on three different types of household waste undertaken at various applied stresses.

Chapter 6 analyses these results and corrects the raw data to take into account the (unwanted) influence of the testing equipment.

Chapter 7 outlines modifications made to a standard groundwater flow model, subsequently used in Chapter 8, to help examine the implications of the results on the flow of leachate in landfills. Chapter 8 also uses the results of the research to consider the feasibility of various leachate control and recirculation systems in achieving the aims of sustainable development by means of the flushing (bio)reactor landfill.

The main conclusions and recommendations of this research are summarised in Chapter 9.

Chapter 2

Literature review and definition of terms

2.1 Summary

The geotechnical and hydrogeological terms used throughout this thesis are defined in this chapter. Where a term has more than one meaning (from different disciplines) these are discussed and clarified.

The literature is reviewed to ascertain the likely nature and magnitude of the pollution load held within landfills and the possible volumes of liquid that may be required to flush out the recalcitrant part of this load. A review of the literature pertaining to the hydrogeology of household wastes is also undertaken, as these properties control the ability to flush liquid through a landfill at the required rate.

2.2 Introduction

2.2.1 Sustainable landfill

Chapter 1 provided an interpretation of how the aims and principles of sustainable development could be applied to the landfilling of (household) wastes. In summary, there is a requirement to shorten the period of time over which landfills have the potential to pollute the environment. At present, in modern day containment sites, the timescale is highly protracted and measured in terms of centuries rather than decades (Harris et al, 1994).

The UK's current definition of sustainable landfilling has been outlined in Section 1.3.5. This thesis is primarily concerned with the *in situ* treatment of wastes to remove the pollution load by operating a landfill as a bioreactor with a high rate of flushing.

To reduce the pollution load of a landfill, pollutants which are initially held in the solid phase must first be transformed into liquid or gaseous phases. Leachate or landfill gas must then be removed from the landfill in order to reduce this pollution load. A key purpose of this thesis is to examine the mechanisms and practicalities of removing or flushing leachate (with its integral pollution load) from sites within an accelerated timescale.

2.2.2 Nature of pollutants within a landfill

The amount of landfill gas or leachate that has to be removed relates to the nature and mass of pollutants held in the solid waste in the first instance. In considering the polluting potential of putrescible wastes, a distinction can be made between the following:

1 the degradable organic carbon content of the waste;
2 releasable nitrogen; and
3 inorganic ions.

By definition, putrescible wastes contain a large proportion of degradable carbon. In the case of household wastes (MSW) the mass of degradable and releasable carbon has been estimated in laboratory scale experiments (Beaven & Walker, 1997) to be up to 185 kg per dry tonne of refuse (~130 kg/t_{wet} for a water content of 30% by wet weight). This compares with a total carbon content of 358 kg/t_{dry}.. The theoretical maximum gas yield of MSW is calculated as 370 m^3/tonne, with more realistic estimates for achievable yields in the field of approximately 200 m^3/tonne (Barlaz & Ham, 1990). Assuming that the gas produced predominantly contains CH_4 and CO_2, then the total gas yield contains a mass of carbon between 107 and 198 kg/t_{wet}.

The mass of nitrogen which can be released from MSW has been estimated by Beaven & Walker (1997) to be up to 2.7 kg/t_{dry} (~1.9 kg/t_{wet}), compared with a total nitrogen content of 10 kg/t_{dry}. Beaven & Walker (1997) also summarised other work which indicated a range of releasable nitrogen of between approximately 1.3 to 1.8 kg/t_{wet} and up to 3.9 kg/t_{dry} (Table 2.1).

Table 2.1 Releasable nitrogen content of refuse determined in laboratory scale experiments

Reference	Releasable N per per tonne of refuse kg/t	Units/ Comment	Waste Stabilised
Knox & Gronow, 1995	1.3	wet weight 2 year old MSW	No
Ehrig & Scheelhaase, 1993	1.6	wet weight	?
Burton & Watson-Craik, 1997	~3.9	dry weight 1-2 month old refuse Total N content ~ 4%	?
Heyer and Stegmann, 1995	1.8	wet weight 8 year old MSW	?
Heyer and Stegmann, 1995	0.7	wet weight 13 year old MSW	?
Brinkmann, et al, 1995	2	dry weight Milled MSW	No
Beaven & Walker, 1997	2.7	dry weight Shredded MSW	probably

Whether the inorganic ion content of wastes is considered to have a polluting potential will largely depend on site location. For example, chloride is likely to have a much larger polluting potential in inland landfills adjacent to relatively small freshwater water courses, than in landfills located near to the coast. The mass of releasable chloride determined by Beaven & Walker (1997) was approximately 2.5 kg/t_{dry}.

2.2.3 Accelerated degradation techniques

It has been demonstrated (e.g. Beaven & Walker, 1997) that methanogenic gas production is required to remove the majority of the degradable organic carbon of MSW. To some extent, methanogenesis and biodegradation are also likely to be required to release nitrogen from the solid into the liquid phase. Techniques to accelerate gas production in landfills are relatively well understood. These include shredding of the refuse prior to landfilling, raising the water content of wastes and the introduction of buffering capacity (e.g. Campbell, 1997; Knox, 1996).

2.2.4 The role of liquid recirculation and flushing in sustainable landfill

Leachate flushing is required to remove the pollution load associated with nitrogen, other inorganic ions (such as chloride) and the residual fraction of organic carbon not

removed by landfill gas production. Further research is needed, however, into the actual volume of liquid required to flush pollutants from a landfill. Assessments to date (e.g. Belevi & Baccini, 1989; Knox, 1990 & 1996a; Walker 1993) have been based on a flushing model which assumes that landfills operate as continuously mixed reactors. In this 'washout' model, any fluid that is introduced into the landfill is assumed to mix instantaneously with the 'bed volume' (the reservoir of water or leachate) existing in the site. Where clean water is introduced, uniform mixing and dilution of the leachate is assumed. The reduction in leachate concentration is related to the number of bed volumes of water that have passed through the landfill. The passage of 4.6 bed volumes of fluid is required to reduce leachate concentrations by two orders of magnitude (e.g. from 1,000 to 10 mg/l). Knox (1996a) suggests that the behaviour of landfills correlates reasonably well with the continuously mixed reactor model and the theory, therefore, forms a useful starting point from which to make predictions about how a site will behave. However, it should be recognised that the theory only applies to conservative parameters where, during washout, there is no net addition to, or removal from, solution.

The number of bed volumes removed can be translated into the volume of fluid required to flush a unit mass of refuse. Estimates for the volume of water required to flush the nitrogen pollution load from waste range from 5 to 7.5 m^3 per $tonne_{wet}$ of waste (Beaven, 1996a; Beaven and Walker, 1997).

The ease with which the required volume of fluid can be flushed through a landfill depends on the hydrogeological properties of the refuse, particularly the hydraulic conductivity. However, the hydrogeological properties of household wastes are in turn dependent on a wide range of factors including:-

1) the composition of the waste;
2) the density of the waste (partially related to depth of burial and stress);
3) the state of degradation; and
4) the degree of saturation.

2.2.5 Overview of chapter

This chapter reviews the available literature on the hydrogeological properties of household waste and, where possible, links these properties to data on the above factors. The following topics are considered.

Section 2.3	Waste composition.
Section 2.4	Waste density.
Section 2.5	Water contents, absorptive capacity and porosity.

Section 2.6 Hydraulic conductivity.
Section 2.7 Total and effective stress.

The subject matter of this thesis spans a number of disciplines, including hydrogeology, soil mechanics and the relatively new (somewhat less precise) subject of landfill science. Each discipline tends to use its own nomenclature to describe the state or some physical attribute of a material. Sometimes different words are used to refer to exactly the same condition, (e.g. porosity in soil mechanics is often called total porosity in hydrogeology); more often than not a totally different condition is being described (e.g. the soil mechanics concept of void ratio is not used in hydrogeology, the term drainable or effective porosity is not used in traditional soil mechanics and the concept of absorptive capacity is only applicable to landfill science). Of potentially greatest confusion is when the same term used in two disciplines is used in different ways. In soil mechanics the water content of a material is defined as the ratio of the mass of water to the mass of dry solids; in landfill science the term is usually taken to mean the ratio of the mass of water to the combined mass of water and dry solids. Water content can also be defined by volume, as in unsaturated flow equations.

Thus this chapter also clarifies the nomenclature used in this thesis and indicates the relationship between differing terms where one exists.

Each section starts with a definition of terms followed by a review of the relevant literature. There is an inevitable overlap between the sections because of the interdependency of the factors being considered. For example, the bulk density of waste is dependent on material composition and water content; the maximum water content is also dependent on waste density.

2.3 Composition of refuse

A description of the nature and composition of any material (even without detailing the nature and geometry of its voids) can give clues to its likely hydrogeological behaviour. For example, a geological material consisting entirely of uniformly graded rounded quartz gravel describes a deposit with a reasonably well defined void structure. The resulting open and well interconnected pore structure leads to a relatively high permeability.

The composition of household waste is considerably more complicated than that of a uniformly graded gravel. Wastes consist of a wide range of highly variable materials

with a wide size distribution. The nature and distribution of pores is as much dependent on density as on composition. For instance, Young (1989) likened the flow of fluid through wastes to that of flow through a doubly porous media (Figure 2.1). Flow can occur between the relatively large voids between individual fragments of waste as well as through the micropores of many individual waste fragments (e.g. paper products). As the overall density of the waste increases the macropores will tend to collapse resulting in more reliance on flow through the micropores or alternatively along the interface between two particles in contact.

Figure 2.1 Section through a double porosity medium

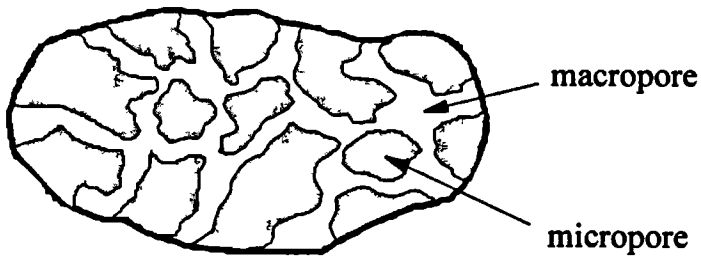

At present it is not possible to take the composition of a waste material and use it, in qualitative or even quantitative terms, to predict the hydrogeological properties of the waste. However, the proper classification and description of wastes is an important part of the experimental work in this thesis if for no other reason than to allow a scientific comparison to be made with other work.

2.3.1 Waste characterisation

The most common method for characterising a waste is to separate the waste into a number of different categories and determine the percentage, by weight, of each component.

As early as 1906, H de Parsons was using a classification system which separated 'general refuse' into four main categories: ashes, garbage (kitchen wastes and other putrescibles), rubbish (paper, wood, metals glass etc.) and street sweepings. The breakdown of wastes from the City of Philadelphia is shown in Table 2.2.

The 1971 report of the working party on refuse disposal (DoE, 1971) gave a more detailed waste classification system which was used to compare wastes over a 30 year period (Table 2.3).

Table 2.2 Composition of waste arisings from the City of Philadelphia in the early 1900s

	US tons	% by weight
Ashes	425,650	51
Garbage	301,643	36
Rubbish	13,975	17
Street Sweepings	93,044	11
TOTAL	834,312	

Collected from a population of 1,385,549.
Source: H de Parsons (1906)

Table 2.3 Breakdown of waste composition over a 30 year period in the UK

	Percentage (% by weight)				Average weight per household per week (kg)			
	1935/6	**1963**	**1967**	**1968**	**1935/6**	**1963**	**1967**	**1968**
Fine dust, ashes and cinders	57.0	38.9	31.0	21.9	9.7	5.5	4.1	2.9
Vegetable and putrescibles	13.7	14.1	15.5	17.6	2.3	2.0	2.0	2.3
Paper	14.3	23.0	29.5	36.9	2.5	3.2	3.8	4.9
Metal	4.0	8.0	8.0	8.9	0.7	1.1	1.0	1.2
Rag and textiles	1.9	2.6	2.1	2.35	0.3	0.4	0.3	0.3
Glassware	3.3	8.5	8.1	9.1	0.5	1.2	1.0	1.2
Unclassified (fines)	5.8	4.9	4.7	2.1	1.0	0.7	0.6	0.3
Plastics	-	-	1.2	1.1	-	-	0.1	0.1
	100.0	100.0	100.0	100.0	17.0	14.1	12.9	13.2

Data modified from reference DoE (1971), Table E pp 23.

There are many other waste classification systems reported in the literature which are variations on the above (e.g. Landva and Clark, 1986; Oweis and Khera, 1990). The most detailed classifications and surveys have been undertaken to assess the potential of a waste to be used in processes other than landfilling. For example, there has been a considerable amount of waste characterisation work undertaken to assess the viability of specific waste incineration schemes (e.g. Royal Commission on Environmental Pollution, 1993). In addition, detailed work has been undertaken on waste

characterisation to assess the viability of recycling schemes (DoE, 1994a) for Local Authorities.

2.3.2 Material classification, water content and particle size distribution (PSD)

The above type of classification has two main problems with regard to waste characterisation in a geotechnical sense. Firstly, most classifications do not routinely determine water contents either of the individual components of wastes or even of the bulk waste. A knowledge of the water content of a waste is essential in geotechnical terms for a wide range of applications. It is used in the determination of waste densities and self weight induced vertical stresses within a landfill. It is also an essential component of a water balance, influencing factors such as the absorptive capacity of a waste. Secondly, very few classifications attempt to measure particle size. Particle size distribution (PSD) curves are widely used to classify geological materials and are used as an empirical guide to a material's geotechnical and hydrogeological behaviour.

A number of workers have produced data on the water content of the constituents of household waste (refer also to Section 2.5). Water content data for a range of materials was summarised by Tchobangolous *et al* (1993) and are reproduced in Table 2.4. These data give an indication of the likely range of water contents of a waste.

Table 2.4 Water contents of individual components of household wastes

Type of waste	Moisture content % by wet weight Range	Typical
Residential (uncompacted)		
Food wastes	50-80	70
Paper	4-10	6
Cardboard	4-8	5
Plastics	1-4	2
Textiles	6-15	10
Rubber	1-4	2
Leather	8-12	10
Yard wastes	30-80	20
Wood	15-40	20
Glass	1-4	2
Tin cans	2-4	3
Aluminium	2-4	2
Other metals	2-4	3
Dirt, ashes etc.	6-12	8
Ashes	6-12	6
Rubbish	5-20	15
Commercial		
Food wastes (wet)	50-80	70

Modified from Tchobangolous *et al* (1993), Table 4.1 pp 70.

In 1994, a comprehensive survey of the composition of household and civic amenity wastes was undertaken in the UK by Warren Spring Laboratory (DoE, 1994a). Data on household waste arisings were collected from a cross section of household types within five carefully chosen and well characterised Local Authorities. A summary of the average composition and water contents from 24 samples is given in Table 2.5.

There are relatively little published data on the size distribution of the various components of waste. Winkler and Wilson (1973) reported PSD curves for municipal refuse from Cambridge, Massachusetts and Middlebury, Vermont in the USA. It was determined that the average size (in terms of the longest dimension) of the individual components of the waste was approximately 20 cm. Warren Spring Laboratory, as part of The UK National Household Waste Analysis Project, undertook a detailed classification of over 30 samples of household waste by category and particle size. Unpublished data indicate that 52.4% by weight of the waste passed through a 80 mm screen (Papworth, 1998).

Table 2.5 Composition and water contents of an 'average' UK household waste

Category	Proportion of material by (wet) weight %		Water Content[1] (wet weight) %
Paper/card	33.6		25.1
Plastic Film	5.1		33.4
Dense Plastic	5.3		11.3
Textiles	2.3		16.1
Misc' Combustibles	7.9		45.0
Misc' Non Combustibles	2.3		8.9
Glass	8.5		0
Putrescibles	20.5		69.1
Ferrous	5.9		8.8
Non-ferrous	1.6		12.3
Fines	7.1		36.9
TOTAL	100.1	BULK	37.8[1]

[1] Based on Leeds County Council Collection March 1993 - ACORN B
Data modified from DoE (1994a)

Kabbe *et al* (1995) determined the particle size distribution of wastes recovered by drill cores from two German landfill sites. The average particle size (by weight) varied from 20 mm for samples recovered from the older of the two landfills, to 60 mm for samples from the younger site (actual ages were not provided). It was inferred that biodegradation of wastes has the effect of reducing particle size.

2.4 Waste density

Figure 2.2 is a schematic representation of refuse divided up into (dry) solids, liquid and air phases. Water content has an important bearing on waste density and this aspect is considered in detail in Section 2.5.

2.4.1 Definition of terms

Density

The bulk density, ρ_{wet}, is defined as the total mass of solids (M_S) and water (M_W) within a unit volume (V_T) of refuse.

$$\rho_{wet} = (M_S+M_W)/V_T \qquad (2.1)$$

The dry density, ρ_{dry}, is defined as the total mass of dry solids within a unit volume of refuse.

$$\rho_{dry} = M_S/V_T \qquad (2.2)$$

The bulk and dry densities are linked as follows:-

$$\rho_{dry} = \rho_{wet} . (1-WC_{wet}) \qquad (2.3)$$

$$\rho_{wet} = \rho_{dry} . (1+WC_{dry}) \qquad (2.4)$$

where WC_{dry} is the dry weight water content and WC_{wet} is the wet weight water content (see Section 2.5.1 below).

Unit weight

The unit weight γ of refuse is defined as the weight of a unit volume, in kN/m^3. It is equal to the bulk density multiplied by the acceleration due to gravity, g. The unit

weight, integrated over depth, can be used to calculate total vertical stresses within a landfill (Section 2.7).

Figure 2.2 Refuse as a three-phase material

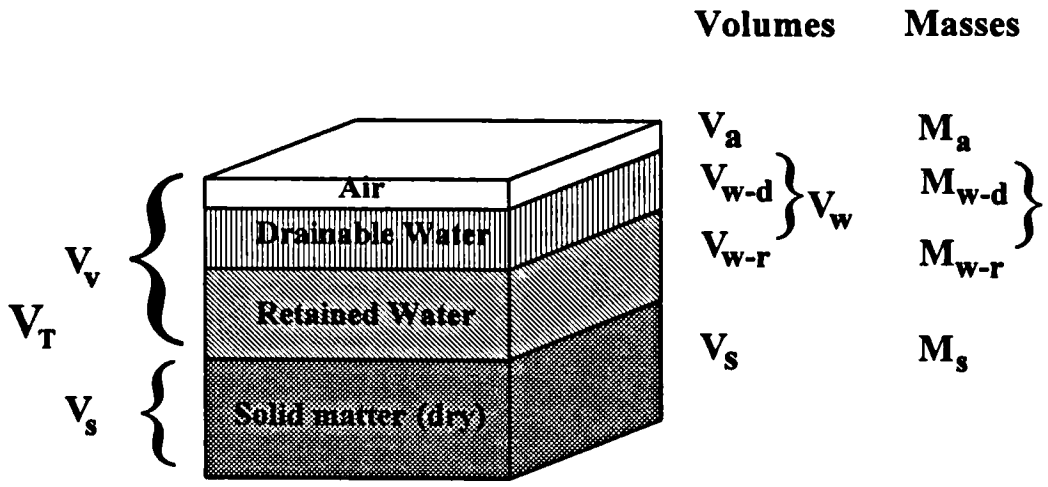

2.4.2 Literature review

Chen *et al* (1977) reported work undertaken by Gupta (1972) that indicated that the hydraulic conductivity of milled refuse was related to its dry density. This finding corresponds to the well documented (e.g. Vaughan, 1994) behaviour of many other geological materials (e.g. clays and peats). In addition, properties such as water content and porosity are also likely to be related to refuse density. One major objective of the research reported in this thesis was to investigate these relationships in more detail under controlled conditions. A review of the literature on waste density is needed to establish the likely range that occur in landfills and to develop an understanding of the factors that can affect it.

General values

A review of the literature on the *in situ* density of wastes indicates a wide range of values for municipal solid waste. Oweis and Khera (1990) reviewed the literature and reported a range of bulk unit weights for municipal wastes of between 2.8 and 10.5 kN/m^3. One reason for this large range of values relates to the wide variety of differing refuse compositions to be found in a landfill.

Theoretical approach

A theoretical approach to calculating the density or unit weight of refuse was suggested by Landva and Clarke (1990). It was recognised that the determination was complicated by the wide diversity of materials present in refuse, and the ability of some materials to absorb water and hence alter their unit weight whilst the overall refuse still remained in a free draining state. A (conceptual) distinction was made between intraparticle voids (i.e. water held within a particle) and interparticle voids (i.e. between particles or macro pores- see Figure 2.1). Water uptake in the intraparticle voids would be equivalent to uptake of absorptive capacity and is the main way in which the unit weight of freely draining refuse can change in the absence of any compression.

Landva and Clarke (1990) calculated the possible maximum and minimum densities for a range of refuse compositions. A possible range of average unit weights was calculated by i) considering the lightest combination of materials and their dry unit weights and ii) the heaviest materials and their saturated unit weights. This yielded possible average unit weights of the constituents of refuse ranging from 3.8 to 16.3 kN/m^3. To calculate the bulk unit weight of refuse these values need to be modified by taking into account the interparticle (macro) porosity. Landva and Clarke (1990) assumed a range of interparticle (dry weight) porosities from 30 to 60% which, when applied to the above range of unit weights, yielded an average bulk unit weight of 1.6 to 2.8 kN/m^3 for the lightest combination and an average of 6.8 to 12 kN/m^3 for the heaviest combination.

Effects of depth of burial on density

Oweis and Khera (1990) reported data relating to the effect of depth of burial on the unit weight of refuse. The results were determined from waste cores taken from the drilling of large diameter (300 mm) holes on a landfill in Southern California. The following conclusions were drawn:

1) the unit weight of the refuse material increased with increasing depth of burial;

2) the dry unit weight of newer and older fill were approximately equal at a given depth (indicating that there was little change as a result of degradation); and

3) at a given depth the wet weight of more recently placed fill was slightly higher than the wet unit weight of older fill, largely because of a higher water content.

The average dry density was calculated as approximately 0.72 t/m^3 at a depth of 5 metres (~17 feet) increasing to approximately 0.99 t/m^3 at a depth of 25 metres (~80 feet). The corresponding wet densities ranged between 0.80 and 0.93 t/m^3 at a depth of 5 metres and between 1.15 and 1.22 t/m^3 at a depth of 25 metres.

Effects of compaction / vibration on density

Ham *et al* (1978) undertook detailed tests on the density of milled and unprocessed refuse in a number of laboratory and field trials. In the laboratory trials samples of milled and unprocessed refuse were subjected to vertical stresses up to 830 kPa (120 psi) and the resulting wet weight densities measured (Figure 2.3). The effects of vibrations produced by site machinery at the tipping face were also simulated. At a constant water content (WC_{dry}) of 45%, the wet weight density of unprocessed waste increased to between 0.8 and 0.95 t/m^3 at applied stresses of between 400 and 830 kPa. The results indicated that the density of the milled refuse was always higher than that of the unprocessed refuse, being between 0.90 and 1.05 t/m^3 for the same applied stress range. Also, at a given stress, higher refuse densities could be achieved by increasing the magnitude of the applied vibratory force.

Figure 2.3 Compressibility tests on refuse

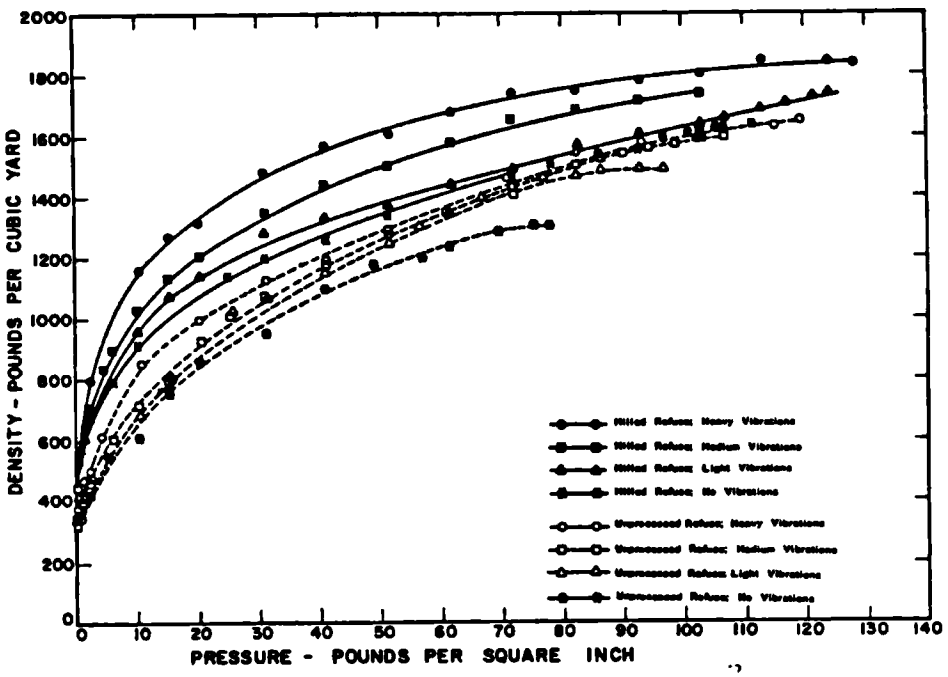

FIG. 2.—Compressibility Tests on Refuse (Wet Weight Density for Refuse at 45% Water on Dry Weight Basis)

NB: 1 psi = 6.895 kPa; 1000 lb/yd^3 = 0.5932 t/m^3: Source: Ham *et al* (1978)

In the field trials three 1,500 m^3 cells were landfilled using a relatively small 14 tonne steel wheeled compactor. One cell was filled with unprocessed waste and two cells with milled (pulverised) waste. The same compaction technique and compaction time (simulating a well compacted landfill) was used to fill Cell 1 with unprocessed waste and Cell 2 with milled waste. The unprocessed waste was compacted to a dry density of 0.48 t/m^3 (ρ_{wet}= 0.66 t/m^3) compared with a dry density of 0.554 t/m^3 (ρ_{wet}= 0.845 t/m^3) for the milled waste. Cell 3 was filled with milled waste but minimal compaction was used: the resulting dry density was 0.477 t/m^3 (ρ_{wet}= 0.758 t/m^3).

Effects of layer thickness on density

Schomaker (1972) reported the effect of layer thickness and number of machine passes on waste density. The highest densities were achieved with thin refuse layers. A density of 0.85 t/m^3 was achieved with a 0.3 metre (1 ft) layer thickness, rapidly reducing to less than 0.3 t/m^3 for a layer thickness over 1.5 metres (5 ft) thick. Data on the water content of the refuse were not reported.

Scott (1977) investigated the effect of layer thickness, ramp angle, machine type, throughput and machine passes on refuse density in 9 test cells varying in capacity from 500 to 3300 tonnes, at Rainham landfill in Essex. The refuse density achieved in the cells varied from 0.55 to 0.78 t/m^3. The main factors that influenced and increased refuse density were the use of shallow refuse ramps and steel wheeled compactors operated with a rate of waste throughput slow enough to allow the machines to compact the waste properly.

More recent work undertaken for Caterpillar (1995) compared the compaction performance of a number of different compactors when making between 3 and 5 passes over a layer of waste. Wet weight densities of between 0.62 and 0.67 t/m^3 were obtained for a Cat 816B and densities of between 0.81 and 1.11 t/m^3 were obtained for a Cat 826. Unfortunately, the water content of the refuse was not reported so actual dry weight densities cannot be calculated. However, assuming the water content of the waste was between 30 and 40% (wet weight) then a range of dry weight refuse densities for each compactor can be estimated. A range of 0.37 to 0.47 t/m^3 is estimated for the Cat 816B and a range of 0.49 to 0.78 t/m^3 for the Cat 826.

Effects of water content and decomposition on density

Harris (1979) undertook British Standard compaction tests on five differing types of pulverised refuse to determine the dry density versus moisture content relationships. Optimum water contents were determined for maximum waste compaction. It was found that there was a large variation in the optimum water content and maximum waste

density depending on the nature of the material. The optimum water contents were higher and the maximum dry densities lower in fresh pulverised waste in comparison with 2 or 14 year old aged pulverised waste.

For example, the maximum dry density of a freshly pulverised waste was 0.76 t/m^3 at a water content (WC_{dry}) of 50%; this indicates a maximum wet density of 1.14 t/m^3. The maximum dry density of 2 and 14 year old decomposed pulverised waste was 1.13 and 1.11 t/m^3 at optimum water contents (WC_{dry}) of 21 and 38% respectively. The maximum wet densities of this older pulverised waste were also higher, at between 1.38 and 1.53 t/m^3.

2.5 Water content, absorptive capacity and porosity

It has already been indicated that the water content of refuse has an important effect on refuse density. This section considers the various methods of calculating water content and the relationship between water content and field capacity and porosity.

2.5.1 Definition of terms

Water Content

In general, fresh refuse will contain some water but will not be saturated. This water, given the notation w-r in Figure 2.2, is held within the matrix of the refuse and is not free draining. It is quantified by means of the original moisture or water content which is determined from the loss in weight of a sample of refuse dried at 105°C. The final weight of the sample after drying gives the mass of dry solids.

In soil mechanics, the water content of a material is defined as the ratio of the mass of water to the mass of dry solids present. It is normally given the symbol w. However, to avoid confusion with an alternative definition of water content generally used in landfill science, the notation WC_{dry} (water content by dry mass) will be used in this thesis.

$$WC_{dry} = M_W/M_S \qquad (2.5)$$

In landfill science, the water content WC_{wet} is often expressed as a ratio of the mass of water to the total mass of water and solids.

$$WC_{wet} = M_W/(M_W+M_S) \qquad (2.6)$$

The relationship between the two water contents is as follows:

$$WC_{dry} = WC_{wet} / (1-WC_{wet}) \quad (2.7)$$

$$WC_{wet} = WC_{dry} / (1+WC_{dry}) \quad (2.8)$$

A further way of expressing the water content of refuse is on a volumetric basis. The volumetric water content WC_{vol} is defined as the ratio of the volume of water to the total volume of air, solids and water.

$$WC_{vol} = \frac{V_w}{V_t} \quad (2.9)$$

Expressing water contents in this form has the advantage that it is possible to relate the water content directly to the drainable porosity. The volumetric water content is related to the wet and dry weight water contents as follows:-

$$WC_{vol} = \frac{V_w}{V_t} = \frac{m_w}{V_t \cdot \rho_w}$$

$$V_w = \frac{m_w}{\rho_w}$$

$$\text{and } V_t = \frac{m_s}{\rho_{dry}} = \frac{m_s + m_w}{\rho_{wet}}$$

$$\Rightarrow WC_{vol} = \frac{m_w \cdot \rho_{dry}}{m_s \cdot \rho_w}$$

$$\Rightarrow WC_{vol} = WC_{dry} \cdot \rho_{dry} / \rho_w \quad (2.10)$$

$$\text{Also, } WC_{vol} = \frac{m_w \cdot \rho_{wet}}{(m_s+m_w) \cdot \rho_w}$$

$$\Rightarrow WC_{vol} = WC_{wet} \cdot \rho_{wet} / \rho_w \quad (2.11)$$

Furthermore, $m_w = m_{wet} - m_{dry}$

$$\text{hence } WC_{vol} = \frac{m_{wet}-m_{dry}}{V_t \cdot \rho_w} = \frac{\rho_{wet}-\rho_{dry}}{\rho_w} = \frac{\gamma_{wet}-\gamma_{dry}}{\gamma_w} \quad (2.12)$$

where the unit weight, γ, is obtained by multiplying the density, ρ, by the acceleration due to gravity, g.

Equations 2.10 and 2.11 enable water contents expressed in ratio of masses to be converted into volumetric terms.

Absorptive Capacity

After landfilling, the moisture content of wastes may increase through the absorption of water by components such as paper, cardboard and textiles. Beyond a certain limit the addition of further water leads to the production of free draining pore fluid, which will tend to move downward under the influence of gravity towards a 'water' table below which the waste is fully saturated. The overall water content (as opposed to simply the absorbed moisture content) of the drained refuse above the water table may be increased, partly by the trapping of leachate in containers which act as isolated voids unable to drain under the influence of gravity. In practice it is very difficult to determine whether an increase in the overall water content is due to true absorption or to fluid trapped in non drainable voids. The increases in water content resulting from both processes are therefore usually combined and referred to as the total absorptive capacity of the refuse (e.g. Knox, 1992).

In addition, to reflect field observations, the total absorptive capacity of refuse has sometimes been split into two components: primary and secondary absorptive capacity. The primary absorptive capacity is taken as the amount of water that can be added to refuse without the creation of any freely draining leachate. Secondary absorptive capacity is taken up more gradually, after leachate production has started, and is probably only fully utilised if the waste becomes completely saturated.

The absorptive capacity, a, of a waste is essentially the difference between two water contents - the original water content (usually at the time of landfilling) and the water content at which there is no further capacity to absorb or hold water. This latter condition is known as field capacity (see below). The absorptive capacity can be expressed in terms of the:

litres of liquid 'absorbed' per wet tonne of waste (litres/t_{wet});
litres of liquid 'absorbed' per dry tonne of waste (litres/t_{dry});
litres of liquid 'absorbed' per unit volume of waste (litres/m^3 or volume %).

The use of absorptive capacity figures in terms of litres per dry tonne is probably of most scientific use and the least likely to be misinterpreted. However, on full scale landfills operators do not tend to measure the water content of the wastes emplaced. Therefore, to

be of any use in water balance calculations, absorptive capacity is usually expressed in terms of litres absorbed per tonne of refuse at its original *in-situ* water content. This is potentially confusing as the absorption of water will increase the wet density of the refuse.

Field capacity

Refuse is referred to as being at field capacity when the total absorptive capacity has been fully utilised and free draining conditions exist. Field capacity is analogous to the term 'specific retention', S_r, used in hydrogeology or soil science. It is defined as the ratio of the volume of water that a material, following saturation, will retain under conditions of gravity drainage, to the total volume.

$$S_r = V_{w\text{-}r}/V_T \qquad (2.13)$$

This is a volumetric water content of the form expressed in Equation 2.9.

Field capacity is often used solely as a qualitative term. However, it is useful to know the water content of a waste at field capacity. It can be expressed as a volumetric water content (specific retention), or alternatively in terms of water contents based on dry or wet weights.

The definition of terms and the varying ways in which water content can be expressed is potentially confusing. This is illustrated below with an example of a hypothetical waste which has a volumetric water content at field capacity of 40%. It is further assumed that this water content remains constant with varying waste dry density (Figure 2.4a). This example is for illustrative purposes only and is not necessarily meant to relate to actual conditions which may be found in a landfill.

The (dry weight) water content WC_{dry} is calculated according to Equation 2.10 and is shown in Figure 2.4b. Whereas the volumetric water content remains constant with changing dry density, WC_{dry} plots as a curve. As WC_{dry} changes with dry density so does the wet density (ρ_{wet}). The relationship is linear and is shown in Figure 2.4c. Finally the (wet weight) water content WC_{wet} also plots as a curve against both wet density (Figure 2.4d) and dry density (not shown).

Figure 2.4 Illustrative relationship between density and water content at field capacity

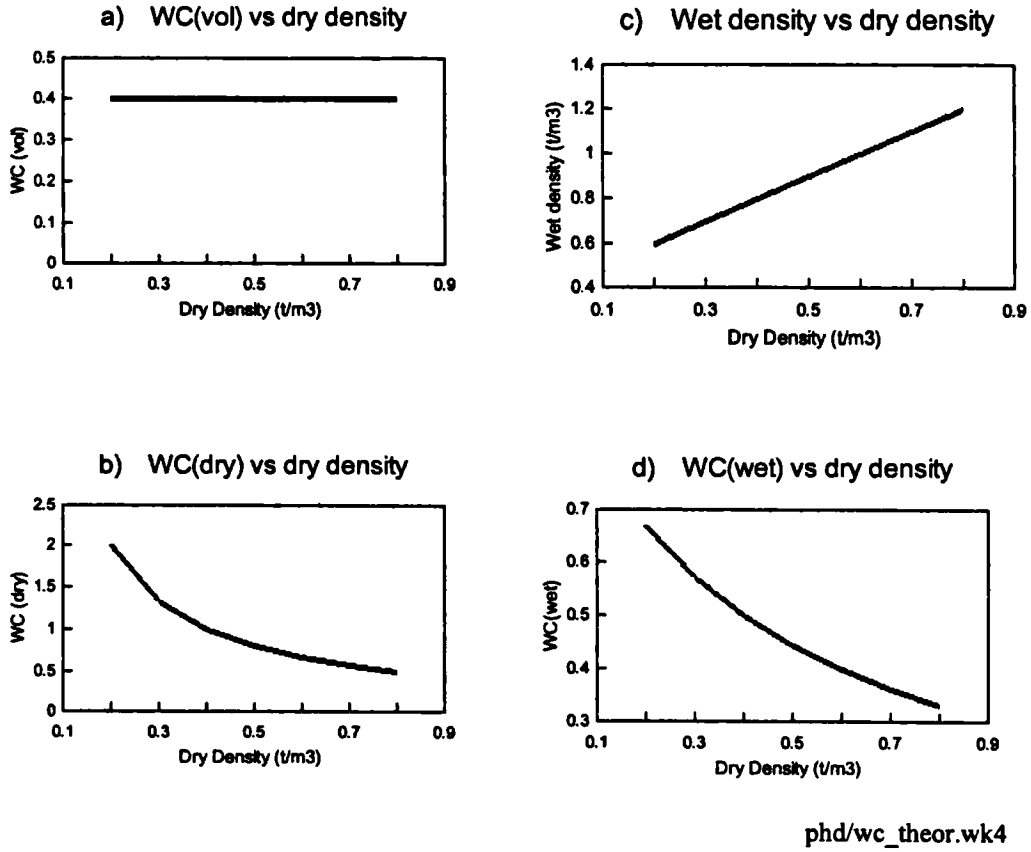

phd/wc_theor.wk4

Void ratio

The void ratio, *e*, is a term used in soil mechanics and is defined as the ratio of the volume of voids to the volume of solids.

$$e = \frac{V_v}{V_s} \tag{2.14}$$

Specific volume

The specific volume, ν, is defined as the actual volume occupied by a unit volume of solids

$$\nu = \frac{V_T}{V_s} = \frac{V_S+V_V}{V_s} = 1+e \tag{2.15}$$

Porosity

The total porosity *n*, is defined as the volume of voids per unit total volume.

$$n = \frac{V_v}{V_T} = \frac{e}{1+e} = \frac{\nu-1}{\nu} \tag{2.16}$$

If the refuse is saturated, or at saturation, all the voids within the refuse are completely filled with liquid. This condition is probably rarely met in practice as air may become trapped in isolated voids (e.g. an upside down glass bottle) and the generation of landfill gas may also reduce the degree of saturation.

Effective porosity

Of greater use is the effective, or drainable porosity n_e, which is analogous to the specific yield S_y used in hydrogeology. The effective porosity of a material is a measure of its capacity to yield water. It is defined as the volume of water released from a unit volume of fully saturated material, when the material is allowed to drain freely under the influence of gravity.

$$S_y = n_e = \frac{V_{w\text{-}d}}{V_T} \qquad (2.17)$$

Storage Capacity

The storage capacity is defined as the volume of water that a fully saturated waste can either absorb or hold in drainable pores. It is an indication of the total absorptive capacity of a waste.

$$S = S_y + S_r - WC_{vol(orig)} \qquad (2.18)$$

Saturation Capacity

For a completely saturated waste, the total volumetric water content is the sum of the volumetric water content at field capacity and the effective porosity. It is an alternative expression to porosity.

$$n = S_y + S_r$$

or

$$(WC_{vol})_{sat} = (WC_{vol})_{fc} + n_e \qquad (2.19)$$

2.5.2 Literature review

Water contents of wastes in landfills

There is a considerable body of data on water contents of waste. However, much of the data have been reported in isolation (from, for example, waste density) and this restricts their usefulness. A review of the literature on the original water content of household waste at the time of collection has already been made in Section 2.3.

Stegmann (1982) reported that the water content of wastes in landfills was highly variable with little correlation between water content and depth of burial. Water contents were reported to lie in the range of 15 to 35% (assumed WC_{vol}) in samples taken from two 20 metre deep boreholes from one particular landfill.

Blight *et al* (1991) also reported a considerable variation in the water content of wastes from vertical profiles within landfills. For example, water contents from the Waterval landfill in South Africa varied from 65 to 125% (assumed WC_{dry}). It was considered that the presence of low permeability intermediate cover layers was primarily responsible for controlling the vertical distribution of water within the landfill.

Unfortunately, in both of the above studies no data is given on waste density, so comparison of the two sets of figures is not possible.

Oweis *et al* (1990) and Oweis and Khera (1990) reported results of dry and wet unit weights of drilled refuse cores against depth within a landfill (see Section 2.4.2). A relationship between water content and depth of burial can be derived by back calculating from these data. The volumetric water content (WC_{vol}) is given by $(\gamma_{wet}-\gamma_{dry})/\gamma_w$ (Equation 2.12), and the water content (WC_{dry}) can be calculated using Equation 2.10. At a depth of 6 metres (20 ft) the average volumetric water content varies between 11 and 25%; at a depth of 25 metres (80 ft) the average volumetric water content varies between 16 and 23%. However, as the dry density of the refuse increases with depth, the dry weight water content WC_{dry} also reduces with depth.

Literature review: Absorptive capacity and field capacity

Work undertaken in the 1970s and early 1980s in the UK, USA, Canada and Europe highlighted the importance of absorptive capacity within water balances for landfill sites. A comprehensive review of water balances was carried out by Knox (1992). Interest in the topic grew as it was realised that careful management of the absorptive capacity of waste in a landfill meant that a site could, in theory at least, be designed and operated to prevent the production of free leachate.

In the context of sustainable landfill, the absorptive capacity and the water content at field capacity are relevant for two reasons:-

1) it is widely recognised (e.g. Knox, 1996) that the biological degradation of putrescible wastes can be enhanced and accelerated by the addition of water (in whatever form) to raise the water content of the waste to a level approaching field capacity.

2) the removal of soluble pollution products from the landfill requires leachate to be flushed from the site. The volume of leachate to be flushed will relate (in simple washout models, e.g. Belevi and Baccini, 1989) to the Bed Volume which, in turn, will relate to the total water content of the landfill.

The majority of studies reported have been undertaken on lysimeter scale experiments, usually less than 10 m^3 in size. Results from a number of studies were summarised by Knox (1992) and are reproduced in Table 2.6.

Table 2.6 Reported values of absorptive capacity for household wastes (MSW)

SOURCE	Test Cell Size and Refuse type	Density	Original WC_{wet}	Final WC_{wet}	Primary Absorptive Capacity	Total Absorptive Capacity
		t/m^3	%	%	l/t_{wet}	l/t_{wet}
Newton (1976)	8 m^3 pulverised MSW	0.5			230	
Robinson *et al*(1981)	8 m^3 pulverised MSW		40			225
Blakey (1982)	300 m^3 crude MSW	0.57				330
Blakey (1982)	0.2 m^3 pulverised MSW	0.76	26		165	290
Campbell (1982)	4000 m^3 crude MSW	0.66	25		100	
	4000 m^3 crude MSW	0.95	25		41	
	4000 m^3 crude MSW	1.01	25		24	
Holmes (1980)	0.2 m^3 drums 17 yr old MSW	0.96	31.5			115
	0.2 m^3 drums 17 yr old MSW	0.64	31.5			307
Harris (1979)	0.2 m^3 drums crude MSW		26.5			570
Fungaroli (1979)	Indoor lysimeter crude MSW	0.33				867
Kinman *et al* (1982)	6 m^3 crude MSW	0.5	35	54		425
Jones & M (1982)	6 m^3 crude MSW	0.4	14.7		345	
Pohland (1975)	1.6 m^3 simulated pulverised MSW	0.4				1300
Rovers & F (1973)	9 m^3 and 1.8 m^3 crude MSW	0.33				372.5

Table modified from Knox (1992)

A number of workers (e.g. Campbell, 1982 & Holmes, 1980) established that there was a relationship between increasing waste density and decreasing absorptive capacity. For instance, Campbell (1982) determined the absorptive capacity of wastes in the field within a number of relatively shallow (~3.5 metre) test cells, each with a nominal capacity of approximately 4,000 m^3. The various cells were filled with wastes at differing densities and leachate produced as a direct response to incident rainfall was measured over a period of 3 years. The absorptive capacity of the waste was calculated from the period of time that elapsed prior to leachate production in each cell. However, no direct measurement of infiltration was made during this time; the infiltration rates

used were obtained from steady state readings of leachate production for similar times of the year in *subsequent* years.

Campbell also reported values for absorptive capacity as m^3 absorbed per tonne of waste as deposited and related this to the density of the waste. These data are re-plotted in Figure 2.5 as water contents expressed on a dry weight and volumetric basis, each as a function of dry density. The calculated absorptive capacity is plotted on the right axis and shows a linear reduction with increasing density. The water content at field capacity calculated on a dry weight basis also reduces with increasing waste density. In contrast, the volumetric water content at field capacity increases with increasing waste dry density. However, this does not mean that the volumetric absorptive capacity increases with waste density, because the original volumetric water content of the waste also increases with density. In fact, the difference between the volumetric water content at field capacity and the original water content of the waste decreases with increasing density (as shown in Figure 2.5).

Figure 2.5 Original water content and water content at field capacity of household waste

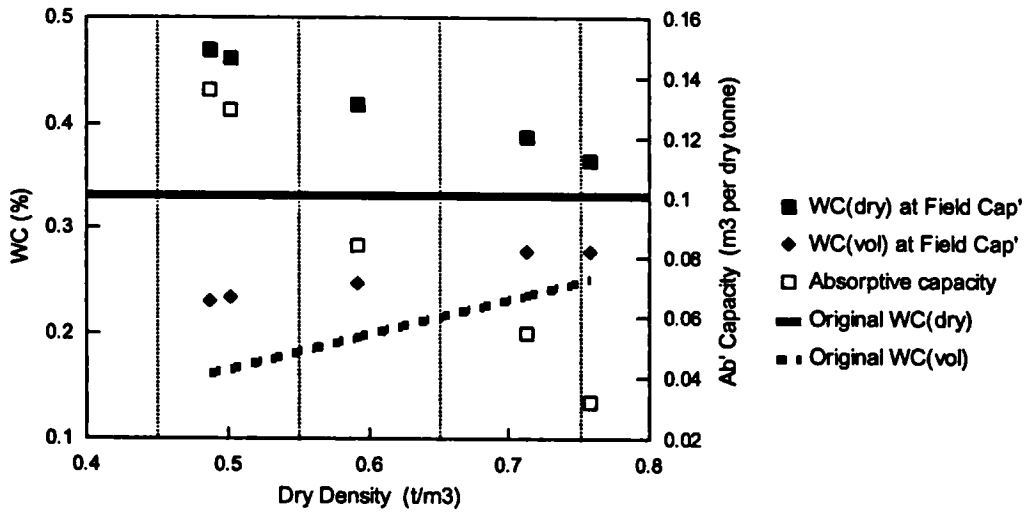

Data modified from Campbell (1982)
absorp.wk4

Much of the German research on absorptive capacity has been reported in terms of volumetric water contents. Stegmann (1982) reviewed West German research on the absorptive capacity of refuse and made particular reference to work undertaken by Franzius (1977). Franzius carried out experiments on shredded MSW and on 10 cm diameter cores of undisturbed waste from a landfill. His data on volumetric water content at field capacity (WC) and volumetric absorptive capacity (RV) are plotted against both wet and dry density in Figure 2.6. The original wet weight water content

(WC_{wet}) was approximately 41% for the shredded MSW and 34% for the undisturbed landfill waste and was assumed not to alter with density.

Figure 2.6 Water capacity (Water content at field capacity) vs density

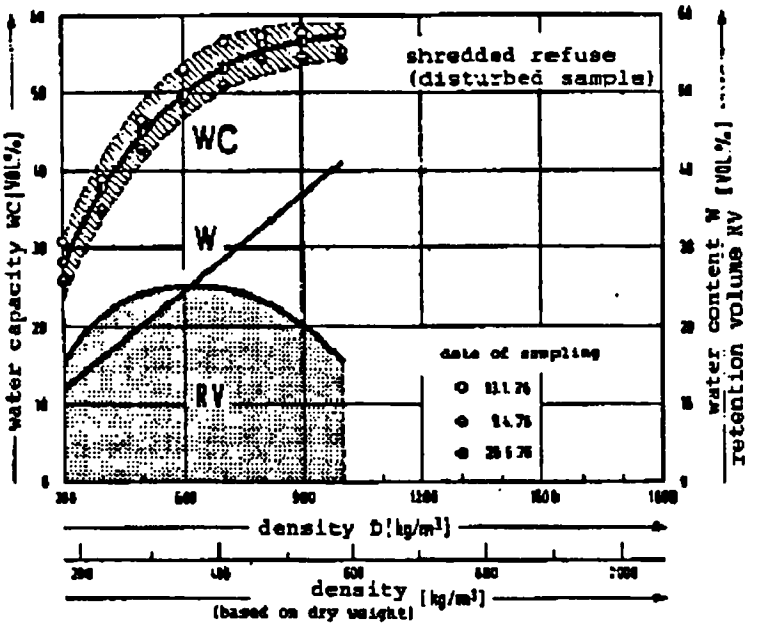

a) Shredded MSW

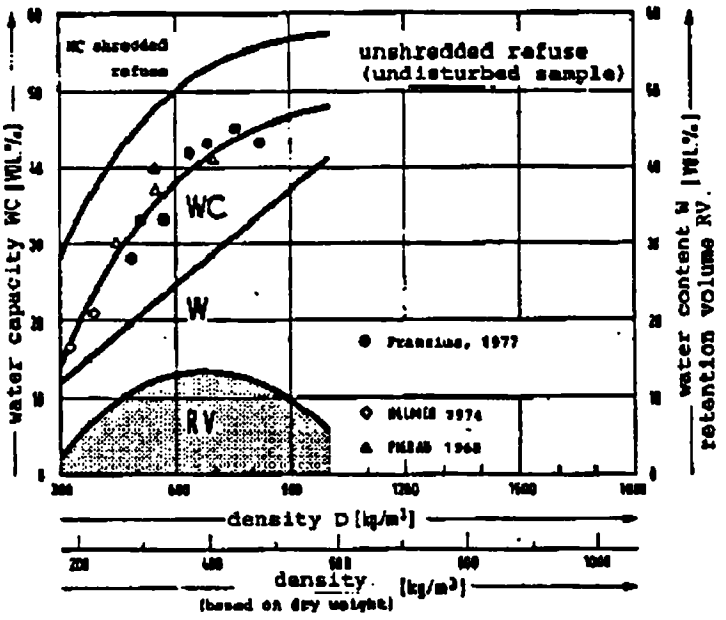

b) Undisturbed MSW

Reference Source: Franzius, 1977

The corresponding variation in this original volumetric water content (W) with density is also plotted on Figure 2.6. The graphs show that in terms of volumetric absorptive capacity (RV=WC-W) there is an optimum waste density at which a maximum amount of water can be absorbed. For both the shredded MSW and the undisturbed landfill waste this occurs at a dry density of slightly under 0.4 t/m^3.

Buivid *et al* (1981) compacted fully saturated MSW to various densities, allowing any water squeezed out of the refuse to drain. The water content is plotted against the compacted wet density in Figure 2.7. The water content of the refuse at field capacity reduced with increasing refuse density from a value of 80% at a wet density of approximately 550 t/m^3 to 55% at a wet density of 940 t/m^3. The basis on which the water content at field capacity has been calculated is not clear but is assumed to be by wet weight.

Figure 2.7 Water content of shredded MSW at field capacity (Buivid *et al*, 1981)

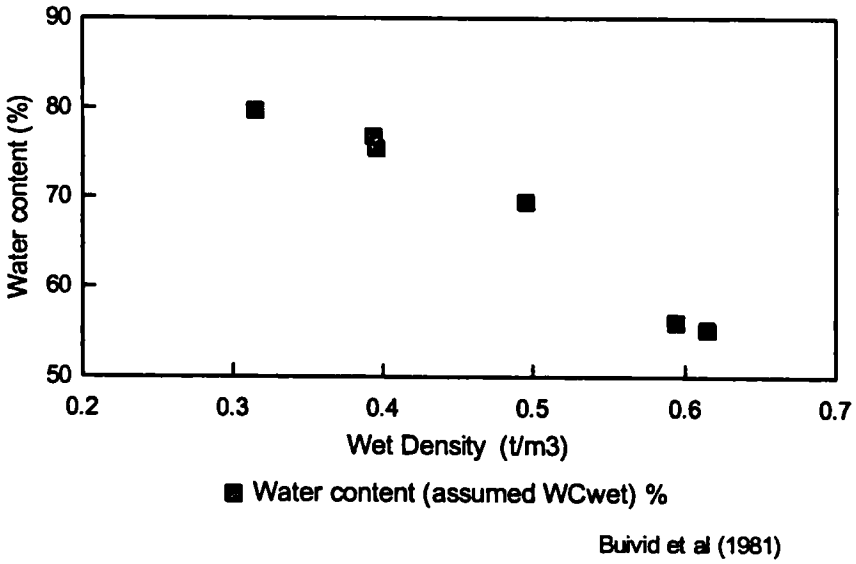

Literature review: Porosity

There are sparse data on specific yield or drainable porosity published in the literature. This reflects the difficulty of measuring the parameter, especially in field conditions.

Knox (1992) reported unpublished work by Holmes (1980) who determined the drainable porosity of crude domestic waste, of various ages, compacted into 200 litre drums at differing waste densities. Specific yields decreased significantly with increasing waste density, from over 40% for waste with an (initial) wet density of below 0.5 t/m^3, to between 15 and 20% at densities over 0.9 t/m^3.

Korfiatis and Demetracopoulos (1984) used refuse cylinders (0.56 m diameter by 1.8 m high) to investigate unsaturated flow through refuse. Saturated water contents of between 50 and 60% (v/v), and a moisture content at field capacity of between 20 and 30% (v/v), were determined for refuse with a dry density of 0.44 t/m^3 . These data indicate that the refuse had a drainable porosity of approximately 30% (Equation 2.19).

Knox (1992) estimated specific yields based on the behaviour of leachate in full scale landfills. Water balance calculations implied specific yields of between 10 and 20% for a number of leachate level fluctuation events on a number of different sites. Knox (1992) also reported the results of a leachate pumping test at Pitsea landfill in Essex. A specific yield of 3% was generated by pumping from a 6 metre depth of refuse.

Oweis *et al* (1990) undertook pumping tests on 30 metre deep waste with a 10.7 metre saturated zone. A fully penetrating well was pumped at a rate of 0.76 l/s for a period of 2.5 days, resulting in 0.88 m and 0.48 metres of drawdown in observation wells at radial distances of 8.5 and 21.8 metres respectively. Analysis of the drawdown curves indicated a specific yield of 5%, although the authors considered that gravity drainage was far from complete and that a long term specific yield of as high as 10% could reasonably be assumed.

Beaven (1996) reported the results of a pumping test on a 9 metre depth of refuse with a 5-6 m saturated zone which yielded a value for specific yield (S_y) of 4%. A further pumping test was undertaken on the same refuse when landfilling had increased the depth of waste to 23 metres and the saturated zone had increased to 6-7 metres. Surprisingly the calculated specific yield in the later test had increased to 7%.

More recently Burrows *et al* (1997) reported the results of over 50 pumping tests at four UK landfill sites. The majority of the tests were of relatively short duration (3-8 hours) and drawdown data from pumping wells only were analysed. However, there were several tests of longer duration (between 2 and 4 weeks) on single wells and on multiple pumped and observation well sets. The determination of specific yields was mainly restricted to the tests where data from observation wells were available. The calculated values of S_y ranged from 9 to 16%.

An extensive series of laboratory based tests on the hydrogeological properties of refuse obtained from varying depths within a landfill was undertaken by Bleiker *et al* (1993). Bulk samples of waste, obtained from the drilling of a well at Keele landfill with a rotary auger, were tested in a small diameter (63 mm) fixed ring with a depth of 19 mm. The material was compressed with applied stresses up to 1,200 kPa and data on the resulting density, porosity and hydraulic conductivity of the samples collected (see also Section 2.6.2). Unfortunately the data on porosity were not related directly to waste density, but were presented graphically as a relationship with hydraulic conductivity. However, the porosity increased from a value of 50% (v/v) at an inferred dry density of approximately 1.2 t/m^3, to 85% (v/v) at an inferred dry density of 0.55 t/m^3. It is assumed that these data relate to total porosity rather than effective porosity. Application of Equation 2.10 then indicates that the saturated water content WC_{dry} varied from 42 to 71%.

2.6 Hydraulic conductivity

The ability to move leachate around a landfill, either to enhance biodegradation by increasing the water content of the waste or as a means to flush soluble pollutants from the landfill, is crucial to the design of a sustainable landfill. In this respect the hydraulic conductivity of the wastes in a landfill is probably the single most important parameter that affects the viability of any scheme.

2.6.1 Definition of terms

Darcy's law

The hydraulic conductivity of saturated waste materials is assumed to obey Darcy's Law: the rate of flow, Q (m^3/s), through a unit cross sectional area, A (m^2), under unit hydraulic gradient, i, is proportional to the hydraulic conductivity, K (m/s) (Darcy, 1856).

$$Q = K.i.A \qquad (2.20)$$

The term transmissivity (T) is often applied to aquifers

$$T = K.b \qquad (2.21)$$

where b is the saturated depth of the aquifer perpendicular to the flow direction.

Intrinsic permeability

Whereas hydraulic conductivity is generally assumed to be a property of the aquifer material alone, its measurement is in fact related to both the properties of the aquifer and of the fluid flowing through the aquifer. The intrinsic permeability is a term better suited to describing the properties of the aquifer alone.

$$k = \frac{K\nu}{g} = \frac{K\mu}{\rho g} \qquad (2.22)$$

where:
- k is the intrinsic permeability (m^2)
- ν is the fluid kinematic viscosity (m^2/s)
- μ is the dynamic viscosity ($N.s./m^2$)
- ρ is the density of the fluid (kg/m^3)
- g is the acceleration due to gravity (m/s^2)

Equation 2.22 combines the physical properties of the fluid with the properties of the material through which it is flowing.

The kinematic viscosity of water is dependent on temperature. At a temperature of 50°C it is approximately 50% of its value at 20°C. The implication of this is that the hydraulic conductivity of wastes in a landfill could apparently vary by a factor of 2 through temperature effects alone.

Unsaturated flow equations

The hydraulic conductivity of an unsaturated material, or soil, will be less than that of the same material when saturated. In summary, the main causes for this are:

1) some pores become air filled, reducing the cross sectional area through which flow can occur;

2) the larger pores empty first, so that flow is restricted to the smaller pores, which are less conductive; and

3) the tortuosity of the flow path through the interlinked pores increases.

e.g. Hillel (1971)

Water in an unsaturated material is held in the pores by surface tension forces and by the physical attraction of the water to the soil particle interfaces. These forces result in a negative water pressure head, or matrix suction head, ψ in the material. The volumetric water content, θ, is related to this suction head. It has been shown that the relationship between θ and ψ exhibits hysteresis; it has a different shape when soils are wetting than when they are drying.

Flow in an unsaturated material moves from areas of high pressure head to low pressure head. This implies that at different points along the flow path both the water content and the hydraulic conductivity will vary. Therefore, hydraulic conductivity is both a function of water content and suction head and is expressed in the following ways:

$$q = -K(\theta)\nabla H \tag{2.23}$$

$$q = -K(\psi)\nabla H \tag{2.24}$$

where ∇H is the hydraulic head gradient, which may include both suctional and gravitational components.

2.6.2 Literature review

Reported data for the hydraulic conductivity of refuse (summary by Knox, 1992), have a large range of values. This relates to the different testing methods used, the type of waste or landfill material tested, the effects of overburden stress and the general heterogeneity of the waste mass.

Field Methods

A limited number of field based trials have been reported. Landva & Clarke (1986, 1990) undertook large-scale percolation tests in pits excavated at the surface of various landfills in Canada. The hydraulic conductivity was estimated on the basis of the rate of water level recession and flow nets applicable to any particular level. Hydraulic conductivities ranging between $4x10^{-4}$ and $1x10^{-5}$ m/s were reported. The unit weights of the refuse excavated from the pits were calculated and generally fell in the range of 10 to 14 kN/m^3. However, there was poor correlation between hydraulic conductivity and refuse density. These data reflect only the permeability of the waste material near the surface of the landfill and in the immediate locality of the test pit.

EMCON (1983) also used a field permeameter to test the hydraulic conductivity of 10 year old refuse. Difficulty was experienced in achieving a complete seal between the surface of the waste and the walls of the permeameter, but an approximate hydraulic conductivity of $1.5x10^{-4}$ m/s was established.

Townsend *et al* (1995) monitored the rate of downward flow from four large-scale infiltration ponds with basal areas ranging from 550 to 1,690 m^3 at a landfill site in Florida, USA. A total of 36,474 m^3 of leachate infiltrated into the landfill through the ponds over a period of 28 months. Steady state infiltration rates were used to calculate the vertical hydraulic conductivity beneath each pond, with values ranging from $3x10^{-8}$ to $4x10^{-8}$ m/s. The authors noted that the calculated values were considerably lower than those produced by many other studies. It was suggested that there may be a number of reasons for this, including the degree and nature of waste compaction, particle size, waste degradation, landfill gas production and soil cover layers. The potential clogging of the base of the lagoons was considered not to have been important, but this was not demonstrated.

Lloyd *et al* (1979) used a point dilution method to determine the hydraulic conductivity of mature domestic refuse. A fluorescein tracer was added to two narrow (<100 mm OD) boreholes in a landfill and the concentration of fluorescein in the boreholes monitored over a period of 14 days. The rate of decay, together with a measured (or inferred) leachate hydraulic gradient at each borehole resulted in calculated hydraulic conductivities of between 4 and 5.5 $x10^{-5}$ m/s.

Indirect methods

Oweis and Khera (1986) indirectly estimated the hydraulic conductivity of refuse in a landfill in New Jersey, Hackensaw Meadows, by applying an analytical solution to the height of leachate in the landfill. Leachate within the (above ground) landfill drained freely to drains at the edge, creating a leachate mound within the landfill. An analytical solution using the height of the mound, the distance between drains and the recharge rate led to an estimated hydraulic conductivity of 2.6 $x10^{-6}$ m/s.

Colden (1990) used tidal stress theory to interpret fluctuations in leachate levels in a landfill at Rhode Island, USA and thereby calculated a bulk hydraulic conductivity of the landfill. A value of $2x10^{-2}$ m/s was calculated. However, this value is exceedingly high in comparison with other data reviewed here.

Pumping tests

The results of hydrogeological pumping tests on landfills have been reported by a number of workers. Oweis and Khera (1990) undertook pumping tests on a 35-metre deep landfill with a 9-metre saturated zone. Oweis and Khera (1986) had previously reported a bulk unit weight of the landfill of approximately 6.8 kN/m^3 based on indirect measurements. Leachate drawdown data were collected from a fully penetrating pumped well and three observation boreholes located at approximately 9, 22 and 61 metres from the pumped well. Two tests were undertaken, the first at a pumping rate of 4.5 m^3/hr (1.26 l/s) for a duration of 24 hours (at which point the pumping well dried up), and a second at a pumping rate of 2.7 m^3/hr (0.76 l/s) which lasted for 2.5 days. Analysis of the drawdown and recovery data from the pumping well and the two nearest observation wells produced a range of hydraulic conductivities between 2.4 $x10^{-5}$ and 9.4 $x10^{-6}$ m/s.

Beaven (1996) reported the results of a pumping test undertaken in 1985 on a 9 metre depth of landfill with a 5-6 metre saturated zone. The pumping test was carried out over a period of 5 days at a pumping rate of 2.9 m^3/hr (0.8 l/s). The drawdown was monitored in a network of observation wells at spacings between 5 and 75 metres from the pumped well. Analysis of the results indicated a hydraulic conductivity of 1 $x10^{-4}$ m/s. The pumping test was repeated 9 years later when the depth of landfill had increased to 23 metres and the depth of the saturated zone to 6-7 metres. A pumping rate of 0.4 m^3/hr (0.11 l/s) was maintained for a period of 12 days and analysis of drawdown data indicated that the hydraulic conductivity of the refuse had decreased by over an order of magnitude to 8 $x10^{-6}$ m/s.

Burrows *et al* (1997) reported the results of over 50 pumping tests at four UK landfill sites. The resulting values of hydraulic conductivity spanned two orders of magnitude from $2.2x10^{-5}$ to 3.9 $x10^{-7}$ m/s, with an average value of 5.6 $x10^{-6}$ m/s. At three out of the

four sites tested the saturated zone of the landfill was between 10 and 20 metres in depth. Most of the tests were of relatively short duration (8 to 16 hours) and used the drawdown data from the pumped well for analysis. There were a small number of longer term (8 day) pumping tests with a 3 week recovery phase which had the benefit of data from observation wells in addition to data from the pumped well.

Cossu *et al* (1997) reported the results of a number of pumping test at Pescantina landfill in North Italy. The landfill had a saturated zone over 16 m deep. The tests were undertaken in previously drilled landfill gas extraction wells- considerable problems were reported with poor well efficiencies and clogging. The tests were of relatively short duration (less than 100 minutes) and provided hydraulic conductivity values of between 1.4 and 1.8 $x10^{-6}$ m/s. A strong anisotropy between horizontal and vertical hydraulic conductivity ($K_h = 4K_v$) was reported, although it is not clear how this was determined.

Giardi (1997) reported the results of a number of pumping tests at Chianni landfill in Italy. Difficulties were experienced in the interpretation of much of the pumping test data as there was often little correlation between the leachate levels in the pumping well and in adjacent monitoring wells. However, a general transmissivity value of $1x10^{-6}$ m^2/s was calculated using Jacob's straight line method (Cooper & Jacob, 1946). No information was provided on the saturated thickness of the landfill but this would appear to have been in excess of 10 metres, indicating that the hydraulic conductivity was less than $1x10^{-7}$ m/s. The average bulk unit weight of the landfill (determined from borehole cores) was 12.7 kN/m^3.

Laboratory studies

A number of laboratory based studies of the hydraulic conductivity of refuse have been undertaken. The tests are invariably complicated by the heterogeneity and large particle size of waste materials which create problems when using standard laboratory sized soil mechanics equipment (such as triaxial cells).

Chen *et al* (1977) reported laboratory permeability tests undertaken by Gupta (1972) which indicated that the hydraulic conductivity of milled refuse was related to the dry density. The hydraulic conductivity reduced from $1x10^{-4}$ m/s for a dry density of 0.24 t/m^3 (15 lbs/ft^3) to below $1x10^{-7}$ m/s for a density of 0.72 t/m^3 (45 lbs/ft^3).

Korfiatis and Demetracopoulos (1985) used laboratory leaching columns to investigate unsaturated flow through refuse. Although the primary aim of the experiment was to determine the relationship between volumetric water content and suction pressure, the

saturated hydraulic conductivity was also measured. Refuse packed to a bulk density of 0.88 t/m^3 had a hydraulic conductivity of between 1.3 x10^{-4} and 8x10^{-3} m/s.

Fungaroli and Steiner (1979) undertook laboratory experiments on shredded MSW of varying particle sizes (between 0.9 and 92 mm D_{50}) and reported hydraulic conductivities as a function of compacted density. Little correlation was found between the hydraulic conductivity and the particle size. However, within a wide scatter of data points there was a correlation between hydraulic conductivity and density. Hydraulic conductivity decreased from approximately 1x10^{-4} m/s for a density of less than 0.1 t/m^3, to 1x10^{-6} m/s for a density of 0.35 t/m^3. It is not clear why the reported densities are so low.

Landva *et al* (1984) undertook limited tests within a 470 mm diameter consolidometer. A variety of materials from different landfills were tested under applied stresses up to 400 kPa. Hydraulic conductivities varied from 6.8x10^{-5} (at an applied stress of 20 kPa) to 6x10^{-9} m/s (at 400 kPa). Unfortunately no data are presented concerning the corresponding waste densities.

Oweis and Khera (1986) reported unpublished work by Fang (1983) who had determined (presumably in the laboratory) the hydraulic conductivity of compacted waste materials. The hydraulic conductivity reduced from 1.5 x10^{-4} m/s at a bulk density of 0.57 t/m^3 to 7 x10^{-6} m/s at a density of 1.14 t/m^3.

Bleiker (1993) determined the hydraulic conductivity of refuse obtained from varying depths within a landfill (see section 2.5.2 on porosity for further details). The hydraulic conductivity of the materials varied between approximately 1x10^{-6} and 5x10^{-9} m/s for dry densities between approximately 0.5 and 1.2 t/m^3. The authors considered that, owing to experimental errors, lower hydraulic conductivities than these might be expected in field conditions. However, the fact that the sample fitted into such a small testing ring indicates that the grain size of the refuse was very small and may well have been reduced by the effects of drilling. Larger cored samples of material were obtained from the Brock West Landfill site and falling head permeability tests carried out. No details are provided of the core diameter, although they were likely to have been 4" or 6" (100 or 150 mm). The samples were tested in a flexible membrane within a rigid walled tube. The membrane was pressurised against the sides of the core whilst falling head tests were undertaken along its length. Hydraulic conductivities between 3x10^{-7} and 1x10^{-8} m/s were obtained, but no data on the density of the refuse were given.

Benson and Othman (1993), investigated the hydraulic characteristics of screened (<1 cm) municipal solid waste composts, compacted to different densities at different water

contents using a Proctor test. At the maximum achieved dry density of 0.93 t/m^3 a hydraulic conductivity of 2 x10^{-10} m/s was determined.

Chen and Chynoweth (1995) undertook hydraulic conductivity measurements on processed municipal refuse packed into laboratory scale columns. Tests were carried out on a typical mixture of paper and plastic produced by a refuse derived fuel (RDF) processing plant. The material had a nominal size of 1.3 x 0.01 cm and represented a very finely shredded waste. The RDF was packed into 120 cm high by 30 cm diameter permeameters at densities of 160, 320 and 480 kg/m^3. It is not clear whether these densities are dry density, but as no data are provided for water content it is likely that they are at 'as received' water contents. In addition, direct comparison with densities of municipal wastes achieved in landfills is not possible as the processing of the RDF would have removed many of the components normally contributing to the overall density. Hydraulic conductivities ranged from 9.5x10^{-4} to 5x10^{-7} m/s. As well as the variation with density, hydraulic conductivities varied with time and hydraulic gradient. This was attributed to a changing pore geometry over time and possibly gas generation.

Rowe and Nadarajah (1996) reported hydraulic conductivity data for the Fresh Kills landfill, New York (reproduced in Figure 2.8). No details are provided on how the hydraulic conductivity measurements were obtained. Despite a considerable amount of scatter the data shows a reduction in hydraulic conductivity with increasing depth within the landfill. The range of hydraulic conductivity values spanned 6 orders of magnitude from 10^{-3} to almost 10^{-9} m/s. The following empirical relationship between hydraulic conductivity (K in m/s) and depth (Z in metres) was derived:-

$$K = 0.00018.e^{-0.269Z} \qquad (2.25)$$

Figure 2.8 Hydraulic conductivity vs depth - Fresh Kills Landfill New York

Fig. 6. Variation in hydraulic conductivity with depth at the Fresh Kills landfill, New York. Based on data and a plot courtesy of the City of New York Department of Sanitation; IT Corporation; and Ogden Environmental and Energy Services, Inc. (personal communication).

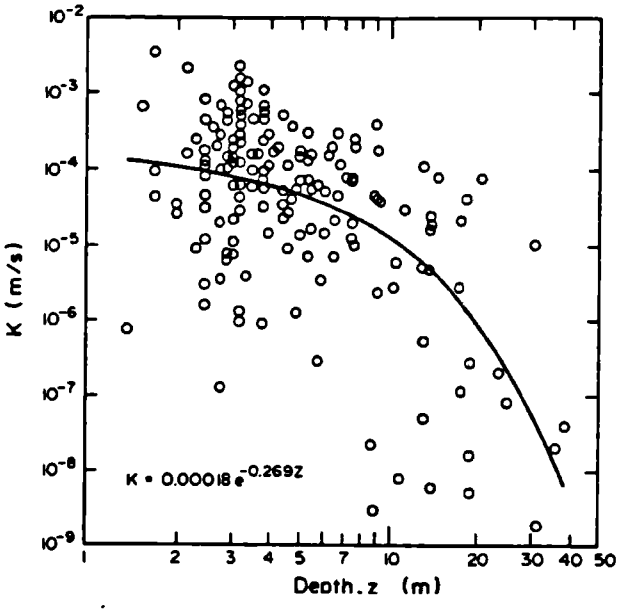

Source: Rowe and Nadarajah 1996

2.6.3 Summary of data relating to hydraulic conductivity

A wide range of hydraulic conductivity values for refuse are reported in the literature, as summarised in Table 2.7. A number of studies (particularly laboratory based) have demonstrated that hydraulic conductivity will decrease with increasing density and increasing applied stress. Whilst these laboratory based experiments have not fully accounted for the problem of sample size it does, nevertheless, suggest that the hydraulic conductivity of refuse in a landfill will decrease with depth of burial.

Reports of field based tests providing hydraulic conductivity measurements have, to date, been relatively limited. Tests, where carried out, appear to have been more successful on wastes with a hydraulic conductivity greater than approximately $1x10^{-6}$ m/s.

Table 2.7 Summary of reported values for hydraulic conductivity of household wastes

SOURCE	Summary of test and refuse type	Density (wet) t/m^3	Applied stress kPa	Hydraulic conductivity m/s
FIELD TESTS				
Lloyd (1977)	Point dilution method in 100 mm boreholes in landfill	N/A	N/A	4-5.5 x10^{-5}
EMCON (1983)	Field permeameter used on 10 year old refuse	N/A	N/A	1.5x10^{-4}
Colden (1990)	Tidal stress theory used to interpret fluctuations in leachate levels in landfill	N/A	N/A	2x10^{-2}
Landva (1986, 1990)	Flow net analysis on seepage from pit in surface of landfill	1-1.4	N/A	4x10^{-4} to 1x10^{-5}
Townsend et al (1990)	Infiltration from large-scale infiltration ponds	N/A	N/A	3-4x10^{-8}
Oweis (1986, 1990)	Pumping test on 35 m deep landfill with 9 metre saturated zone.	0.68	N/A	2.4x10^{-5} to 9.4x10^{-6}
Beaven (1996)	Pumping test on 9 metre deep landfill repeated when depth increased to 23 metres	N/A	N/A	1x10^{-4} 8x10^{-6}
Burrows (1997)	Numerous pumping tests on 3 landfills, ?approx. 20 metre deep with ?10 m saturated zone	N/A	N/A	2.2x10^{-5} to 3.9 x10^{-7} Av' 5.6 x10^{-7}
LABORATORY TESTS				
Chen (1977)	Laboratory tests on milled refuse	0.24 (dry) 0.72 (dry)	N/A N/A	1x10^{-4} 1x10^{-7}
Fungaroli (1979)	Laboratory tests on shredded MSW of varying particle sizes	0.1[1] 0.35[1]	N/A N/A	1x10^{-4} 1x10^{-6}
Korfiatis (1985)	Flow through refuse investigated	0.88	N/A	~1x10^{-4}
Landva (1984)	Wastes excavated from landfill tested in 470 mm diameter oedometer	N/A N/A	20 400	6.8x10^{-5} 6x10^{-9}
Oweis & Khera (1986)	Waste materials	0.57 1.14	N/A N/A	1.5x10^{-4} 7x10^{-6}
Bleiker (1993)	Refuse recovered from boreholes in landfill tested in laboratory	0.5 (dry) 1.2 (dry)	N/A N/A	1x10^{-6} 5x10^{-9}
Chen & Chynoweth (1995)	Processed (RDF) waste packed into columns at different densities	0.16 0.48		9.5x10^{-4} 5x10^{-7}

[1] Reason for very low recorded densities is unclear

2.7 Stress and stiffness

2.7.1 Total and effective stress

The total vertical stress σ_v exerted on a lift of refuse at depth z is derived from the weight of overburden above.

$$\sigma_v = \int_0^z \gamma(z)dz \qquad (2.26)$$

where the unit weight of refuse may itself be related to depth of burial.

If the unit weight is constant then the total vertical stress at depth z is $\gamma.z$ (kN/m^2 or kPa).

If the refuse is saturated, the effective stress σ' actually exerted on the matrix or fabric of the refuse is reduced by the action of the pressure of water, u in the pore spaces according to Terzaghi's equation

$$\sigma' = \sigma - u \qquad (2.27)$$

(Terzaghi, 1936)

A more rigorous analytical and experimental investigation into action of effective stress in soils led Skempton (1960) to propose more accurate expressions for effective stress in fully saturated soils as follows:

i) for shear strength

$$\sigma' = \sigma - \left(1 - a.\frac{\tan\psi}{\tan\phi'}\right)u_w \qquad (2.28)$$

where a is the effective contact area of the particles, ψ is the angle of intrinsic friction of the solid substance comprising the particles, ϕ' is the angle of shearing resistance of the porous medium, and u_w is the pore water pressure.

ii) for volume change

$$\sigma' = \sigma - \left(1 - \frac{C_s}{C}\right)u_w \qquad (2.29)$$

where C_s is the compressibility of the solid substance comprising the particles, and C is the compressibility of the porous medium.

Skempton concluded that for most soils both equations reduce to the form $\sigma' = \sigma - u_w$, or in other words Terzaghi's equation was applicable in most situations. With regard to Equation 2.28, $\tan\psi / \tan\phi'$ for most soils may be in the range of 0.15 to 0.3, but the interparticle contact area *a* is very small (typically << 0.1%, Mitchell, 1993) at pressures experienced in most geotechnical engineering applications. Also, under these low pressure conditions C_s/C is extremely small. Whereas it was concluded that Terzaghi's equation could be used with confidence in most situations for soils, this was not the general case for saturated concrete and rocks, where a is not negligible and C_s/C is typically in the range 0.1 to 0.5.

The extent to which these equations reduce to Terzaghi's equation when applied to household wastes is uncertain. This is related in part to the difficulty of describing in geotechnical terms the complexity and variable make up of household waste. Intuitively, household wastes are more akin to (compressible) soils rather than competent rocks and concrete, in which case Terzaghi's equation should be acceptable. However, the highly compressible nature of the wastes may result in high surface contact areas, a, developing particularly at high refuse densities. Furthermore, wastes are not made up of one predominant constituent or mineral, as is the case for many soils (e.g. silica in a sand), which makes comparing the compressibility of the refuse with the compressibility of the individual particles difficult. Some components of refuse, for example paper and some plastics, may be relatively compressible and could be of similar compressibility to the bulk refuse, again particularly at high refuse densities when many of the macro voids have collapsed. This could result in a reduction in the influence of pore water pressure on the effective stress in Equation 2.27.

In the absence of further work on this topic, which is beyond the scope of this thesis, it will be assumed that Terzaghi's equation is applicable to household waste materials.

2.7.2 Stiffness

Stiffness is a measure of the compressibility of a material. The stiffness of refuse may be quantified by means of the one-dimensional constrained modulus, M_0, which is defined as:

$$M_0 = \frac{\Delta\sigma'_v}{\Delta\varepsilon_v} \qquad (2.30)$$

where $\Delta\varepsilon_v$ is the increase in vertical compressive strain which results from an increase in vertical effective stress of σ'_v under conditions of zero lateral displacement. Units of kPa are used in this thesis for stiffness. The higher the value of stiffness, the less compressible the material.

Chapter 3

Equipment design and construction

3.1 Summary

The rationale for developing a large-scale, purpose built compression cell to test the geotechnical and hydrogeological properties of waste under loads equivalent to a 50 metre depth of landfill is presented. The dimensions of the compression cell are justified in terms of the ability to test representative samples of waste, the effect of sidewall friction and particle bridging on the vertical transmission of stress and on economic and operational constraints. The design, construction and operation of the compression cell are described and details are given of the monitoring systems used to determine the geotechnical and hydrogeological properties of the waste.

3.2 Introduction

Chapter 1 of this thesis developed the concept of a high rate flushing bioreactor as a possible method of achieving a sustainable landfill. In Chapter 2 the hydrogeological and geotechnical properties of wastes that may have a bearing on the operation of a high rate flushing bioreactor were considered and the relevant literature reviewed. Although a number of workers have recognised that waste density and depth of burial will effect the hydrogeological properties of the waste, a fundamental study under controlled conditions had not previously been carried out on representative samples of waste.

3.2.1 Need for purpose built equipment

There have been relatively few laboratory experiments on refuse which simulate depths of burial to over 40 metres. In 1990, prior to the commissioning of the research reported herein, the main laboratory study had been undertaken (by Landva *et al,* 1984) using a 438 mm diameter consolidation press to investigate the properties of refuse retrieved from auger cores taken from landfill sites (see Section 2.6.2). Since then Bleiker *et al* (1993) have also reported a major laboratory-based study. However, both set of experiments were undertaken using bench scale geotechnical testing equipment of limited size which required the waste to undergo some degree of processing (e.g. shredding) or size reduction (e.g. during the process of drilling). No studies have investigated all aspects of the hydrogeological properties of refuse included in Chapter 2, or considered the results in the context of a high rate flushing bioreactor.

A number of field scale well pumping tests have been used to determine the hydrogeology of landfills. However, it is impossible to relate the hydrogeological data obtained in these large-scale tests to the physical properties of the wastes being tested. Furthermore, it is difficult to interpret the data when there are considerable spatial variations and heterogeneities in the hydrogeological properties.

There was, therefore, a need for further research into the fundamental hydrogeological properties of waste. The research needed to be carried out in a controlled way to realistically simulate the conditions to be expected in full-scale landfill sites. However, it was not considered necessary to recreate the large-scale heterogeneities that occur in landfill sites. An understanding of the effects of larger scale variations could be developed by simulating the juxtaposition of various types of waste or cover material in a future experimental or theoretical model (a topic beyond the scope of this thesis). The approach taken was to determine the individual properties and behaviour of specific and well characterised wastes. Thus, the following design criteria for the test cell were established:

1) the cell should be large enough to accommodate the heterogeneous nature of the materials to be tested without the need for particle size reduction

2) the cell should be capable of simulating loads on the material being tested equivalent to a minimum 50 metre depth of landfill

3) the cell should allow for determination of the absorptive capacity and effective porosity of the material being tested at different applied loads and

4) the cell should allow for determination of the hydraulic conductivity of the material being tested at different applied loads.

To fulfil these requirements a purpose built compression cell was required. The various elements of the design are discussed in Section 3.3.

Other factors that are likely to have an impact on the hydrogeological properties of refuse include:-

1) vertical and horizontal anisotropy;

2) the effect of biodegradation; and

3) the degree of saturation, that in turn may be related to gas production.

These aspects were not investigated by the research reported herein, although recommendations for further work into these factors are made in Chapter 9.

3.3 Design Requirements

3.3.1 Diameter of cell

The diameter of the cell needed to be large enough to be able to hold (and test) representative samples of household waste without the need for particle size reduction by techniques such as shredding or pulverisation.

Household waste is generally placed and disposed of in black plastic refuse bags with an approximate capacity of 60 litres and a diameter (when full) of approximately 50 cm. The firsts requirement was that the diameter of the compression cell should be large enough for a number of these bags to be placed side by side to replicate packing within a landfill site.

The second consideration relates to the compression of the wastes in the cell. It has been determined (e.g. Lambe, 1951) that if the diameter of a compression cell is less than approximately 10 to 20 times the particle size of the material being compressed, then it is possible that the particles will combine to form arch structures that will artificially resist compression. This feature will be more significant for relatively non compressible particles, such as quartz grains. The relatively compressible nature of the majority of materials found in refuse may mean that there is very limited scope for arching or bridge structures to develop. The average size (in terms of the longest dimension) of the

individual components of samples of municipal waste from the USA was determined by Winkler and Wilson (1973) to be approximately 200 mm (see Section 2.3.2). Also Jessberger and Kockel (1991) reported that 85% by weight of MSW passed through a 100 mm screen.

The diameter chosen for the compression cell was 2 metres. This was considered large enough to accept representative samples of waste and would also accommodate between 10 and 15 black plastic refuse bags laid side by side in a layer. Being between 10 and 20 times the average particle size of the constituents of refuse, bridging effects would be negligible.

3.3.2 Height

The vertical height of the compression cell was related to a number of factors:-

1) the pre-determined diameter of the cell (2 metres);

2) the need to maintain a sufficient flow path length for the determination of vertical hydraulic conductivity:

3) the highly compressible nature of refuse, meaning that the depth of a sample could be reduced over the course of a test to perhaps one half of its original depth; and

4) consideration of sidewall friction effects.

Length of vertical flow path

The main purpose of the experiments was to determine the hydrogeological properties of wastes, with an emphasis on hydraulic conductivity. Vertical hydraulic conductivity was obtained by measuring the hydraulic gradient whilst vertical flow was induced through the refuse. The height of the testing cylinder needed to be sufficient for vertical flow paths to be representative.

Although, theoretically, hydraulic gradients should exist and be measurable over very short distances, it was considered that a minimum cell height of between 1 and 1.5 metres would be required for reliable hydraulic gradient measurements. This length can be related to average particle size. Daniel (1994), citing the standards of ASTM D2434 and D5084, reported that the minimum sample length should be at least 6 times larger than the largest particle in the specimen. Using data provided by Jessberger and Kockel (1991) a cell height of 1 to 1. 5 metres would provide a flow path of between at least 10 and 15 times the average particle size (see above). In practice the average particle

dimension in the vertical orientation is likely to be considerably smaller than the overall average. Natural packing will tend to orientate the longest dimensions of a particle along an x-y (horizontal) plane, leaving the shortest dimension to fill the z (vertical) plane. Vertical compression will then further reduce the length of the vertical (z) dimension.

With piezometers installed at vertical spacings of 300 mm (reduced to 150 mm in an early modification to the cell), at least four head measurements could be used to determine the hydraulic gradient over a flow path length of between 1 and 1.5 metres.

Compressible nature of refuse

A further factor relating to the height of the cell was the highly compressible nature of refuse. Ham *et al* (1978), among others, had demonstrated that household waste could exist in a very loose state but could be compacted to high densities. Some of Ham's compression experiments on loose waste resulted in the waste density increasing by a factor of four. On this basis, an initial height of 4 metres of loosely compacted refuse would be required to end up with a minimum refuse height of 1 metre in the compression cell.

Reduction of transmitted stress due to sidewall friction

The vertical height of standard oedometers used for consolidation tests on (generally) clay type samples is usually restricted to approximately one quarter of its diameter so that the effects of side wall friction are negligible. Application of this rule to the design of the compression cell would have restricted the vertical height to 0.5 metres. This was considered unacceptable for the reasons outlined above in relation to representative flow path length, the measurement of hydraulic gradients and waste compression. In addition, the economics of the project did not allow an increase in the overall diameter of the cell to achieve an increased vertical depth. Therefore the approach taken attempted to measure and/or quantify the transmission of applied stress over the depth of waste in the cell.

Ham *et al* (1978) in their work on the density of refuse (Section 2.4.2), compacted waste into a rectangular cell approximately 0.6 metres square and 0.9 metres high. To determine the effect that the sidewalls of the container had on compaction, tests were also undertaken without the container. Refuse was initially placed in the container and loaded with a stress of approximately 9 kPa (320 kg on a cross sectional area of 0.6 m x 0.6 m = 0.36 m^2). At this stage it was possible to remove the container whilst maintaining the sample of refuse intact and proceed with the compaction tests. It was found that for unprocessed refuse at applied stresses between 35 and 620 kPa (without

induced vibrations) an increase in density of between 6 and 17% was seen in the tests without the supporting chamber. It was assumed that this the result of removing both the effects of sidewall friction and the effect of particle bridging. The test was repeated using milled refuse where a smaller increase in density, between 4 and 8%, was recorded when the container was not used. The greater increase in density of the unprocessed refuse (compared with that of milled refuse) was interpreted as an indication of the influence of particle size on bridging effects. Ham *et al* (1978) assumed that the milled refuse was not being affected by particle bridging. This indicates that sidewall friction had a relatively limited effect (of only 4 to 8%) on refuse density when the container was in place.

Theoretical approach to calculating the effect of sidewall friction

Figure 3.1 is a simple model illustrating the stresses that act on a thin layer of waste at depth z within the compression cell, and Figure 3.2 is a representation of the forces.

Figure 3.1 **Conceptual model of stresses acting on a layer of thickness δz at depth z within the compression cell**

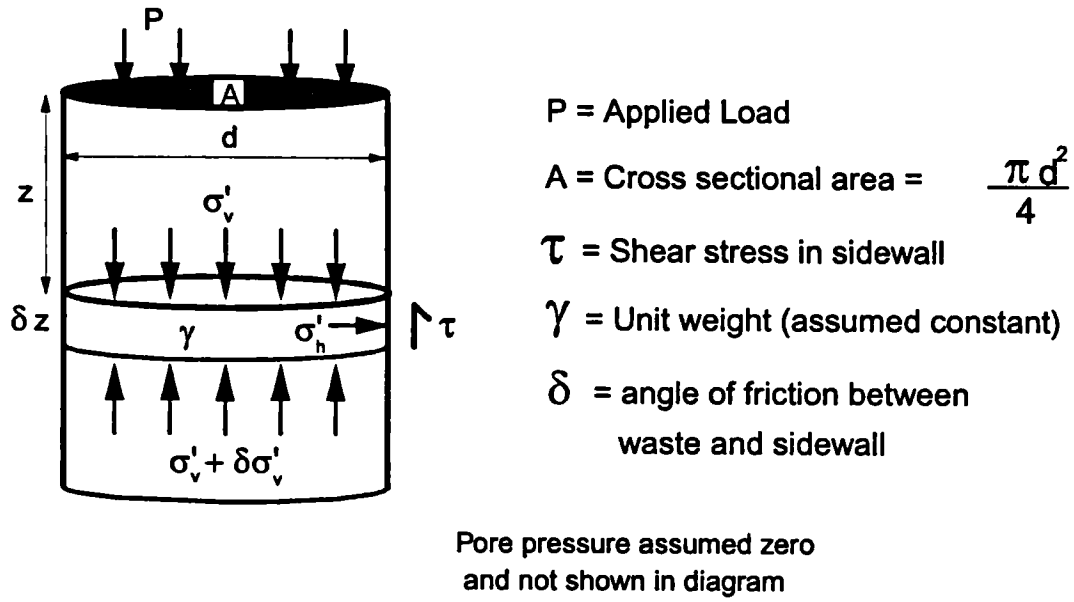

Figure 3.2 Forces acting on layer of thickness δz at depth z within the cell

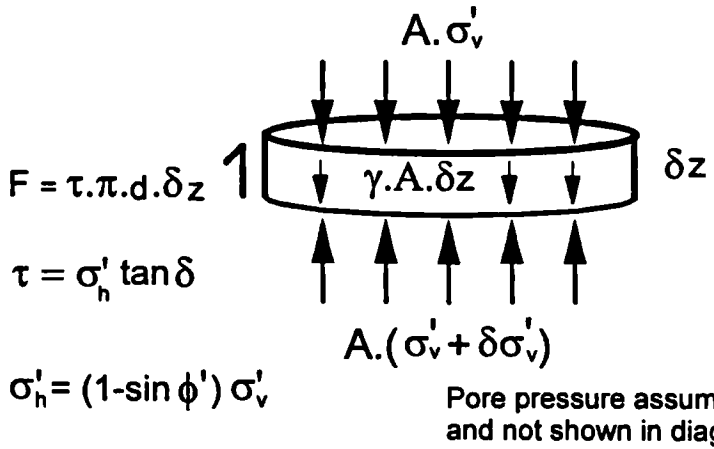

The difference $A.\delta\sigma'_v$ between the total vertical force applied to the top of a layer of vertical thickness δz and the total vertical force transmitted at the bottom of the layer is equal to the difference between the force due to the weight of refuse within the layer and the frictional forces exerted around the edge of the layer.

The shear stress τ is equal to the product of the normal effective stress σ'_h and the tangent of the angle of friction (δ) between the refuse and wall of the compression cell. The frictional force F is:-

$$F = \sigma'_h.\tan(\delta)\pi.d.\delta z \qquad (3.1)$$

The forces acting on the layer can be balanced as follows:

$$A.\delta\sigma'_v = \gamma.A.\delta z - \pi.d.\delta z.(\sigma'_h \tan\delta)$$

Rearranging and setting $A = \frac{\pi d^2}{4}$

$$\delta z\,(\gamma d - 4\sigma'_h.\tan\delta) = d.\delta\sigma'_v$$

or

$$\frac{d\sigma'_v}{dz} = \gamma - \frac{4\sigma'_h.\tan\delta}{d} \qquad (3.2)$$

The horizontal effective stress may be related to vertical effective stress (Jaky, 1944) by:

$$\sigma'_h = (1-\sin\phi')\sigma'_v \qquad (3.3)$$

$$\frac{d\sigma'_v}{dz} = \gamma - \left[\frac{4(1-\sin\phi').\tan\delta}{d}\right]\sigma'_v \qquad (3.4)$$

Assuming that ϕ', δ and γ remain constant and are independent of depth, z, within the cell then let

$$B = \left[\frac{4(1-\sin\phi').\tan\delta}{d}\right] \qquad (3.5)$$

Substituting B in Equation 3.4 gives:

$$\frac{d\sigma'_v}{dz} = \gamma - B.\sigma'_v \qquad (3.6)$$

Integrating with respect to vertical effective stress and depth gives

$$\int_P^{\sigma'_v} \frac{d\sigma'_v}{\gamma - B.\sigma'_v} = \int_0^z dz \qquad (3.7)$$

where P is the applied surface load, or

$$\sigma'_v = \frac{\gamma}{B}(1 - e^{-Bz}) + P.e^{-Bz} \qquad (3.8)$$

This equation relates the vertical effective stress (σ_v') at depth z in the cell to the internal angle of friction of the waste (ϕ') and to the angle of friction (δ) between the waste and the wall of the compression cell. The equation shows that the vertical effective stress has two components: one that relates to the density of the waste in the cell and (more significantly) one that relates to the applied load. The derivation of the equation assumed that the unit weight of the waste was constant. Although in theory the density of the waste will reduce with depth in the cell in response to the reduction in transmitted vertical effective stress, this has little bearing on the calculated effective stress for the applied surface loads being considered.

Internal angle of friction of refuse, ϕ'

The internal angle of friction of refuse is a subject of considerable debate. Jessberger and Kockel (1991) reported values for the internal angle of friction of refuse ranging from approximately 20° to 40°, with an apparent reduction in the angle as refuse ages. However, they also reported that the mobilised internal angle of friction increased with increasing strain within a refuse sample. An example was given of a mobilised friction

angle of 19° within a sample of refuse strained by 5% increasing to 46° when strained at 20%. They noted that even at 20% strain the refuse had not failed and that this might not occur until strains of approximately 50% had been reached.

Determination of side wall friction angle δ

A simple experiment gave an indication of the angle of friction between household waste and the walls of the compression cell. Approximately 1 tonne of loosely compacted household waste was placed on the smooth metal back (body) of a tipper lorry. The body was slowly raised until the refuse just started to move and the angle of the body to the horizontal was measured as 27°. It is usual that once movement has started, the angle of friction reduces slightly, perhaps in this case to a value of 25°.

Calculation of reduction in vertical stress with depth in cell

The calculated reduction in vertical stress with depth within a compression cell of 2 metres diameter is recorded in Table 3.1 for the full range of ϕ' and δ discussed above. The unit weight of the waste in the cell was set at a constant 10 kN/m^3. The range of possible values of effective stress is restricted as it is not possible for the sidewall friction angle to be greater than the internal angle of friction of the waste (i.e. $\delta \leq \phi'$). Also, the term B in Equation 3.5 tends to a maximum when $\delta = \phi' = 38°$, such that the ratio of transmitted effective stress (σ_v') to applied load (p) also tends to minimum when $\delta = \phi' = 38°$. For this worst case situation, 33% of the applied load is transmitted to a depth of 2 metres. The best possible case ($\phi' = 50°$ and $\delta = 15°$) results in over 80% of the applied load being transmitted.

Table 3.1 Calculated reduction in vertical effective stress with depth for varying values of ϕ' and δ

			P = 150 kPa		P = 450 kPa	
Internal friction angle	Sidewall friction angle	Depth in cell	Calculated effective stress	Ratio of stress to load	Calculated effective stress	Ratio of stress to load
ϕ' degrees	δ degrees	z metres	σ'_v kPa	σ'_v/P	σ'_v kPa	σ'_v/P
20	15	0	150	1.00	450	1.00
20	15	1.0	114	0.76	325	0.72
20	15	2.0	88	0.59	237	0.53
20	20	0	150	1.00	450	1.00
20	20	1.0	101	0.67	287	0.64
20	20	2.0	70	0.47	186	0.41
30	15	0	150	1.00	450	1.00
30	15	1.0	124	0.82	353	0.78
30	15	2.0	103	0.69	279	0.62
30	20	0	150	1.00	450	1.00
30	20	1.0	113	0.75	321	0.71
30	20	2.0	87	0.58	232	0.51
30	25	0	150	1.00	450	1.00
30	25	1.0	102	0.68	290	0.65
30	25	2.0	72	0.48	190	0.42
40	15	0	150	1.00	450	1.00
40	15	1.0	133	0.89	381	0.85
40	15	2.0	119	0.79	323	0.72
40	20	0	150	1.00	450	1.00
40	20	1.0	124	0.83	356	0.79
40	20	2.0	105	0.70	283	0.63
40	25	0	150	1.00	450	1.00
40	25	1.0	116	0.77	331	0.74
40	25	2.0	92	0.61	246	0.55
50	15	0	150	1.00	450	1.00
50	15	1.0	142	0.94	406	0.90
50	15	2.0	134	0.90	368	0.82
50	20	0	150	1.00	450	1.00
50	20	1.0	136	0.90	389	0.86
50	20	2.0	124	0.82	337	0.75
50	25	0	150	1.00	450	1.00
50	25	1.0	130	0.86	371	0.82
50	25	2.0	113	0.75	307	0.68
38	38	0	150	1.00	450	1.00
38	38	1.0	90	0.60	254	0.57
38	38	2.0	57	0.38	147	0.33

For γ = 10 kN/m^3 Calculations based on Equation 3.8

Effect of pore water pressure on sidewall friction

Burland and Roscoe (1969) investigated the effects of sidewall friction in a tall oedometer with a height to diameter ratio in excess of 2:1. The oedometer consisted of a $1\frac{1}{2}$ inch (3.8 cm) diameter polished brass tube with a 1 inch (2.5 cm) diameter load cell mounted on its lower plate. The tube was filled with kaolin clay and a vertical load applied in increments. For each load increment the stress transmitted to the lower load cell was measured against time. It was found that the amount of stress transmitted reduced with time, indicating that the sidewall friction force increased with time (each stress increment lasted from between 24 to 72 hours). It was concluded that the magnitude of wall friction appeared to increase significantly during the process of secondary consolidation. It was also noted that the magnitude of wall friction is much larger for decreasing applied stress than for increasing applied stress.

These effects can be explained by the fact that the frictional shear force on the side of the waste in the compression cell is related to the horizontal effective stress. If the horizontal effective stress is low then the frictional shear force will also be low. According to one dimensional consolidation theory and Terzaghi's effective stress equation (Equation 2.27), a load applied to a saturated material will first be supported by an increase in the pore water pressure within the material with little or no increase in effective stress. This means that directly after the application of an applied load the horizontal effective stress would remain low and, therefore, the magnitude of wall friction would also be low. As pore water pressures dissipated the sample would consolidate, effective stresses would increase, and the magnitude of wall friction would also increase.

This mechanism would probably also occur within the compression cell during the compression of wastes. Wastes tested in the compression cell were often compressed with a water content at field capacity (e.g. see Sections 4.3.5 and 6.4.6). In practice these water contents were not too different from the water content at complete saturation. Within the context of the compression tests this means that the magnitude of sidewall friction may initially be less than indicated in Table 3.1.

Final decision on height of the compression cell

Because vertical hydraulic conductivity was to be determined by the measurement of hydraulic gradient it was considered that a minimum of approximately 1 metre depth of waste was required. Although this was the minimum acceptable for a highly compressed sample of waste, the required height of the compression cell would depend on the amount of compression expected during the tests. Although Ham *et al* (1978) measured fourfold increases in the density of waste during compression tests, it was felt that the increase could be restricted to a factor of approximately 2 by lightly pre-compacting

wastes into the cell. On this basis the cell needed a minimum working height of 2 metres, giving a diameter to height ratio of approximately 1:1.

At the design stage there was considerable uncertainty as to how significant sidewall friction effects might be. For a 2 metre depth of waste, the theoretical approach indicated that for likely values of ϕ' and δ, side wall friction could reduce the applied stress at the base of the waste by up to about 50% (the maximum possible reduction was 66%). For these effects to have been eliminated from the experiment the diameter to height ratio would have had to have been reduced significantly, from approximately 1:1 to between 2:1 and 3:1. This would have increased the diameter of the cell to over 4 metres, which would not have been viable for both economic and operational reasons.

A final height of 3 metres was chosen. This would allow a maximum 2.5 metre depth of waste to be placed in the cell as at least 0.5 metres of free space was required for operational and practical reasons (e.g. additional height was needed when loading waste into the cell at the start of a set of experiments, see Section 4.3.3).

3.3.3 Applied load to simulate required depth of landfill

The compression cell needed to simulate depths of landfill of up to 50 metres (see Section 3.2.1). Assuming an average unit weight of waste in a landfill of 10 kN/m^2, the cell needed to be capable of generating a minimum applied stress of 500 kPa. The force required over the cross sectional area of the 2 metre diameter cell was 1,570 kN, equivalent to a mass of approximately 160 tonnes.

The cell also needed to be capable of applying the load in stages, with each increment of load being kept constant over a prolonged period of time.

3.3.4 Monitoring requirements

The main purpose of the experiment was to determine various geotechnical and hydrogeological properties of wastes under different applied loads. Therefore, the design of the compression cell had to include facilities for measuring the parameters listed in Table 3.2. In addition, analysis of the possible effects of sidewall friction (Section 3.3.2) indicated that there could be a significant reduction of stress with depth within the cell. This meant that, where possible, parameters should be measured as a function of depth in addition to being measured as an overall average for the waste in the cell.

Table 3.2 Monitoring requirements of compression cell

Parameter	Required Quantities	Measured Quantities
Water content[1]	Mass of dry solids	Assumed to remain constant during test and derived from a laboratory water content test on an initial sample of waste
	Mass of water	i) Total mass of waste in cell (subtract mass of dry solids) and/or ii) All water inputs and outputs to cell to maintain a water balance
Water content at field capacity[1]	Mass of dry solids	As above
	Mass of water after waste has been saturated and allowed to drain under influence of gravity	As above
Dry density[1,2]	Mass of dry solid	Assumed constant (see above)
	Volume occupied	Elevation of upper platen
Wet density[1,2]	Total mass of waste	Total mass of waste in cell
	Volume occupied	Elevation of upper platen
Effective porosity[2]	Water added/ drained	Water added or drained
	Change in saturated volume of waste	Change in hydrostatic water level in waste (multiply by cross sectional area)
Hydraulic conductivity[2]	Rate of vertical flow through waste	Rate of vertical flow into and out of waste
	Vertical hydraulic gradient	Piezometric levels taken at different elevations in waste

[1] Parameters to be measured against time
[2] Parameter to be measured against depth

3.4 Design Elements

3.4.1 Introduction

A purpose built compression cell was designed by Enviropower Ltd in November 1990, to fulfil the requirements outlined in Section 3.3. The original design was slightly amended by Sherwen Engineering Company Ltd after being awarded the contract to build the cell. The design consists of a 3 metre high testing cylinder supported within a steel frame with an overall height of approximately 8 metres. Material in the cylinder is compressed by a 2 metre diameter platen. The movement of the platen and the cylinder

itself is controlled by hydraulics. Specific features of the design are outlined in more detail below.

3.4.2 Steelwork

The compression cell consists of a steel cylinder 2 metres in diameter and 3 metres high (Figures 3.3 and 3.4). The cylinder is suspended vertically within a steel support frame which has an overall height of approximately 8 metres. The frame including the compression cell is mounted on load cells which provide a continuous readout of the weight of the cell and its contents (see below). The base of the cylinder is sealed by a 2 metre diameter lower platen seated on a water tight 'O' ring. Refuse in the cylinder is compressed by an upper platen, just under 2 metres in diameter, which can be moved vertically up and down inside the testing cylinder. The upper platen is connected to, and moved by two 200 mm diameter hydraulically operated pistons which are mounted on the upper part of the steel support frame. The connection points between the upper platen and the load pistons allow the upper platen to tilt slightly in one plane to accommodate small amounts of differential compression.

With the upper platen fully raised the test cylinder can be rotated on a central pivot to a horizontal orientation. Whilst in this position refuse can be ejected from the column by a hydraulically operated telescopic piston which pushes the lower platen up to the top of the cylinder. The cylinder can also be tilted to an angle of approximately 45° to the vertical to facilitate initial placement of refuse at the start of a series of tests.

Although the cylinder can be rotated about its central pivot point, the cell is designed to prevent any of the applied load being transmitted onto this pivot point during testing. The pivot point is not connected directly to the testing cylinder but to a square collar loosely embracing it. The lower platen and base of the cylinder sit on a lower member of the support frame. It is onto this that the forces exerted by the upper platen are transmitted. Prior to rotation the testing cylinder is first raised off the basal support frame to provide enough clearance. This lifting is accomplished using four "jack up" hydraulic rams which sit on the square collar and act on a steel ring connected to the cylinder (see Figure 3.5).

There are two lines of 20 piezometer ports running up the side of the cylinder at spacings of between 150 mm and 400 mm. The original design for these points consisted of a boss with a 2" diameter BSP female thread, but in a subsequent modification these were altered to stainless steel flanges. Piezometer tubes are installed horizontally through these ports (see Section 3.6.6). The piezometer ports are also used to measure differential compression at various depths within the column (Section 3.6.4).

Figure 3.3 Schematic section through compression cell

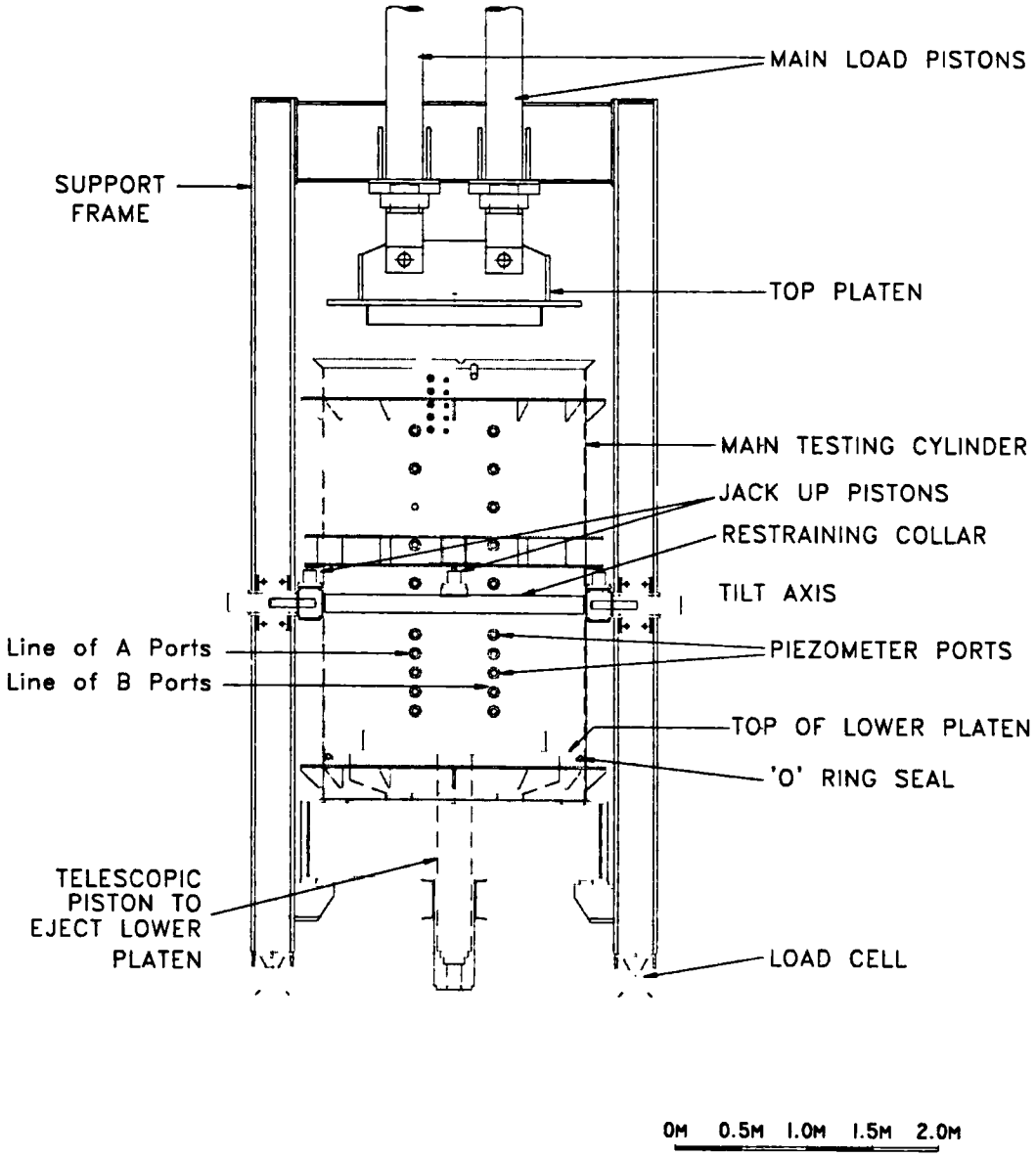

Figure 3.4 Compression cell as built

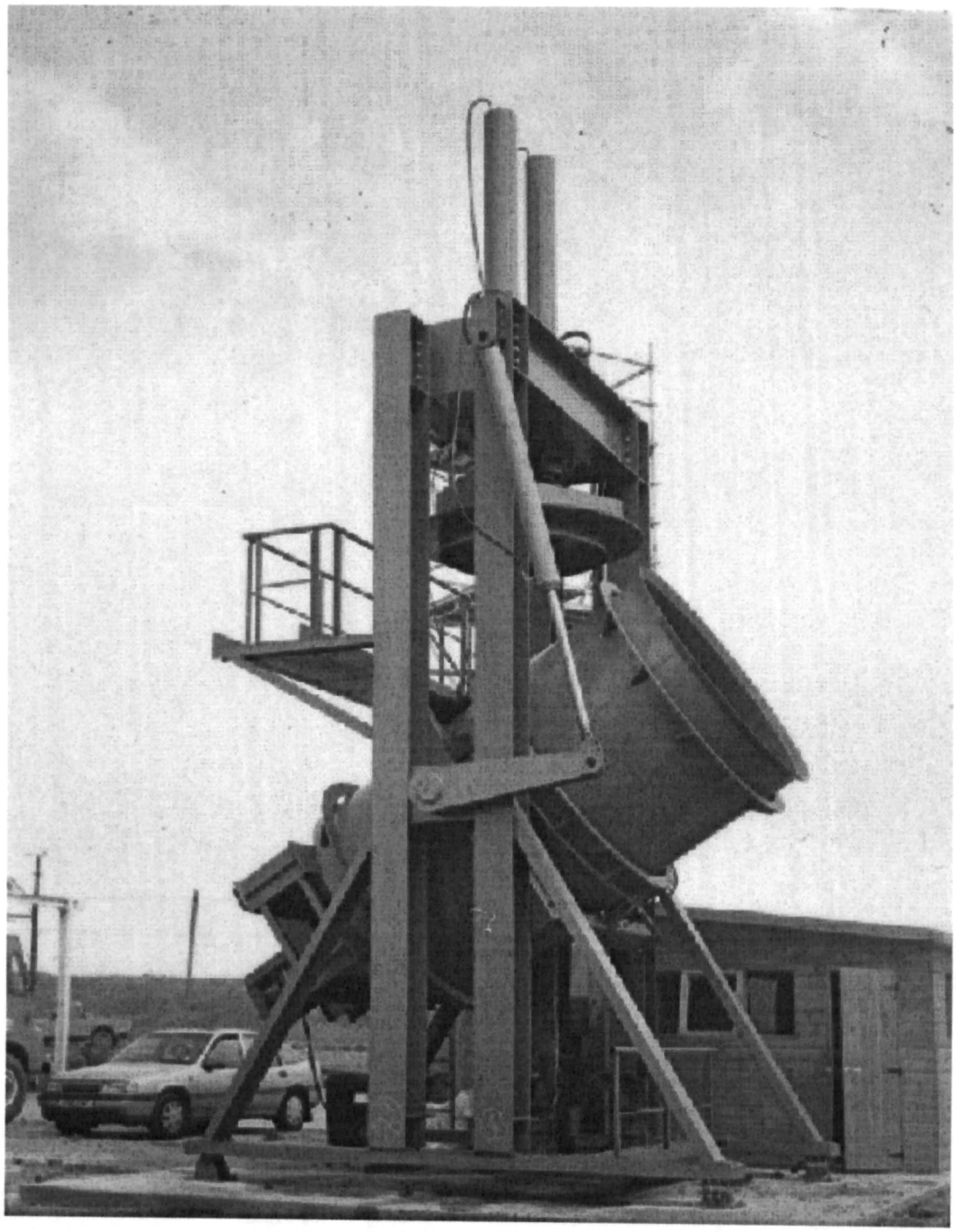

Figure 3.5 **Compression cell showing operation of "jack up" cylinders prior to rotation of testing cylinder**

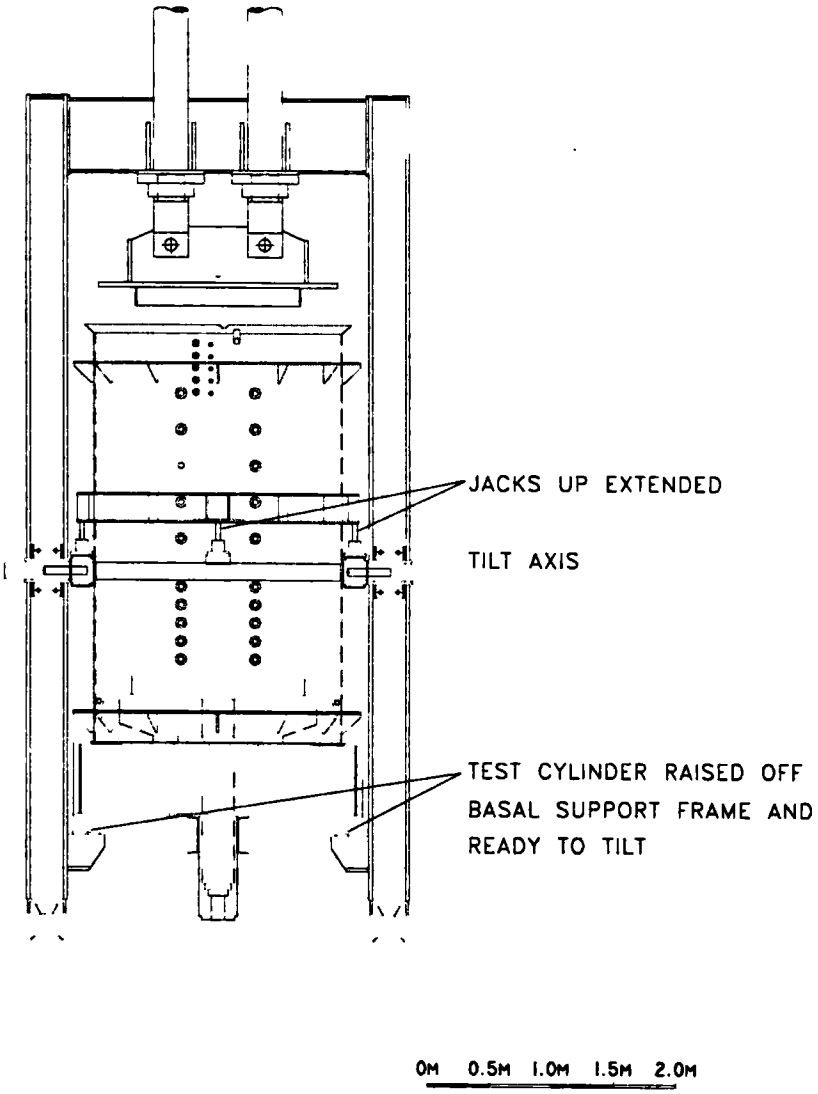

3.4.3 Hydraulics

The compression cell is operated by a hydraulic system controlling four groups of pistons. These are:-

1) two 250 mm diameter pistons with a 2.5 metre stroke which move the upper load platen: these are referred to as the "load" pistons or cylinders;

2) one two-stage telescopic piston with a three metre stroke which raises and lowers the lower platen within the testing cylinder: this is referred to as the "eject" cylinder;

3) four 75 mm diameter pistons which are used to raise and lower the testing cylinder within its restraining collar prior to rotation: these are referred to as the "jack up" cylinders; and

4) one 140 mm diameter piston which rotates the cell from a vertical to horizontal orientation: this is referred to as the "rotate" cylinder.

A summary of the purpose and dimensions of the various cylinders is provided in Table 3.3.

The hydraulic pistons are part of a system comprising a control panel, a 1,000 litre oil reservoir tank, two electrically operated oil pressure pumps and a bank of solenoid operated valves which direct the oil to the appropriate hydraulic cylinders. The hydraulic system has a maximum operating pressure of 190 bar, regulated by a system pressure relief valve (see Figure 3.6).

Assuming minimal friction losses in the seals within the two main load cylinders, the maximum possible applied stress that can be exerted through the upper platen is given by:-

$$F = P_1 . A_1 + F_{plat} = P_2 . A_2$$

where:-

F	=	The total force (kN)		
P_1	=	Hydraulic Pressure	= 190 bar	= 19,000 kPa
A_1	=	Cross sectional area of both load cylinder bores	= $2x\pi x(0.125)^2$	= 0.0982 m^2
F_{plat}	=	Dead weight of upper platen and cylinder rods	= 28.85 kN	
P_2	=	Applied load through upper platen		
A_2	=	Cross sectional area of upper platen	= $\pi x(1)^2$	= π m^2

$$P_2 = \frac{19{,}000 \times 2.\pi.(0.125)^2 + 28.85}{\pi}$$

$$= 603 \text{ kPa}$$

The two oil pressure pumps have different specifications but each consists of a three phase electrical motor which drives a hydraulic pump unit. (see Appendix A).

The high capacity "fast" pump is used to operate the eject and tilt cylinders. It is also used with the load cylinders when there is a requirement to move the top platen relatively rapidly, usually at the start or end of a series of tests. The pump can operate at a pressure of up to approximately 230 bar with a nominal pumping rate of 15 l/min.

The low capacity "load" pump is mainly used during long term refuse compression tests to maintain the required pressure in the two load cylinders connected to the upper platen. It is also used to operate the jack up cylinders. The pump is a rotary piston pump and can operate at pressures in excess of 250 bar with a nominal pumping rate of 0.9 l/min. It is continuously rated and is designed for uninterrupted operation over a period of many weeks during load tests. The operating pressure of the hydraulic system is controlled by a manually adjustable pressure relief valve and a pressure gauge. The pressure within the hydraulic circuit can be regulated between 1,000 and 19,000 kPa (10 and 190 bar), equating to applied stresses on the refuse of between 25 and 603 kPa. Oil is pumped continuously around the system by the load pump and any oil not required to maintain the selected pressure in the load cylinders is returned to the reservoir tank. This ensures that there is never any pressure drop in the load cylinders as a consequence of the refuse in the test cell compressing.

Table 3.3 Hydraulic cylinder summary

Piston/ Cylinder	Number of pistons	Purpose	Bore	Rod Diam.	Max.[1] Force	Stroke
			mm	mm	kN	mm
Load (dual acting)	2	Compress refuse through upper platen	250	200	1,854	2,500
Eject	1	Eject refuse from cylinder by raising lower platen	200 /165 (8" /6.5")	125[1] (5")	597	3,000
Jack Up	4	Raise test cylinder within restraining collar prior to tilting	75 (3" imp)	50 (2" imp)	336	75
Rotate (dual acting)	1	Rotate test cylinder from vert' to horizontal orientation for filling and discharging refuse from cell	140 (5.5" imp)	75 (3" imp)	292	1,800

The movement of the load and rotate cylinders, which are dual acting, is controlled in both directions by hydraulic pressure. Retraction of the jack up and eject cylinders rely, respectively, on the weight of the testing cylinder and the bottom platen to displace hydraulic fluid under atmospheric pressure back into the reservoir tank.

[1] The eject cylinder is a two stage telescopic piston comprising two cylinders and one rod.

Table 3.4 summarises the oil capacity of each set of cylinders and the approximate time taken for the full stroke of each set to be achieved using either the fast or load pumps.

Table 3.4 Use of hydraulic cylinders with different pumps

Piston	Number of pistons	Oil capacity of bore when cylinder(s) fully expanded litres	Approx. time to expand fully cylinder(s) using Fast Pump	Approx. time to expand fully cylinder(s) using Load Pump
Load	2	245	16 min	270 min
Eject	1	52	3.5 min	58 min
Jack Up	4	1.3	5 secs	1.4 min
Rotate	1	28	1.8 min	31 min

Figure 3.6 Schematic diagram of part of the hydraulic circuit used to control the operation of the compression cell

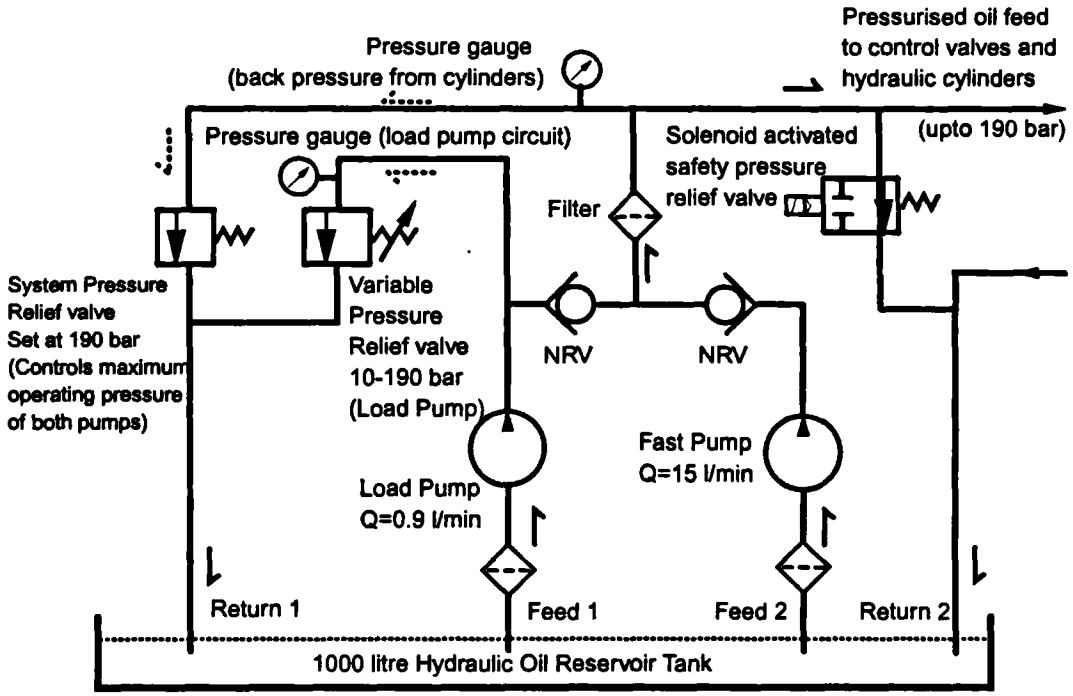

3.4.4 Ancillaries - Water flow systems

In order to determine the hydrogeological properties of the waste, facilities are required to introduce water into, and drain leachate from the compression cell. Measurements of both the quantity of water added (or drained) and the rate of flow through the refuse are required.

The introduction of water or leachate into the cell is achieved by using two 450 litre water header tanks situated on a scaffold tower adjacent to the compression cell. The tanks can be located up to 3 metres above the top of the testing cylinder. The tanks are connected through pipework to two rings of six evenly spaced 25 mm (1" imp) diameter ports on the lower platen. A similar arrangement of two rings of ports exists on the upper platen and is connected to pipework to take the return flow of water passing upwards through the compression cell back to the main reservoir tank.

On both the upper and lower platen the inner set of ports is separated from the outer set by a 150 mm high annular ring, or skirt, located on the inner (i.e. facing the waste) surface of the platen. This is illustrated in Figure 3.7 for the lower platen. This divides the waste in the test cell into two equal areas comprising a central cylindrical core and an outer annulus (the skirt has a radius of 0.71 metres). The purpose of these skirts was to provide some degree of hydraulic separation between the water being fed into and removed from the central core and outer annulus of waste using the two rings of ports. By monitoring and comparing the flow rates through the central core and outer annulus of waste it was intended to assess the impact of edge effects: if edge effects were significant then higher flow rates would be expected in the outer annulus of waste. In practice it was difficult to achieve sufficient control over the flow and head distribution within the cell to interpret the resulting data with any degree of confidence.

In addition to the upward flow of water through the outer ports in the upper platen, water can also pass through the 2 mm annulus between the outer edge of the platen and the inner surface of the testing cylinder.

Any leachate collecting above the upper platen is returned to a 8,500 litre reservoir tank by gravity overflow through pipes connected to a number of ports on the side of the column. Water from the reservoir tank is pumped to the header tanks using a 3 phase open impeller electrical pump. The pump is capable of pumping at a rate of approximately 6 l/sec (22 m^3/hr) at a lift of 9 metres. A schematic representation of this flow system is given in Figure 3.7.

Figure 3.7 Schematic representation of flow system through cell

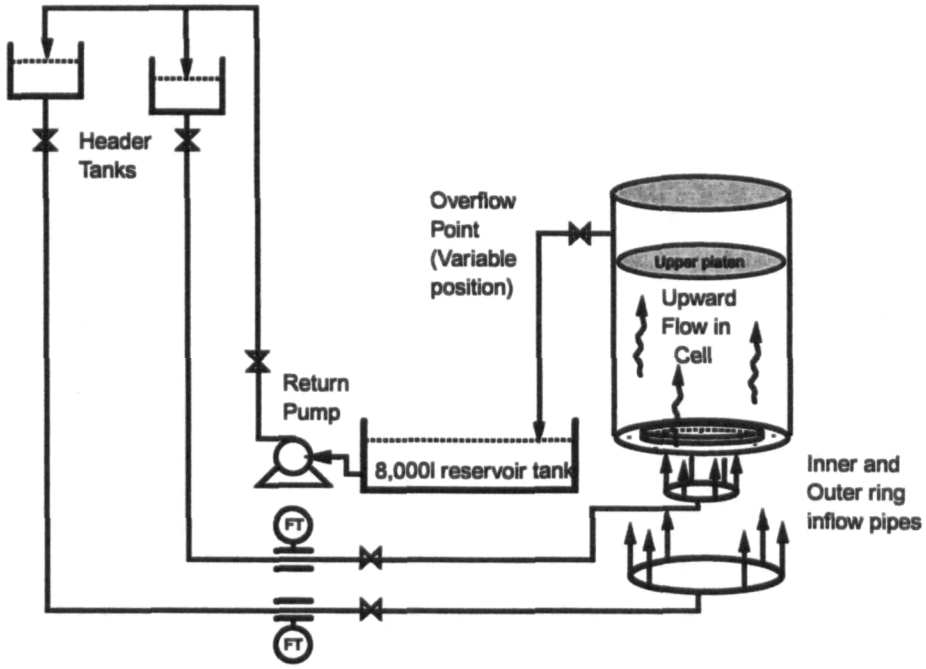

3.4.5 Operation of the Cell

A control panel (Figure 3.8) is used to regulate the hydraulic operations of the cell. The panel has a series of on/off switches which activate the hydraulic components of the system, and a number of indicator lights that show the operational status.

The panel is powered by a 110v supply and must be activated by a key operated locking system. The panel will not operate if any of the emergency stop buttons have been left on, or if any of the safety control sensors are energised (see below). After switching on, the key can be removed from the panel.

Before most of the hydraulic cylinders can be operated, the load or fast pump must be switched on. Movement of any cylinder is then accomplished by pressing the relevant button on the control panel activating a solenoid connected to a bi-directional valve which controls the flow of hydraulic oil. In general the button must be held in manually for the length of time it takes for the action to be completed. The load cylinders are an exception - an "inch hold" switch allows the button to act as an "on" switch.

Proximity limit switches are located at various positions on the compression cell to ensure that the various movements of the cell are synchronised. Unless the relevant proximity switches are activated the solenoids controlling the bi-directional hydraulic valves will not operate. For example, for the main load cylinders to operate the Tilt Up proximity switch must be activated to confirm the cylinder is in a vertical orientation,

the Ready to Load switch must be activated to confirm the Jack Up cylinders are fully retracted and the Platen Sealed switch must be on to confirm the lower platen is sealed.

Figure 3.8 Control Panel Schematic

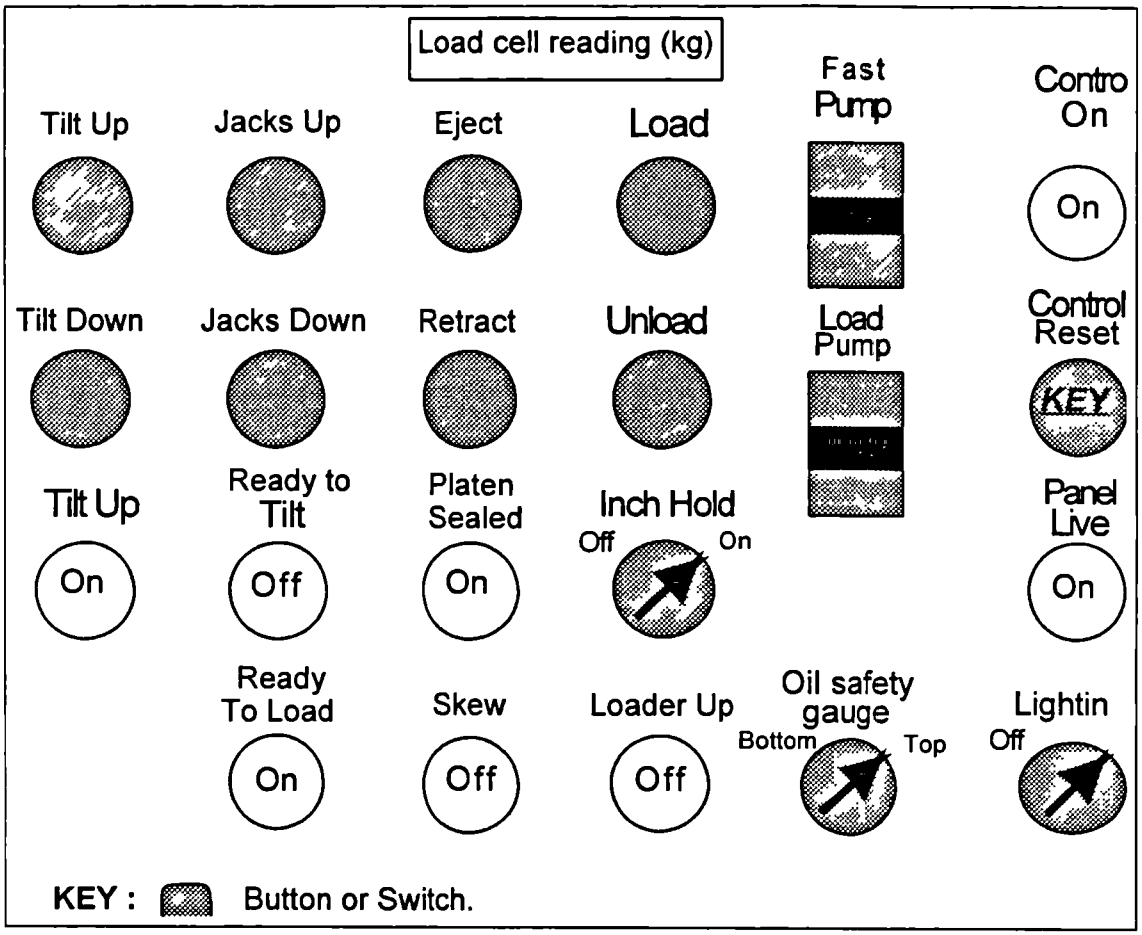

Panel settings during compression testing

The hydraulic operating pressure is controlled by two pressure relief valves (Figure 3.6) The maximum system pressure is controlled by a pre-set pressure relief valve (at 190 bar) which will regulate the pressure generated by both the Fast and Load pumps. A second variable pressure relief valve is used to control the circuit pressure (up to 190 bar) when the load pump is being used. It is this valve that controls the load applied to the waste in the cell through the upper platen.

In addition to the proximity limit switches there are a number of other safety devices that will shut down the whole panel. These are:-

1) three emergency stop buttons;

2) hydraulic oil low level sensors on the reservoir tank (in case of leaks);

3) a temperature sensor on the oil reservoir tank: (the energy put into the system to maintain high hydraulic operating pressures can cause the oil temperature to increase); and

4) a skew limit switch on the upper platen: If the upper platen tilts too much, the switch will activate.

3.5 Construction

3.5.1 Introduction

Invitations to tender for the construction of the compression cell were sent out to five companies in December 1990. Temporary planning permission to construct and locate the cell at Pitsea landfill in Essex was granted by Basildon District Council in January 1991.

A contract for the work was awarded to Sherwen Engineering Company Ltd of Mile End Green, Dartford, Kent in February 1991. The value of the contract was £67,000 + VAT. This did not include items such as ground works and the purchase and installation of ancillary pumps, flow meters and monitoring equipment for the experiment.

Sherwen Engineering Company modified and improved the design of the cell and produced detailed engineering drawings. Construction of the cell was finished by July 1991, although commissioning was not completed until October 1991 when the first tests were undertaken.

Between January 1992 and October 1995 a number of modifications were made to the cell. These were:

adaptation of the seal (which was found to leak) between the lower platen (basal plate) and the walls of the compression cylinder;

modification of the fixing points that connect the two main load pistons to the upper platen;

installation of additional piezometers and monitoring ports;

modification of the load cell weighing system; and

modification to the guides used to ensure the testing cylinder returned to the correct position when it was lowered (Jacks down) following rotation.

3.6 Monitoring systems

3.6.1 Reference systems

The measurement of hydraulic or piezometric head required an easy to use reference datum. It was decided that ground level would be used as this datum. The elevations (above datum) of all major reference and monitoring points on the cell are summarised in Table 3.5.

The volume occupied by waste in the compression cell was obtained by the position of the upper platen within the testing cylinder. The elevation of the upper platen was measured by taking readings off a 4 metre high calibrated measuring staff attached to the top of the platen. Readings were taken against a reference point situated on the underside of the top cross beam of the main support frame.

The calculated depth of waste (D) within the compression cell is given by:

$$D = 4{,}405 \text{ mm} - (A+B) - S$$

or

$$D = 3{,}477 \text{ mm} - (A+B) - S'$$

where

A+B is the total depth, in mm, of material other than refuse (e.g. the gravel drainage layers) in the cell

S is the staff reading, in mm, when set on the top of the upper platen

S' is the staff reading, in mm, when set on top of the upper platen cut out arm

Table 3.5 Reference levels of various points on the compression cell

	Height above ground level mm	Abbreviation
Compression Cell		
Bottom edge of Column	1,530	B
Top Rim of Cylinder	4,900	RM
Top Lip of Cylinder	4,980	L
Top of Lower Platen inside Cylinder	1,900	
Top of Flow Divider on Lower Platen	2,050	
Top of Floor Grill to Walkway	4,330	WK
Top of Safety Railings of Walkway	5,490	RL
Staff measurement reference point	6,340	RF
Piezometer Ports		
A1 and B1	2,200	
A1a and B1a	2,350	
A2 and B2	2,500	
A2a and B2	2,650	
A3 and B3	2,800	
A4 and B4	3,200	
A5 and B5	3,500	
A6 and B6	3,800	
A7 and B7	4,100	
A8 and B8	4,400	
Scaffold Tower		
Top of Concrete Block	2,180	CB
1st Deck (Lower)	6,340	DL
1st Deck fixing point	6,375	
2nd Deck (Upper)	8,340	DU
2nd Deck fixing point	8,375	

NOTE
Length of cut out arm on upper platen = 928 mm
Thickness of upper platen = 35 mm

3.6.2 Load cells

The purpose of the load cells was to provide an instantaneous readout of the total mass of material (waste + water) in the testing cylinder at any time. This would not only allow accurate determination of the wet and dry density of the waste in the cell, but would also provide a useful check on the flow rate measurements (i.e. how much water had been added to the cell over a period of time). It was therefore unfortunate that the load cell system gave continual problems throughout its life, reducing the reliability of this useful cross checking technique.

The original specification for the load cells was to measure the total weight of the whole compression cell and its contents to an accuracy of ±5 kgf. The overall mass of the empty compression cell was approximately 18 tonnes. It was estimated that a further 10

tonnes would be added when the testing cylinder was full of waste and/or water. During normal operation the weight of the compression cell was evenly distributed onto four mounting points, such that each load cell needed to be capable of withstanding at least a 7 tonne load.

Initially two load cells (manufactured by Thames Side, Model T90-103) were installed under two corners of the support frame with pivoted mountings under the other two. Each load cell had a capacity of 10 tonnes and an output of 2mV/V at full load. The supply voltage was 10 volts.

The combined error was specified as $<\pm 0.05\%$ of full load, or $<\pm 5$ kg, with the repeatability specified as $<\pm 0.025\%$. The cells were temperature compensated resulting in an additional error of $<\pm$ 0.008% of full load per °C, or $<\pm$ 0.8 kg per °C. However, it was not possible to be certain that the load cells ever met these specifications for the reasons outlined below.

The cells were connected to a load cell amplifier (see calibration techniques, Section 3.7.1).

Problems with the load cells

A number of problems were encountered with the load cells and these were not entirely resolved during the period of the research. It was noted that the cells did not produce stable readings and drifted over a period of time. This effect was to some extent masked by shorter term fluctuations caused by lateral wind loading on the side of the compression cell.

Two additional load cells were installed in August 1994 under the previously pivoted mounting points, and this was successful in removing the major effects of lateral wind loading. However, it did not solve the problem relating to drifting readings, although it did make the nature of the problem clearer. It was observed that the combined load cell reading could fluctuate by up to approximately 300 kg and that this was related, to some extent, to temperature changes.

A different load cell amplifier was installed and a faulty load cell identified and repaired but these actions contributed little to resolving the overall problem. It was thought that temperature induced expansion of the compression cell support frame might be applying lateral forces to the load cells, held in position in their mountings by fixing pins. These lateral forces might affect the load cell readings, but it was not possible to test this hypothesis within the timescale of the research.

These problems meant that more reliance had to be placed on other monitoring systems. For example, if water was being added to, or drained from the cell, the readout from the load cells should have provided an accurate measure of the volumes involved. This was probably the case where the measurement was undertaken over a relatively short period of time (i.e. minutes rather than hours or days). However, for longer periods of time more reliance had to be placed on the direct measurement of flow through flow meters or, for example, by the fall in the level of water in header tanks (see Section 3.6.5).

The main loss of data probably related to the long term water balance of wastes in the cell. As tests were carried out over a period of many weeks or months it was not possible to account for all water inputs and outputs to the cell (for example rainfall and evaporation) so the main way of determining the water content at any particular time was by using the load cells. Fluctuation in the load cell readings of ±150 kg would not have obscured major trends in the water content of the waste, but could have obscured more subtle changes caused by, for example, gas production in the cell.

3.6.3 Total earth pressure cells

The total vertical stress at different depths within the refuse was measured using three vibrating wire oil filled total stress cells. The cells used were manufactured by Soil Instruments Ltd (reference 6P/1.21). They had a diameter of 300 mm, a maximum thickness of 6.4 mm and an operating range of 0 to 7 bar (i.e. 0 to 700 kPa). The readout from the cells was logged manually using a vibrating wire readout unit, also manufactured by Soil Instruments.

One of the cells was installed in the lower gravel layer, and the other two installed in the middle and near the top of the waste. The cell in the gravel layer was installed within a pocket of sharp sand (approximately 50 to 75 mm thick) and the cells in the waste were installed within a pocket comprising an inner layer of vermiculite (mica) chippings and/or an outer layer of sand.

The use and correction of the data produced by the total stress cells is discussed in Sections 3.7.2 and 6.4.

3.6.4 Differential compression

In addition to measuring the total compression (Section 3.6.1) attempts were made in some experiments to measure the compression at different levels within the waste using the two vertical lines of piezometer ports in the side of the test cell. In general, compression was undertaken on waste which had previously been allowed to drain freely

under the influence of gravity. This meant that it was possible to undo the piezometer ports during compression without there being too significant a loss of leachate.

Strings were inserted through each piezometer port and wedged into the refuse at the level of the base of the port. Downward displacement of the refuse at the location of the port was translated into a reduction in the length of the string remaining outside the compression cell (Figure 3.9).

Figure 3.9 **Insertion of strings into refuse through piezometer ports to measure differential compression**

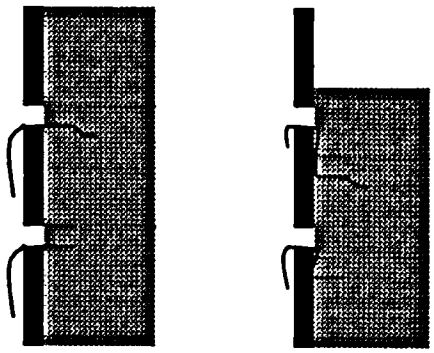

In practice this system had a number of problems. The main problem related to the fixing of the strings into the refuse in a way that prevented them from working loose. In addition, if the string was not inserted at the very bottom of the piezometer port the initial downward movement of the refuse would result in a lengthening of the string. These problems were compounded by the general difficulty of measuring the strings, especially during periods of inclement or windy weather.

3.6.5 Water flow rates and quantities

A number of methods were used to monitor the flow and volume of water passing into or out of the compression cell. The method used depended on the actual flow rate encountered during a test.

Three electromagnetic flow meters with totalisers (model Discomag 6531) were obtained from Endress & Hauser Ltd (Appendix A). The meters had a nominal bore of 25 mm and were suitable for measuring flow rates in the range of approximately 0.25 l/s to 2.5 l/s (15 l/min to 150 l/min).

In general, two of the meters were connected into the pipework leading to the inner and outer ring of the lower platen (see Section 3.4.4 and Figure 3.7). This allowed the

volume and flow rate of water passing into or draining from the compression cell to be monitored. The remaining meter was usually only used during constant head hydraulic conductivity tests and was connected to the pipework taking the combined return flow from above the upper platen.

At flow rates less than approximately 0.25 l/s, alternative monitoring systems were used. When only the volume of water added to, or drained from the waste was required, this was obtained from the direct measurement of the loss of water from header tanks, or the addition of water to collection tanks. Alternatively, the change in the total mass of the waste in the cell (i.e. the change in the water content) could be obtained using the load cells.

When flow rates were required these changes in volume (or mass) were measured over a set period of time.

3.6.6 Piezometric heads

The accurate measurement of piezometric head within the compression cell was a critical part of the monitoring undertaken. Changes in leachate levels were used to determine effective porosity, and measurement of hydraulic gradients was required to determine hydraulic conductivity.

Piezometers were installed into the waste by inserting lengths of 12 mm diameter nylon tubing through the piezometer ports. The last 50 to 100 mm of the nylon tube was perforated with approximately 2 to 4 mm diameter holes to increase the open area available for fluid flow. Piezometer tubes were inserted to a horizontal distance of approximately 500 to 750 mm from the line of A ports, and to a distance of between 100 and 200 mm from the line of B Ports (see Figure 3.3). A searcher bar (15 mm diameter metal rod) was used to pre-drill a hole prior to inserting the nylon tube itself. This tended to become increasingly difficult as the waste became more compacted at higher applied loads.

Cable glands fitted into the piezometer ports were used to create a water tight seal around the tubes leading into the waste. The horizontal piezometer tube was turned through 90°, by an elbow compression fitting, to connect to vertical tubes running in cable ducts up each side of the compression cell. Measurement of hydraulic head within these tubes was made against tapes that were related to the reference datum (i.e. ground level - Section 3.6.1). Any air or gas bubbles collecting in the piezometer tubes were removed prior to measurements being taken. It was sometimes necessary to add a coloured dye to the liquid in the tubes for the purpose of clarity.

3.7 Calibration techniques

3.7.1 Load cells

The load cells were calibrated by filling the test cylinder with a known volume of water. The total volume of the testing cylinder was approximately 9.4 m^3 (π m^2 x 3 m), which when filled with water, gave a calibration weight of approximately 9 tonnes. This exceeded the anticipated maximum weight of refuse that would be used in the tests.

The depth of water within the cell could be measured to an accuracy of approximately ±2 mm which meant that the overall accuracy of the calibration weight was better than ± 0.1%:

Total mass of water used in calibration:	~ 9,000 kg
Depth of water measured to:	± 2 mm
Volume of water measured to:	± 6.28 litres
Error	± 6 kg
Calibration Accuracy	± 6 kg/ 9,000 kg = ± 0.07%

After calibration a further correction had to be made to the load cell reading depending on the elevation of the upper platen. The amount of hydraulic oil in the main load cylinders increased during testing as the waste compressed and the cylinder rods extended.

Volume of both 200 mm (8") rods:

$$V = 2 \times \pi \frac{0.2^2}{4} \times E, \quad \text{where E is the extension of the rod in metres}$$

$$V = 62.8 \text{ litres per metre of rod extension.}$$

Taking the density of hydraulic oil as 0.87 t/m^3 the required correction to the load cell reading is approximately 55 kg per metre of rod extension. A slightly higher correction of 60 kg per metre of rod extension was determined experimentally (Figure 3.10) and this correction factor was subsequently applied to all data collected. The position of the platen was related to the measuring staff readings (see Section 3.6.1), such that:-

For S readings

Correction = - (S - 915mm) x 0.060 kg

For S' readings

Correction = - (S' + 13 mm) x 0.060 kg

Figure 3.10 The effect of the elevation of the upper platen depth on load cell readout

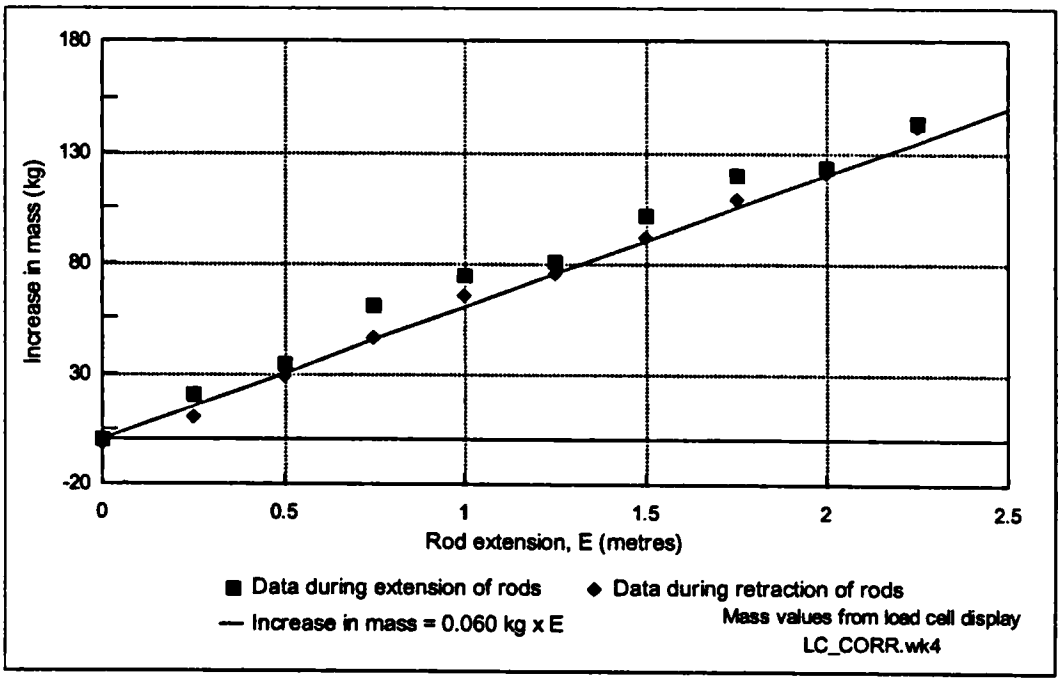

3.7.2 Earth pressure cells

The output (in period units) from the vibrating wire earth pressure cells was calibrated in a pressurised water tank by the manufacturer, Soil Instruments Ltd. The calibration constants were programmed into the vibrating wire readout unit to give a reading in kPa. The cells were usually sent back for re-calibration after each set of tests.

Although accurate results would be expected from cells if installed in a fluid, additional corrections are usually required when earth pressure cells are inserted in a soil; the presence of the cell in the soil alters the stress field in its vicinity, leading to misleading results.

Many authors have attempted to quantify the necessary correction factors that should be applied to the readings from earth pressure cells in a variety of settings (e.g. Taylor, 1947; Tory and Sparrow, 1967; Shad, 1989.) . The main factors that influence the readings are:-

- the dimensions of the pressure cell;
- the relative stiffness of the soil and the cell;
- the void ratio and particle size of the soil; and

- the direction of the applied stress relative to cell orientation.

The important factor relating to the dimension of the cell is its aspect ratio, defined as the ratio of the thickness of the cell to its diameter. Taylor (1947) suggested that when a cell is introduced into a soil it results in an over-reading of the stress field. Peattie and Sparrow (1954) proposed that the cell over-read was related to the aspect ratio: cells with a large aspect ratio would over-read more than cells with a low aspect ratio.

The aspect ratio of a cell is not the only physical property of the cell which influences the correction factor. Whereas the inclusion of a stiff body into a soil will lead to an over-reading of the stress field, deflection of the acting face of the cell can lead to stress relief and a potential under-reading. The significance of any deflection is related to the relative stiffnesses of the soil and cell. Tory and Sparrow (1967) proposed a flexibility factor, F, for cell designs comprising a diaphragm mounted on a stiff peripheral ring.

$$F = \frac{E_{soil}.D^3}{E_{cell}.t^3} \qquad (3.1)$$

where E_{soil} is the Young's modulus of the soil
E_{cell} is the Young's modulus of the cell material
D is the diameter of the cell
t is the thickness of the diaphragm

Tory and Sparrow (1967) produced curves of cell error for various combinations of flexibility factors and aspect ratios (Figure 3.11). It can be seen that cells with a low aspect ratio (<0.1) and a flexibility factor below approximately 2, accurately record the stress field (i.e. ± 5%). As the flexibility factor increases, cells with a low aspect ratio progressively under-read the actual stress field.

These results strictly apply to diaphragm type earth pressure cells, with two parallel plates oriented perpendicular to the direction of stress measurement. However, the vibrating wire pressure cells used were oblate; the thickness of the cells increased from 3 mm at the circumference of the cell (where the two plates were welded together) to 6.4 mm in the centre of the cells.

With a diameter of 300 mm the aspect ratio of the cells is 0.02. This low aspect ratio suggests that the cells will not over-read stress (to within 5%) and that the only possible significant error is an under-read. It is not considered appropriate to calculate a flexibility factor for the cells (because of the different nature of the cell design) and

therefore it is not possible to quantify the magnitude of any under read by the method of Tory and Sparrow (1967). However, it is noted that the magnitude of any under-read is related to the stiffness of the material in which the pressure cell is embedded, and if the stiffness of that material changes (for example as a consequence of increasing applied stress) then the correction factor will also change.

Figure 3.11 Variation of cell error with flexibility factor

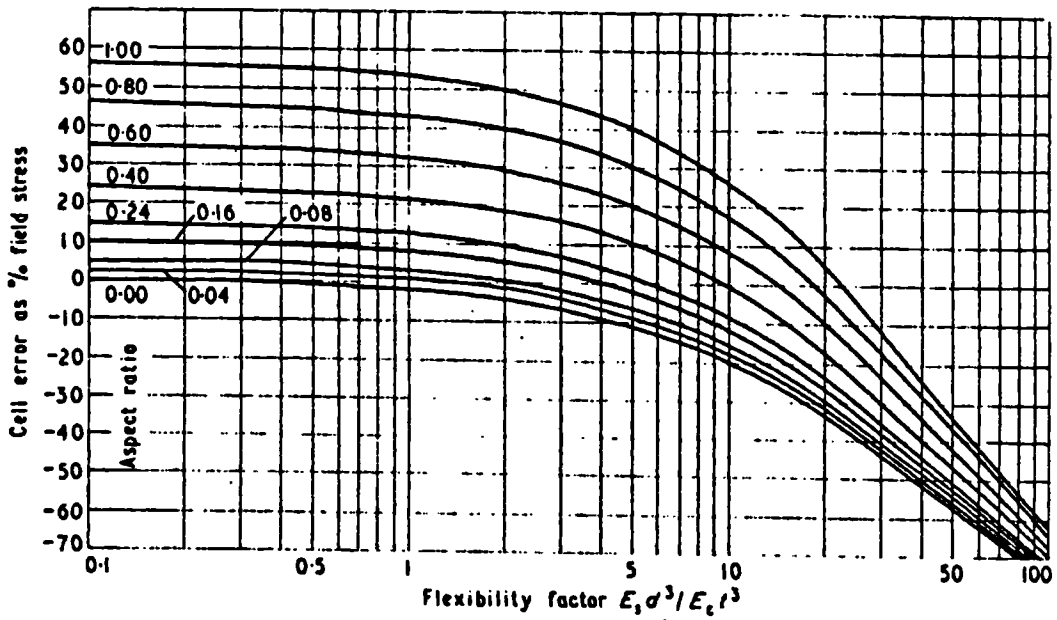

Source: Tory and Sparrow (1967)

Taylor (1947) considered the effect of soil void ratio and particle size on total stress readings in experiments on sands and concluded that they were only important in extreme circumstances. Clayton and Bica (1993) also concluded that fine grained soils with high void ratios had very little effect on stress measurements.

It has been suggested that the diameter of the pressure cell (or diaphragm) should be a minimum of 50 times the dimensions of the largest particle in the soil, and that individual large particles should be kept away from the pressure cell face (Shad, 1989; Clayton and Bica, 1993). With an average particle size of approximately 100 mm for household waste (Jessberger and Kockel, 1991), the first of these requirement was impossible to achieve. The installation of the pressure cells in pockets of vermiculite chippings and/or sand (Section 4.3.3) would have prevented individual particles from coming into contact with the pressure cells and would have distributed the stress field more evenly across the cell.

As it was neither possible to quantify the effect of these factors on the recorded stress, nor calculate flexibility factors, a direct calibration of the pressure cells was attempted. The calibration was only undertaken for a pressure cell installed in gravel. This would allow a correction to be applied to the stress recorded in the lower gravel layer, making it possible (in combination with the stress applied through the upper platen) to calculate an average stress in the waste.

The pressure cell was installed in sand and gravel layers in a 490 mm ID testing rig as shown in Figure 3.12. The overall depth of material in the cell was 150mm, giving a diameter to depth ratio of approximately 3.25:1 (i.e. sidewall friction effects were negligible). A stress was applied through a top plate and the corresponding stress recorded by the pressure cell recorded. Figure 3.13 shows that earth pressure cell over reads the actual applied stress by approximately 17%.

Figure 3.12 Calibration of total pressure cells in gravel

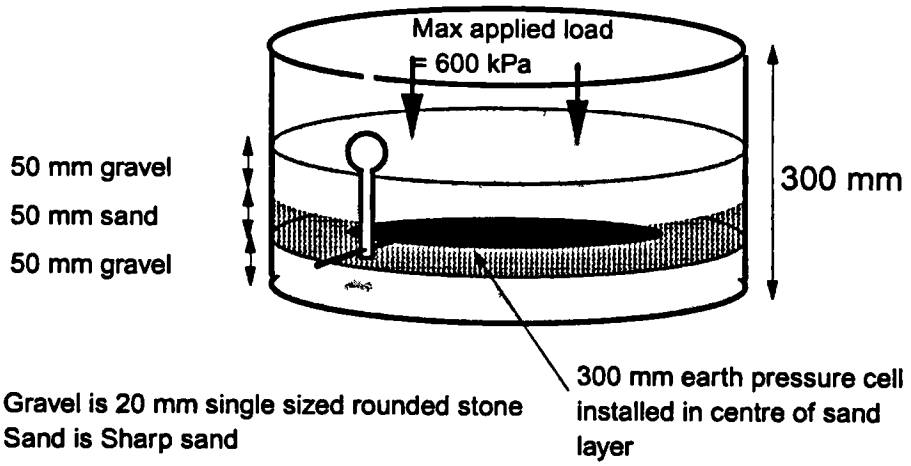

Figure 3.13 Calibration results of earth pressure cell installed in gravel

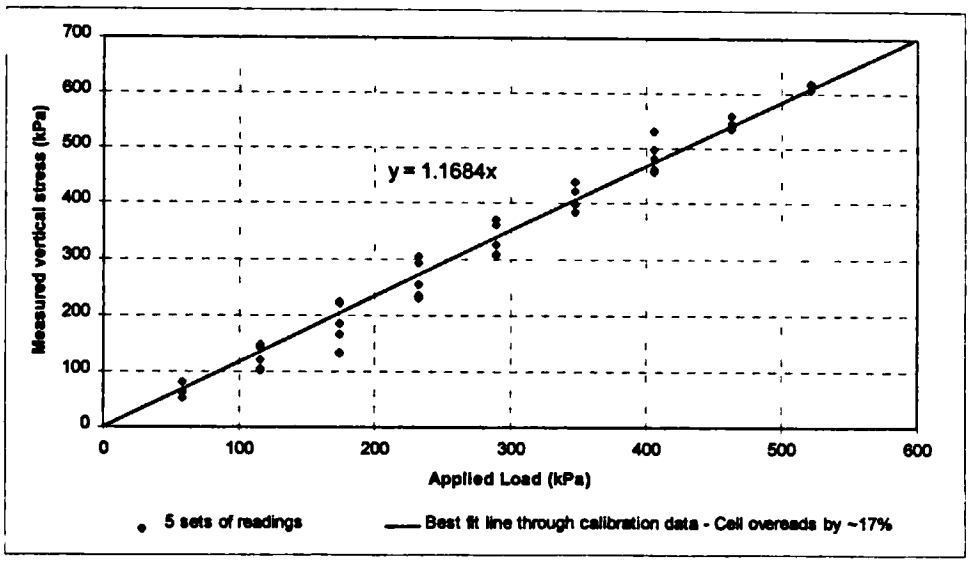

3.7.3 Flow meters

The electromagnetic flow meters were calibrated in the factory by the manufacturers. Their accuracy was confirmed during the process of filling the compression cell with water; the volume was calculated by measuring the depth of water in the cell and this compared favourably with the totaliser reading of the meters.

Chapter 4

Testing Methodology

4.1 Summary

In this Chapter the methodologies used in the compression tests on various types of household waste are outlined. The method of material classification is described, together with the protocol for loading the waste into the compression cell. The methodologies used to determine the absorptive capacity, effective porosity and hydraulic conductivity at various applied loads are also included.

4.2 Introduction

The experimental programme using the Pitsea compression cell lasted for more than four years and inevitably the testing methods and protocols evolved over this time. The methodologies described below represent the general practice adopted for the majority of tests. Where there were any significant changes to the practices used in a particular test this is highlighted with the relevant results in Chapter 5.

4.3 Testing Methodology

4.3.1 Sample selection

Tests were undertaken on three different types of household waste. The first was crude or unprocessed waste, which forms the majority of household waste landfilled in the UK. The second was pulverised or processed waste. This was chosen because the landfilling of shredded waste has been advocated as a way of speeding up the microbiological stabilisation (i.e. degradation) of landfills. The use of shredded waste could be an important component of sustainable landfill practice. In addition large quantities of pulverised waste were landfilled in the 1960s and 1970s so that the hydrogeological properties of many existing sites may be largely controlled by this type of waste. The last type investigated was aged and partially degraded waste excavated from a landfill. This type was chosen to provide an indication of how the properties of waste may change following degradation in a landfill.

4.3.2 Waste characterisation

Full physical classifications were made of the wastes tested. These classifications were initially undertaken at Warren Spring Laboratory and then, latterly, at AEA Technology Harwell, when the material recovery unit which undertook the work moved.

The samples were sorted and analysed according to a procedure described by Poll (1988). The waste was passed over a number of screens to grade the samples by size. The waste was then hand sorted into 11 material categories (e.g. paper, plastics, textiles etc.) to produce a matrix classification based on size and component. Results were reported in terms of proportion by as received weight.

The bulk water content of the waste was also determined.

4.3.3 Loading of waste into compression cell

The placing of waste into the compression cell prior to the start of a set of tests was a major task. The following steps were usually taken:

1) All hydraulically controlled movements of the compression cell were tested and the lower platen seal checked to ensure it was water tight.

2) Plastic mesh (~ 1cm mesh size) was placed over the ports in the lower platen prior to the placement of a layer of 10-20 mm gravel. The gravel was required to facilitate the even distribution of water from the ports to the lower layers of refuse.

The depth of the gravel layer varied from 150 mm to 200 mm. The weight of gravel added to the cell was recorded using the load cells.

3) A total earth pressure cell was installed horizontally in a central position in the lower gravel layer. The cell was installed within a pocket of sand. The cable from the cell was passed through a cable gland installed in one of the ports on the lower platen. The cable from a second total stress cell was passed through another cable gland on the lower platen in preparation for installing the stress cell into the middle of the refuse.

4) Waste was loaded into the compression cell using a lorry mounted hydraulic grab. Sub-samples of the refuse were taken during the filling process for size and material classification (see section 4.3.2). The cell was rotated, without disturbing the gravel layer, to an angle of approximately 30° to the vertical to allow waste to be placed into the top of the cell. The refuse was loosely placed in the cell and every so often the cell was returned to an upright position and the refuse raked level. In this way the cell would be filled with refuse to a depth of approximately 2.5 metres. At this point, with the cell returned to an upright position the weight of refuse in the cell was recorded.

5) A second earth pressure cell was installed in a horizontal plane near the top of the waste in the cell. The cell's cable, already installed through a gland in the lower platen (see 3 above), was pulled tight.

6) The upper platen was used to compact the waste lightly. Two procedures were adopted: either the refuse was packed to a specified starting *in situ* density (e.g. ~ 0.5 t/m^3 for crude domestic waste) or the waste was compacted using the lowest possible operational pressure (~5 bar) in the hydraulic circuit, which equates to an applied load of approximately 25 kPa. In either case the final packed bulk density of the refuse was calculated as the ratio of the mass of refuse at its original water content to the volume occupied in the compression cell. Usually the depth of refuse in the cell at this stage was slightly over 1 metre. This means that the effects of sidewall friction should have been relatively low (refer to Table 3.1) and that a reasonably even packing density would have been achieved.

7) Further waste was added to the cell, raked level and then compressed to achieve the overall initial packing density as determined in 6) above. This was undertaken a number of times until it was no longer possible to place any more refuse in the compression cell. In practice a total depth of refuse of approximately 2.5 metres was achievable.

8) The final weight of refuse in the cell was determined using the load cell readout when the cell had been returned to an upright position. The original bulk density of the waste in the cell was calculated. The water content of the subsamples sent for material classification was used to calculate the mass of dry solids in the cell and the dry density.

9) The final earth pressure cell was installed in a horizontal plane near the top of the refuse in the cell. The cable from the pressure cell was passed out through a port in the upper platen.

10) A final 150 mm to 200 mm layer of 10 to 20 mm gravel was placed on top of the waste.

The refuse in the cell was now ready for testing.

4.3.4 General testing methodology

The general principle of testing was that a constant load be applied to the refuse through the upper platen and the consequent compression of the waste be monitored. After all compression had ceased a series of tests was carried out to determine the hydrogeological properties of the waste- principally hydraulic conductivity and effective porosity. In addition, data on the absorptive capacity of the waste and its water content at field capacity was also generated. The waste was then drained prior to the applied load being increased, compression monitored and the hydrogeological properties determined. This cycle of increasing the applied load was generally repeated up to 5 times, until a maximum applied load of 603 kPa had been achieved. The general increments of loading used are given in Table 4.1

Table 4.1 Increments of applied load used in compression tests

Hydraulic Operating Pressure **Bars**	Applied Load **kPa**	Waste type where increment of applied load was used
10	40	DM1-3, PV1-2, AG1
25	87	DM2-3, PV1-2, AG1
50	165	DM1-3, PV1-2, AG1
100	322	DM1-3, PV1-2, AG1
(150)	(478)	PV1
190	603	DM2-3, PV1-2, AG1

See Table 5.1 for description of waste types

The detailed methodology used for each type of test is outlined below.

4.3.5 Compression tests

Compression tests were undertaken by increasing the load applied to the top of the waste through the upper platen. Generally, compression would be undertaken on waste that was at field capacity, following the end of a set of saturation tests.

Bulk compression of the waste in the cell was monitored as a function of time by measuring the downward movement of the upper platen. Measurements were taken manually from a vertical measuring staff attached to the upper platen. The vertical movement of the platen was measured to an accuracy of ± 0.5 mm. The frequency of monitoring was reduced as the test progressed and the rate of compression reduced. Initially, at the start of the compression test readings were taken every 10 to 15 seconds, but this rapidly reduced to perhaps one reading every hour by the end of the first day. Thereafter the taking of only one or two readings a day was sufficient to monitor compression accurately.

The applied load was maintained until compression had ceased. For practical purposes this was taken to be when the rate of change of refuse depth had fallen to less than 1% in 24 hours. This normally took between 2 and 7 days.

Readings from the three vibrating wire earth pressure cells were recorded manually at intervals during the period of the test.

The average dry density at the end of compression was calculated using the original mass of dry solids in the cell. The average wet density of the waste was calculated using the load cell output to determine the bulk mass of waste in the cell. There may have been some errors in this measurement bearing in mind the problems experienced with the load cells (see below and Section 3.6.2).

Leachate squeezed out of the refuse was collected and its volume recorded. However, in practice it was difficult to collect all of the displaced leachate as it tended to seep out of the piezometer ports which were being used to measure differential compression.

Differential compression was measured within the waste by means of lengths of string secured at various heights in the refuse through the piezometer ports. The vertical movement of waste at each piezometer port was indicated by the reduction in the length of string outside the port. New strings were inserted into the refuse at the start of each compression stage.

At the end of each compression stage, prior to the start of any hydrogeological tests, the cell was made watertight. Piezometer tubes were installed at various heights into the refuse through the piezometer ports and any ports not in use were blanked off.

Errors in density measurements

Volume of waste in cell

	Measuring staff readings recorded to accuracy of	±1 mm
	Depth of waste generally	> 1,000mm
⇒	Error in determining waste volume	< ±1%

Initial mass of waste in cell

	Maximum (short term) fluctuations in load cell readings	±50 kg
	Mass of waste loaded into compression cell	~2,500 to 6,500 kg
⇒	Error in initial mass of waste in cell	<±0.75 to 2%

Initial water content of waste (laboratory determination)

	Error estimated to be	<±5% (of value)

Initial mass of dry solids

	(Mass of waste in cell) x (1-water content)	
⇒	Error	<± 6 to 7%

Dry density

	(Mass of dry solids) / (Volume of waste)	
⇒	Error	<± 7 to 8%

Bulk mass of waste in compression cell

	Maximum (long term) fluctuations in load cell readings	<±150 kg
	Mass of waste (at field capacity) in compression cell	~ 3,000 to 6,500 kg
⇒	Error in wet mass of waste in cell	<±2 to 5%

Wet density

	(Bulk mass of waste) / (Volume of waste)	
⇒	Error in bulk density	<±3 to 6%

4.3.6 Absorptive capacity and water content at field capacity

Absorptive capacity could only be determined once during each set of tests on a particular type of waste. This was either at the original placement density, or at the density achieved after the first compression stage at an applied stress of 40 kPa.

The absorptive capacity was determined by saturating and then draining the waste to field capacity. Water was passed into the bottom of the compression cell through the

lower platen. The piezometers were used to monitor the increase in leachate head within the cell before the waste was drained, again through the lower platen.

The difference between the volume of water added to saturate the refuse and the volume removed during drainage was used to determine the absorptive capacity.

The water content of the waste at field capacity was determined from the wet weight of the refuse, which, for the majority of tests, was obtained from the load cells. This could be determined whenever the waste in the cell had been drained to field capacity

4.3.7 Effective porosity

The effective porosity of the waste was determined whilst the applied load on the waste was maintained. Small increments of water were introduced into, or drained from the cell and the resulting change in hydrostatic head in the waste was measured. The water was introduced or drained through the lower platen and the piezometers up the side of the cell were used to measure piezometric head.

The volume of water added (or drained) in an increment was measured using either the electromagnetic flow recorders or by direct measurement from the header tanks. A further check on this volume was given by the load cell readings.

In general, piezometric levels were allowed to stabilise before readings were taken. However, during some tests at high applied stresses the low permeability of the waste meant that this was not possible. Furthermore, it was sometimes not possible to remove the accumulation of gas in some piezometer tubes, thus preventing true piezometric readings from being taken.

The cumulative volume (V) of water added (or drained) was plotted against hydrostatic leachate head (h), to indicate the level to which the waste in the cell had become saturated. The slope of the line (S) through these data points at any particular elevation within the waste is directly related to the drainable porosity.

$$S = \frac{\Delta V \text{ (litres)}}{\Delta h \text{ (mm)}}$$

$$n_e = \frac{\Delta \text{ volume of water added}}{\Delta \text{ volume of waste saturated}} = \frac{\Delta V \times 100\%}{\Delta h.\pi.r^2}$$

(r = radius of compression cell = 1m)

$$n_e = \frac{S}{\pi} \times 100\%$$

Errors in effective porosity measurements

The estimated errors in the calculated effective porosity varied. The errors were smaller at lower applied stresses (with lower waste densities and higher permeabilities) than at higher applied stresses.

Low applied stress

At lower applied stresses the volume of water added to the waste was measured using the flow meters. Water levels return to hydrostatic conditions rapidly after a volume of water had been added.

Error in volume of water added	<±5%
Depth of saturated zone measured to	<±50 mm in overall depth of approximately 1,000mm
Error in change in saturated volume	<±5%
Error in effective porosity at low applied stresses	<±10% (of value)

High applied stresses

At higher applied stresses the rate at which water entered into, or drained from the waste reduced to below the operational range of the flow meters. The change in volume was either determined from the load cell readings or by direct measurement of flow into or out of leachate tanks. It was more difficult to achieve hydrostatic conditions in the waste, especially during draining. The errors relating to the change in saturated volume are correspondingly higher.

Estimated error in volume of water added (load cells)	<±20%
Estimated error in volume of water added (direct measurement)	<±5%
Estimated error in change in saturated volume	<±50%
Error in effective porosity at high applied stresses	<±80%

Although the effective porosity error is high it tended to apply to effective porosity values, n_e, below 2% (see Chapter 5). Therefore, the estimated maximum absolute error (of approximately 1.6%) in effective porosity at high applied stresses is similar to the absolute error in effective porosity at low applied stress, where a typical value of n_e might be in the range of 10 to 15% (see Table 5.20).

4.3.8 Constant head hydraulic conductivity tests

Hydraulic conductivity was generally determined by means of a constant head test undertaken whilst a given applied vertical stress was maintained on the refuse in the cell. Tests lasted from one or two hours up to several days. Water from header tanks, located on a scaffold tower at an elevation of 8.9 metres above datum (7 metres above the base

of the waste), was fed into the cell through the bottom platen. A constant head was maintained in the header tanks, at the level of an overflow pipe, by continually pumping leachate into the tanks. Water on entering the cell was allowed to pass upwards through the waste to the level of an overflow port situated above the position of the upper platen.

The flow rate into (and generally out of) the waste was measured using the electromagnetic flow meters. At high vertical stresses and low refuse permeability the flow rate of water into the column was small, and flow rates were measured by turning off the leachate feed into the tanks and directly measuring the drop in head in the tanks over a set period of time. During this process the head could drop by up to 0.5 metres. In a few tests the water flowing out of the waste was not removed at a constant head from an overflow pipe, but was allowed to build up on top of the upper platen within the 2-metre diameter compression cell. This generally occurred when the rate of flow through the waste was relatively low (below ~ 5 litres/minute), which meant that the head increased at a rate that was generally less than 0.1 metres per hour.

The hydraulic conductivity was determined by the application of Darcy's Law:-

$$K = \frac{Q}{i.A}$$ where Q = Flow rate; i = Hydraulic gradient; A = Cross sectional area (π m^2).

The vertical hydraulic gradient (i) in the waste was determined from readings of head taken from the piezometers up the side of the column. The piezometric head (in mm AD) was plotted against the elevation (in mm AD) of the respective piezometer; the slope of the line (Δhead/Δelevation) at any particular elevation within the waste is the hydraulic gradient. Successive readings of flow rate and gradient were taken until stable conditions became established.

Errors in hydraulic conductivity measurements (constant head method)

The potential errors in the hydraulic conductivity measurements increased with increasing applied stress as the flow rates through the waste reduced. The errors were related to a reduced accuracy in the measurement of flow rates and an increased uncertainty about the effect of preferential peripheral flow up the sides of the testing cylinder. Daniels (1994) undertook a comprehensive review of laboratory hydraulic conductivity tests, including those carried out in fixed wall permeameters. It was recognised that sidewall flow can occur in any rigid-wall permeameter, because a greater percentage of macropores exist near the perimeter of the test specimen. It was considered that the potential error was greatest for low hydraulic conductivity materials.

However, it was also concluded that sidewall leakage is rarely a problem for compressible soils that have been subjected to stresses of at least 50 kPa.

Figure 4.1 shows waste DM3 being ejected from the compression cell after being subjected to an applied load of over 600 kPa. The edge of the waste, where it had been in contact with the wall of the testing cylinder is clearly visible. Although the structure of the waste shows evidence of partings in a plane perpendicular to the applied load, the edge is generally very smooth. The compressible nature of the waste meant that it had been pressed tight up against the cylinder wall.

It was considered that the potential errors in hydraulic conductivity measurements caused by sidewall flow were negligible at low effective stresses (where there were relatively large macropores in the waste resulting in high hydraulic conductivities). For the reasons discussed above errors in hydraulic conductivity measurements may be greater at high effective stresses (and lower hydraulic conductivities) but because of the relatively compressible nature of the wastes tested it was considered unlikely that peripheral flow was a major factor in the experiments. However, it was not possible to verify this assertion by any direct measurement of peripheral flow during the course of this research. Consequently, solely for the purpose of plotting error bars on graphs of hydraulic conductivity versus stress, it was assumed that the hydraulic conductivity may have been overestimated by a maximum of 50% at high effective stresses.

Figure 4.1 Extrusion of waste DM3 from the compression cell

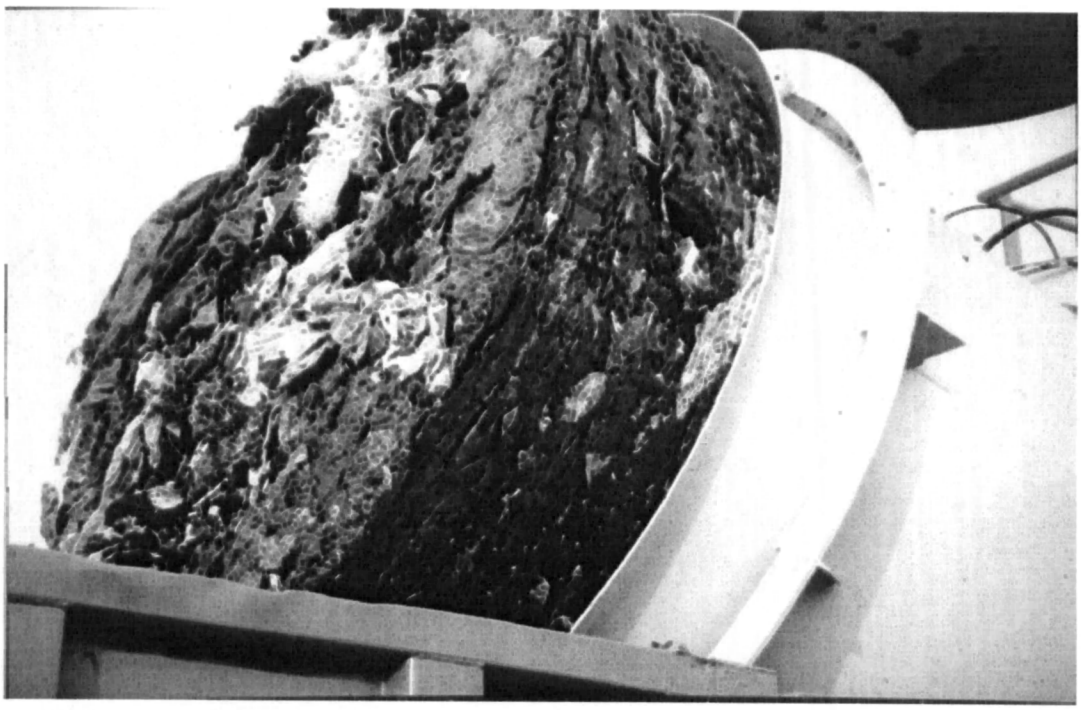

Further work is required to quantify the actual effect of peripheral flow on hydraulic conductivity measurements. The compression cell includes facilities to separate and measure the flows from an inner core and outer annulus of waste (each with the same cross sectional area). However, during the course of the research attempts to develop a suitable experimental technique taking benefit of these facilities were not successful.

Low applied stresses

At low applied stresses the flow rate through the waste was measured by the flow meters.

Estimated error in flow rates	$\leq \pm$ 5%
Estimated error in hydraulic gradient	$\leq \pm$ 5%
Estimated error caused by peripheral flow	0%
Estimated error in hydraulic conductivity measurement at low applied stresses	$\leq \pm$ 10%

High applied stresses

At high applied stresses the flow rate was determined by the direct measurement of the volume of water lost from the header tanks over a set period time. Although this method was generally as accurate as taking measurements by flow meters, at flow rates below approximately 0.1 litres/minute (which indicated a hydraulic conductivity below $1x10^{-7}$ m/s) the potential errors increased. Firstly, any leak in the pipework system (slight leaks at joints were difficult to stop) started to become significant and, secondly, limitations in the length of time that the test could be run meant there was some question as to whether the flow had reached equilibrium.

Estimated error in flow rates	$\leq \pm$ 20%
Estimated error in hydraulic gradient	$\leq \pm$ 5%
Estimated error caused by peripheral flow	$<$ - 50%
Estimated error in hydraulic conductivity at high applied stresses	$<$ + 30% $<$ - 80%

4.3.9 Falling head hydraulic conductivity test

This test was carried out on waste PV2 at an applied stress of 603 kPa because the rate of flow of water passing into the waste was exceedingly low and a constant head test was not practicable. The test was undertaken by measuring the fall in head within the leachate supply hose to the bottom platen (see Figure 4.2). The depth of the saturated zone (L) was obtained from piezometers installed at varying depths in the waste. Piezometers at the base of the waste registered a water level; the piezometer at the lowest level, which did not register a water level, was taken to represent the start of the unsaturated zone.

Errors in hydraulic conductivity measurements (falling head method)

As a falling head test was used on only one occasion, the errors relating to that test are considered with the results (Section 5.7.10).

Figure 4.2 Schematic representation of falling head hydraulic conductivity test

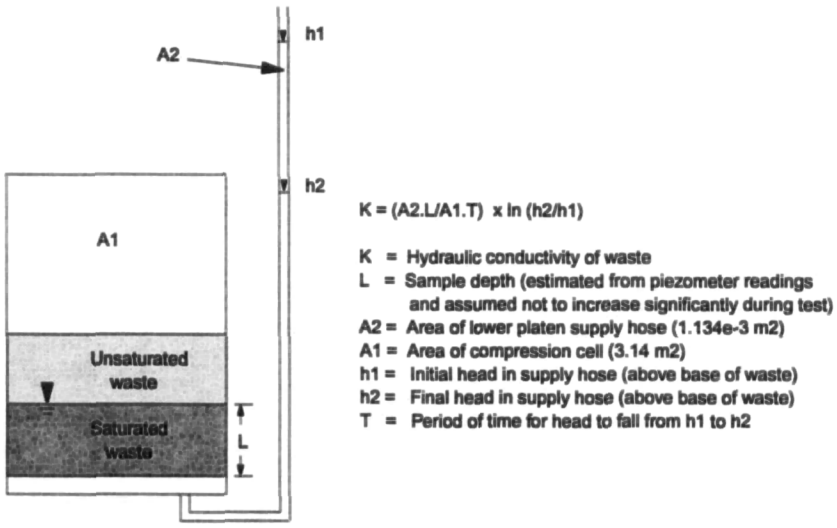

Chapter 5

Results

5.1 Summary

Results from compression tests on three different types of waste (crude, pulverised and aged household wastes) are presented. Each waste type was characterised in terms of its composition, initial water content and the density at which it was placed in the compression cell.

The waste was subjected to an applied load which was increased, in stages, to a maximum of 603 kPa. At each increment of applied load the average density, water content, effective porosity and vertical hydraulic conductivity was determined. These results, together with data on the transmission of total vertical stress and differential compression, are presented in this Chapter.

5.2 Introduction

Three general types of household waste were tested within the compression cell as follows:

1) Crude, unprocessed fresh household waste

2) Pulverised and processed shredded waste

3) Aged, partially degraded waste excavated from a landfill.

Overall, six individual series of tests were undertaken on these wastes. A summary of the tests undertaken and the test codes allocated is given in Table 5.1.

Results for each series of tests are presented in turn, as follows-

Section 5.3 Test code DM1	Crude waste
Section 5.4 Test code DM2	Crude waste
Section 5.5 Test code DM3	Crude waste
Section 5.6 Test code PV1	Pulverised (processed) waste
Section 5.7 Test code PV2	Pulverised (processed) waste
Section 5.8 Test code AG1	Partially degraded waste.

Table 5.1 Summary of materials tested and test codes

Refuse / Test Reference	Description
DM1	Crude domestic refuse obtained direct from tipping face of landfill in October 1991. Compression tests undertaken at original 'as placed' water content. Water content at start of compression ~51% (dry weight)
DM2	Crude domestic refuse as used in DM1. Original waste emptied from compression cell and reused. Compression tests undertaken after refuse brought up to field capacity by fully saturating and draining refuse. Water content at start of compression ~ 112% (dry weight).
DM3	Crude domestic refuse obtained direct from tipping face of landfill in February 1995. Compression tests undertaken after refuse brought up to field capacity by fully saturating and draining refuse. Water content at start of compression ~102% (dry weight). Drainable porosity and permeability determined when compression stopped at the end of each stress increment.
PV1	Processed (pulverised) refuse. Crude domestic refuse pulverised and passed through a 150-mm filter. Heavy fines (including some putrescibles) removed . Compression tests undertaken after refuse brought up to field capacity by fully saturating and draining refuse. Water content at start of compression ~ 141% (dry weight). Drainable porosity and permeability determined when compression stopped at the end of each stress increment.
PV2	Processed (pulverised) refuse as used in PV1. The waste had been stored in a covered skip for a period of 12 months. Compression tests undertaken at original 'as placed ' water content. Water content at start of compression ~ 66% (dry weight).
AG1	Aged municipal solid waste (MSW) obtained from Rainham landfill, Essex in July 1995. The waste dated from the late 1960's and contained a mixture of soil, crude MSW and pulverised MSW.

The various data sets collected are presented in each section. No attempt is made to compare results in this Chapter, but a summary of all data is presented in Section 5.9.

5.3 Crude household waste (Test series DM1)

Crude household waste was tested in the compression cell between October 1991 and January 1992 and was designated a test code DM1. A compression test in which the applied stress was increased in stages was carried out on the waste at its original water content. No tests to determine the hydrogeological properties of the waste were carried out. After completion the waste was ejected from the cell into a skip, where it was re-used for test series DM2 (Section 5.4).

5.3.1 Waste source

The material used in the test was crude household waste. It was obtained directly from Basildon District Council refuse collection vehicles as they discharged their loads at the tipping face of Pitsea landfill site on 21st October 1991. Approximately 10 tonnes of refuse was collected from 7 or 8 vehicles using a lorry equipped with a hydraulically operated grab. The waste was placed on an area of hardstanding and samples taken from different positions to mix the waste and to provide a more representative sample for testing. This practice was not used in subsequent tests as it was felt that the possible benefits of mixing the sample were outweighed by factors such as the waste being disturbed and the general impracticalities of the operation (e.g. litter). One sub-sample of approximately 4.5 tonnes was taken for loading into the compression cell and another sub-sample of approximately 3.5 tonnes taken for material classification (Section 5.3.2).

5.3.2 Waste characterisation

The 3.5 tonne sub-sample of the waste was sent to Warren Spring Laboratories for material classification. The compositional analysis of the waste is summarised in Tables 5.2 and 5.3. The bulk water content of the waste (WC_{wet}) was determined as 33.7%.

5.3.3 Loading of waste into compression cell

A layer of 20 mm single sized stone was placed in the bottom of the compression cell and levelled to a depth of 100 mm. A total of 4.600 tonnes (as measured by the load cells) of waste was placed into the cell in five stages. At the end of each stage the waste was compressed to achieve an approximate wet density of 0.7 t/m^3. There was an element of rebound in the refuse after each stage. No total stress cells were installed in the waste and an upper layer of gravel was not utilised. The loading process is summarised in Table 5.4.

5.3.4 Changes in average waste density in response to changes in applied stress

The upper platen was used to apply a stress to the top of the waste in the cell and compression of the waste was measured against time. A given stress was maintained until further compression was negligible, whereupon the applied stress was increased. There were four stages of increasing applied stress and one stage where the applied stress was removed and rebound was measured. The results are summarised in Table 5.5. The maximum wet density attained at the end of compression at an applied stress of 322 kPa was 0.90 t/m^3.

Table 5.2 Size and category analysis of waste used in tests DM1 and DM2

CATEGORY ASSAY %

Size mm	Wt %	Pa/Cd	PIF	DP	Tx	Mc	Mnc	Gl	Put	Fe	nFE	<10
+160	27.6	74.1	10.3	2.7	6.5	3.6	-	-	1.3	1.5	-	-
-160+80	29.1	25.2	6.5	8.9	1.07	22.6	1.1	8.7	8.3	15.4	1.6	-
-80+40	17.6	30.9	5.1	4.6	1.7	6.8	2.6	6.1	26.5	10.8	4.9	-
-40+20	11.4	14.1	0.8	1.9	-	1.4	1.3	8.6	69.7	1.4	0.9	-
-20+10	8.1	3.4	0.3	0.5	-	1.5	1.4	11.6	81.1	-	0.3	-
-10	6.2	-	-	-	-	-	-	-	-	-	-	100.0
Total	100.0	35.1	5.7	4.4	2.6	9.1	1.0	5.5	22.0	7.0	1.5	6.2

CATEGORY DISTRIBUTION

Size mm	Pa/Cd	PIF	DP	Tx	Mc	Mnc	Gl	Put	Fe	nFe	<10
+160	58.3	49.5	16.8	69.5	10.9	-	-	1.7	6.1	-	-
-160+80	20.9	32.9	59.1	18.7	72.7	30.7	46.0	11.0	64.3	32.7	-
-80+40	15.5	15.7	18.3	11.8	13.3	44.6	19.4	21.2	27.3	58.8	-
-40+20	4.6	1.5	4.9	-	1.8	13.9	17.8	36.3	2.3	7.1	-
-20+10	0.8	0.4	1.0	-	1.3	10.9	16.9	29.8	-	1.4	-
-10	-	-	-	-	-	-	-	-	-	-	100.0
Total	100.0	100.0	100.0	100.0	100.0	100.0	100.0	100.0	100.0	100.0	100.0

Water Content (WC_{wet}) of Refuse = 33.7%

Key

Pa/Cd	Paper and card	Mc	Miscellaneous Combustibles	Fe	Ferrous metal
PIF	Plastic Film	Mnc	Misc' Non combustibles	nFe	Non Ferrous Metal
DP	Dense plastics	Gl	Glass	<10	Material < 10mm size
Tx	Textiles	Put	Putrescibles		

Table 5.3 Detailed compositional analysis of waste used in tests DM1 and DM2

Category	Wt%	Category	Wt%
Newspapers	9.7	Brown glass bottles	0.3
Magazines	4.0	Green glass bottles	1.8
Other Paper	12.9	Clear glass bottles	0.4
Liquid containers	0.6	Clear glass jars	0.8
Card packaging	3.4	Other glass	2.2
Other Card	4.5	Garden waste	0.4
Refuse sacks	1.3	Other putrescible material	19.6
Other plastic film	4.4	Steel beverage cans	0.4
Clear plastic beverage bottles	0.9	Steel food cans	4.8
Coloured plastic beverage bottles	-	Batteries	0.3
Other plastic bottles	1.3	Other steel cans	0.4
Food packaging	0.9	Other ferrous metals	1.1
Other dense plastic	1.3	Aluminium beverage cans	0.4
Textile	2.6	Foil	0.8
Disposable nappies	5.1	Other non-ferrous metal	0.3
Other Misc' combustibles	3.9	-10 mm fines	6.2
Misc' non combustibles	1.0		
		TOTAL	100.0

Table 5.4 Summary of the loading of waste into compression cell for Test DM1

Loading Stage	Cumulative Weight of refuse in comp' cell kg	Depth of refuse following compression metres	Average wet density following compression t/m³	Depth of refuse following rebound metres	Average wet density following rebound t/m³
1	1,240	1.0	0.39	1.0	0.39
2	2,352	1.0	0.75	1.2	0.62
3	3,227	1.55	0.66	1.8	0.57
3a	3,227	1.3	0.79	1.6	0.64
4	N/R	1.4	N/D	1.7	N/D
5	4,600	none	N/D	2.09	0.70

N/R Not recorded (due to oversight)
N/D Not determined

Table 5.5 Compression of waste DM1 at varying applied stresses

Stage number	Duration	Applied Stress	Final depth of refuse	Wet density	Dry density[1]
	days	kPa	mm	t/m³	t/m³
Initial	N/R	0	2,089	0.70	0.45
1	7	40	2,018	0.73	0.48
2	6	165	1,751	0.84	0.55
3 (Recovery)	69	0	1,812	0.81	0.53
4	7	165	1,748	0.84	0.55
5	10	322	1,629	0.90	0.59

[1] Dry density calculated using a water content (WC_{wet}) of 33.7%

5.4 Crude household waste (Test series DM2)

Crude household waste was tested in the compression cell between March 1992 and August 1992 and was designated a test code DM2. A compression test, in which the applied stress was increased in stages, was carried out on the waste after its water content had been raised to field capacity. The hydrogeological properties of the waste were determined prior to the application of any load and at an applied stress of 40 kPa. Thereafter, the failure of the lower platen hydraulic seal prevented any further hydrogeological testing.

5.4.1 Waste source

The waste used in test DM2 was the same waste as used in test DM1. The original source of the waste is described in Section 5.3.1.

5.4.2 Waste characterisation

See Section 5.3.2.

5.4.3 Loading of waste into the compression cell

The waste used in test DM1 was emptied into a covered skip in January 1992 and re-used for test DM2. The waste was reloaded into the compression cell on 11 March 1992. The process of loading (using a hydraulically operated grab) loosened the previously compacted waste such that the waste was placed into the cell in an unconsolidated state.

A total of 4,040 kg of waste was loaded into the cell in three stages. As the compression cell load cells were not working properly at the time, the mass was determined by using the landfill site's weigh bridge. Vibrating wire earth pressure (stress) cells were installed in the bottom, middle and top of the refuse (see Figure 5.1).

The waste was loaded at an average bulk density of 0.54 t/m^3. The water content (WC_{wet}) of the waste was not determined but was assumed not to have changed significantly from test DM1 and was taken as approximately 34%.

5.4.4 Absorptive capacity

The absorptive capacity of the waste was determined on 18/19 March 1992 (test DM2C0ST1) prior to any compression tests. The waste was saturated completely and then allowed to drain under conditions of gravity drainage for a period of 24 hours. The absorptive capacity was calculated from the volume of water retained.

Volume of water added to saturate waste	4,405 litres
Volume of water drained	2,799 litres
Amount of water retained	1,606 litres
Mass of waste at original WC_{wet} = 34%	4,040 kg
Dry mass of waste	2,666 kg
Total absorptive capacity of waste at a bulk density of 0.54 t/m^3	398 litres/tonne

Figure 5.1 The loading of waste DM2 into the compression cell

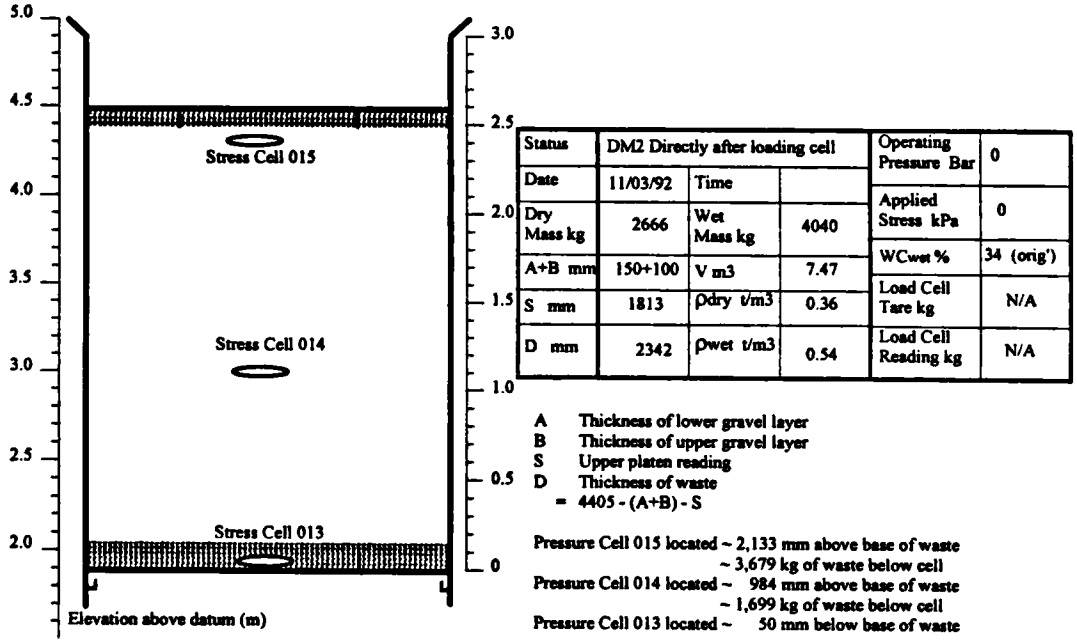

5.4.5 Changes in average waste density in response to changes in applied stress

The waste was subjected to five stages of compression, with applied stresses of 40, 87, 165, 322 and 603 kPa. Each compression stage was carried out with the waste at field capacity and under conditions of gravity drainage.

The final average dry density of the waste at the end of each compression stage is recorded in Table 5.6: over the test it increased from 0.36 to 0.73 t/m^3. The average wet density of the waste at the end of each compression stage is more difficult to calculate because of the changing water content of the waste (see Section 5.4.6). The wet density initially increased from 0.54 t/m^3 to 0.76 t/m^3 when the original water content of the waste was increased to field capacity (at zero applied stress), and finally to 1.14 t/m^3 at an applied stress of 603 kPa (see Figure 5.2).

5.4.6 Water content at field capacity

During certain compression stages it was noticed that water was being squeezed out of the waste. As the waste was at field capacity at the start of each compression stage this indicates that the water content at field capacity was reducing during compression.

However, because the load cells were not working no data on the bulk weight of the refuse could be collected and it was, therefore, not possible to determine directly the changes in water content of the waste in response to the increases in applied stress.

Figure 5.2 Average dry and wet densities of DM2 at varying applied stresses

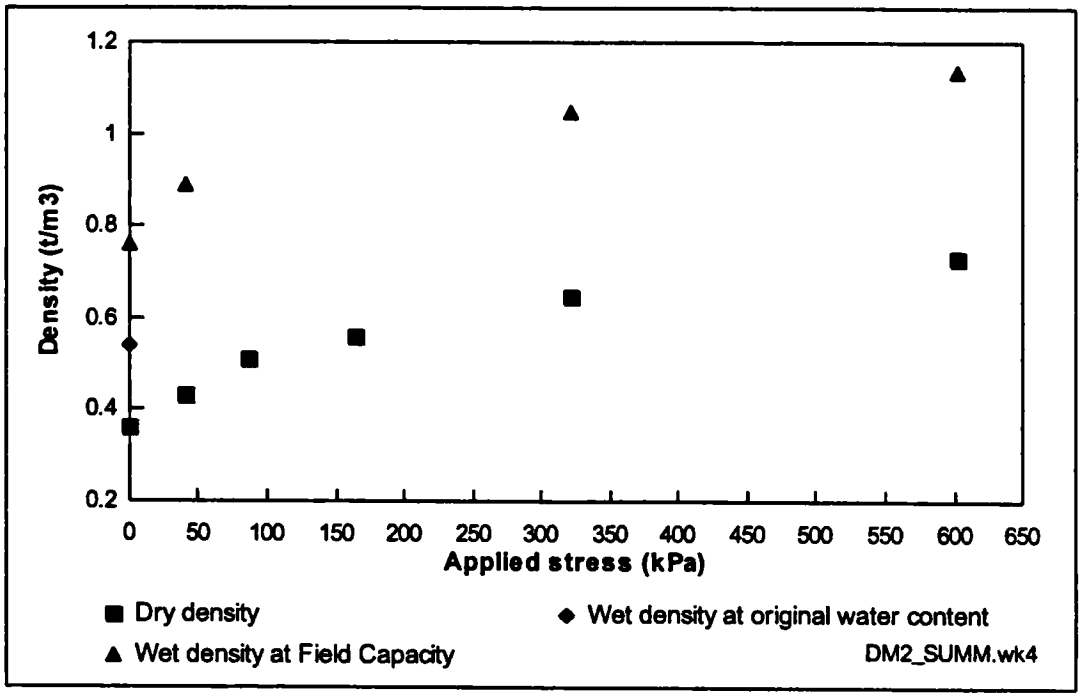

The initial water content (WC_{dry}) at field capacity prior to any compression was 112% (see Table 5.6). At the end of the compression stage at an applied stress of 603 kPa the waste was ejected into a skip and weighed using the landfill site's weigh bridge. The mass of wet waste (still at field capacity) was 4,166 kg; the water content (WC_{dry}) was determined as 56.3% (WC_{wet} = 36.0%), indicating that the water content at field capacity had reduced significantly.

In addition, data were collected on the volume of leachate squeezed out of the waste during certain of the compression stages. However, it was only possible to use these data with any degree of certainty to calculate field capacities for the first and last compression stages. This was because the recirculation of water through the waste was not monitored continuously and, consequently, the bulk water content of the waste was not tracked during hydraulic conductivity testing.

Table 5.6 Water contents at field capacity of DM2

Stage	Applied Stress (kPa)	Assumed bulk mass of refuse at start of stage (kg)	Water squeezed from waste during stage (litres)	Assumed bulk mass of refuse at end of stage (kg)	Water Content WC_{dry} at end of stage (%)	Dry Density[2] at end of stage t/m³	Comment
0	0	4,040	-1,606	5,646	112	0.36	Waste saturated and then drained to field capacity
1	40	5,646	131	5,515	107	0.43	Waste re-saturated and then drained to field capacity at end of stage
2	87		N/D			0.51	Waste not re-saturated
3	165		N/D			0.56	Waste not re-saturated
4	322	4,637[1]	322	4,315[1]	61.9	0.65	Saturation test at end of stage aborted after seal on lower platen breached
5	603	4,315	149	4,166	56.3	0.73	Waste mass obtained at end of test using site's weigh bridge.

[1] Assumed values because waste was re-saturated at end of stage
[2] See Section 5.4.5
N/D Not determined

5.4.7 Differential compression (String data)

Differential compression was measured at various depths within the waste at applied stresses of 87, 165, 322 and 603 kPa, using strings inserted into the waste through piezometer ports. The results for each compression stage are shown in Figures 5.3 to 5.6.

A more detailed analysis of the results is made in Chapter 6. An attempt is made to reconcile them with the earth pressure cell and hydrogeological data but it is noted, at this point, that there are almost certainly errors with the measurements due to the problem of anchoring the end of the strings in the waste (Section 3.6.3).

Figure 5.3 Differential compression of waste DM2 at applied stress of 87 kPa

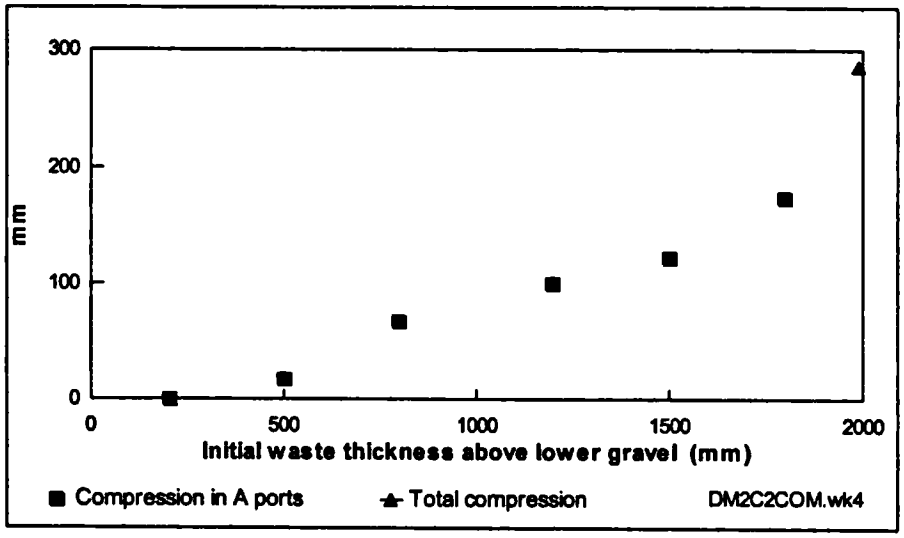

Figure 5.4 Differential compression of waste DM2 at applied stress of 165 kPa

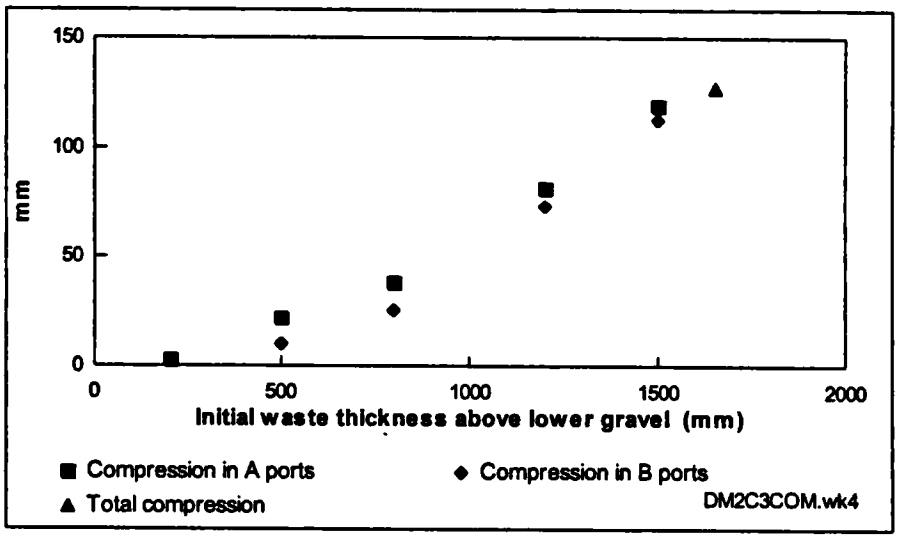

Figure 5.5 Differential compression of waste DM2 at applied stress of 322 kPa

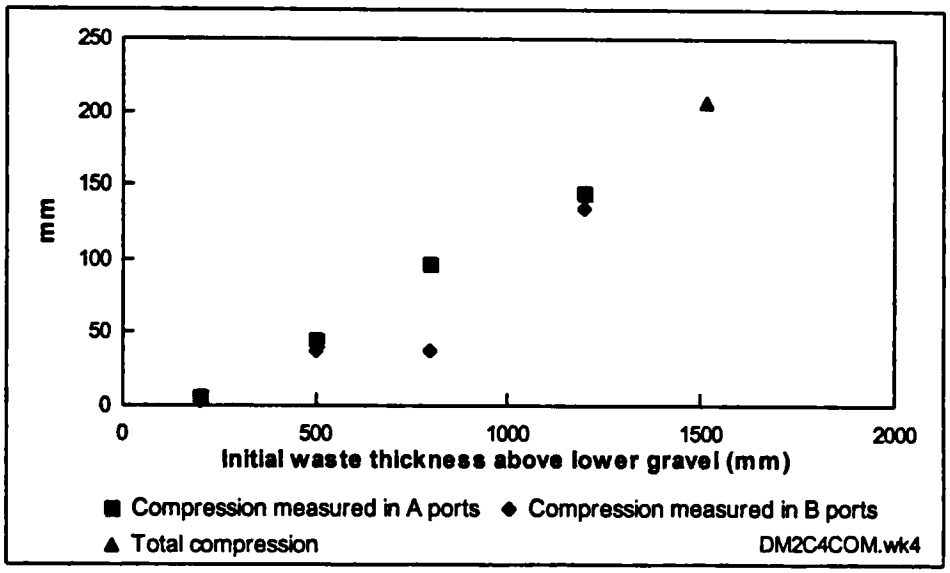

Figure 5.6 Differential compression of waste DM2 at applied stress of 603 kPa

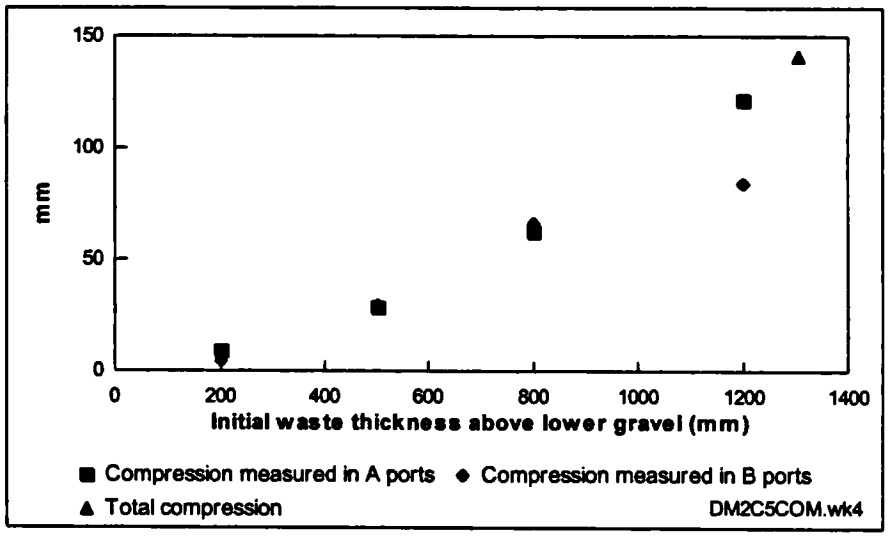

5.4.8 Earth pressure cell data

Measurements of transmitted total vertical stress were obtained from the three earth pressure cells throughout the experiment. An example of the transient variations in recorded stress from the cells during compression at an applied stress of 87 kPa is shown in Figure 5.7. The applied stress was controlled by the oil pressure in the hydraulic circuit. There were two periods when the applied stress dropped below 87 kPa - once when the hydraulic pressure dropped from 25 to 15 bar (~56 kPa) and once when a power failure shut the whole system down.

The maximum recorded total vertical stress during each compression stage is shown in Figure 5.8. Data correction and analysis of the data is undertaken in Section 6.4.

Figure 5.7 Uncorrected pressure cell data during compression of DM2 at an applied stress of 87 kPa

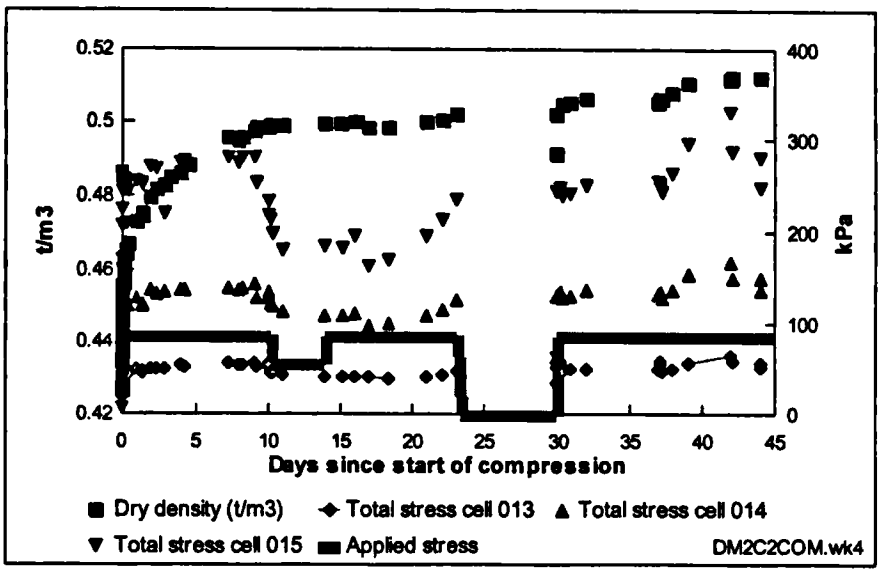

Figure 5.8 Maximum total stresses recorded during each compression stage of DM2

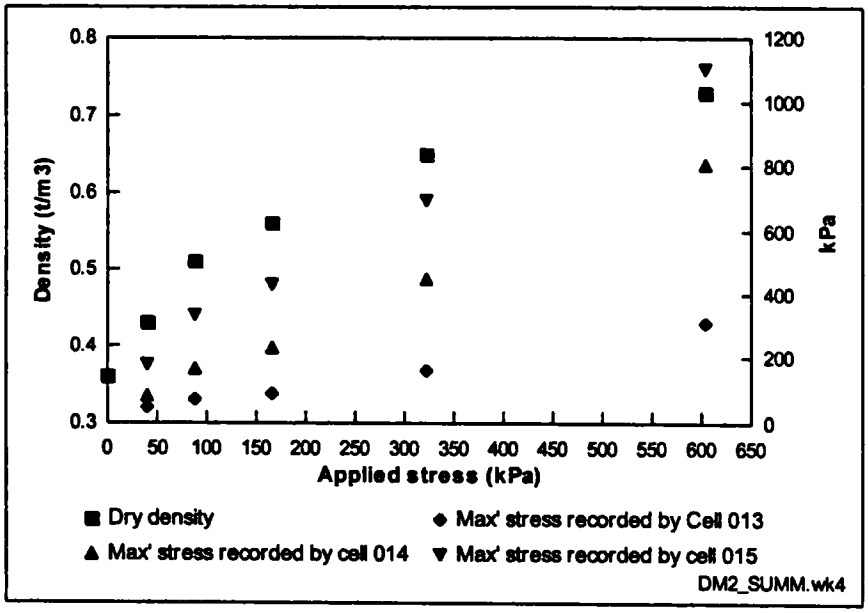

5.4.9 Effective porosity

The effective porosity of the waste was determined prior to the first compression stage and after compression at 40 kPa. At the end of the 40 kPa compression stage the water seal on the lower platen started to leak, preventing any further saturation tests until the lower seal was re-designed at the end of tests on DM2. Figures 5.9 and 5.10 show examples of data from effective porosity tests on the waste prior to compression and after compression at an applied stress of 40 kPa and Table 5.7 summarises the results for a number of tests in each stage. Although there is considerable uncertainty in the data for the tests undertaken with zero applied load (due to the possible flotation of the unconfined waste) the effective porosity generally decreases from approximately 18% to 11%.

Table 5.7 Effective porosity of DM2 at varying applied stresses

Stage	Test	Applied Stress kPa	Effective Porosity %	Comment
DM2C0St1	Drain	0	27.6[1]	Lower 2 m of waste in cell
DM2C0St2	Fill	0	36.2[1]	Upper 1 m of waste in cell.
DM2C0St3	Fill	0	39.8[1]	Upper 0.5 m of waste in cell.
DM2C0St3	Fill	0	**17.5**	Lower 1.5 m of waste in cell.
DM2C1St1	Fill	40	6.0	Upper 1.1 m of waste in cell.
DM2C1St1	Fill	40	18.2	Lower 0.4 m of waste in cell.
DM2C1St2	Fill	40	**11**	Average for all waste in cell

[1] Effective porosity values probably being affected by upper surface of waste not being confined by upper platen.
Values in bold considered to be most reliable.

Figure 5.9 Effective porosity determination of DM2 prior to compression

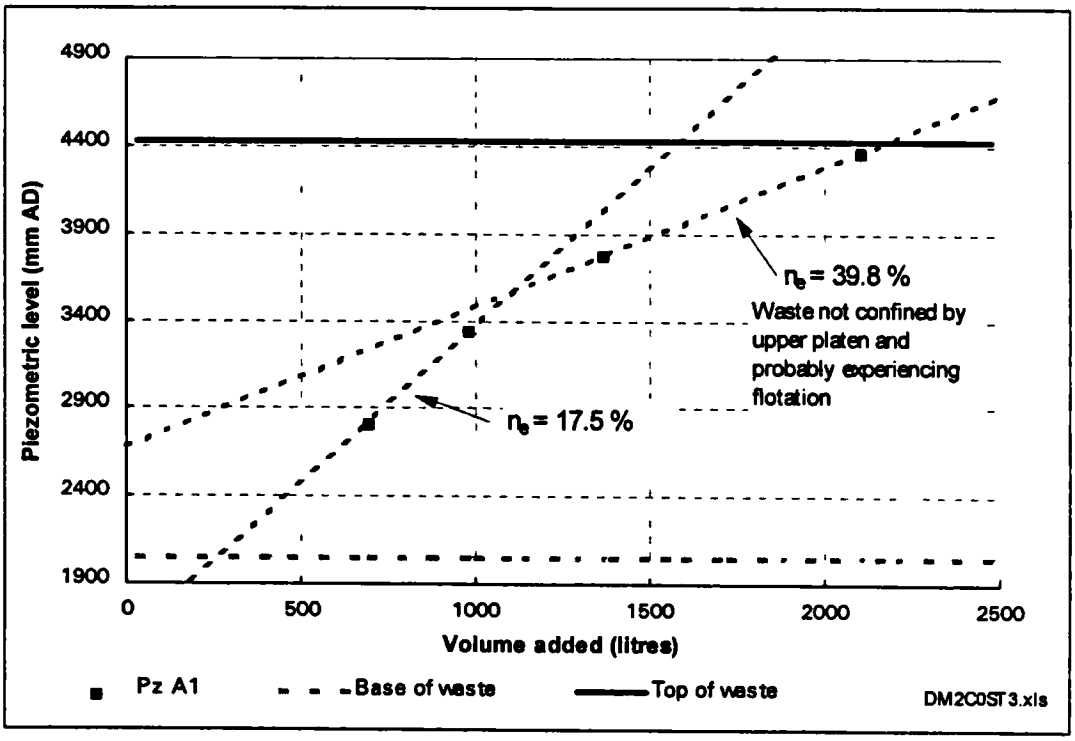

Figure 5.10 Effective porosity determination of DM2 at an applied stress of 40 kPa

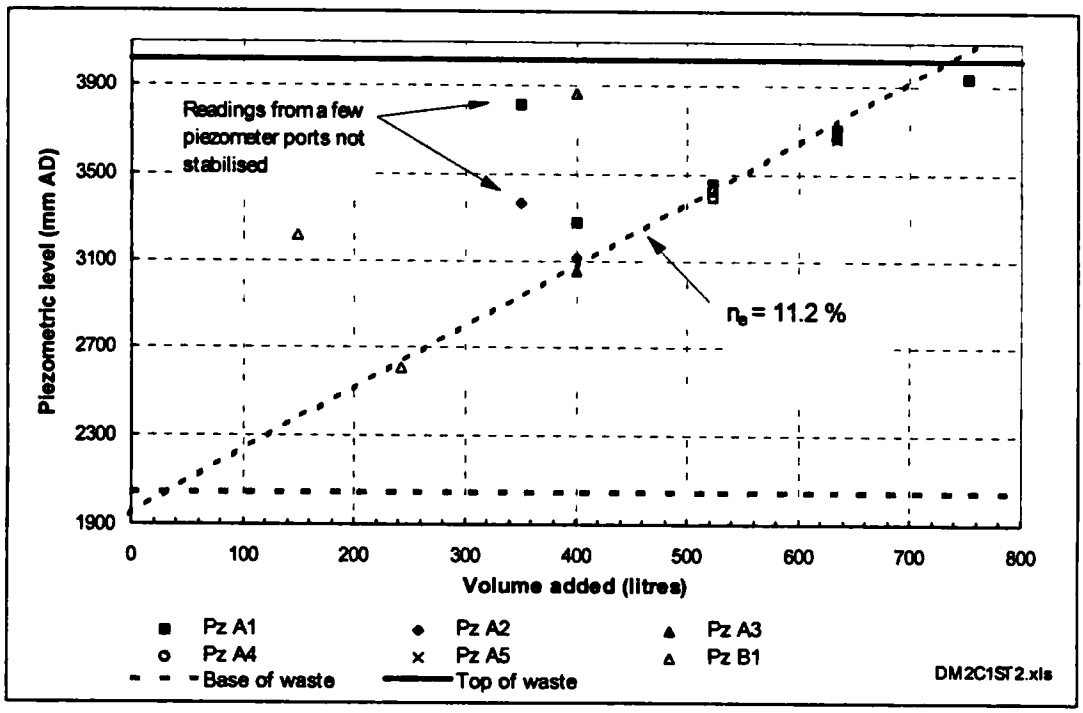

5.4.10 *Hydraulic conductivity*

As with the effective porosity tests, hydraulic conductivity was only determined prior to any compression and after compression at 40 kPa. The hydraulic conductivity of the bottom 1.2 metres of waste with zero applied load was 6.5×10^{-4} m/s (Figure 5.11). This was the same order of magnitude as the value of 2×10^{-4} m/s calculated for the middle part of the waste at an applied stress of 40 kPa (Figure 5.12).

Figure 5.11 Constant head hydraulic conductivity test on DM2 prior to compression

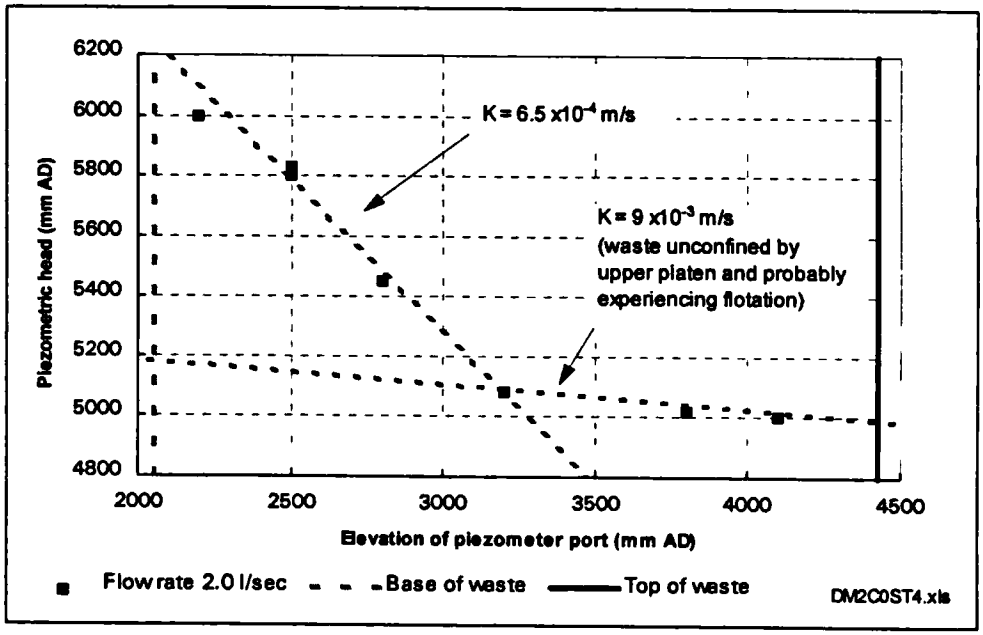

Figure 5.12 Constant head hydraulic conductivity test on DM2 at an applied stress of 40 kPa.

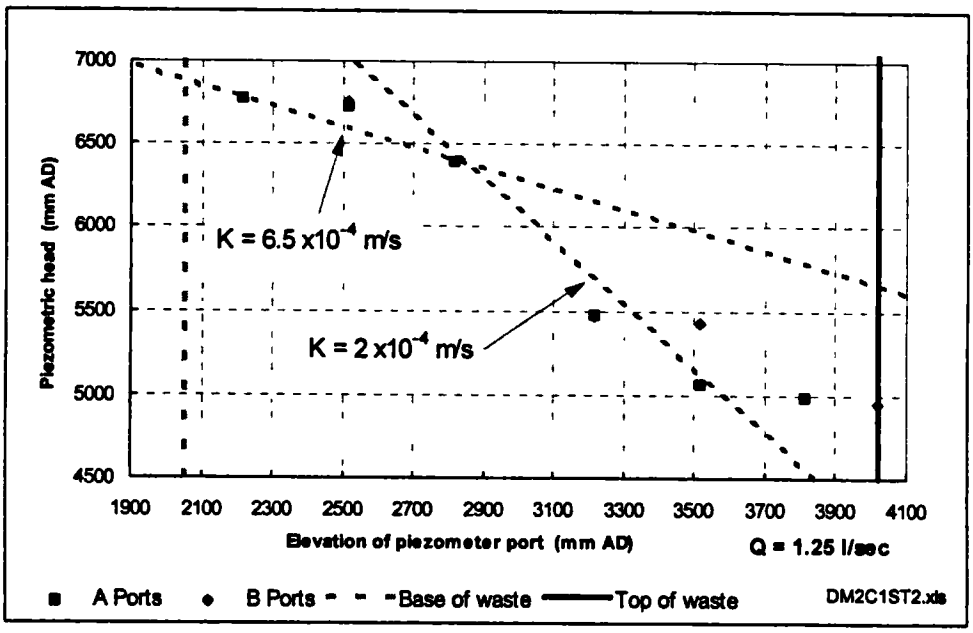

NB Piezometric levels at bottom of waste probably affected by leak in bottom platen hydraulic seal during the test.

5.5 Crude household waste (Test series DM3)

Crude household waste was tested in the compression cell between February 1995 and May 1995 and was designated a test code DM3. A compression test, in which the applied stress was increased in stages, was carried out on the waste after its water content had been raised to field capacity. The hydrogeological properties of the waste were determined at the end of each compression stage.

5.5.1 Waste source

The material used in tests DM3 was crude household waste. It was obtained directly from refuse collection vehicles as they discharged their loads at the tipping face of Pitsea landfill site on 7th February 1995. The waste was collected using a lorry equipped with a hydraulically operated grab and transported to the compression cell. A number of trips were made. Each load was split, with some waste being loaded into the compression cell and some waste being placed into a skip for subsequent transport to AEA Technology, Harwell for material classification.

5.5.2 Waste characterisation

A bulk sample weighing 1.91 tonnes was delivered to AEA Technology Harwell on 2 March 1995 for analysis. It had a bulk water content (WC_{wet}) of 34%. The compositional size analysis of the sample is recorded in Table 5.8.

Table 5.8 Size and category analysis of waste DM3

CATEGORY ASSAY %												
Size mm	Wt %	Pa/Cd	PIF	DP	Tx	Mc	Mnc	Gl	Put	Fe	nFE	-10
+160	39.0	62.7	4.0	7.1	10.5	14.0	-	0.8	-	0.7	-	-
-160+80	26.4	35.4	6.8	7.5	4.4	18.5	1.3	7.0	9.3	7.7	2.1	-
-80+40	15.2	30.2	6.3	8.4	1.3	5.3	5.0	9.2	25.8	5.4	3.2	-
-40+20	10.0	1.8	0.7	3.4	0.8	4.2	10.9	21.6	44.2	1.1	1.2	-
-20+10	4.5	6.0	0.2	1.5	-	5.6	5.6	27.8	52.9	-	0.5	-
-10	4.9	-	-	-	-	-	-	-	-	-	-	100.0
Total	100.0	39.8	4.4	6.4	5.5	11.8	2.4	7.0	13.2	3.2	1.2	4.9

Water Content (WC_{wet}) of Refuse = 34%

Key					
Pa/Cd	Paper and card	Mc	Miscellaneous Combustibles	Fe	Ferrous metal
PIF	Plastic Film	Mnc	Misc' Non combustibles	nFe	Non Ferrous Metal
DP	Dense plastics	Gl	Glass	Put	Putrescibles
Tx	Textiles	-10	Material <10 mm in size		

5.5.3 Loading of waste into the compression cell

The waste was loaded into the compression cell over a two day period from 7th to 8th February 1995. A total of 4,048 kg of waste was added in six stages. The waste in each stage was levelled out and compacted to a nominal density of 0.5 t/m^3 (0.33 t/m^3 dry density) using the upper platen. However, as the waste rebounded at the end of each compression stage it was sometimes compacted to a density in excess of 0.5 t/m^3. The maximum density reached during the loading process was 0.56 t/m^3 - this occurred during the last compression stage after all the waste had been added to the cell. Three total stress cells were installed at the locations depicted in Figure 5.13.

Figure 5.13 The loading of waste DM3 into the compression cell

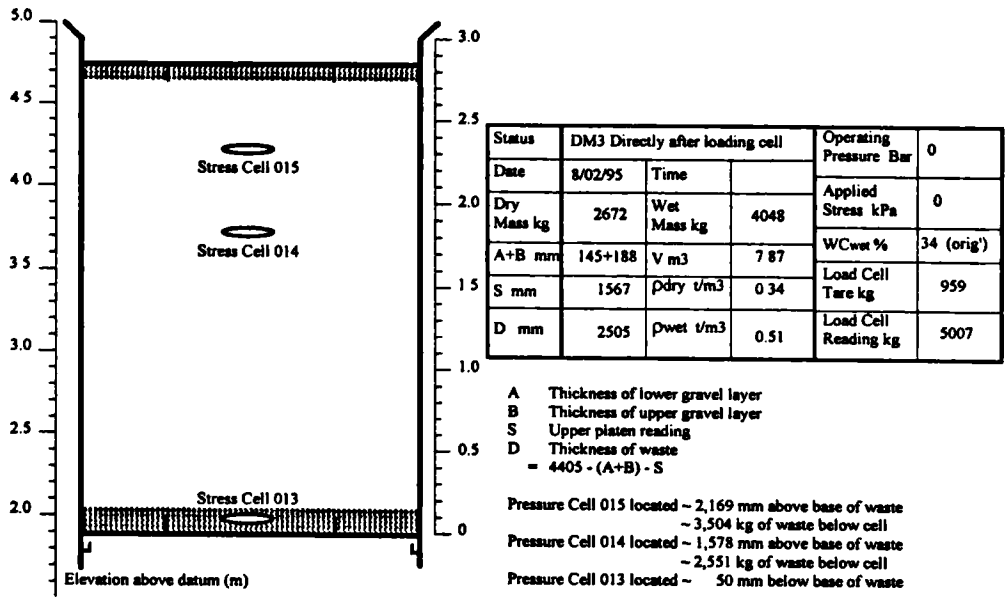

Status	DM3 Directly after loading cell			Operating Pressure Bar	0
Date	8/02/95	Time		Applied Stress kPa	0
Dry Mass kg	2672	Wet Mass kg	4048	WCwet %	34 (orig')
A+B mm	145+188	V m3	7 87	Load Cell Tare kg	959
S mm	1567	ρdry t/m3	0 34	Load Cell Reading kg	5007
D mm	2505	ρwet t/m3	0.51		

5.5.4 Absorptive capacity

The absorptive capacity of the waste was determined after the waste had been compressed to an average dry density of 0.38 t/m^3 at an applied stress of 40 kPa. The waste was saturated and then allowed to drain over a period of 5 days.

Volume of water added to saturate waste	4,919 litres
Volume of water drained	3,552 litres
Amount of water retained	1,367 litres
Mass of waste at original WC_{wet} = 34%	4,048 kg
Dry mass of waste	2,672 kg
Total absorptive capacity of waste at a bulk density of 0.59 t/m^3	338 litres/tonne

5.5.5 Changes in average waste density in response to changes in applied stress

The waste was subjected to six stages of compression, with applied stresses of 40, 87, 165, 244, 322 and 603 kPa. During compression the waste was maintained under conditions which allowed gravity drainage.

The final average dry density of the waste at the end of each compression stage is recorded in Table 5.9 showing an increase from 0.32 to 0.72 t/m^3.

Table 5.9 Changes in dry density and water content at field capacity of DM3

Stage	Applied Stress (kPa)	Status[1]	Wet mass of waste at end of stage (kg)	Change in water held in waste in stage[1] (litres)	ρ_{dry} at end of stage (t/m^3)	WC_{dry} at end of stage (%)	WC_{wet} at end of stage (%)	WC_{vol} at end of stage (%)
0	-	Loading	4048	0	0.32	51.5[4]	34.0[4]	16.5[4]
1	40	Comp'n	4048	0	0.38	51.5[4]	34.0[4]	16.5[4]
1	40	S&D	5415	+1367	0.39	101.4	50.3	39.9
2	87	Comp'n	5316	-113	0.42	99.0	49.7	41.6
2	87	S&D	5404	+88	0.43	102.3	50.6	44.0
3	165	Comp'n	5100	-304	0.49	90.8	47.6	44.5
3	165	S&D	5071	-29	0.50	89.8	47.3	44.9
4	244	Comp'n	5006	-131[3]	0.53	87.4	46.6	46.3
5	322	Comp'n	4706	-300	0.59	76.1	43.2	44.9
5	322	S&D	4666	-40	0.62	74.6	42.7	46.3
6	603	Comp'n	4322	-344	0.72	61.8	38.2	44.4

[1] S&D indicates that waste was saturated and then drained to field capacity during stage.
[2] Change in water content of waste determined by load cell readings. Some inaccuracies in method due to drift in load cell readings.
[3] Direct measurement of water squeezed from waste. Difference in load cell readings = -65 litres.
[4] Not at field capacity

The average wet density of the waste at the end of each compression stage is linked to its water content (Section 5.5.6). At an applied stress of 40 kPa the wet density increased from 0.59 to 0.79 t/m^3 (Figure 5.14) because the water content of the waste was brought up to field capacity by saturation followed by gravity drainage. Thereafter, it increased to a maximum density of 1.15 t/m^3 at an applied stress of 603 kPa.

There was a negligible increase in dry density (from 0.389 to 0.393 t/m^3) resulting from the process of increasing the water content of the waste whilst under an applied stress of 40 kPa.

Figure 5.14 Average dry and wet densities of DM3 at varying applied stresses

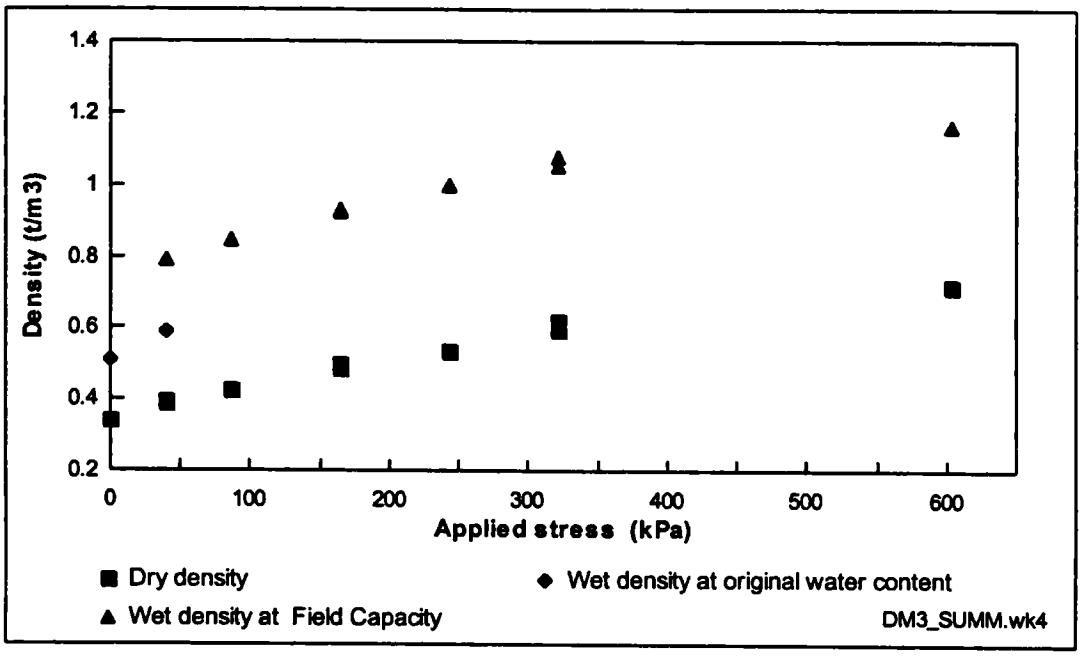

5.5.6 Water content at field capacity

The changes in the water content of the waste at field capacity throughout the various stages of compression are summarised in Table 5.9. During the compression stages water was generally squeezed out of the waste, reducing the water content, WC_{dry}, from approximately 103% to 62% as the density of the waste increased. However, when the water content is expressed in volumetric terms (WC_{vol}) there is no definitive change with increasing applied stress and density; WC_{vol} remains in a range between approximately 41% and 46%.

5.5.7 Differential compression (String data)

Differential compression was measured at various depths within the waste at applied stresses of 40, 87, 165, 244, 322 and 603 kPa, using strings inserted into the waste through piezometer ports. The differential compression of the waste measured in this way for each compression stage is shown in Figures 5.15 to 5.20.

Further analyses of these data are made in Chapter 6 and Appendix B.

Figure 5.15 **Differential compression of waste DM3 at applied stress of 40 kPa**

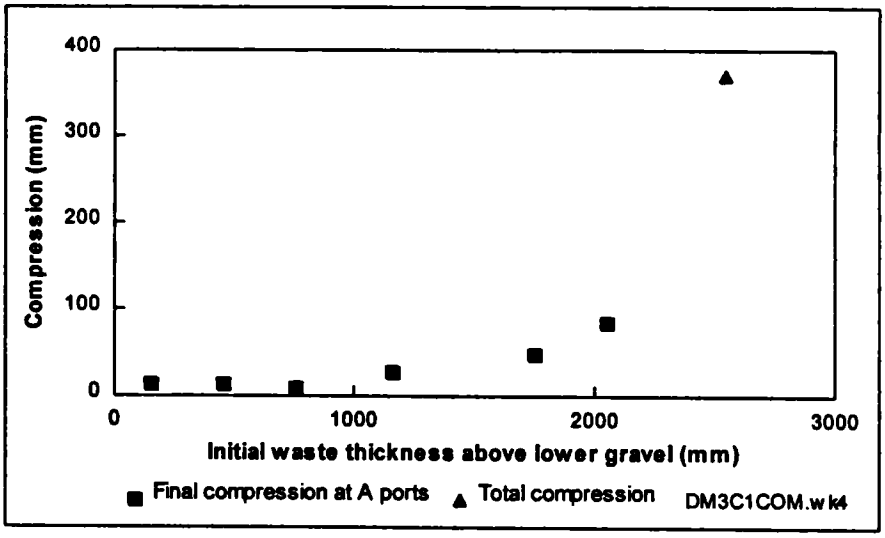

Figure 5.16 **Differential compression of waste DM3 at applied stress of 87 kPa**

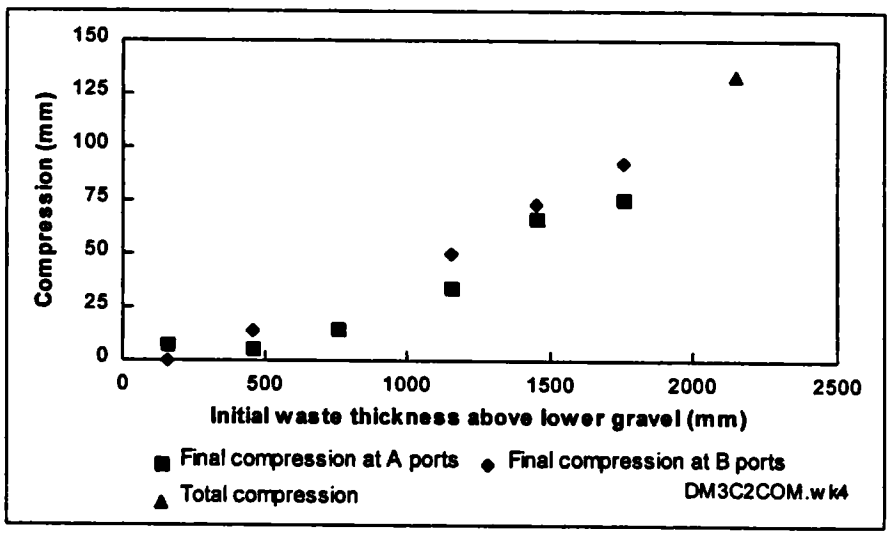

Figure 5.17 **Differential compression of waste DM3 at applied stress of 165 kPa**

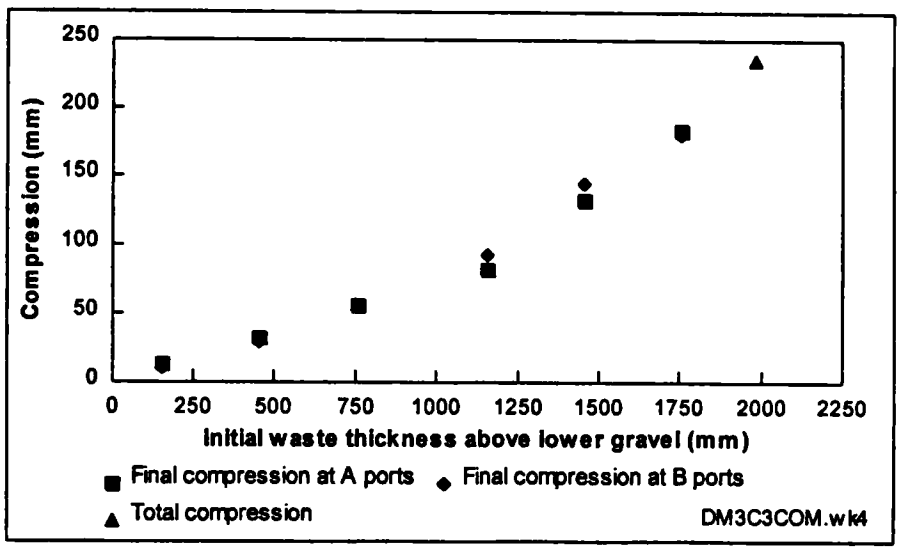

Figure 5.18 **Differential compression of waste DM3 at applied stresses of 244 kPa**

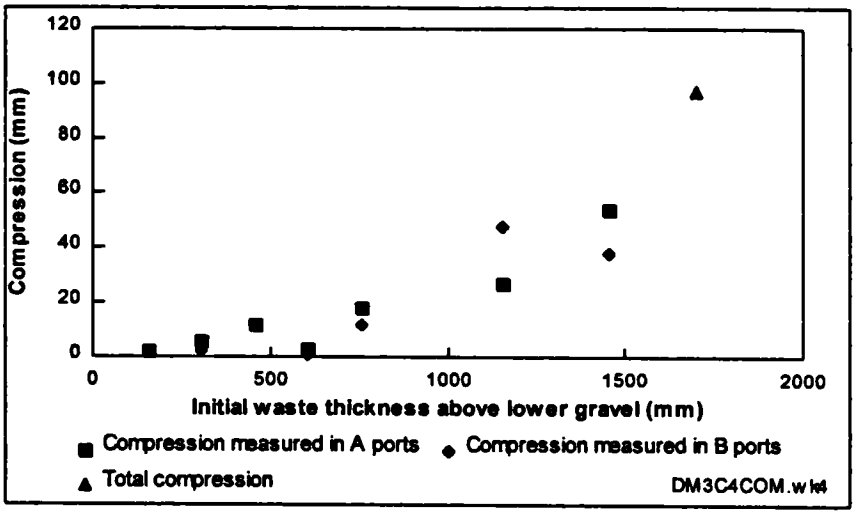

Figure 5.19 **Differential compression of waste DM3 at applied stress of 322 kPa**

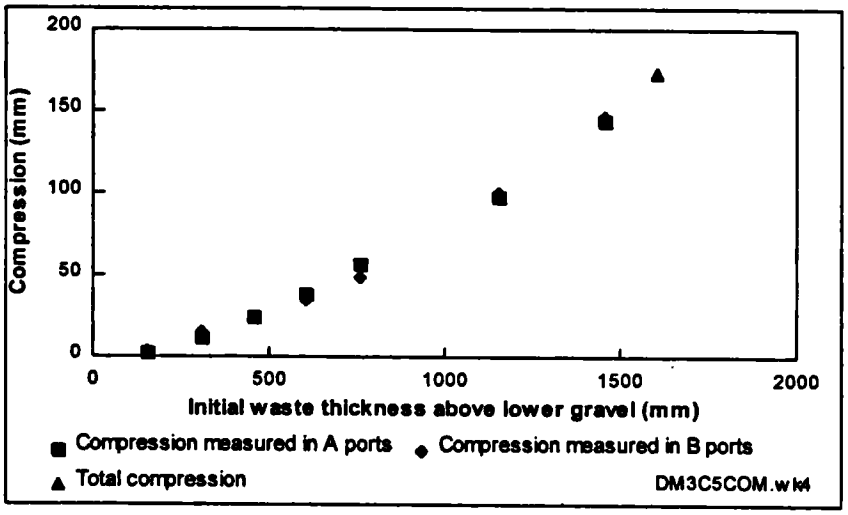

Figure 5.20 **Differential compression of waste DM3 at applied stress of 603 kPa**

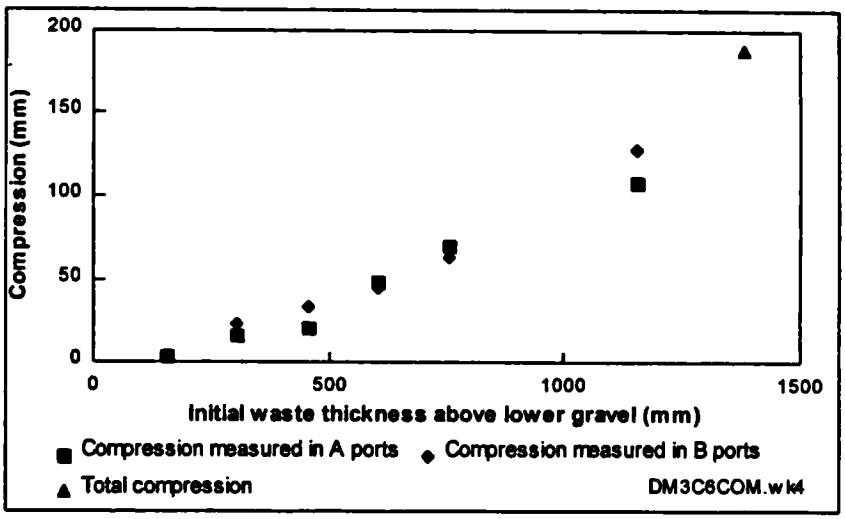

5.5.8 Total stress cell data

The maximum total vertical stress recorded by the three earth pressure cells during the six stages of compression is shown in Figure 5.21. The application of correction factors and the general validity of the data are discussed in Chapter 6.

Figure 5.21 Maximum total stresses recorded during each compression stage of DM3

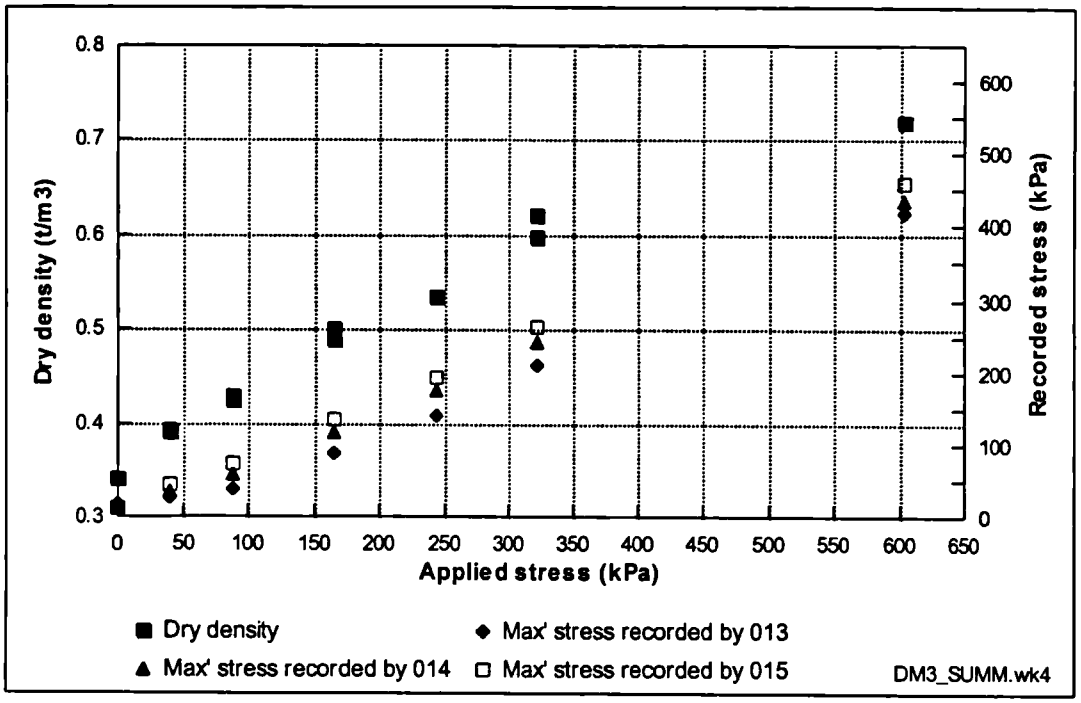

5.5.9 Effective porosity

The effective porosity of the waste was determined after compression at applied stresses of 40, 87, 165, 322 and 603 kPa. Figures 5.22 to 5.27 show, for each compression stage, the average piezometric head plotted against the volume of water either added to or drained from the waste. The gradient of the line through the data at any point is directly related to the drainable porosity. More than one test was undertaken at each compression stage, as summarised in Table 5.10. In general the effective porosity reduced with increasing applied stress. At an applied stress of 40 kPa the effective porosity was approximately 14.6%; at an applied stress of 603 kPa the effective porosity was approximately 1.5%.

Data produced during the draining of the waste at an applied stress of 40 kPa is shown in Figure 5.23. The waste was drained over a period of 5 days during which time approximately 1,000 litres drained from a waste thickness of 1,908 mm, indicating a bulk drainable porosity of 14.7%. This compares favourably with a porosity of 14.6% determined from the subsequent re-saturation of the waste in test DM3C1SAT2 (see Table 5.10).

Figure 5.23 also illustrates the potential problem that arises from determining effective porosity from piezometric readings that have not been given long enough to stabilise. This is particularly the case for data involving the draining, rather than the saturating, of waste. The error bars (plotted only for the A ports for clarity) represent the range of piezometric readings recorded; the actual data point plotted is the mean of all values. The second data point on the graph (at 200 litres drained) was taken after the waste had been allowed to drain overnight for approximately 18 hours. Each of the next five data points on the graph (from 270 to 510 litres drained) were taken after the waste had been allowed to drain for between 1 and 3 hours. The average piezometric level recorded in the A ports after 510 litres had been removed was 3,014 mm AD. The waste was then allowed to drain (without removing any further leachate from the cell) for a further 48 hours, whereupon piezometric levels were taken again. Over this period of time the average level in the A ports had increased by over 300 mm to 3,318 mm AD. This value was greater than the maximum piezometric level recorded in any A port (plotted as an error bar on Figure 5.23) from the previous set of readings. This indicates that the increase in levels over the 48 hours must have been in part from gravity drainage from the unsaturated zone, rather than resulting entirely from the stabilisation of hydraulic heads (to hydrostatic conditions).

If the effective porosity of the upper part of the waste is calculated using the level of 3,014 mm AD (at 510 litres drained) a value of 9.8% is derived. This is not a true effective porosity, as the waste had not completely drained. An effective porosity of 14.4% is calculated for the upper part of the waste if a level of 3,318 mm AD (at 510 litres drained) is used. This is very similar to the average effective porosity of 14.6% to 14.7% calculated above.

Figure 5.22 Total storage capacity of waste DM3 with no confining stress

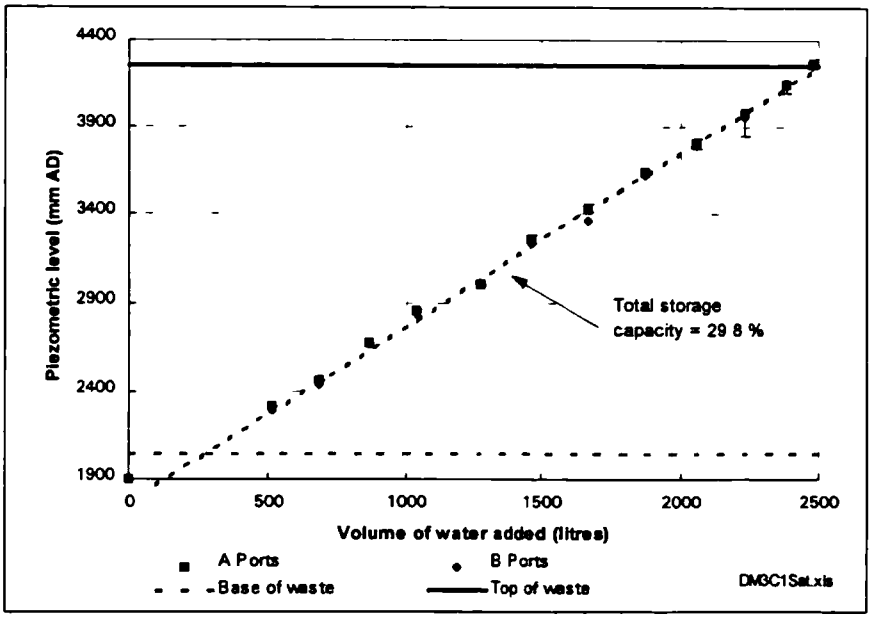

Figure 5.23 **Effective porosity determination of DM3 at an applied stress of 40 kPa**

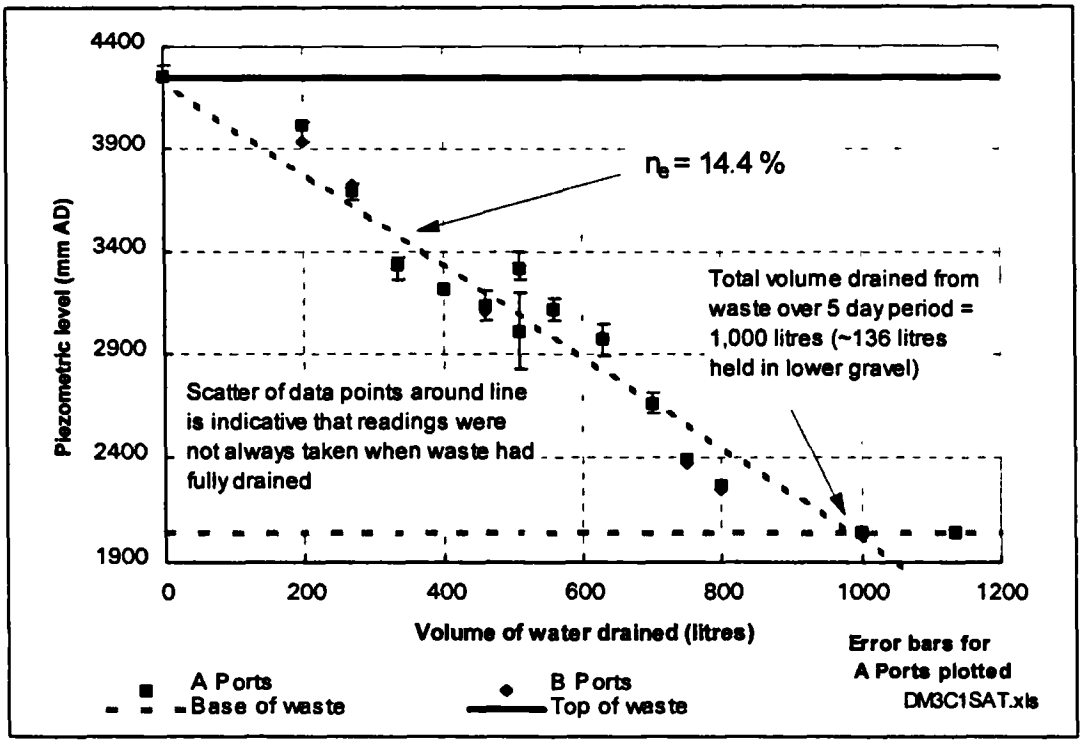

Figure 5.24 **Effective porosity determination of DM3 at an applied stress of 87 kPa**

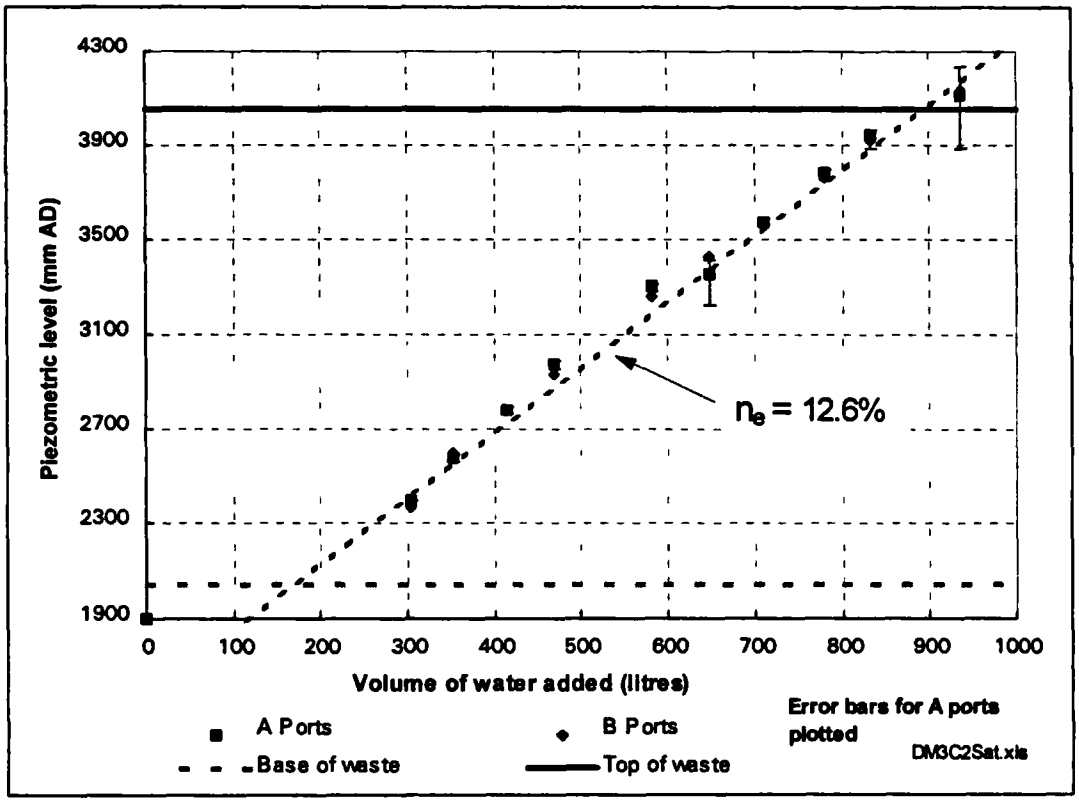

Figure 5.25 **Effective porosity determination of DM3 at an applied stress of 165 kPa**

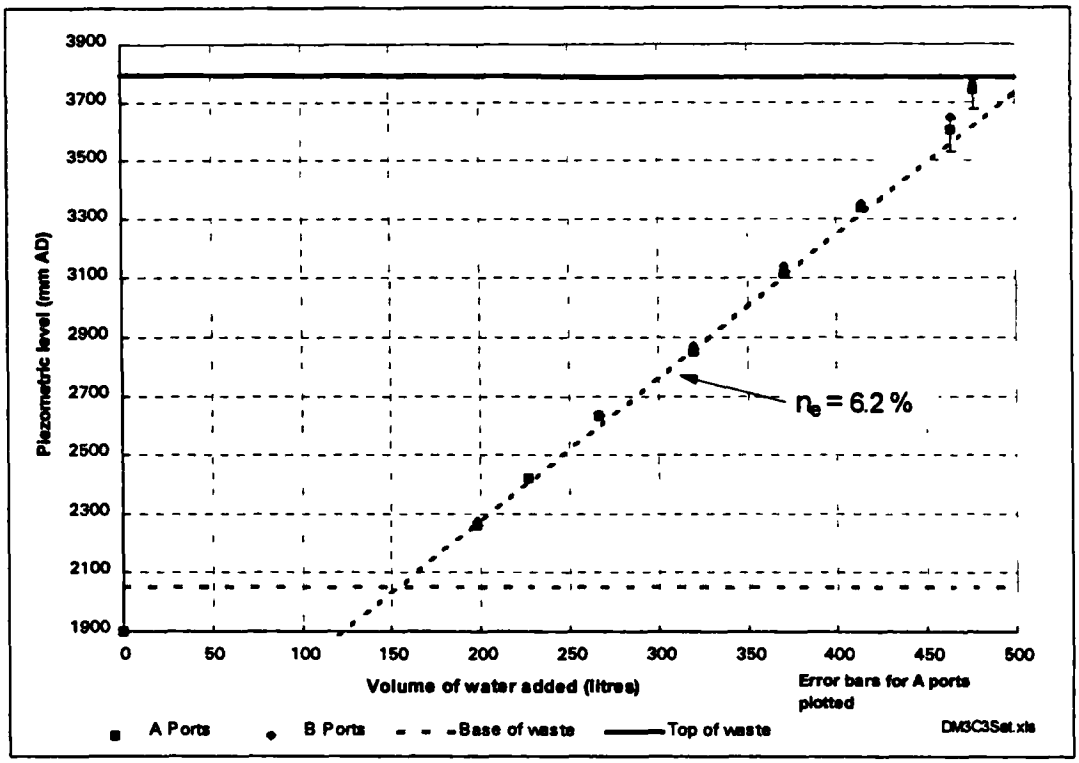

Figure 5.26 **Effective porosity determination of DM3 at an applied stress of 322 kPa**

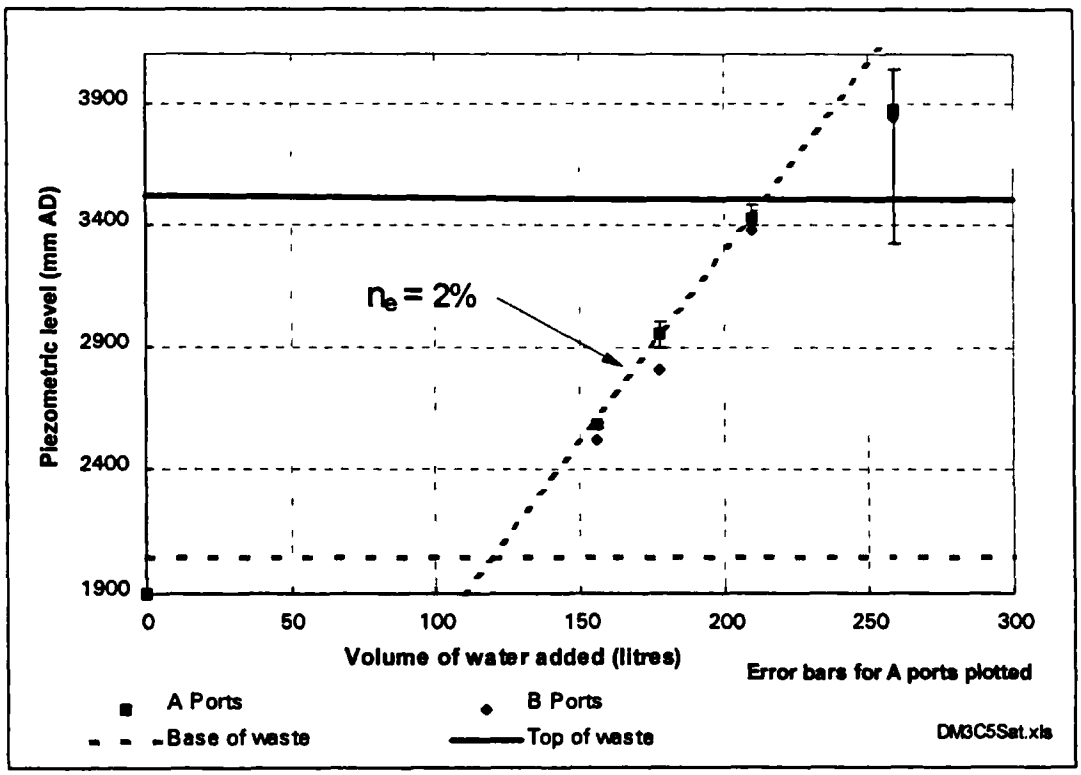

Figure 5.27 Effective porosity determination of DM3 at an applied stress of 603 kPa

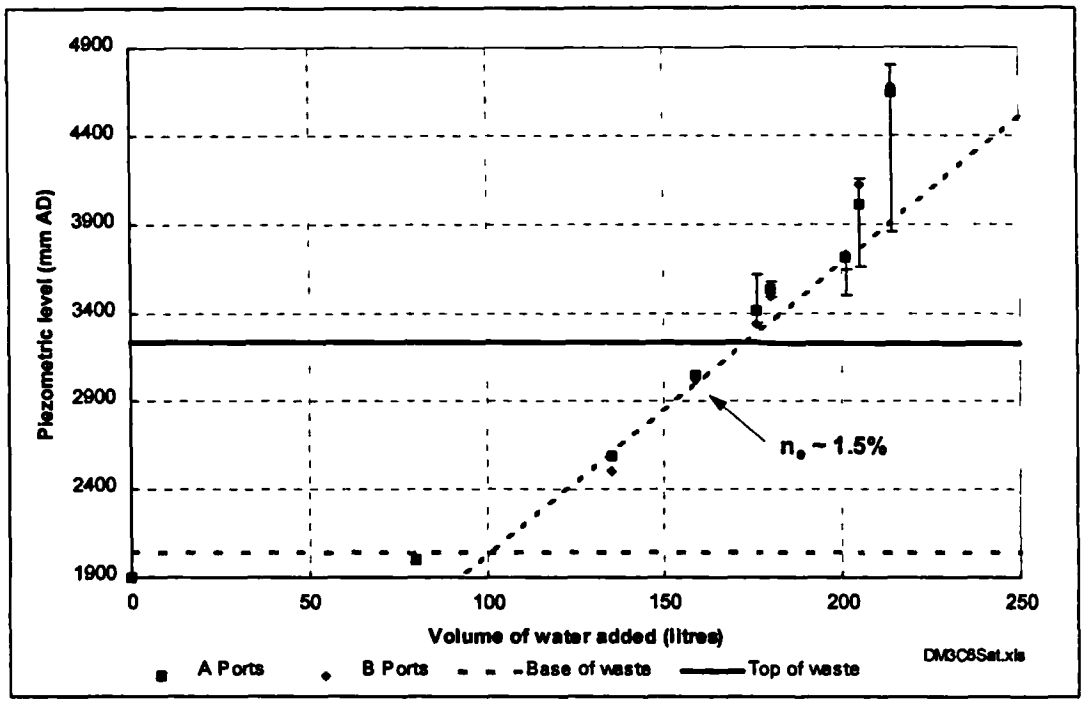

Table 5.10 Effective porosity of DM3 at varying applied stresses

Stage	Test type	Applied Stress kPa	Effective Porosity %	Comment
DM3C1St1	Fill	40	N/D	Total storage capacity = 29.8%
DM3C1St1	Drain	40	**14.7**	Average 5 day drainage for all waste in cell.
DM3C1St1	Drain	40	14.4	48 hour drainage for upper waste in cell
DM3C1St2	Fill	40	**14.6**	Average for all waste in cell.
DM3C2St1	Fill	87	**12.6**	Average for all waste in cell.
DM3C2St1	Fill	87	10.3	Upper waste (1,205-1,955 mm above base).
DM3C2St1	Fill	87	13.7	Middle waste (805-1,205 mm above base).
DM3C2St1	Fill	87	9.4	Lower waste (305-805 mm above base).
DM3C2St1	Drain	87	**12.3**	Average for all waste in cell.
DM3C2St2	Fill	87	11.4	Average.
DM3C3St1	Fill	165	**6.2**	Average
DM3C3St1	Drain	165	5.0	Average. Drainage occurs over 30 hours.
DM3C3St2	Fill	165	7.8	Average.
DM3C5St1	Fill	322	**2**	Average. Many piezometric readings not stable due to production of gas in cell
DM3C6St1	Fill	603	**1.5**	Average. Low hydraulic conductivity means that over 6 days piezometric readings had not stabilised.

5.5.10 *Hydraulic conductivity*

The vertical hydraulic conductivity of waste DM3 was determined after compression at applied stresses of 40, 87, 165, 322 and 603 kPa. Graphs of piezometric head plotted against elevation are shown in Figures 5.28 to 5.32 for each of the compression stages. The gradient of a line plotted through the data points is the hydraulic gradient which, according to Darcy's Law (Equation 2.20), is directly related to the hydraulic conductivity.

Any variation in hydraulic gradient with depth in the waste (represented by a deviation from linearity) indicates a variation in hydraulic conductivity (assuming that the rate of flow, Q, and the cross sectional area, A, through which the flow takes place remain constant).

The data plotted in Figures 5.28 to 5.32 clearly indicate variations of hydraulic gradient with depth and hence variation in vertical hydraulic conductivity with depth. At each compression stage lower hydraulic conductivities are recorded in the waste near the top of the cell than at the bottom.

The results are summarised in Table 5.11.

Figure 5.28 **Constant head hydraulic conductivity test on DM3 at an applied stress of 40 kPa**

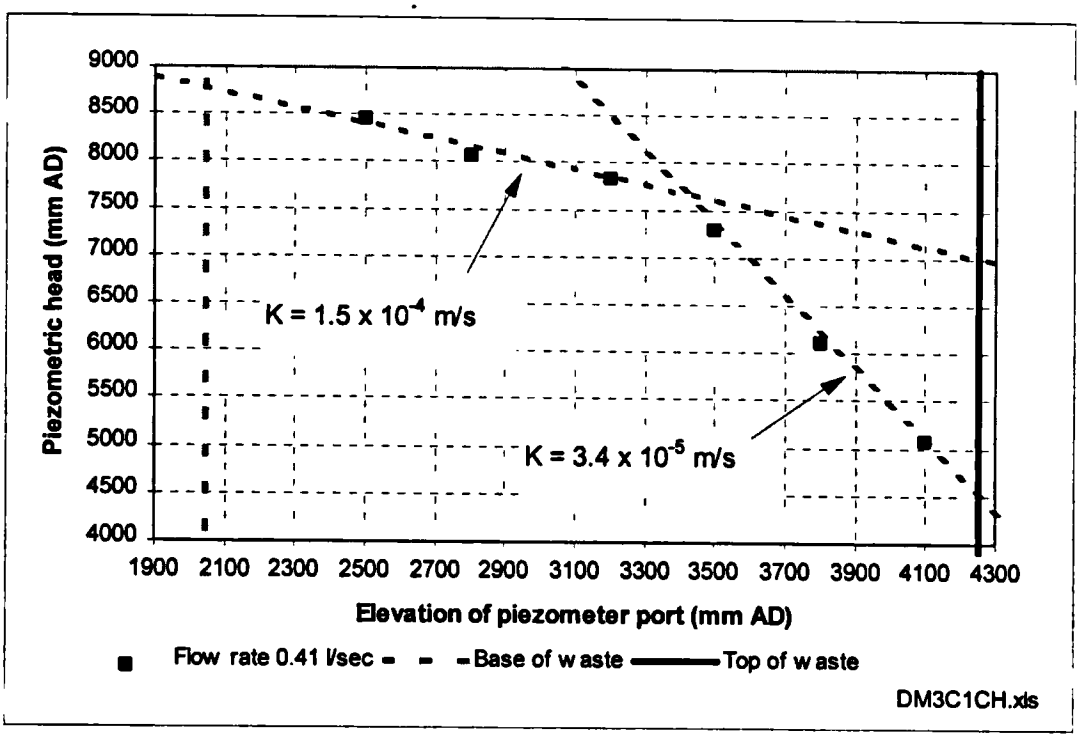

Figure 5.29 **Constant head hydraulic conductivity test on DM3 at an applied stress of 87 kPa**

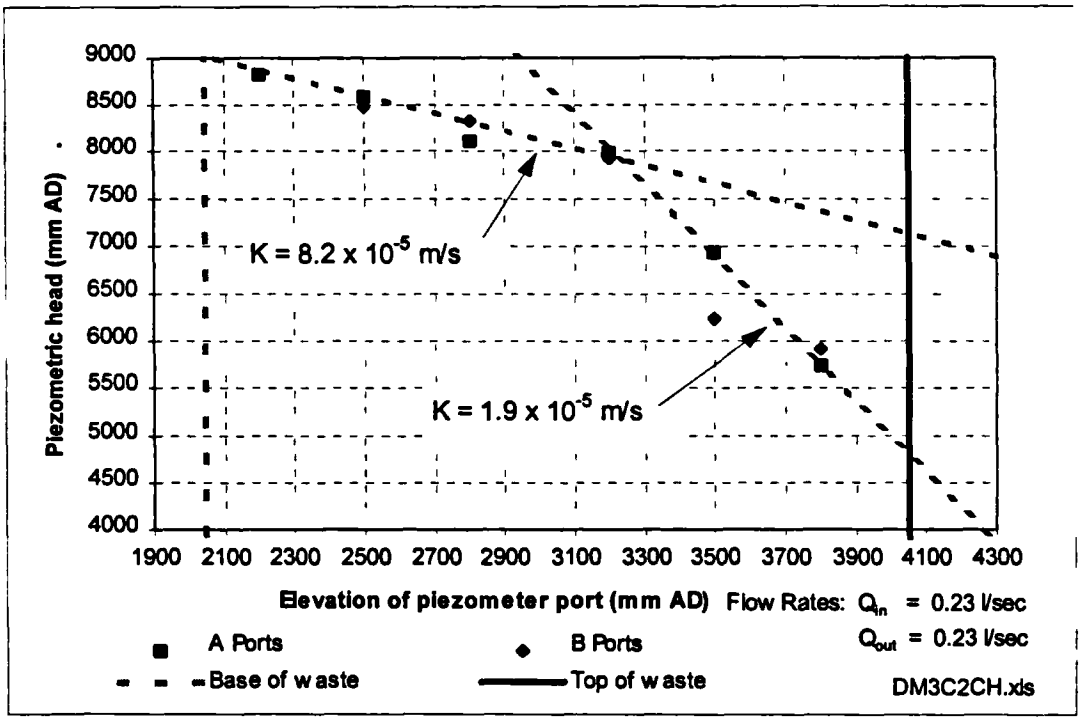

Figure 5.30 **Constant head hydraulic conductivity test on DM3 at an applied stress of 165 kPa**

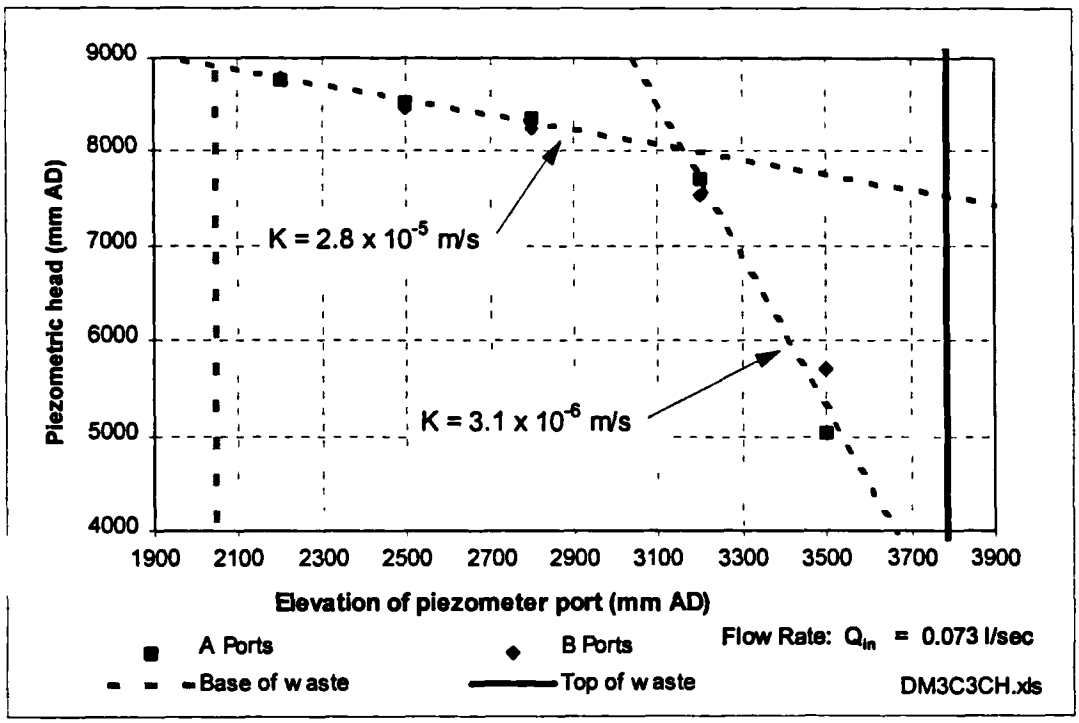

Figure 5.31 **Constant head hydraulic conductivity test on DM3 at an applied stress of 322 kPa**

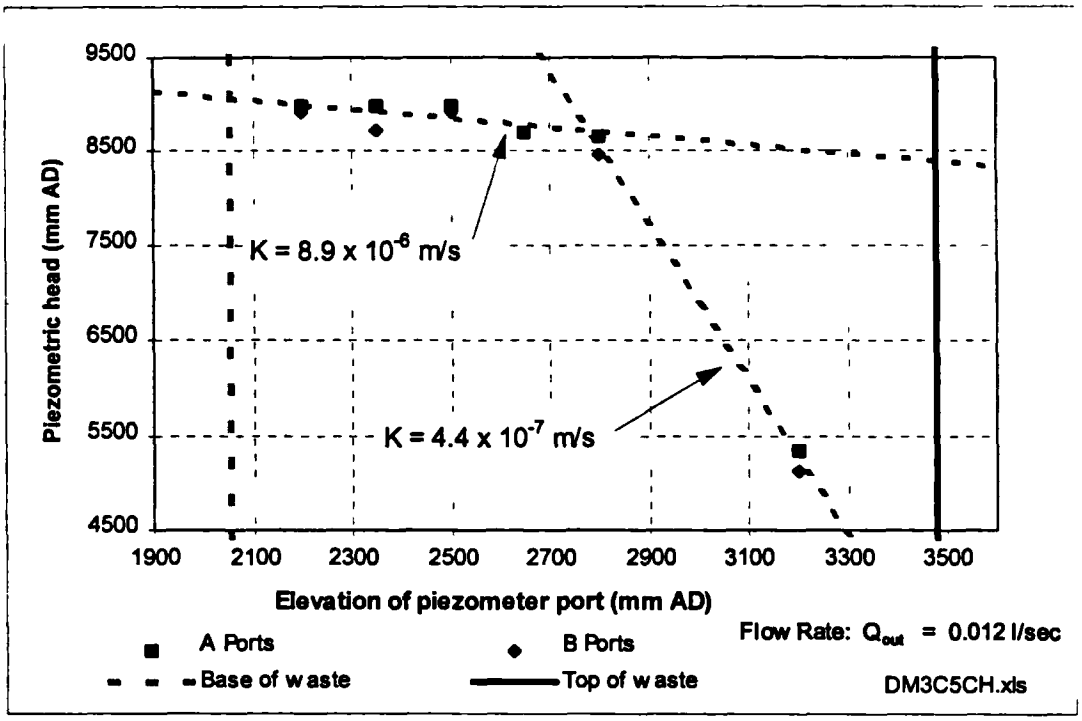

Figure 5.32 **Constant head hydraulic conductivity test on DM3 at an applied stress of 603 kPa**

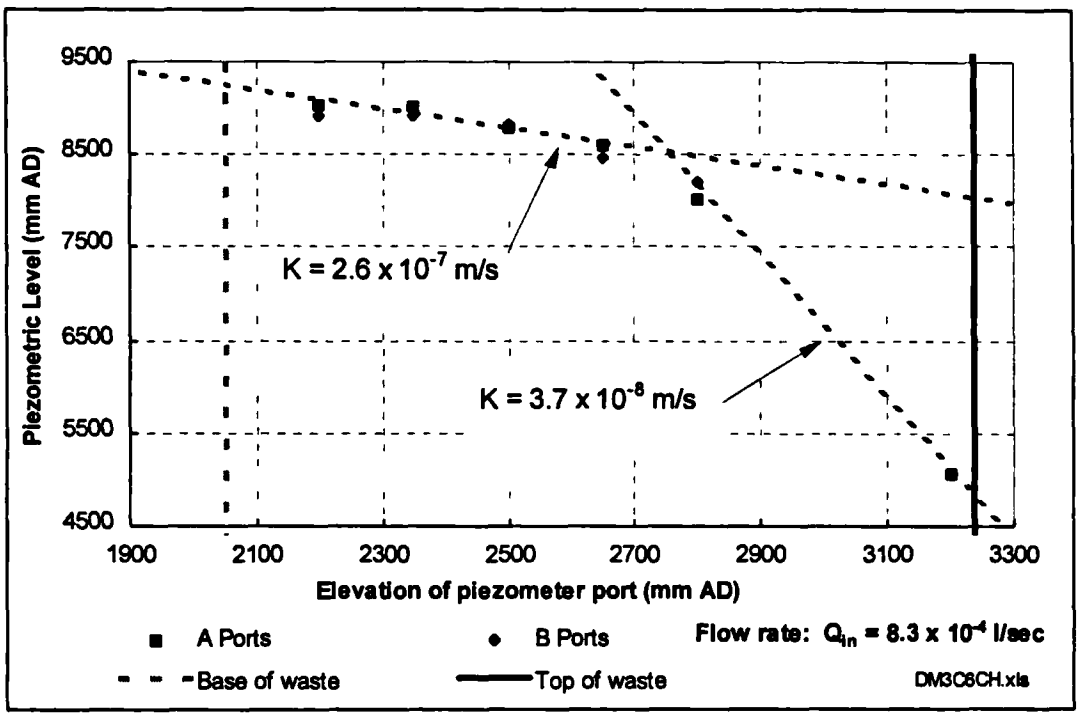

Table 5.11 Hydraulic conductivity of DM3 at varying applied stresses

Stage	Applied Stress kPa	Hydraulic Conductivity m/s	Comment
DM3C1	40	$3.4x10^{-5}$	Upper 0.8 m of waste in cell
	40	$1.5x10^{-4}$	Lower 1.0 m of waste in cell
DM3C2	87	$1.9x10^{-5}$	Upper 0.8 m of waste in cell
	87	$8.2x10^{-5}$	Lower 1.0 m of waste in cell
DM3C3	165	$3.1x10^{-6}$	Upper 0.6 m of waste in cell
	165	$2.8x10^{-5}$	Lower 0.9 m of waste in cell
DM3C5	322	$4.4x10^{-7}$	Upper 0.6 m of waste in cell
	322	$8.9x10^{-6}$	Lower 0.9 m of waste in cell
	322	$8x10^{-7}$	Average for all waste in cell[#]
DM3C6	603	$3.7x10^{-8}$	Upper 0.4 m of waste in cell
	603	$2.7x10^{-7}$	Lower 0.8 m of waste in cell
	603	$1x10^{-7}$	Average for all waste in cell[#]

[#] Hydraulic conductivity based on average hydraulic gradient across all waste in cell.

5.6 Pulverised waste (Test series PV1)

Pulverised or processed waste was tested in the compression cell between August 1993 and April 1994 and was designated a test code PV1. A compression test, in which the applied stress was increased in stages, was carried out on the waste after its water content had been raised to field capacity. The hydrogeological properties of the waste were determined at the end of each compression stage.

5.6.1 Waste Source

A pulverised, or processed, waste stream was obtained from Reprotech Ltd's waste pelletising plant at Pebersham, East Sussex in August 1994. Crude domestic waste was received at the plant and passed over a 50 mm screen to remove fines. The remaining fraction was then passed over a 130 mm screen. Material which was held back on this screen was passed through a hammer mill and then over a 140 mm screen. The material which passed through this final screen was combined with the 50 to 130 mm fraction to create a composite waste mix which was used in the tests. Therefore, this material did not include the fines screened out at the beginning of the process or any material which could not be pulverised to a size below 140 mm.

5.6.2 Waste characterisation

Approximately 300 kg of the processed waste stream was sent to Warren Spring Laboratory for compositional/ size analysis. The results of this analysis are presented in Table 5.12.

5.6.3 Loading of waste into compression cell

The waste was received from Reprotech in two covered skips, containing 1.94 and 2.54 tonnes respectively. The waste was combined on a hardstanding and then split into three fractions. One fraction was loaded into the compression cell, a second was sent to Warren Spring Laboratory for analysis, and the remainder was placed in a covered skip to be stored for subsequent testing (PV2).

A total of 2,400 kg of waste was placed in the cell to a total depth of approximately 2.13 metres. The top and bottom gravel layers were both 200 mm deep. Three earth pressure cells were installed in the waste. Cell 013 was installed in the lower gravel layer, Cell 014 in the middle of the waste and Cell 015 in the top of the waste. Unfortunately, no details were kept of the exact position of the cells, although Cell 015 was probably located within the top 250 mm of waste.

The reliability of the load cell readings throughout the tests on PV1 are questionable (see Section 3.6.2). There were a number of instances when the load cell readings jumped (sometimes by 200-300 kg) without any change in the contents of the cell. However, when the compression cell was emptied at the end of the PV1 set of tests, the load cells gave a reading of -1,238 kg. This negative value represents the mass of the lower gravel layer in the cell as the load cells were zeroed just prior to waste being loaded into the cell. The depth of the upper and lower gravel layers was approximately the same (200 mm) so the mass of the two layers should also have been approximately the same. The mass of the upper gravel layer was 1,375 kg (recorded as the tare weight) and this is similar to the above value of 1,238 kg for the lower gravel layer. It can be concluded that, whereas at any particular moment in time the load cell readings may have been recording an error of perhaps as much as ±150 kg, there is no evidence of a consistent drift in the readings over time.

Table 5.12 Size and category analysis of waste used in tests PV1 and PV2

CATEGORY ASSAY %

Size mm	Wt %	Pa/Cd	PIF	DP	Tx	Mc	Mnc	Gl	Put	Fe	nFE	<10
+160	7.7	29.2	28.6	8.7	29.0	4.1	-	-	0.3	-	-	-
-160+80	34.1	40.2	12.0	12.0	3.6	6.8	-	-	0.3	23.4	1.7	-
-80+40	34.4	56.2	5.3	7.0	6.5	3.6	1.6	-	15.0	2.1	2.8	-
-40+20	13.3	76.9	1.2	2.9	0.2	4.3	1.4	6.8	5.3	1.0	-	-
-20+10	5.2	65.4	0.5	4.6	-	2.8	6.9	6.9	9.2	2.8	0.9	-
-10	5.2	-	-	-	-	-	-	-	-	-	-	100.0
Total	100.0	49.0	8.3	7.8	5.7	4.6	1.1	1.3	6.5	9.0	1.6	5.2

CATEGORY DISTRIBUTION

Size mm	Pa/Cd	PIF	DP	Tx	Mc	Mnc	Gl	Put	Fe	nFe	<10
+160	4.6	26.5	8.6	39.0	6.9	-	-	0.4	-	-	-
-160+80	28.0	49.4	57.3	21.5	50.6	-	-	1.7	89.0	36.1	-
-80+40	39.5	22.0	31.0	39.0	26.8	50.0	-	79.6	7.9	60.9	-
-40+20	20.9	1.9	5.0	0.5	12.5	16.8	71.6	10.9	1.5	-	-
-20+10	7.0	0.3	3.1	-	3.2	33.3	28.4	7.4	1.6	3.0	-
-10	-	-	-	-	-	-	-	-	-	-	100.0
Total	100.0	100.0	100.0	100.0	100.0	100.0	100.0	100.0	100.0	100.0	100.0

Water Content (WC_{wet}) of Refuse = 28.8%

Key

Pa/Cd	Paper and card	Mc	Miscellaneous Combustibles	Fe	Ferrous metal
PIF	Plastic Film	Mnc	Misc' Non combustibles	nFe	Non Ferrous Metal
DP	Dense plastics	Gl	Glass	<10	Material <10 mm size
Tx	Textiles	Put	Putrescibles		

5.6.4 Absorptive capacity

The absorptive capacity of the waste was determined prior to the waste being compressed.

Corrected load cell reading at end of loading	2,400 kg
Corrected load cell reading at start of PV1C1COM following saturation and draining of waste	3,617 kg
Amount of water retained	1,217 litres
Mass of waste at original WC_{wet} = 28.8%	2,400 kg
Dry mass of waste	1,709 kg
Total absorptive capacity of waste at a bulk density of 0.54 t/m^3	507 litres/tonne

5.6.5 Changes in average waste density in response to changes in applied stress

The waste was subjected to six stages of compression, with applied stresses of 40, 87, 165, 244, 322 and 603 kPa. During compression, the waste was maintained under conditions which allowed gravity drainage.

The final average dry density of the waste at the end of each compression stage is recorded in Table 5.13 and increased from 0.26 to 0.60 t/m^3.

Table 5.13 Changes in dry density and water content at field capacity of PV1

Stage	Applied Stress (kPa)	Status[1]	Wet mass of waste at end of stage[2] (kg)	Change in water held in waste in stage[2] (litres)	ρ_{dry} at end of stage (t/m^3)	WC_{dry} at end of stage (%)	WC_{wet} at end of stage (%)	WC_{vol} at end of stage (%)
0	-	Loading	2400	0	0.26	40.4[3]	28.8[3]	10.4[3]
0	-	S&D	3617	+1217	0.26	111.6	52.8	28.6
1	40	Comp'n	3540	-77	0.30	107.1	51.7	32.1
1	40	S&D	3516	-24	0.31	105.7	51.4	32.5
2	87	Comp'n	3368	-148	0.35	97.1	49.3	33.8
2	87	S&D	3465	+97	0.35	102.8	50.7	35.9
3	165	Comp'n	3119	-346	0.41	82.5	45.2	34.1
3	165	S&D	2894	-225	0.45	69.3	40.9	31.0
4	322	Comp'n	2672	-222	0.50	56.3	36.0	28.1
4	322	S&D	2680	+8	0.53	56.8	36.2	30.2
5	603	Comp'n	2662	-18	0.60	55.8	35.8	33.5

[1] S&D indicates that waste was saturated and then drained to field capacity during stage.
[2] Change in water content of waste determined by load cell readings. Some inaccuracies in method due to drift in load cell readings.
[3] Not at field capacity.

5.6.6 Water content at field capacity

The changes in the water content of the waste at field capacity throughout the various stages of compression are also summarised in Table 5.13. Water was squeezed out of waste during each compression stage, reducing the water content (WC_{dry}) at field capacity from approximately 112% to 56% as the density of the waste increased.

Changes in the volumetric water content (WC_{vol}) at field capacity did not follow a clear downward trend, but fluctuated within a relatively narrow range of 29 to 36%.

5.6.7 Differential compression (String data)

Differential compression was measured at various depths within the waste at applied stresses of 40, 87, 165, 322 and 603 kPa, using strings inserted into the waste through piezometer ports. The differential compression of the waste measured in this way for each compression stage is shown in Figures 5.33 to 5.37.

Figure 5.33 Differential compression of waste PV1 at applied stress of 40 kPa

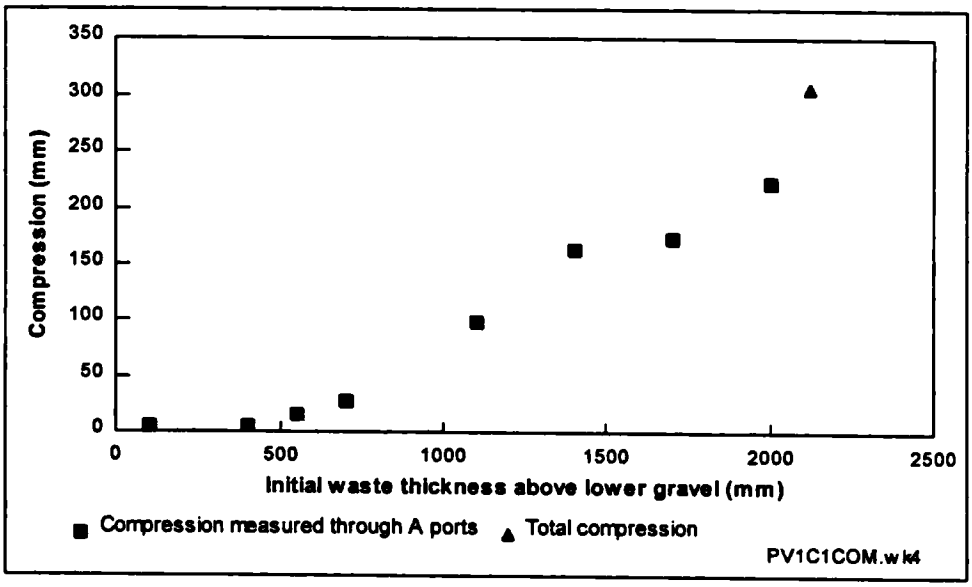

Figure 5.34 Differential compression of waste PV1 at applied stress of 87 kPa

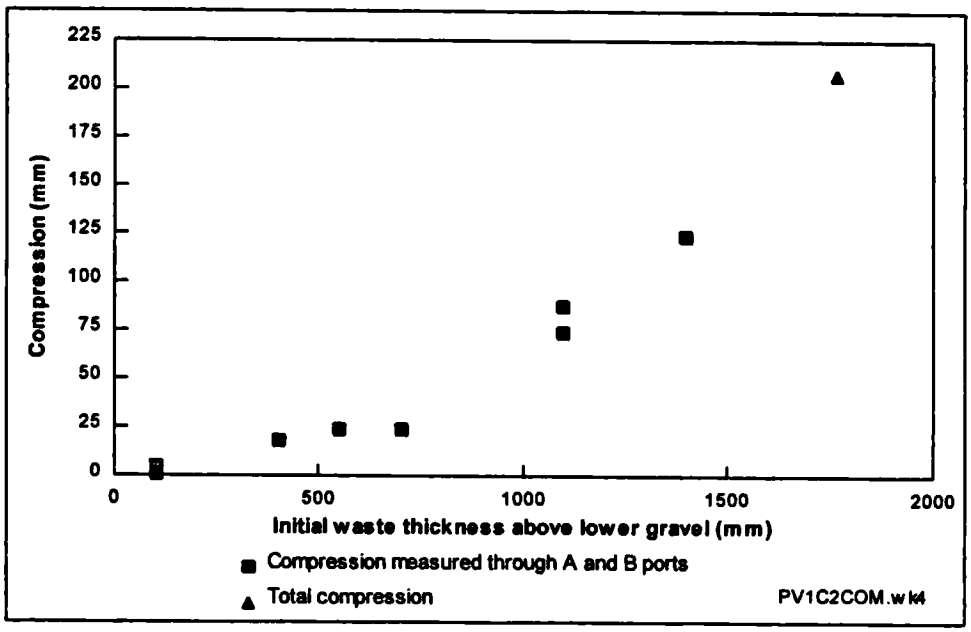

Figure 5.35 Differential compression of waste PV1 at applied stress of 165 kPa

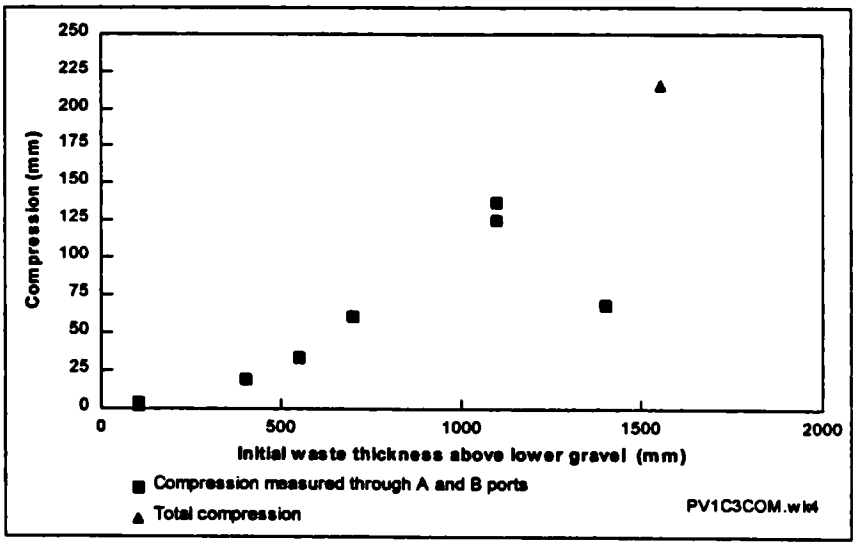

Figure 5.36 Differential compression of waste PV1 at applied stress of 322 kPa

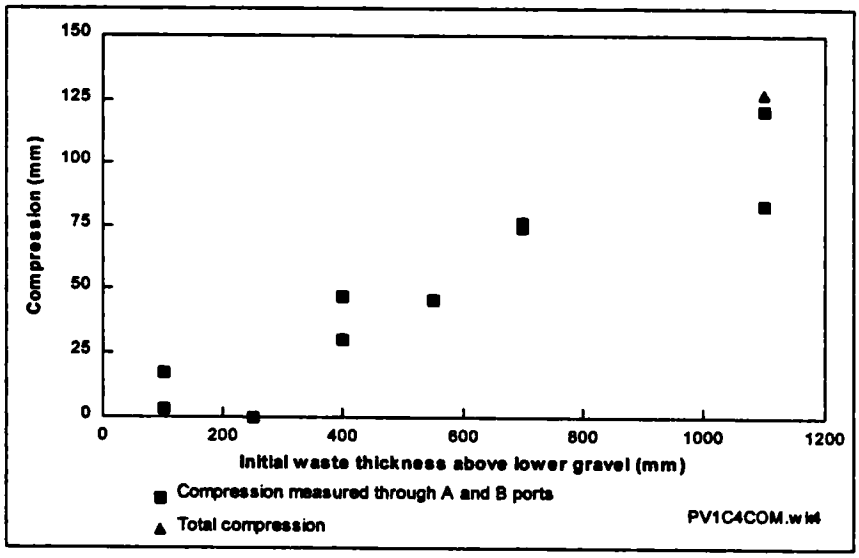

Figure 5.37 Differential compression of waste PV1 at applied stress of 603 kPa

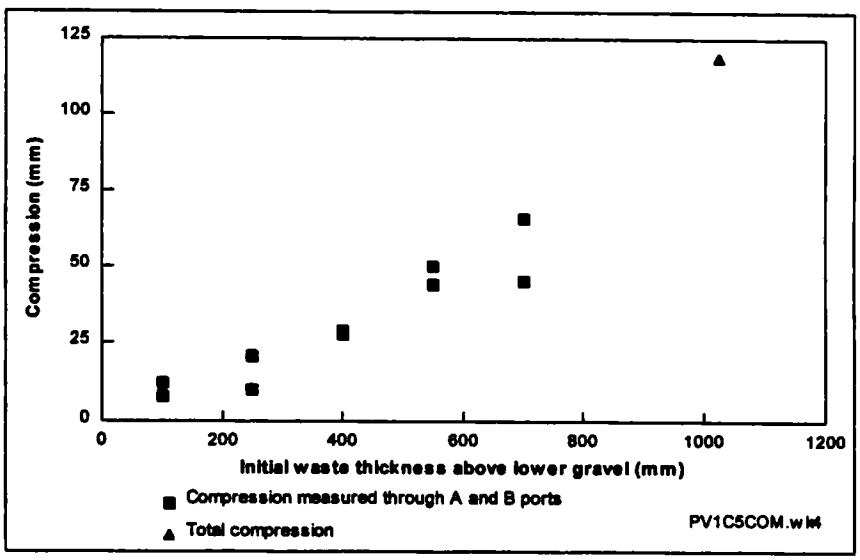

5.6.8 Total stress cell data

The maximum total vertical stress recorded by the three earth pressure cells during the six stages of compression is shown on Figure 5.38. The results are considered further in Chapter 6.

Figure 5.38 Maximum total stress recorded during each compression stage of PV1

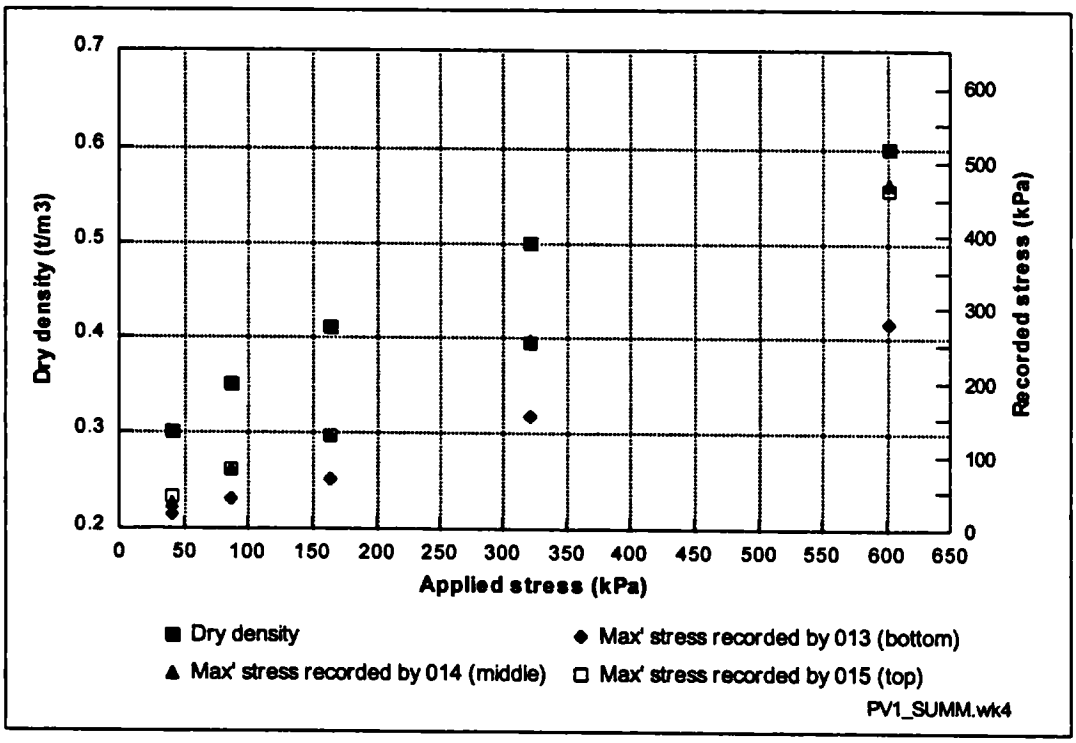

5.6.9 Effective porosity

The effective porosity of the waste was determined after compression at applied stresses of 40, 87, 165 and 322 kPa. Figures 5.39 to 5.43 show the most reliable test undertaken at any particular applied stress; results from other tests are summarised in Table 5.14. It was not possible to obtain a value of effective porosity at an applied stress of 603 kPa as the waste appeared to be fully saturated after the compression stage (piezometers were registering readings) and the low permeability of the waste prevented draining.

The results indicate a reduction in effective porosity at higher applied stresses. The effective porosity reduced from approximately 28% at zero applied load to 2% at an applied stress of 322 kPa.

Figure 5.39 Effective porosity determination of PV1 with no confining stress

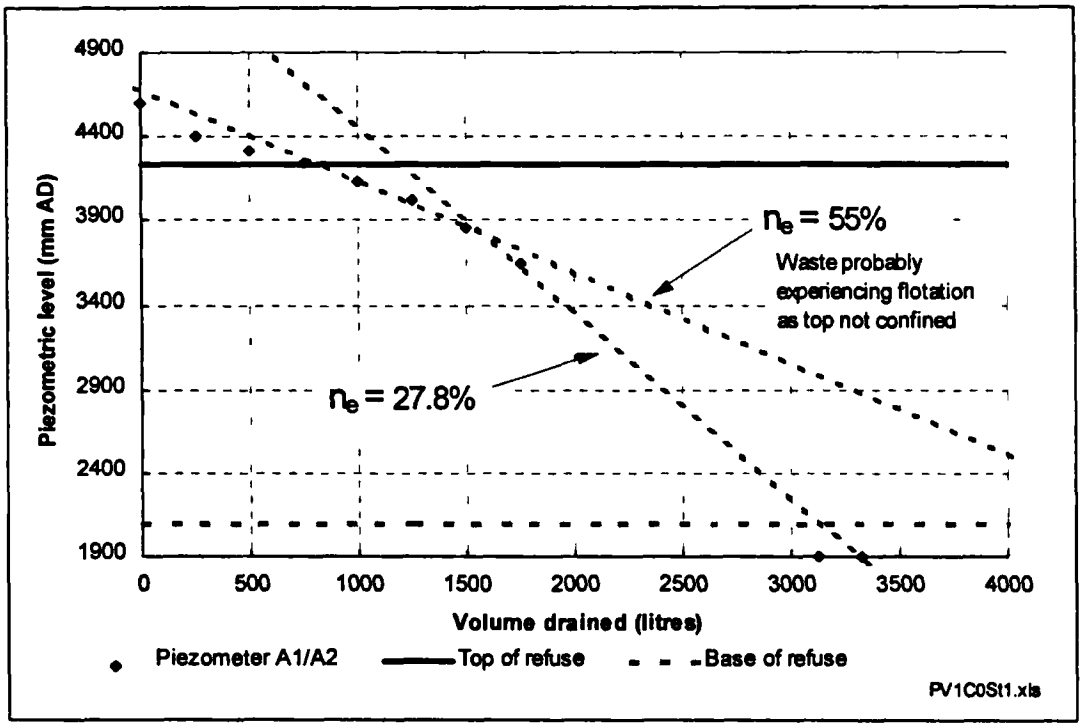

Figure 5.40 Effective porosity determination of PV1 at an applied stress of 40 kPa

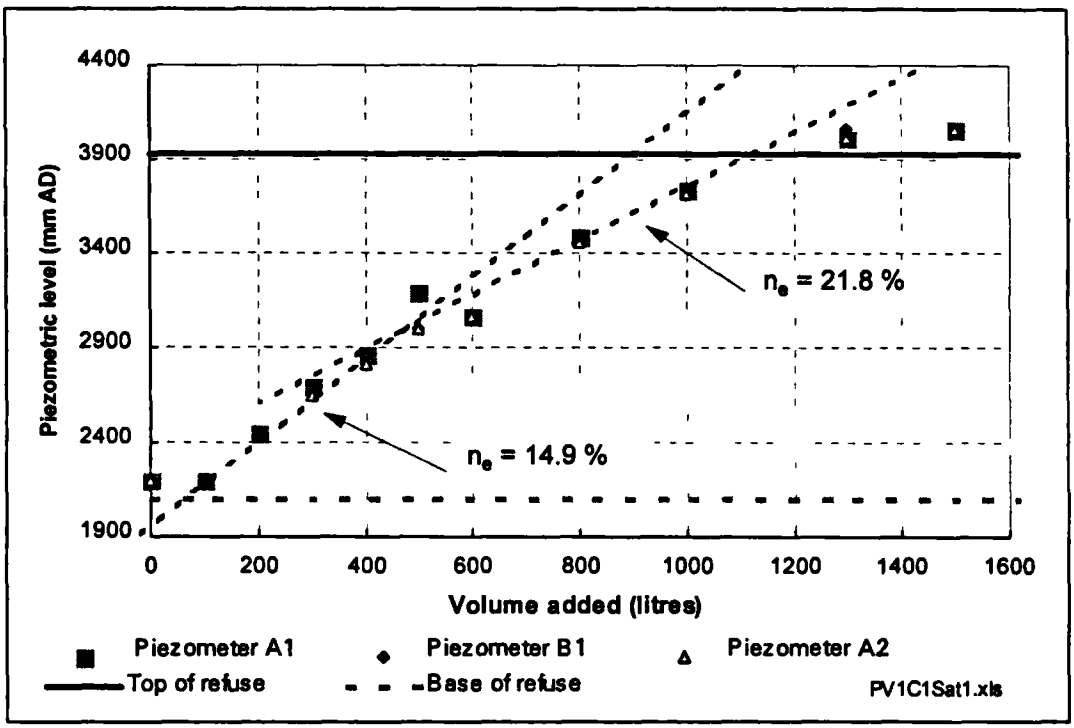

Figure 5.41 **Effective porosity determination of PV1 at an applied stress of 87 kPa**

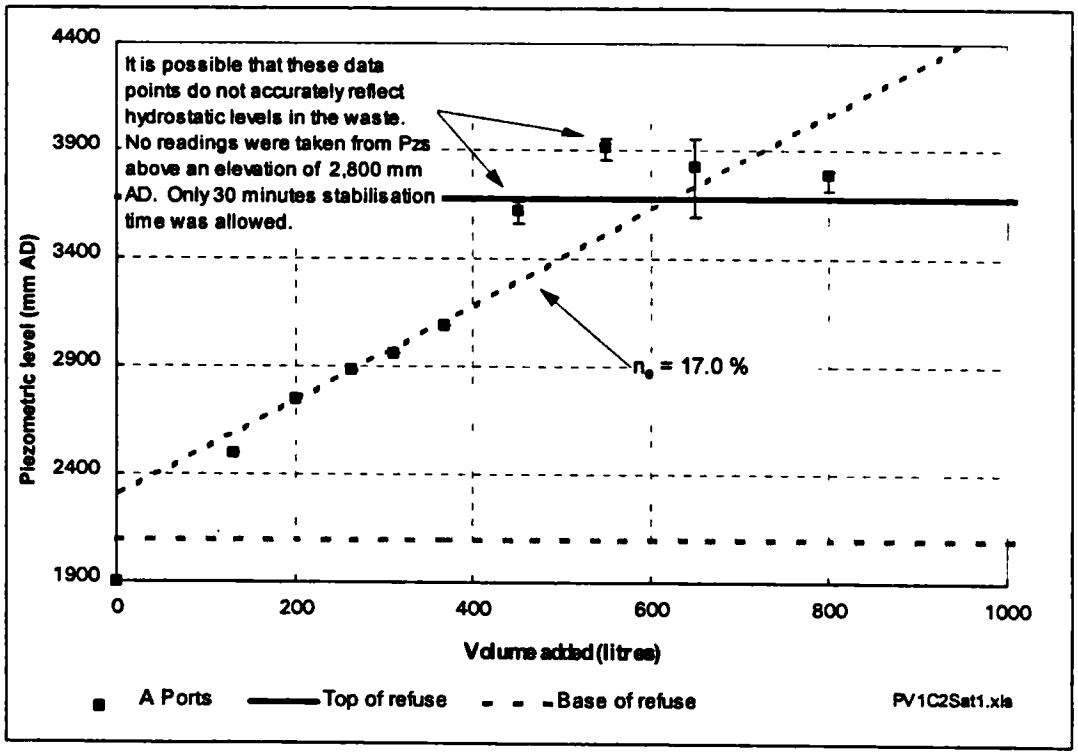

Figure 5.42 **Effective porosity determination of PV1 at an applied stress of 165 kPa**

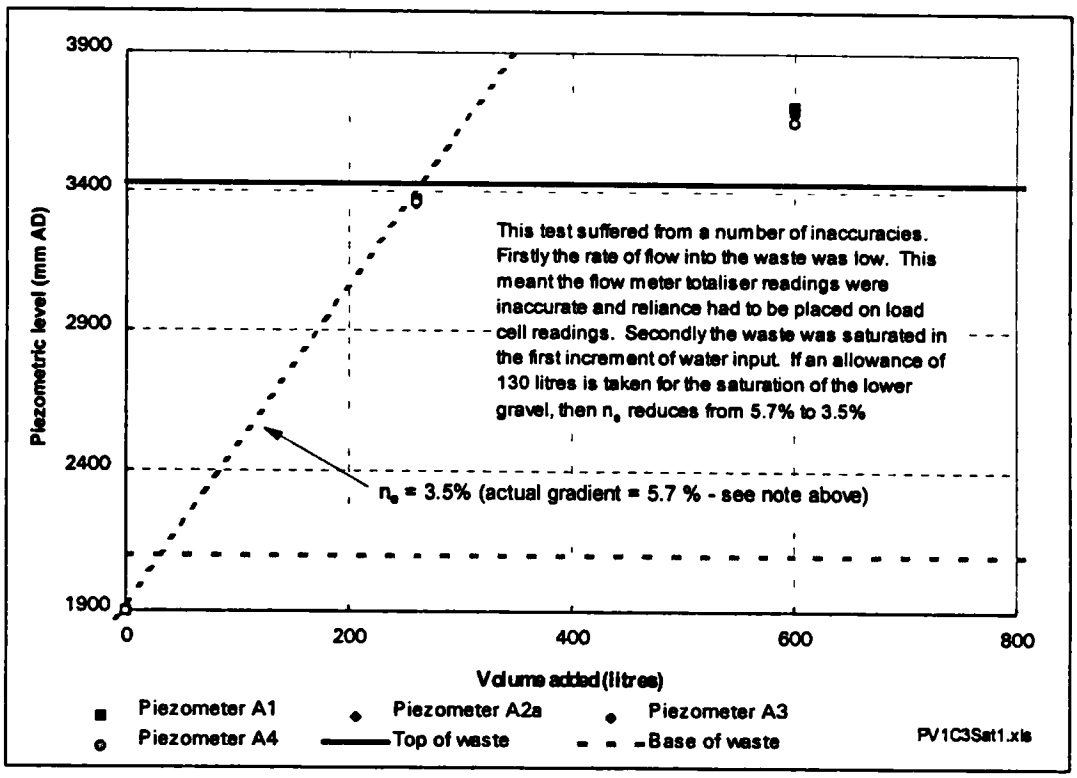

Figure 5.43 Effective porosity determination of PV1 at an applied stress of 322 kPa

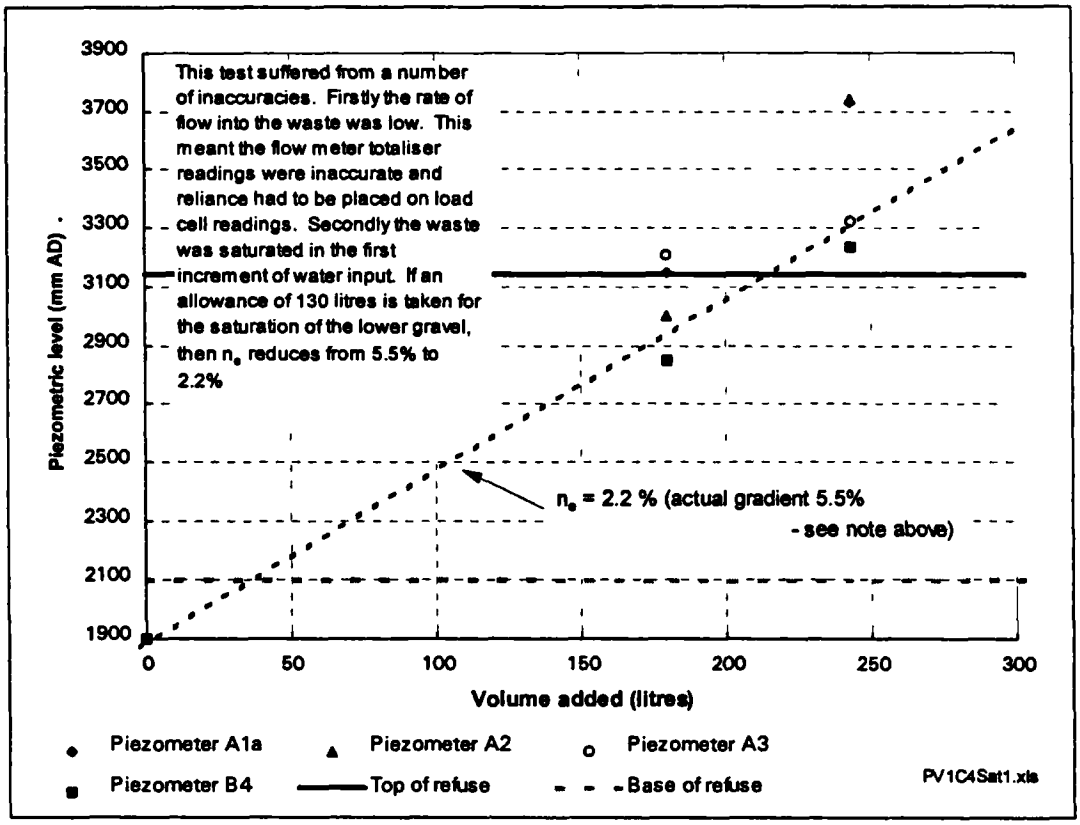

Table 5.14 Effective porosity of PV1 at varying applied stresses

Stage	Test Type	Applied Stress kPa	Effective Porosity %	Comment
PV1C0St1	Fill	0	N/D	Total storage capacity = 60.3% - flotation
PV1C0St1	Drain	0	55	Top 0.5 metres of waste - flotation
PV1C0St1	Drain	0	**27.8**	Bottom 1.5 metres of waste
PV1C1St1	Fill	40	**21.8**	Value for top of waste
PV1C1St1	Fill	40	14.9	Value for bottom of waste.
PV1C1St1	Drain	40	23.0	Average value for all waste in cell.
PV1C2St1	Fill	87	**17.0**	Average value for all waste in cell.
PV1C2St1	Drain	87	12.5	Average value for all waste (Drainage time probably not long enough)
PV1C3St1	Fill	165	**3.5**	Average value for all waste in cell.
PV1C4St1	Fill	322	**2.2**	Average value for all waste in cell
PV1C5St	-	603	**<1**	Waste would not drain

Values in **bold** considered to be most reliable values

5.6.10 Hydraulic conductivity

The vertical hydraulic conductivity of the waste was determined after compression at applied stresses of 40, 87, 165, 322 and 603 kPa.

Graphs of piezometric head plotted against elevation are shown in Figures 5.44 to 5.49 for each of the compression stages.

The vertical hydraulic conductivity of the waste reduced by three orders of magnitude from approximately $3x10^{-5}$ m/s at an applied stress of 40 kPa to less than $4.8 x10^{-8}$ m/s at an applied stress of 603 kPa (see Table 5.15).

There was little evidence of any significant variation in hydraulic gradient and, therefore, hydraulic conductivity with depth in the waste.

Table 5.15 Hydraulic conductivity of PV1 at varying applied stresses

Stage	Applied Stress kPa	Hydraulic Conductivity m/s	Comment
PV1C0	0	$3.3x10^{-4}$	No confining load and waste may have been experiencing flotation
PV1C1	40	$3.4x10^{-5}$	Average for all waste in cell
PV1C2	87	$1.2x10^{-5}$	Average for all waste in cell
PV1C3	165	$2.4x10^{-6}$	Average for all waste in cell
PV1C4	322	$\sim 2x10^{-7}$	Average for all waste in cell
PV1C5	603	$<4.8x10^{-8}$	Average for all waste in cell

Figure 5.44 **Constant head hydraulic conductivity test on PV1 with no confining stress**

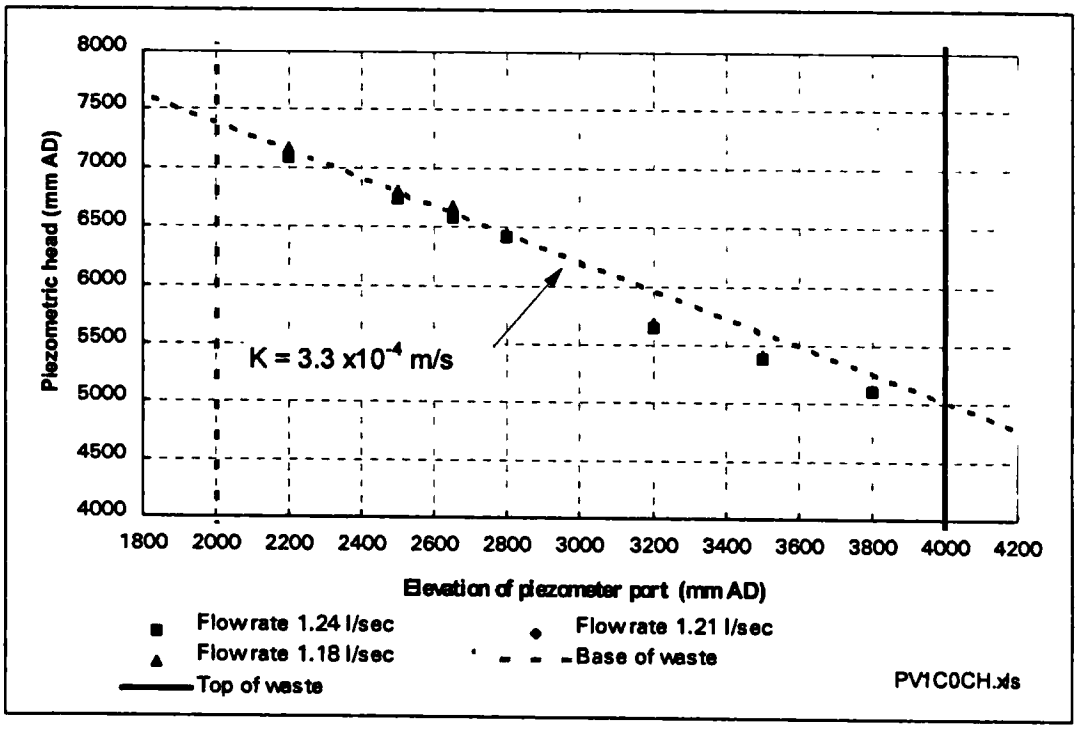

Figure 5.45 **Constant head hydraulic conductivity test on PV1 at an applied stress of 40 kPa**

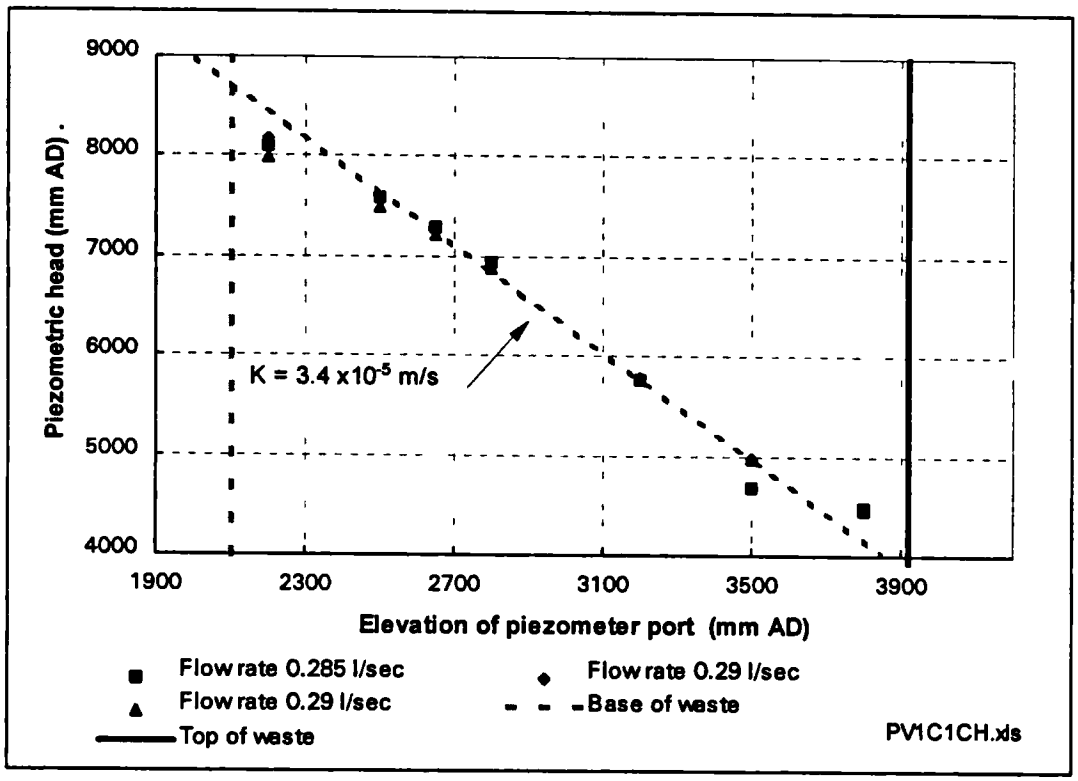

Figure 5.46 **Constant head hydraulic conductivity test on PV1 at an applied stress of 87 kPa**

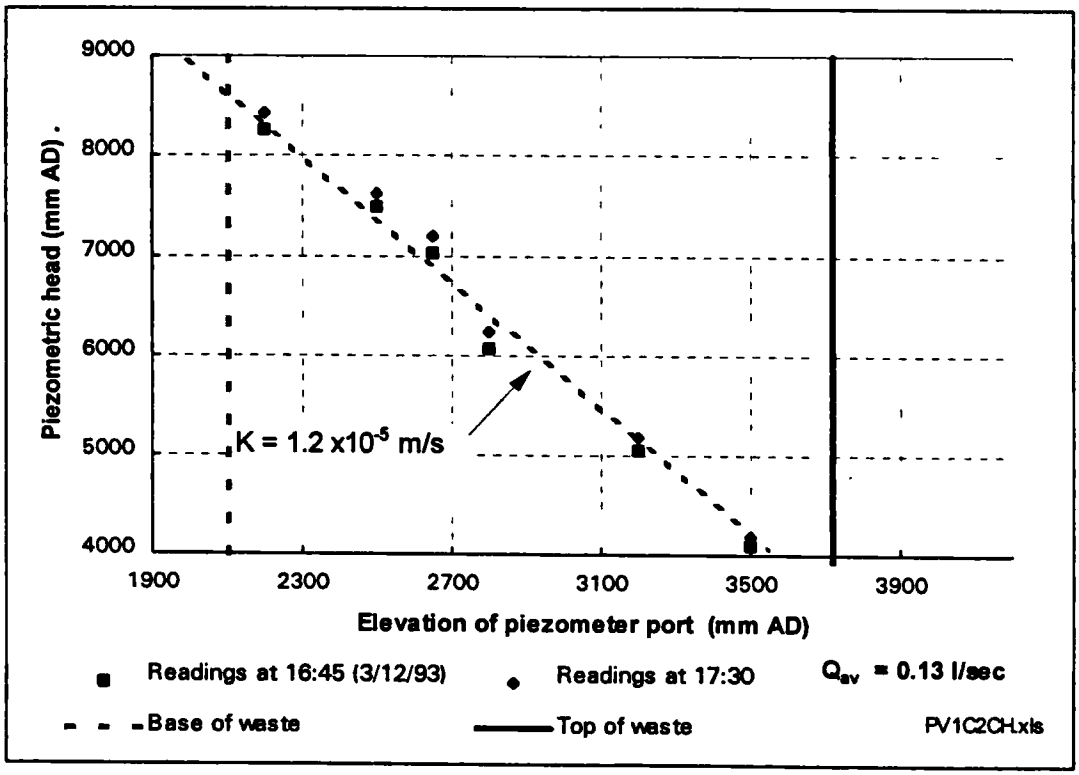

Figure 5.47 **Constant head hydraulic conductivity test on PV1 at an applied stress of 165 kPa**

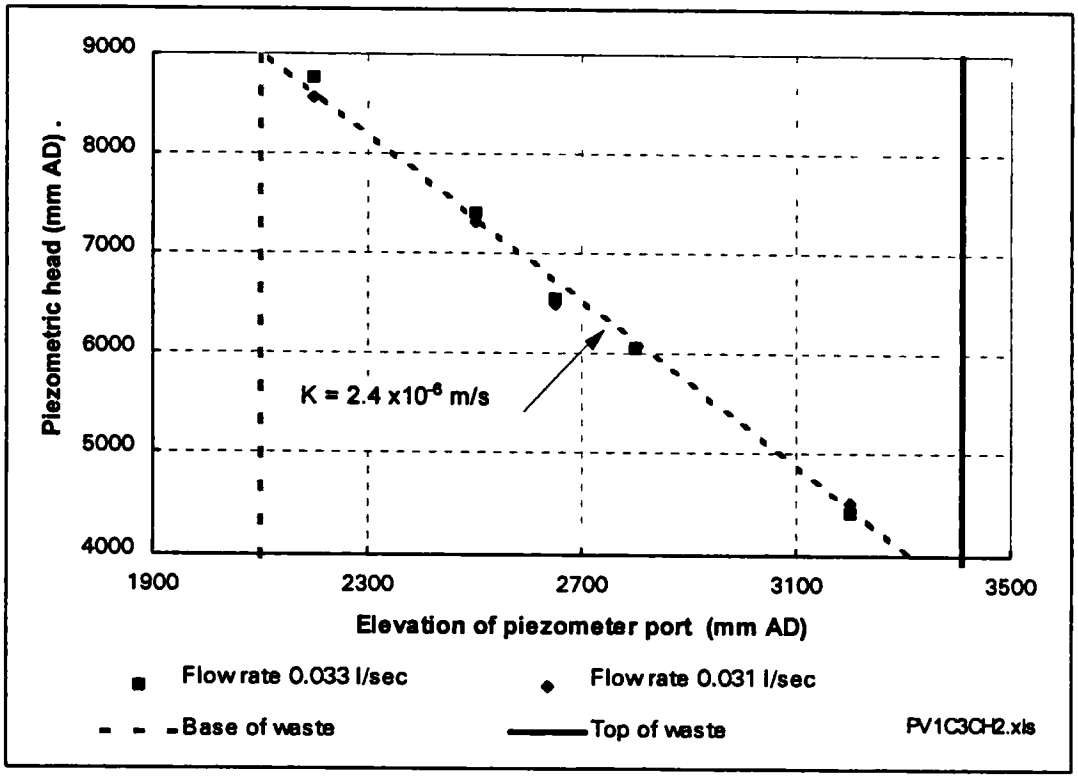

Figure 5.48 **Constant head hydraulic conductivity test on PV1 at an applied stress of 322 kPa**

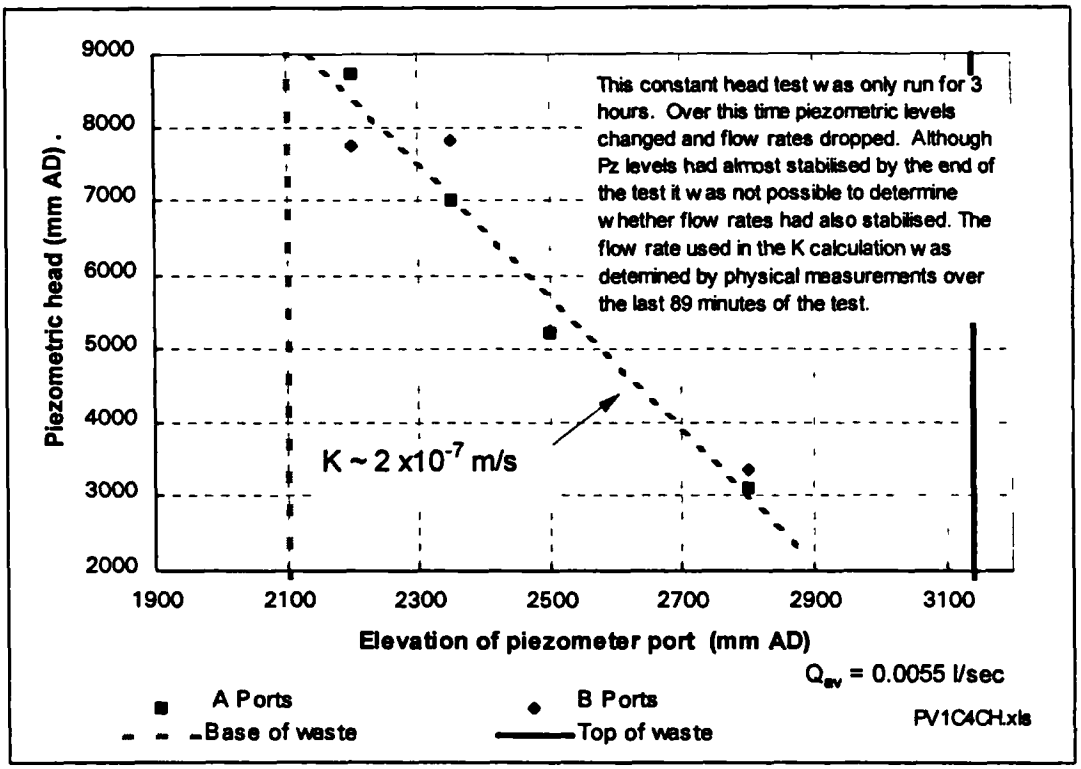

Figure 5.49 **Constant head hydraulic conductivity test on PV1 at an applied stress of 603 kPa**

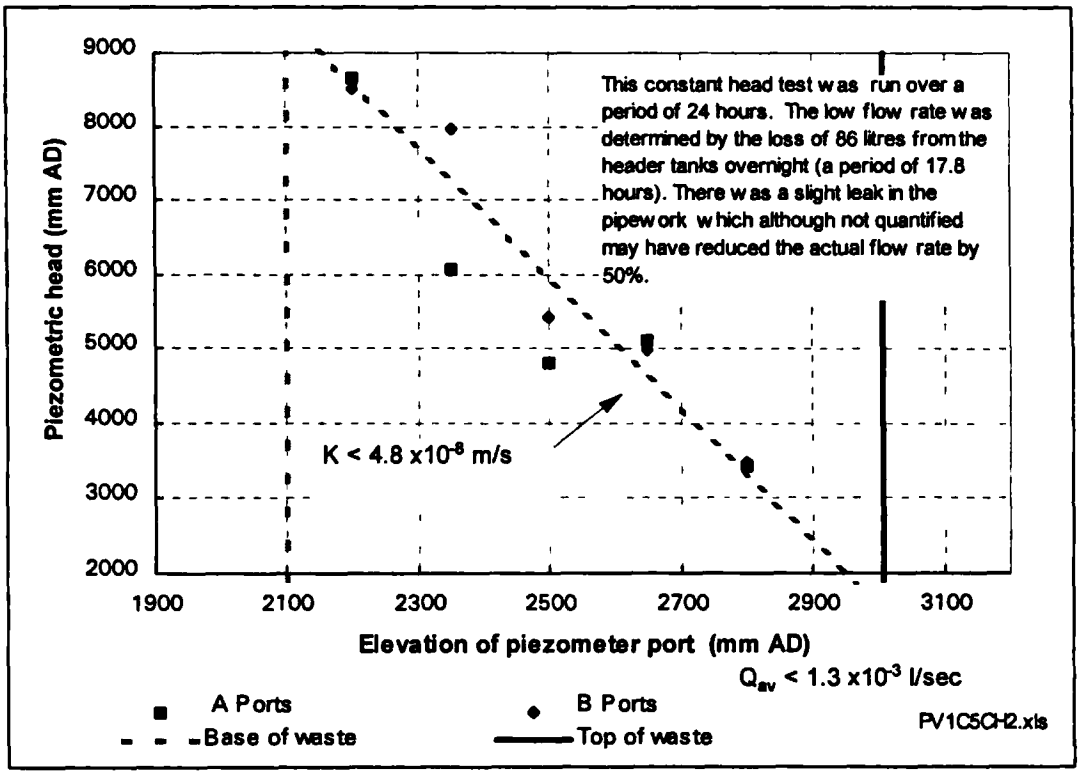

5.7 Pulverised waste (Test series PV2)

5.7.1 Waste Source

Waste type PV2 was obtained from the same source and at the same time as waste PV1 (Section 5.6.1). It was stored in a tarpaulin covered skip prior to use.

5.7.2 Waste characterisation

See Section 5.6.2 and Table 5.12 for the main material and size characterisation of the waste. Additional samples of the waste were taken just prior to loading into the compression cell and the water content (WC_{wet}) was re-determined as 39.7%.

5.7.3 Loading of waste into compression cell

A total of approximately 2,333 kg of waste was loaded into the compression cell on 15 August 1994. The waste was lightly compacted with the upper platen (in three stages) to an overall bulk density of 0.32 t/m^3. Three total pressure cells were installed in the waste at the positions shown in Figure 5.50.

Figure 5.50 The loading of waste PV2 into the compression cell

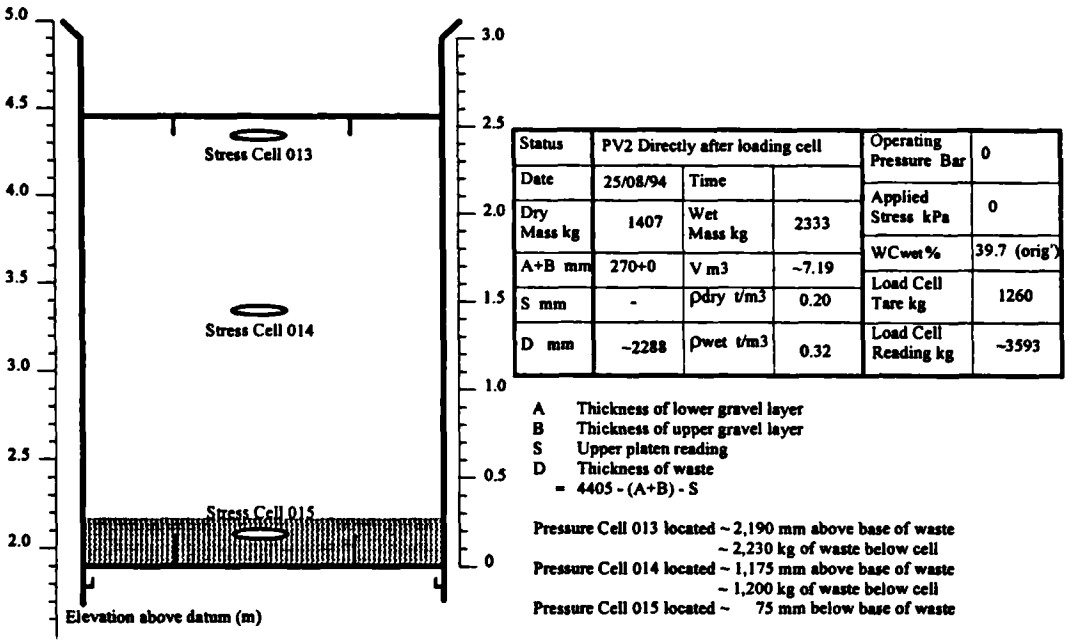

Status	PV2 Directly after loading cell			Operating Pressure Bar	0
Date	25/08/94	Time		Applied Stress kPa	0
Dry Mass kg	1407	Wet Mass kg	2333	WCwet %	39.7 (orig')
A+B mm	270+0	V m3	~7.19	Load Cell Tare kg	1260
S mm	-	ρdry t/m3	0.20	Load Cell Reading kg	~3593
D mm	~2288	ρwet t/m3	0.32		

5.7.4 Absorptive capacity

The absorptive capacity of the waste was not determined as no hydrogeological testing of the waste was undertaken until after compression at an applied stress of 603 kPa.

5.7.5 Changes in average waste density in response to changes in applied stress

The waste was subjected to five stages of compression, at applied stresses of 40, 87, 165, 322 and 603 kPa. During compression the waste was maintained under conditions which allowed gravity drainage.

The final average dry density of the waste at the end of each compression stage increased from 0.20 to 0.62 t/m^3, as recorded in Table 5.16.

Table 5.16 Changes in dry density of waste PV2 at different applied stresses

Stage	Applied Stress (kPa)	Status	Wet mass of waste at end of stage[1] (kg)	ρ_{dry} at end of stage (t/m^3)
0	-	Loading	2,333	0.20
1	40	Comp'n	2,002	0.28
2	87	Comp'n	2,161	0.35
3	165	Comp'n	2,293	0.41
4	322	Comp'n	2,303	0.51
5	603	Comp'n	1,913	0.62

[1] Waste (probably) not at field capacity
Change in water content of waste determined by load cell readings - some inaccuracies expected.
Some variations in wet mass expected as compression cell was open to the elements.

5.7.6 Water content at field capacity

The water content at field capacity was not determined at any stage during the testing of the sample.

5.7.7 Differential compression (String data)

The differential compression of the waste, measured using strings inserted through piezometer ports, is shown in Figures 5.51 to 5.55. Unlike tests on other wastes, the strings were not replaced in the piezometer ports at the start of each new compression stage.

Figure 5.51 Differential compression of waste PV2 at applied stress of 40 kPa

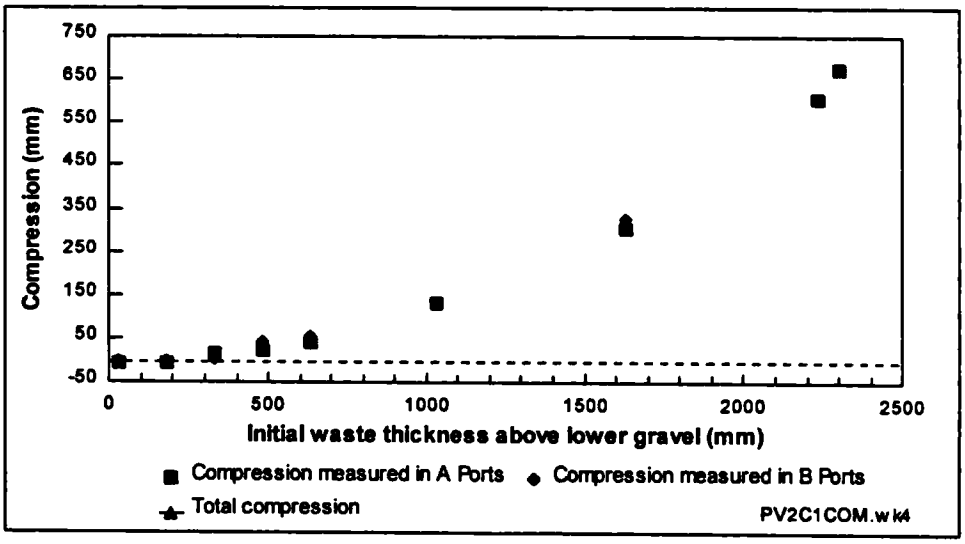

Figure 5.52 Differential compression of waste PV2 at applied stress of 87 kPa

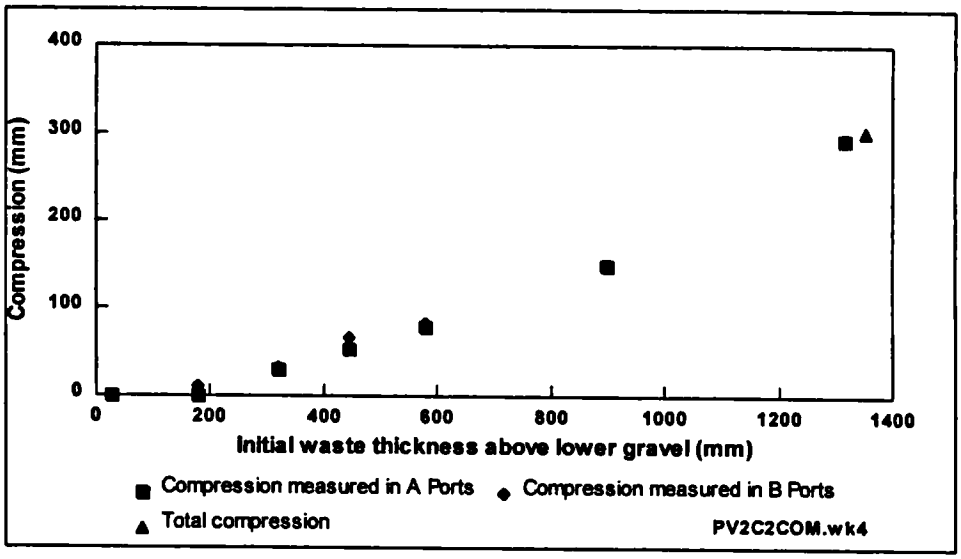

Figure 5.53 Differential compression of waste PV2 at applied stress of 165 kPa

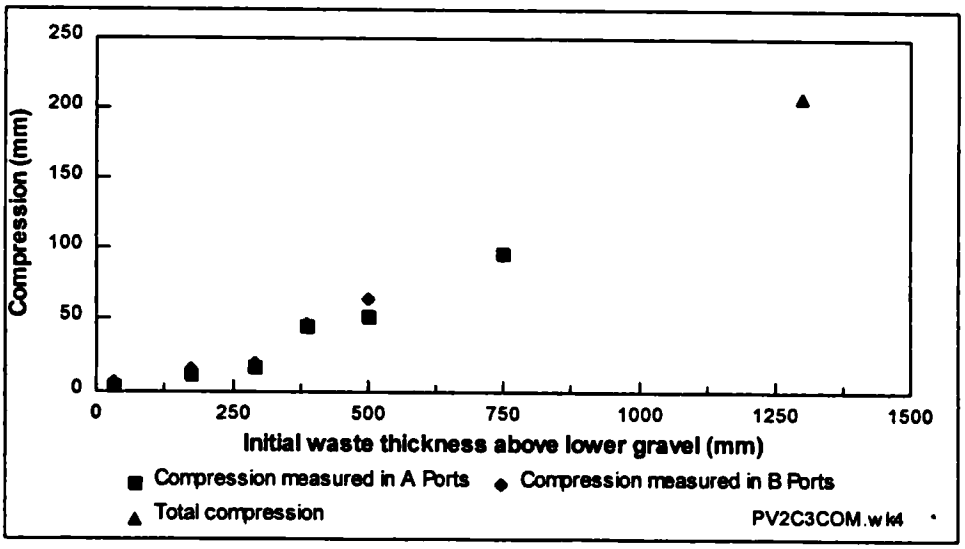

Figure 5.54 Differential compression of waste PV2 at applied stress of 322 kPa

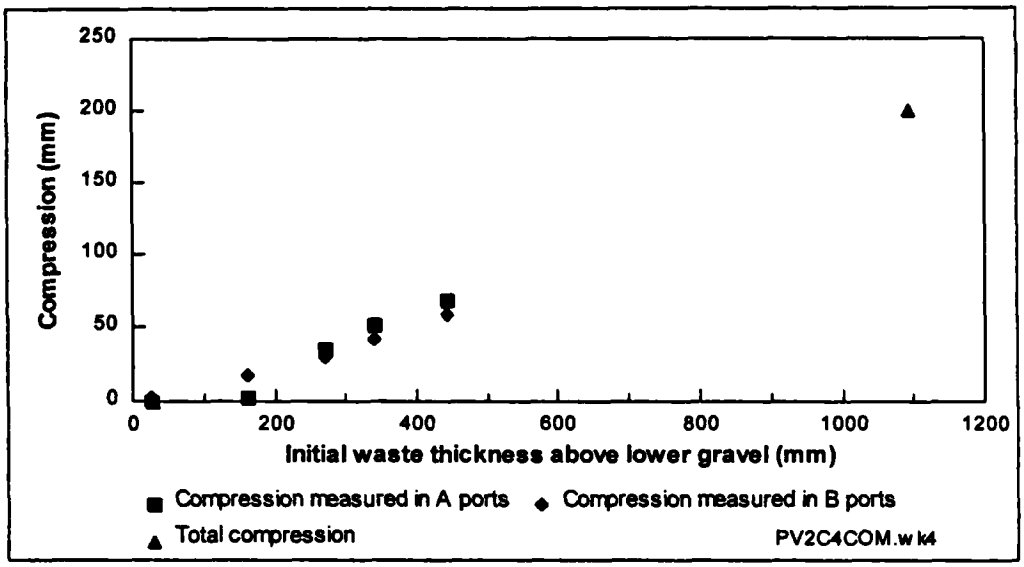

Figure 5.55 Differential compression of waste PV2 at applied stress of 603 kPa

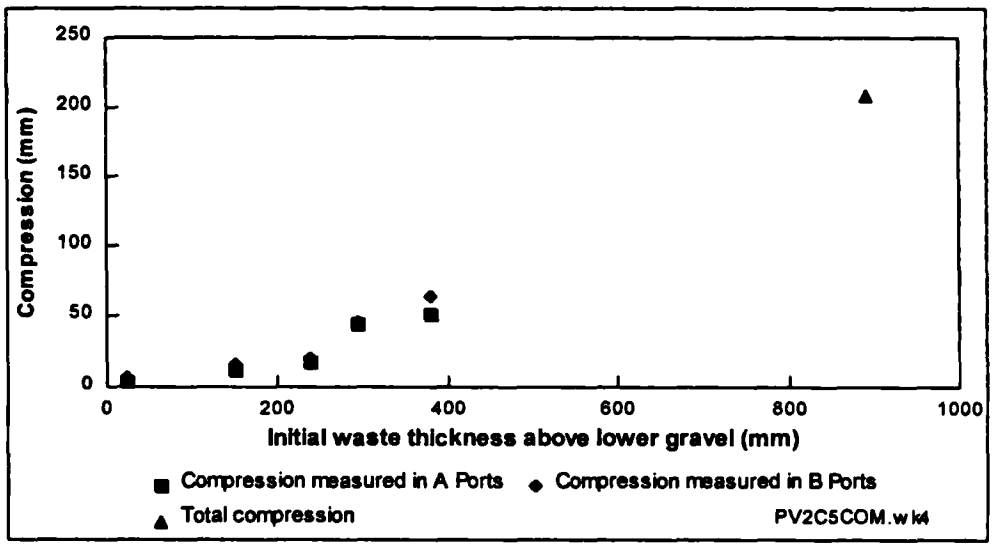

5.7.8 Total stress cell data

The maximum total vertical stress recorded by the three earth pressure cells during the five stages of compression is shown on Figure 5.56.

Figure 5.56 Maximum total stress recorded during each compression stage of PV2

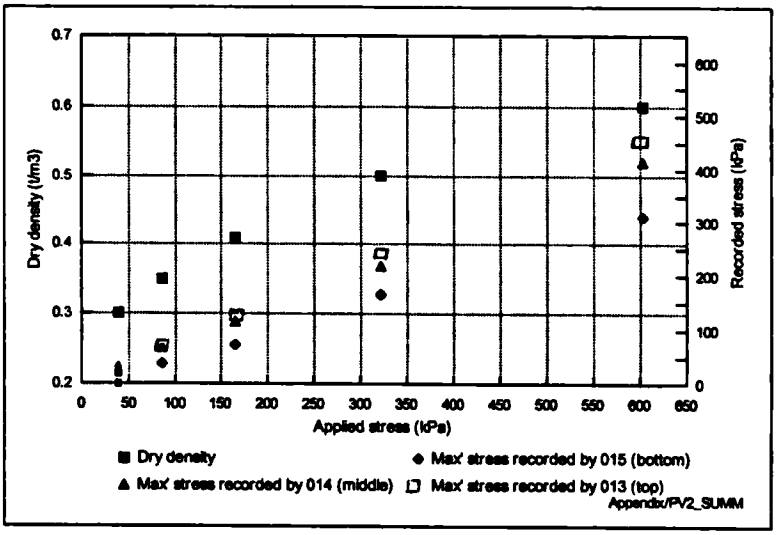

5.7.9 Effective porosity

Waste PV2 was saturated following compression at an applied stress of 603 kPa (see Figure 5.57). The total storage capacity of the lower 300 mm of waste was calculated as 7.9%. As the waste had not been brought up to field capacity before, it is not possible to know how much of the water added was being taken up as absorptive capacity and how much was filling drainable voids.

It was not possible to determine either the total storage capacity or the effective porosity of the upper part of the waste. The addition of water to increase the level of saturation above the bottom 300 mm of waste resulted in the development of elevated pore water pressures, which did not dissipate over a period of several days.

5.7.10 Hydraulic conductivity

The lack of dissipation of the elevated pore water pressures in the effective porosity test (Section 5.7.9) was indicative of low hydraulic conductivities in the upper part of the waste. This low hydraulic conductivity meant that the flow rate in a constant head permeability test was too low to be measured within the time available for the test. Therefore, a falling head analysis was undertaken (see Section 4.3.9), which indicated that the vertical hydraulic conductivity of the upper part of the waste was approximately 1×10^{-9} m/s (see Figure 5.58). This value was at least an order of magnitude lower than any other measurement of hydraulic conductivity. It is not certain whether there was a problem with the testing methodology (e.g. air locks in pipes) that contributed to the low value. However, in the absence of other supporting experimental evidence, little emphasis is placed on this hydraulic conductivity measurement in subsequent analyses in this thesis.

Figure 5.57 **Total Storage capacity of waste PV2 determined at an applied stress of 603 kPa**

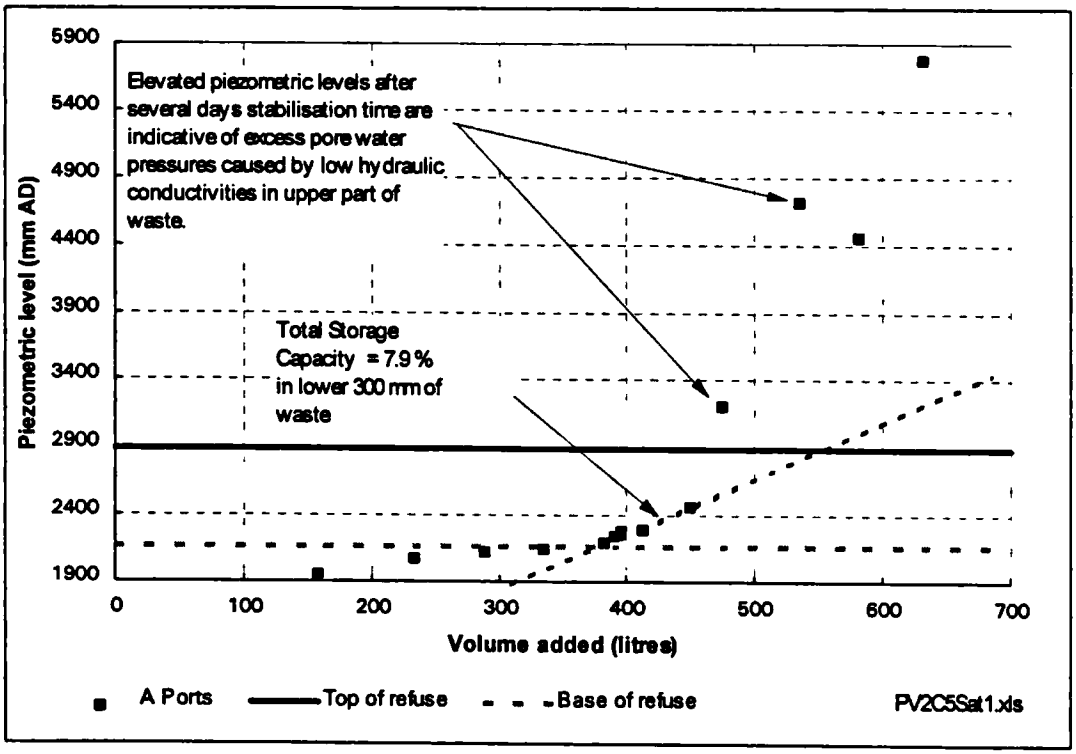

Figure 5.58 **Falling head hydraulic conductivity test for waste PV2 at an applied stress of 603 kPa**

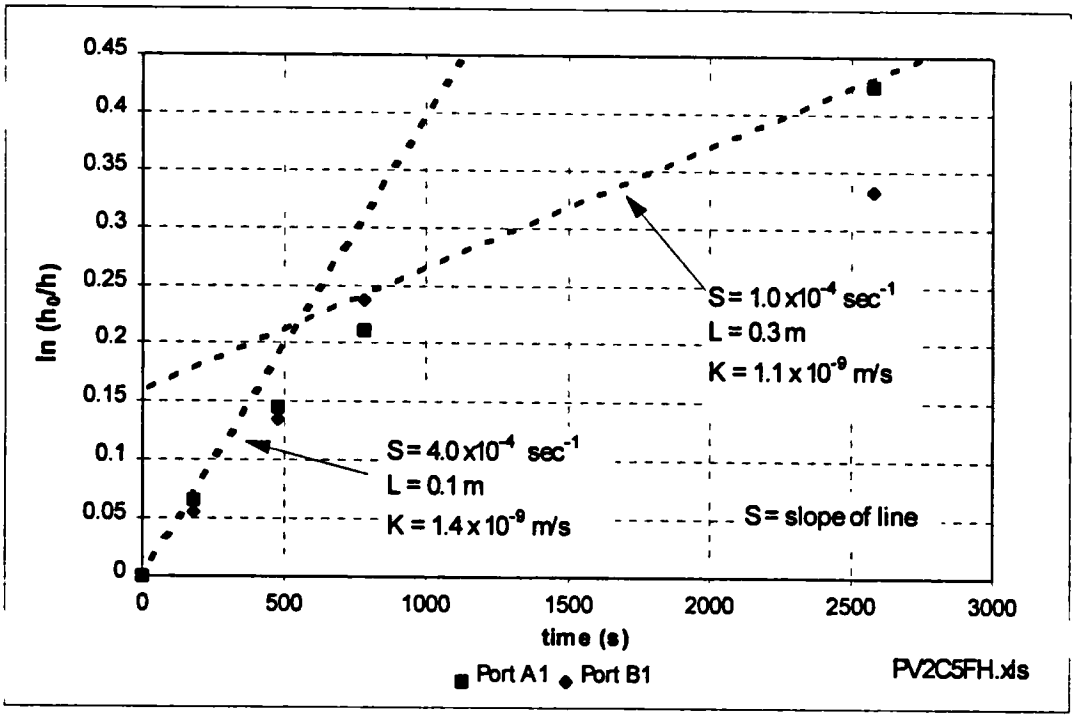

5.8 Aged waste (Test series AG1)

Aged waste was tested in the compression cell between July 1995 and January 1996 and was designated a test code AG1. The water content of the waste was raised to, and maintained at field capacity whilst the waste was subjected to a compression test in which the applied stress was increased in stages. The hydrogeological properties of the waste were determined at the end of each compression stage.

5.8.1 Waste Source

Approximately 10.2 tonnes of waste was excavated from Cleanaway Ltd's Rainham landfill site in Essex during early July 1995. An area of the site was chosen which was believed to contain domestic wastes at least 20 years old. The material excavated had the appearance of old household waste, with newspapers from 1964 being recovered. It was also noted that the material contained a large proportion of soil-like material.

5.8.2 Waste characterisation

A 3.74 tonne bulk sample of the waste was analysed by AEA Technology in early August 1995. The waste had a water content (WC_{wet}) of 41.6%. The results of the material classification are shown in Table 5.17. It was reported that the sample contained fragments of newspapers that were dated November 1976, and garden wastes in the form of leaves were clearly visible. The waste also contained a large proportion of fines (~34% by weight) which passed through a 10 mm sieve.

Table 5.17 Size and category analysis of waste used in tests AG1

CATEGORY ASSAY %												
Size mm	Wt %	Pa/Cd	PlF	DP	Tx	Mc	Mnc	Gl	Put	Fe	nFE	<10
+160	6.3	7.0	16.7	2.2	4.2	45.2	7.6	0.5	2.9	13.9	-	-
-160+80	10.8	26.7	8.8	5.6	3.7	32.9	-	8.8	1.3	12.2	-	-
-80+40	16.7	33.0	3.6	3.6	0.8	9.8	46	12.3	24.0	8.4	0.4	-
-40+20	18.1	19.9	1.4	2.1	0.0	5.9	2.5	16.1	50.3	1.8	0.0	-
-20+10	14.2	9.0	0.8	0.7	-	3.1	5.7	10.6	69.9	-	0.2	.
-10	33.9	-	-	-	-	-		-	-	-	-	100.0
Total	100.0	13.7	3.0	1.8	0.8	9.5	2.5	7.5	23.3	3.9	0.1	33.9

Water Content (WC_{wet}) of Refuse = 41.6%

Key					
Pa/Cd	Paper and card	Mc	Miscellaneous Combustibles	Fe	Ferrous metal
PlF	Plastic Film	Mnc	Misc' Non combustibles	nFe	Non Ferrous Metal
DP	Dense plastics	Gl	Glass	<10	Material <10 mm size
Tx	Textiles	Put	Putrescibles		

5.8.3 Loading of waste into compression cell

A total of 6.55 tonnes of waste was loaded into the compression cell as shown in Figure 5.59. The waste was lightly compacted in stages with the upper platen using a hydraulic pressure of less than 5 bar (~25 kPa), which resulted in an *in situ* bulk density of approximately 0.9 t/m^3.

Figure 5.59 The loading of waste AG1 into the compression cell

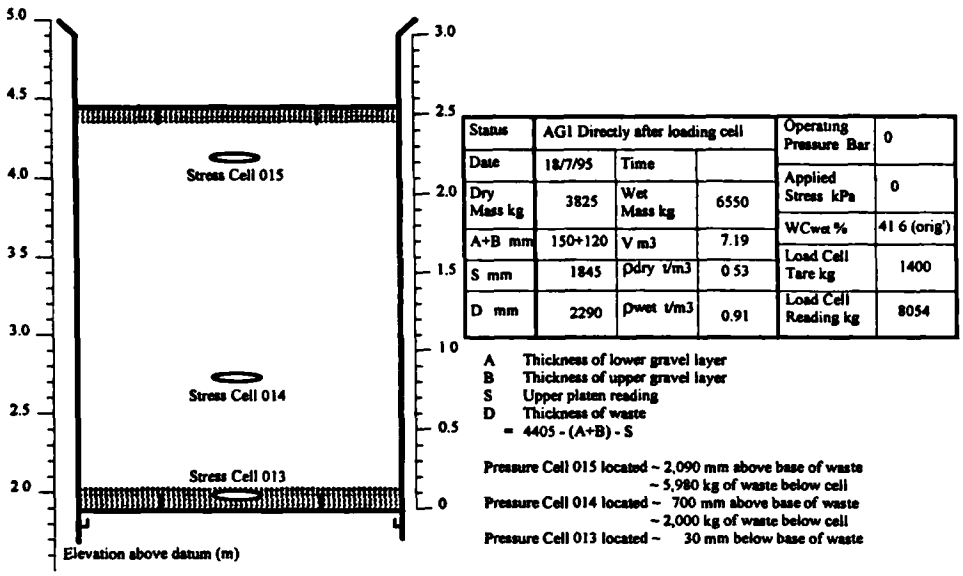

5.8.4 Absorptive capacity

The absorptive capacity of the waste was determined after compression at an applied stress of 40 kPa, where a dry density of 0.62 t/m^3 was achieved.

Volume of water added to saturate waste	1,157 litres
Volume of water drained	972 litres
Amount of water retained	185 litres
Mass of waste at original WC_{wet} = 41.6%	6,550 kg
Dry mass of waste	3,825 kg
Total absorptive capacity of waste at a bulk density of 1.09 t/m^3	35 litres/tonne

5.8.5 Changes in average waste density in response to changes in applied stress

The waste was subjected to six stages of compression, with applied stresses of 40, 87, 165, 244, 322 and 603 kPa. During compression the waste was maintained under conditions which allowed gravity drainage.

The final average dry density of the waste at the end of each compression stage is recorded in Table 5.18 and increased from 0.53 to 0.95 t/m^3.

Table 5.18 Changes in dry density and water content at field capacity of AG1

Stage	Applied Stress (kPa)	Status[1]	Wet mass of waste at end of stage[2] (kg)	Change in water held in waste in stage[2] (litres)	ρ_{dry} at end of stage (t/m^3)	WC_{dry} at end of stage (%)	WC_{wet} at end of stage (%)	WC_{vol} at end of stage (%)
0	-	Loading	6,550	0	0.53	71.2[3]	41.6[3]	37.9[3]
1	40	Comp'n	6,697	+147	0.62	75.1	42.9	46.7
1	40	S&D	6,708	+11	0.64	75.4	43.0	48.1
2	87	Comp'n	6,464	-244	0.69	69.0	40.8	47.3
2	87	S&D	6,664	+200	0.69	74.2	42.6	51.5
3	165	Comp'n	6,247	-417	0.77	63.3	38.8	48.5
3	165	S&D	6,345	+98	0.77	65.9	39.7	50.7
4	322	Comp'n	5,964	-381	0.86	55.9	35.9	48.1
4	322	S&D	5,915	-49	0.86	54.6	35.3	45.6
5	603	Comp'n	5,763		0.95	50.7	33.6	47.9

[1] S&D indicates that waste was saturated and then drained to field capacity during stage.
[2] Values based on load cell readings
[3] Not at field capacity

5.8.6 Water content at field capacity

The water content (WC_{dry}) at field capacity reduces with increasing applied stress and waste density, from approximately 75% at an applied stress of 40 kPa to 51% at an applied stress of 603 kPa (see Table 5.18). However, the volumetric water content (WC_{vol}) remains relatively constant in the range of 46% to 50%.

5.8.7 Differential compression (String data)

Differential compression was measured at various depths within the waste at applied stresses of 40, 87, 165, 322 and 603 kPa, using strings inserted into the waste through piezometer ports. The differential compression of the waste measured in this way for each compression stage is shown in Figures 5.60 to 5.64.

Further analyses of these data are made in Chapter 6 and Appendix B.

Figure 5.60 Differential compression of waste AG1 at applied stress of 40 kPa

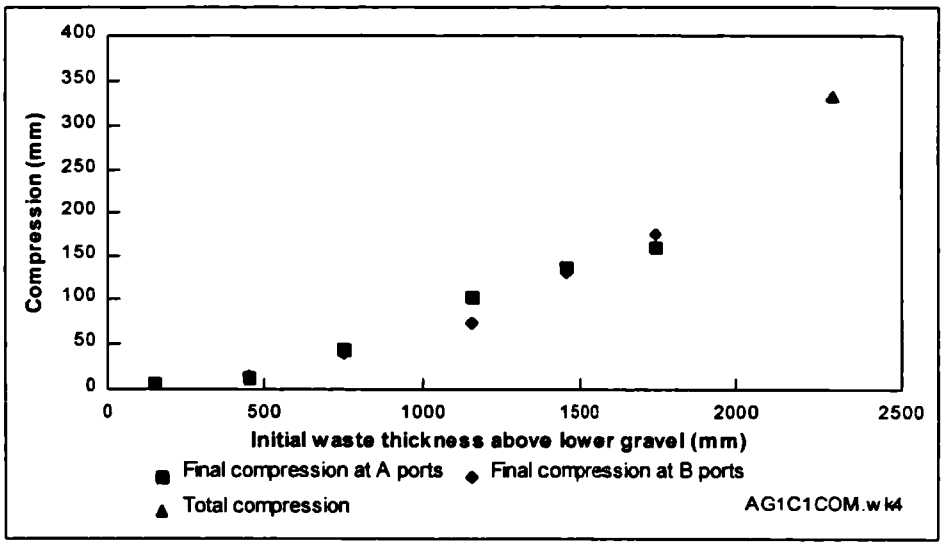

Figure 5.61 Differential compression of waste AG1 at applied stress of 87 kPa

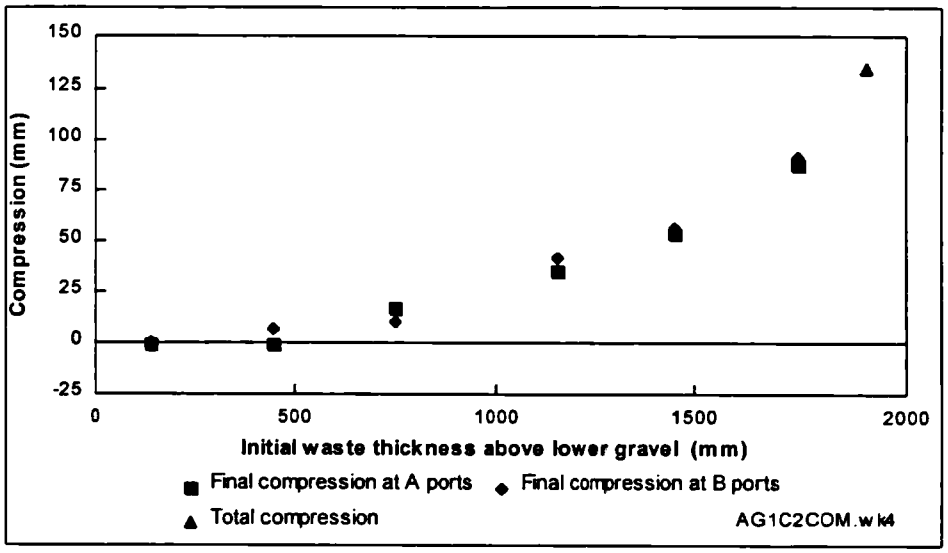

Figure 5.62 Differential compression of waste AG1 at applied stress of 165 kPa

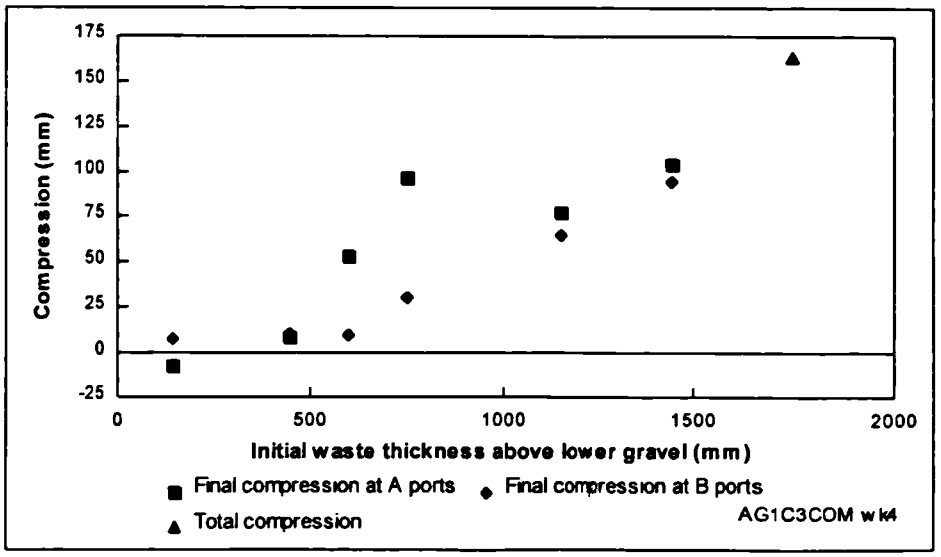

Figure 5.63 Differential compression of waste AG1 at applied stress of 322 kPa

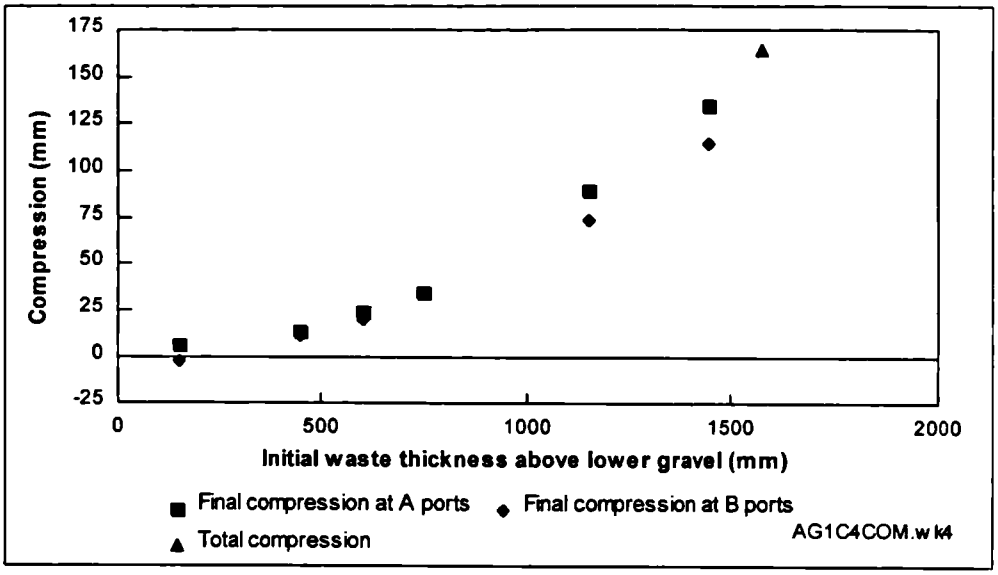

Figure 5.64 Differential compression of waste AG1 at applied stress of 603 kPa

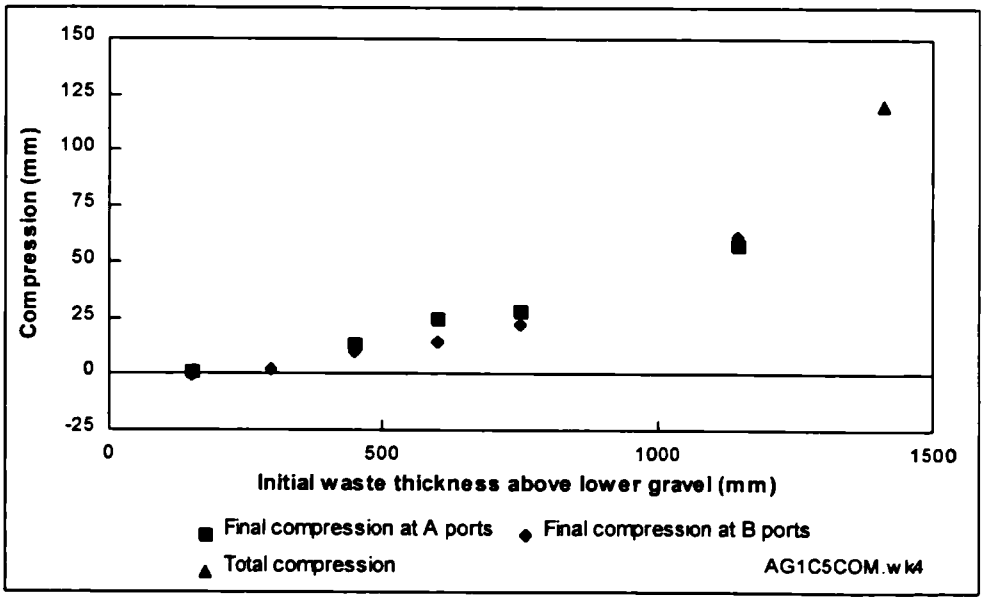

5.8.8 Total stress cell data

The maximum total vertical stress recorded by the three earth pressure stress cells during the six stages of compression is shown in Figure 5.65.

Figure 5.65 Maximum total stress recorded during each compression stage of AG1

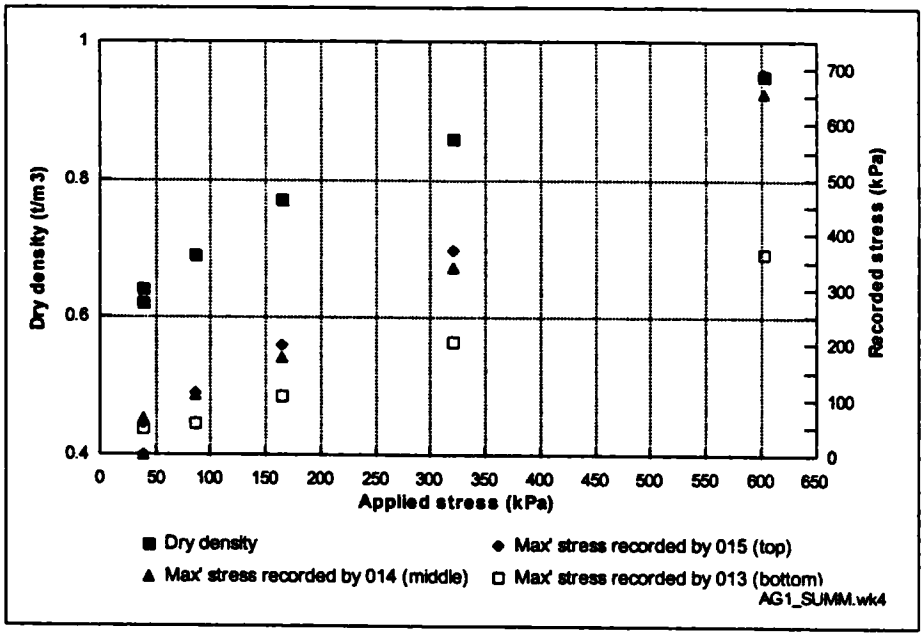

5.8.9 Effective porosity

The effective porosity of the waste was determined after compression at applied stresses of 40, 87, 165, 322 and 603 kPa (Figures 5.66 to 5.73). The effective porosity reduced from approximately 16% at an applied stress of 40 kPa to less than 1% at 603 kPa (see Table 5.19 for summary).

Figure 5.66 Total storage capacity of waste AG1 at an applied stress of 40 kPa

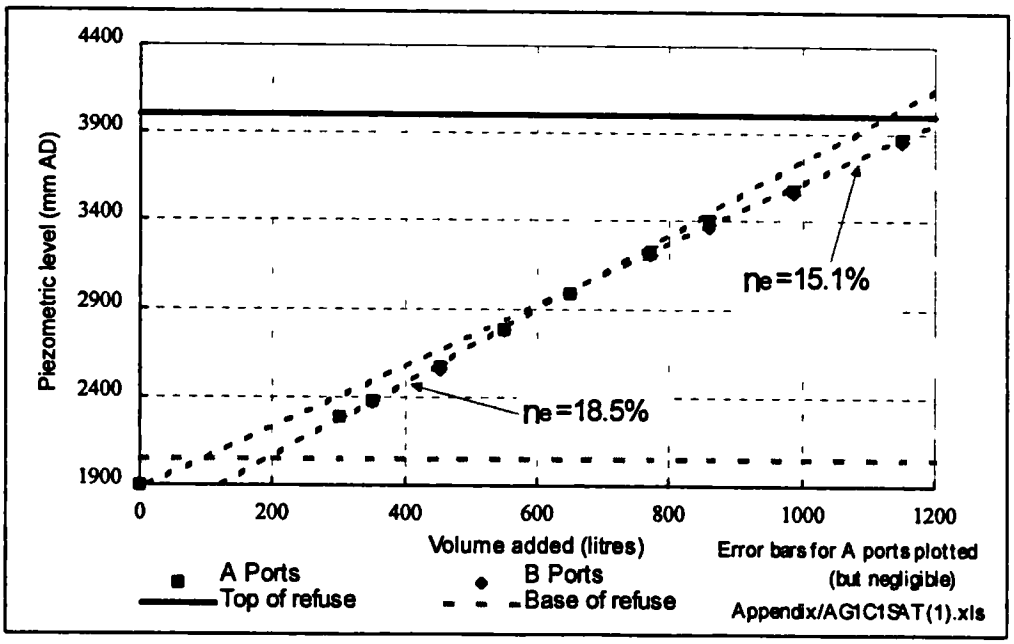

Figure 5.67 **Effective porosity determination of AG1 at an applied stress of 40 kPa**

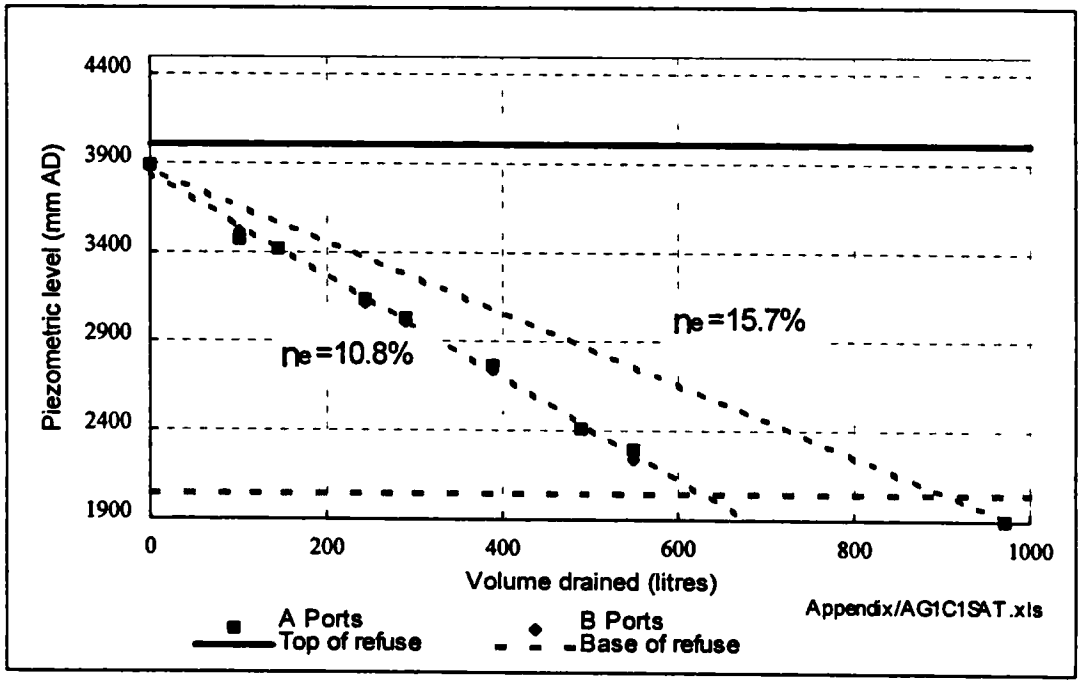

Figure 5.68 **Effective porosity determination (by saturation) of AG1 at an applied stress of 87 kPa**

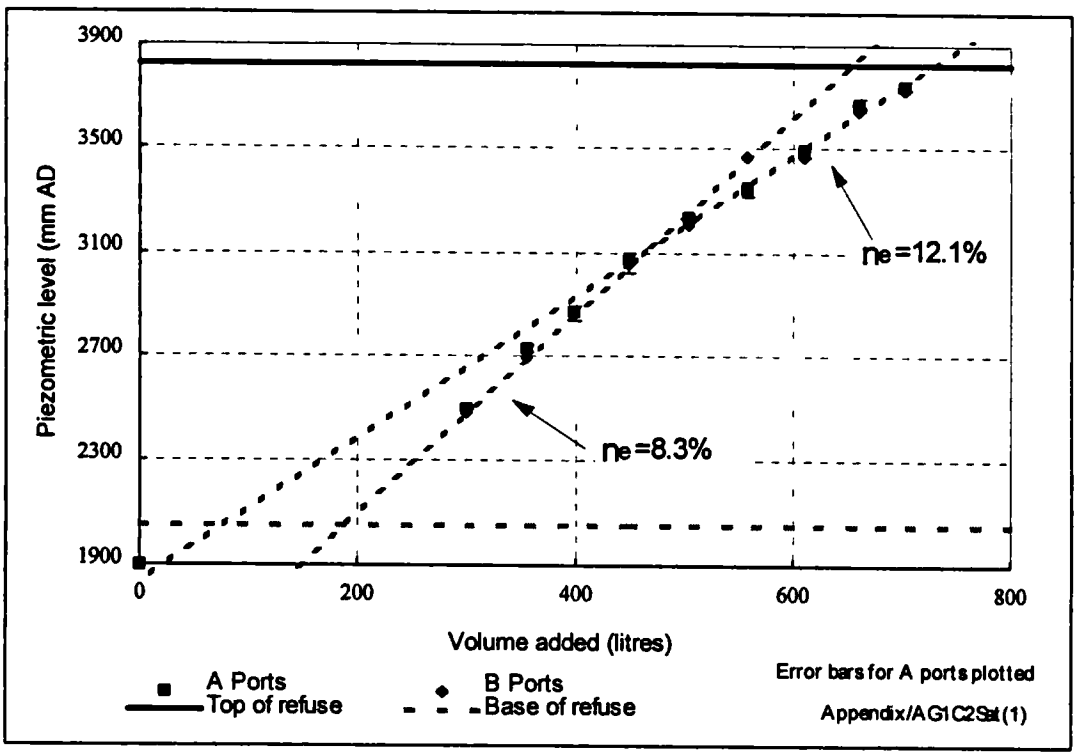

Figure 5.69 **Effective porosity determination (by draining) of AG1 at an applied stress of 87 kPa**

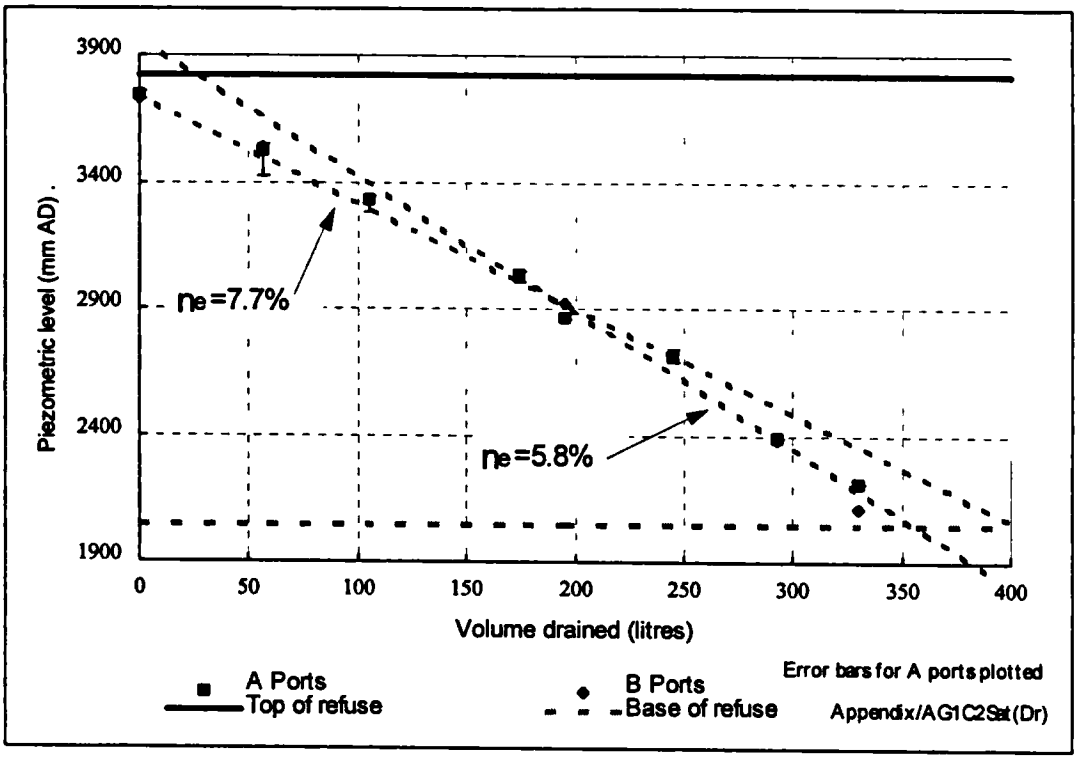

Figure 5.70 **Effective porosity determination (by saturation) of AG1 at an applied stress of 165 kPa**

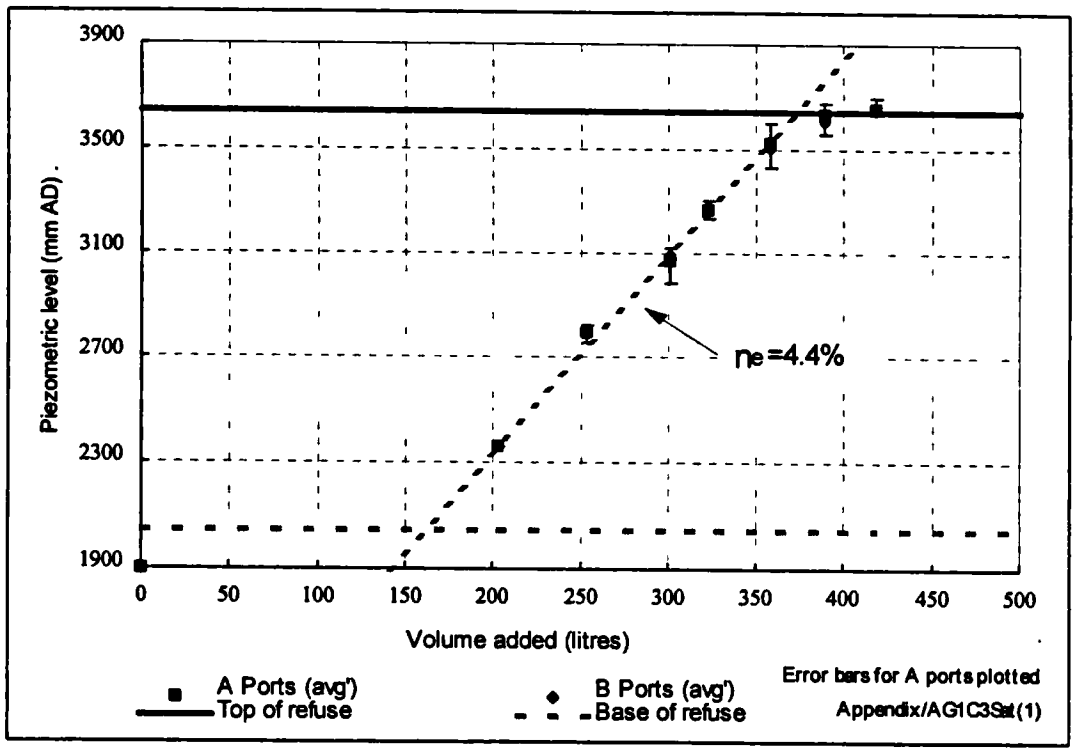

Figure 5.71 **Effective porosity determination (by draining) of AG1 at an applied stress of 165 kPa**

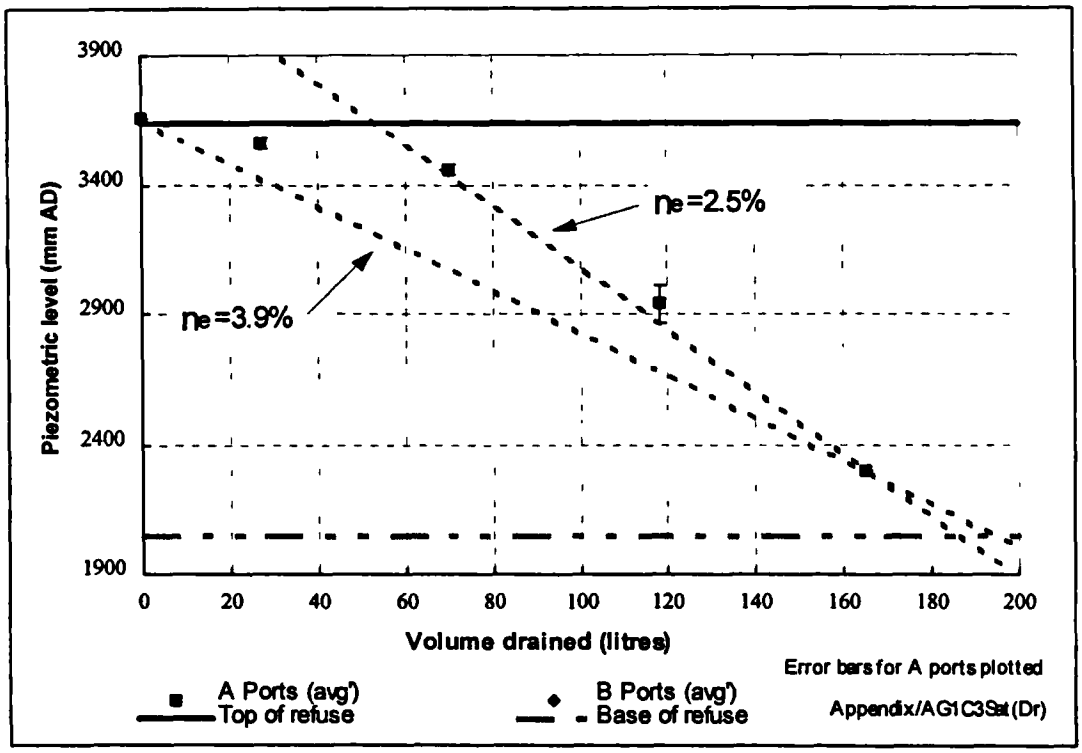

Figure 5.72 **Effective porosity determination of AG1 at an applied stress of 322 kPa**

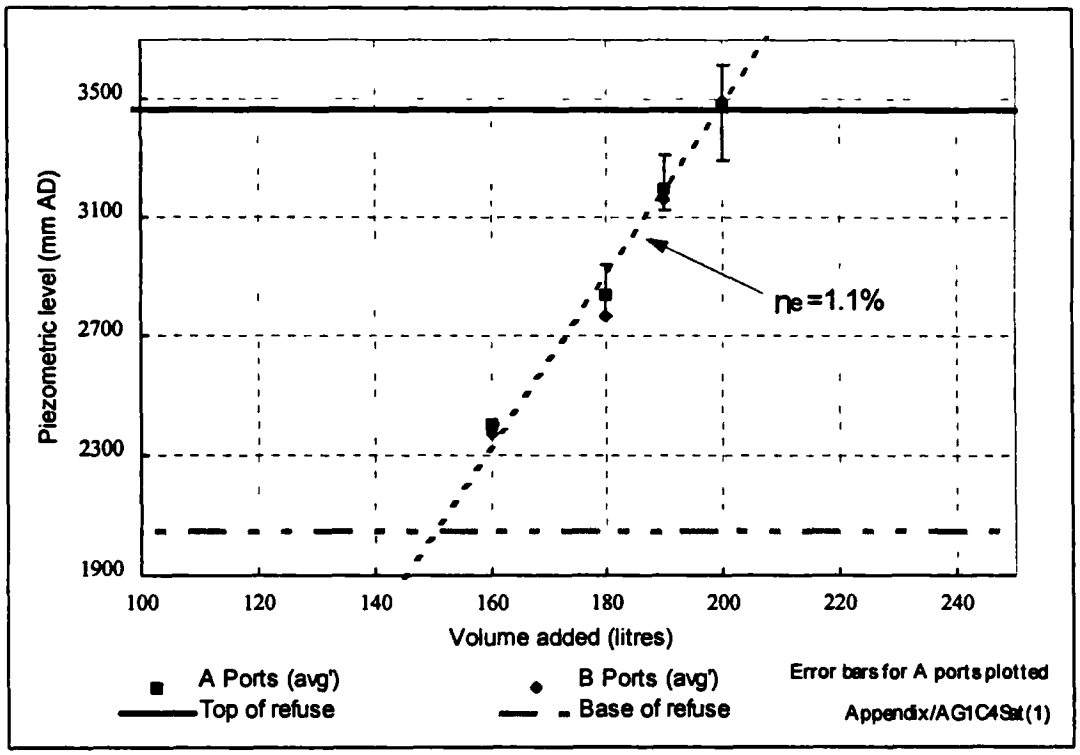

Figure 5.73 Effective porosity determination of AG1 at an applied stress of 603 kPa

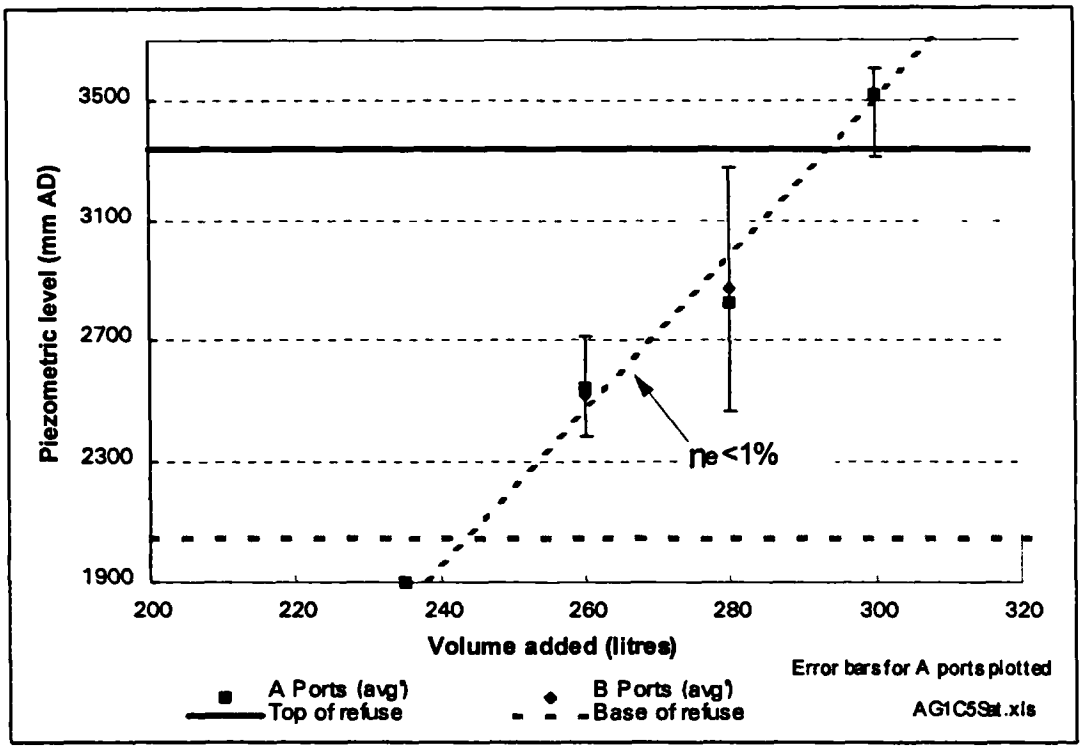

Table 5.19 Effective porosity of AG1 at varying applied stresses

Stage	Test type	Applied Stress kPa	Effective Porosity %	Comment
AG1C1St1	Fill	40	N/D	Average total storage capacity = 16.8%
AG1C1St1	Drain	40	**15.7**	Average for all waste in cell.
AG1C2St1	Fill	87	**10.2**	Average for all waste in cell.[1]
AG1C2St1	Fill	87	12.1	Upper waste (1,100-1,800 mm above base).
AG1C2St1	Fill	87	8.3	Lower waste (400-1,100 mm above base).
AG1C2St1	Drain	87	7.7	Upper waste (1,100-1,800 mm above base).
AG1C2St1	Drain	87	5.8	Lower waste (200-1,100 above base).
AG1C3St1	Fill	165	**4.4**	Average for all waste in cell
AG1C3St1	Drain	165	3.9	Average. Drainage occurs over 24 hours.
AG1C4St1	Fill	322	**1.1**	Average for all waste in cell.
AG1C5St1	Fill	603	**<1**	Average. Low hydraulic conductivity means that piezometric readings had not stabilised.

Values in **bold** considered to be most representative

[1] Based on average hydraulic gradient

5.8.10 *Hydraulic conductivity*

The vertical hydraulic conductivity of the waste was determined after compression at applied stresses of 40, 87, 165, 322 and 603 kPa.

Graphs of piezometric head plotted against elevation are shown in Figures 5.74 to 5.78 for each of the compression stages.

The vertical hydraulic conductivity of the waste reduced by four orders of magnitude from approximately $1.5x10^{-4}$ m/s at an applied stress of 40 kPa, to $1x10^{-8}$ m/s at an applied stress of 603 kPa (see Table 5.20).

Table 5.20 Hydraulic conductivity of AG1 at varying applied stresses

Stage	Applied Stress kPa	Hydraulic Conductivity m/s	Comment
AG1C1	40	$1.5x10^{-4}$	All waste in cell
AG1C2	87	$6.7x10^{-5}$	Upper 0.7 m of waste in cell
	87	$3.2x10^{-5}$	Lower 0.7 m of waste in cell
AG1C3	165	$6.0x10^{-6}$	All waste in cell
AG1C4	322	$5.0x10^{-7}$	All waste in cell
AG1C5	603	$1.1x10^{-8}$	Upper 0.4 m of waste in cell
	603	$6.0x10^{-8}$	Lower 0.8 m of waste in cell

Figure 5.74 Constant head hydraulic conductivity test on AG1 at an applied stress of 40 kPa

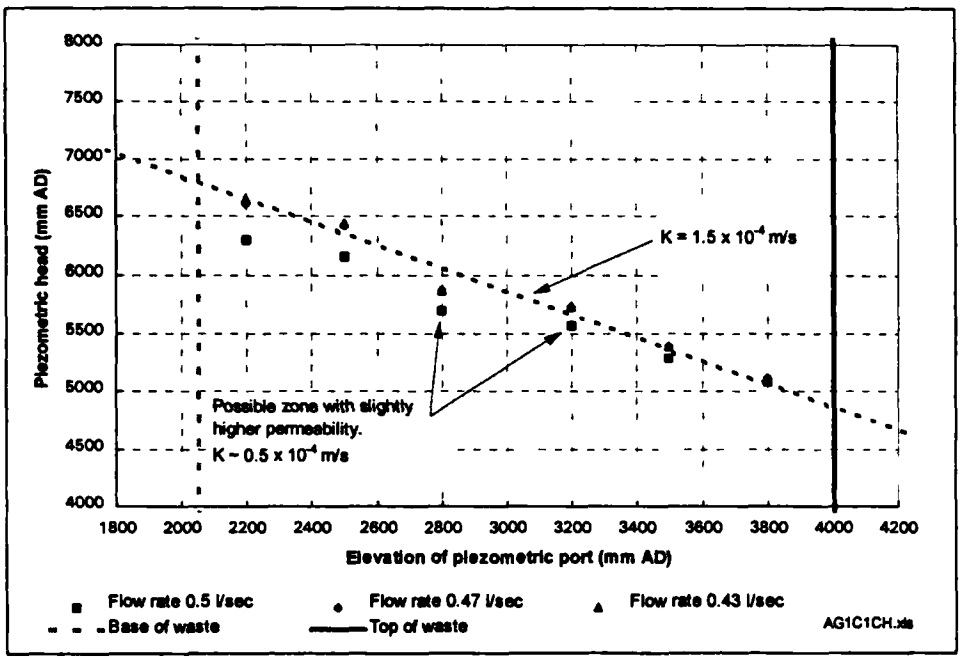

Figure 5.75 **Constant head hydraulic conductivity test on AG1 at an applied stress of 87 kPa**

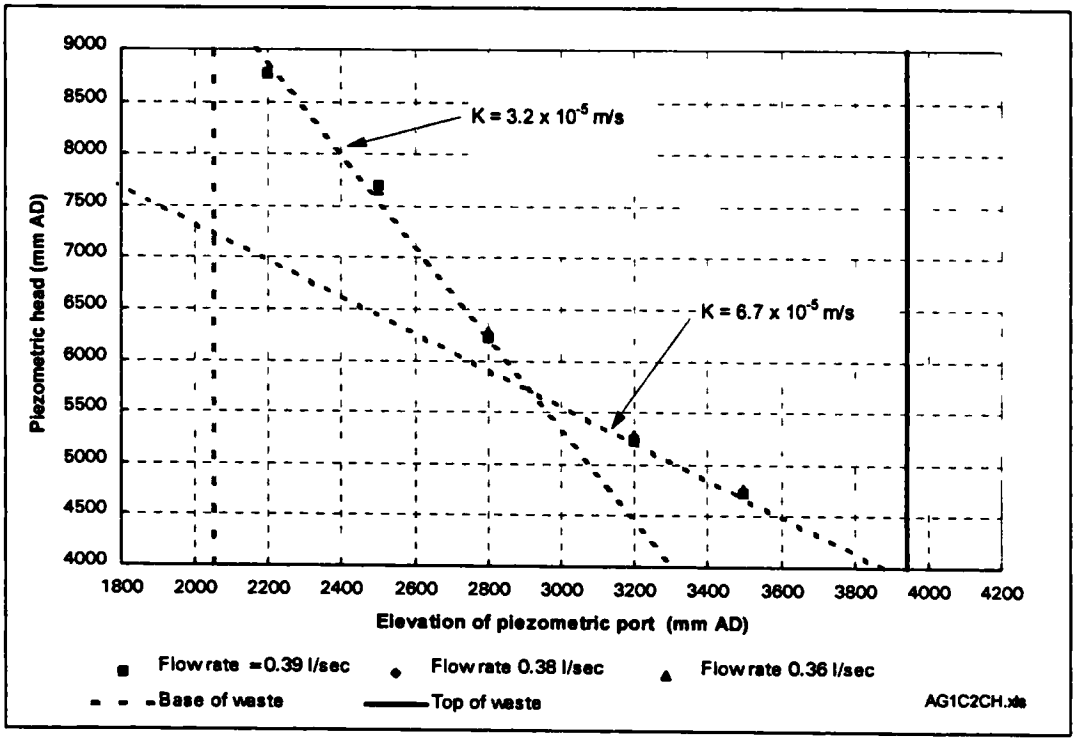

Figure 5.76 **Constant head hydraulic conductivity test on AG1 at an applied stress of 165 kPa**

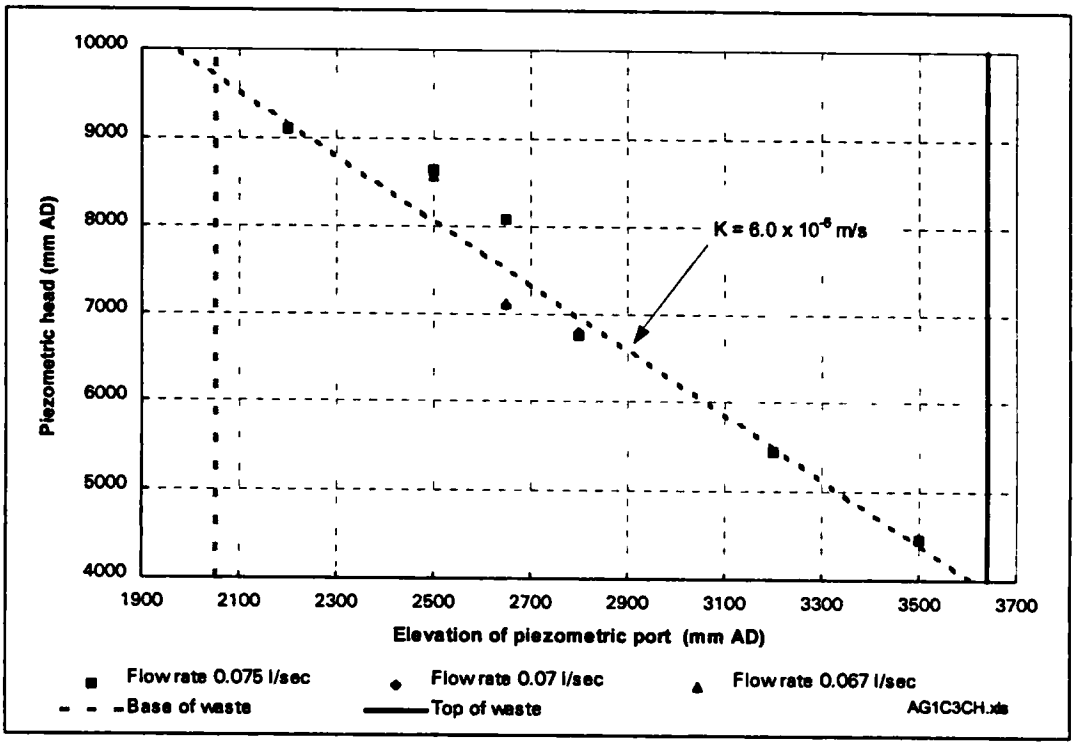

Figure 5.77 **Constant head hydraulic conductivity test on AG1 at an applied stress of 322 kPa**

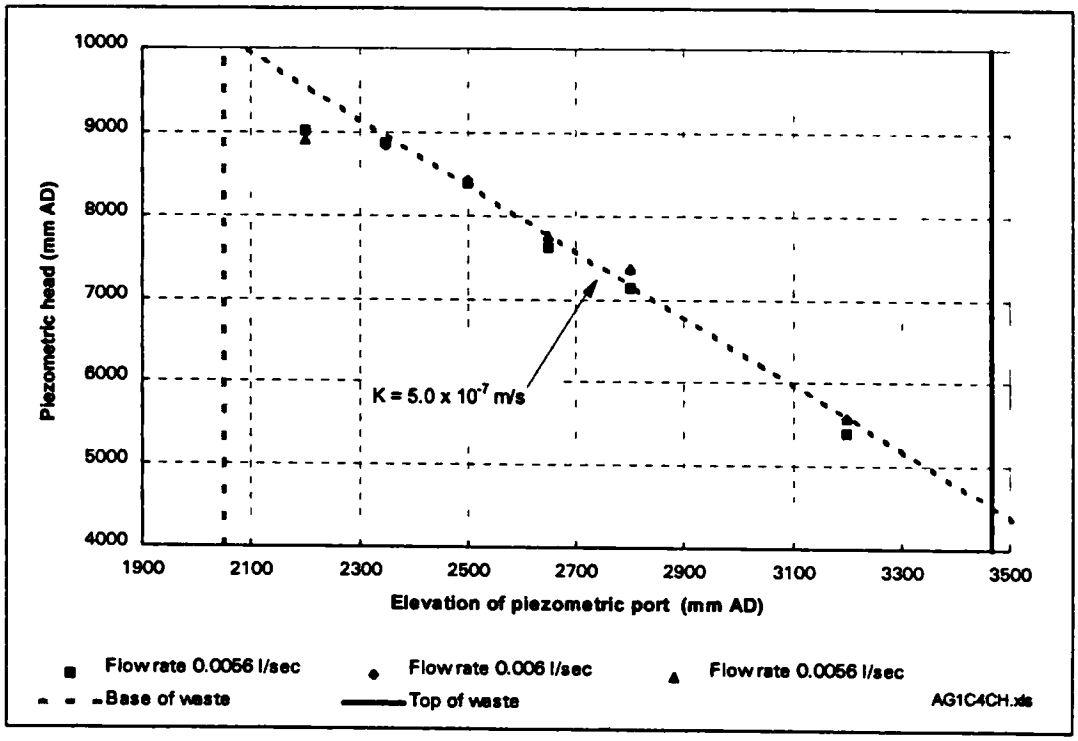

Figure 5.78 **Constant head hydraulic conductivity test on AG1 at an applied stress of 603 kPa**

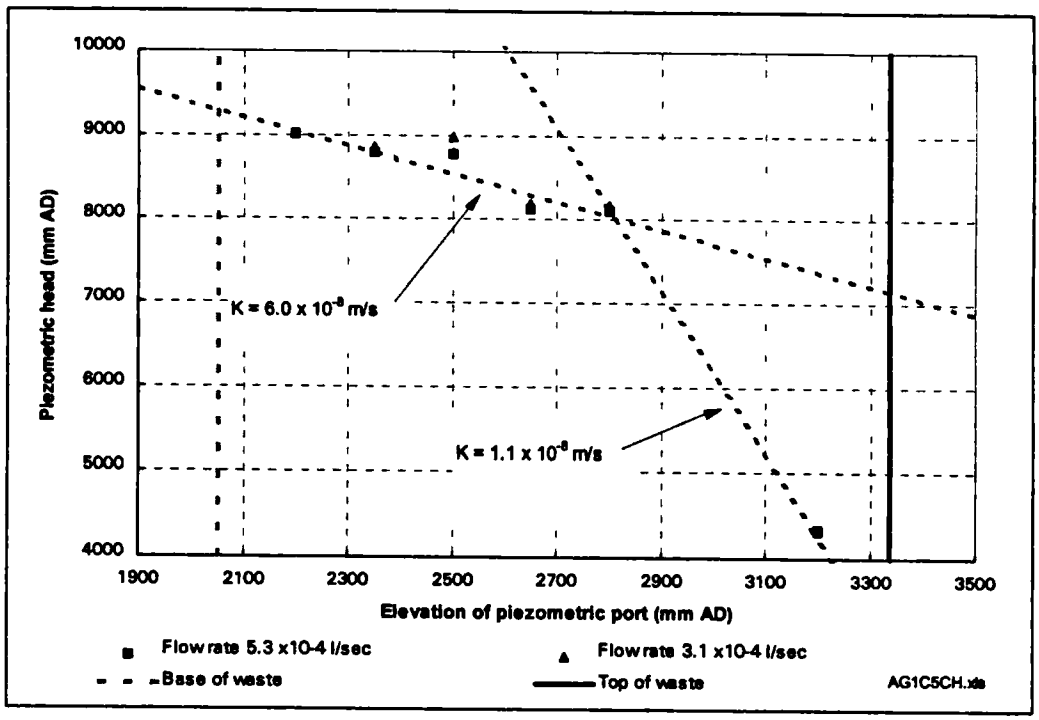

5.9 Summary of experimental results

Table 5.21 summarises the results obtained from the various tests on the six waste types presented in Sections 5.3 to 5.8 above.

Table 5.21 Summary of results

Applied Stress σ_{app} kPa	Waste Type	Avg' dry density ρ_{dry} t/m³	Avg' wet density ρ_{wet} t/m³	Water Content WC_{wet} %	Drainable Porosity n_e %	Hydraulic Conductivity K m/sec
0	DM1	0.45	0.70	33.7	ND	ND
0	DM2	0.36	0.76	52.8[1]	17.5	6.5×10^{-4}
0	DM3	0.34	0.51	34.0	ND	ND
0	PV1	0.26	0.54	52.8[1]	27.8	3.3×10^{-4}
0	PV2	0.20	0.32	39.7	ND	ND
0	AG1	0.53	0.91	41.6[1]	ND	ND
40	DM1	0.48	0.73	ND	ND	ND
40	DM2	0.43	0.89	51.7[1]	11	2×10^{-4}
40	DM3	0.39	0.79	50.3[1]	14.6	1.5×10^{-4} to 3.4×10^{-5}
40	PV1	0.31	0.63	51.4[1]	23	3.4×10^{-5}
40	PV2	0.28	0.40	29.7	ND	ND
40	AG1	0.64	1.09	42.9[1]	15.7	1.5×10^{-4}
87	DM1	ND	ND	ND	ND	ND
87	DM2	0.51	ND	ND	ND	ND
87	DM3	0.42	0.84	49.7[1]	12.6	1.9×10^{-5} to 8.9×10^{-5}
87	PV1	0.35	0.71	50.7[1]	17	1.2×10^{-5}
87	PV2	0.35	0.53	34.9	ND	ND
87	AG1	0.69	1.21	42.6[1]	10.2	3.2×10^{-5} to 6.7×10^{-5}
165	DM1	0.55	0.84	ND	ND	ND
165	DM2	0.56	ND	ND	ND	ND
165	DM3	0.49	0.94	47.3[1]	6.2	3.1×10^{-6} to 2.8×10^{-5}
165	PV1	0.45	0.76	40.9[1]	3.5	2.4×10^{-6}
165	PV2	0.41	0.65	36.5	ND	ND
165	AG1	0.77	1.28	39.7[1]	4.4	6.0×10^{-6}
322	DM1	0.59	0.90	ND	ND	ND
322	DM2	0.65	1.05	38.2[1]	ND	ND
322	DM3	0.62	1.08	42.7[1]	2	4.4×10^{-7} to 8.9×10^{-7}
322	PV1	0.53	0.83	36.2[1]	2.2	2×10^{-7}
322	PV2	0.51	0.83	38.8	ND	ND
322	AG1	0.86	1.34	35.9[1]	1.1	5.0×10^{-7}
603	DM1	ND	ND	ND	ND	ND
603	DM2	0.73	1.14	36.0[1]	ND	ND
603	DM3	0.72	1.16	38.2[1]	1.5	3.7×10^{-8} to 2.7×10^{-7}
603	PV1	0.60	0.94	35.8[1]	<1	$<4.8\times10^{-8}$
603	PV2	0.62	0.99	37.5	ND	(1.1 to 1.4×10^{-9})[2]
603	AG1	0.95	1.42	33.6[1]	<1	1.1×10^{-8} to 6.0×10^{-8}

ND Not determined. [1] At Field Capacity [2] Unreliable -determined by falling head test

Chapter 6

Data interpretation and analysis

6.1 Summary

Results from earth pressure cells are analysed to quantify the reduction in transmitted vertical stress within the waste due to side-wall friction. The data are used to calibrate an analytical method, which is then used to calculate the stress transmitted to any particular depth within the waste in the compression cell.

The variation in waste density, effective porosity, water content at field capacity, and hydraulic conductivity that was reported against applied stress in Chapter 5 is related here to average effective stress. Empirical relationships are suggested between density and effective stress, and hydraulic conductivity and effective stress. A relationship between stress and depth within an unsaturated landfill is also derived.

Changes in average density are related to changes in average stress to determine the constrained modulus of the waste. At each stress stage the specific volume and dry density of the waste are used to deduce the average dry density of the particles making up the waste. An increase in average dry particle density is shown to occur with increasing stress.

6.2 Introduction

The results presented in Chapter 5 were generally reported against the applied load exerted on the waste through the upper platen. However, it is more appropriate to relate the results to the actual effective stress in the waste, which will be less than the applied load due to the effects of sidewall friction.

It is assumed that at the end of a compression stage the applied vertical stresses are transmitted through the waste as effective stresses by interparticle contact. This is because during compression the waste is free to drain downwards under the influence of gravity, and it is assumed that there was sufficient time to allow excess pore water pressures to dissipate.

Two approaches were used to determine the average vertical effective stress in the waste at various stages of compression. First, the data on differential compression were analysed to provide density profiles in the waste at the end of each compression stage (Section 6.3). This approach did not lead to a viable way of determining a relationship between reduction in stress and depth in the cell. A second method, using the stress readings from the earth pressure cells installed in the waste and the lower gravel layer, was more successful (Section 6.4).

6.3 Analysis of differential compression data.

The compression of wastes DM2, DM3 and AG1 at different vertical heights has been analysed in Appendix B. The waste within the compression cell was considered to be made up of a number of slabs, with the top and bottom of each slab being defined by piezometer ports through which strings had been inserted into the waste (see Section 3.6.4, and Chapter 5). The analyses track the decrease in height and the increase in density of individual slabs with increasing applied stress. The resulting dry density profiles for wastes DM2, DM3 and AG1 are shown in Figures 6.1 to 6.3.

For all three of the wastes the differential compression (string) data indicate that considerable vertical variations in waste density developed in the compression cell, especially at higher applied stresses. For example, the dry density of DM3 ranged from 0.47 t/m^3 at the bottom of the cell to 1.18 t/m^3 at the top at an applied stress of 603 kPa. Taken at face value, these variations imply that the effects of sidewall friction must be considerable and that only a small proportion of the applied load is being transmitted to the lower regions of the waste. However, evidence from a number of other sources indicates that the string data are unreliable and that vertical density gradients in the waste are less than indicated in Figures 6.1 to 6.3. For example -

1) At an applied stress of 603 kPa the top slab of waste DM3 reached a calculated dry density of 1.18 t/m^3. If a minimum water content, WC_{wet}, of 30% is assumed, then the bulk density is calculated as 1.7 t/m^3. This is greater than the maximum theoretical density of refuse reported (as unit weights) in Section 2.4.2.

2) The effective porosity data for wastes DM3 and AG1 (presented in Sections 5.5.9 and 5.8.9) do not support the density profiles of Figures 6.2 and 6.3. Any increase in waste dry density should be reflected by a decrease in effective porosity (see Section 6.6 on changes in particle density). However, there is little evidence that at a given applied stress there is much, if any, variation in effective porosity with depth. For example, at an applied stress of 165 kPa the effective porosity of waste DM3 showed little variation with depth from a value of approximately 6.2% (Figure 5.25). According to the slab analysis (Figure 6.2) the dry density of waste DM3 at an applied stress of 165 kPa varied from 0.40 to 0.69 t/m^3. There are many other examples of discrepancies between the effective porosity and density profiles of wastes DM3 and AG1. For example, the effective porosity of waste AG1 at an applied stress of 165 kPa showed little variation with depth from a value of 4.4% (Figure 5.65), whereas according to the slab analysis (Figure 6.3) the dry density increased from 0.60 to 1.1 t/m^3.

3) The variations in hydraulic conductivity of wastes DM3 and AG1 with depth also do not correlate with the density profiles of Figures 6.2 and 6.3. There is evidence of an increase in hydraulic conductivity with depth (especially in waste DM3), indicative of a reduction in waste density, but not to the extent suggested by the string data. For example, the density profile of waste DM3 at an applied stress of 322 kPa indicates a range of densities from 0.44 to 0.95 t/m^3 (Figure 6.2). The lower density (at the base of the compression cell) is similar to the calculated density at the top of the waste after compression at an applied stress of 40 kPa. However, the hydraulic conductivities of the wastes, which were calculated to have a similar density in the two compression stages, do not correlate well; the minimum hydraulic conductivity recorded at an applied stress of 40 kPa was 3.4×10^{-5} m/s (Figure 5.28), whereas the maximum hydraulic conductivity recorded at an applied stress of 322 kPa was 8.9×10^{-6} m/s (Figure 5.31).

Overall, it is considered that the differential compression (string) data are unreliable and cannot be used to quantify the extent to which vertical density gradients developed in the waste in the cell. This is unfortunate because it was a way of deriving a relationship between transmitted stress and depth in the cell. The possible experimental problems with the technique were discussed in Section 3.6.4.

Figure 6.1 Calculated dry density profile of DM2 at varying applied stresses

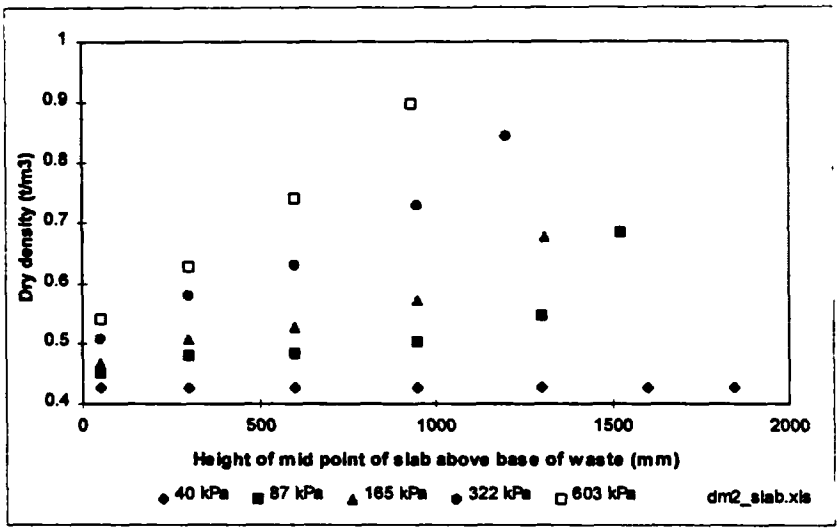

Figure 6.2 Calculated dry density profile of DM3 at varying applied stresses

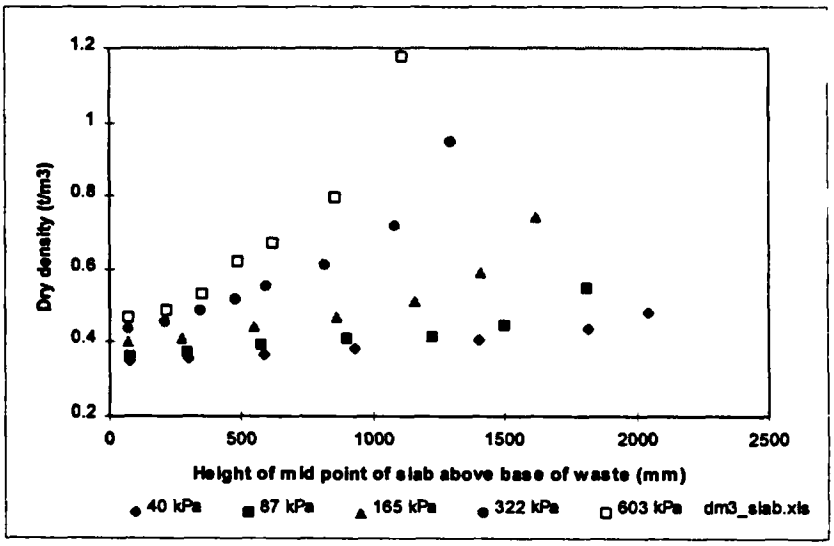

Figure 6.3 Calculated dry density profile of AG1 at varying applied stresses

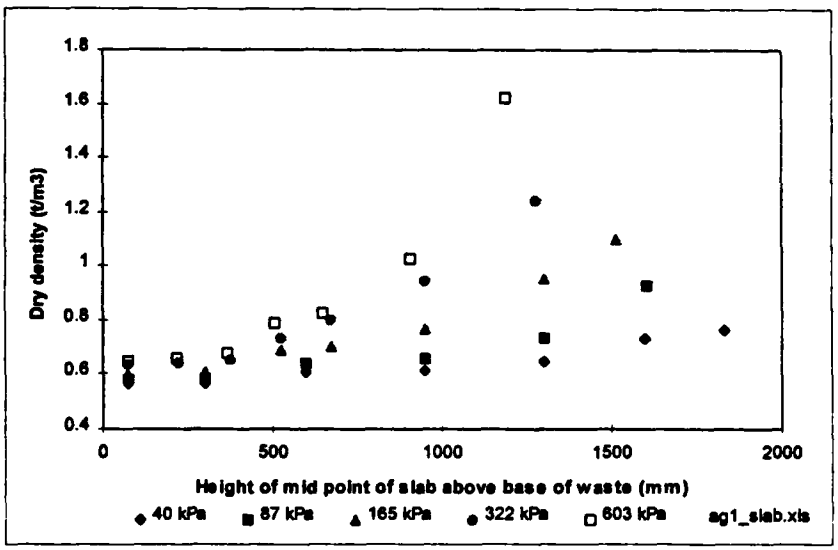

6.4 Analysis of total earth pressure cell data

Data from three total earth pressure cells were collected from tests on all waste types, apart from waste DM1. One cell was installed in the basal gravel layer and two in the waste.

The difficulties of using and interpreting data from earth pressure cells were discussed in Section 3.7.2. It is considered that there are insufficient data to justify a theoretical approach to calculating cell action factors for any of the cells. Two alternative approaches have been taken to analysing the data.

1) Direct comparison of stress data from the two cells installed in the waste - Section 6.4.1

2) Application of a calibrated correction factor to the stress readings from the cell installed in the lower gravel - Section 6.4.2.

6.4.1 Comparison of stress readings from earth pressure cells located in waste

In each test there were two earth pressure cells at different elevations within the waste. The correction factors (cell action factors) that should be applied to the readings from each of these cells are unknown. However, as the two cells were of similar type and were installed in a similar manner, it is reasonable to assume that the correction factor for each cell will be similar and that a relative comparison of the data from each cell may be valid. The stress recorded by the lower cell in the waste should be less than that recorded by the upper cell due to the effects of sidewall friction. The larger the vertical distance between the two cells, the larger the difference in readings should be.

The estimated vertical distances between the earth pressure cells during tests on wastes DM2, DM3, PV2 and AG1, together with actual stress readings, are shown in Tables 6.1 to 6.4.

For each compression stage the ratio of the stress recorded by the middle (waste) earth pressure cell to that of the upper cell is plotted against the estimated distance between the two cells in Figure 6.4. Lines showing the theoretical reduction in stress, according to Equation 3.8 (where P = 300 kPa and γ =10 kN/m^3) are also shown. The maximum reduction in stress (where $\delta = \phi' = 38°$) is plotted, together with the case for $\delta = 20°$ and $\phi' = 40°$. Data from DM3 and PV2 generally fall between these two curves, whilst the data from AG1 lies above the top curve. Data for DM2 are not shown as they fall well below the curve for the theoretical maximum reduction in stress.

Table 6.1 Separation distances and stresses recorded by total earth pressure cells in waste DM2

Applied Stress kPa	Stress in Cell 015 (top) σ_{rec-15} kPa	Stress in Cell 014 (middle) σ_{rec-14} kPa	Stress in Cell 013 (gravel) σ_{rec-13} kPa	Ratio of σ_{rec-14} / σ_{rec-15}	Distance between Cell 015 and Cell 014[1] metres	Distance between Cell 015 and Cell 013[2] metres
40	179	83	43	0.46	0.78-0.96	1.83
87	331	167	67	0.50	0.69-0.81	1.54
165	428	230	87	0.54	0.58-0.74	1.40
322	697	450	162	0.65	0.50-0.64	1.21
603	1101	807	312	0.73	0.40-0.57	1.08

[1] The larger distance in the range is calculated by assuming a uniform waste density in the column at the end of each compression stage. The smaller distance is taken from the slab analysis (Appendix B) which computes the development of density gradients in the waste.
[2] Based on total reduction in waste thickness.

Table 6.2 Separation distances and stresses recorded by total earth pressure cells in waste DM3

Applied Stress kPa	Stress in Cell 015 (top) σ_{rec-15} kPa	Stress in Cell 014 (middle) σ_{rec-14} kPa	Stress in Cell 013 (gravel) σ_{rec-13} kPa	Ratio of σ_{rec-14} / σ_{rec-15}	Distance between Cell 015 and Cell 014[1] metres	Distance between Cell 015 and Cell 013[2] metres
40	43.6	33.9	26.3	0.78	0.48-0.51	1.90
87	74.3	58.8	39.2	0.79	0.42-0.46	1.72
165	135	117.3	88.3	0.87	0.35-0.40	1.48
322	264.4	241.9	210.6	0.91	0.26-0.32	1.20
603	461.3	437	419	0.95	0.22-0.28	1.03

[1] The larger distance in the range is calculated by assuming a uniform waste density in the column at the end of each compression stage. The smaller distance is taken from the slab analysis (Appendix B) which computes the development of density gradients in the waste.
[2] Based on total reduction in waste thickness

Table 6.3 Separation distances and stresses recorded by total earth pressure cells in waste PV2

Applied Stress kPa	Stress in Cell 013 (top) σ_{rec-13} kPa	Stress in Cell 014 (middle) σ_{rec-14} kPa	Stress in Cell 015 (gravel) σ_{rec-15} kPa	Ratio of σ_{rec-14} / σ_{rec-13}	Distance between Cell 013 and Cell 014[1] metres	Distance between Cell 013 and Cell 015[1] metres
40	19.7	30.4	17.3	1.54	0.73	1.62
87	67	67	37.7	1.00	0.58	1.29
165	127	114.6	73.3	0.90	0.50	1.11
322	245	218.2	164.8	0.89	0.40	0.89
603	456.6	414.8	312.5	0.91	0.33	0.73

[1] Based on total reduction in waste thickness

Table 6.4 Separation distances and stresses recorded by total earth pressure cells in waste AG1

Applied Stress kPa	Stress in Cell 015 (top) σ_{rec-15} kPa	Stress in Cell 014 (middle) σ_{rec-14} kPa	Stress in Cell 013 (gravel) σ_{rec-13} kPa	Ratio of σ_{rec-14} / σ_{rec-15}	Distance between Cell 015 and Cell 014[1] metres	Distance between Cell 015 and Cell 013[2] metres
40	56.1	64.6	48.3	1.15	1.13-1.15	1.76
87	111.2	110	57.8	0.99	1.03-1.07	1.63
165	197.9	175.4	106.3	0.89	0.89-0.96	1.46
322	371.2	338.9	203.2	0.91	0.77-0.86	1.31
603	690	657	365	0.95	0.68-0.78	1.18

[1] The larger distance in the range is calculated by assuming a uniform waste density in the column at the end of each compression stage. The smaller distance is taken from the slab analysis (Appendix B) which computes the development of density gradients in the waste.

[2] Based on total reduction in waste thickness

Figure 6.4 **Transmission of stress between upper and middle (waste) earth pressure cells**

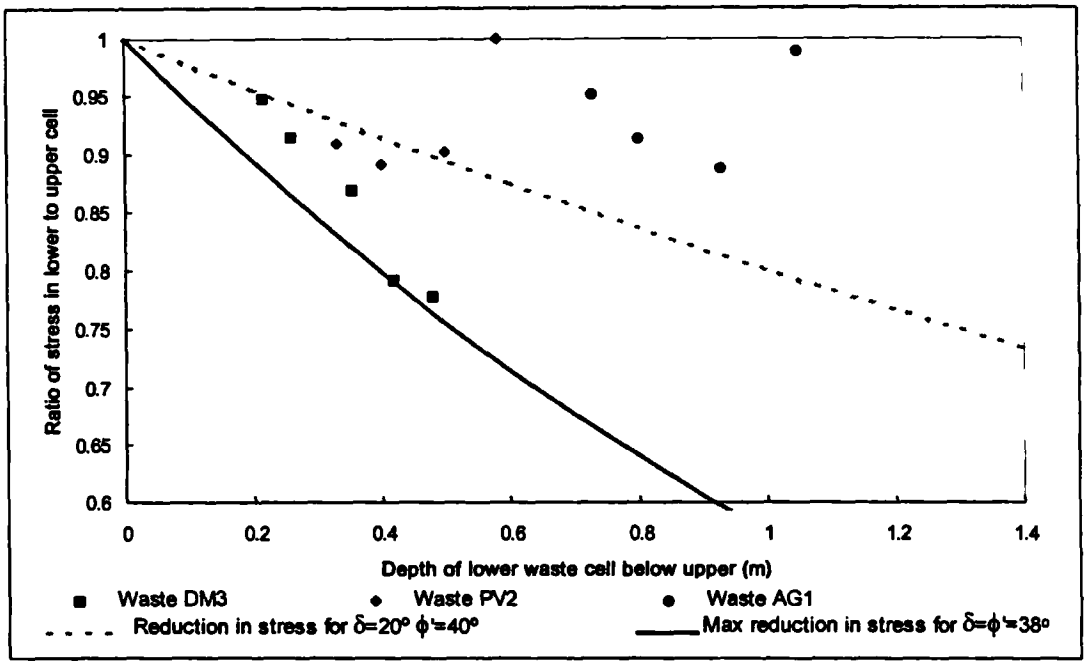

6.4.2 Stress readings from earth pressure cell in lower gravel

Laboratory calibration of the earth pressure cell installed in the layer of gravel (Section 3.7.2) indicated an over reading of the actual stress by approximately 17%. The readings of stress from the cells installed in the gravel in wastes DM3, PV2 and AG1 (as recorded in Tables 6.2 to 6.4) and from waste PV1 have been corrected accordingly.

Figure 6.5 shows the ratio of the corrected stress (in the basal gravel) to the applied stress, plotted against the vertical distance between the upper platen and the cell the lower gravel. The theoretical reduction in stress curves have also been plotted. The majority of the data points lie between the curve of the theoretical maximum reduction in stress ($\delta=\phi'=38°$) and the curve for $\delta = 20°$ and $\phi'= 40°$ ($P = 300$ kPa; $\gamma =10$ kN/m^3).

6.4.3 Correlation of stress readings with theoretical model

Data from Figures 6.4 and 6.5 have been combined into Figure 6.6 and are compared with the theoretical reduction in vertical stress with depth for varying values of δ and ϕ'. A reasonable fit is achieved with $\delta=30^o$ and $\phi'=40°$ (for $P= 300$ kPa; $\gamma =10$ kN/m^3). This fit is then used (e.g. see Section 6.4.4) as the basis for applying a consistent and repeatable correction to the actual transmitted vertical stress in the various tests. The theoretical model (with $\delta=30^o$ and $\phi'=40°$) is used to calculate the transmission of the applied load (P) to a given depth within the waste in the compression cell .

Figure 6.5 Corrected vertical stress in basal gravel with depth for all wastes

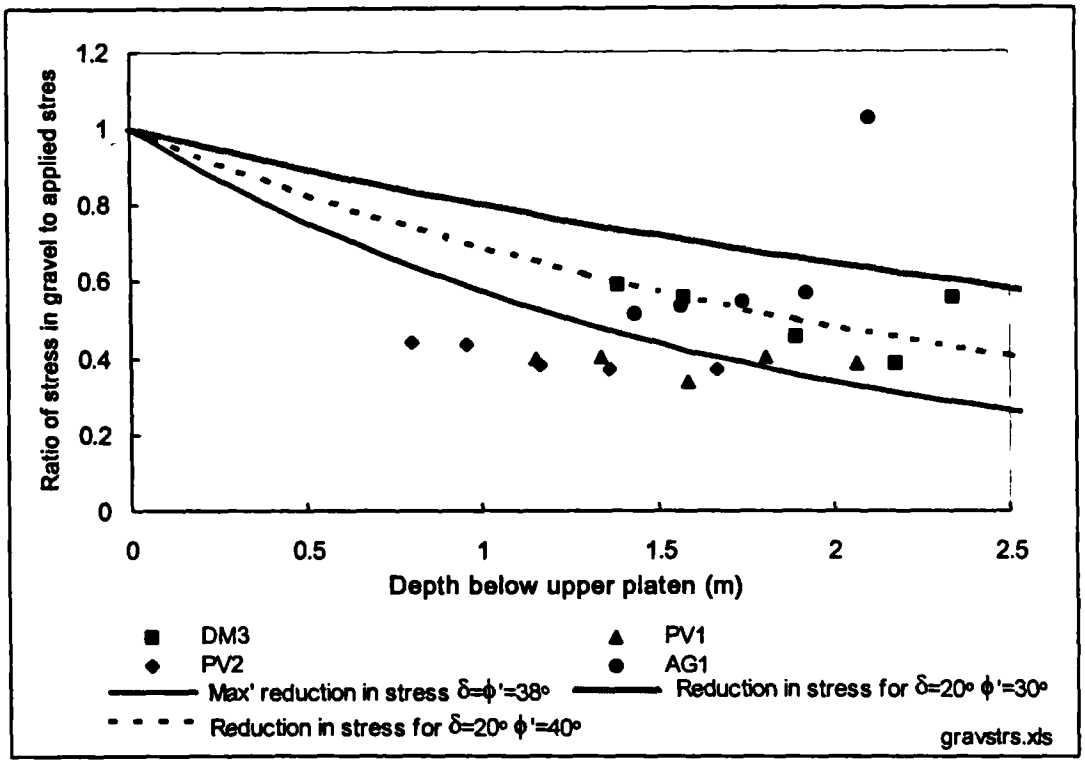

Figure 6.6 Ratio of transmitted stress vs depth in cell

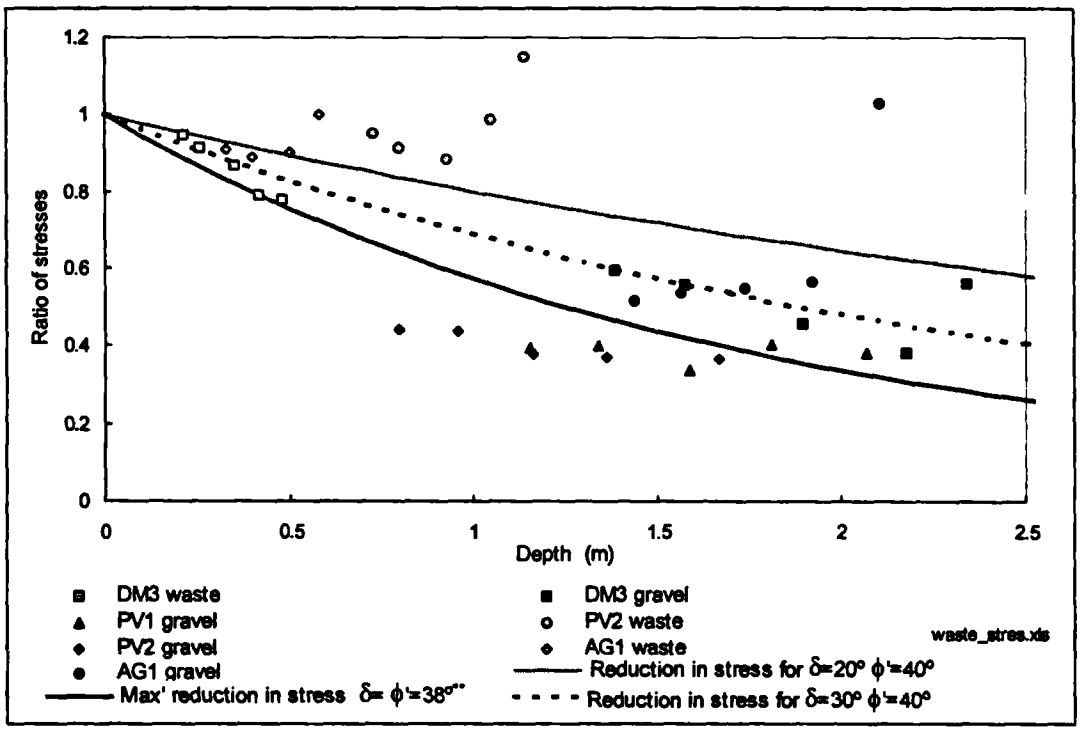

**Applied stress = 300 kPa

6.4.4 Average vertical stress in waste at different applied loads

The average vertical stress in the waste at a given applied load is obtained by applying the theoretical model of stress reduction in the compression cell (with values of δ=30° and ϕ'=40° derived in Section 6.4.3) to the average thickness of waste at the end of each compression stage (see Table 6.5). Using this technique the calculated average stress ranges between 73 and 89% of the applied stress.

Table 6.5 Estimated average vertical effective stress in wastes at varying applied loads

Applied Stress kPa	Thickness of waste and upper gravel metres	Av' depth of waste below upper platen metres	Calculated* average stress in waste kPa	Ratio of calculated to applied stress
Waste DM2				
40	2.07	1.03	34.5	0.86
87	1.76	0.88	67.9	0.78
165	1.62	0.81	125	0.76
322	1.41	0.70	247	0.77
603	1.27	0.63	471	0.78
Waste DM3				
40	2.3	1.15	34.0	0.85
87	2.1	1.05	64.9	0.75
165	1.85	0.93	120	0.73
322	1.53	0.77	241	0.75
603	1.34	0.67	463	0.77
Waste PV1				
40	2.02	1.01	34.6	0.87
87	1.76	0.88	67.9	0.78
165	1.54	0.77	127	0.77
322	1.29	0.64	253	0.79
603	1.11	0.55	486	0.81
Waste PV2				
40	1.61	0.81	35.5	0.89
87	1.29	0.64	72.4	0.83
165	1.09	0.55	136	0.83
322	0.88	0.44	273	0.85
603	0.72	0.36	523	0.87
Waste AG1				
40	2.03	1.01	34.6	0.87
87	1.87	0.94	66.8	0.77
165	1.70	0.85	123	0.75
322	1.58	0.79	239	0.74
603	1.41	0.70	458	0.76

* Based on $\delta = 30^{o}$, $\phi' = 40°$ and $\gamma = 10$ kN/m^3

6.4.5 Waste density in relation to effective stress

Tables 6.6 to 6.10 record the average densities and effective porosities of the different waste types against average effective stress. The average densities of wastes DM3, PV1 and AG1 are also plotted against average effective stress in Figures 6.7 to 6.9. Error bars for stress are plotted for each point. The maximum possible stress at a point (represented by the positive error bar) is the applied stress. The minimum possible stress (represented by the negative error bar) is calculated using the theoretical model with values of $\delta=\phi'=38°$ (see Section 6.4.3).

The data points for waste DM3 in Figure 6.7 have been matched to power law curves within an Excel (version 7.0) spreadsheet. It was determined by trial and error that of the curve fitting options available in Excel (including an exponential relationship) the data best fitted a power curve. This type of relationship (probably unrealistically) predicts zero density at zero effective stress; it can be compared to the Soil Mechanics relationship between void ratio (v) and effective stress $v=v_0-\lambda \ln \sigma'$ that predicts infinite void ratio, and hence zero density at zero effective stress. It is recognised that the void ratio relationship should not be used at low effective stresses (below ~5 kPa) and this restriction should also be applied to the empirical relationships below.

The following relationships between density and effective stress were derived; they are considered valid up to effective stresses of approximately 500 kPa and should certainly not be used at effective stresses much below 10 kPa:-

The dry density of the waste, $\rho_{dry} \approx 0.16 (\sigma_v')^{0.248}$; (6.1)

the density of the waste at field capacity, $\rho_{FC} \approx 0.45 (\sigma_v')^{0.156}$; (6.2)

and the saturated waste density, $\rho_{sat} \approx 0.67(\sigma_v')^{0.09}$. (6.3)

where density is in units of t/m^3 and effective stress is in units of kPa.

Similarly, the following relationships for waste PV1 were established:-

The dry density of the waste, $\rho_{dry} \approx 0.12 (\sigma_v')^{0.263}$; (6.4)

and the density of the waste at field capacity, $\rho_{FC} \approx 0.39 (\sigma_v')^{0.137}$. (6.5)

where density is in units of t/m^3 and effective stress is in units of kPa.

It was not possible to fit any type of curve to the saturated waste density data for PV1, mainly due to the reduction in saturated density between approximately 70 and 130 kPa. Over this stress range there is a considerable reduction in the voidage of the waste (the effective porosity reduces from approximately 17 to 4%). The water held in voids is

replaced by waste with a lower density than water, thereby causing an overall reduction in the saturated density of the waste (see also Section 6.7 on particle densities).

The following relationships for waste AG1 were established:-

The dry density of the waste, $\rho_{dry} \approx 0.36(\sigma_v')^{0.157}$; (6.6)

the density of the waste at field capacity, $\rho_{FC} \approx 0.82\,(\sigma_v')^{0.091}$; (6.7)

and the saturated waste density, $\rho_{sat} \approx 1.10\,(\sigma_v')^{0.041}$. (6.8)

where density is in units of t/m^3 and effective stress is in units of kPa.

Table 6.6 Effective porosity and density of waste DM2 at different average stresses

Applied stress kPa	Average stress in waste kPa	Effective porosity %	Dry density t/m^3	Density at field capacity t/m^3	Saturated density t/m^3
40	34.5	17.5	0.43	0.89	1.07
87	67.9	11	0.51	nd	nd
165	125	nd	0.56	nd	nd
322	247	nd	0.65	1.05	nd
603	471	nd	0.73	1.14	nd

Table 6.7 Effective porosity and density of waste DM3 at different average stresses

Applied stress kPa	Average stress in waste kPa	Effective porosity %	Dry density t/m^3	Density at field capacity t/m^3	Saturated density t/m^3
40	34.0	14.7	0.39	0.79	0.94
87	64.9	12.5	0.42	0.84	0.97
165	120	6.5	0.49	0.94	1.01
322	241	2	0.60	1.08	1.10
603	463	1.5	0.72	1.16	1.18

Table 6.8 Effective porosity and density of waste PV1 at different average stresses

Applied stress kPa	Average stress in waste kPa	Effective porosity %	Dry density t/m^3	Density at field capacity t/m^3	Saturated density t/m^3
40	34.6	23.0	0.31	0.64	0.87
87	67.9	17.0	0.35	0.71	0.88
165	127	3.5	0.45	0.76	0.80
322	253	2.2	0.53	0.83	0.85
603	486	<1	0.60	0.93	0.93

Table 6.9 Effective porosity and density of waste PV2 at different average stresses

Applied stress kPa	Average stress in waste kPa	Effective porosity %	Dry density t/m³	Density at field capacity t/m³	Saturated density t/m³
40	35.5	nd	0.28	nd	nd
87	72.4	nd	0.35	nd	nd
165	136	nd	0.41	nd	nd
322	273	nd	0.51	nd	nd
603	523	nd	0.62	nd	nd

Table 6.10 Effective porosity and density of waste AG1 at different average stresses

Applied stress kPa	Average stress in waste kPa	Effective porosity %	Dry density t/m³	Density at field capacity t/m³	Saturated density t/m³
40	34.6	15.7	0.64	1.12	1.28
87	66.8	10.2	0.69	1.21	1.31
165	123	4.4	0.77	1.28	1.32
322	239	1.1	0.86	1.35	1.36
603	458	<1	0.95	1.42	1.42

Figure 6.7 Average density of DM3 vs effective stress

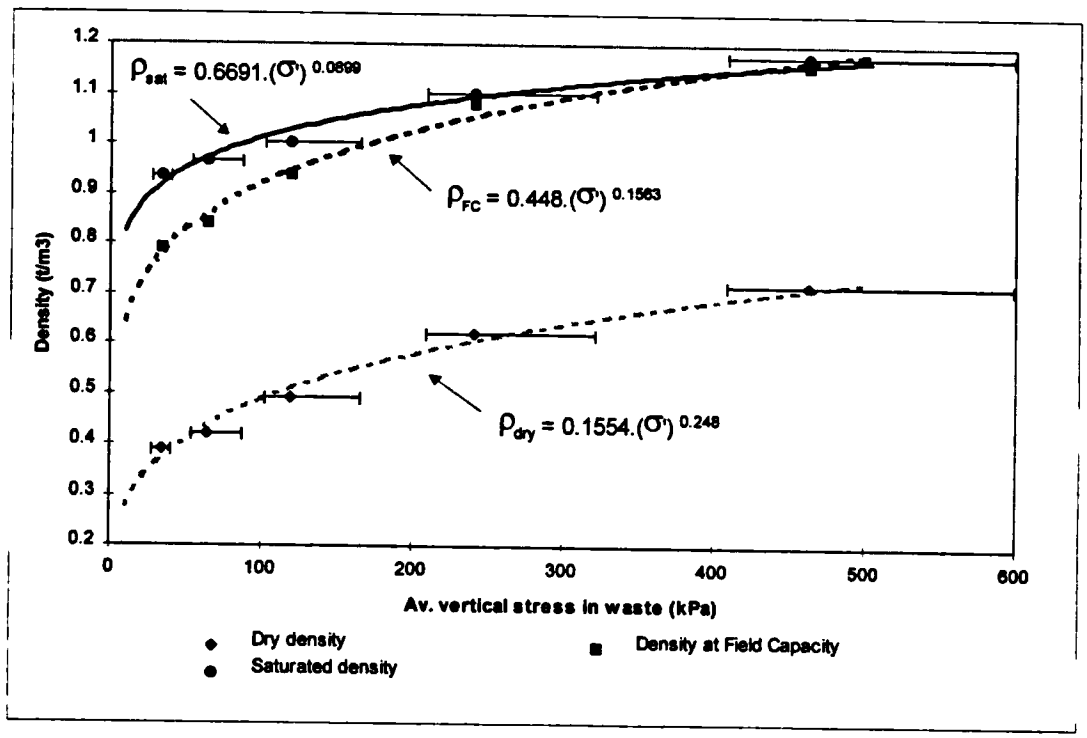

Figure 6.8 Average density of PV1 vs effective stress

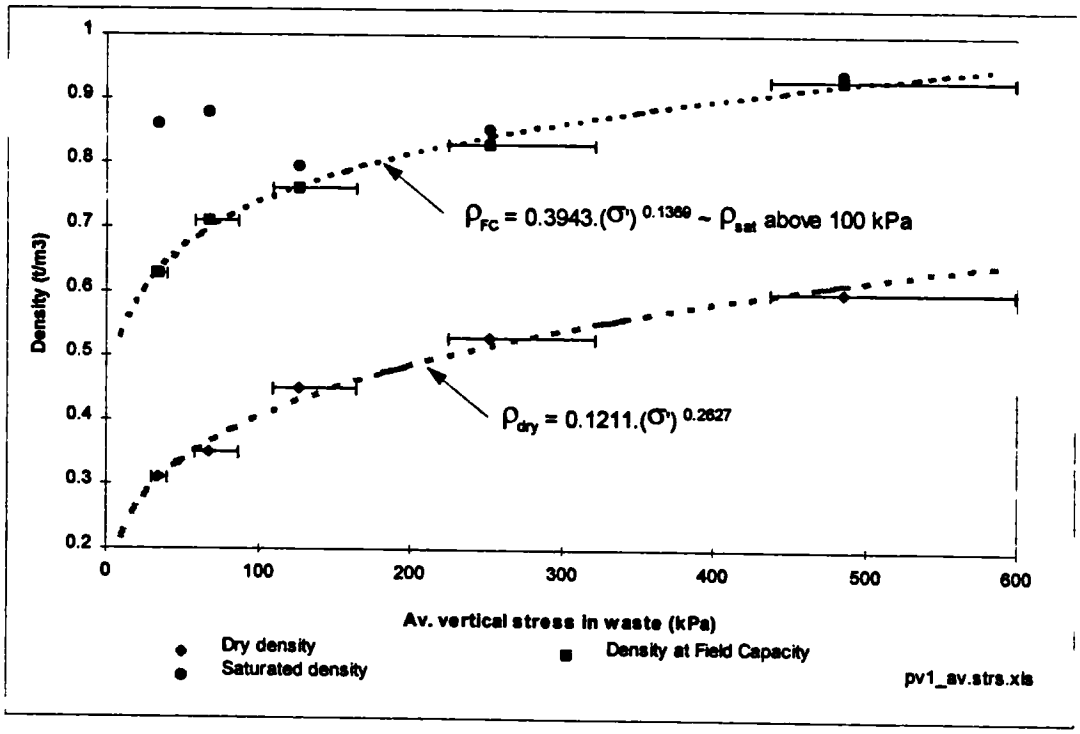

Figure 6.9 Average density of AG1 vs effective stress

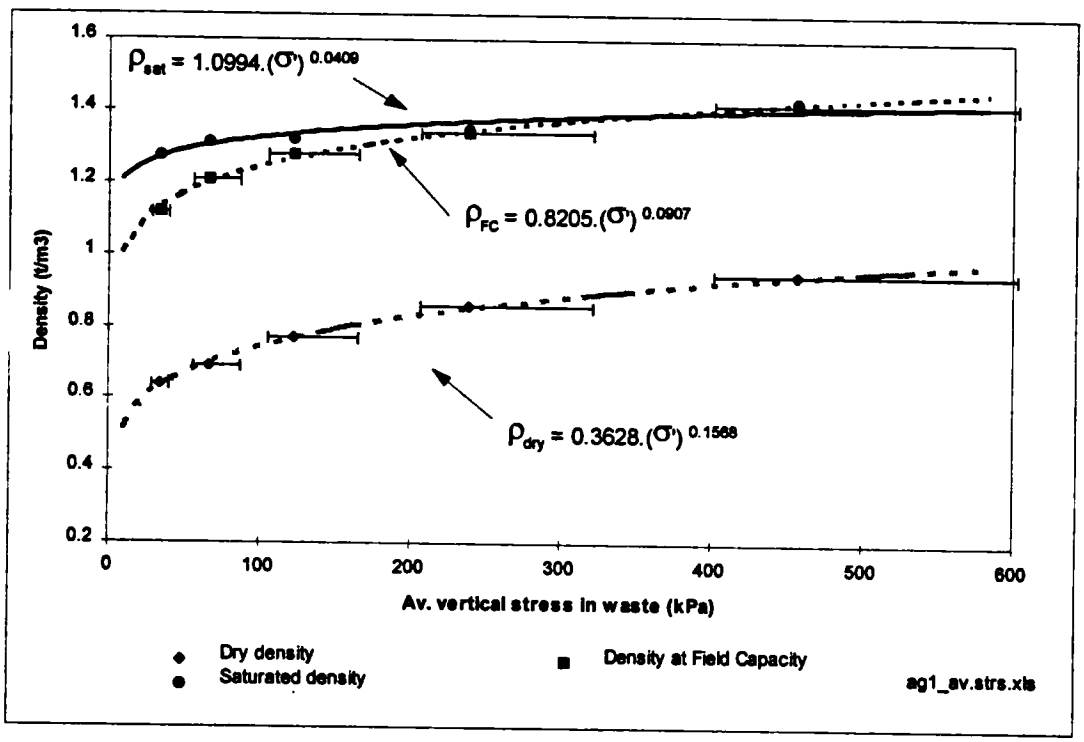

6.4.6 Effective porosity and water contents in relation to effective stress

Tables 6.11 to 6.13 summarise the water content at field capacity, the effective porosity and total saturation capacity for wastes DM3, PV1 and AG1 at various average stresses.

Figures 6.10 to 6.12 plot effective porosity, volumetric water content at field capacity, and total saturation capacity of wastes DM3, PV1 and AG1 against average stress. As previously noted (Sections 5.5.6, 5.6.6 & 5.8.6), the volumetric water content at field capacity is relatively independent of stress - values vary by a maximum of 5% (as a water content). The effective porosity of all waste types reduces very rapidly (from over 15% to less than 5%) as stresses increase up to approximately 100 kPa. Smaller reductions in effective porosity occur as stresses increase above 100 kPa.

The total saturation capacity (which is the sum of the effective porosity and water content at field capacity) reduces over the stress range 0 to 100 kPa. It then remains at a relatively constant value at higher stresses, mainly reflecting the water content at field capacity.

The water contents at field capacity expressed as a dry weight (WC_{dry}) for wastes DM3, PV1 and AG1 have been plotted against average stress in Figures 6.13 to 6.15. In wastes DM3 and PV1 the water content at field capacity at low average stresses was considerably greater than the original water content of the waste, indicating a large absorptive capacity. In comparison, waste AG1 (Figure 6.15) had a very limited absorptive capacity. It is not surprising that the absorptive capacity of AG1 was already exhausted, as the waste was excavated from the surface layers of a 20 year old landfill and would have been subjected to considerable volumes of infiltrating water.

Figures 6.13 to 6.15 indicate that the water contents at field capacity of all three wastes reduce with increasing stress. Consequently, if any of the wastes were at field capacity at low stresses (as was the case for waste AG1; wastes DM3 and PV1 would require additional water) then subsequent increases in stress would squeeze water out of the matrix of the waste. The implication of this finding is that increasing the depth of a landfill may result in water that was previously held as absorptive capacity being released as leachate.

Table 6.11 Effective porosity and volumetric water contents of waste DM3 at different average stresses

Applied stress	Average stress in waste	Dry density	WC_{dry} at FC	WC_{vol} at FC	Effective porosity	Total saturation capacity
kPa	kPa	t/m³	%	%	%	%
40	34.0	0.39	101.4	39.9	14.7	54.5
87	64.9	0.42	99	41.6	125.	54.2
165	120	0.49	90.8	44.5	6.5	50.7
322	241	0.60	76.1	44.9	2	46.9
603	463	0.72	61.8	44.4	1.5	45.9

Table 6.12 Effective porosity and volumetric water contents of waste PV1 at different average stresses

Applied stress	Average stress in waste	Dry density	WC_{dry} at FC	WC_{vol} at FC	Effective porosity	Total saturation capacity
kPa	kPa	t/m³	%	%	%	%
40	34.6	0.31	107.1	32.1	23.0	55.1
87	67.9	0.35	97.1	33.8	17.0	50.8
165	127	0.45	82.5	34.1	3.5	37.6
322	253	0.53	56.3	28.1	2.2	30.3
603	486	0.60	55.8	33.5	<1	34.5

Table 6.13 Effective porosity and volumetric water contents of waste AG1 at different average stresses

Applied stress	Average stress in waste	Dry density	WC_{dry} at FC	WC_{vol} at FC	Effective porosity	Total saturation capacity
kPa	kPa	t/m³	%	%	%	%
40	34.6	0.64	75.4	48.1	15.7	63.8
87	66.8	0.69	69	47.3	10.2	57.5
165	123	0.77	63.3	48.5	4.4	52.9
322	239	0.86	55.9	48.1	1.1	49.2
603	458	0.95	50.7	47.9	<1	48.9

Figure 6.10 Volumetric water contents vs effective stress for DM3

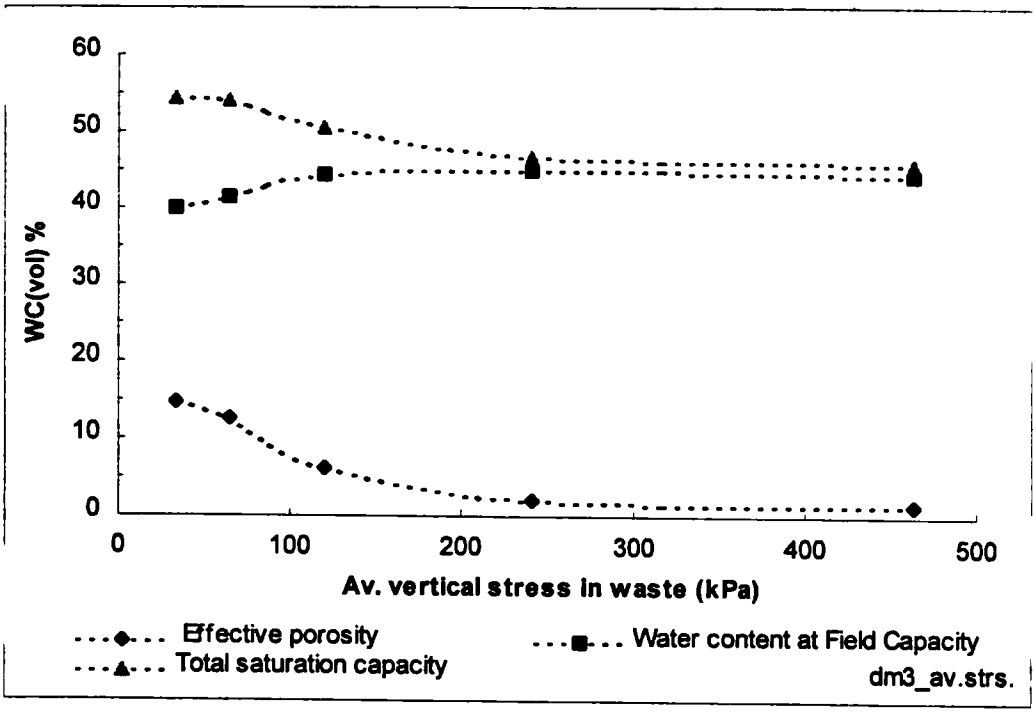

Figure 6.11 Volumetric water contents vs effective stress for PV1

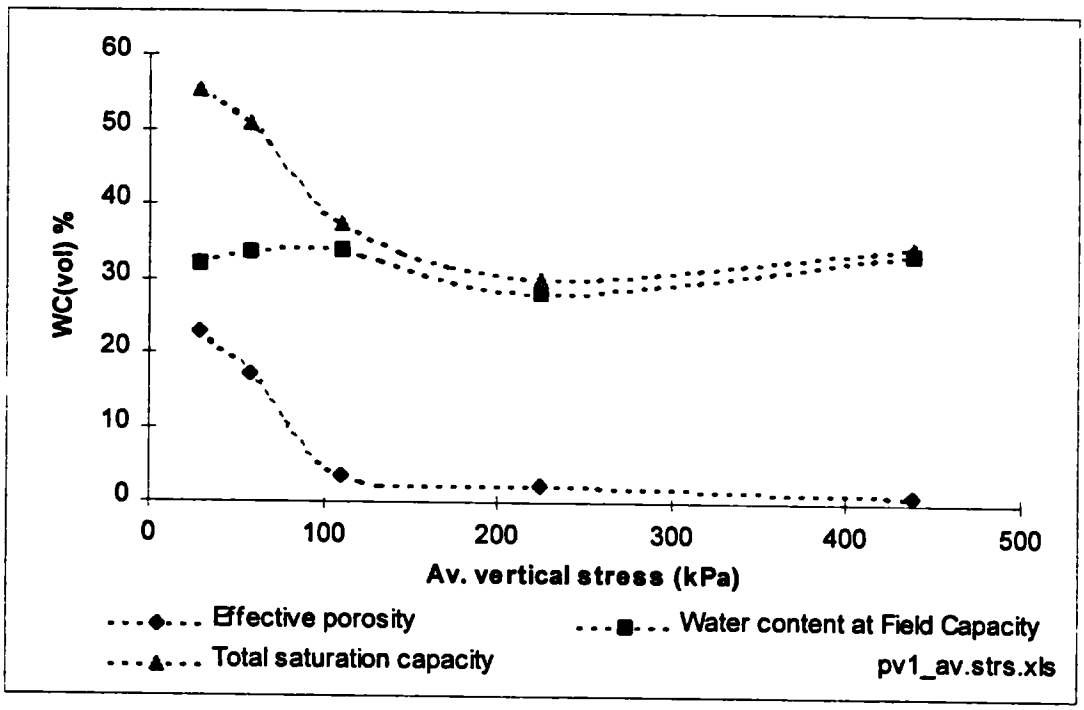

Figure 6.12 Volumetric water contents vs effective stress for AG1

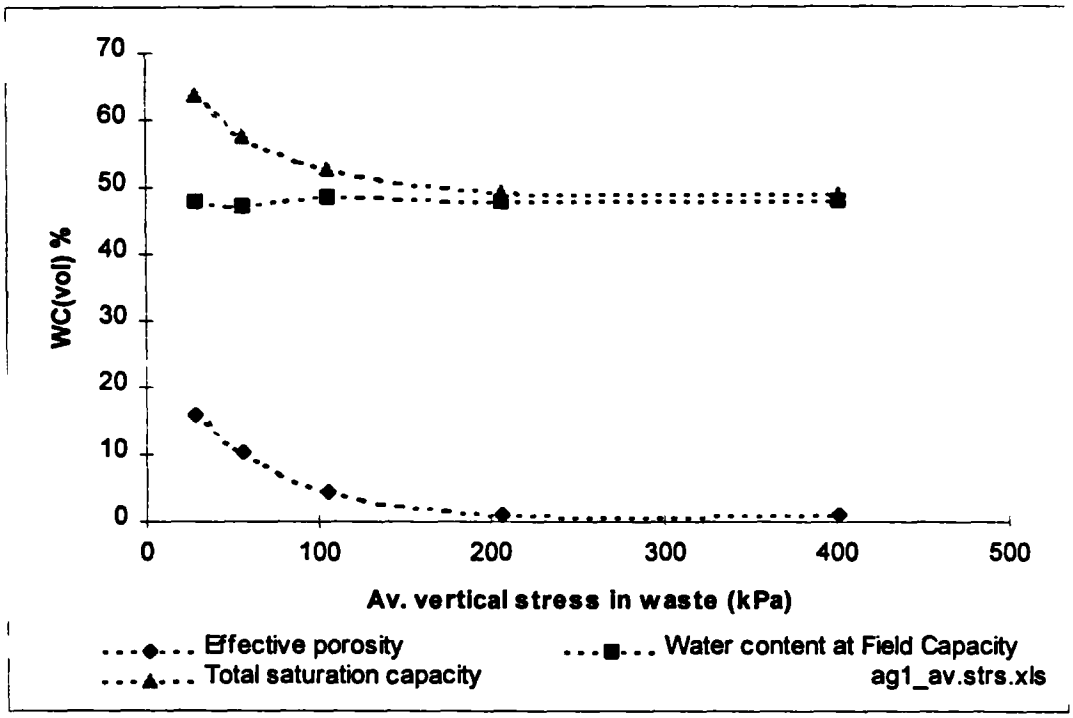

Figure 6.13 Water content at field capacity of DM3 vs effective stress

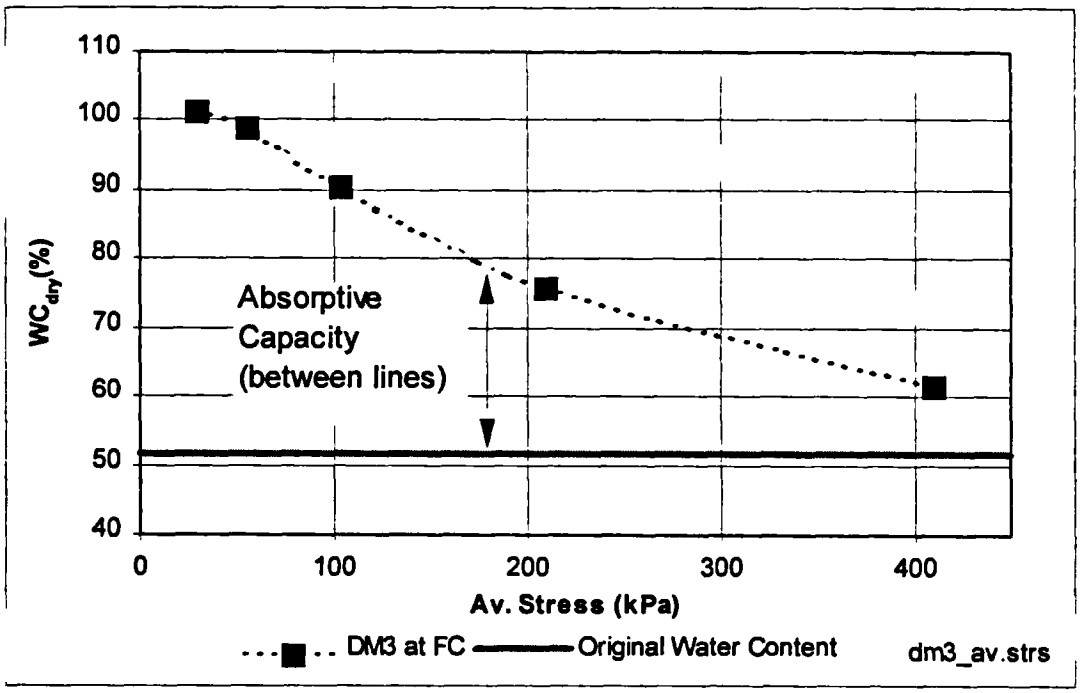

Figure 6.14 Water content at field capacity of PV1 vs effective stress

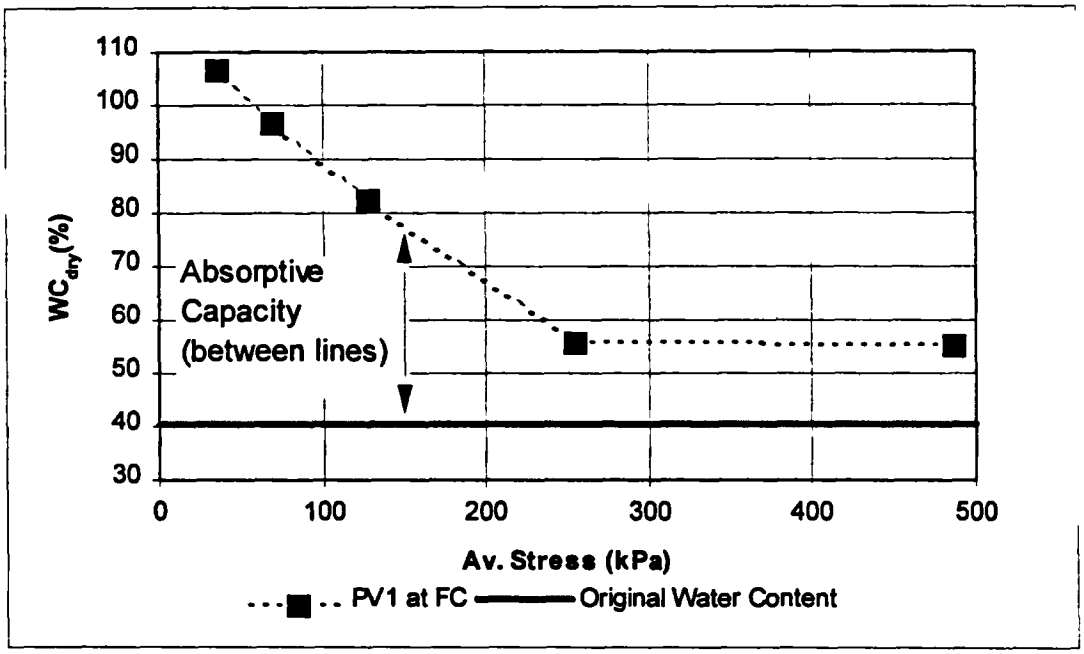

Figure 6.15 Water content at field capacity of AG1 vs effective stress

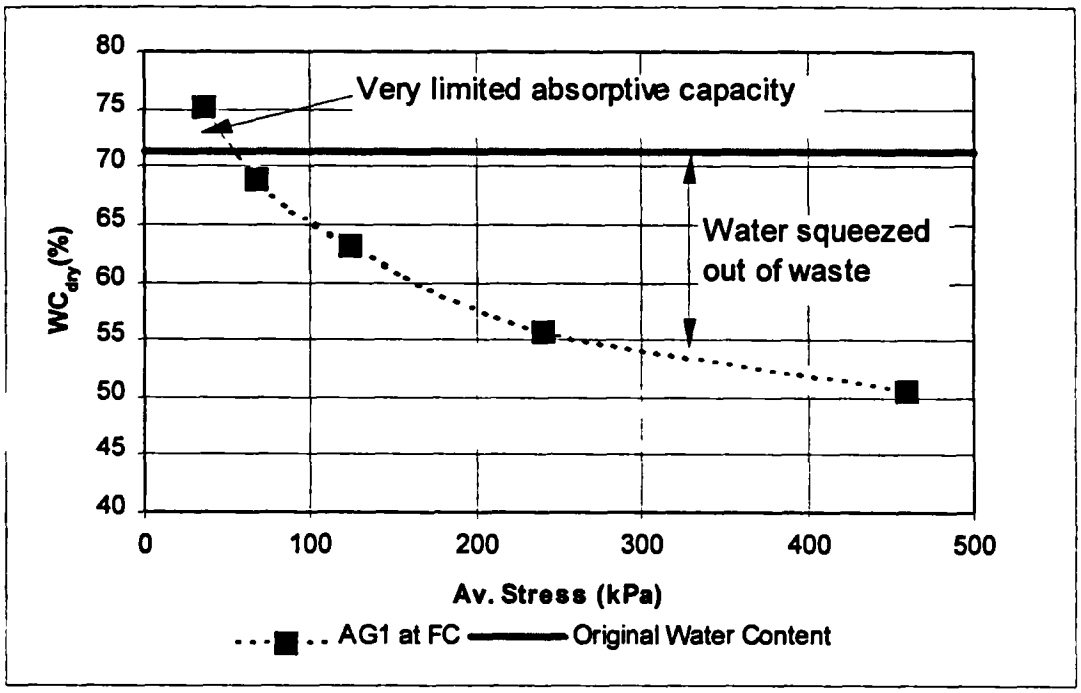

6.4.7 Relationship between hydraulic conductivity and effective stress

Hydraulic conductivity was measured at different applied stresses for wastes DM3, PV1 and AG1. Waste DM3 showed evidence of zones of different hydraulic conductivity at varying depths. The average transmitted vertical stress in the waste was calculated as described in Section 6.4.4 and is recorded against hydraulic conductivity in Tables 6.14 to 6.16.

The recorded average vertical stress is based on the conditions in the waste prior to the start of the constant head hydraulic conductivity tests. During these tests a hydraulic gradient was generated across the waste leading to the development of pore water pressures. The magnitude of these pressures are recorded in Tables 6.14 to 6.16. These pressures mean that the average effective stress in the waste during the hydraulic conductivity tests would have been less than that both prior to, and after the test. The influence of the pore water pressure on effective stress is more significant at lower applied stresses (where the calculated effective stresses are sometimes negative) than at higher applied stresses. Nevertheless, in Figures 6.16 to 6.18 the hydraulic conductivity of wastes DM3, PV1 and AG1 has been plotted against the average effective stress in the waste prior to the hydraulic conductivity tests. The error bars for stress encompass the applied stress as the maximum possible value and the transmitted stress calculated according to Equation 3.8, with $\delta=\phi'=38°$ as a minimum. This is justifiable because the density and hydraulic conductivity of a soil will tend to reflect the maximum effective stress to which it has been exposed. During the research few tests were undertaken on the amount of rebound that occurs in a waste when the vertical stress is reduced. It is recognised there this is an area that requires further work. Waste DM1 (at its original as-placed water content) rebounded by 18% when the applied stress was reduced from 165 to 0 kPa (Table 5.5). However, subsequent tests (not reported here) on an aged wet waste, indicated that the amount of rebound was less than 3% when the applied stress was reduced from 600 to 87 kPa.

Negative error bars have been plotted for hydraulic conductivity. Section 4.3.8 discussed possible errors with hydraulic conductivity measurements and indicated that at high applied stresses and low hydraulic conductivities the errors are mainly negative (due to problems of small leaks, peripheral flow etc.) Negative error bars have been plotted which vary from 80% (of the measurement) for readings between $1x10^{-7}$ and $1x10^{-8}$ m/s, to 10% for readings above $1x10^{-5}$ m/s.

The data in Figures 6.16 to 6.18 are plotted on a log-log scale and have been matched to power law curves in an Excel (version 7.0) spreadsheet. Initially a good match between the data from DM3 and an exponential law curve was achieved, with:-

$$K \text{ (in m/s)} = 1x10^{-4}\, e^{-0.0155\sigma'} \qquad (\sigma' \text{ in kPa}).$$

However, it was not possible to achieve a reasonable match between the data from PV1 and AG1 and an exponential law curve, and consequently a power law relationship between hydraulic conductivity and effective stress was adopted. All wastes show a very rapid reduction in hydraulic conductivity with increasing applied stress. The best fit lines for the three waste types are as follows:-

DM3: $K = 2.1(\sigma')^{-2.71}$ (6.9)

PV1: $K = 65(\sigma')^{-3.4}$ (6.10)

AG1 $K = 36(\sigma')^{-3.34}$ (6.11)

where K is in m/s and σ' is in kPa. The relationships are considered valid up to effective stresses of approximately 500 kPa and should not be used at stresses below 10 kPa:

There is a wider scatter of data points in the plot for DM3 because two measurements of stress and hydraulic conductivity were taken for each compression stage. One data point shown on Figure 6.16 was eliminated from the best fit line as it fell well outside the general trend.

Considering the size of the error bars, a wide number of gradients could be plotted through the points. An approximate worst case fit (which for the purpose of this thesis is considered to be the fit which gives the lowest hydraulic conductivity at a given stress) has been plotted for each waste type and gives the relationships:-

DM3: $K = 17(\sigma')^{-3.26}$ (6.12)

PV1: $K = 2000(\sigma')^{-4.4}$ (6.13)

AG1 $K = 305(\sigma')^{-3.9}$ (6.14)

The data points from all waste types have been combined onto one graph (Figure 6.19), and give the following best fit curve:-

$$K = 10(\sigma')^{-3.1} \qquad (6.15)$$

This relationship gives a hydraulic conductivity of $1x10^{-7}$ m/s at a stress of 380 kPa, and a hydraulic conductivity of $1x10^{-8}$ m/s at a stress of 800 kPa (which is outside the recommended range for effective stress).

An approximate worst case fit for this plot gives:

$$K = 80(\sigma')^{-3.63} \qquad (6.16)$$

This relationship gives a hydraulic conductivity of $1x10^{-7}$ m/s at a stress of 284 kPa, and a hydraulic conductivity of $1x10^{-8}$ m/s at a stress of 535 kPa.

Table 6.14 Average stress and hydraulic conductivity for DM3

Applied Stress kPa	Depth range of waste below upper platen metres	Av' depth of zone below upper platen metres	Calculated* average stress in waste kPa	Average pore water pressure kPa	Hydraulic conductivity of waste in zone m/s
40	0.19-0.99	0.59	36.6	22	$3.4x10^{-5}$
40	1.35-2.35	1.85	31.6	31	$1.5x10^{-4}$
87	0.19-0.99	0.59	73.4	33	$1.9x10^{-5}$
87	1.17-2.17	1.67	55.8	55	$8.2x10^{-5}$
165	0.19-0.79	0.49	139	32	$3.1x10^{-6}$
165	0.99-1.89	1.44	102	60	$2.8x10^{-5}$
322	0.19-0.79	0.49	268	39	$4.4x10^{-7}$
322	0.66-1.56	1.11	212	65	$8.9x10^{-6}$
603	0.19-0.59	0.39	517	38	$3.7x10^{-8}$
603	0.57-1.37	0.97	412	65	$2.7x10^{-7}$

* Based on $\delta = 30^{o}$, $\phi' = 40^{o}$

Table 6.15 Average stress and hydraulic conductivity for PV1

Applied Stress kPa	Depth range of waste below upper platen metres	Av' depth of zone below upper platen metres	Calculated* average stress in waste kPa	Average pore water pressure kPa	Hydraulic conductivity of waste in zone m/s
40	0.2-2.02	1.11	34.2	37	$3.3x10^{-4}$
87	0.2-1.76	0.98	66.1	41	$3.4x10^{-5}$
165	0.2-1.54	0.87	123	42	$2.4x10^{-6}$
322	0.2-1.29	0.75	243	36	$2.2x10^{-7}$
603	0.2-1.11	0.66	466	35	$4.8x10^{-8}$

* Based on $\delta = 30^{o}$, $\phi' = 40^{o}$

Table 6.16 Average stress and hydraulic conductivity for AG1

Applied Stress kPa	Depth range of waste below upper platen metres	Av' depth of zone below upper platen metres	Calculated* average stress in waste kPa	Average pore water pressure kPa	Hydraulic conductivity of waste in zone m/s
40	0.12-2.03	1.08	34.3	30	$1.5x10^{-4}$
87	0.12-1.87	1.00	65.8	34	$5.0x10^{-5}$
165	0.12-1.70	0.91	121	42	$6.0x10^{-6}$
322	0.12-1.58	0.85	234	49	$5.0x10^{-7}$
603	0.12-1.41	0.77	446	56	$3.5x10^{-8}$

* Based on $\delta = 30^{o}$, $\phi' = 40^{o}$

Figure 6.16 Hydraulic conductivity of DM3 vs effective stress

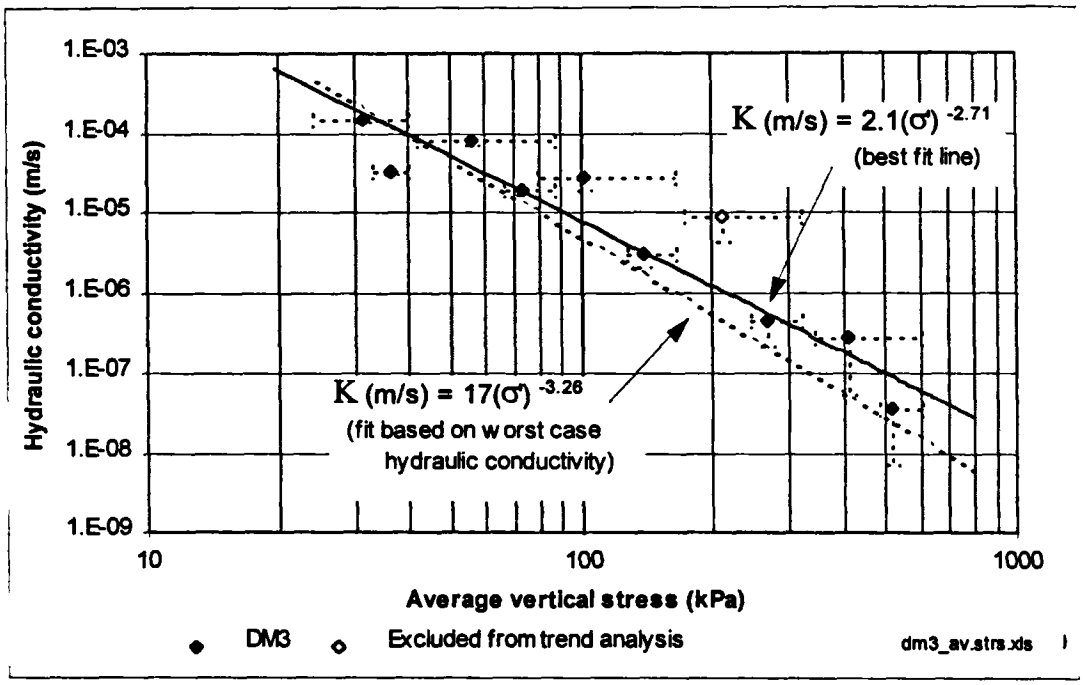

Figure 6.17 Hydraulic conductivity of PV1 vs effective stress

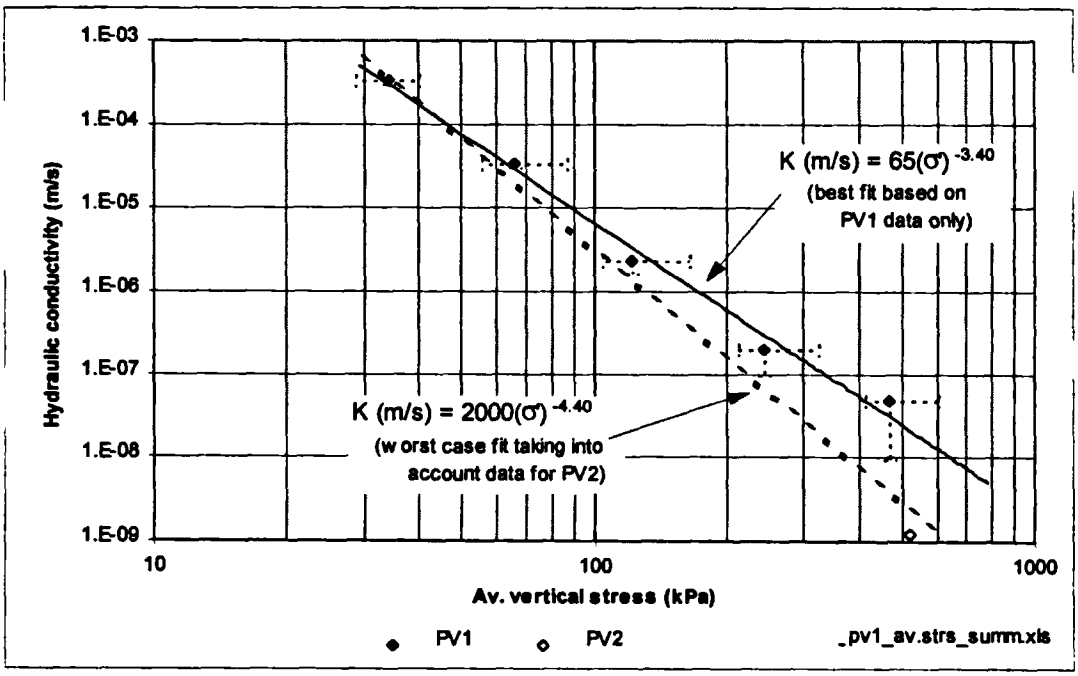

Figure 6.18 Hydraulic conductivity of AG1 vs effective stress

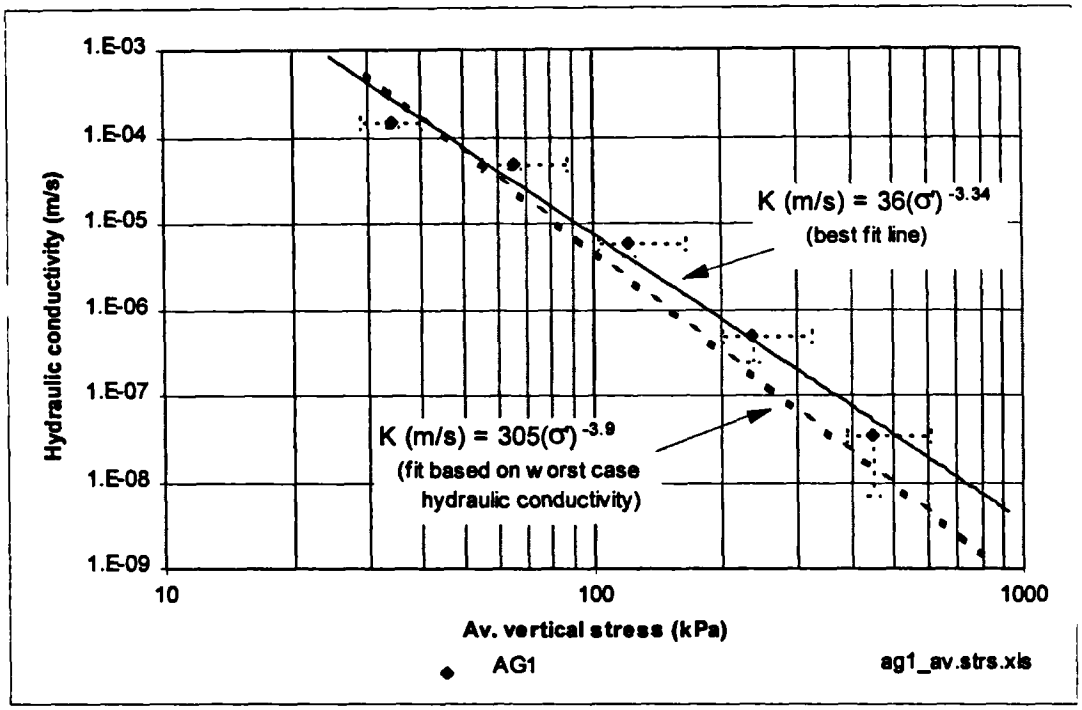

Figure 6.19 Hydraulic conductivity of all wastes vs effective stress

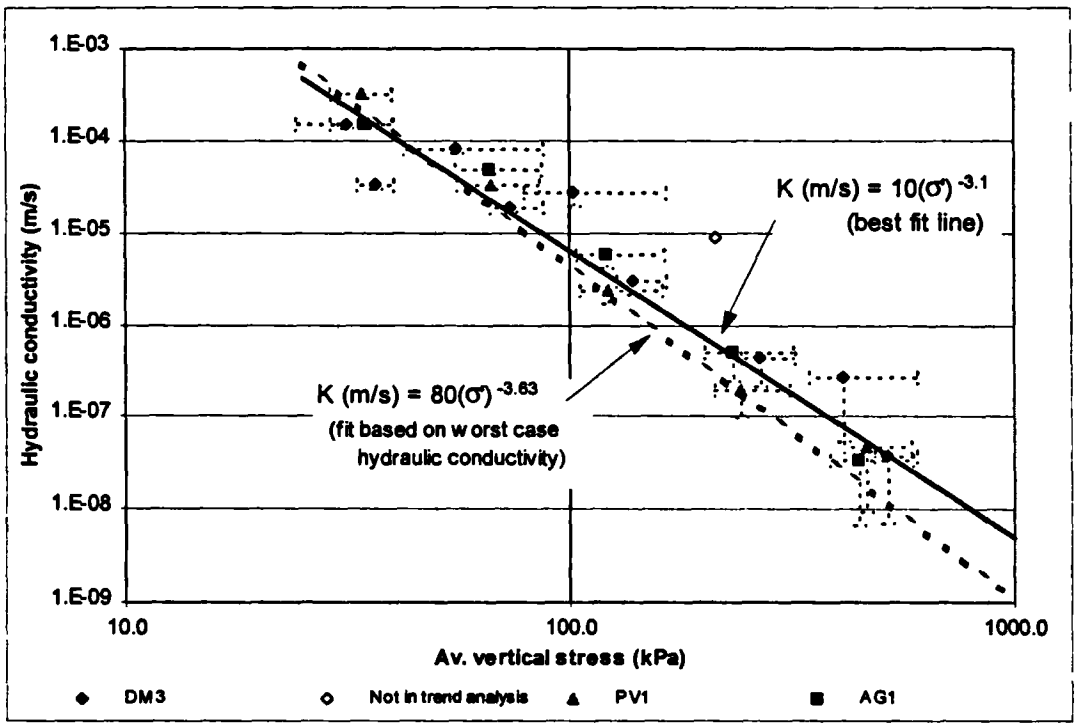

6.5 Relationship between depth of burial and stress

It is possible to estimate the vertical effective stress that will arise from self weight effects at depth z within an unsaturated landfill by utilising an appropriate relationship (e.g. Equation 6.2) between density and effective stress.

Consider a layer of waste of thickness δz and of mass δm, at depth z within a landfill. The effective stress acting on the top of the layer is σ_v' and the stress on the base of the layer is $\sigma_v' + \delta\sigma_v'$.

$$\delta\sigma_v' = \delta m.g,$$

but $\delta m = \rho_{av}.\delta z$ (per unit area)

where ρ_{av} is the average density of the waste in depth δz.

Integrating with respect to vertical effective stress and depth gives

$$\int_0^{\sigma_v'} d\sigma_v' = \int_0^z \rho g.dz \qquad (6.17)$$

ρ is a function of σ'_v, so

$$\int_0^{\sigma_v'} \frac{d\sigma_v'}{\rho g} = \int_0^z dz = z \qquad (6.18)$$

$$z = \int \frac{1}{\rho}.d\sigma'_v \qquad (6.19)$$

Therefore the area under a graph of $1/(\rho.g)$ plotted against σ_v' gives the unsaturated depth z required to generate a particular stress σ_v', assuming that the correct relationship between density and stress has been used.

Alternatively, as $\rho_{FC} \approx 0.45\ (\sigma_v')^{0.156}$, for the case of waste DM3, Equation 6.18 can be rewritten as

$$\int_0^{\sigma_v'} d\sigma_v' = \int_0^z 0.45.g.(\sigma_v')^{0.156}.dz$$

$$\text{or} \quad \int_0^{\sigma'_v} \frac{1}{0.45g}(\sigma'_v)^{-0.156} d\sigma'_v = \int_0^z dz$$

$$\therefore \quad z = \frac{1}{0.38g}(\sigma'_v)^{0.844}$$

$$\text{or} \quad \sigma'_v = (0.38g.z)^{1.185} \tag{6.20}$$

The density of waste PV1 at field capacity is related to effective stress by:-

$$\rho_{FC} \approx 0.39\,(\sigma_v')^{0.137}$$

which leads to the relationship:-

$$\sigma'_v = (0.34g.z)^{1.16} \tag{6.21}$$

Likewise the density of waste AG1 at field capacity is given by:-

$$\rho_{FC} \approx 0.82\,(\sigma_v')^{0.091}$$

leading to:-

$$\sigma'_v = (0.75g.z)^{1.10} \tag{6.22}$$

6.6 Waste stiffness

Values of constrained modulus (M_0, Equation 2.30) are calculated using the average stress in the waste for each compression stage. Tables 6.17 to 6.22 summarise the results for the various waste types.

Table 6.17 The constrained modulus of waste DM1

Stage	Applied load increment	Average stress increment	Increase in effective stress	Average effective stress in stage[1]	Thickness of waste at start of stage	Compression of waste during stage	Constrained Modulus $=\Delta\sigma_v'.t/\rho$
			$\Delta\sigma_v'$	$\sigma_{v(av)}'$	t	ρ	M_0
	kPa	kPa	kPa	kPa	mm	mm	kPa
1	0-40	0-34.6	34.6	18.1	2,089	71	1,018
2	40-165	34.6-122	87.7	79.3	2,018	267	663
3	165-0	122-0	-122	62	1,751	-61	3,511
4	0-165	0-122	122	62	1,812	64	3,454
5	165-322	122-237	115	180	1,748	119	1,689

[1] Includes self weight of sample

Table 6.18 The constrained modulus of waste DM2

Stage	Applied load increment	Average stress increment	Increase in effective stress	Average effective stress in stage[1]	Thickness of waste at start of stage	Compression of waste during stage	Constrained Modulus $=\Delta\sigma_v'.t/\rho$
			$\Delta\sigma_v'$	$\sigma_{v(av)}'$	t	ρ	M_0
	kPa	kPa	kPa	kPa	mm	mm	kPa
1	0-40	0-34.5	34.5	18.3	2,377	407	201
2	40-87	34.5-67.9	33.4	51.2	1,990	334	199
3	87-165	67.9-125	57.1	97	1,653	135	699
4	165-322	125-247	122	187	1,515	207	893
5	322-603	247-471	224	360	1,308	141	2,078

[1] Includes self weight of sample

Table 6.19 The constrained modulus of waste DM3

Stage	Applied load increment	Average stress increment	Increase in effective stress	Average effective stress in stage[1]	Thickness of waste at start of stage	Compression of waste during stage	Constrained Modulus $=\Delta\sigma_v'.t/\rho$
			$\Delta\sigma_v'$	$\sigma_{v(av)}'$	t	ρ	M_0
	kPa	kPa	kPa	kPa	mm	mm	kPa
1	0-40	0-34	34	23.5	2,554	370	235
2	40-87	34-64.9	30.9	58.0	2,147	142	467
3	87-165	64.9-120	55.1	101.1	1,983	235	465
4	165-322	120-241	121	188.6	1,701	270	762
5	322-603	241-463	222	359.4	1,382	188	1,632

[1] Includes self weight of sample

Table 6.20 The constrained modulus of waste PV1

Stage	Applied load increment	Average stress increment	Increase in effective stress	Average effective stress in stage[1]	Thickness of waste at start of stage	Compression of waste during stage	Constrained Modulus $=\Delta\sigma_v'.t/\rho$
			$\Delta\sigma_v'$	$\sigma_{v'(av)}$	t	ρ	M_0
	kPa	kPa	kPa	kPa	mm	mm	kPa
1	0-40	0-34.6	34.6	23.0	2,124	306	240
2	40-87	34.6-67.9	33.3	56.8	1,769	208	283
3	87-165	67.9-127	59.1	103.0	1,555	216	425
4	165-322	127-253	126	194.6	1,216	127	1,206
5	322-603	253-486	233	373.8	1,025	119	2,007

[1] Includes self weight of sample

Table 6.21 The constrained modulus of waste PV2

Stage	Applied load increment	Average stress increment	Increase in effective stress	Average effective stress in stage[1]	Thickness of waste at start of stage	Compression of waste during stage	Constrained Modulus $=\Delta\sigma_v'.t/\rho$
			$\Delta\sigma_v'$	$\sigma_{v'(av)}$	t	ρ	M_0
	kPa	kPa	kPa	kPa	mm	mm	kPa
1	0-40	0-35.5	35.5	21.4	2,288	675	120
2	40-87	35.5-72.4	36.9	57.6	1,613	323	184
3	87-165	72.4-136	63.6	107.9	1,290	208	394
4	165-322	136-273	137	208.1	1,082	200	741
5	322-603	273-523	250	401.7	882	158	1,396

[1] Includes self weight of sample

Table 6.22 The constrained modulus of waste AG1

Stage	Applied load increment	Average stress increment	Increase in effective stress	Average effective stress in stage[1]	Thickness of waste at start of stage	Compression of waste during stage	Constrained Modulus $=\Delta\sigma_v'.t/\rho$
			$\Delta\sigma_v'$	$\sigma_{v'(av)}$	t	ρ	M_0
	kPa	kPa	kPa	kPa	mm	mm	kPa
1	0-40	0-34.6	34.6	27.7	2,290	334	237
2	40-87	34.6-66.8	32.2	61.4	1,909	135	455
3	87-165	66.8-123	56.2	105.5	1,754	164	601
4	165-322	123-239	116	191.1	1,581	165	1,112
5	322-603	239-458	219	357.9	1,458	120	2,661

[1] Includes self weight of sample

Figure 6.20 shows the relationship between the constrained modulus (M_0) and vertical effective stress for all waste types during first loading. There is an approximate linear increase in stiffness of all wastes with increasing effective stress. The stiffest waste is AG1 ($M_0 \approx 7\sigma_v'$); the most compressible waste is PV2 ($M_0 \approx 3.5\sigma_v'$).

Figure 6.20 Constrained modulus vs vertical effective stress for all wastes

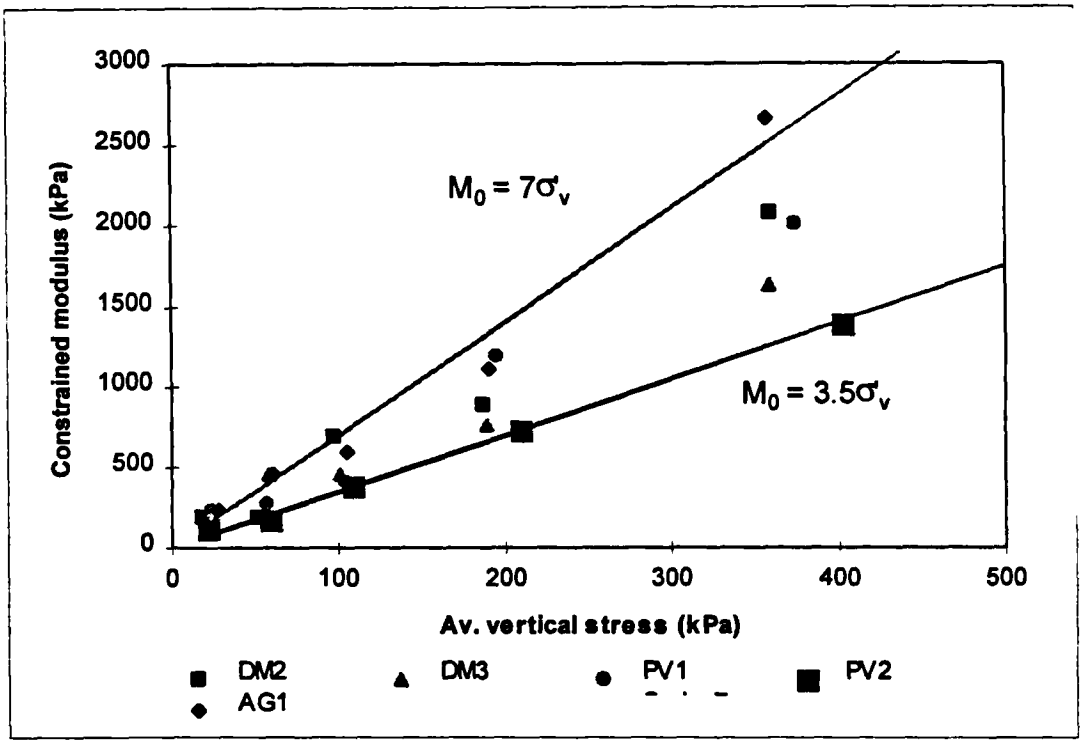

6.7 Specific volume and dry particle density

The specific volume, v, of the waste at each stage of compression can be determined from the percentage of total voids in the sample. The total voids approximates to the sum of the water content at field capacity, expressed in volumetric terms (WC_{vol}), and the effective porosity, n_e.

$$v = \frac{V_s+V_v}{V_s} = \frac{1}{\left(1-(WC_{vol}+n_e)\right)} \qquad (6.23)$$

The average density of the waste particles, ρ_s, is

$$\rho_s = \frac{m_s}{V_s} \qquad (6.24)$$

where m_s is the mass and V_s is the volume of dry solids. Also as

$$\rho_{dry} = \frac{m_s}{V_s+V_v}$$

$$\rho_s = \nu.\rho_{dry} \quad (6.25)$$

Tables 6.23 and 6.24 indicate that the average particle density of wastes DM3 and PV1 increase with applied stress. The change in particle density with increasing applied stress is less in waste AG1 (Table 6.25), which probably reflects the greater proportion of fines and soil-like material in the sample. In conventional soil mechanics it is assumed that the solid particles are incompressible and the particle density does not change significantly. The finding that the particle density of the wastes tested varied with applied stress is important in that it may cast doubt on the applicability of some soil mechanics theories to household wastes.

A check on the validity of the above findings can be made by considering the necessary reduction in the volume of voids required to maintain a constant particle density as the dry density increases. Assuming the particle density of waste DM3 remained constant at 0.876 t/m^3, at an applied stress of 603 kPa the specific volume would need to be 1.27. This implies that the voids in the sample would have been reduced to 19% by volume. Assuming that these voids were filled with water, the volumetric water content (WC_{vol}) would be 19% and the water content (WC_{dry}) 26.8%. The actual water content (WC_{dry}) at an applied stress of 603 kPa was 61.8%. The discrepancy between these two values in terms of the volume of water held in the waste is 972 litres (mass of dry solids = 2,672 kg - Section 5.5). This is well outside the limits of experimental error in determining the mass of the waste and therefore indicates that a constant particle density is not feasible.

Table 6.23 Specific volume and average particle density of waste DM3

Applied Stress	Average Stress	Dry Density	Effective porosity	WC at FC	Volume voids	Volume solids	Specific volume	Particle density
		ρ_{dry}	n_e	WC_{vol}	V_v	V_s	ν	ρ_s
kPa	kPa	t/m^3	%	%	%	%		t/m^3
40	34.0	0.39	14.4	41.1	55.5	44.5	2.247	0.876
87	64.9	0.43	12.6	43	55.6	44.4	2.252	0.968
165	120	0.50	6.5	44.5	51.0	49.0	2.041	1.020
322	241	0.62	2	45	47.0	53.0	1.887	1.170
603	463	0.71	1.5	44	45.5	54.5	1.835	1.303

Table 6.24 Specific volume and average particle density of waste PV1

Applied Stress	Average Stress	Dry Density	Effective porosity	WC at FC	Volume voids	Volume solids	Specific volume	Particle density
		ρ_{dry}	n_e	WC_{vol}	V_v	V_s	v	ρ_s
kPa	kPa	t/m³	%	%	%	%		t/m³
40	34.6	0.31	14.6	33	47.6	52.4	1.908	0.592
87	67.9	0.35	12.3	36	48.3	51.7	1.934	0.677
165	127	0.45	6.2	31	37.2	62.8	1.592	0.717
322	253	0.53	2	30	32.0	68.0	1.471	0.779
603	486	0.60	1.5	34	35.5	64.5	1.550	0.930

Table 6.25 Specific volume and average particle density of waste AG1

Applied Stress	Average Stress	Dry Density	Effective porosity	WC at FC	Volume voids	Volume solids	Specific volume	Particle density
		ρ_{dry}	n_e	WC_{vol}	V_v	V_s	v	ρ_s
kPa	kPa	t/m³	%	%	%	%		t/m³
40	34.6	0.62	15.4	46.7	62.1	37.9	2.639	1.636
87	66.8	0.69	10.0	47.3	57.3	42.7	2.342	1.616
165	123	0.77	4.4	48.5	52.9	47.1	2.123	1.635
322	239	0.86	1	48.1	49.1	50.9	1.965	1.690
603	458	0.95	1	47.9	48.9	51.1	1.957	1.859

Chapter 7

A stress dependent hydraulic conductivity flow model

7.1 Summary

A new module is written for the USGS' three dimensional groundwater flow programme MODFLOW. The module varies the hydraulic conductivity in the model according to the effective stress at each cell. As effective stress is related to pore water pressure, the hydraulic conductivity varies according to changes in modelled water head.

The new module is verified against two analytical solutions for flow in an aquifer where the hydraulic conductivity varies with effective stress. The first solution concerns vertical infiltration through a landfill, and the second, steady state flow to a pumped well in a confined aquifer.

7.2 Introduction

In Chapters 1 and 2 the importance of fluid movement in removing the polluting potential of landfills was discussed. This research has shown that the hydraulic conductivity of household wastes is related to effective stress. Consequently, in the absence of pre-compaction, the hydraulic conductivity of wastes will usually decrease with increasing landfill depth. It was considered to be helpful and necessary to develop a groundwater flow model that takes this finding into account in order to assess its implications on both the ability to flush wastes and on general leachate control systems.

The model chosen for this purpose was MODFLOW, published by the United States Geological Survey (USGS). A new module was written and a small part of the original model re-written to allow hydraulic conductivity to vary with effective stress. A pre and post processor package, Groundwater Vistas was used as a graphical interface to create the data files used by MODFLOW and to examine the output data files created by successful (i.e. converged) simulation runs.

7.3 MODFLOW and Groundwater Vistas

MODFLOW is a multi-layered three dimensional numerical groundwater flow model. The model simulates steady state and non steady (transient) flow in an irregularly shaped flow domain in which layers can be confined or unconfined. Flow in each layer is only two dimensional, but layers are linked together hydraulically to create the three dimensional capability of the model. Each layer is discretised into variably sized rectangular blocks or cells; the hydgrogeological properties of each individual cell are defined and flow through the overall system solved using a finite-difference approximation to the governing finite difference equations. The main outputs from the model are groundwater head and volumetric flow. Additional sources of water can be added to, or removed from, the model in a variety of forms including wells, drains, constant head cells and areal recharge.

The model has become an industry standard for modelling groundwater flow. The first version of the model was made available in 1983 (McDonald and Harbaugh, 1984) and since then there have been frequent updates and additions to the code. The programme is written in FORTRAN and both the source code and compiled executable files are available free of charge from the USGS (http://www.water.usgs.gov/software/).

The data input (and output) files required by MODFLOW are long and cumbersome to create and use. It is normal to use a pre-processor to create MODFLOW data files, and a post processor to display and analyse the output. Groundwater Vistas (marketed by Environmental Simulations Ltd) is a graphical interface which combines both of these functions into one programme. Groundwater Vistas also incorporates a windows based version of MODFLOW which runs seamlessly as part of the package. Groundwater Vistas displays the model design in both plan and cross-sectional views using a split window (i.e. both views are visible at the same time). Results are presented as contours, colour floods, velocity vectors, and detailed mass balance analyses.

The latest version of MODFLOW (MODFLOW-96, version 3.2) was modified for this research. Documentation relating to this version of the model includes both user's and programmer's manuals (Harbaugh and McDonald, 1996 & 1996a).

7.4 Structure of MODFLOW

MODFLOW is based on a modular structure consisting of a Main Program which calls a series of independent subroutines called modules or packages (McDonald and Harbaugh, 1984). Each package deals with a specific feature of the hydrologic system that is to be simulated. The packages can be split into five general groups:-

1) The Basic (BAS) package (obligatory)

The Basic Package handles a number of administrative tasks for the model. It reads data on the number of rows, columns, layers, and stress periods (see point 4 below), on the major options to be used, and on the location of input data for those options. It allocates space in computer memory for model arrays; reads data specifying initial and boundary conditions; reads and implements data establishing the discretization of time; sets up the starting head arrays for each time step; calculates an overall water budget; and controls model output according to user specification (McDonald and Harbaugh, 1984).

2) Block centred flow (BCF) package (obligatory)

The block centred Flow (BCF) Package computes the conductance components of the finite-difference equation which determine flow between adjacent cells. It also computes the terms that determine the rate of movement of water to and from storage.

3) Solver (e.g. SIP) package (obligatory)

A solver package is required to solve the linear equations that describe the flow system in the model. There are a number of different mathematical approaches and solutions to the problem resulting in the availability of different packages, such as the Strongly Implicit Procedure (SIP) or Slice-Successive Over-relaxation (SOR) package. However, all solvers are based on iterative techniques.

4) Stress packages (e.g. RCH or WEL)

Stress, in MODFLOW terms, relates to the input or removal of water from the model. Therefore, stress packages replicate the processes they are intended to represent by controlling part of the water budget into individual elements of the model. For example, the well package (WEL) simulates the operation of pumping wells by removing a set volume of water (per unit time) from each cell of the

model containing an active well. There are currently at least eight different stress packages, including packages for recharge, drains, rivers and aquifer compaction (which releases water from storage).

5) ***Hydrogeological parameter packages***
This group of packages modifies the hydrogeological parameters initially specified within the Basic package. At present the only package published by the USGS which belongs to this group is the horizontal flow barrier package, simulating thin, vertical low-permeability geologic features that impede the horizontal flow of groundwater. The aquifer compaction package does not belong to this group as, although it assumes the specific yield of interbeds are reducing during compaction (thereby releasing water from storage), the actual changes in storativity are not carried through into the equations governing rates of flow.

MODFLOW divides the period of simulation into a series of "stress periods" within which specified stress parameters are constant. Each stress period, in turn, is divided into a series of time steps. The finite-difference flow equations are formulated and solved to yield the head at each node at the end of each time step, thus allowing transient situations to be modelled.

The output from a MODFLOW simulation includes the distribution of head and a volumetric cell by cell flow analysis. These data can be used to produce contours of head, flow velocity vectors and mass balances of flow.

7.5 Conceptual design of a stress dependent hydraulic conductivity (SDK) package

Implementation of a stress dependent hydraulic conductivity (SDK) package requires that the hydraulic conductivity at each cell in the model is allowed to vary according to the effective stress. However, the effective stress at any point in the model is related to the head, and the head in turn will be dependent on the hydraulic conductivity (see Figure 7.1). This results in a loop of inter-related parameters that in general can only be solved by iteration.

The existing program structure was therefore modified (see Figure 7.2) to incorporate a new SDK package that calculates the effective stress and hydraulic conductivity, throughout the model, only after an initial head distribution has been produced (based on the initial user-defined values of hydraulic conductivity). The new values of hydraulic

conductivity across the model will alter the head distribution; this is re-calculated by re-formulating the finite difference flow equations and re-invoking the solver package.

The SDK package is then called again and the process of calculating revised values of effective stress and hydraulic conductivity repeated. Solving of the head distribution, followed by the calling of the SDK package is continued until the maximum difference between successive values of calculated hydraulic conductivity at every cell is less than a user-defined tolerance. At this point the model will move on to the next time step or stress period if one has been defined.

Figure 7.1 Relationship and dependency of model variables

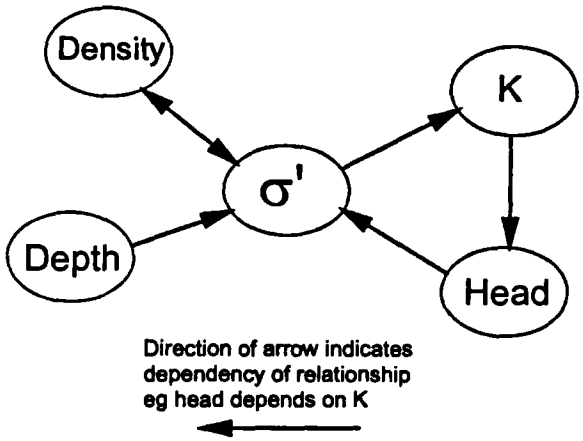

Figure 7.2 Existing and revised program structure

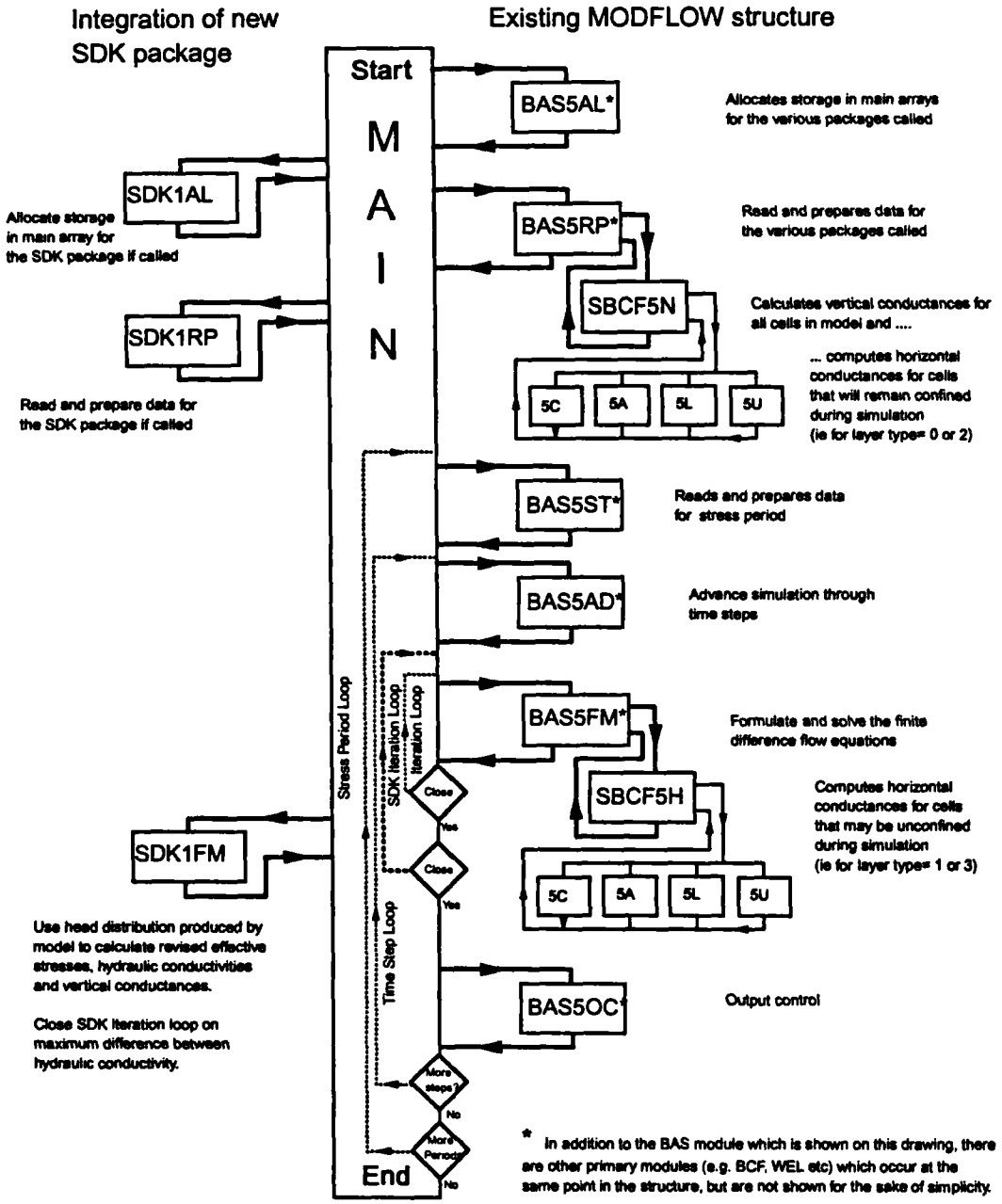

7.6 Programming

7.6.1 Revision of programme module MAIN

The full listing of the program modifications is given in Appendix C.
The major alterations to the MAIN code involve calls to the three new modules listed below:

Module SDK1AL	allocates storage space to the new arrays required by the package SDK1FM;
Module SDK1RP	reads and prepares input data; and
Module SDK1FM	calculates effective stress and hydraulic conductivity and checks to see whether the maximum difference between hydraulic conductivity has met the convergence criterion (ISDKFLAG=1).

The other alteration to the MAIN code involves the looping of the program to recalculate heads, depending on the status of the flag ISDKFLAG, which is returned by module SDK1FM.

7.6.2 Module SDK1AL

This program allocates storage for 7 new arrays required by module SDK1FM. Storage space is required for each cell of the model for:-

HYOLD	the old value of hydraulic conductivity;
ESMID	the effective stress;
PWP	the pore water pressure;
DEN	the average density;
ISDKCF	a flag to indicate whether the SDK package applies to the cell;
SATD	the saturated density of cells that are not stress dependent; and
USATD	the unsaturated density of cells that are not stress dependent.

7.6.3 Module SDK1RP

This program reads in data required by module SDK1FM.

The relationship between density (both unsaturated at field capacity and saturated) and effective stress was established in Chapter 6 to have the form:

$$\rho_{FC} = VAR1\ (\sigma_v')^{VAR2} \qquad (7.1)$$

$$\rho_{sat} = VAR3\ (\sigma_v')^{VAR4} \qquad (7.2)$$

where VAR1 .. VAR 4 are constants

Likewise, the relationship between hydraulic conductivity and effective stress had the form:

$$K = VAR5\ (\sigma_v')^{VAR6} \qquad (7.3)$$

where VAR5 and VAR 6 are constants.

Table 7.1 shows the structure of the SDK data input files.

Table 7.1 Format of data input files to SDK module

Line 1:	Blank for free text	
Line 2:	**VAR1**	is the unsaturated density to stress constant
Line 3:	**VAR2**	is the unsaturated density to stress power term
Line 4:	**VAR3**	is the saturated density to stress constant
Line 5:	**VAR4**	is the saturated density to stress power term
Line 6:	**VAR5**	is the stress to hydraulic conductivity constant
Line 7:	**VAR6**	is the stress to hydraulic conductivity power term (if IKFLAG=1)
Line 8:	**DCFACT**	is the conversion factor from model units to metres; i.e. if model units are cm, then DCFACT=0.01
Line 9:	**TCFACT**	is the number of seconds in a model unit: i.e. if model units are days, then TCFACT = 864000.
Line 10:	**HYCLOSE**	is the maximum allowable variation in hydraulic conductivity between two iterations (expressed as a ratio)
Line 11:	**DENW**	is the density of water/leachate in t/m^3
Line 12:	**TSSURF**	is the surcharge at the surface of the site/model in kPa
Line 13:	**NSDKLAY**	number of layers where the SDK package does not apply

If NSDKLAY>0 then:-

Line 14 to line 14+(NSDKLAY-1) **LAYNUM, USTD, STD**

where LAYNUM is the number of the layer that is inactive
USTD is the unsaturated density of each cell in the layer
STD is the saturated density of each cell in the layer

Line (14+NSDKLAY) **NSDKCELL** Number of cells where SDK is not active.

If NSDKCELL >0 then there are NSDKCELL lines of format:-

I, J, K, IFLAG, USTD, STD

where I, J, K, identify the row, column and layer of the cell
IFLAG indicates whether the SDK package is active(1) or inactive(0)
USTD and STD are as defined above.

7.6.4 Module SDK1FM

This module undertakes the following major tasks:

1) The values of hydraulic conductivity (HY) carried over from the MAIN module are copied into an array HYOLD.

2) The effective stress (ESMID) is calculated as the difference between the total stress (TSMID) and the pore water pressure (PWP) at each cell in the model. The program works from the top layer downwards, so that the calculated total stress at the bottom of a cell becomes the total stress at the top of the underlying cell . In calculating total stresses, consideration is given to whether a cell is saturated or unsaturated and to whether the density of the cell is itself stress dependent or not. The simulation is stopped if the effective stress at any cell becomes negative.

3) The hydraulic conductivities (HY) of cells specified as being stress dependent are re-calculated according to the effective stress. If the calculated hydraulic conductivity of any cell is greater than $1x10^{-4}$ m/s, it is reset to $1x10^{-4}$ m/s.

4) The maximum difference (expressed as a percentage variation) between the new hydraulic conductivity (HY) and the old hydraulic conductivity (HYOLD) at any cell is compared with the convergence value (HYCLOSE): if convergence in all cells has been met, the flag ISDKFLAG is set to 1.

5) The vertical conductance of cells in all layers, except for the bottom one (see below), is re-calculated according to the new hydraulic conductivity distribution.

6) The density, effective stress, pore water pressure, hydraulic conductivity and vertical conductance for each cell is written to the output file. Head is not written as this is undertaken within the original program structure.

Calculation of stresses

Figure 7.3 depicts a small volume, or cell of waste at average depth z within a landfill. The diagram shows both the relevant physical and model parameters that affect the hydraulic conductivity of the cell.

Figure 7.3 Consideration of a small volume of waste at depth z in a landfill

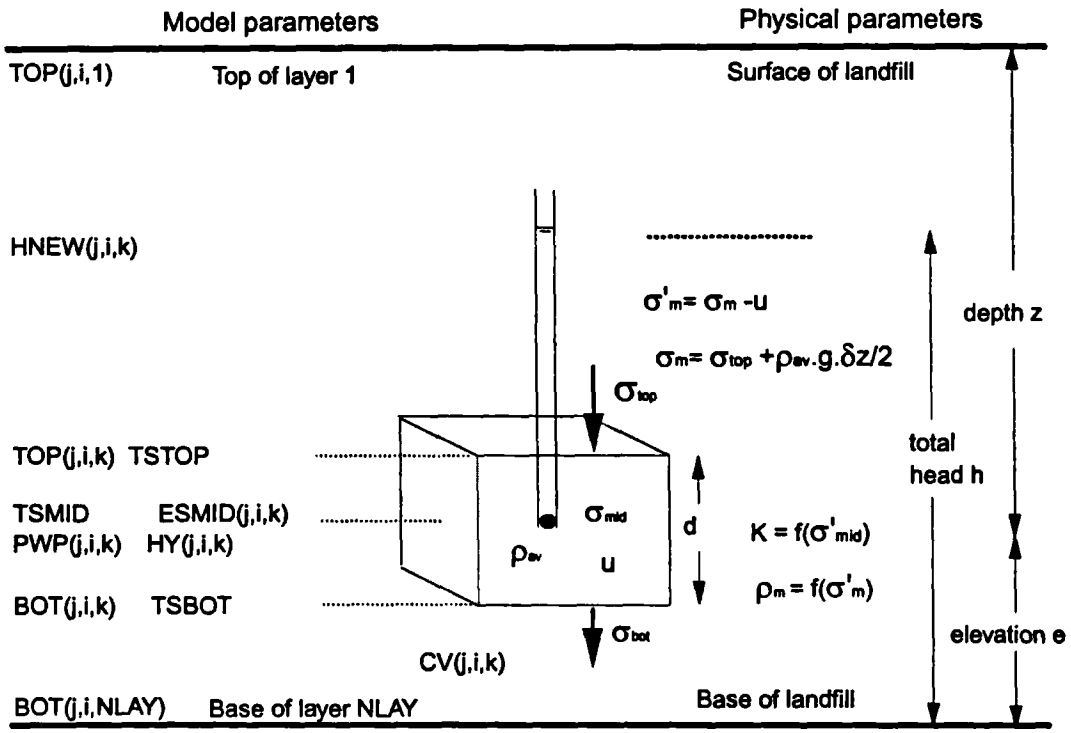

HY = Hydraulic conductivity, ESMID = Effective stress, CV = Vertical leakance
For a full description of model parameters, see Appendix C.

Table 7.2 List of variables relating to Figure 7.3

Variable	Mathematical Symbol	Model variable
Average effective stress	σ'_m	ESMID(j,i,k)
Average total stress	σ_m	TSMID
Total stress at top of cell	σ_{top}	TSTOP
Total stress at base of cell	σ_{bot}	TSBOT
Pore water pressure	u_m	PWP(j,i,k)
Av' density of cell	ρ_{av}	DEN(j,i,k)
Height of cell	d	D=(TOP(j,i,k)*BOT(j,i,k))*DCFACT
Acceleration due to gravity	g	G=9.81
Stress to density constant	a	VAR1 (unsat) or VAR3 (sat)
Stress to density power term	b	VAR2 (unsat) or VAR4 (sat)

The total stresses acting on the cell are:-

$$\sigma_{bot} = \sigma_{top} + \rho_{av}.g.d \tag{7.4}$$

The total stress at the mid point of the cell (σ_m) approximates to:-

$$\sigma_m = \frac{\sigma_{top}+\sigma_{bot}}{2} \tag{7.5}$$

or $$\sigma_m = \sigma_{top} + \rho_{av}.g.\frac{d}{2} \tag{7.6}$$

The average density of the cell is (from Chapter 6) of the form,

$$\rho_{av} = a(\sigma'_m)^b \tag{7.7}$$

or $$\rho_{av} = a(\sigma_m - u_m)^b \tag{7.8}$$

where the average pore water pressure, u_m = (h-e).ρ_w.g

Substitution of Equation 7.8 into Equation 7.6 results in:

$$\sigma_m = \sigma_{top}+a(\sigma_m - u_m)^b.g.\frac{d}{2} \tag{7.9}$$

This equation can be solved by iterative techniques (see below) to determine σ_m for both unsaturated and saturated cells.

Calculation of stresses in unsaturated cell

For the case of an unsaturated cell, the pore water pressure, u_m, is zero and Equation 7.9 reduces to:

$$\sigma_m = \sigma_{top}+a(\sigma_m)^b.g.\frac{d}{2} \tag{7.10}$$

Within the model, Equation 7.10 is represented by the following variables (refer also to Table 7.2):

$$TSMID = TSTOP + A\ (TSMID)^{VAR2} \tag{7.11}$$

or $$TSTOP - TSMID + A\ (TSMID)^{VAR2} = 0 \tag{7.12}$$

where A = VAR1xGxD/2

Equation 7.10 is solved for TSMID by an iterative technique within the program. By starting at the top layer in the model and working downwards, TSTOP for the cell in question is always known (see below and Equation 7.15). If the correct value of TSMID is substituted into Equation 7.11, the two sides of the equation will balance each other out, resulting in zero (Equation 7.12). If an incorrect value of TSMID is used in Equation 7.10, the difference between the two sides of the equation will result in an error (TSERR) where,

$$TSERR = TSTOP\text{-}TSMID + A\,(TSMID)^{VAR2} \qquad (7.13)$$

The program makes an initial guess of TSMID for the cell and calculates the error, TSERR. If TSERR is greater than 0.1 kPa, a revised value of TSMID is obtained by halving the error and adding it to the initial value of TSMID. TSERR is then recalculated and the process repeated until the error is less than 0.1 kPa.

Once the correct value of TSMID has been obtained, calculation of the following is possible:

$$ESMID(j,i,k) = TSMID \quad (\text{as } PWP = 0)$$

$$DEN(j,i,k) = VAR1*ESMID(j,i,k)^{VAR2} \qquad (7.14)$$

$$TSBOT = TSTOP+DEN(j,i,k)*G*D \qquad (7.15)$$

$$HY(j,i,k) = VAR5*(ESMID(j,i,k))^{VAR6} \qquad (7.16)$$

The total stress at the bottom of the cell (TSBOT) is carried forward as the total stress (TSTOP) at the top of the underlying cell, so that the calculation of effective stress can be continued throughout the model

Calculation of stresses in saturated cells

The process of calculating the effective stress at the mid point of saturated cells is based on Equation 7.9 and is similar to that adopted for unsaturated cells.

The total stress error (TSERR) calculated during the iterative process of determining the average total stress (TSMID) is:

$$TSERR = TSTOP\text{-}TSMID + A\,(TSMID\text{-}PWP(j,i,k))^{VAR4} \qquad (7.17)$$

where A is redefined as A = VAR3xGxD/2

When the average total stress (TSMID) has been determined the effective stress is calculated as:

$$ESMID(j,i,k) = TSMID - PWP(j,i,k) \quad (7.18)$$

with Equations 7.14 to 7.16 being used to calculate the average density, hydraulic conductivity and total stress at the base of the cell.

Vertical conductance

The module also recalculates vertical conductance using the revised hydraulic conductivity values. Vertical conductance is used to calculate the volume of water that flows from a cell downwards to an underlying layer. It therefore does not apply to any cells in the lowest layer of a model. Vertical conductance is the product of vertical leakance and the plan area of the cell.

The vertical leakance of a cell is the harmonic mean of the hydraulic conductivity between the cell and the one below it, divided by the vertical distance between the mid points of the two cells.

$$\text{Harmonic mean of K} = \frac{2 \times HY(j,i,k) \times HY(j,i,k+1)}{HY(j,i,k) + HY(j,i,k+1)}$$

$$\text{Vertical distance} = 0.5 \times (TOP(j,i,k) - BOT(j,i,k+1))$$

$$\text{Plan area of cell (j,i,k)} = DELR(j) \times DELC(i)$$

where DELR(j) is the row grid spacing of the cell

and DELC(i) is the column grid spacing of the cell

7.7 Verification of model

The SDK package was verified against two mathematical solutions for flow in an aquifer where the hydraulic conductivity varies with effective stress (Powrie and Beaven, 1999). The first solution concerned vertical infiltration through a landfill, and the second steady state flow to a pumped well in a confined aquifer.

An attempt was also made to verify the model against an analytical solution for flow to a well in an unsaturated aquifer (Powrie and Beaven, 1999). This proved unsuccessful because the original MODFLOW program was unable to model the seepage face, at the

interface of an aquifer and well screen in unconfined pumped wells (e.g. Hantush, 1962). The seepage face is the zone through which water enters a well above the standing water level in the well. MODFLOW calculates (correctly) that the cells above the water level in the well are unsaturated. However, all unsaturated cells in MODFLOW are assumed to take no part in any flow and are turned off. This has the effect of creating an impermeable barrier to flow into the well above the standing water level.

7.7.1 Vertical flow

Powrie and Beaven (1999) gave a set of equations (reproduced below) that described the saturated vertical flow of water from an irrigation system at the surface of a landfill, to a leachate collection system at the base of the site. Figure 7.4 shows a layer of thickness δz whose upper surface is at a depth z below the surface of a landfill, of overall depth D. The hydraulic head (measured above the base of the landfill) at depth z is h, and the hydraulic head at depth $z+\delta z$ is $h-\delta h$. Therefore, the hydraulic gradient at depth z is $\delta h/\delta z$.

Figure 7.4 Analysis of vertical infiltration through a landfill

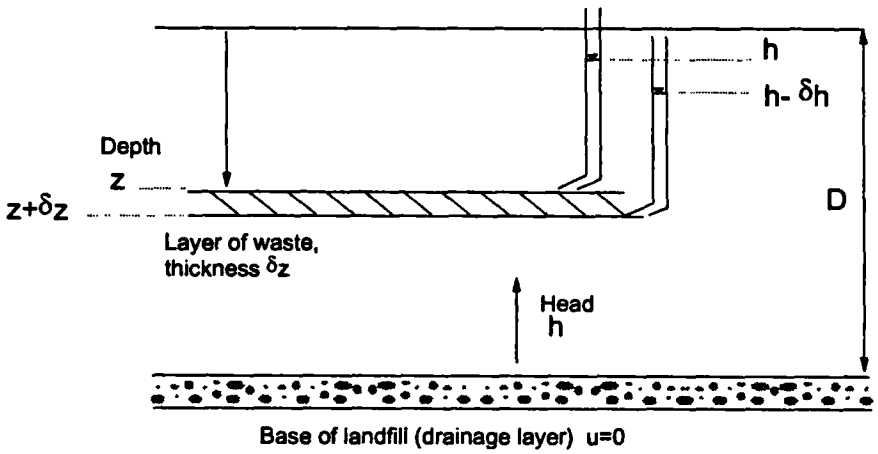

Source: Powrie and Beaven (1999)

The changes in vertical total stress ($\delta\sigma_v$), pore water pressure (δu) and vertical effective stress ($\delta\sigma_v'$) that take place over the depth increment δz are as follows:

$$\delta\sigma_v = \rho_{sat}.g.\delta z \qquad (7.19)$$

$$\delta u = \rho_w.g.(\delta z-\delta h) \qquad (7.20)$$

$$\delta\sigma_v' = \delta\sigma_v-\delta u \qquad (7.21)$$

while from Darcy's Law,

$$v = (q/A) = K.i = K.(\delta h/\delta z), \text{ or}$$

$$\delta h = v.(1/K).\delta z \tag{7.22}$$

where v (or q/A) is the infiltration rate.

The saturated density (in t/m^3) and hydraulic conductivity (in m/s) may be related to the vertical effective stress according to

$$\rho_{sat} = C.(\sigma_v')^D \tag{7.23}$$

and $$K = A.(\sigma_v')^B \tag{7.24}$$

where in both cases σ_v' is in kPa.

such that the hydraulic conductivity can be related to density by

$$K = A\left(\frac{\rho_{sat}}{C}\right)^{\frac{B}{D}} \tag{7.25}$$

Substitution of Equations 7.19, 7.20 and 7.22 into Equation 7.21 leads to:

$$\delta\sigma_v' = g\delta z\left[\rho_{sat} + \rho_w\left(\frac{v}{K} - 1\right)\right]$$

and substitution of Equations 7.23 and 7.24 leads to

$$\delta\sigma_v' = g\delta z\left[C(\sigma_v')^D + \rho_w\left(\frac{v}{A(\sigma_v')^B} - 1\right)\right]$$

or

$$\frac{d\sigma_v'}{dz} = g\left[C(\sigma_v')^D + \rho_w\left(\frac{v}{A(\sigma_v')^B} - 1\right)\right] \tag{7.26}$$

Equation 7.26 is a first-order differential equation that can be solved if an initial value of σ_v' is known at an initial depth z_0. The equations were resolved by finite difference techniques in a spreadsheet as illustrated in Figure 7.5 (see also footnote[1] on page 238). It is assumed that at depth =0, the total vertical stress = the surcharge (representing for example the effect of restoration layers) and the pore water pressure (u) =0. An infiltration rate (q/A) is entered into cell reference B12 and from this the distribution of

pore water pressure, effective stress, density and hydraulic conductivity is calculated. The infiltration rate is altered by trial and error until the desired value of head is calculated in the basal drainage layer (at depth D). The analysis works for negative values of recharge, indicating upward flow from the basal layer to the surface, in addition to downward flow. In the example given in Figure 7.5, an infiltration rate of $1x10^{-5}$ m/s results in a head of 0.33 m in the base of a 10 metre deep landfill, with a 60 kPa surcharge (i.e. the basal drainage layer is virtually dewatered).

To verify the SDK MODFLOW package the spreadsheet analysis was used to calculate infiltration through a 30 metre deep landfill with a 60 kPa surcharge. The maximum vertical infiltration rate was calculated for various values of head in the basal drainage layer and is plotted on Figure 7.6.

Figure 7.5 Example of vertical flow spreadsheet analysis for a 10 m deep landfill

	A	B	C	D	E	F	G	H	I	J
1	A	2.1	Depth	Vertical	dσ'	Density	Vertical	Pore water	Head	Hyd. Cond.
2	B	-2.71	z	Eff. stress			Total stress	pressure	h	K
3	C	0.6691	metres	kPa	kPa	t/m3	kPa	kPa	m	m/s
4	D	0.0899	0	60	1.38	0.967	60.00	0	10	3.19E-05
5	Surcharge (kPa)	60	0.5	61.38	1.48	0.969	64.74	3.37	9.84	3.00E-05
6	Initial density (t/m3)	0	1	62.86	1.60	0.971	69.49	6.63	9.68	2.81E-05
7	G	9.81	1.5	64.46	1.74	0.973	74.26	9.79	9.50	2.62E-05
8	Total depth (D)	10	2	66.20	1.89	0.975	79.03	12.83	9.31	2.44E-05
9	Increase in total	0%	2.5	68.09	2.06	0.978	83.81	15.73	9.10	2.26E-05
10	stress due to cover		3	70.15	2.25	0.980	88.61	18.46	8.88	2.09E-05
11			3.5	72.40	2.48	0.983	93.42	21.02	8.64	1.92E-05
12	TRY v (q/A) (m/s)	1.00E-05	4	74.88	2.74	0.986	98.24	23.36	8.38	1.75E-05
13			4.5	77.62	3.04	0.989	103.08	25.46	8.10	1.59E-05
14			5	80.66	3.40	0.993	107.93	27.28	7.78	1.43E-05
15			5.5	84.05	3.82	0.997	112.80	28.75	7.43	1.28E-05
16			6	87.87	4.33	1.001	117.69	29.82	7.04	1.13E-05
17			6.5	92.21	4.95	1.005	122.60	30.39	6.60	9.95E-06
18			7	97.16	5.73	1.010	127.53	30.37	6.10	8.83E-06
19			7.5	102.89	6.71	1.015	132.48	29.59	5.52	7.39E-06
20			8	109.60	7.98	1.021	137.46	27.86	4.84	6.23E-06
21			8.5	117.58	9.66	1.027	142.46	24.89	4.04	5.15E-06
22			9	127.24	11.97	1.034	147.50	20.27	3.07	4.16E-06
23			9.5	139.21	15.27	1.043	152.58	13.37	1.86	3.26E-06
24			10	154.47	20.22	1.053	157.69	3.22	0.33	2.46E-06

$C23+0.5

$D23+$E23

Eq. 7.26 0.5*$B$7*($B$3*POWER(D24,$B$4)+1*($B$12/($B$1*POWER(D24,$B$2))-1))

Eq. 7.23 MAX($B$6,$B$3*(POWER($D24,$B$4)))

Eq. 7.19 $G23+($C24-$C23)*(1+$B$9)*$F23*9.81

Eq. 7.20 $B$7*($I24-($B$8-$C24))

Eq. 7.22 $I23-($B$12*($C24-$C23)/$J23)

Eq. 7.25 ($B$1*POWER(($F24/$B$3),($B$2/$B$4)))

[1] Equation 7.26 etc. was solved in the spreadsheet in Figure 7.5 (and subsequently in various analyses throughout Chapter 8) using Euler's method. It is known that Euler's method provides an approximate solution to this type of finite difference equation, and consequently the accuracy of the solution was checked using the more precise Runge-Kutta method. For the conditions specified in Figure 7.5 the Runge-Kutta method required an infiltration rate of $9.18x10^{-6}$ m/s to produce a 0.33 metre head at the base of the 10 metre deep landfill; the calculated effective stress was 146.8 kPa. Therefore, it should be noted that the vertical flow analyses reported in Chapter 8 may contain errors of approximately 10% in infiltration rates and approximately 5% in effective stress. This is considered acceptable for the purposes of this thesis.

The same 30 metre deep landfill was modelled using Groundwater Vistas and SDK MODFLOW. A slight alteration was made to the programming previously described to provide a better correlation with the results of the spreadsheet analysis. The code that prevented hydraulic conductivity (calculated from the effective stress) increasing above $1x10^{-4}$ m/s was removed (see Section 7.6.4, point 3).

A model with 60 layers, each 0.5 metres thick, and 10 rows and 10 columns was established. The elevation of the top of the upper layer was set at 30 metres, and the base of the lower layer at 0 metres. Irrigation at the top of the model was simulated by setting constant head cells in the upper layer to 30 metres. The head in the basal drainage layer was simulated by setting constant head cells in the lower layer to the appropriate value.

The data input file for the SDK package is shown in Table 7.3.

The model was run with different values of head in the basal drainage layer and the flow into the constant head cells converted into an equivalent infiltration rate. These are plotted on Figure 7.6 for six different values of head and indicate good correlation with the results from the finite difference spreadsheet analysis.

Table 7.3 SDK MODFLOW data file for vertical flow problem

```
Input data file for module SDK -Vertical infiltration problem
  0.6691   VAR1
  0.0899   VAR2
  0.6691   VAR3
  0.0899   VAR4
  2.1      VAR5
 -2.71     VAR6
  1.0      DCFACT
  1.0      TCFACT
  0.001    HYCLOSE
  1.0      DENW
 60.0      Surface Surcharge (kPa)
  0        Number of LAYERS where SDK Module does not apply
  0        Number of CELLS where SDK Module to be switched ON/OFF
```

There is a slight discrepancy between the calculated flow rates, with decreasing values of head in the basal drainage blanket. The reason for this is illustrated by the vertical profile of pore water pressures and effective stresses (Figure 7.7). With the drainage blanket being totally dewatered (i.e. zero head on the base of the site and zero pore water pressure) there is a very rapid reduction in pore water pressure and a large hydraulic gradient directly above the drain. This results in rapid vertical variations in effective stress and hydraulic conductivity. In terms of modelling (for both the spreadsheet analysis and MODFLOW), a better match and solution would be obtained by increasing

the number of layers in the vicinity of the drainage layer. The implications of the large vertical gradients above the drainage layer are discussed in Section 8.5.8.

Figure 7.6 Comparison of infiltration rates between models

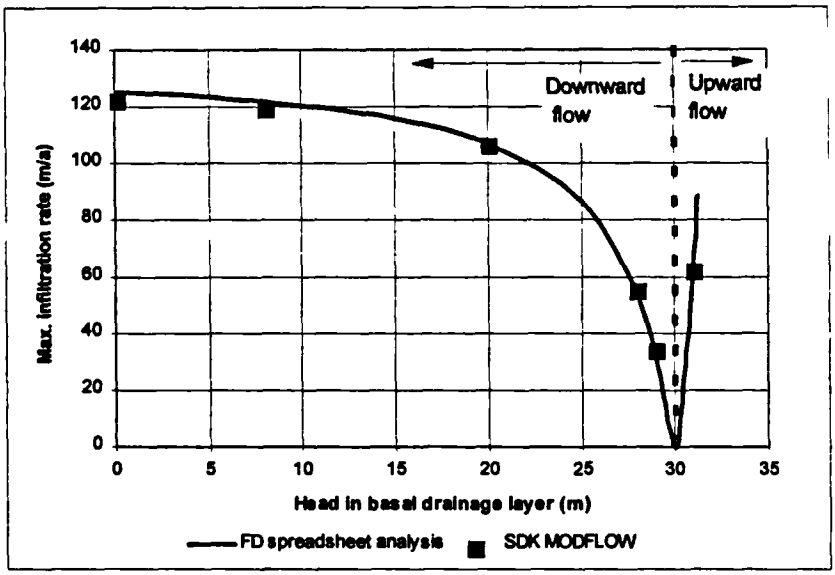

Figure 7.7 Comparison of pore water pressures and effective stresses between models: drainage blanket completely dewatered (PWP=0)

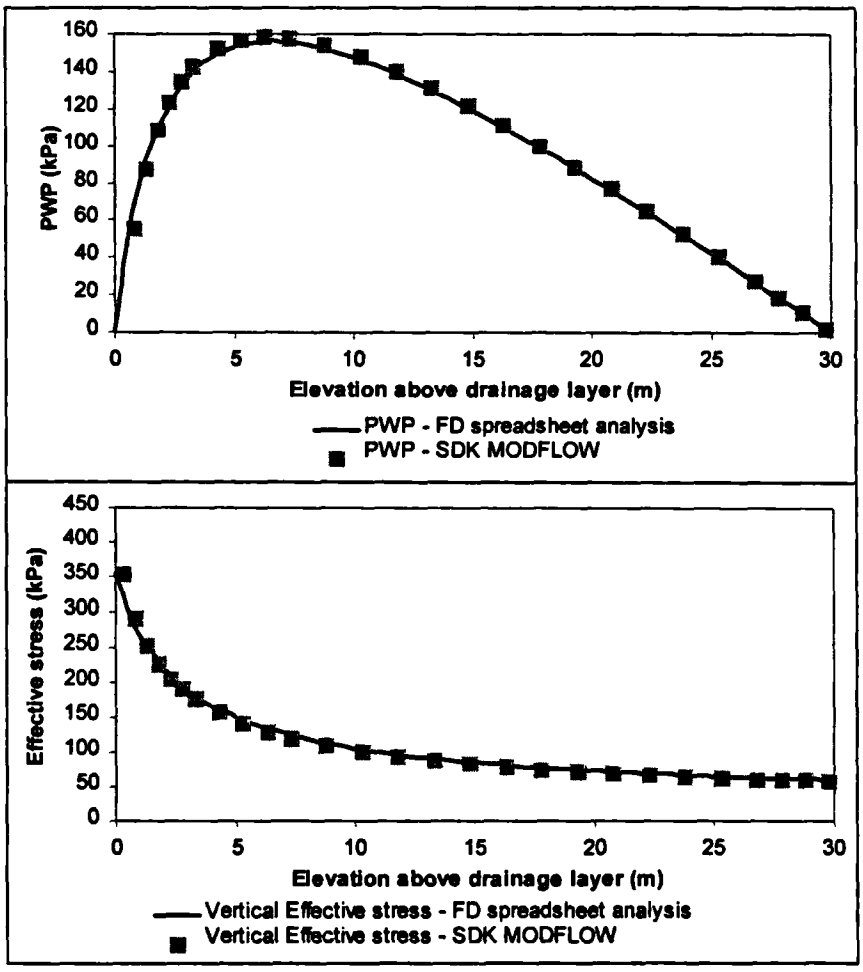

7.7.2 Flow to a confined well

Powrie and Beaven (1999) also provided a closed-form analytical solution relating the discharge from a confined well to the drawdown in an aquifer where the hydraulic conductivity varies with effective stress (Figure 7.8).

The solution assumed that neither the unsaturated (γ_1) or saturated (γ_2) unit weight of the aquifer varied with head, and that the hydraulic conductivity (K) varied with effective stress according to the relationship:-

$$K = A.(\sigma_v')^B$$

where A and B are constants.

Figure 7.8 Confined well analysis

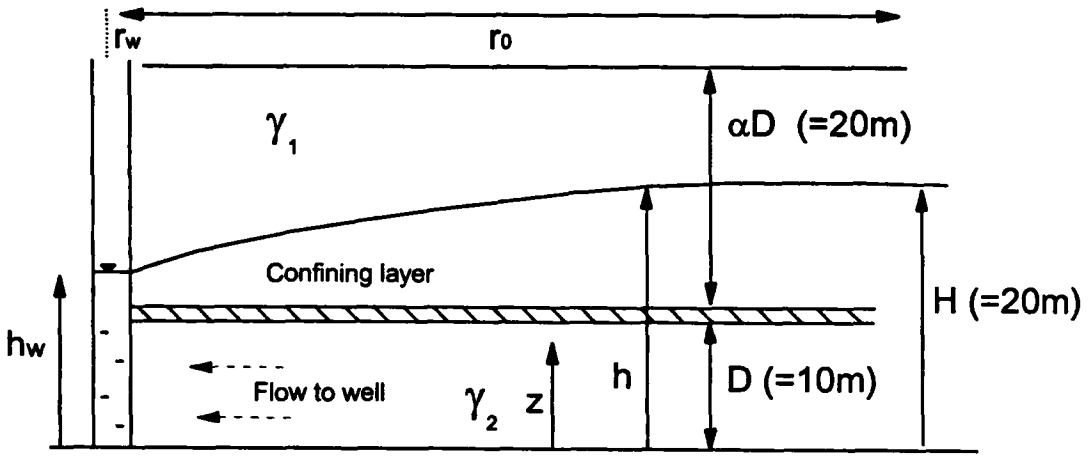

Source: Powrie and Beaven (1999)

The discharge from the well (q) was related to the head in the well (h_w) by the following equation:

$$q = \frac{2\pi.A}{E\gamma'_2(-B-1)(-B-2)\ln\left(r_0/r_w\right)}\left\{\begin{matrix}(C-EH-\gamma'_2 D)^{(B+2)}-(C-EH)^{(B+2)}- \\ (C-Eh_w-\gamma'_2 D)^{(B+2)}+(C-Eh_w)^{(B+2)}\end{matrix}\right\} \quad (7.27)$$

where: γ_w is the unit weight of water

$\gamma_1' = \gamma_1-\gamma_w$

$\gamma_2' = \gamma_2-\gamma_w$

$C = \gamma_1(1+\alpha).D$

and $E = \gamma_1-\gamma_2'$

MODFLOW

The above was modelled using SDK MODFLOW. As in the case of the vertical flow correlation, the code that prevented the hydraulic conductivity increasing above $1x10^{-4}$ m/s was removed (see Section 7.6.4, point 3).

Grid design

The problem illustrated in Figure 7.8 involves radial flow to a well, which is not an ideal configuration for a block centred finite difference grid. A suitably accurate model was created by increasing the size of the cells from the well outwards towards the boundaries (see Figure 7.9). In addition, it was only necessary to model a 90° quadrant centred on the well.

The dimensions of the smallest cell in the model are based on the perimeter, P, of the well, which is assumed to have a drilled diameter, d, of approximately 0.30 m.

$$P = \pi.d$$
$$= 0.942 \text{ m}$$

Since only a 90° quadrant is to be modelled, the active perimeter is reduced to 0.24 m. Within the model the pumped well is represented by sixteen cells of dimensions 0.03 m x 0.03 m (see Figure 7.9). As only two sides of this block of cells are involved in flow, this configuration (2 sides x4 cells x0.03m) accurately represents the length of the active perimeter of the well. An attempt was made initially to model the pumped well by a single cell. This was abandoned, however, as the convergence of flow into this one cell resulted in general instability in model runs.

The dimensions of the cells were increased towards the boundaries of the model, which were set at a minimum distance of 50 metres from the pumped well. There is a convention within MODFLOW (to reduce problems with model stability) that the size of a row or column must be less than 1.5 times the size of its neighbour. Except in the immediate vicinity of the well, multiplication factors were restricted to a range of 0.8 to 1.2. The final dimensions of the model grid are summarised in Table 7.4 and illustrated in Figure 7.9.

Figure 7.9 MODFLOW grid design to simulate flow to a well

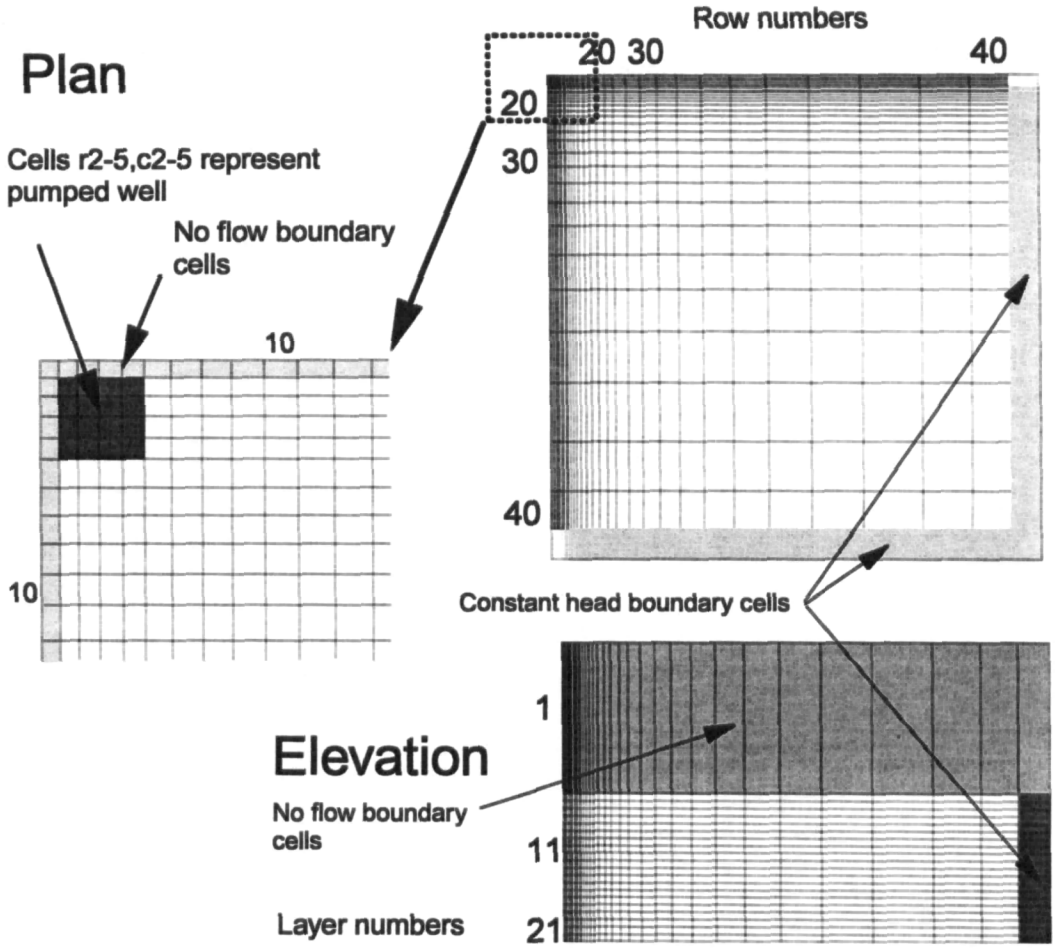

The 10 metre deep saturated zone of the landfill was replicated in the model by 20 layers, each 0.5 metres deep. The confining layer in the landfill was replicated by a single layer, which for the conditions specified above was set to a depth of 10 metres. The base of layer 21 had an elevation of 0 m, and the top of layer 1 an elevation of 20 m (2,000 cm, see below).

Finally, dimensions of centimetres (for length) and seconds (for time) were used. Trial runs using dimensions of metres had failed - it appeared that MODFLOW did not accept grid spacings of less than unity.

Table 7.4 Design of finite difference grid

Row/Column Number	Spacing in cm	Multiplication Factor[1]	Total distance from well (cm)	Total distance from well (m)
1 (No-flow boundary)	3	-	-3	-0.03
2 (cell r2,c2 = Well)	3	1.0	0	0
3 (cell r3,c3 = Well)	3	1.0	0	0
4 (cell r4,c4 = Well)	3	1.0	0	0
5 (cell r4,c4 = Well)	3	1.0	0	0
6	4	1.4 (RD)	4	0.04
7	5	1.3 (RD)	9	0.09
8	6	1.3 (RD)	15	0.15
9	7	1.3 (RD)	22	0.22
10	8	1.2 (RD)	30	0.30
11	9	1.2 (RD)	39	0.39
12	10	1.2 (RD)	49	0.49
13	12	1.2 (RD)	61	0.61
14	14	1.2 (RD)	75	0.75
15	16	1.2 (RD)	91	0.91
16	18	1.1 (R)	109	1.09
17	20	1.1 (R)	129	1.29
18	22	1.1 (R)	151	1.51
19	24	1.05 (R)	175	1.75
20	28	1.15 (R)	203	2.03
21	33	1.15 (R)	236	2.36
22	39	1.2 (RD)	275	2.75
23	46	1.2 (RD)	321	3.21
24	55	1.2 (R)	376	3.76
25	66	1.2 (R)	442	4.42
26	79	1.2 (R)	521	5.21
27	94	1.2 (R)	615	6.15
28	112	1.2 (R)	727	7.27
29	134	1.2 (R)	861	8.61
30	161	1.2 (R)	1022	10.22
31	193	1.2 (R)	1215	12.15
32	232	1.2 (R)	1447	14.47
33	278	1.2 (R)	1725	17.25
34	334	1.2 (R)	2059	20.59
35	401	1.2 (R)	2460	24.60
36	481	1.2 (R)	2941	29.41
37	577	1.2 (R)	3518	35.18
38	692	1.2 (R)	4210	42.10
39	554	0.8 (R)	4764	47.64
40	443	0.8 (R)	5207	52.07
41 (Boundary cells)	354	0.8 (R)	5561	55.61

[1] The multiplication factor is applied to the dimensions of the previous cell to obtain current cell size

RD Spacing rounded down to nearest whole number

R Standard rounding rules apply

Boundary Conditions

Two types of boundary condition were specified for the model: no-flow cells and constant head cells. No-flow cells were set along row 1 and column 1 for all layers to simulate the boundaries of the modelled quadrant. Constant head cells were set at 2,000 cm along row 35 and column 35 for Layers 2 to 21 to replicate the initial head of 20 metres in the saturated zone. The whole of layer 1 was specified as no-flow cells to represent the confining layer.

Hydrogeological Parameters

As the model was run in the steady state the only additional parameter which needed to be set was the hydraulic conductivity. Although the SDK package recalculates hydraulic conductivity according to effective stress, the model uses the initially defined values to calculate a head distribution from which effective stresses are calculated. Setting the user defined values of hydraulic conductivity to sensible values will speed up convergence of the model. The hydraulic conductivity was set at 3.6×10^{-4} cm/sec, which represented an estimated average effective stress of 130 kPa in the aquifer.

Simulation of constant head in pumped well

A constant drawdown in the pumped well was modelled by specifying constant head cells in r2-5, c2-5 in layers 2 to 21. For example, a constant drawdown of 4 metres equates to a constant head in the pumped well of 16 m, requiring the specification of constant head cells of 1,600 cm.

SDK input data

The data input file for the SDK module of MODFLOW is shown in Table 7.5.

Results of simulations

A comparison was made between the results of the confined well analysis generated by the analytical solution and SDK-MODFLOW. The value of $\ln(r_0/r_w)$, (required by the analytical solution) was obtained from the configuration of the MODFLOW model as $\ln(5561/12) = 6.14$.

Figure 7.10 indicates that excellent correlation was obtained between the analytical solution and SDK MODFLOW, with the difference between the calculated flow rates at different drawdowns being less than 2.3%.

Table 7.5 SDK MODFLOW data file for confined well analysis

```
Input data file for module SDK -Confined well analysis
     1.1        VAR1
     0.0        VAR2
     1.1        VAR3
     0.0        VAR4
     2.1        VAR5
    -2.71       VAR6
     0.01       DCFACT
     1.0        TCFACT
     0.001      HYCLOSE
     1.0        DENW
     0.0        SURFACE SURCHARGE (kPa)
    0           NUMBER OF LAYERS WHERE SDK MODULE DOES NOT APPLY
    0           NUMBER OF CELLS WHERE SDK MODULE TO BE SWITCHED ON/OFF
```

Table 7.6 Analytical model data input for confined well

D	$= 10$ m	$\ln(r_0/r_w)$	$= 6.14$
α	$= 1$	A	$= 2.1$
$\gamma_1 = \gamma_2$	$= 10.79$ kN/m^3	B	$= 2.71$
γ_w	$= 9.81$ kN/m^3		

Figure 7.10 Comparison of calculated flow rates for confined well

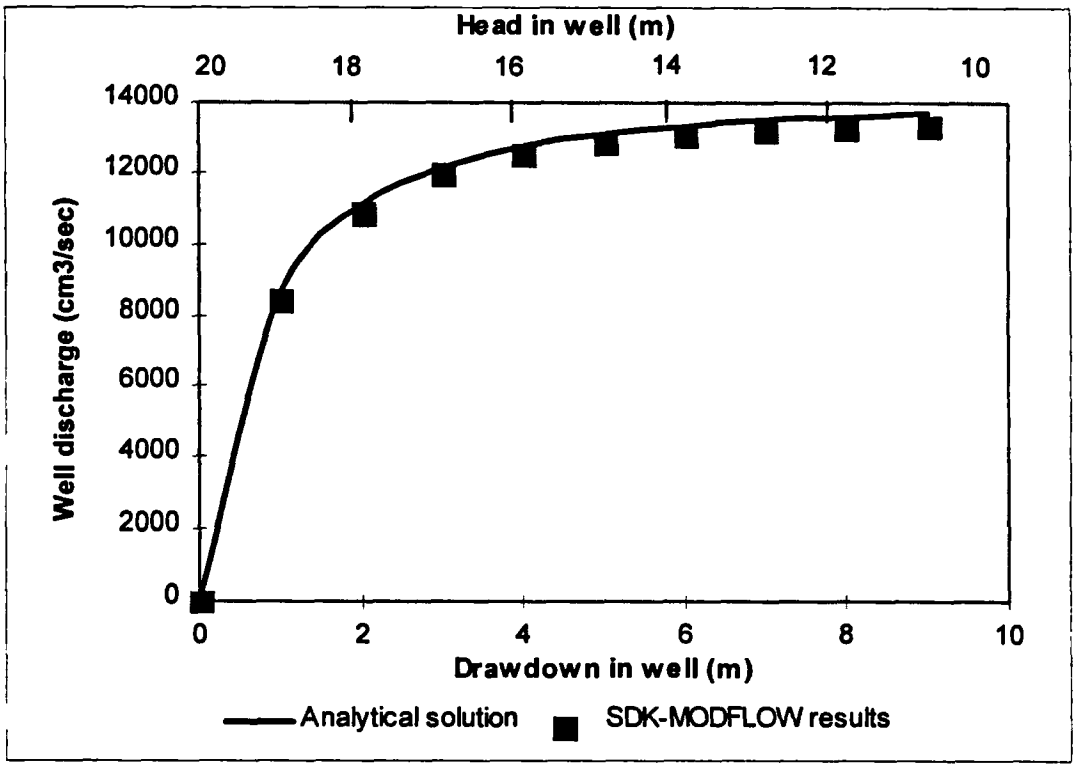

7.8 Limitations of model

The SDK package has the following limitations and restrictions:-

1) The package has been written to work only with MODFLOW layer type 3. This layer type allows fluctuation between confined and unconfined conditions, and calculates the transmissivity of an unconfined layer based on the saturated thickness.

2) In calculating the increase in stress with depth, the model assumes that the tops of all layers remain at a constant level. Therefore any settlement (or rebound) is not accounted for, and the model effectively 'introduces' (or removes) mass to make up any settlement. This introduces an error into the calculation of effective stress with depth.

3) The relationship between waste density, hydraulic conductivity and effective stress is assumed to be perfectly elastic. This means that it is not possible to take into account:
i) pre-compaction of waste to an initial density at the tipping face, or
ii) the fact that the physical properties of saturated waste will almost certainly not return to their initial values after a cycle of dewatering and re-wetting.

4) The simulation aborts if at any time the effective stress at any cell is calculated to be negative. This places restrictions on modelling scenarios such as the injection of leachate into wells at high pressures. Furthermore, it is possible that during the iteration process of recalculating effective stress and hydraulic conductivity after a head distribution has been produced, negative effective stresses may be calculated even though there may be no negative values in the final solution.

5) Any cell in the model that is calculated to be dry (at any time during the head iteration procedure) is converted by MODFLOW into a no-flow cell and is prevented from taking any further part in the simulation. There are two exceptions to this. The first is that cells that have been switched off can be re-wetted (during the head iteration procedure) if the head in adjacent cell(s) meets certain user defined criteria (McDonald *et al*, 1992). Secondly, there is an option to allow recharge (precipitation) to pass through unsaturated layers to the first active layer in the model. Unfortunately, these exceptions do not help in the modelling of the following situations:-

   i) Seepage faces in a well pumping from an unconfined aquifer. The cells above the water level in the well are switched off preventing water entering the well through the seepage face. An unsuccessful attempt was made to

validate the SDK package against an analytical solution for flow to a well in an unconfined aquifer (Powrie and Beaven, 1999), and it was at this point that the problem relating to the way in which MODFLOW treats dry cells became clear.

ii) The downward movement of water or leachate in a system where there is a large increase (moving downwards) in hydraulic conductivity between any two layers. The low hydraulic conductivity of the upper layer will limit the rate of flow into the lower layer, which having a relatively high hydraulic conductivity will become unsaturated and switch off. This means that in its present form MODFLOW, with or without the SDK package, is unsuitable for modelling the impact of low permeability daily cover in landfills.

6) Although the package is capable of transient simulations, it should be noted that it does not calculate changes in storage in response to changes in effective stress. Consequently, it will not take into account the release of water from consolidating waste during dewatering, and will give misleading results. It is possible that this limitation could be partially overcome by incorporating the existing aquifer compaction package of MODFLOW (Leake and Prudic, 1991) but this has not been investigated herein.

Chapter 8

Discussion and application of results to sustainable landfilling

8.1 Summary

The practicalities of operating different types of leachate recirculation and flushing schemes in landfills are considered using the results reported in this thesis. Two simple flushing models - continuously mixed reactor, and fill and drain - are assessed to determine the possible volume of leachate that must be flushed to bring a waste to a stable non-polluting state. This volume will depend on the nature of the waste, the contaminant to be flushed and the sensitivity of the landfill's surrounding environment to the contaminant. It is demonstrated (using the continuously mixed reactor model) that approximately 2.7 m^3 of leachate per unit volume (i.e. per m^3) of household waste is required to reduce the concentration of ammoniacal nitrogen in the leachate to below 10 mg/l. This is independent of the waste density. This value is used to calculate a minimum flushing rate (in terms of specific flushing rate) if the requisite volume of leachate is to be removed over a period of 30 years.

Various leachate flushing schemes in different depths of landfill are evaluated against this minimum flushing rate. Downward vertical flushing through both unsaturated and saturated wastes is considered. In the latter case, the option of upward vertical flow is also investigated. MODFLOW is used to assess the feasibility of using leachate wells to flush wastes horizontally.

For saturated flow the main factor affecting the viability of a given recirculation scheme is the relationship between hydraulic conductivity and effective stress. Schemes that are demonstrated to work if it is assumed that hydraulic conductivity varies reversibly with

effective stress, fail if it is assumed the hydraulic conductivity reflects either the maximum historical stress exerted on the waste or the pre-compaction density at the tipping face. Further research is required into this subject.

The findings are considered in relation to the design and engineering of a high rate flushing (bio)reactor as a sustainable landfill. Potential problems, such as high leachate heads and source of flushing water, are discussed and possible solutions suggested.

8.2 Introduction

The importance of fluid movement in the removal of the pollution load of landfills was discussed in Chapters 1 and 2. Increasing the water content of biodegradable wastes generally accelerates the degradation process; intractable and potentially polluting soluble degradation products have to be flushed from the waste by leachate recirculation and treatment. Using the data provided by this research it is now possible to examine the feasibility and practicalities of different leachate recirculation and flushing schemes in various landfill settings.

The data can also be used to develop an understanding of the scope and/or limitations of leachate control measures in existing landfill sites.

8.3 General considerations

Results from tests on three general types of household waste have been reported. Although there are variations in the composition, the physical behaviour of all the wastes was generally very similar.

8.3.1 Relationship between the hydrogeological properties and density of household waste

Probably the single most important finding of this research is the extent to which the hydrogeological properties of household wastes vary with waste density. As density increases there are very significant reductions in drainable porosity and hydraulic conductivity.

Figure 8.1 shows these reductions, as a function of dry density, for crude household waste DM3. The effective porosity, water content at field capacity and total saturation capacity are all expressed as a volumetric water content (WC_{vol}). At low densities it is

surmised that the relatively high drainable porosity is created by the presence of large macro-pores within the waste. Increases in density are caused by the collapse of these macro-pores, leading to the rapid reduction in drainable porosity. The majority of the macropores have collapsed at dry densities above 0.5 t/m^3. At a water content (WC_{dry}) of 51.5% (the original water content of waste DM3 as deposited) this is equivalent to a wet density of 0.76 t/m^3. At field capacity this is equivalent to a density of approximately 0.95 t/m^3.

Figure 8.1 Hydrogeological properties of waste DM3 in relation to dry density

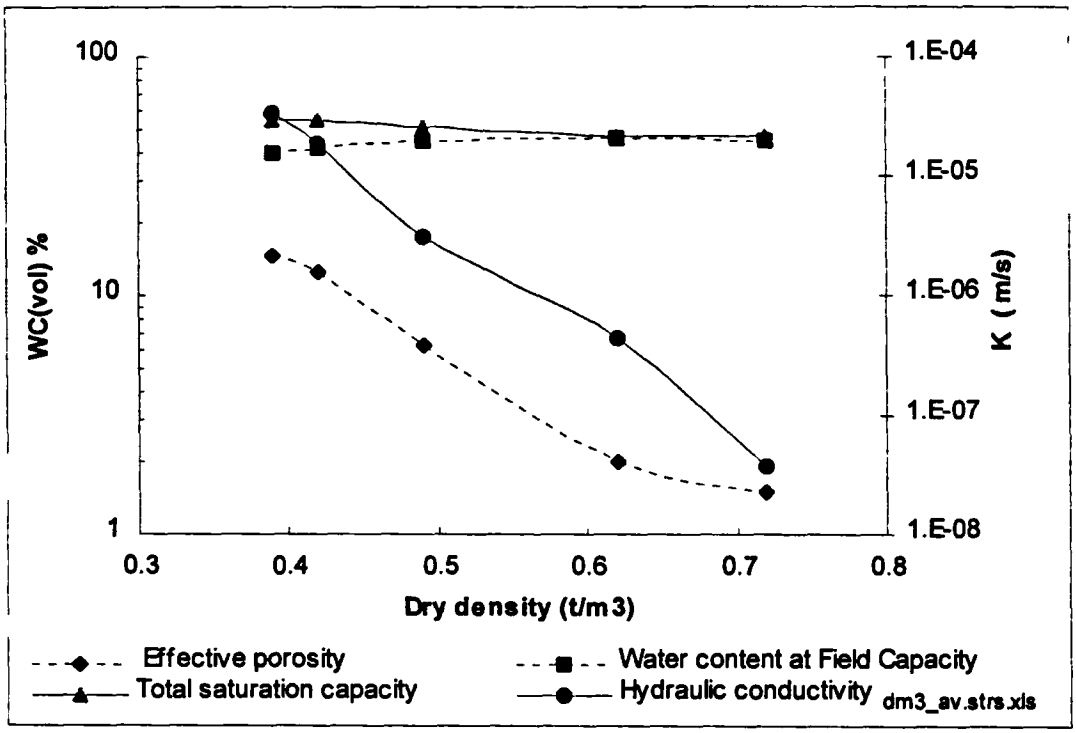

In addition, as the constituents of the waste are relatively compressible the contact area between individual particles will increase as the macro-pores collapse. Flow through the waste at low densities is probably dominated by intergranular flow through macro-pores. As the density of the waste increases this changes to predominantly fissure flow, along the interface of individual particles, and/or intraparticle flow through the matrix of particles (i.e. through paper). This change in the mechanism of flow is marked by the rapid reduction in hydraulic conductivity.

It is not possible to make a direct comparison between the density of the three types of household waste (crude, processed and aged) and the absolute values of drainable porosity or hydraulic conductivity because of the very different composition and unit weights of the individual constituents of the waste. However, all three waste types behave in a similar manner to that shown in Figure 8.1.

There is a good correlation between the hydraulic conductivity (and to a lesser extent effective porosity) and effective stress of all the household wastes tested, as illustrated by Figure 6.19 and Figures 6.10 to 6.12.

8.3.2 Relationship between density of household waste and compactive effort

The initial control over the density of waste in a landfill relates to the tipping method and amount of compactive effort that is applied to the waste.

Field scale trials by Scott (1977) indicated that the *in situ* density of crude household waste placed with a dozer or small compactor was between 0.57 and 0.79 t/m^3. A report undertaken for Caterpillar® (1995) suggests that densities of approximately 0.65 t/m^3 could be achieved with relatively small compactors such as the Cat® 816 (gross weight 20.8 tonnes) or the Bomag 601. Waste densities of between 0.8 and 1.11 t/m^3 could be achieved with medium sized compactors such as the Cat® 826 (gross weight 33.3 tonnes) and densities up to 1.2 t/m^3 with large compactors such as the Cat® 836 (gross weight 45.5 tonnes). Direct comparison of these findings with the results from this research is slightly tentative, as the Cat® survey did not include compositional analyses of the waste or even the water content at which the waste was deposited.

8.3.3 Relationship between density of household waste and effective stress

The second major control over the density of waste in a landfill is effective stress. Section 2.7 briefly considered the applicability of effective stress theory to household waste. Although it is likely that Terzaghi's Equation (Equation 2.26) can correctly be applied to household wastes it was considered that further work was required to establish this as a certainty. The need for additional work is accentuated by the finding that the average particle density of household wastes is not constant (Section 6.7).

At sites where a minimal amount of compactive effort has been used at the tipping face, the density of waste at any point in the landfill can be related to the effective stress generated by self weight effects.

From the surface of the landfill down to the leachate table there will be a progressive increase in effective stress and waste density as shown in Figure 8.2 for a 30 m deep landfill. The increase in vertical stress with depth has been calculated using the finite difference technique described in Section 7.7.1 (see also footnote on page 238).

The increases in vertical stress and density in both the unsaturated and saturated zones have been based on data obtained for waste DM3 (see Section 6.4.5). It is assumed there

is a 20 kPa surface surcharge and the increase in stress in the unsaturated zone is based on the relationship:

$$\rho_{FC} = 0.45\ (\sigma_v')^{0.156} \quad \text{(from Eq 6.2).} \tag{8.1}$$

The calculated increase in total stress for a given increment in depth is increased by an estimated 10% to take into account the presence of cover material in the site.

The calculated total stress at the base of the unsaturated zone is taken as a surcharge to the saturated zone. The spreadsheet (Section 7.7.1) is again used to calculated the increase in effective stress with depth. The pore water pressure is assumed to be hydrostatic, and the density is related to the vertical effective stress by

$$\rho_{waste} = 0.6691\ (\sigma_v')^{0.0899} \quad \text{(from Eq 6.3)} \tag{8.2}$$

The increase in total stress for a given increment in depth is again increased by an arbitrary 10%.

Figure 8.2 Changes in effective stress and waste density in a 30 m deep landfill

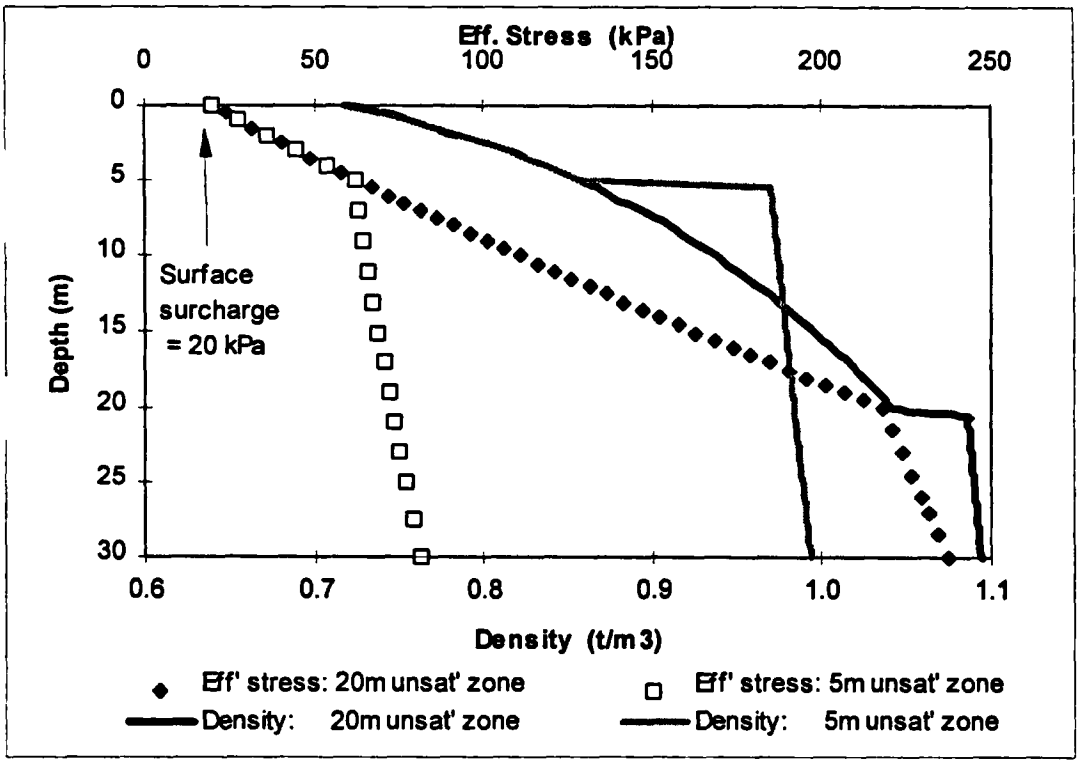

Two examples are shown, for sites with 5 metre and 20 metre deep unsaturated zones. The vertical effective stress at a depth of 5 metres is calculated to be approximately 63 kPa and the unsaturated density to be 0.86 t/m^3. At an unsaturated depth of 20 metres the vertical effective stress is 218 kPa and the density 1.04 t/m^3. On entering the

saturated zone there is a sudden increase in the bulk density of the (now saturated) waste. The greatest increase occurs at a depth of 5 metres, where the bulk density rises to 0.97 t/m^3. At a depth of 20 metres the density increases to 1.086 t/m^3.

Below the leachate table the changes in effective stress and density with depth are less pronounced because the density of the saturated waste (including the 10% additional component from cover) is around unity. Under hydrostatic conditions an increase in total stress with depth is approximately matched by an increase in the pore water pressure, resulting in little change in effective stress.

The calculated effective stress at any point in a landfill is not the only factor controlling waste density. Firstly (as discussed in Section 8.3.2) if the waste has been pre-compacted at the tipping face, there may be only negligible increases in density with depth. The pre-compacted density can be equated to an effective stress (see for example Figure 6.7) and it is reasonable to assume that there will be no change in density until the effective stress increases above this value.

Secondly, it is a well established fact in soil mechanics that the density of a compressible soil is related to the historical maximum effective stress experienced by the soil. For example, Figure 8.2 shows that the effective stress at the base of a 30 metre deep landfill with a 25 metre deep saturated zone is approximately 82 kPa, which equates to a saturated density of 0.99 t/m^3. However, if directly after the completion of landfilling there was only a 10 metre deep saturated zone (which subsequently increased to 25 metres over time), the effective stress and waste density at the base of the site would have been approximately 237 kPa and 1.1 t/m^3 respectively. It is likely that this higher waste density would be maintained as leachate levels increased and effective stresses reduced - i.e. the rebound on reducing the effective stress is small.

In summary, therefore, the effective stress distribution within a landfill (calculated from the depth and leachate level) can only be used to calculate the likely minimum waste density at any point.

8.4 Application of results to leachate control in existing landfills

Whilst the primary aim of this thesis is to consider the implications of the research to sustainable landfilling, the results are also relevant to existing landfills with leachate control problems.

The majority of landfills engineered before the start of the 1990s would not have incorporated specific leachate control infrastructure into their design. Increases in leachate levels in many of these sites, and especially in those sites designed on the principle of containment, may have occurred to an extent where retrospective leachate control measures are required.

In all but the shallowest of sites (less than 10 metres) the only recognised way to control leachate is by the installation and operation of leachate extraction wells. Whilst specific site assessments are required to determine the individual hydrogeological properties, this research can be used to gain valuable insights into the nature of the problem.

8.4.1 Estimation of leachate volumes

At sites where there is a requirement to lower leachate levels an important consideration is the actual volume of leachate that needs to be removed. The volume of leachate combined with the time available to remove it will have a large influence on the disposal option adopted. If the volume and rate of removal are relatively small, the use of a tanker may be the most economical and practicable option as it involves little capital expense. For larger volumes and rates of removal it is likely that the option chosen will involve either disposal to sewer and/or on-site leachate treatment.

To calculate the volume of leachate to be removed from a landfill both the saturated volume of waste requiring dewatering and the drainable porosity of that waste must be defined. The volume of waste to be dewatered can be estimated from an assessment of leachate levels within the site.

It has been shown that the drainable porosity of waste can vary from less than 1% to over 20% depending on the density of the waste and the effective stress.

The effective porosity within the saturated zone of a landfill of any depth can be calculated from the average effective stress in the saturated layer, taken to occur at the average depth. The average effective stress is determined by means of the spreadsheet analysis described in Section 7.7.1 and the technique described in Section 8.3.3. The stress at the base of the unsaturated zone is used as a surcharge to the saturated zone. The variables used in the analysis are summarised in Table 8.1.

Table 8.1 Variables used to calculate average effective stress in Table 8.2

Surface surcharge:		10 kPa
Density relationship:	Unsaturated	$\rho = 0.45(\sigma_v')^{0.156}$
	Saturated	$\rho = 0.6691(\sigma_v')^{0.0899}$
Increase in total stress per depth increment (z)		$d\sigma_v = 1.1(\rho.z)$ (10% increase for daily cover)

The effective porosity is given (from Section 6.4.6) by:-

$$n_e = 578\ (\sigma_v')^{-0.9812} \qquad \text{(valid for } \sigma_v' > 30 \text{ kPa}$$
$$n_e \sim 15\% \text{ for } \sigma_v' < 30 \text{ kPa)}$$

The calculated average effective porosity in the saturated zone for various depths of landfill and different depths of unsaturated zone (assuming no pre-compaction) is shown in Table 8.2. The values are based on the average effective stress in the saturated zone; if effective stresses had historically been higher than indicated, perhaps as a result of lower leachate levels, then effective porosity values would have been lower. Consequently the values of effective porosity shown in Table 8.2 should be taken as maximum values.

Table 8.2 Maximum average effective porosity in various depths of landfill

Landfill Depth = 10 m

		Saturated (unsaturated) depth in metres	
		10(0)	5(5)
Stress at top of sat' zone	kPa	10	50
Av. Eff' stress in sat' zone	kPa	-ve	51
Average effective porosity	%	>15	12.2

Landfill Depth = 20 m

		Saturated (unsaturated) depth in metres			
		20(0)	15(5)	10(10)	5(15)
Stress at top of sat' zone	kPa	10	50	97	148
Av. Eff' stress in sat' zone	kPa	-ve	54	103	152
Average effective porosity	%	>15	11.5	6.1	4.2

Landfill Depth = 30 m

		Saturated (unsaturated) depth in metres				
		30(0)	25(5)	20(10)	10(20)	5(25)
Stress at top of sat' zone	kPa	10	50	97	203	259
Av. Eff' stress in sat' zone	kPa	-ve	56	108	212	264
Average effective porosity	%	>15	11.1	5.8	3	2

Landfill Depth = 40 m

		Saturated (unsaturated) depth in metres					
		40(0)	35(5)	30(10)	25(15)	10(30)	5(35)
Stress at top of sat' zone	kPa	10	50	97	148	318	378
Av. Eff' stress in sat' zone	kPa	-ve	59	114	168	330	384
Average effective porosity	%	-	10.6	5.5	3.8	2	1.7

It can be seen that effective porosity is primarily a function of the depth of the unsaturated zone rather than landfill depth because the unit weight of the waste is similar to the unit weight of water and there is little increase in effective stress in the saturated zone. For example, the average effective porosity of 20 m and 40 m deep landfills with 5 metre unsaturated zones is 13 and 10% respectively. This reduces to 4.3 and 3.8% when the unsaturated zone is 15 metres deep. Therefore, if the objective is to dewater a saturated zone (for example 5 metres thick) at the base of a landfill, overall landfill depth becomes important. The average effective porosity of a 5 metre saturated zone at the base of a 10 metre deep landfill is approximately 15%, compared with less than 2% for the same depth at the base of a 40 metre deep landfill. If both sites were dewatered the shallow site could potentially yield seven times more leachate.

8.4.2 Leachate control in existing sites using wells

In many existing landfills the only dewatering option that can be installed retrospectively is vertical wells. The removal of leachate from vertical wells involves radial flow and is, in comparison to the essentially one dimensional flow to basal drains, relatively inefficient. The feasibility of using vertical wells in various landfill settings can be assessed by using the hydrogeological results of this research in standard steady state solutions of radial flow to wells.

The drawdown in a pumped well at steady state can be related to the hydraulic conductivity and saturated depth of the aquifer, the recharge rate, and the radius of capture of the pumped well by the following expression:-

$$r_v^2 . \ln \frac{r_v}{r_w} - 0.5(r_v^2 - r_w^2) = \frac{K}{P}(H^2 - h_w^2) \qquad (8.3)$$

(e.g. Bouwer, 1978)

where
- K is the hydraulic conductivity of the (refuse) aquifer
- P is the recharge rate
- r_v is the radius of capture (influence) of the well
- r_w is the radius of the well
- H is the initial saturated thickness (or maximum head on base)
- h_w is the head in the well

Equation 8.3 has been used to calculate the approximate spacing of leachate wells (Table 8.3) that would be required to control leachate levels in various depths of landfills. The necessary spacings are considered for different recharge rates. The lowest infiltration rate of 50 mm/annum is taken to represent possible recharge through a high quality low

permeability clay cap; the highest rate of 500 mm/a is taken as the approximate maximum effective rainfall in most parts of the UK. The depths of landfill considered are 10, 20 and 40 metres, with leachate being controlled (at the midpoint between wells) at 1, 2 and 5 metres above the base of the site. It is assumed that the wells are completely dewatered to create the maximum possible drawdown.

The hydraulic conductivity is calculated from the average effective stress in the saturated layer. The average effective stress is determined in the same way as in Section 8.4.1. (see also Table 8.1). Two values of hydraulic conductivity are considered, based on the best and worst case fit of hydraulic conductivity plotted against effective stress for waste DM3 (see Figure 6.7). The relationships used are:-

$$K\ (m/s) = 2.1(\sigma_v')^{-2.71} \quad \text{(from Eq. 6.9 - best case, i.e. greatest K), and}$$
$$K\ (m/s) = 17(\sigma_v')^{-3.26} \quad \text{(from Eq. 6.12 - worst case, i.e. smallest K)}$$

The results of the analysis, which assumes no pre-compaction of the waste, are shown in Table 8.3. The analysis does not take into account the effects of well losses, caused by friction as leachate enters the well. These losses reduce the yield of a well at a given drawdown, meaning that the grid spacings will in reality be smaller than those calculated. This is especially applicable to the calculations based on small saturated depths.

As there is a limit to the number of wells that can be installed and operated in a given area, the efficacy of using vertical wells to control leachate levels is related to the required grid spacing. For example, a grid spacing of 2.3 metres is calculated as required to maintain leachate levels to within 1 metre of the base of a 40 metre deep landfill with 500 mm/annum of infiltration. This equates to approximately 1,900 wells per hectare and is clearly totally impracticable. Table 8.4 shows the number of wells required per hectare for various grid spacings.

Leachate control by wells in shallow sites where the hydraulic conductivity of the waste is greater than approximately $1x10^{-6}$ m/s is feasible. For example, a grid spacing of approximately 40 metres is calculated as necessary to maintain a maximum 1 metre head in a 10 metre deep landfill with an infiltration rate of 100 mm/annum. In deeper sites, where the hydraulic conductivity falls below approximately $1x10^{-7}$ m/s, the control of leachate levels to within 1 or 2 metres of the base of the site is impracticable. For example, the grid spacing needed to control leachate levels to within 2 metres in the base of a 40 m deep landfill with an infiltration rate of 100 mm/a is between 8 and 14 metres (i.e. at least 50 wells per hectare before adjusting for the effects of well losses).

Table 8.3 Well spacings required to control leachate heads in various depths of landfill

Landfill Depth = 10 m Max. Permissible Leachate Head (m)	Total stress at top of sat' zone (kPa)	Av. Eff stress in sat zone (kPa)	Av. K in saturated zone # (m/s)	P = 50 mm/a radius/grid spacing* (m)	P = 100 mm/a radius/grid spacing* (m)	P = 500 mm/a radius/grid spacing* (m)
5	50	51	4.91×10^{-5}	327/580	237/420	113/200
			4.57×10^{-5}	317/562	230/408	109/193
2	78	79	1.52×10^{-5}	81/144	59/105	28/50
			1.11×10^{-5}	70/125	51/91	25/44
1	87	88	1.15×10^{-5}	38/67	28/49	13/24
			7.94×10^{-6}	32/57	23/42	11/20
Landfill Depth = 20 m Max. Permissible Leachate Head (m)	Total stress at top of sat' zone (kPa)	Av. Eff stress in sat zone (kPa)	Av. K in saturated zone # (m/s)	P = 50 mm/a radius/grid spacing* (m)	P = 100 mm/a radius/grid spacing* (m)	P = 500 mm/a radius/grid spacing* (m)
5	148	152	2.58×10^{-6}	84/149	61/108	29/51
			1.32×10^{-6}	61/108	45/80	22/38
2	181	183	1.56×10^{-6}	29/51	21/37	10.3/18
			7.20×10^{-7}	20/36	15/26	7.3/13
1	192	193	1.35×10^{-6}	14/26	10.6/19	5.3/9.4
			6.03×10^{-7}	10.1/18	7.5/13	3.7/6.6
Landfill Depth = 40 m Max. Permissible Leachate Head (m)	Total stress at top of sat' zone (kPa)	Av. Eff stress in sat zone (kPa)	Av. K in saturated zone # (m/s)	P = 50 mm/a radius/grid spacing* (m)	P = 100 mm/a radius/grid spacing* (m)	P = 500 mm/a radius/grid spacing* (m)
5	378	384	2.08×10^{-7}	27/47	19/34	9.5/16.8
			6.38×10^{-8}	16/28	11.5/20	5.7/10
2	415	418	1.66×10^{-7}	10.6/19	7.8/13.8	3.9/6.9
			4.86×10^{-8}	6.2/11	4.6/8.2	2.3/4.1
1	428	429	1.54×10^{-7}	5.6/10	4.2/7.4	2.1/3.8
			4.44×10^{-8}	3.3/5.8	2.5/4.4	1.3/2.3

The range of hydraulic conductivity values is provided by Equations 6.9 and 6.12

* Radius is the effective radius of influence of the pumping well. Infiltration over the area encompassed by the radius provides enough water to satisfy the discharge rate of the well. The **grid spacing** is the square root of the area. It indicates the approximate spacing of wells in a block centred grid that would be required to achieve the leachate head target for the various situations.

Solution based on Equation 8.3 with r_{well} = 0.15 m; h_{well} = 0 m. Well losses not accounted for, but could be considerable, especially when attempting to control leachate at a level of 1 or 2 m above the base.

Table 8.4 Number of wells per hectare for various grid spacings

Grid spacing metres	Approx. number of wells per ha	Grid spacing metres	Approx. number of wells per ha
2	2,500	25	16
5	400	30	11
10	100	40	6
15	44	50	4
20	25	100	1

The analysis indicates that in deeper sites, even with relatively low infiltration rates, an operationally feasible number of wells will not control leachate levels to within 1 or 2 metres of the base. Control of (rising) leachate levels would only be achieved after a deep saturated depth (e.g. 5 metres) had developed.

8.5 Application of results to the flushing of wastes in a sustainable landfill

A sustainable landfill has been defined in this thesis as one where the wastes deposited are brought to a stable non-polluting state within 30 to 50 years after cessation of landfilling operations. This means that a site will be in equilibrium with the surrounding environment and any future emissions will be controlled and rendered harmless by naturally occurring attenuation mechanisms. The concentrations of potential contaminants in the leachate will have achieved 'completion criteria' that will reflect the local site conditions.

For landfills containing biodegradable wastes a combination of measures to accelerate degradation and to flush out contaminants will be required to bring the site to a stable non-polluting state; for non degradable but nevertheless polluting wastes, contaminants will still need to be flushed. The amount of flushing required at a landfill will depend on site location as well as waste inputs. For example, a landfill located adjacent to the coast may have higher completion criteria for chloride than for a site located adjacent to a small inland waterway. Therefore, wastes in the inland site may need to be flushed more than similar wastes in the coastal landfill before a stable non-polluting state is reached.

This thesis does not investigate the relative merits (in terms of sustainable development) of landfilling versus any other waste management option, such as recycling or incineration. The approach being taken is that any material landfilled, no matter what its source or how much pre-treatment it has already received, should be subjected to the

requirement that its ability to pollute the surrounding environment must be removed within a sustainable timescale. To achieve this the wastes in a landfill will need to be flushed.

In order to flush wastes, there are a number of factors to consider:-

a) the water content of the wastes need to be raised to at least field capacity and preferably to saturation capacity. This is discussed in Section 8.5.1;

b) the rate of flushing is principally determined by the bed volume of the site and the length of time required to remove the contaminants. Sections 8.5.2 and 8.5.3 explore this in more detail;

c) the feasibility of achieving the required flushing rates is related to the hydraulic conductivity of the waste, as reviewed in Section 8.5.4;

d) the practicalities of various types of leachate recirculation systems. Sections 8.5.5 and 8.5.6 review the different types of collection and abstraction systems. Section 8.5.7 to 8.5.11 considers vertical flushing systems; Section 8.5.12 considers horizontal flushing through wells; and

e) the impact of waste type and precompaction density on flushing, explored in Sections 8.5.13 and 8.5.14.

The hydrogeological data obtained as a result of this research are used in the discussion of these factors.

8.5.1 Raising the water content of wastes to field capacity

To bring biodegradable material such as household waste to a stable non-polluting state the first stage is to accelerate degradation rates. Various techniques have been demonstrated to work in field scale trials, of which raising the water content of the waste to field capacity is perhaps the most important (e.g. Knox, 1996).

The water content of wastes can either be increased before the waste is placed or retrospectively within the body of the landfill as a whole. If water is added before wastes are landfilled then the volume to be added can be controlled by weight. The optimum amount of water to be added depends on the *in situ* density of the waste following landfilling. This is related to the ultimate depth of burial and, hence, the stress to which the waste will be subjected. The data relating the water content (WC_{dry}) at field

capacity of waste DM3 to stress (shown in Figure 6.13) has been reproduced in Figure 8.3 as the volume of water to be added to a tonne of waste at a particular surcharge. For example, a tonne of waste surcharged by a stress of 100 kPa (approximating to a depth burial of 10 metres) should have 260 litres of water added to ensure it is at field capacity following burial.

Figure 8.3 Volume of water required to bring waste DM3 to field capacity

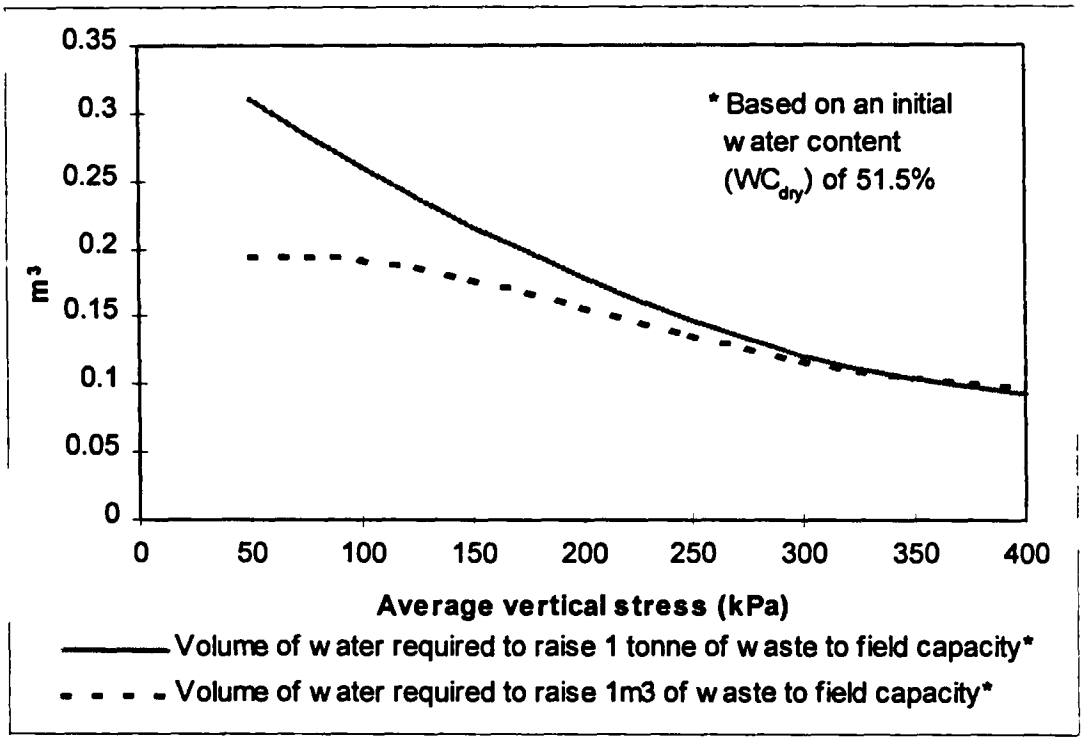

If water is to be added within the body of the site (perhaps by irrigation systems) then it is more convenient to relate the volume required to waste volume rather than mass. The amount of water required to bring a unit volume of waste up to field capacity has been calculated using the relationship between stress and dry density (Figure 6.7), and is also shown on Figure 8.3. In this case, a unit volume of waste experiencing a stress of 100 kPa would require the addition of approximately 192 litres of water to bring it up to field capacity (assuming its original water content -expressed as WC_{dry}- had not altered during its time in the landfill). The volumes required to bring the waste up to field capacity are obviously highly dependent on the initial water content of the waste. Figure 8.3 has been based on waste DM3 with an initial water content (WC_{dry}) of 51.5%. If the original water content were different, for example WC_{dry}= 60% , then the volumes of water required to bring the waste to field capacity at a stress of 100 kPa are calculated as 193 litres per tonne, or 153 litre per m^3.

8.5.2 Estimation of the bed volume of a landfill

The bed volume of a landfill is the volume of water or leachate that is active in the exchange of contaminant ions during leachate recirculation (see Section 2.2.4). It has generally been considered to be the total water content of the landfill (e.g. Knox 1996a).

The total water content of wastes in a landfill undergoing leachate recirculation will then depend on a number of factors, including:-

the average density of the waste (related to the effective stress)

whether the waste is unsaturated or saturated, in which case the total water content will be the saturation capacity.

If leachate recirculation is taking place through unsaturated waste, the bed volume can be based on the water content at field capacity. Examination of Figures 6.10 to 6.12 indicates that the volumetric water content of wastes at field capacity is relatively independent of stress. This is a useful finding as it makes calculating the approximate bed volume of a landfill relatively easy.

Over the stress range 0 to 450 kPa:-

the volumetric water content at field capacity of waste DM3 varied from 40 to 45%;

the volumetric water content at field capacity of waste AG1 varied from 45 to 50%; and

the volumetric water content at field capacity of waste PV1 varied from 35 to 40%.

From these values a reasonable approximation to the bed volume of unsaturated wastes is 40% of the total volume. For example, a 100,000 m^3 landfill cell (e.g. a 10 metre waste depth over an average plan area of 1 ha) would have a bed volume of approximately 40,000 m^3.

The bed volume of saturated wastes can be equated to the total saturation capacity, which is the sum of the volumetric water content at field capacity and the effective porosity. The saturation capacities of wastes DM3, PV1 and AG1 in relation to effective stress are shown in Figures 6.10 to 6.12. Generally there is a reduction in the saturation capacity (and hence bed volume) of saturated waste over a stress range from 0 to 150 kPa, mainly as a result of rapidly decreasing effective porosities. For example, the total saturation capacity of waste DM3 reduced from approximately 55% to 45% over the stress range from 0 to 200 kPa. At higher stress levels, due to very low effective

porosities, the bed volume is little different to that of unsaturated waste and is relatively independent of stress.

It is probable that the important difference between recirculation through saturated and unsaturated wastes is not the difference in the size of the bed volume, but the variation in the flow regime that will occur. In saturated waste (that have not been pre-compacted) at an effective stress of less than 100 kPa, the effective (drainable) porosity comprises over 10% of the total saturation capacity and hence the bed volume. Flow of recirculating leachate will predominantly occur through these large pores and there will be a relatively large volume of mobile leachate that can take part in exchange (diffusion) mechanisms with contaminants held in the micropores (matrix) of the waste. The mechanism of flow through unsaturated waste is not clear. However, it is probable that most of the flow will occur along the surface of and/or the interfaces between particles. It is suggested that, with a smaller volume of mobile leachate and a potentially smaller contact area with waste particles, diffusion of contaminants from the matrix of the waste will not occur as readily as in saturated wastes.

8.5.3 Estimation of flushing volumes and flushing rates

The estimated volume of fluid required to remove soluble degradation products from a landfill will depend on a number of factors including the flushing model used. The flushing rate will depend on the flushing volume and the time scale over which the removal of the contaminant is to be achieved.

Washout models

The majority of flushing models that have been applied to landfills to date are based on the assumption that landfills operate as continuously mixed reactors (see Section 2.2.4). These continuously mixed reactor models assume that at the start of flushing all of the contaminant to be removed is held within the bed volume of the landfill. Therefore, during the flushing process it is assumed that no further degradation is taking place and no additional degradation products (e.g. ammonia from the process of ammonification) are being released into the system. As 'clean' water (i.e. clean compared with the contaminant being removed) is introduced it is assumed to mix instantaneously with the bed volume diluting its concentration. A volume of leachate is removed, equivalent to the volume of clean water introduced, thereby keeping the water content or bed volume of the landfill constant.

The reduction in concentration of a contaminant held in solution in a continuously mixed reactor is given by the following expression:-

$$C_v = C_0 e^{-BV} \qquad (8.4)$$

(e.g. Knox, 1996a)

where C_0 is the initial concentration of a conservative parameter, and
C_v is the concentration after BV bed volumes of leachate have been flushed

Therefore, the flushing of 2.3 bed volumes is required to achieve a 10 fold reduction in concentration; a 100 fold reduction requires 4.6 bed volumes and a reduction of three orders of magnitude requires 6.9 bed volumes.

Assuming that all degradation products are in solution prior to the removal of any leachate, then the total volume of leachate to be removed to achieve a given reduction in concentration becomes highly dependent on the actual bed volume of the site.

An alternative flushing mechanism to the continuously mixed reactor is the 'fill and draw' approach. This is only applicable to saturated waste as it involves repeated cycles of flooding and draining. After the initial flooding of the waste it is assumed that the contaminant to be removed is held in solution at equal concentrations in drainable and non-drainable micro-pores.

When the waste is drained the mass of the contaminant held in solution in the drainable pores is removed. The waste is then re-saturated with clean water and it is assumed that the remaining mass of contaminants held within the micro-pores becomes evenly distributed throughout the waste, leading to a uniform concentration of a now slightly diluted leachate across both micro and macro pores. The cycle of draining and refilling is repeated until the required reduction in concentration has been achieved. The number of cycles needed to achieve this is highly dependent on the ratio of drainable to non-drainable pores. An example of an analysis based on this flushing model is given in Appendix D.

The relative merits of the two flushing models are compared below. The flushing volume required to reduce the ammoniacal nitrogen concentration of a unit volume of waste to below 10 mg/l is calculated using each model. The two models are highly idealised representations of the flushing process. In reality, the processes involved in flushing a landfill site will be considerably more complicated, but it is considered that the models can be used to give an indication of the likely flushing volumes required.

Assuming a constant dry density of 0.45 t/m^3 and taking the amount of releasable nitrogen in household waste as 2.7 kg/t_{dry} (Section 2.2.2 & Beaven and Walker, 1997), the initial mass of nitrogen in 1 m^3 of waste is 1.215 kg. It is also assumed that this mass of nitrogen is held in solution (as ammoniacal nitrogen) within any water present within

the unit volume of waste. The initial concentration of NH_3-N will consequently depend on the bed volume of the waste.

The volume of leachate that requires flushing through a unit volume of waste (at a dry density of 0.45 t/m^3) to reduce the concentration of ammoniacal nitrogen in the leachate to less than 10 mg/l is summarised in Table 8.5 for the continuously mixed reactor and fill and draw models. The results are also shown in Figure 8.4. Various bed volumes, ranging from 0.3 m^3 to 0.6 m^3, for the unit volume of waste are considered, with the initial concentration of ammoniacal nitrogen varying from 4,050 mg/l to 2,025 mg/l.

For the continuously mixed reactor model the total volume of leachate to be flushed is directly proportional to the bed volume. Despite the higher initial concentration of ammonia in the leachate at lower bed volumes, a smaller total volume of leachate requires flushing than for a higher bed volume with a lower initial ammonia concentration. For the range of bed volumes considered the volume to be flushed varies from 1.8 to 3.2 m^3.

Table 8.5 Flushing volumes to reduce the NH_3-N concentration in a unit volume of waste to < 10 mg/l

		CMR model		<---------- Fill and draw models ---------->					
				30% drainable pores *		20% drainable pores *		10% drainable pores *	
Bed Vol. m^3	Initial N conc' in leach' mg/l	No. of BVs to 10 mg/l	Vol. flushed m^3	No. of cycles to <10 mg/l	Vol flushed m^3	No. of cycles to <10 mg/l	Vol. flushed m^3	No. of cycles to <10 mg/l	Vol. flushed m^3
0.3	4050	6.0	1.80	27	2.43	43	2.58	88	2.64
0.35	3471	5.8	2.05	23	2.42	36	2.52	76	2.66
0.4	3038	5.7	2.29	20	2.4	32	2.56	66	2.64
0.45	2700	5.6	2.52	18	2.43	28	2.52	59	2.66
0.5	2430	5.5	2.75	16	2.4	25	2.5	53	2.65
0.55	2209	5.4	2.97	14	2.31	23	2.53	48	2.64
0.6	2025	5.3	3.19	13	2.34	21	2.52	44	2.64

* The percentage of drainable pores relates to the total volumetric water content (not the total waste volume)

The volume of leachate to be removed using the fill and draw model is independent of bed volume, although the total number of fill and draw cycles is not. However, the ratio of drainable pores to the total water content affects both the volume of leachate to be removed and the number of fill and draw cycles. The volume of leachate to be removed varies from approximately 2.4 m^3 for 30% drainable pores, to 2.65 m^3 for 10% drainable pores. At low bed volumes the volume of leachate to be removed is more than that required by the continuously mixed reactor model, but at bed volumes over 0.5 m^3 it is less.

Figure 8.4 **Flushing volumes to reduce the ammoniacal nitrogen concentration in a unit volume of waste to < 10 mg/l**

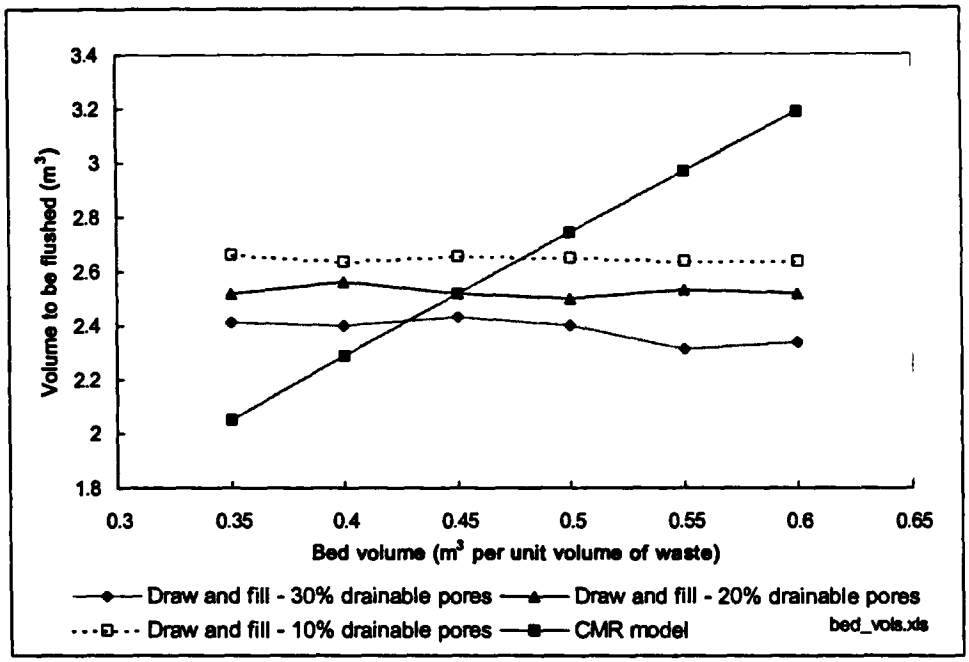

The number of fill and drain cycles required with 30% drainable pores varies from 13 to 27; this increases to a maximum of 88 with 10% drainable pores. In practice each fill and drain cycle would mean that the landfill would need to be fully saturated and then drained. This suggests that large numbers of such cycles would not be practicable. However, as the cycles could be undertaken over a period of approximately 30 years, in certain circumstances (especially for relatively shallow sites) between 20 and 30 cycles could be feasible.

The example above usefully illustrates the key features and differences between the continuously mixed reactor and fill and drain flushing models. However, the workings assume a constant dry density of 0.45 t/m^3 and are therefore slightly unrealistic.

The volume of leachate needing to be flushed through waste DM3 at various dry densities (between 0.39 and 0.72 t/m^3) has been calculated in Table 8.6 and is shown in Figure 8.5. At each density the ratio of drainable to total pores has been calculated from the effective porosity and the volumetric water content at field capacity: it varies from approximately 27% at a dry density of 0.39 t/m^3 to 3% at a dry density of 0.72 t/m^3.

The bed volume of the waste assuming unsaturated flow is taken as the volumetric field capacity, and the bed volume assuming saturated flow as the sum of the field capacity and effective porosity. The mass of nitrogen in a unit volume of waste is calculated (from the dry density), and the initial concentration of ammoniacal nitrogen calculated

from the bed volume. The volume of leachate to be flushed (to reduce NH_3-N concentrations to below 10 mg/l) from both a unit volume and a dry tonne of waste are reported.

Figure 8.5 shows that in terms of volume to be flushed there is surprisingly little difference between the continuously mixed reactor and fill and drain models, especially at dry densities above 0.5 t/m^3.

Table 8.6 Flushing volumes to reduce NH_3-N concentrations in a unit volume of waste at various dry densities to <10 mg/l

		Average stress (kPa)				
		Dry density (t/m^3)				
		35	65	120	241	463
		0.39	0.42	0.49	0.60	0.72
WC_{vol} at FC	(%)	39.9	41.6	44.5	44.9	44.4
Drainable porosity	(%)	14.7	12.5	6.5	2	1.5
Ratio of drainable to total pores	(%)	26.9	23.1	12.7	4.3	3.3
Unsaturated BV per m^3 of waste	(m^3)	0.399	0.416	0.445	0.449	0.444
Saturated BV per m^3 of waste	(m^3)	0.546	0.541	0.51	0.469	0.459
Mass of N in 1 m^3 of waste*	(kg)	1.053	1.134	1.323	1.62	1.944
CMR models						
NH_3-N conc. in unsaturated BV	(mg/l)	2,639	2,726	2,973	3,608	4,378
Number of **unsaturated** BVs to reduce concentration to 10 mg/l		5.58	5.61	5.69	5.89	6.08
Flushing volume per m^3 of waste	(m^3)	2.22	2.33	2.53	2.64	2.70
Flushing volume per dry tonne	(m^3)	5.70	5.55	5.17	4.41	3.75
NH_3-N conc in saturated BV	(mg/l)	1,929	2,096	2,594	3,454	4,235
Number of **saturated** BVs to reduce concentration to 10 mg/l		5.26	5.35	5.56	5.84	6.05
Flushing volume per m^3 of waste	(m^3)	2.87	2.89	2.83	2.74	2.78
Flushing volume per dry tonne	(m^3)	7.37	6.89	5.79	4.57	3.86
Fill and draw model						
NH_3-N conc in saturated BV	(mg/l)	1,929	2,096	2,594	3,454	4,235
Number of fill and drain cycles to reduce concentration to <10 mg/l		16	19	41	141	194
Flushing volume per m^3 of waste	(m^3)	2.35	2.38	2.67	2.82	2.91
Flushing volume per dry tonne	(m^3)	6.03	5.65	5.44	4.70	4.04

BV = Bed volume

* Based on 2.7 kg N/t_{dry}

The volume to be flushed from a dry tonne of waste decreases with increasing dry density, indicating that more efficient use of water is made if the waste is placed at higher densities. However, at dry densities above approximately 0.49 t/m^3 the fill and draw technique becomes impracticable because the required number of cycles becomes excessive (over 40). As this density equates to an effective stress of approximately 120 kPa it is unlikely that the fill and drain approach could be used in landfills over 10 -15 metres deep.

For both the continuously mixed reactor and the fill and drain model the volume of leachate to be flushed per unit volume of waste is within a narrow band of between 2.2 and 2.9 m^3 (average 2.65 m^3), irrespective of dry density. This is a useful finding: it is easier to make an assessment of the volumes of leachate that would need to be flushed from a landfill on the basis of airspace consumed than on the mass or density of wastes deposited.

Figure 8.5 Flushing volumes to reduce NH_3-N concentrations in a unit volume of waste at various dry densities to <10 mg/l

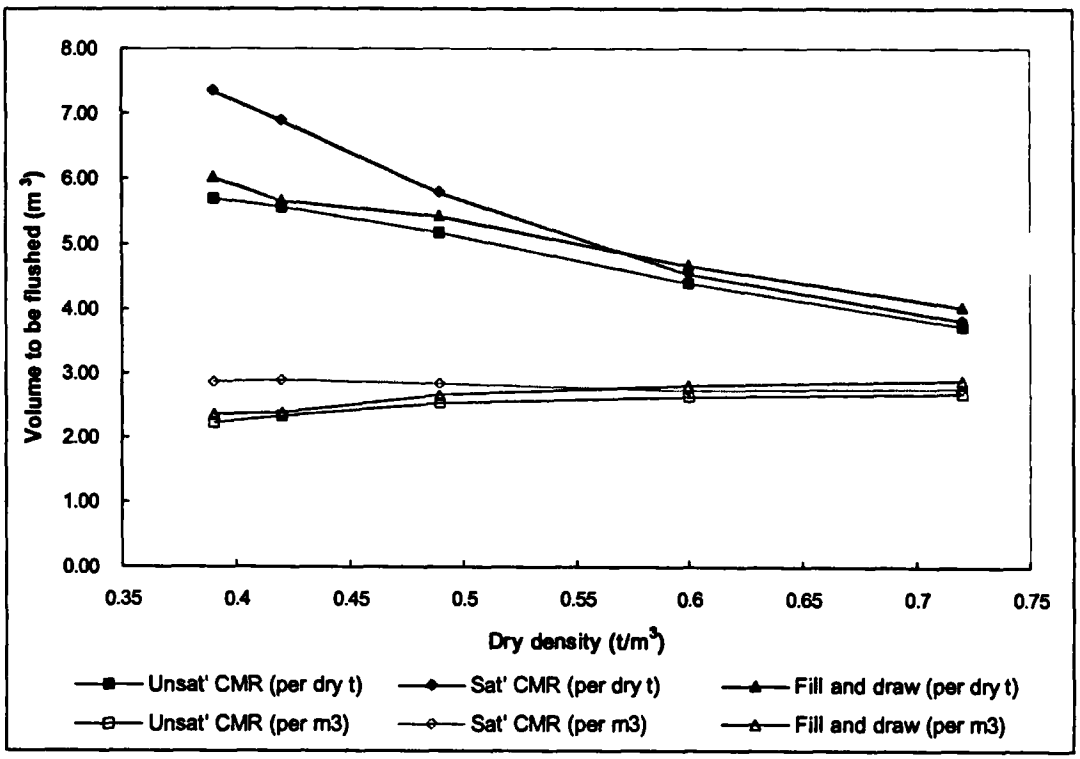

The examples given above are based on the hydrogeological properties of waste DM3 and an assumed need to reduce ammoniacal nitrogen concentrations to 10 mg/l. It is probable that the volumes required to flush other contaminants to acceptable levels will vary. Further work is therefore required to provide better estimates of the volume of leachate that will need to be flushed through landfills

However, within this thesis it will be assumed that to achieve the necessary completion criteria approximately 2.7 m^3 of leachate requires flushing for every m^3 of waste in a landfill. Furthermore, this volume of leachate must be flushed within a finite period of time, approximately 30 years, if the requirements of sustainable development are to be met. It is useful at this point to introduce a new term that reflects this rate of flushing.

The specific flushing rate, which is defined as the volumetric flow rate per unit volume of waste and has (typical) units of sec^{-1}, gives an approximate indication of the effectiveness of the flushing arrangement. The inverse of the specific flushing rate is the time taken to flush 1 m^3 of waste with 1 m^3 of water: the smaller the specific flushing rate, the longer this will take.

Examples of specific flushing rates required to flush various volume of water through a unit volume of waste over various time-spans are given in Table 8.7.

Table 8.7 Specific flushing rates required to flush various volumes of leachate through a unit volume of waste over different time-spans

The specific flushing rate that results in 2.7 m^3 of leachate passing through 1 m^3 of waste in 30 years is given by:-

$$\frac{2.7\ (m^3/m^3)}{30\ (years)} = 0.09\ years^{-1} = 2.85 \times 10^{-9}\ sec^{-1}$$

The specific flushing rate that equates to various flushing volumes and timescales are given below.

Volume to be flushed	Time-span 5 years	10 years	30 years	50 years
1.5 m^3	$9.51 \times 10^{-9}\ sec^{-1}$	$4.76 \times 10^{-9}\ sec^{-1}$	$1.59 \times 10^{-9}\ sec^{-1}$	$9.51 \times 10^{-10}\ sec^{-1}$
2.7 m^3	$1.71 \times 10^{-8}\ sec^{-1}$	$8.56 \times 10^{-9}\ sec^{-1}$	**$2.85 \times 10^{-9}\ sec^{-1}$**	$1.71 \times 10^{-9}\ sec^{-1}$
5.0 m^3	$3.17 \times 10^{-8}\ sec^{-1}$	$1.59 \times 10^{-8}\ sec^{-1}$	$5.28 \times 10^{-9}\ sec^{-1}$	$3.17 \times 10^{-9}\ sec^{-1}$

In some cases it is more appropriate to relate the rate of flushing to a vertical infiltration rate.

The volume of leachate (V) to be removed per unit area of landfill is given as:-

$$V\ (m^3) = 2.7\ (m^2) \times \text{depth of landfill (m)}$$

$$\text{and the flushing rate (m/a)} = \frac{2.7\ (m^2) \times \text{depth of landfill (m)}}{30\ (years)}$$

leading to the empirical relationship that

$$\text{Flushing rate (m/a)} \sim \frac{\text{Depth of landfill (m)}}{10\ (a)} \qquad (8.5)$$

Therefore, a 30 metre deep landfill would require a (minimum) infiltration or flushing rate of approximately 3 m/annum and a 60 metre deep site a rate of 6 m/annum. If flushing were carried out over a period of 50 years then the minimum flushing rate would be given by:-

$$\text{Flushing rate (m/a)} \sim \frac{\text{Depth of landfill (m)}}{18\ (a)}$$

It is considered that further work on the applicability of flushing models to landfills is required as a priority. For example, the relative merits of the continuously mixed reactor and plug flow (which has not been considered here) models need exploring. Also, it is generally assumed that the contaminants being flushed are conservative whereas it is probable that many will be reactive, with either net additions or net losses into the leachate as a function of ongoing degradation. Work is also required on the factors controlling the dissipation of contaminants from micro to macro pores.

8.5.4 Estimation of hydraulic conductivity

The ability to achieve the required flushing rates will depend heavily on the hydraulic conductivity of the waste. Assuming (from Section 8.5.3) a minimum vertical flushing rate of between 1 and 10 metres per year, and a hydraulic gradient equal to one, then the waste must have a minimum hydraulic conductivity of between $3x10^{-8}$ m/s (for a rate of 1 metre per year) and $3x10^{-7}$ m/s (for 10 m/yr).

Figure 6.16 showed the relationship between hydraulic conductivity and average vertical stress for waste DM3; Figure 6.19 combined the data for all wastes tested in a similar plot. Using the best and worst case fit lines through these data sets, an indication of the maximum effective stress that will maintain a given hydraulic conductivity can be calculated. This has been done for hydraulic conductivities of $3x10^{-7}$ m/s and $3x10^{-8}$ m/s in Table 8.8. To flush leachate through a site at a rate of 10 m/a under unit hydraulic gradient, the average effective stress in the worst case must not exceed approximately 200 kPa.

Table 8.8 Maximum possible effective stress that maintains various hydraulic conductivities

Hydraulic conductivity m/s	Waste DM3 Best fit line $K=2.1(\sigma')^{-2.71}$	Waste DM3 Worst case fit $K=17(\sigma')^{-3.26}$	All wastes Best fit line $K=10(\sigma')^{-3.1}$	All wastes Worst case fit $K=80(\sigma')^{-3.63}$
$3x10^{-7}$	335	239	267	209
$3x10^{-8}$	785	484	561	395

The hydraulic conductivities measured in this research are based on fully saturated waste samples. The hydraulic conductivity of unsaturated wastes could be at least an order of magnitude lower. Unsaturated flow in a landfill could occur either by the recirculation of leachate through the unsaturated zone, or within the nominally saturated zone when part of the pore space has become occupied by landfill gas. Further work is required into this topic, but the potential implications on recirculation are considered further in Sections 8.5.7 and 8.6.8.

8.5.5 Leachate recirculation - collection systems

In order to flush liquid through landfills there is a need for efficient leachate collection and injection systems. In new sites leachate collection systems will almost certainly be based on a network of horizontal drains laid either directly in the waste or within a drainage blanket at the base of the site. In older sites, without the benefit of a leachate collection infrastructure, the use of leachate extraction wells will almost certainly be required.

This section briefly summarises the hydraulic performance and limitations of the various types of leachate collection systems. The relative merits of operating flushing in unsaturated and saturated wastes are discussed in Section 8.5.8. However, it is noted here that the operation of any type of gravity collection system relies on the build up of a head of leachate at some point, whether in the surrounding waste or (as in the case of total drainage blankets) in the drainage system itself.

Horizontal drains.

Leachate drains are the most common type of leachate collection system. They are especially applicable to new sites where they can be incorporated into the collection system at the base of the site. The drains may or may not be installed into a drainage layer depending on the anticipated infiltration rate and the hydraulic conductivity of the waste. There are a number of analytical solutions that calculate the appropriate spacing of leachate at the base of a landfill (e.g. Oweis, 1990; Giroud 1995 & McEnroe, 1989).

For illustrative purposes, the following analytical solution for steady state flow to parallel drains on a flat grade is adopted.

$$L = \sqrt{\frac{(h_2^2 - h_1^2).K}{P}} \qquad (8.6)$$

(modified from Bouwer, 1978)

where

- 2L is the distance between parallel spaced drains (m)
- h_2 is the maximum desired leachate level above base (m)
- h_1 is the leachate level in the drain (m)
- P is the recharge rate (due to infiltration), in m^3 /s per m^2- i.e. in m/s, and
- K is the hydraulic conductivity of the refuse (m/s)

The operation of this type of system relies on horizontal flow in a saturated zone that builds up on an impermeable base. The drain spacing required to maintain a particular maximum leachate head is related to the recharge rate and the hydraulic conductivity of the 'aquifer' material between the drains.

Table 8.9 shows the drain spacings required to maintain different leachate heads at varying recharge rates (expressed in mm/annum) and depths of landfill.

For landfills up to 40 m deep and at low infiltration rates (e.g. 50 mm/annum), leachate drains laid directly into the waste do not need to be spaced any closer than 20 metres to control leachate levels to within 2 metres of the base of the site. At higher infiltration rates (associated with a flushing bioreactor) drains spaced at 20 metres or more in waste can only control leachate levels in shallow sites (where the waste has not been pre-compacted and maintains a hydraulic conductivity of 10^{-6} m/s or greater).

In deeper sites, where the hydraulic conductivity of the waste falls significantly below $1x10^{-6}$ m/s, then the drains need to be installed in a layer of a high permeability drainage stone at the base of the site to control leachate levels effectively.

Table 8.9 Drain spacings for various depths of landfill and infiltration rates

Landfill Depth = 10 m					P =	
Max. Permissible Leachate Head (m)	Total stress at top of sat' zone (kPa)	Av. eff stress in sat zone (kPa)	Av. K in saturated zone # (m/s)	50 mm/a Drain spacing* (m)	1,000 mm/a Drain spacing* (m)	10,000 mm/a Drain spacing* (m)
5	50	51	4.91×10^{-5}	1,760	393	124
			4.57×10^{-5}	1,698	380	120
2	78	79	1.52×10^{-5}	392	88	28
			1.11×10^{-5}	335	75	24
1		Drainage Layer	1×10^{-4}	502	112	36
			1×10^{-5}	159	36	11
Landfill Depth = 20 m					**P =**	
Max. Permissible Leachate Head (m)	Total stress at top of sat' zone (kPa)	Av. eff stress in sat zone (kPa)	Av. K in saturated zone # (m/s)	50 mm/a Drain spacing* (m)	1,000 mm/a Drain spacing* (m)	10,000 mm/a Drain spacing* (m)
5	148	152	2.58×10^{-6}	403	90	29
			1.32×10^{-6}	289	65	20
2	181	183	1.56×10^{-6}	125	28	9
			7.20×10^{-7}	85	19	6
1		Drainage Layer	1×10^{-4}	502	112	36
			1×10^{-5}	159	36	11
Landfill Depth = 40 m					**P =**	
Max. Permissible Leachate Head (m)	Total stress at top of sat' zone (kPa)	Av. eff stress in sat zone (kPa)	Av. K in saturated zone # (m/s)	50 mm/a Drain spacing* (m)	1,000 mm/a Drain spacing* (m)	10,000 mm/a Drain spacing* (m)
5	378	384	2.08×10^{-7}	115	26	8
			6.38×10^{-8}	63	14	4
2	415	418	1.66×10^{-7}	41	9	3
			4.86×10^{-8}	22	5	2
1		Drainage Layer	1×10^{-4}	502	112	36
			1×10^{-5}	159	36	11

The range of hydraulic conductivity values is provided by Equations 6.9 and 6.12
* Drain spacing = 2L from Equation 8.6

Operation and efficiency of leachate pumping wells

The principle of operating leachate extraction wells in landfills for recharge rates up to 500 mm/annum has already been examined in Section 8.4.2 (see Table 8.3).

The same principle is applicable for higher recharge rates. Equation 8.3 has been applied to a pumped well assumed to be part of a network of wells spaced on a 20 metre grid. The analytical solution is based on steady state flow where the volume of leachate extracted from a well is matched by the recharge over the catchment area of the well.

The well yield has been calculated assuming full drawdown in the well and for various saturated depths in a 40 m deep landfill (i.e. the full saturated depth is assumed to occur at a radius of 11.3 metres from the well). Inevitably this leads to significant components of vertical flow where large saturated depths are involved. Although the analysis is based on horizontal flow it has been proved, for other analytical solutions of radial flow to a well (e.g. Hantush, 1962 for the Dupuit-Forchheimer well discharge formula), that the components of vertical flow do not alter the accuracy of the calculated discharge rate. It is therefore considered that the following analysis can be used as a reasonable approximation.

The results of an analysis on a 40 m deep landfill with various depth of saturation are shown in Table 8.10. For each depth of saturation two values of hydraulic conductivity have been calculated from the average effective stress in the saturated zone and Equations 6.9 and 6.12. As a worst case scenario, two values of hydraulic conductivity have also been based on the stress (440 kPa) at the base of a 40 metre deep unsaturated landfill:- Equation 6.9 gives a value of 1.44×10^{-7} m/s and Equation 6.12 gives 4.1×10^{-8} m/s.

If the hydraulic conductivity is related to the average effective stress then large saturated thicknesses (above 20-25 m) lead to low effective stresses, high hydraulic conductivities and large pumping rates. At low saturated thicknesses (below 10-15 m) well yields are reduced considerably and approach the values calculated with the worst case hydraulic conductivity (based on a stress of 440 kPa). Even then pumping rates in excess of 1 m^3/day are possible for saturated depths over 20 metres.

The data in Table 8.10 are plotted on Figure 8.5 as recharge rate against saturated depth. It illustrates that the achievement of the required minimum flushing rate (of 4 m/a, from Eq 8.5) is mainly dependent on the depth of saturated zone within the landfill.

Table 8.10 Maximum well yields, expressed as a recharge rate, for varying saturated depths in a 40 metre deep landfill

Saturated Depth	Av. eff. stress in sat. zone	Max. well yield based on $K=2.1(\sigma')^{-2.71}$		Max. well yield based on $K=1.44\times10^{-7}$ m/s		Max. well yield based on $K=17(\sigma')^{-3.26}$		Max. well yield based on $K=4.1\times10^{-8}$ m/s	
m	kPa	m/a*	m^3/d	m/a*	m^3/d	m/a*	m^3/d	m/a*	m^3/d
35	61	2,641	2,894	11.4	12.5	2,268	2,487	3.2	3.6
30	119	326	357	8.4	9.2	195	214	2.4	2.6
25	173	79	87	5.8	6.4	38	42	1.7	1.8
20	228	24	26	3.7	4.1	10	11	1.1	1.2
15	283	7.5	8.2	2.1	2.3	2.8	3.0	0.60	0.65
10	338	2.0	2.2	0.93	1.0	0.68	0.74	0.27	0.29
5	395	0.34	0.37	0.23	0.26	0.10	0.11	0.066	0.073
1	440	0.01	0.011	0.009	0.01	0.003	0.003	0.003	0.003

* Well yield is expressed as an equivalent infiltration rate over the area of influence of each well in addition to a pumping rate in m^3/day. This is based on a radius of influence of 11.3 metres (20 metre grid) giving an area of influence of 400 m^2. For example, a recharge rate of 10 m/a equates to a well yield of 400 m^3/annum (10.96 m^3/day).

The analysis is based on Equation 8.3, and takes no account of well losses.

Pumping from a small saturated zone will not produce large enough well yields to achieve the required flushing rate. A minimum saturated depth of between approximately 15 and 20 metres is required for most cases examined; the worst case situation (of $K=4.1\times10^{-8}$ m/s) requires a saturated depth slightly in excess of a 35 m to give a recharge rate of 4 m/a.

Figure 8.6 Maximum yield, expressed as a recharge rate, of a pumped well located in a 20 metre grid of wells in a 40 m deep landfill

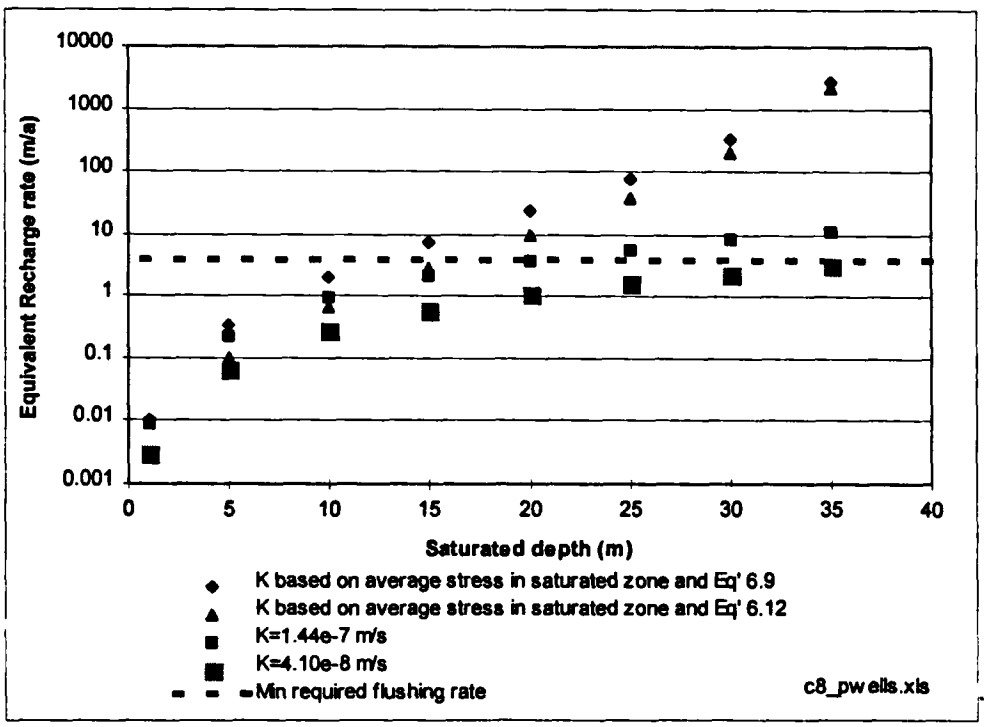

8.5.6 Leachate recirculation - injection systems

In order to recirculate or flush liquid within a landfill, there is an equal need to introduce liquid into the site as to extract leachate.

The various ways in which liquid can be introduced into a landfill are discussed below. The potential advantages and disadvantages of the various techniques are summarised in Table 8.11.

Spray irrigation

Spray irrigation has previously been used (e.g. Ettala, 1987) as a method to remove excess leachate from a site by evapo-transpiration. By increasing the application rate, infiltration as well as evapo-transpiration will occur. Technology exists for irrigation over large areas with the use of, for example, large central pivot irrigators (Hanna *et al*, 1983).

Irrigation ponds

Irrigation ponds have been used on a relatively small scale as a means to recirculate leachate into operational sites in the US (Townsend *et al*, 1995). The technique proved reasonably successful, although infiltration rates reduced over time.

Injection trenches

The majority of leachate recirculation trials undertaken in the UK have used pipes buried in the surface of the site as a means to introduce leachate (e.g. Blakey *et al* 1997; Knox, 1996). Pipes should ideally be installed in a trench backfilled with drainage aggregate. They should be laid on a level and operated in a way that results in the pipe and trench being (periodically) flooded. This will ensure there is a potential for infiltration to occur from the full length of the injection system. Otherwise, if liquid is injected into the system at a relatively slow rate, it will infiltrate into the landfill in close proximity to the injection point, and will not become widely distributed.

Injection layers

A wider areal distribution of leachate can be achieved by installing injection pipes within a layer of drainage stone, rather than in trenches. There are no known documented examples of this type of system, although a rectangular area or pad of scrap car tyres was placed in a site in Essex (Keeling, 1999) to allow leachate re-injection. To counteract the effects of settlement (particularly differential), this type of system would benefit from being constructed as a number of hydraulically separated pads, each with its own individual injection pipework. Each pad should be operated in a similar way to injection trenches - i.e. by flooding to ensure the recirculating leachate is properly distributed.

Table 8.11 Available methods for introducing leachate into landfills

Method	Advantages	Disadvantages
Spray irrigation	Creates even distribution over surface	Evaporation
	Rate of irrigation (up to maximum before ponding occurs) can be regulated	Requires relatively flat and horizontal surface
	Irrigation surface can be 'hoed' or broken up if area becomes clogged and infiltration rates fall	Has to be undertaken before capping layer placed: No operations in same area
	Rainbows in sunshine	Possible public health issues - e.g. smells, ideal conditions for flies
Irrigation ponds	Creates even distribution over surface	Evaporation
	Maximum infiltration rate always achieved	Requires flat and horizontal bunded surface
		Has to be undertaken before capping layer placed: No operations in same area
		Recharge rate reduces over time
		Possible public health issues - e.g. smells, ideal conditions for flies
Injection trenches	Can be placed at any location in site	Limited areal distribution
	Operations not affected - landfilling can continue over the top	Access to (buried) pipes may be difficult
		Settlement may damage system (e.g. rupture of pipes)
		Maintenance (e.g. clogging) and repairs not possible
Injection blankets	Can be placed at any location in site	Access to (buried) system may be difficult
	Operations not affected - landfilling can continue over the top	Settlement may damage system (e.g. rupture of pipes)
	Good areal distribution	Maintenance (e.g. clogging) and repairs not possible
	Effects of settlement can be minimised by creating a number of hydraulically isolated injection areas	
Injection wells	Can be installed retrospectively	Clogging
	Individual areas and levels can be targeted	Well Efficiency
	Could be used to flush horizontally rather than vertically	

Injection wells

Vertical wells or sumps can be used to re-inject leachate into sites. They can be installed with well screen at particular horizons to target flow, or with screen throughout their full depth. It is possible that the wells could (at different times) have a number of purposes:- leachate injection, leachate abstraction and landfill gas extraction.

8.5.7 Vertical flushing - downward unsaturated flow

This section examines flushing through predominantly unsaturated waste. Section 8.5.8 then examines the significant benefits, in terms of flushing rates, efficiency and control, that are obtained by recirculating leachate through saturated sites.

One of the major restrictions often placed on the concept of a flushing bioreactor (or on the recirculation of leachate through wastes) is that flushing should be carried out without the build up of any leachate heads within the landfill. The industry has spent the last decade engineering and operating sites on the principle of 'zero' or at least minimal leachate heads. Consequently there is an understandable reluctance to the suggestion that large volumes of liquid should be introduced and recirculated through the site. This is reflected to a certain extent in the current draft of the landfill directive (EC, 1998) which aims to prohibit the introduction of liquid wastes to new sites.

There is a view that if leachate recirculation has to take place it should not result in the build up of leachate heads in the landfill; this means that recirculation would have to take place through unsaturated wastes. It will be argued in Section 8.6.1 that engineering measures can be taken to mitigate against the effects of high heads and, therefore, restricting recirculation to unsaturated wastes is unnecessary.

If leachate recirculation is to be through unsaturated waste then the leachate has to be evenly introduced at the surface. Assuming uniform downward vertical seepage, a complete leachate under-drainage system at the base of the site is then required to collect it.

The maximum infiltration rate can be directly equated to the minimum hydraulic conductivity that occurs in any vertical section through the site. In the absence of any low permeability cover or loads of 'abnormal' wastes, this will occur at the base of the site.

The stress at the base of various depths of unsaturated landfill (with a 30 kPa surcharge) has been calculated using the same methods described in Section 8.4.1. A range of hydraulic conductivities has been calculated from these stresses using Equations 6.9 and 6.12 to represent the maximum unsaturated infiltration rate possible. These data are

plotted on Figure 8.7, together with the approximate minimum flushing rate (from Equation 8.5) for the various depths of landfill. As the calculated values of hydraulic conductivity have been based on flow through saturated waste, error bars have been applied to the infiltration rates. These represent a possible order of magnitude reduction in the hydraulic conductivity due to flow through unsaturated waste.

Figure 8.7 Flushing rates through various depths of unsaturated landfill

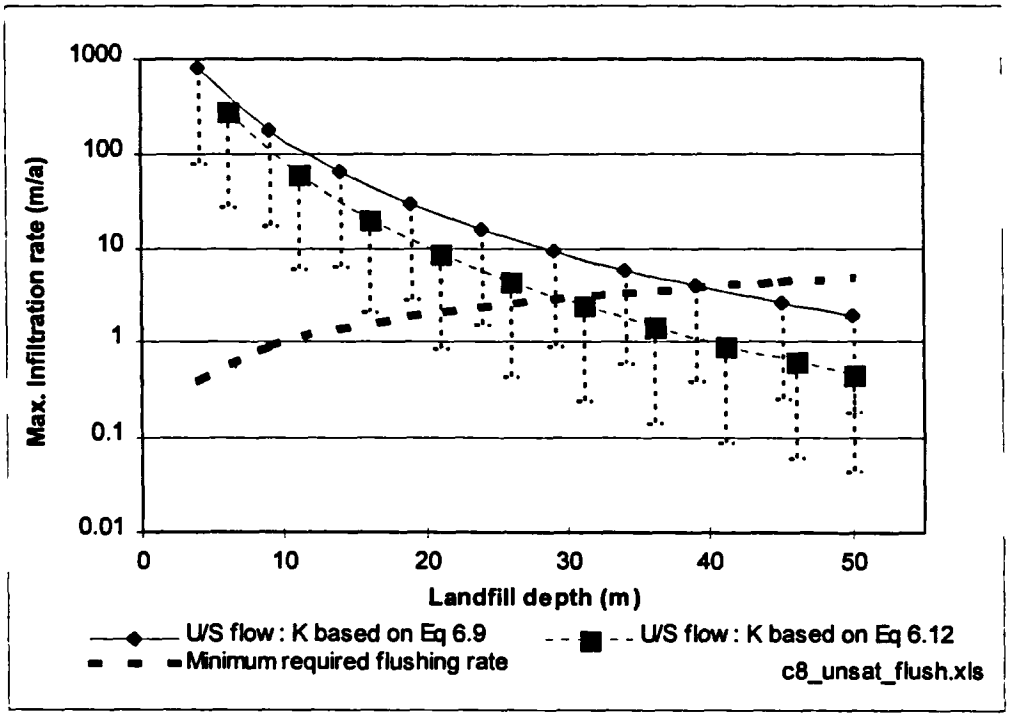

Figure 8.7 indicates that, in the absence of waste pre-compaction, the required rate of flushing through unsaturated wastes can only be achieved by limiting landfill depth. Taking into account the possible reduction in hydraulic conductivity caused by unsaturated flow, landfills would need to be less than approximately 20 metres deep.

If the objective is to flush approximately 2.7 m^3 of leachate per unit volume of waste in around 30 years, it can also be concluded that there is little point attempting this by unsaturated flushing in landfills more than approximately 35 metres deep. The maximum attainable flushing rate would mean it probably taking several hundred years to achieve.

8.5.8 Vertical flushing - benefit of operating with a saturated zone

Significant increases in flushing rate, for a given depth of landfill, can be achieved by recirculating leachate through saturated rather than unsaturated waste. The most obvious advantage is that there is no longer the reduction in the hydraulic conductivity of the

waste that occurs in unsaturated materials. This fact alone could lead to an immediate order of magnitude increase in flushing rates, although the action of gas generation within the saturated zone may reduce the extent of this benefit.

In addition, Powrie and Beaven (1999) showed that even higher vertical flushing rates could be achieved if leachate heads in the body of a landfill (but not in the basal drainage layer) were allowed to increase above that associated with a hydrostatic increase in water pressures. The analysis was undertaken with the finite difference technique already described in Section 7.7.1 (see also footnote on page 238). It has been re-worked here, using the variables shown in Table 8.12, to calculate the maximum flushing rate through various depths of landfill (Figure 8.8). It is assumed that leachate is introduced at the top of the landfill at zero pore water pressure and abstracted from a dewatered basal drainage layer (where the pore water pressure is also zero).

The relationship between density and effective stress was based on Equation 6.3, (with a 10% increase for the presence of cover - see Section 8.4.1). It was assumed that the hydraulic conductivity of the saturated waste was allowed to vary reversibly with effective stress. Hydraulic conductivity was calculated from Equation 6.12, representing the worst case fit for waste DM3. At low effective stresses this relationship produces unrealistically high hydraulic conductivities. Therefore, below a stress of 40 kPa, the hydraulic conductivity was set to 1×10^{-4} m/s.

Table 8.12 Variables used in saturated downward flow analysis

Surface surcharge:	30 kPa
Density relationship: Saturated	$\rho = 0.6691(\sigma_v')^{0.0899}$
Increase in total stress per depth increment (z)	$d\sigma_v = 1.1(\rho.z)$ (10% increase for cover)
Hydraulic conductivity	$K=17(\sigma_v')^{-3.26}$ for $\sigma_v'>40$ kPa $K=1 \times 10^{-4}$ m/s for $\sigma_v'<40$ kPa

Figure 8.8 compares maximum infiltration rates through saturated and unsaturated landfills of various depths. At shallow depths the saturated and unsaturated flushing rates converge (excluding error bars). In deep landfills the saturated infiltration rate is considerably higher than the unsaturated rate. This is principally because saturation keeps the effective stresses in the body of the landfill low and the hydraulic conductivity high. Figure 8.9 shows the variation in effective stress, pore water pressure, and hydraulic conductivity with depth in a 30 metre deep landfill. From the surface of the landfill to a depth of approximately 25 metres, the increase in pore water pressure is only slightly less than hydrostatic, and there is very little increase in effective stress. Consequently, high hydraulic conductivities are maintained.

Figure 8.8 **Comparison of maximum flushing rates through saturated and unsaturated landfills.**

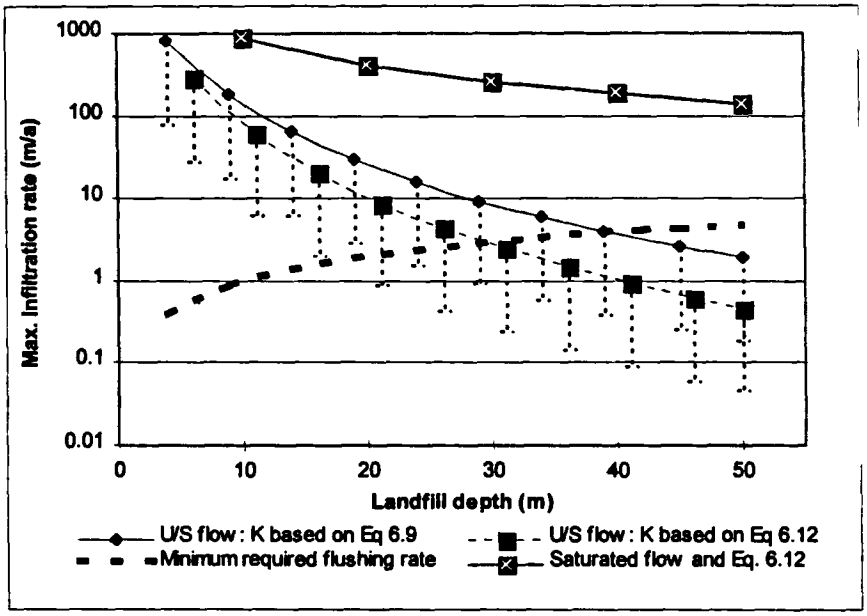

In the bottom 5 metres of the landfill the influence of the dewatered basal drainage blanket is seen in a rapidly decreasing pore water pressure. This leads to rapid increases in effective stress and reductions in hydraulic conductivity. The hydraulic gradient also increases and, in terms of vertical flow rate, this compensates for the reduction in hydraulic conductivity. For example, the hydraulic conductivity in the bottom 0.5 metre increment is approximately 1×10^{-7} m/s, which is similar to the value calculated at the base of an unsaturated landfill. However, the saturated hydraulic gradient over this same depth increment is 24 (compared with 1 for the unsaturated case).

Figure 8.9 **Variation in vertical effective stress, pore water pressure and hydraulic conductivity with depth in a 30 m deep landfill with saturated downward flow**

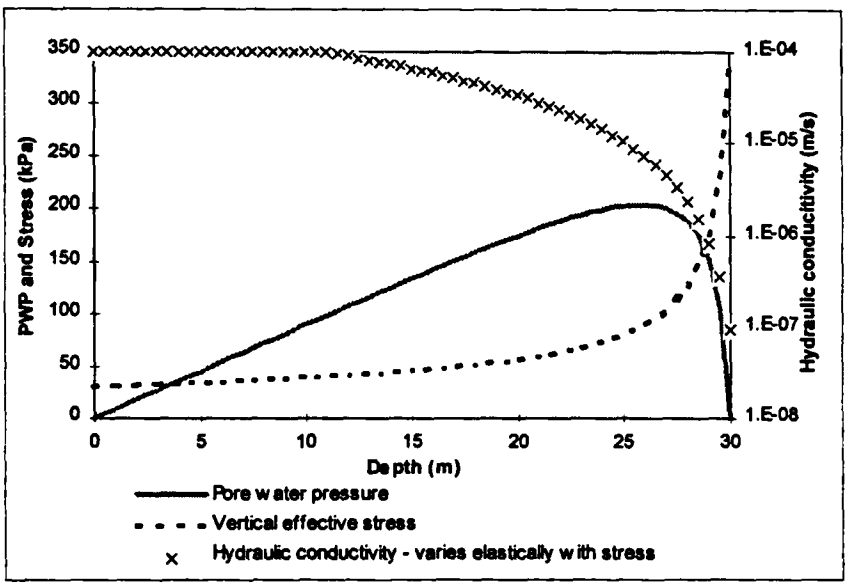

If the hydraulic conductivity at any depth is based on the maximum historical effective stress, then the potential saturated flushing rates could be considerably lower than shown in Figure 8.9.

Figure 8.10 shows the maximum flushing rate through various depths of landfill, where the variation in hydraulic conductivity with depth (Figure 8.11) has been based on the variation in stress in an unsaturated landfill.

Figure 8.11 shows that the rate of reduction in pore water pressure with depth near to the drainage layer is less pronounced than shown in Figure 8.9, resulting in a more gradual increase in effective stress. More importantly, the hydraulic gradient at entry into the drainage layer is approximately 4. This restricts the maximum flushing rate to between 4 and 5 times that for unsaturated flow, as shown in Figure 8.10.

It is clear that the full benefits of operating leachate recirculation through saturated wastes, in terms of enhanced recirculation rates, can only be obtained if measures are taken to prevent the establishment of elevated effective stresses and hence low hydraulic conductivities in the landfill.

Figure 8.10 **Maximum flushing rates through saturated and unsaturated landfills:- hydraulic conductivity based on unsaturated stress distribution.**

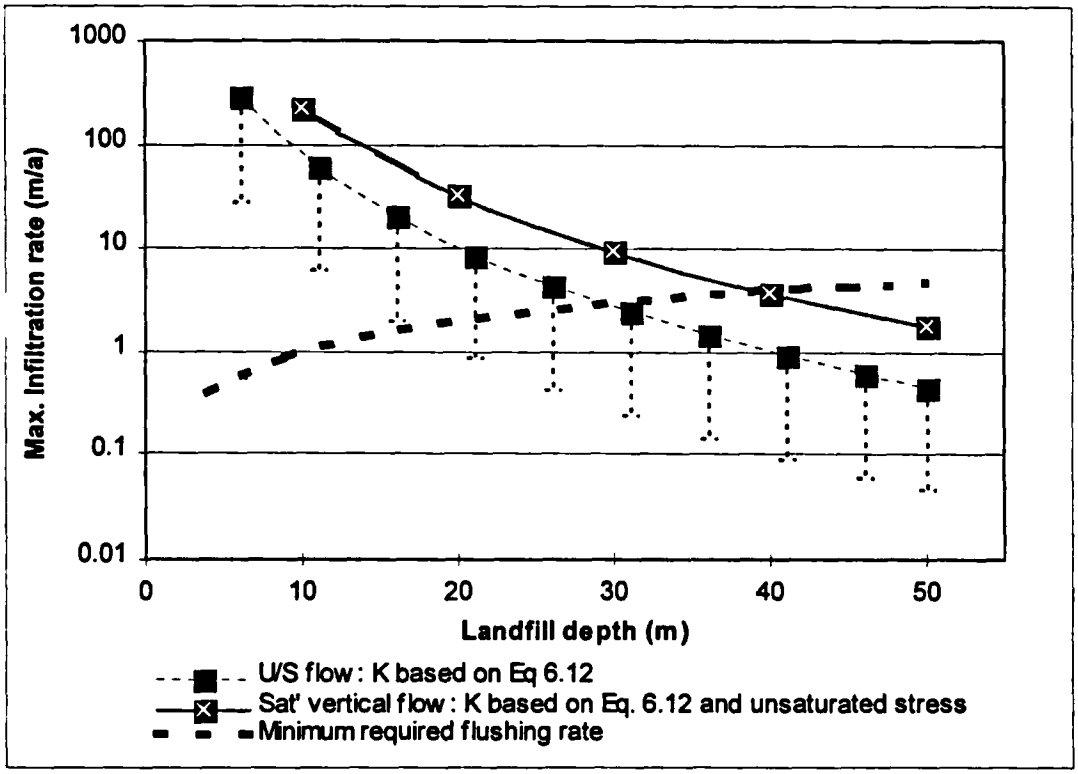

Figure 8.11 **Variation in vertical effective stress and pore water pressure with depth in a 30 m deep landfill with saturated downward flow:- hydraulic conductivity based on unsaturated stress distribution**

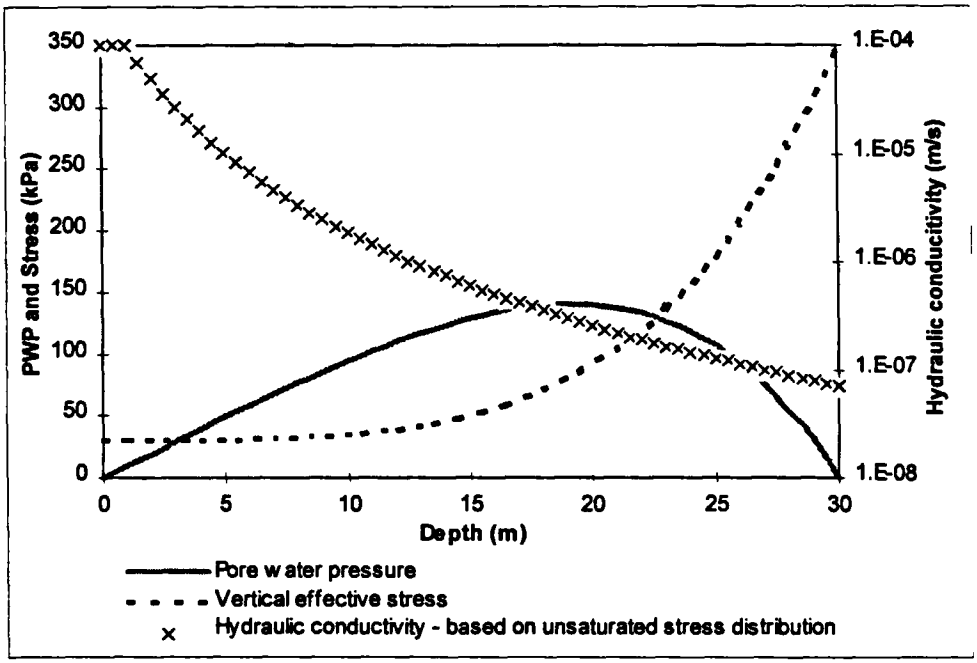

If waste is placed in a landfill and brought up to final levels without the build up of any leachate, when recirculation is attempted the flushing rates will probably be restricted to that shown in Figure 8.10 (assuming no rebound in the waste). However, if water is continually introduced into a landfill (perhaps from a basal drainage layer) as the site is being raised and a leachate table is maintained a few metres below the surface, then relatively high hydraulic conductivities would be preserved. This would result in maximum flushing rates being nearer to that illustrated in Figure 8.8.

It could be argued that such measures are unnecessary in sites less than approximately 40 metres deep as the minimum required flushing rate can be achieved in shallower sites even if the hydraulic conductivity of the waste is based on unsaturated stresses (as in Figure 8.10). However, the required flushing rate is, as stated, a minimum; to achieve the objectives not only will flushing have to continue at the rate specified but over the full time involved - i.e. 30 years. Flushing at a higher rate would mean that the objective could to be met more quickly or even if there were periods of time when recirculation was not taking place. Furthermore, it provides more operational flexibility by allowing the site to be split into phases with flushing being rotated between them. One advantage of this mode of operation would be to allow leachate from different phases at different stages of the flushing process to be blended to produce a leachate with a relatively constant strength over time. The design and operation of a leachate treatment plant on

the basis of a balanced flow is easier than if the strength of the leachate is going to reduce over time.

A further benefit of operating leachate recirculation through saturated (rather than unsaturated) wastes is that there is no longer the need to rely on downward vertical flow. Upward vertical flow could be achieved by introducing leachate into the base of a site and removing it from near the surface. The possible benefits of this mode of operation are investigated in Section 8.5.9.

Saturated flow also allows an element of horizontal flow to be introduced by, for example, introducing leachate to one side of a site and removing it from another. This may accelerate flushing of waste which would otherwise be in a region of low flow (perhaps as a result of being overlain by a low permeability layer - see Section 8.5.11).

Finally, saturated conditions may enhance the process of diffusion and the transfer of contaminants from fluid held in the matrix of the waste to a more mobile phase.

8.5.9 Vertical flushing - upward flow

There are potential benefits of operating of a leachate recirculation scheme based on upward flow between a basal injection layer and a collection layer located at, or near, the top of the landfill. It has already been demonstrated in Section 8.5.8 that the downward flushing of leachate into a dewatered drainage blanket leads to the development of high effective stresses above the drain and low hydraulic conductivities. The operation of upward flushing would preserve low effective stresses and high hydraulic conductivities and could lead to higher flushing rates.

The finite difference analysis technique (Section 7.7.1 and footnote on page 238) has been used to calculate the vertical infiltration rates that occur with various leachate heads in the basal drain of a 30 m deep landfill. The previous analyses were undertaken assuming that the drain was totally dewatered (i.e. zero pore water pressure). It is still assumed that leachate is either introduced or removed from the surface of the landfill under a head of 30 m AD.

Table 8.13 Variables used in upward and downward flow analysis

Surface surcharge:	30 kPa
Density relationship:	$\rho = 0.6691(\sigma_v')^{0.0899}$
Increase in total stress per depth increment (z)	$d\sigma_v = 1.1 \times \rho.z$ (10% increase for cover)
Hydraulic conductivity	$K=17(\sigma_v')^{-3.26}$ for $\sigma_v'>40$ kPa $K=1\times10^{-4}$ m/s for $\sigma_v'<40$ kPa

Figure 8.12 shows the results of the analysis for a waste whose hydraulic conductivity varies with effective stress. The maximum infiltration rate occurs when the drainage layer is dewatered. However, as the leachate head in the drain increases, there is initially only a small reduction in performance; a reduction in the average hydraulic gradient is compensated by increases in hydraulic conductivity at the base of the site as effective stresses reduce. It is not until the head in the basal layer exceeds approximately 20 m that there is a significant reduction in infiltration rate. The implication is that the leachate recirculation scheme can be operated to maintain relatively high hydraulic conductivities at the base of the site (i.e. by not dewatering the drainage layer) without a significant loss in recirculation rates.

When the head in the basal layer exceeds 30 m AD, upward flow starts. The analysis breaks down when effective stress is less than zero. The maximum head in the basal layer is constrained by the need (of the analysis if not in reality) to maintain positive effective stresses. Negative effective stresses create a potential for the waste to become fluidized with a possible risk of flotation.

The analysis indicates that zero effective stress occurs at the base of the site with a head of 31.5 m AD. This leads to an upward flow rate of 156 m/a. A larger basal head, and hence a larger upward infiltration rate, could be achieved if there was a greater surcharge at the surface of the site. This point is in effect considered in Section 8.5.10 when the depth of the upper collection drain below the surface of the site is varied.

Figure 8.12 **Infiltration rate through a 30 m deep landfill for various heads in a basal drainage layer: hydraulic conductivity varies with effective stress**

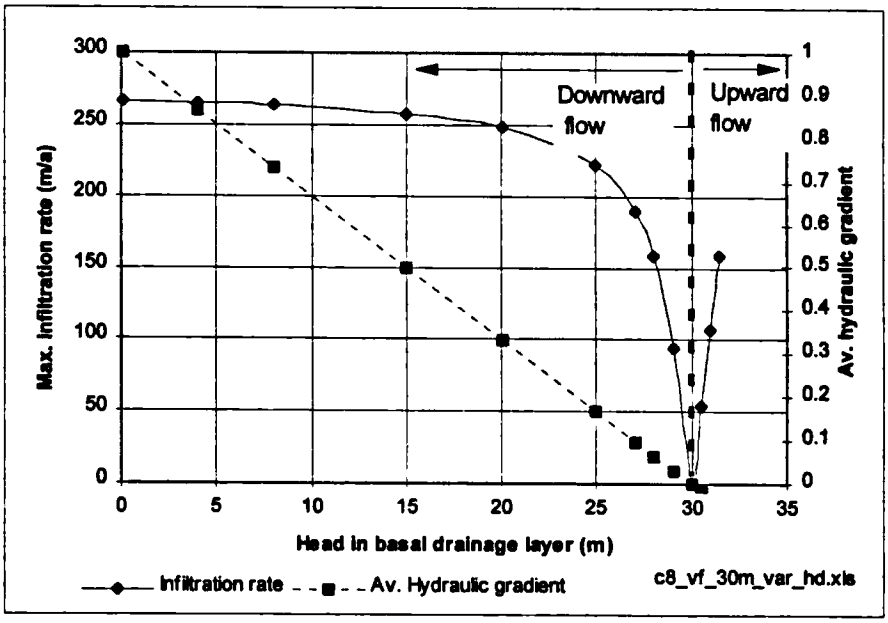

Figure 8.13 shows the results of a repeat analysis where the variation of hydraulic conductivity with depth is based on the effective stress distribution that results from the dewatering of the basal drainage layer. This distribution results in low hydraulic conductivities at the base of the site. In this example subsequent increases in the leachate head in the basal drainage layer lead to a proportional decrease in flow rate. It suggests that once the basal drainage layer has been dewatered, irreversible reductions in hydraulic conductivity lead to the loss of any benefit (in terms of flushing rate) of operating with a higher leachate head in the basal drain.

Finally, Figure 8.14 shows the results of an analysis where the variation of hydraulic conductivity with depth is based on the effective stress distribution for unsaturated waste. This perhaps represents a landfill being raised to final levels before any leachate is introduced. The potential flushing rates are considerably lower. Although the hydraulic conductivity at the base of the site is similar to that of the previous examples, it is considerably lower throughout the remaining depth of landfill. This prevents the development of large hydraulic gradients into the drain, thereby keeping flow rates down.

Figure 8.13 **Infiltration rate through a 30 m deep landfill for various heads in a basal drainage layer: hydraulic conductivity based on effective stress distribution with zero head in drainage layer**

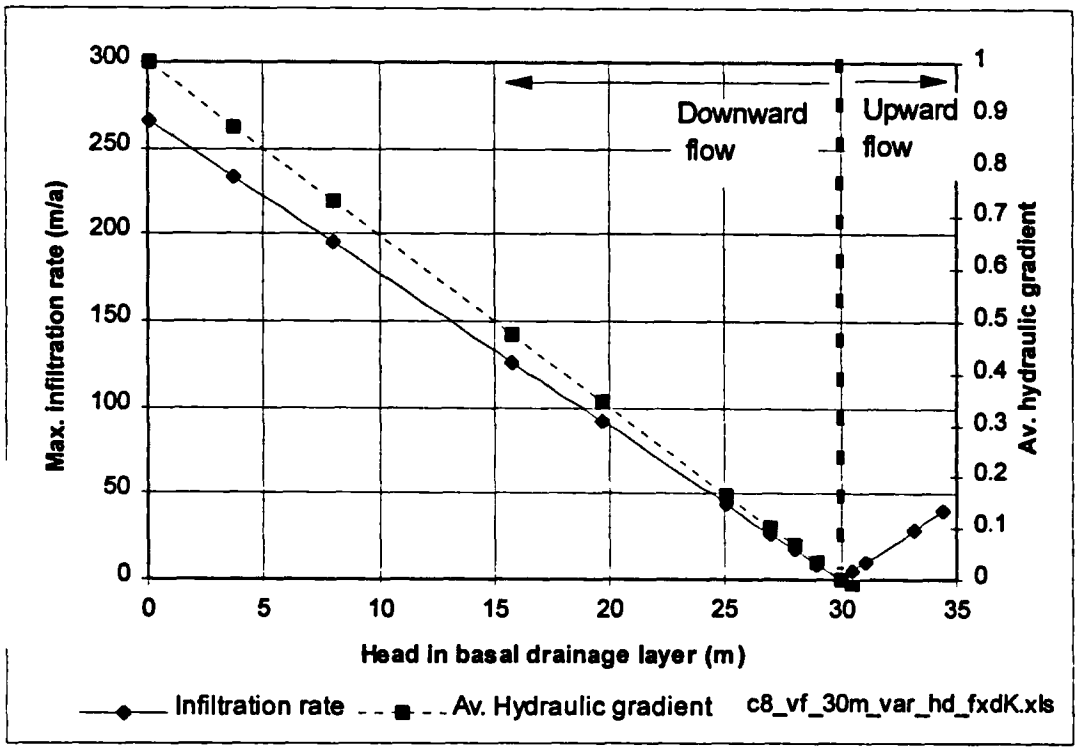

Figure 8.14 **Infiltration rate through a 30 m deep landfill for various heads in a basal drainage layer: hydraulic conductivity based on unsaturated stress distribution**

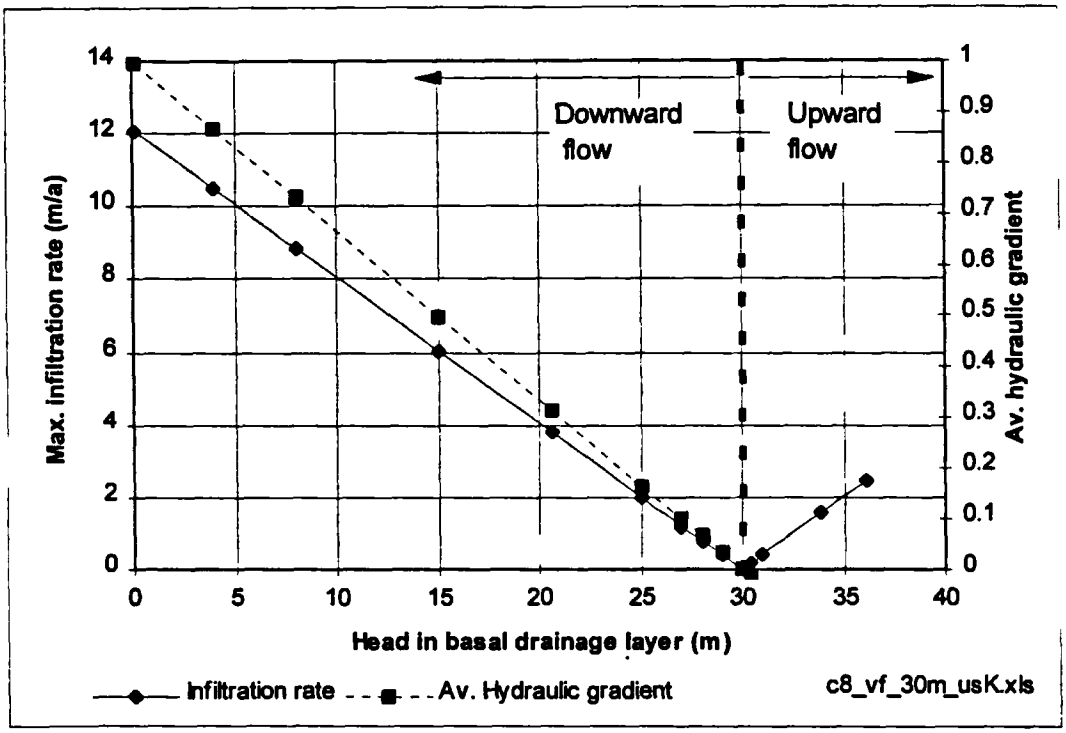

8.5.10 Vertical flushing - combined upward and unsaturated downward flow

In Section 8.5.9, the maximum rate of upward flow was restricted by the maximum head in the basal layer that did not create negative effective stresses. This maximum basal head could be increased if the surface surcharge was also increased. For example, for the analysis shown in Figure 8.12 where a 30 kPa surcharge was applied, the maximum basal head was 31.5 m AD. If the surcharge is increased to 50 kPa the maximum possible head increases to 34.5 m AD, and if increased to 100 kPa, to 40 m AD. The higher basal heads create a larger hydraulic gradient and larger flows, although the potential increase in flows is offset to some extent by lower hydraulic conductivities.

An alternative to increasing the surcharge at the top of the 30 m deep landfill is to move the upper collector drain to a lower level in the landfill. The waste overlying the drain then acts as a surcharge. This a sensible option as most landfill sites are domed above surrounding ground levels and it would be difficult to operate saturated (particularly upward) flushing above these levels.

The maximum upward flow rate in a 30 m deep landfill has been calculated according to the elevation of the upper collection drain. The stress at the collector drain is taken as the surcharge to the analysis, and is based on the assumption that the overlying waste is unsaturated.

Figure 8.15 shows the results from an analysis where hydraulic conductivity is allowed to vary reversibly with effective stress according to Equation 6.12. As the length of the vertical flow path between the two drains varies according to the elevation of the collector drain, the maximum flushing rate has been expressed as a specific flushing rate (see Table 8.7). The maximum upward specific flushing rate increases as the depth of the collector drain below the surface also increases.

Based on the total unsaturated stress and hydraulic conductivity at the upper collector drain, the maximum rate of downward unsaturated flushing has been calculated and is also shown on Figure 8.15. At drain depths above approximately 5 metres the maximum downward specific flushing rate exceeds the upward rate. For depths in excess of 7 metres the maximum upward specific flushing rate exceeds the downward unsaturated rate, although it is not until the drain is at a depth of approximately 20 metres, that the maximum possible rate falls to near the minimum required specific flushing rate of 2.85×10^{-9} sec^{-1}.

It is also feasible that the downward vertical flushing to the upper collector drain could be through saturated rather than unsaturated waste, in which case the overall maximum flushing rate could be higher than indicated above. Calculations have not been undertaken for this scenario, but an indication of possible rates can be obtained by combining results for maximum upward flow rates from this Section, with the results for downward saturated flow from Section 8.5.8.

Figure 8.15 **Specific flushing rates according to the depth of an upper collector drain in a 30 m deep landfill: hydraulic conductivity varies with effective stress**

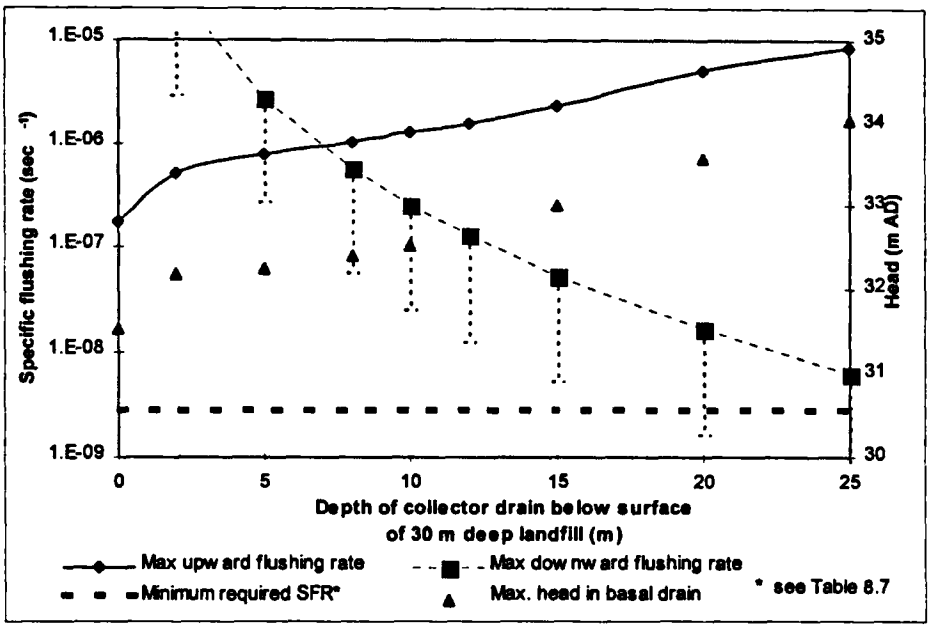

The variation in effective stress, pore water pressure and hydraulic conductivity with depth during upward flow are shown in Figure 8.16 for a drain located at a depth of 10 metres, and in Figure 8.17 for a drain at 20 metres. The maximum rate of upward flow is constrained by the need to prevent negative effective stresses at the base, and the analysis is therefore based on zero effective stress in the basal layer. The hydraulic conductivity in this layer (and for all layers where the effective stresses are less than 40 kPa) is consequently set to $1x10^{-4}$ m/s.

The hydraulic conductivity of the waste at or just above the upper collector drain is related to the stress caused by the overburden of waste above the drain. The deeper the drain, the lower the hydraulic conductivity. There is a rapid increase in pore water pressure and hydraulic conductivity, and a decrease in effective stress directly below the drain. These changes are more extreme the deeper the drain; the analyses (particularly for the drain located at a depth of 20 metres) had to be altered to work on 0.1 metre depth increments because of this.

Figure 8.16 **Variation in vertical effective stress, pore water pressure and hydraulic conductivity with depth in a 30 m deep landfill with saturated upward flow to a drain located at a depth of 10 m**

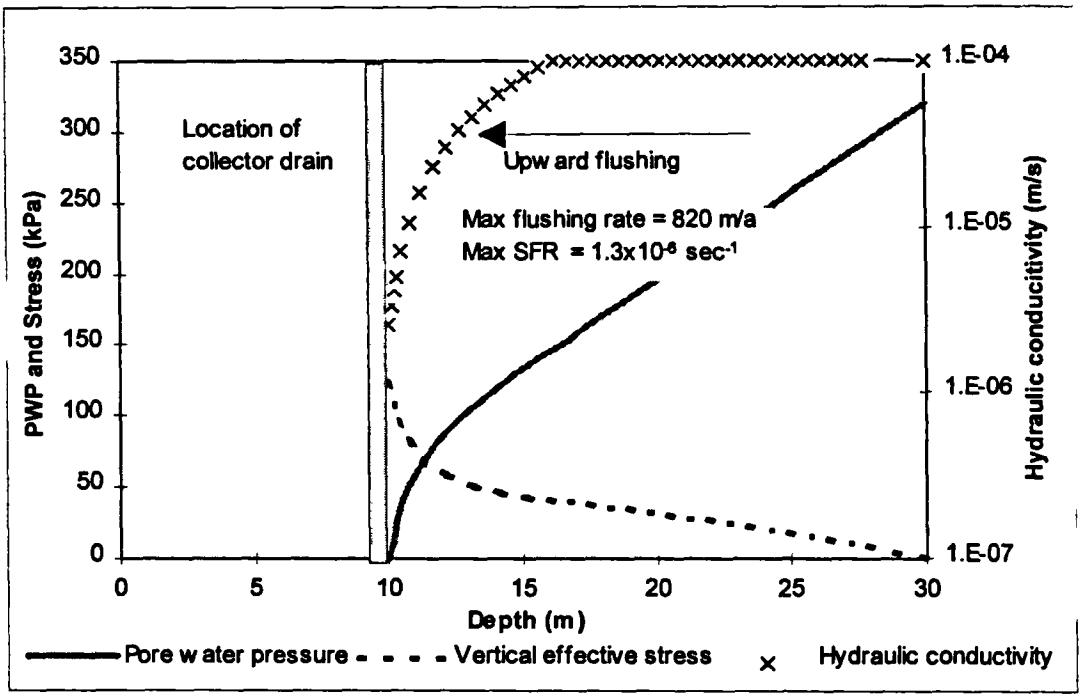

Figure 8.17 **Variation in vertical effective stress, pore water pressure and hydraulic conductivity with depth in a 30 m deep landfill with saturated upward flow to a drain located at a depth of 20 m**

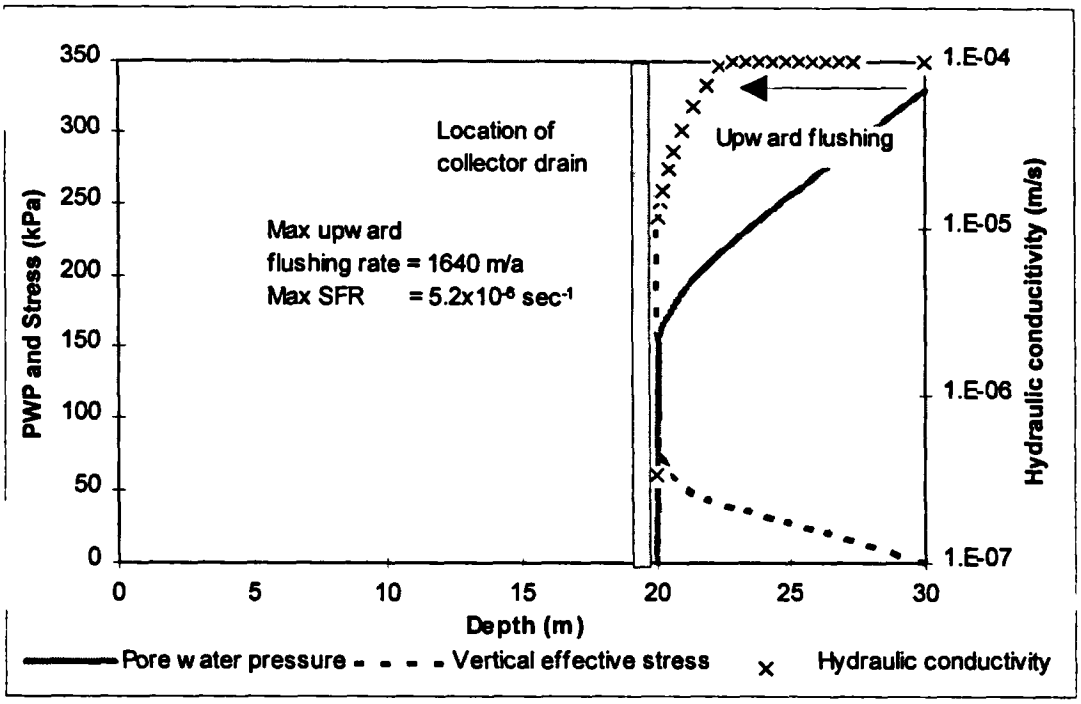

Figure 8.18 shows a repeat analysis where the hydraulic conductivity and maximum waste density is based on that calculated to occur under hydrostatic conditions (e.g. if each layer of waste is saturated directly after placement). Unlike that shown in Figure 8.15, the maximum upward specific flushing rate initially decreases as the depth of the collector drain increases because the hydraulic conductivity in the saturated zone reduces. The specific flushing rate reaches a minimum at a drain depth of approximately 12 metres, and then gradually rises as the increased hydraulic gradient (caused by the shortening vertical flow path length and increasing head in the basal drain) is able to compensate for the reduction in hydraulic conductivity. Over the full depth range the specific flushing rate is still well in excess of the specified minimum required.

If the analysis is run with hydraulic conductivities and waste densities based on an unsaturated stress distribution (e.g. if the waste is placed dry), the calculated upward specific flushing rate is slightly less than the minimum required specific flushing rate when the collector drain is at the surface of the landfill (Figure 8.19). The calculated specific flushing rate increases as the depth of the drain increases, and intersects the unsaturated downward specific flushing rate curve at a depth between 12 and 18 m.

Over this depth range the calculated specific flushing rate through both the saturated and unsaturated waste is between 4 and 10 times higher than the required minimum. This exceeds the maximum flushing rate for the case of downward saturated flow. Figure 8.13 (where the hydraulic conductivity was also based on the same unsaturated stress distribution) showed that the maximum infiltration rate for downward saturated flow, with the injection drain at the surface, was 12 m/a. This is only 4 times larger than the required minimum flushing rate of 3 m/a (from Equation 8.5).

Therefore, the highest flushing rates through a landfill may possibly be obtained by the operation of a leachate recirculation system involving both upward vertical saturated flow and downward unsaturated flow to a collector drain located within the body of the site.

Figure 8.18 **Specific flushing rates according to the depth of an upper collector drain in a 30 m deep landfill: hydraulic conductivity based on effective stress under hydrostatic conditions**

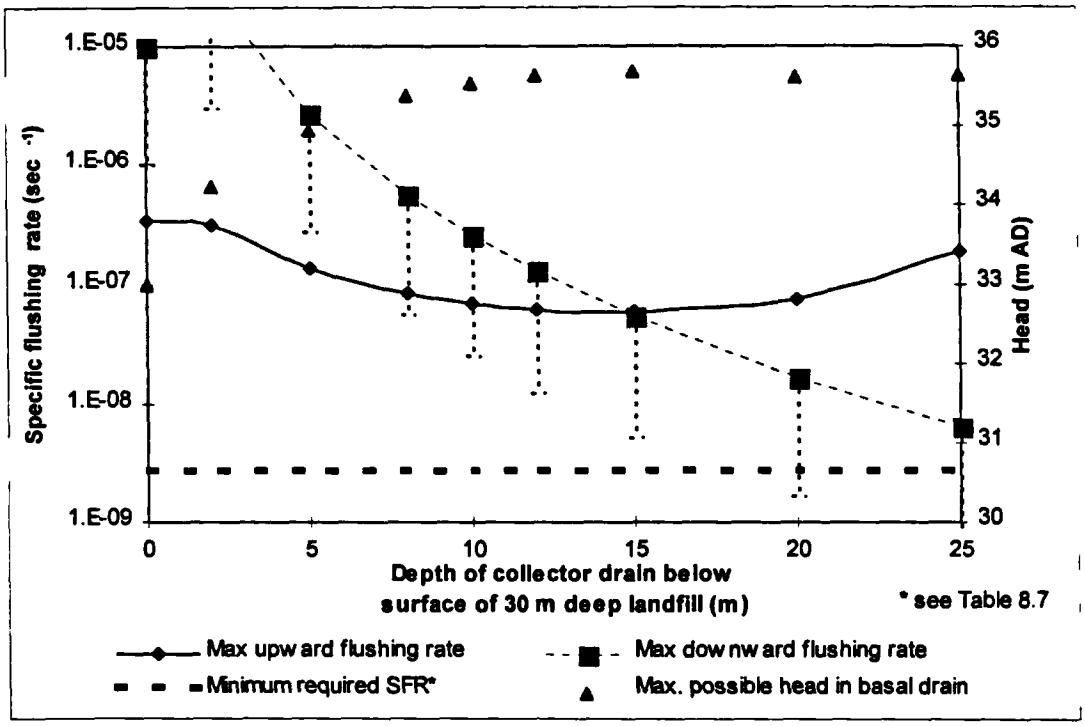

Figure 8.19 **Specific flushing rates according to the depth of an upper collector drain in a 30 m deep landfill: hydraulic conductivity based on unsaturated effective stress**

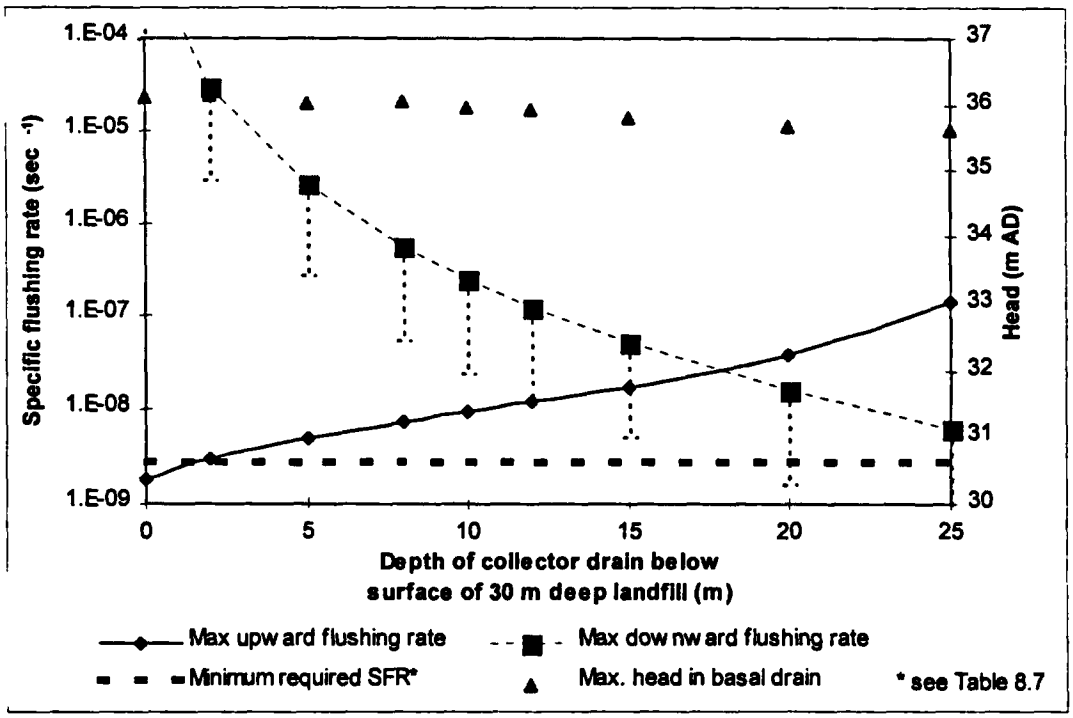

8.5.11 *Vertical flushing - impact of barriers and routes of preferential flow*

The presence of horizontal layers of low permeability material in a landfill will severely restrict vertical flushing rates. Assuming saturated conditions, the depth of a low permeability layer will affect the maximum infiltration rate. Table 8.14 shows the infiltration rates and specific flushing rates through a 30 metre deep landfill with a 0.5 metre thick layer with a hydraulic conductivity of $1x10^{-9}$ m/s. For both upward and downward flushing, the maximum possible specific flushing rate increases with the depth of the low permeability layer (Figure 8.20), because the potential hydraulic gradient across the layer increases. However, in all cases the maximum specific flushing rate is less than the specific flushing rate required to flush the wastes in a sustainable timescale (see Table 8.7).

Table 8.14 Maximum infiltration and specific flushing rates through a 30 m deep landfill with a 0.5 m thick low permeability layer at various depths

Depth of barrier m	Max Hyd gradient across low K layer	Max infiltration rate m/a	Max downward SFR* sec^{-1}	Max upward inf rate m/a	Max upward SFR* sec^{-1}
5	11	0.35	$3.67x10^{-10}$	0.065	$6.8x10^{-11}$
10	21	0.66	$7x10^{-10}$	0.077	$8.2x10^{-11}$
15	31	0.98	$1x10^{-9}$	0.09	$9.7x10^{-11}$
20	41	1.29	$1.37x10^{-9}$	0.11	$1.2x10^{-10}$
25	51	1.61	$1.7x10^{-9}$	0.14	$1.5x10^{-10}$

* SFR = Specific flushing rate

Figure 8.20 Variation in specific flushing rate through a landfill with a low permeability layer

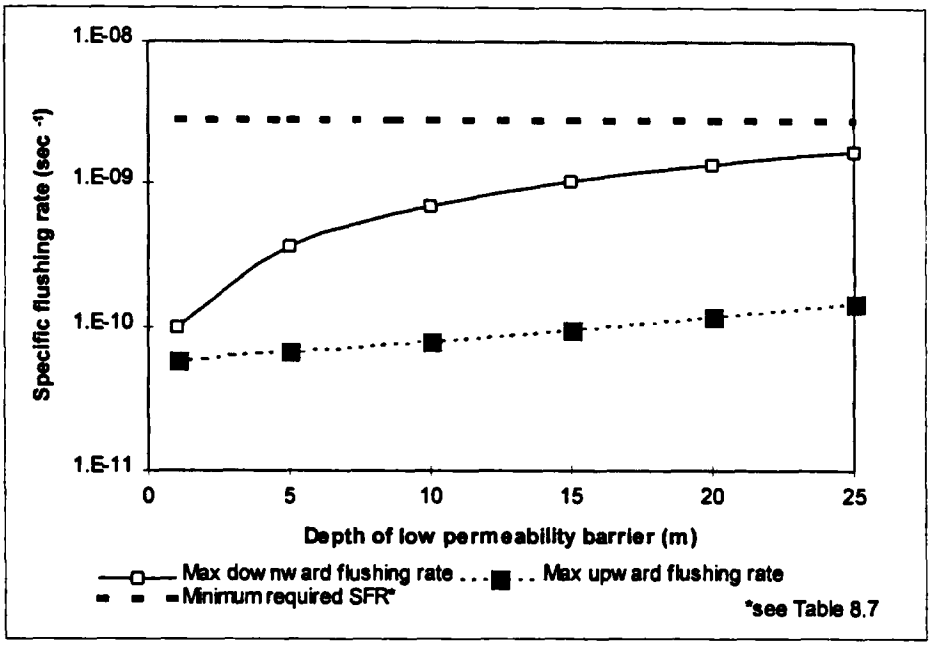

Figure 8.21 (produced using the spreadsheet analysis - Section 7.7.1) shows the variation in vertical effective stress, pore water pressure and hydraulic conductivity with depth for the maximum rate of downward flow through a 30 m deep landfill with a low permeability layer at a depth of 15 metres. Because the low permeability layer impedes the downward flow of leachate waste above it is saturated and the increase in pore water pressure with depth is virtually hydrostatic. There is little change in effective stress and the hydraulic conductivity remains constant at $1x10^{-4}$ m/s.

Waste below the low permeability layer is unsaturated as the rate of infiltration through the layer is not high enough to lead to saturated conditions. The hydraulic gradient (which controls the rate of flow) across the low permeability layer is therefore 15.5 m/0.5 m = 31.

With zero pore water pressures directly below the low permeability layer there is an immediate increase in effective stress, which continues to increase with depth. There is a concomitant decrease in hydraulic conductivity, but not (in this case) to an extent to lead to the development of saturated conditions.

Figure 8.21 Downward flow through a 30 m deep landfill with a low permeability layer at a depth of 15 m

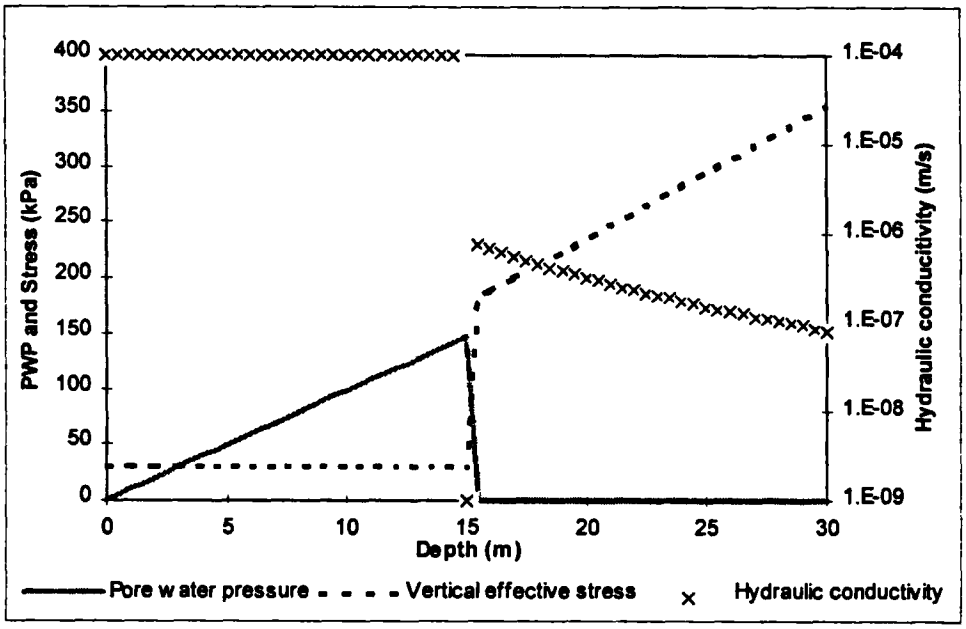

Figure 8.22 shows the variation in vertical effective stress, pore water pressure and hydraulic conductivity with depth for the maximum achievable rate of upward flow with a low permeability layer at a depth of 15 metres. The maximum flow rate was calculated when the effective stress at the base of the site was just above zero; this occurs with a

hydraulic head of 31.45 m above the base. There is a negligible upward loss in head from the base of the site to the low permeability layer, and the reduction in pore water pressure is therefore hydrostatic. From the surface of the landfill, where the leachate head is 30 m AD, down to the low permeability layer there is also a negligible increase in leachate head. The change in leachate head between the base and the surface therefore occurs across the low permeability layer, leading to a hydraulic gradient of 1.45 m/0.5 m = 2.9.

Figure 8.22 **Upward flow through a 30 m deep landfill with a low permeability layer at a depth of 15 m**

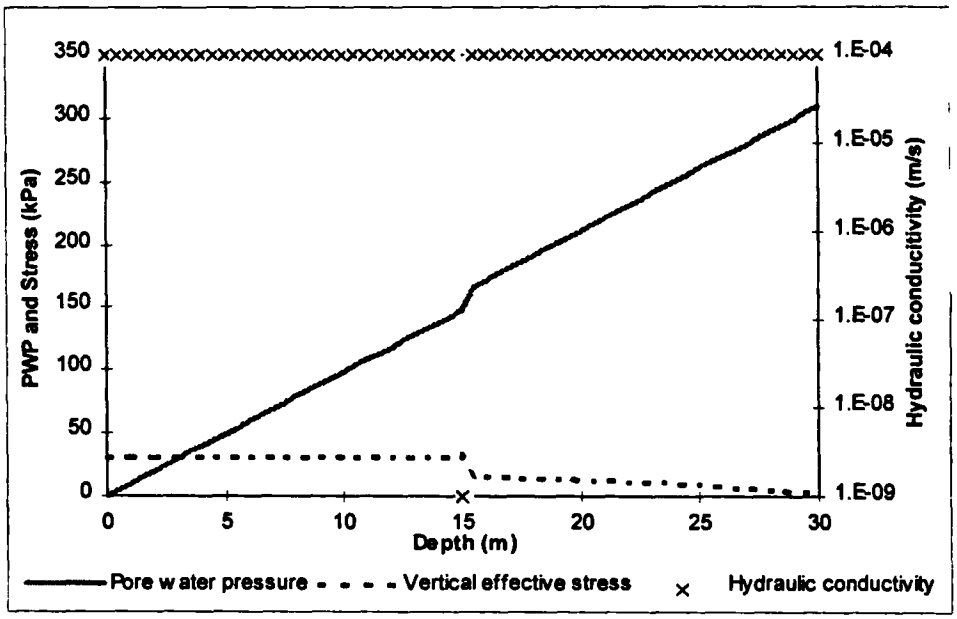

The rate of upward flow, governed by the hydraulic gradient across the low permeability layer, is more dependent on the maximum leachate head possible to avoid negative effective stresses, than on the location of the drainage layer.

This is illustrated by Figure 8.23, which shows the results of an analysis where the variation of hydraulic conductivity and density with depth is based on the unsaturated stress distribution. The maximum upward specific flushing rate is higher than that shown in Figure 8.20 even though the hydraulic conductivity of the waste over the full depth is considerably lower. The higher waste densities mean that a higher head is possible at the base, resulting in higher hydraulic gradients (up to 9.2) across the low permeability layer and therefore higher flow rates.

Figure 8.23 **Variation in specific flushing rate through a landfill with a low permeability layer where the hydraulic conductivity and density of the waste are related to the stress under unsaturated conditions**

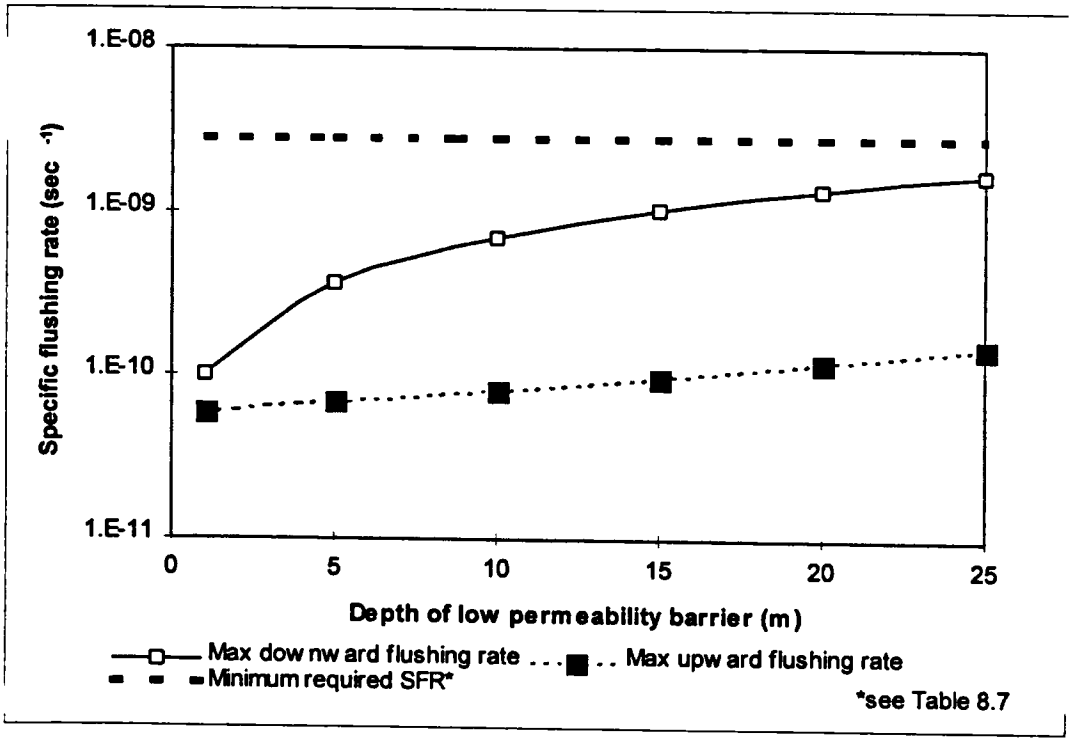

8.5.12 Horizontal flushing - injection and abstraction wells

The potential use of vertical wells to flush wastes by both injecting and abstracting leachate from a landfill is investigated below. There are two obvious advantages of such a system. Firstly, the wells and the flushing infrastructure can be installed after landfilling has been completed. Secondly, wells can also be replaced as and when their performance reduces, perhaps as a result of clogging. Thirdly, the impact of low permeability layers on flushing rates would be reduced by the predominantly horizontal flow paths associated with a vertical well system.

The factors controlling the performance of leachate wells have already been considered in Section 8.4.2. It can be concluded from that Section that in terms of well yield, depth of saturation is as important as hydraulic conductivity. For vertical wells to have a role in the flushing of wastes they will need to be operated with large saturated depths.

Figure 8.22 shows an orthogonal grid of wells spaced at a distance of 20 metres. This spacing was chosen on the basis that implementation of a well field system at this spacing on most landfills should be practicable. Reference to Table 8.3 indicates that at smaller grid spacings the number of wells required per hectare increases dramatically. Whilst this does not necessarily rule out the use of smaller grid spacings, the costs may become prohibitive.

In Figure 8.24(a) alternate lines of wells are operated as either injection or abstraction wells, resulting in parallel ridges and troughs of leachate head. The zone of influence of each well is bounded by a rectangle (20 m x 40 m) with an area of 800 m^2. Potential areas of stagnation (where flow rates approach zero) exist at the mid point between any two adjacent injection or abstraction wells. Flow through these stagnant areas can be increased by either rotating the pumping grid through 90^0 (so the lines of injection or abstraction wells run from top to bottom) or by adopting the pumping configuration shown in Figure 8.24(b). In this case injection or abstraction wells are operated along diagonal lines. The area of influence of each well is still 800 m^2 but it is delimited by a square with sides 28.3 metres long. The operation of this pumping configuration results in a pattern of leachate domes centred around the injection wells and leachate depressions around the abstraction wells. Potential areas of stagnation exist at the midpoint between any four wells.

Model set-up

MODFLOW and Groundwater Vistas was used to model the area between four of the wells shown in Figure 8.24 for a 30 metre deep landfill. A similar approach to that described in Section 7.4.10 was used. A square model grid was established with a well located at each corner (although only one quarter of each well was modelled - see Figure 8.25).

Figure 8.24 Different pumping configurations from a block centred grid of wells

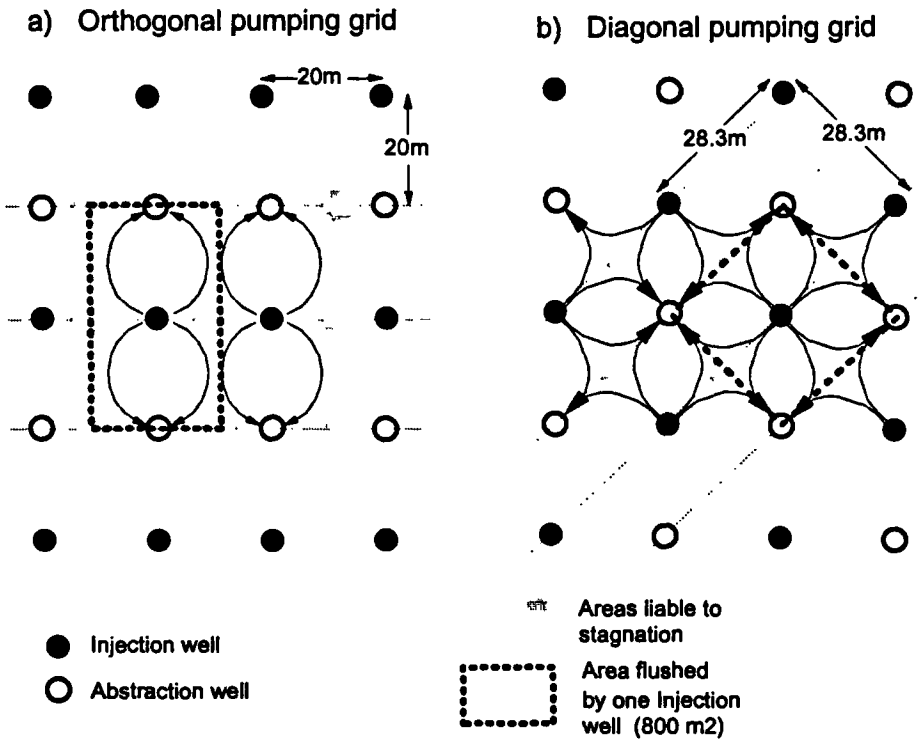

Figure 8.25 MODFLOW grid design to simulate operation of injection and abstraction wells

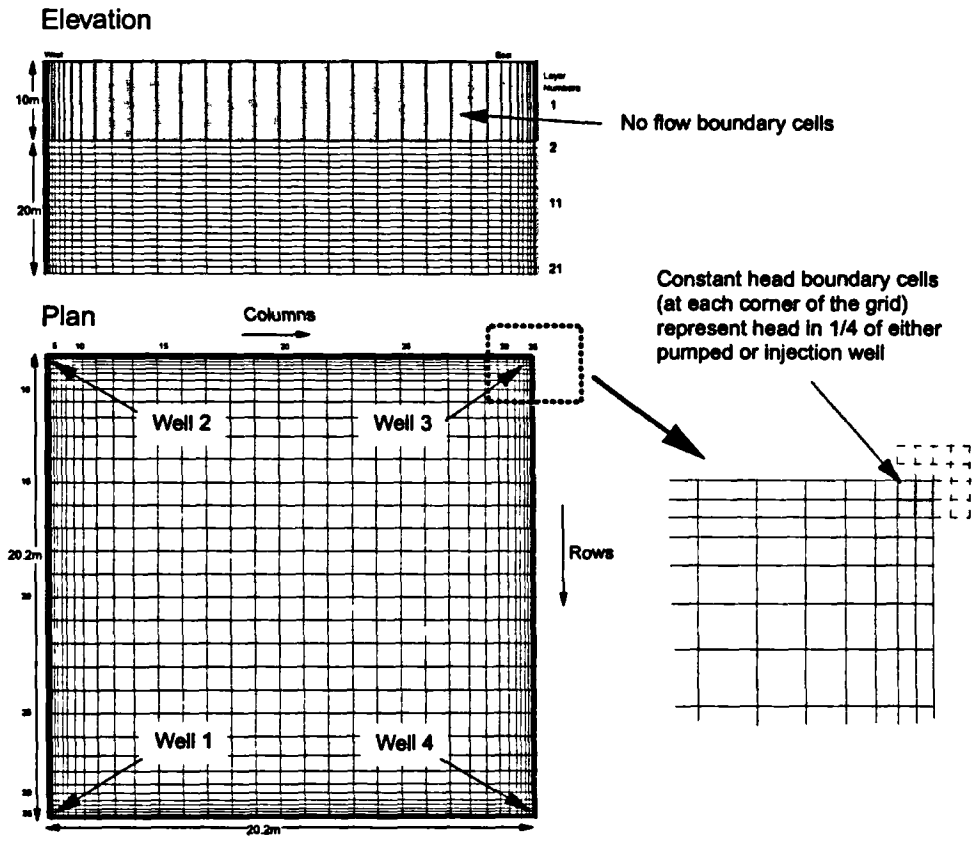

Table 8.15 Design of finite difference model grid for four wells

Row/Column Number	Spacing in cm	Total distance from well (m)	Row/column number	Spacing in cm	Total distance from well (m)
1	5	-0.05	21	100	11.5
2	5	0.0	22	100	12.5
3	6	0.06	23	100	13.5
4	8	0.14	24	100	14.5
5	11	0.25	25	100	15.5
6	13	0.38	26	100	16.5
7	16	0.54	27	80	17.3
8	21	0.75	28	70	18.0
9	30	1.05	29	55	18.55
10	40	1.45	30	40	18.95
11	55	2	31	30	19.25
12	70	2.7	32	21	19.46
13	80	3.5	33	16	19.62
14	100	4.5	34	13	19.75
15	100	5.5	35	11	19.86
16	100	6.5	36	8	19.94
17	100	7.5	37	6	20.0
18	100	8.5	38	5	20.05
19	100	9.5	39	5	20.1
20	100	10.5			
21	100	11.5			

The wells are assumed to have a drilled diameter of 0.25 m, and a total active perimeter of approximately 0.8 m. Each well is represented in the model by four constant head cells with dimensions of 0.05 m x 0.05 m. The size of cells is increased away from each well (see Table 8.15).

As previously noted (Section 7.9), MODFLOW cannot accurately model seepage faces into unconfined wells. Therefore, a confined flow situation through the bottom 20 metres of a landfill was modelled with 21 layers. The top layer was 10 metres thick (representing the confining layer) and the saturated zone was divided into 20 layers, each one metre thick. The injection of leachate under a 30 metre head, and abstraction at a head of 21 metres, was simulated by the appropriate setting of the constant head cells in the wells. The use of these levels maintains confined and saturated conditions in the lower 20 metres of waste.

The model was run with two different relationship between hydraulic conductivity and effective stress.

Firstly, the standard MODFLOW package was used with fixed values of hydraulic conductivity; these were based on the increase in vertical stress with depth in an unsaturated landfill.

The distribution of stress with depth was obtained using the spreadsheet analysis described in Section 7.7.1 with a surcharge of 40 kPa. Values given by Equation 6.2 (the relationship between the density of waste DM3 at field capacity and effective stress) were increased by 10% to take into account the presence of cover material to give:-

$$\rho = 0.495(\sigma_v')^{0.156} \qquad (8.7)$$

Equation 6.12, the worst case fit of the data on Figure 6.16 was taken as the relationship between hydraulic conductivity and effective stress:-

$$K = 17(\sigma_v')^{-3.26} \qquad (8.8)$$

The resulting variation in hydraulic conductivity with depth is shown in Figure 8.26 and was used to enter fixed values of hydraulic conductivity into the 21 layers in MODFLOW.

Secondly, the new SDK MODFLOW package was used to model a situation where hydraulic conductivity is allowed to vary elastically (i.e. reversibly) with effective stress.

Effective stress was calculated from Equation 6.3 (the relationship between the saturated density of waste DM3 and effective stress) with densities being increased by 10% to take into account the presence of cover material to give:-

$$\rho = 0.74(\sigma_v')^{0.0899} \qquad (8.9)$$

This relationship was applied uniformly throughout the model, which was surcharged by a stress of 40 kPa. The data file used for the SDK MODFLOW package is shown in Table 8.16.

Table 8.16 SDK MODFLOW data input file: injection and abstraction wells

```
Input data file for module SDK - Flow to 4 wells in a 30 m deep landfill
     0.7400     VAR1
     0.0899     VAR2
     0.7400     VAR3
     0.0899     VAR4
    17.0000     VAR5
    -3.2600     VAR6
     0.0100     DCFACT
     1.0000     TCFACT
     0.0100     HYCLOSE
     1.0000     DENW
    40.0000     SURFACE SURCHARGE (kPa)
    0           NUMBER OF LAYERS WHERE SDK MODULE DOES NOT APPLY
    0           NUMBER OF CELLS WHERE SDK MODULE TO BE SWITCHED ON/OFF
```

Figure 8.26 **Variation in hydraulic conductivity with depth, based on unsaturated stress distribution**

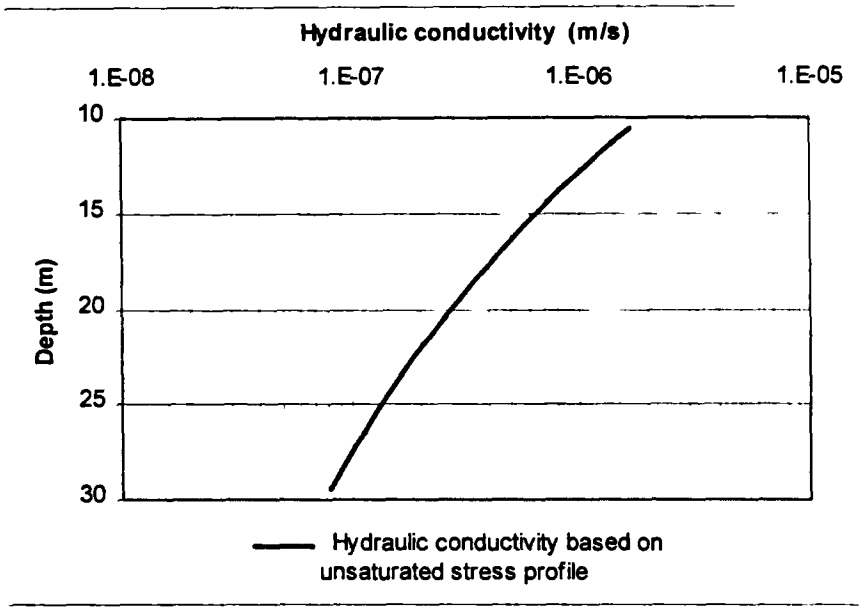

Model runs

The model was initially run to simulate the head distribution and flow rate that would result from the well configuration shown in Figure 8.24a. Leachate was injected into two adjacent wells (Wells 1& 2, Figure 8.25) and abstracted from two others (Wells 3& 4).

The head distribution for (the middle layer of) the model with fixed hydraulic conductivities is shown in Figure 8.27. A symmetrical pattern of contours indicates flow from a general ridge of high heads on the left to a trough on the right. The head at the centre point between all four wells is 25.5 m AD, which is the average of the head at the injection well (30 m AD) and the head at the abstraction well (21 m AD). The main loss in head occurs in close proximity to the wells, such that there is only a 1.5 metre difference in levels between the midpoint of the two injection wells (26.3 m AD) and the midpoint of the two abstraction wells (24.7 m AD).

The head distribution for the model with varying hydraulic conductivities is shown in Figure 8.28. The contours are no longer completely symmetrical. The head at the centre point between all four wells is 28.3 m AD, which is approximately 2.8 metres above the average of the input and output heads. The reason for this is that there is a greater loss in head around the abstraction wells than around the injection wells. Figure 8.29 shows a profile of head in layer 11 (at a depth of 19.5 metres) along column 2 (see Figure 8.25) between injection well 2 and abstraction well 3. The lower heads around the abstraction well, in comparison with the injection well, results in higher effective stresses, lower hydraulic conductivities and hence larger head losses in the vicinity of the well.

Figure 8.27 Head distribution for injection wells and abstraction wells on parallel grid, with hydraulic conductivity based on unsaturated stress distribution

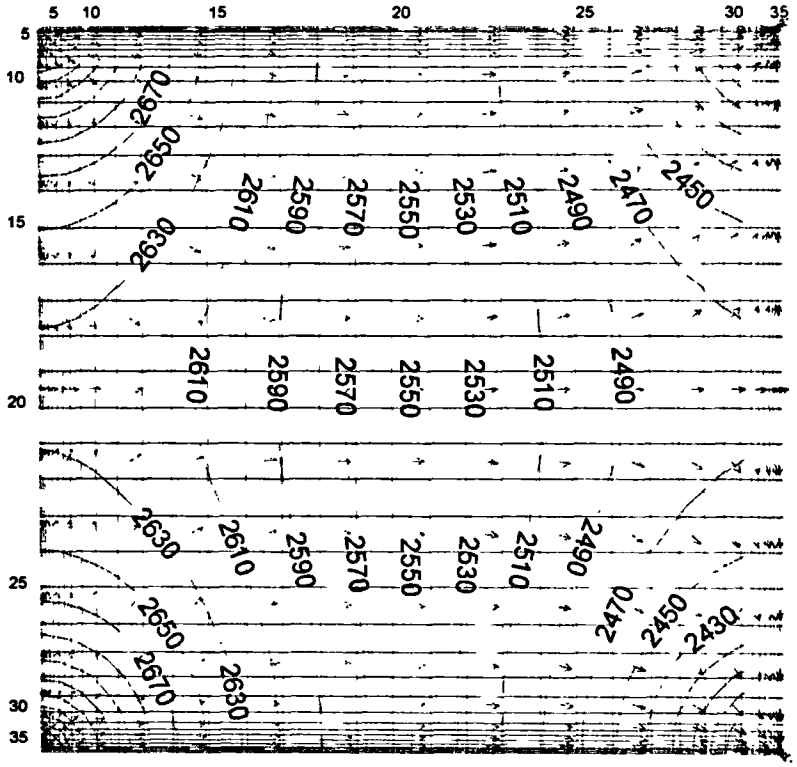

NB: Contours of head in cm above base (cm AD)

Figure 8.28 Head distribution for injection wells and abstraction wells on parallel grid with hydraulic conductivity varying with effective stress

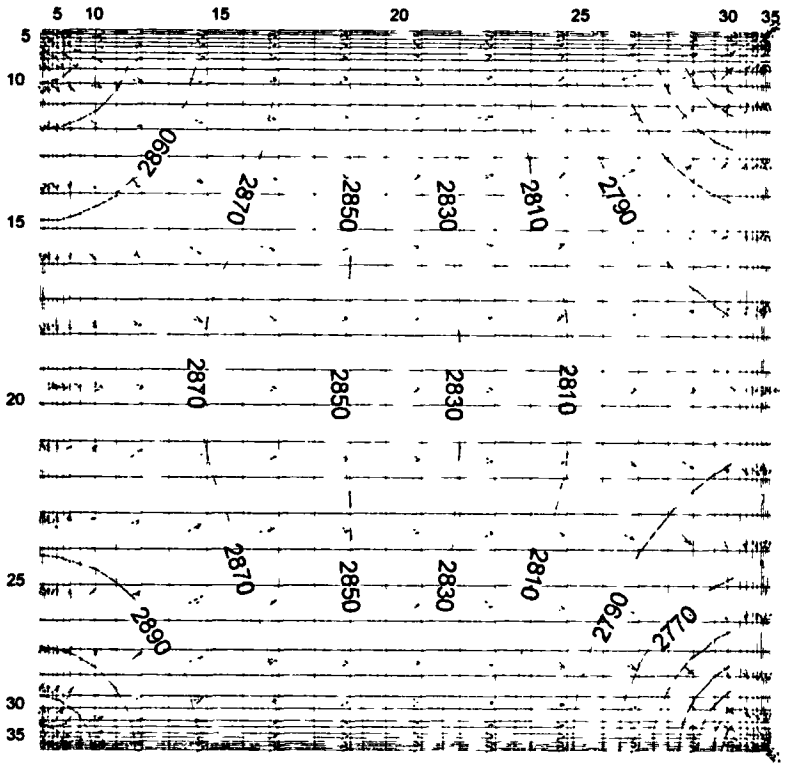

NB: Contours of head in cm above base (cm AD)

Figure 8.29 Head distribution along column 2 between injection and abstraction well

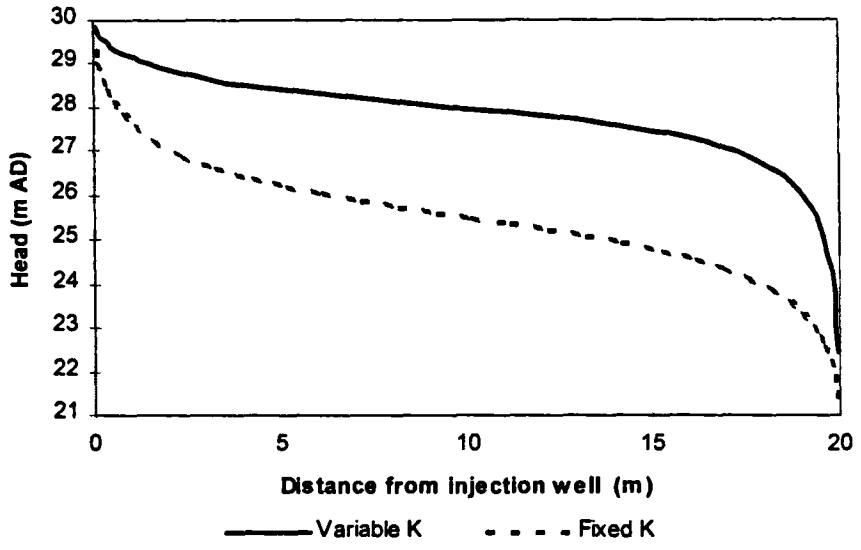

The steady state flow rate of each injection and abstraction well is obtained from the mass balance summary of the model.

The following flow rates were calculated:-

Fixed hydraulic conductivity model: 4.3 m^3/day per well
Variable hydraulic conductivity model : 65.4 m^3/day per well

Not surprisingly, the pumping rate of the wells in the model with the fixed hydraulic conductivities is considerably lower than in the model with the variable (and higher) hydraulic conductivities.

The area of influence of each well is 800 m^2 (see Figure 8.24), and with a saturated depth of 20 metres each well could influence flow through 16,000 m^3 of waste.

Section 8.5.2 indicated that a total of approximately 2.7 m^3 of liquid was required to flush contaminants from a unit volume of waste. This value was calculated from consideration of both continuously mixed reactor and fill and draw models. Although there must be some doubts about the applicability of these models to the flushing of wastes by wells, this volume is nevertheless a useful starting point from which to assess the feasibility of using wells to flush wastes.

Assuming that each well is responsible for flushing 16,000 m^3 of waste, then approximately 43,200 m^3 must be pumped through each well. In average terms it will take:-

10,050 days (27.5 years) at 4.3 m^3/ day to recirculate 43,200 m^3, and
660 days, (1.8 years) at 65.4 m^3/ day to recirculate 43,200 m^3.

Even at the lower flow rate the required volume of leachate could be recirculated within 30 years.

However, as the hydraulic conductivity reduces with depth, the local rate of flow of leachate into or out of a well also reduces. Figure 8.30 shows the variation of flow rate with depth for a well in the fixed hydraulic conductivity model. The flow rate (of 0.8 m^3/day) in the top metre of the well is 20 times higher than the flow rate (of 0.04 m^3/day) in the bottom metre of the well. The average flow rate is 0.215 m^3/day per metre, over 5 times higher than the rate at the base of the well. There are smaller variations in the rate of flow with depth for a well in the variable hydraulic conductivity model (see Figure 8.31), with the flow rate in the top metre of the well being only twice that in the bottom metre of the well.

In addition to the variation of well flow rate with depth, there will be considerable differences in the extent to which wastes get flushed depending on the distance to a well. Waste located near a well will have a large volume of liquid passing through it and waste at the mid point between two wells relatively little.

An indication of the flushing rate through wastes is given by the specific flushing rate (see Table 8.7). The specific flushing rate in close proximity to the wells is very high. For example, the flow rate through the cell (r8,c8, L11) at a radial distance of approximately 1 metre from the well was calculated as 4.5×10^{-8} m^3/sec (for the fixed hydraulic conductivity model, with an average pumping rate of 4.3 m^3/day). The volume of the cell was 4.41×10^{-2} m^3 (0.21 m x 0.21 m x 1 m), giving a specific flushing rate of 1.02×10^{-6} sec^{-1}. The time to flush the equivalent of 2.7 m^3 per unit volume of waste through this cell is therefore:-

$= 2.7/1.02 \times 10^{-6}$
$= 2.65 \times 10^{6}$ seconds $=$ 30.6 days

Waste near to the injection well will similarly have been flushed with relatively clean water (or treated leachate) and in this time would almost certainly have reached a stable non-polluting state. However, despite the high specific flushing rate in close proximity

to the abstraction wells, wastes will have been flushed by predominantly undiluted leachate and would take considerably longer to reach the completion criteria.

Figure 8.30 **Variation of flow rate with depth into pumped / injection well: hydraulic conductivity based on unsaturated stress distribution**

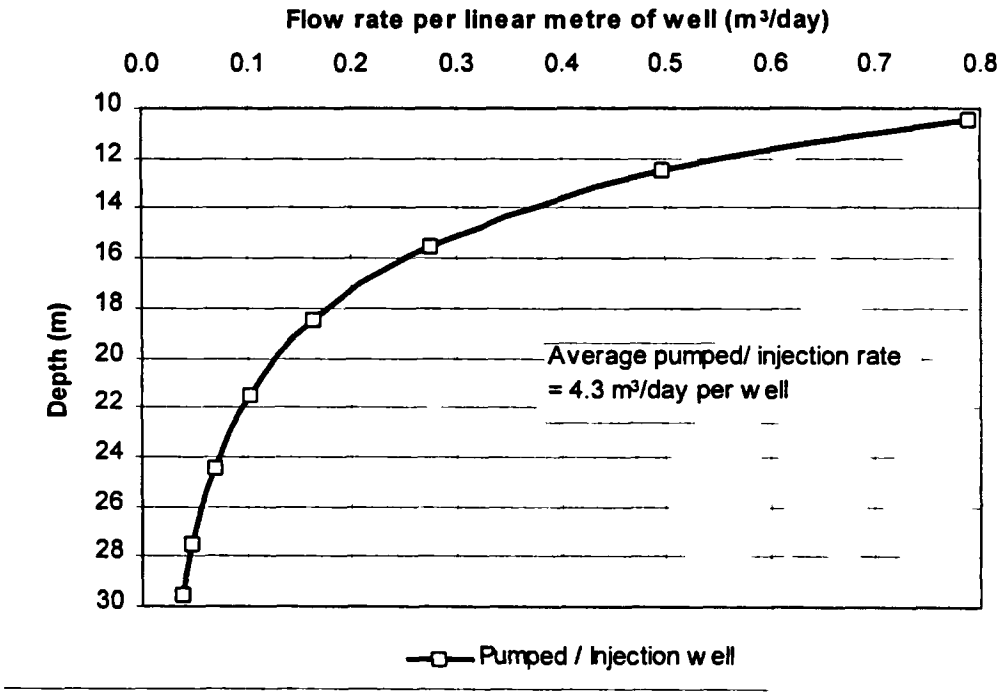

Figure 8.31 **Variation of flow rate with depth into pumped/ injection well: hydraulic conductivity varies with effective stress**

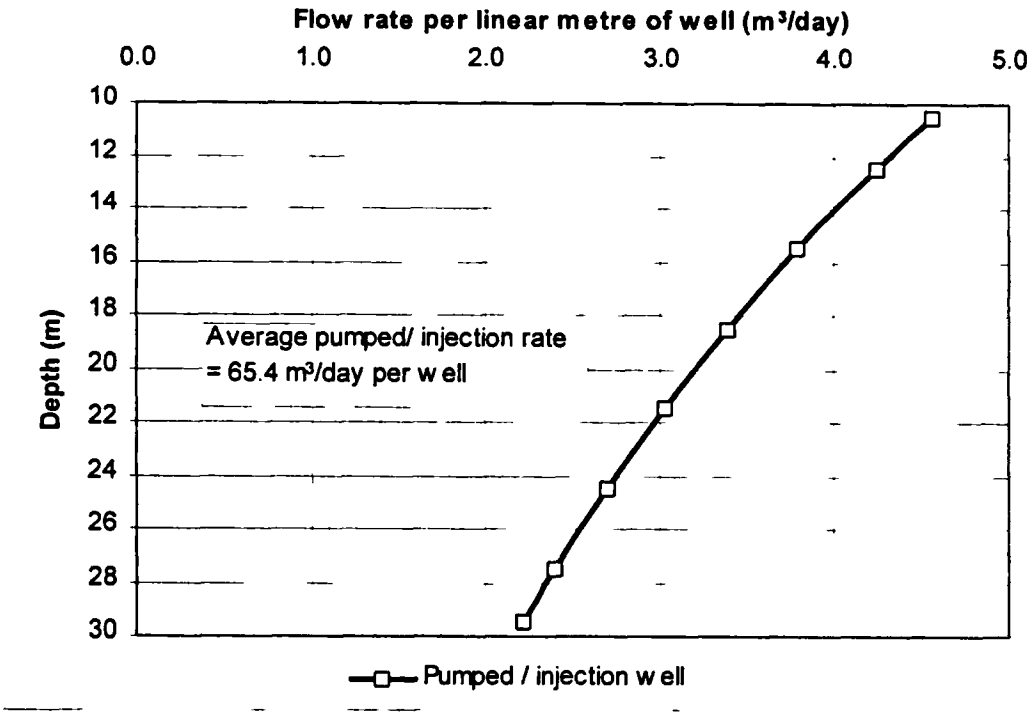

Figure 8.24 indicated the potential regions between wells where stagnant conditions could develop. To provide an indication of the flushing rate in these regions and at other locations between the wells, the specific flushing rate at three positions has been calculated (see Table 8.17).

Table 8.17 Location of model cells where specific flushing rate is calculated

Location of element	Dimensions	Volume of element (per layer)	Comment
r20, c20	1 m x 1 m	1 m^3	Central point between four wells
r1-6, c20	0.48 m x 1 m	0.48 m^3	Mid point between injection and abstraction well
r20, c1-6	1 m x 0.48 m	0.48 m^3	Mid point between injection wells

Figure 8.32 shows the variation in specific flushing rate with depth for the fixed hydraulic conductivity model. The minimum required specific flushing rate of 2.85×10^{-9} sec^{-1} to achieve flushing in 30 years (Table 8.7) is also shown.

At all locations there is a reduction in specific flushing rate with increasing depth in the landfill. This is consistent with the reduction in hydraulic conductivity with depth and the reduction in flow rate shown in Figure 8.30. This trend is repeated in the model with the variable hydraulic conductivity, as shown in Figure 8.33.

The specific flushing rate (in Figure 8.32) at the mid point of the four wells (r20, c20) and at the midpoint between an injection and abstraction well (r1-6, c20) are broadly similar, and well above the required value of 2.85×10^{-9} sec^{-1}. However, the specific flushing rate at the midpoint between the two injection wells (r20, c1-6), indicated as an area prone to stagnation on Figure 8.24, varies from 3.46×10^{-8} sec^{-1} at the top of the saturated zone to 1.68×10^{-9} sec^{-1} at the bottom.

To flush this area of relatively low flow the lines of injection and abstraction wells could be rotated through 90°. The specific flushing rate of the waste which had the lowest rate of $1.68 \times 10^{-9} sec^{-1}$ could thereby be increased by almost an order of magnitude to a rate of $1.29 \times 10^{-8} sec^{-1}$.

An alternative way to increase the rate of flow through the low specific flushing rate areas would be to switch to a diagonal pumping configuration, as shown in Figure 8.24(b).

Figure 8.32 **Variation of specific flushing rate with depth at various localities in fixed hydraulic conductivity model**

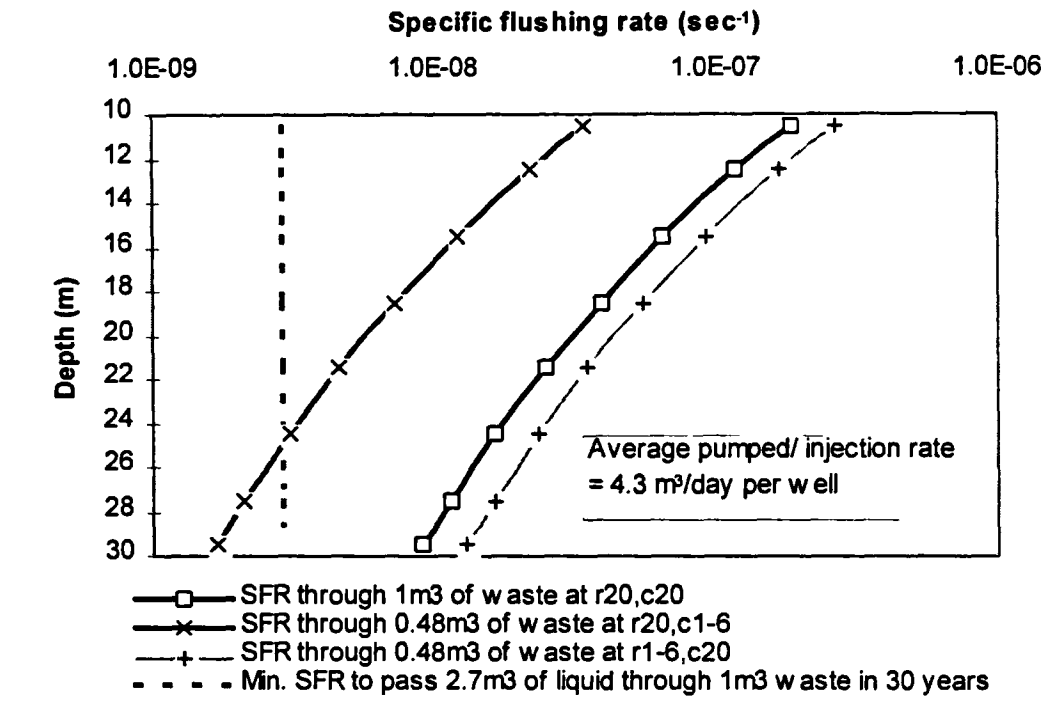

Figure 8.33 **Variation of specific flushing rate with depth at various localities in variable hydraulic conductivity model**

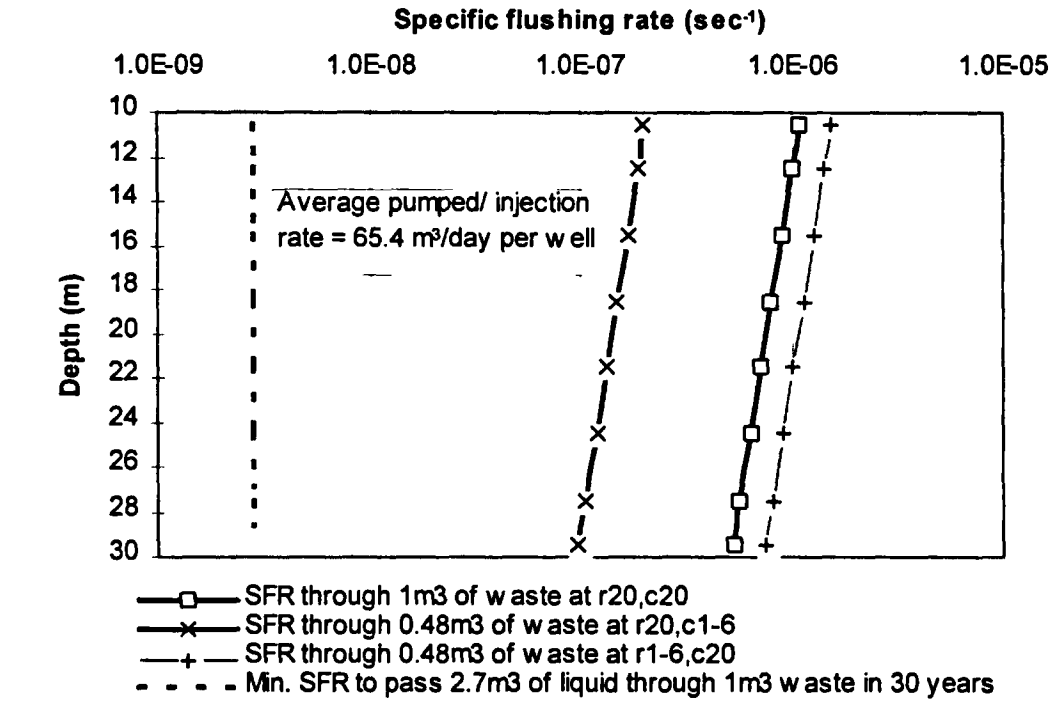

The head distribution with a diagonal pumping configuration in the model with fixed hydraulic conductivities is shown in Figure 8.34. Again (as was the case for the parallel lines of wells) the head at the centre point between the wells is 25.5 m AD. The point represents a no, or low, flow zone between the two cones of leachate depression centred around the abstraction wells and the two domes of elevated leachate head around the injection wells. The midpoint between each well along the model boundaries now lies on a direct flow path between each well.

Figure 8.35 shows the head distribution from the model run with the variable hydraulic conductivities. The head at the centre point between the wells is 28.4 m AD, which is the same as that produced by the variable hydraulic conductivity model for the lines of injection and abstraction wells. There is again a greater head loss in the vicinity of the abstraction wells compared with the injection wells and this leads to a diagonal symmetry in the contour pattern.

The steady state flow rate for each injection and abstraction well were calculated as follows:-

Fixed hydraulic conductivity model:	4.7 m^3/day per well
Variable hydraulic conductivity model:	70.2 m^3/day per well

These values are slightly higher than the modelled flow rates for the lines of abstraction and injection wells.

Figures 8.36 and 8.37 show the variation in well flow rate with depth from the fixed and variable hydraulic conductivity models respectively. The profiles are very similar to Figures 8.30 and 8.31.

Figures 8.38 and 8.39 show the specific flushing rate at various cells or locations in the model. The main feature of these figures is the exceedingly low specific flushing rate calculated at cell r20,c20 at the centre of each model. However, because the flow rates are so low there are significant errors in the flow rate mass balance for the cell, and the resulting pattern may be an artefact of these errors. Consequently, the specific flushing rate through a larger volume of waste at the centre of the model is considered. The specific flushing rate through 9 m^3 (per 1 metre layer) of waste from cells r19-21,c19-21 is also shown on Figures 8.38 and 8.39. For the case of the fixed hydraulic conductivity model, the specific flushing rate varies from 1.2×10^{-8} sec^{-1} at the top of the model to 5.6×10^{-10} sec^{-1} at the bottom of the model, a variation that reflects the different well flow rates with depth.

Figure 8.34 **Head distribution for diagonally oriented abstraction and injection wells: hydraulic conductivity based on unsaturated stress distribution**

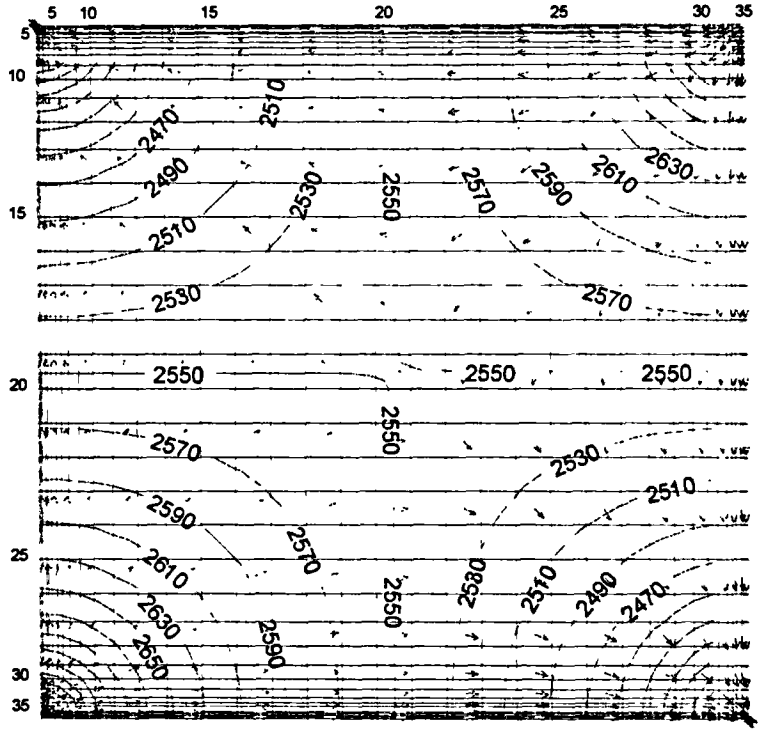

NB: Contours of head in cm above base (cm AD)

Figure 8.35 **Head distribution for diagonally oriented abstraction and injection wells: hydraulic conductivity varies with effective stress**

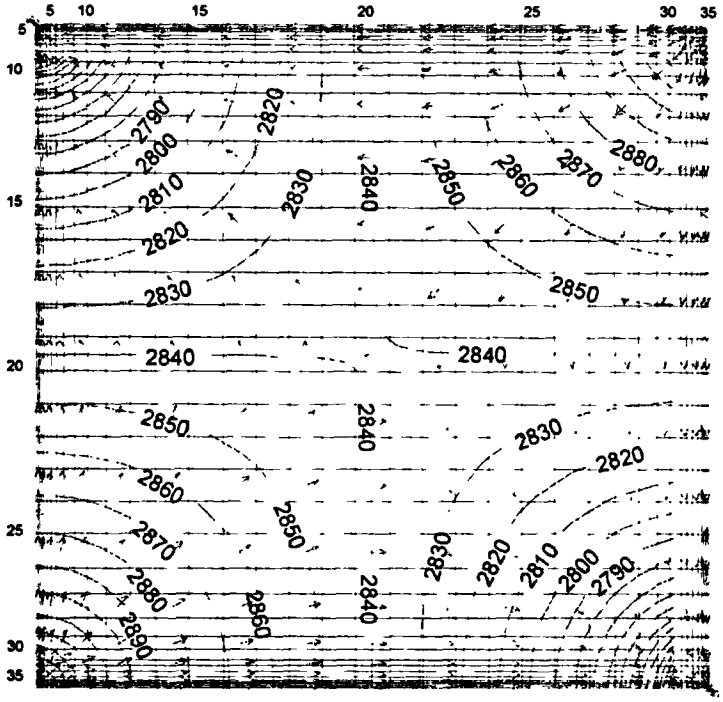

NB: Contours of head in cm above base (cm AD)

Figure 8.36 **Variation of flow rate with depth for diagonally oriented abstraction and injection wells: hydraulic conductivity based on unsaturated stress distribution**

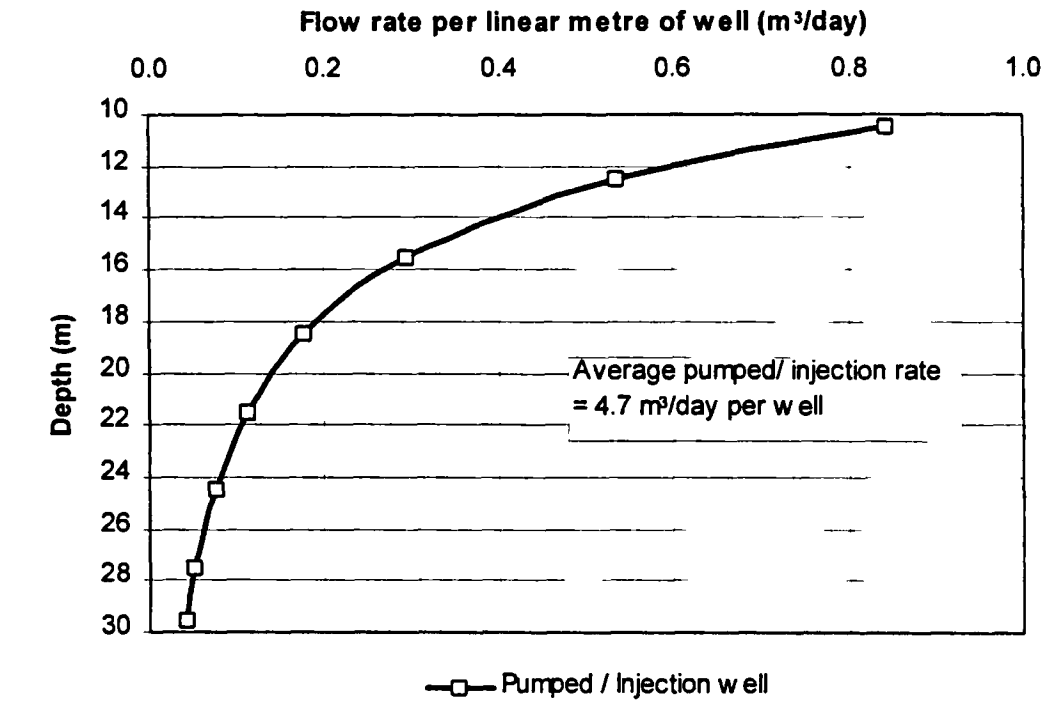

Figure 8.37 **Variation of flow rate with depth for diagonally oriented abstraction and injection wells: hydraulic conductivity varies with effective stress**

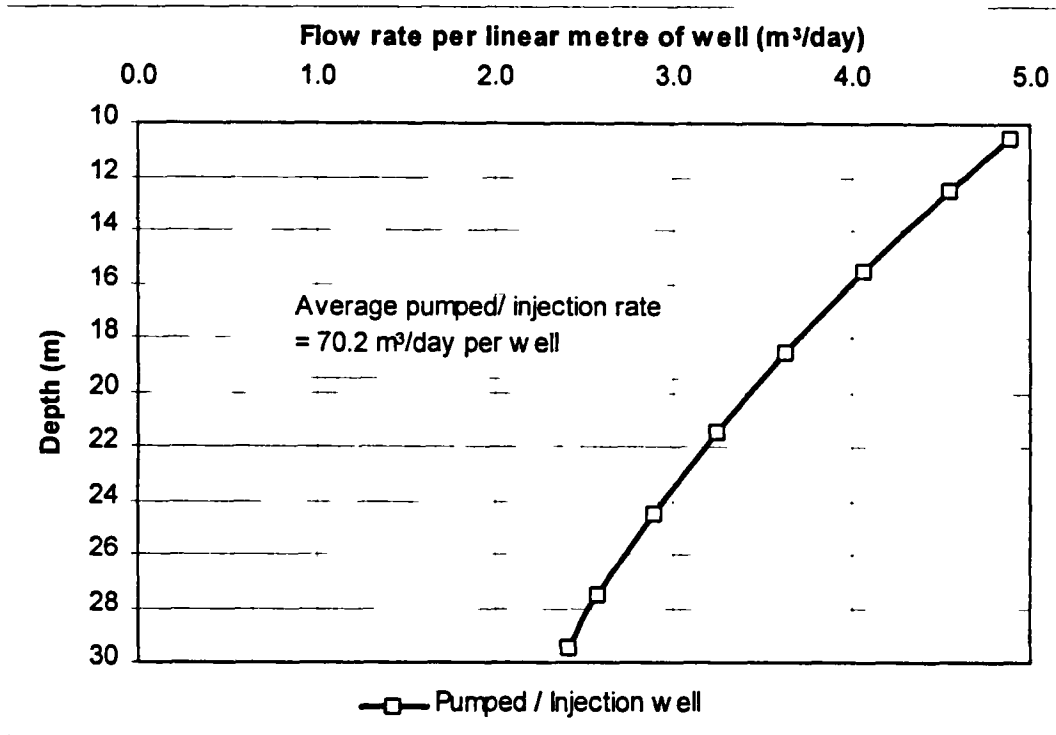

Figure 8.38 **Variation in specific flushing rate with depth for diagonally oriented abstraction and injection wells: hydraulic conductivity based on unsaturated stress distribution**

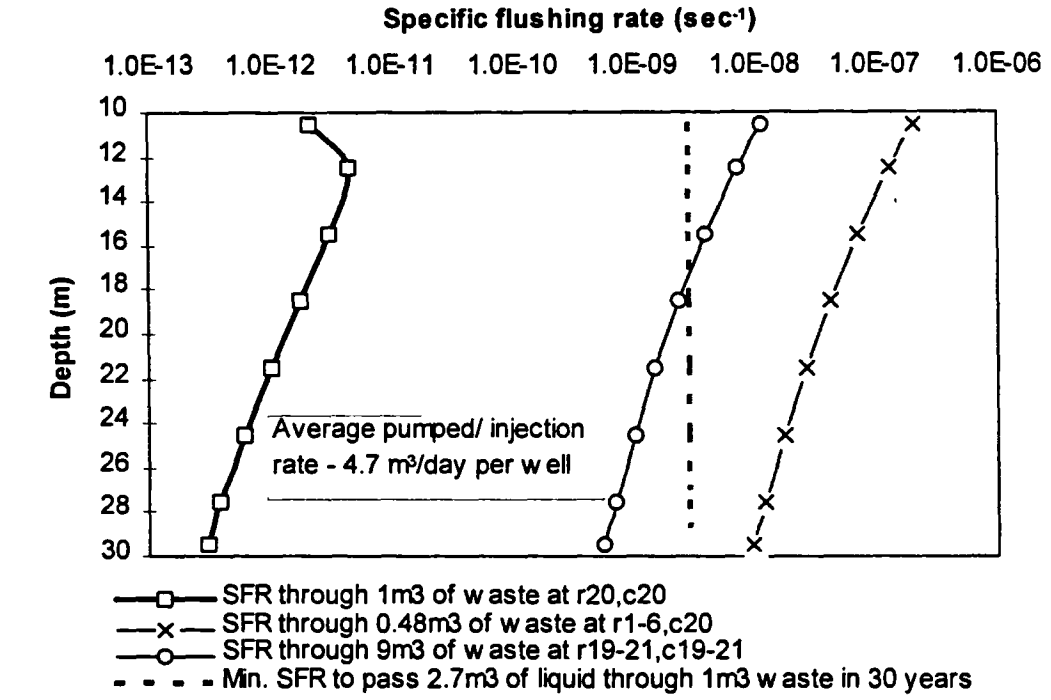

Figure 8.39 **Variation in specific flushing rate with depth for diagonally oriented abstraction and injection wells: hydraulic conductivity varies with effective stress**

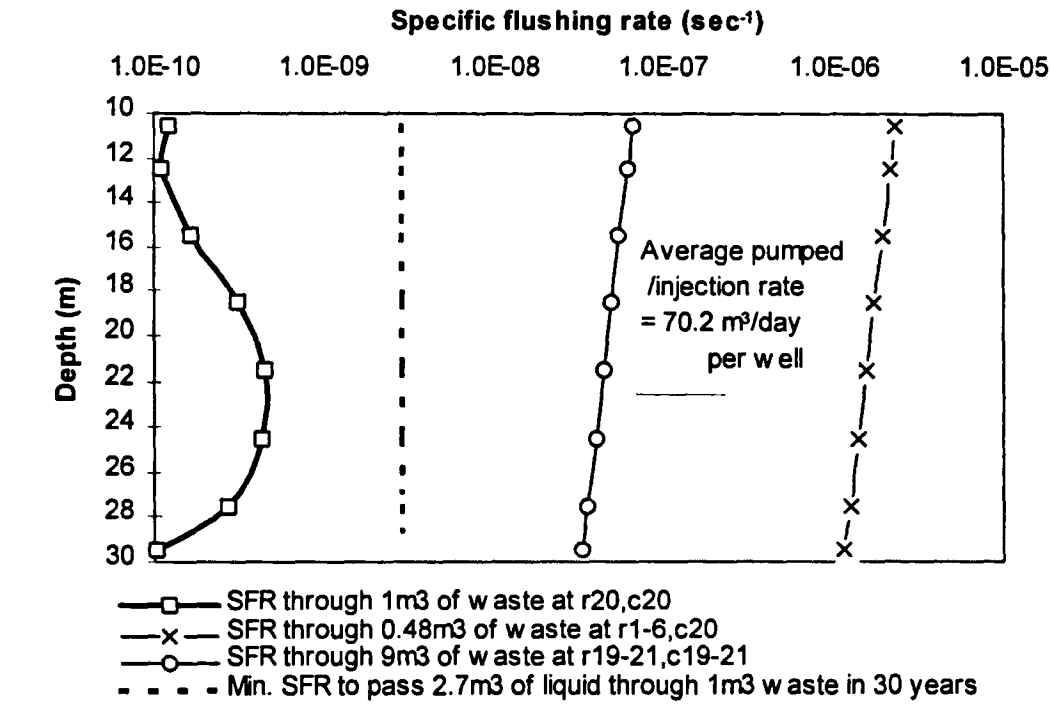

The specific flushing rate at the mid point between any two adjacent wells (e.g. at r1-6,c20) varies from $2x10^{-7}$ sec^{-1} at the top of the model to $9.8x10^{-9}$ sec^{-1} at the bottom. When the wells are operated along parallel lines (as in Figure 8.24a) the specific flushing rate between an injection and abstraction well is slightly lower, varying from $2.7x10^{-7}$ sec^{-1} at the top of the model to $1.3x10^{-8}$ sec^{-1} at the bottom (Figure 8.32).

Impact of horizontal layers of low or high permeability material on flushing

At the beginning of this section, it was recognised that the impact of low permeability layers on vertical flushing rates could be largely overcome by the predominantly horizontal flow associated with a well field system. A strictly horizontal low permeability layer would concentrate flow through the waste lying directly below and above the layer and would accentuate the flushing of this waste. This has not been considered any further. However, the corollary to this potential benefit is that horizontal layers of high permeability (perhaps a buried hard-core road) may attract flow, thereby reducing the flushing of adjacent wastes.

This premise was tested by modifying the fixed hydraulic conductivity model comprising two lines of injection and abstraction wells (Figure 8.24a). A 5 m x 5 m area in the middle of layer 12 (r18-22,c18-22) at an average depth of 20.5 m was assigned a hydraulic conductivity of $1.5x10^{-5}$ m/s, approximately 100 times higher than that of the waste in the layer. The flow rate of each well was calculated as 4.36 m^3/day, little changed from the rate of 4.3 m^3/day for the model without the high permeability layer. Figure 8.40 shows the variation of specific flushing rate with depth at the centre point of the model (r20,c20). It can be seen that the effect of the high permeability layer is to draw flow away from waste located within 3-4 metres above and below the layer.

Figure 8.40 Variation of specific flushing rate with depth in a landfill with an area of high permeability at a depth of 20.5 metres

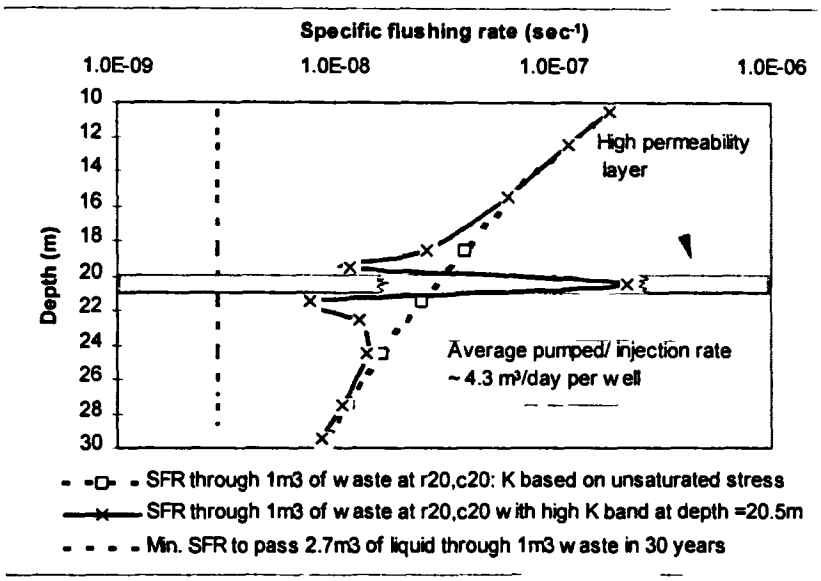

Summary of findings relating to wells.

1. The analyses have been undertaken assuming confined conditions in a landfill. The actual operation of wells in an unconfined state should result in higher rates of flow and flushing than those indicated. The effects of gas generation on flow are unknown.

2. The rates of flushing are highly dependent on the relationship between hydraulic conductivity and effective stress. Very large flushing rates are achieved if hydraulic conductivity varies reversibly with effective stress. However, the required flushing rates can still be achieved with wells at realistic spacing and large saturated depths, even if the hydraulic conductivity is based on the unsaturated stress distribution (i.e. no increase in K when σ_v' is reduced). This has been tested by modelling a 30 m deep landfill with a minimum hydraulic conductivity (at the base) of slightly less than $1x10^{-7}$ m/s. However, it is probable that wells could successfully be used in slightly deeper sites as well.

3. The optimum configuration of a flushing system based on wells is an orthogonal grid with alternate lines of wells being operated as either injection or abstraction wells. The orientation of these lines would need to be rotated through 90^0 at various times to flush areas of low flow.

4. The main problem that has been identified is the potential for rates of flushing to vary with depth. The flushing of wastes (at the required rate) at the base of a 30 metre deep landfill with fully penetrating wells will result in the waste near the top of the site being flushed at a rate approximately 20 times higher. This is an inefficient mode of operation. There are two obvious solutions to this problem. Firstly, multiple wells could be installed at a given location with each well being screened at different depths in the landfill. It would then be possible to regulate the rate of flushing at different depths. Secondly, pre-compaction could be used in an attempt to create a waste with a uniform density and hydraulic conductivity with depth. This is investigated further in Section 8.5.13.

8.5.13 Impact of waste pre-compaction on flushing

The potential impact of waste pre-compaction at the tipping face was not considered in the preceding sections. Flushing rates were calculated for a) conditions where the hydraulic conductivity varied reversibly with effective stress and b) a fixed hydraulic conductivity profile based on the possible historical maximum effective stress.

The maximum hydraulic conductivity of a waste will probably reflect the density of waste compaction at the tipping face. This density can be equated to an effective stress (e.g. see Figure 6.7) and it can be assumed that there will be no further increase in density, or reduction in hydraulic conductivity, until that effective stress is exceeded.

Table 8.18 shows the relationship between dry, saturated and compacted density of waste DM3, for densities at the tipping face between 0.5 and 1.2 t/m^3. Figure 8.41 shows the relationship between dry density and hydraulic conductivity. A best fit line has been drawn through the data and has been used to indicate the hydraulic conductivity at different bulk densities for a range of probable water contents. A minimum water content (WC_{dry}) of 40% has been assumed, with the maximum water content being taken as the water content at field capacity, which reduces with increasing dry density (Figure 6.13). For, example a waste compacted to a bulk density of 1 t/m^3 could have a hydraulic conductivity in the range of $9x10^{-5}$ to $1x10^{-7}$ m/s. If it is assumed that waste DM3 (at its original water content, WC_{dry}, of 51.5%) were compacted at the tipping face to a density of 1 t/m^3, this would represent a dry density of 0.66 t/m^3 (Table 8.18). Figure 6.7 indicates that this dry density represents an effective stress of 340 kPa. Based on the worst case fit of hydraulic conductivity to effective stress (Equation 6.12) this represents a hydraulic conductivity of $9.5x10^{-8}$ m/s (this is an alternative approach to using the data from Figure 8.41, which is based on the best fit of the data). Assuming the original (as tipped) water content of the waste did not change, then the depth at which the stress of 340 kPa would be exceeded is 34.6 metres. Below this depth there would be further increases in waste density and a reduction in hydraulic conductivity. However, from the surface of the landfill to this depth, it could be assumed that the density and hydraulic conductivity will remain relatively constant.

This is potentially useful in operating vertical wells to flush waste. The MODFLOW model of four wells (2 lines) was rerun with a fixed hydraulic conductivity of $9.5x10^{-8}$ m/s in all layers to represent waste compacted to a wet density of 1 t/m^3. The average flow rate to or from each well was calculated as 0.9 m^3/day compared with 4.3 m^3/day for the model with hydraulic conductivity increasing from $8.44x10^{-6}$ to $8.03x10^{-8}$ m/s. This flow rate was distributed evenly over the full 20 metre depth of the well. The specific flushing rate in all layers at the centre point of the model (r20c20) was $1.07x10^{-8}$ sec^{-1}, which is above the minimum required rate of $2.85 x10^{-9}$ sec^{-1}.

Table 8.18 Relationship between tipping densities and saturated densities for DM3

Compacted density* at tipping face t/m³	Dry density t/m³	Density at FC t/m³	Saturated density t/m³
0.50	0.330	0.720	0.879
0.60	0.396	0.808	0.939
0.70	0.462	0.890	0.993
0.75	0.495	0.930	1.018
0.80	0.528	0.968	1.042
0.85	0.561	1.006	1.066
0.90	0.594	1.043	1.088
0.95	0.627	1.079	1.109
1.00	0.660	1.115	1.130
1.05	0.693	1.150	1.150
1.10	0.726	1.18#	1.18#
1.15	0.759	1.20#	1.20#
1.20	0.792	1.23#	1.23#

Calculations based on Equations 6.1 to 6.3

* Based on original water content WC_{dry} = 51.5%

\# Value is average of density at field capacity and saturated density, as the density at field capacity is calculated to be slightly higher than the saturated density (see Figure 6.7).

Figure 8.41 Relationship between density of waste DM3 and hydraulic conductivity

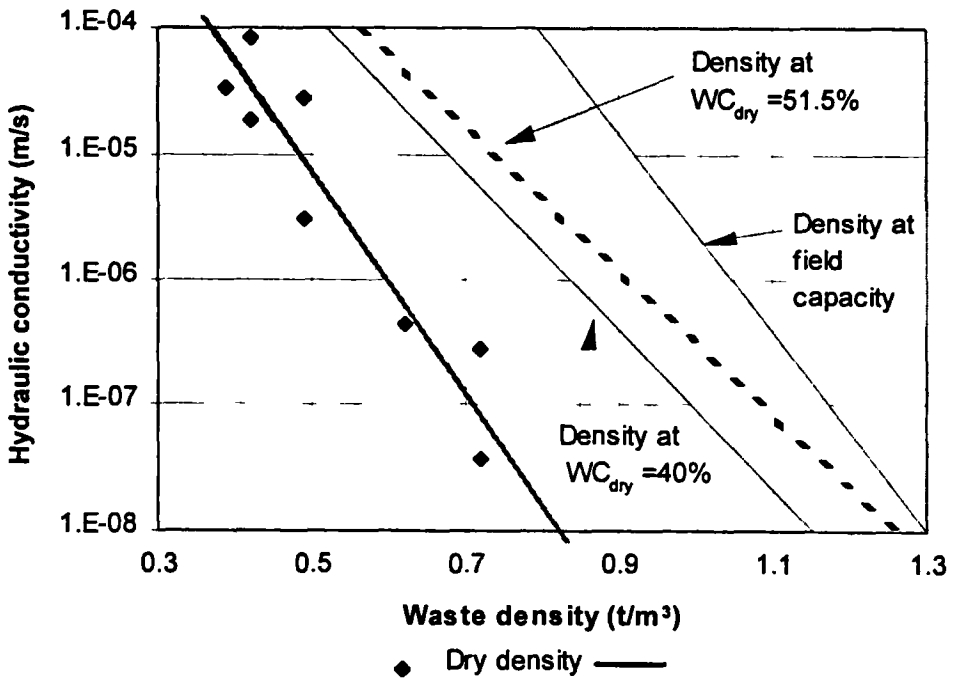

Powrie and Beaven (1999) investigated the effect of waste pre-compaction on maximum downward vertical infiltration rates through various depth of landfills. Their analysis (reproduced as Figure 8.42) was based on the data pertaining to waste DM3 reported in this thesis. Taking the best fit relationship between hydraulic conductivity and vertical effective stress (Figure 8.42a) it can be seen that it is only for highly compacted wastes (above 1.1 t/m^3) that the minimum flushing rate will not be achieved in landfills between 0 and 30 metres deep. For sites between 30 and 60 metres deep a pre-compaction wet density of less than 1.0 t/m^3 is required. For the worst case relation between hydraulic conductivity and stress, lower pre-compaction densities are required, with a maximum density of 0.9 t/m^3 for sites over 30 metres deep.

Figure 8.42 **Infiltration rate for a) $K=2.1(\sigma')^{-2.71}$ and b) $K=17(\sigma')^{-3.26}$ against landfill depth for various pre-compacted waste densities**

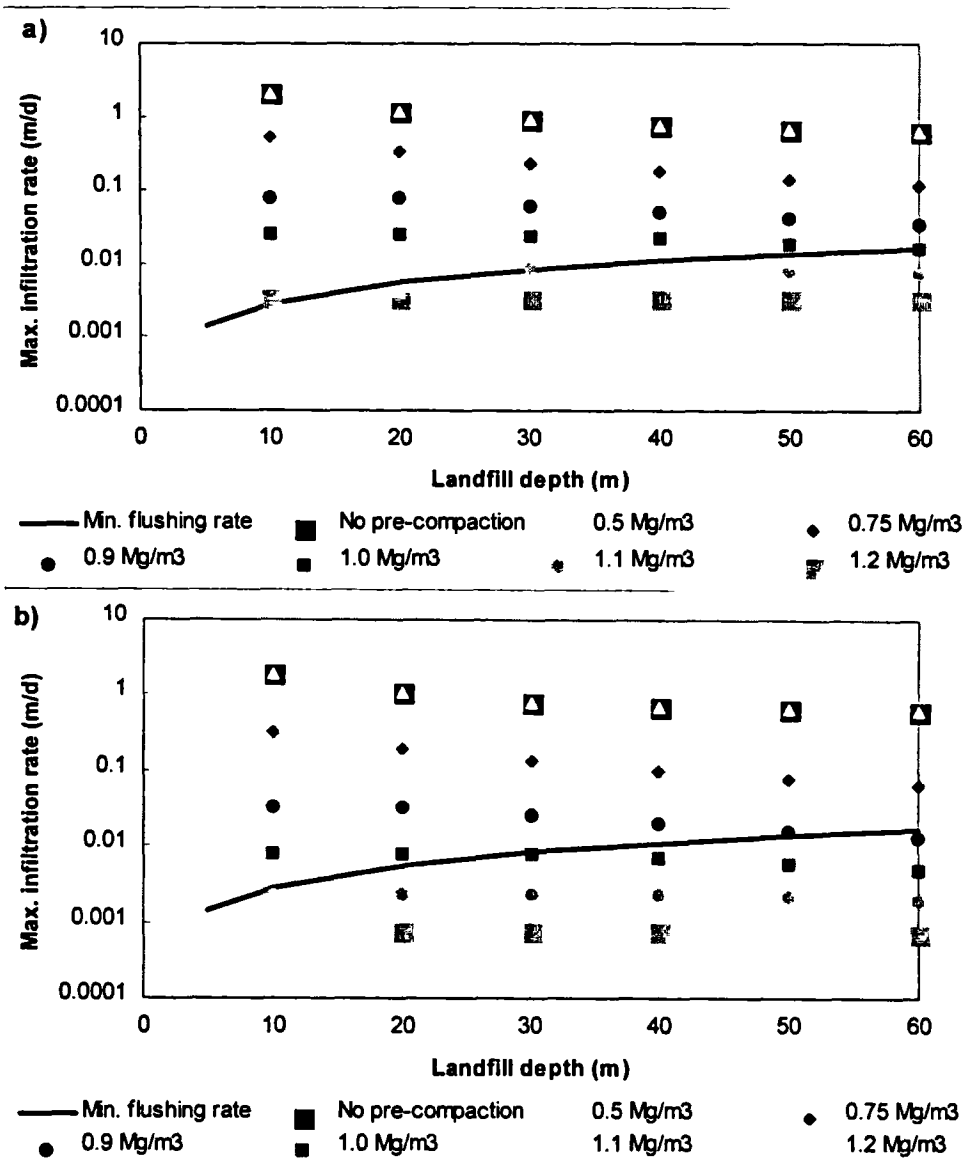

All waste densities at a water content (WC_{dry}) of 51.5% (assumed WC of waste as deposited)

Source: Powrie and Beaven, 1999

In Section 2.4.2 and 8.3.2 the relationship between the density of household waste and compactive effort, including type of plant, was discussed. Large compactors, such as the Cat[R] 836, used to their full potential can achieve waste densities up to 1.2 t/m^3, which according to Figure 8.42 would restrict the ability to flush wastes in virtually any landfill setting. The use of compactors equivalent to the Cat[R] 826, which can achieve waste densities between 0.8 and 1 t/m^3, may be the largest type of machine that should be used to prevent over compaction of wastes at the tipping face. However, before definitive conclusions can be made on this subject further research is required to link the waste density achieved by different machines to the hydrogeological properties of those wastes.

8.5.14 Impact of waste type on flushing

Discussion so far have been based on the results relating to crude household waste DM3. This section considers the results for the other wastes investigated in the large scale compression cell.

Figure 6.19 plotted hydraulic conductivity against effective stress for all waste types tested. In general terms it can be seen that, at a given stress, the difference between the hydraulic conductivity of the various wastes falls within the margin of experimental error. It has been shown that in terms of flushing waste, one of the key variables is the extent to which hydraulic conductivity varies reversibly with effective stress. This factor alone has a much larger bearing on flushing rates than the small variations in hydraulic conductivity between the various waste types. Furthermore, the majority of the flushing analyses were based on the worst case fit of hydraulic conductivity to effective stress for waste DM3. This relationship gives slightly lower hydraulic conductivities at a given stress than the best fit line through the data for all waste types. Consequently, it is reasonable to apply the results of the previous analyses to other waste types if required.

However, it is possible that the differences in the relationship between density and effective stress for the various waste types have more of a bearing on the flushing models. For example, the density at field capacity of waste DM3 at a stress of 100 kPa is approximately 0.92 t/m^3; that of waste PV2 is 0.74 t/m^3; and that of waste AG1 is 1.25 t/m^3. Therefore, the increase in unsaturated vertical stress with depth will be very different depending on the landfilled waste.

Of perhaps even greater significance is whether the average unit weight of saturated waste is greater or less than that of water. If it is less than water, then there will be a reduction in effective stress with increasing depth within the saturated zone and there may be potential problems associated with negative effective stresses and fluidisation.

This potential problem would apply in particular to the processed waste PV2, as the saturated density is below 1 t/m^3 at stresses up to at least 600 kPa.

However, it is noted that during the processing of this waste the heavy oversized and undersized components of the waste were removed. The density of waste PV2 cannot therefore be likened to that of a shredded waste where there has been no separation out of materials. However, it may have relevance if future recycling and waste management processes result in a waste of this type (probably not very likely, as the material left behind is more likely to have recycling value than the material taken out). It is probable that if waste DM3 had been shredded the relationship between density and effective stress would have been similar to that of waste DM3 in its crude state. In addition, waste AG1 contained a large proportion of soil material; the compositional analysis (Table 5.17) indicated that almost 34% (by weight) of the sample was classified as fines, i.e. that passing through a 10 mm screen. This is a large proportion and may not be very representative of the amount of soil material in many landfills. The previous flushing analyses, based on DM3, included a 10% allowance for cover material. Therefore the results of these analyses would not be altered too much, even if they were based on the density to stress relationship of waste AG1.

8.6 Technical constraints and possible solutions to the operation of a high rate flushing sustainable landfill

The preceding sections have included many examples that suggest the flushing of household wastes within landfills is feasible within a sustainable time-span. A number of potential problems and limiting factors were identified and these are discussed further below.

8.6.1 Saturation of wastes

There are considerable benefits to the operation of a high rate flushing (bio)reactor through saturated, rather than unsaturated wastes (Section 8.5.8). However, this will result in leachate heads within the body of the landfill. Although the leachate recirculation system can be operated to prevent pore water pressures or heads developing in the basal drainage blanket, active pumping would be required and could not be relied on as the only means of control. Furthermore, if it was considered important to preserve relatively high hydraulic conductivities at the base of the site the basal drain should not be dewatered. Consequently, the landfill would have to be engineered to contain high leachate heads.

At present many sites are engineered with a single composite liner system comprising a low permeability barrier overlain by a leachate collection system. This by itself in most situations would not be a sufficient safeguard against high heads.

During the 1980s double liner systems, comprising two flexible membrane liners (FMLs) each overlain by a drainage layer, were engineered into landfills in mainland Europe and the US (e.g. Schevon and Damas, 1986). In general the practice was stopped when it was recognised that the drainage layer between the two FMLs tended to spread any leachate leaking from the upper FML over a wide area. As a result composite liners, where an FML is directly underlain by a low permeability layer (e.g. Giroud *et al*, 1989a), become an Industry standard for lining (e.g. DoE, 1995a).

A lining system incorporating a drainage layer between two composite liners is one solution to the problem of high leachate heads in landfills (e.g. Rowe, 1995). A possible design is shown in Figure 8.43. The hydraulic break, effected by the drainage layer between the composite liners, prevents high leachate heads on the upper liner being transmitted to the lower. Consequently, the heads on the lower liner should be no higher than those exerted on the liners in existing landfills. Because of the large leachate heads on the upper liner, there is perhaps an even greater need for an excellent quality of engineering with closely controlled QA/ QC systems. A geophysical leak detection

system could be incorporated into the engineering specification (e.g. White *et al*, 1995) to prevent leaks remaining undetected at the time of construction.

Figure 8.43 Design of a double composite liner to mitigate the effects of high leachate heads

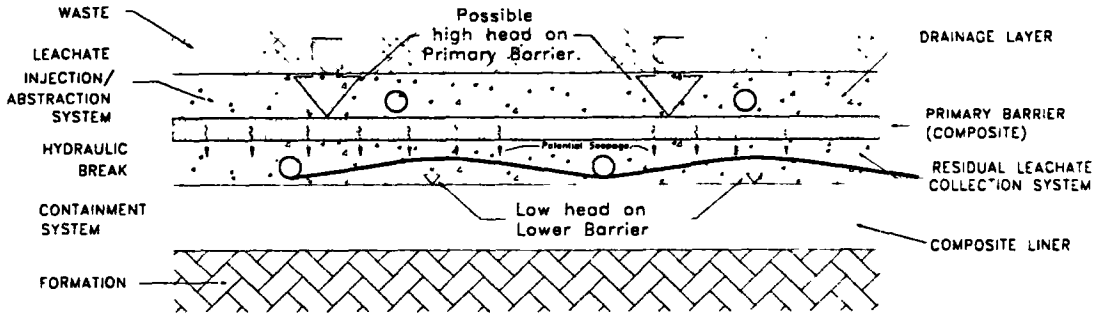

Hall (1997) considered the design of leachate drainage layers in landfills with high rates of infiltration (associated with a flushing bioreactor). The impact on the environment from potential leakage through a double composite liner with these high infiltration rates was compared with that occurring in existing designs. It was shown that the potential contaminant loading over the polluting life of a site was considerably lower in the flushing bioreactor landfill. In addition, it was possible to be more confident about the predictions for the flushing bioreactor as the performance of the liners had to be gauged over a period of decades rather than centuries.

It is recognised that problems of slope stability and leachate containment might militate against the maintenance of saturated conditions at sites where the waste rises above the level of the surrounding ground. Flushing of these wastes may have to be undertaken with a separate recirculation system based on vertical unsaturated flow (Section 8.5.10).

8.6.2 Maximum depth of landfill and density of waste

Landfill depth need not be a limiting factor in flushing bio(reactor) designs. The key to the successful flushing of wastes is the maintenance of sufficiently high hydraulic conductivities (preferably above 1×10^{-7} m/s) by preventing effective stresses becoming too great. The hydraulic conductivity at the base of an unsaturated site over approximately 20 metres deep will be too low. However, low effective stresses (below approximately 200 kPa) and high hydraulic conductivities can be maintained in deep landfills if large saturated zones are established, with the thickness of the unsaturated zone being kept to less than approximately 15-20 metres.

Operationally, this could be achieved whilst landfilling was in progress by introducing liquid into the basal drainage blanket and flooding the landfill from the bottom.

Pre-compacting the waste at the tipping face can lead to waste densities that will preclude rapid flushing. It is potentially very difficult to specify a maximum waste density as it would be highly dependent on both waste composition and water content at the time of landfilling. However, to allow sustainable flushing the maximum density of waste DM3 must not be (for the worse case hydraulic conductivity/ stress relationship) less than 0.9 t/m^3 for sites up to 30 m deep or less than 1 t/m^3 for sites from 30 m to 60 m deep. There is not enough good quality data linking machine type and mode of operation with waste composition and the density at which the waste is placed. Consequently it is difficult to make definitive statements about the type of machines that should be used at the tipping face to achieve a particular target density. There is evidence, however, that the largest models of waste compactors used to their full potential will compact waste to a density that precludes flushing at the rates required. It appears that medium sized compactors (e.g. Cat 826) achieve waste densities that are more appropriate to those required for flushing.

8.6.3 Pre-treatment of wastes

The shredding of wastes prior to landfilling has two main benefits. Firstly, it will reduce the average particle size in the waste and increase the surface area exposed to microbiological breakdown, thereby accelerating rates of degradation. Secondly, the more homogeneous waste mass would help to create relatively uniform hydrogeological characteristics. This would aid the even distribution of circulating liquids so that all parts of the waste would be flushed.

Any differences between the hydrogeological properties of shredded and crude wastes are relatively minor, and consequently the use of shredded waste should not significantly affect the ability to flush it.

8.6.4 Low permeability barriers and preferential flow routes

The presence of material in the landfill that creates either barriers to flow or preferential flow routes will adversely affect the uniform distribution of flow. Wherever possible, these materials should be excluded from the landfill, or placed in a separate area. For example, the use of low permeability daily cover that creates horizontal barriers to flow should be prohibited. Alternative covers could be used, such as biodegradable foams or hessian sheets. Similarly, any operational practice that resulted in the development of preferential flow routes would have to be changed. For example, the more permeable material used in site roads would need to be removed. Where it is found that there are

impediments to vertical flushing of waste, horizontal flushing could be undertaken using wells.

8.6.5 Source of flushing fluid

A problem that is often raised with the concept of a high rate flushing bioreactor is the volume of water required to flush the wastes (e.g. Reeds, 1997). It is held that it is difficult to justify this use of water within the context of other water demands, water shortages and increased water conservation measures.

Any landfill over approximately 5 metres deep will require a supply of water additional to that which could come from incident rainfall (in a 30 year period). On the basis that it may take 2.7 m^3 of water to flush a unit volume of waste, a landfill with an airspace of 1 million m^3 would require approximately 2.7 million m^3 (2,700 Ml) of water. Over a period of 30 years this means that the annual requirement for water would be approximately 90,000 m^3, or 247 m^3 per day.

It is useful to consider this volume of water in the context of the total water supply in England and Wales. The estimated per capita production of household waste is 0.35 tonnes per year (Royal Commission on Environmental Pollution). If it is assumed that this waste is landfilled at an average wet density of 1 t/m^3, then the amount of water required to flush an individual's annual production of waste is approximately 0.95 m^3. The average per capita consumption of water in England and Wales is 154 litres per day (WSA, 1996), or 56.2 m^3 per year. This means that an individual would require an additional 6 days' supply of water to provide for the flushing of their waste. This represents an increase of just 1%. It is equivalent to the amount of water used to fill approximately 12 baths or the amount used by a garden sprinkler in just one hour.

An alternative way of estimating the amount of water required is to look at the total volume of waste requiring flushing in comparison with the total volume of supply. Although household waste represents a relatively small proportion of wastes going to landfill, it does represent a much higher proportion of the wastes that need flushing. Overall, approximately 137 million tonnes of controlled wastes are landfilled (DoE, 1992). It can be assumed that perhaps between 75 and 100 million tonnes of this waste is bioreactive and/or requires flushing. The total amount of water required to flush 100 million tonnes of waste is approximately 270 million m^3 (270,000 Ml). The estimated total daily volume of water abstracted for public water supply in England and Wales in 1994 was 16,735 Ml (WSA, 1996). This indicates that the annual volume of water supplied was approximately 6,100 million m^3. The volume of water required to flush the total quantity of bioreactive waste is 4.4% of existing supply.

Thus, between 1% and 4.4% additional water would be required to flush waste assuming that none of it could be re-used. It is shown below that, of the possible 2.7 m^3 of water required to flush a unit volume (or approximately 1 tonne) of waste, only a fraction needs to be from new sources of water. Furthermore, there is no suggestion that high quality potable water supplies need be, or even should be, used to flush wastes. If water is to be used it could be from lower quality sources such as untreated surface or groundwater or even sewage effluent. An effluent from a sewage treatment plant was added to the wastes at Landfill 2000 and, although not used for flushing, proved to be beneficial in accelerating the degradation (Blakey *et al*, 1997). However, even if the full volume of water had to be supplied from new sources it is argued that this is both justifiable and, within the context of the volumes of water used to treat sewage, an excellent use of the resource.

A very approximate comparison can be made between the annual carbon pollution load in sewage and in solid wastes disposed to landfill. A measure of the pollution load of sewage is the population equivalent, which is defined as a daily biochemical oxygen demand (BOD) of 60g (e.g. DoE, 1997). The national population equivalent, including the input from industry, is 81.9 million. As 1 gramme of organic carbon generates a biochemical oxygen demand of approximately 1.1 grammes, the total organic carbon load in sewage is approximately 1.64 million tonnes per annum. If a maximum of 15% by weight of the 75-100 million tonnes of biodegradable waste disposed to landfill (see above) is in the form of degradable carbon (e.g. Beaven and Walker, 1995), then the annual carbon pollution load going to landfill is between approximately 11 to 15 million tonnes. If this pollution load was reduced in a landfill operated as a high rate flushing bioreactor, then it would largely be converted into CH_4 and CO_2 in landfill gas. However, Beaven and Walker (1995) showed in laboratory columns that approximately 5% of the carbon load of MSW was not released into gas and required flushing from the waste. Consequently, the annual carbon pollution load going to landfill that may require flushing from a high rate flushing bioreactor is estimated at between 0.5 and 0.75 million tonnes, approximately half the load treated in sewage. A similar comparison between the annual nitrogen pollution load in sewage and in solid wastes disposed to landfill has not been undertaken because of a lack of data on the load in sewage, but would probably indicate that the load to landfill was slightly larger. It can, therefore, be concluded that the total pollution load in sewage is broadly similar in size to the part of the load in landfills that may require flushing and treatment.

In terms of the volumes of water required to treat these respective loads, virtually all the public water supply (i.e. that returned to the sewers) is used in the treatment of the load

held in sewage. Therefore, existing sewage treatment is based on processes that use between 20 and 100 times as much water as that being proposed for landfills (see above).

Although approximately 2.7 m^3 of water is required per unit volume of waste, a considerable proportion of this can be recycled treated leachate. Leachate treatment plants are in operation which can both nitrify and then denitrify (e.g. Robinson et al 1997). This treated leachate could then be reintroduced into the landfill to flush further nitrogen from the site. Alternatively, Knox & Gronow (1995) demonstrated in a pilot scale study that denitrification of a nitrified leachate could be supported by the residual carbon content of young waste within a landfill, without inhibiting methanogenesis. This process would avoid the need for an external source of carbon required in conventional denitrification plants. The reintroduction of leachate into the site is likely to be beneficial in terms of maintaining levels of trace nutrients and reintroducing methanogens, both of which may encourage further degradation.

The only unequivocal requirement for new water is that needed to saturate the waste initially. This is nearer to a maximum of 0.2 m^3 per unit volume, i.e. only 7% of the actual flushing volume required. The limiting factor on the extent to which treated leachate could be used to flush contaminants from the site is likely to relate to the build up of inorganic ions in the recirculating leachate. Too high a concentration of ions may adversely affect the microbiology of the landfill, the ability to treat the leachate and the ability to discharge the treated leachate to the surrounding environment. The actual volumes of new water required will therefore be between 0.2 and 2.7 m^3 per unit volume. Furthermore, any water supplied in excess of approximately 0.2 m^3 will be returned to the water cycle as treated leachate.

8.6.6 Design and operation of leachate collection and distribution system

The technical constraints on the design and operation of leachate collection and distribution systems are related to the following operational requirements. The system needs to:-

1) flush wastes at the required rates (including a margin of safety);

2) ensure an even distribution of flushing water, so that all wastes are flushed;

3) cope with large and potentially differential waste settlements;

4) allow the rate of leachate flow to be controlled and provide operational flexibility;

5) regulate, where possible, the quality of leachate being produced; and

6) minimise the effects of clogging.

The benefit of operating flushing through a saturated zone, and the requirement for unsaturated flushing in parts of the site above surrounding ground levels, means that there will have to be more than one recirculation system in operation.

For unsaturated flushing, water could be introduced at the top of the site by a variety of means. The method chosen will very much depend on topography, whether there are any adverse environmental impacts from the operation, and what other use or activity is going on at the surface of the site. The infiltrating water could be collected in a drainage layer serviced by a network of perforated pipes within the body of the landfill. This layer could also form part of the saturated flow recirculating system for waste underlying it. It could either act as an injection layer, with leachate being extracted from a layer at the base of the site, or if upward flow were adopted it could be used to extract leachate.

Both the upper and basal drainage system should be based on a number of discrete 'drainage' zones which can be isolated and operated independently of each other. This would help prevent short circuiting of leachate around the drainage system and allow control over the flushing mechanism so that hydraulic gradients could be set up in virtually any direction. This would require more pumping chambers or more complicated pipework systems than would normally be implemented at a landfill, but would provide considerably more control over the flushing process. It would also allow a small part of the site to be flushed initially, with other parts being brought into service later on. This would help solve the problem of unequal loading on the treatment plant and allow leachate from established cells to be used to encourage methanogenesis in more recently placed refuse.

Finally, any leachate drainage or injection system located within the body of the waste is likely to suffer badly from differential settlement. By separating the system into discrete zones with multiple injection/abstraction points the long term integrity of the overall system is more likely to be preserved. Risks of clogging could be minimised by using aggregates with a large grain size, 20-40 mm or above (e.g. Powrie *et al,* 1997; Rowe *et al* 1997).

8.6.7 Regulation of leachate quality to accelerate refuse degradation

A potential problem with establishing saturated conditions shortly after waste deposition is the risk of generating high strength acid leachate which then inhibits methanogenesis. Possible ways of preventing this from occurring might include:-

1) seeding of the landfill with methanogenic waste (e.g. Cossu, 1995) and/or with wastes with buffering capacity;
2) introducing methanogenic leachate from another source (e.g. an adjacent cell); and
3) introducing liquid into the landfill via the basal collection system to create upward flow within the landfill. This would push a front of methanogenic leachate from older wastes upwards into the younger more acidogenic zones.

8.6.8 Accelerated waste degradation and effect of gas production on flushing

It may also be necessary to investigate the effects of the depth of the saturated zone on gas release once methanogenic conditions have become established. For instance, it is unclear whether the activity of methanogens is pressure limited, or to what extent methanogens are affected by high partial pressures of CO_2 and CH_4 in the leachate. Further research is also required to investigate the effect of gas production on leachate flow. It is probable that gas liberated from the waste may occupy the large pores in the waste thereby blocking the main leachate flow routes. During the period when rapid waste degradation and gas production is in progress leachate recirculation may not be feasible. Solutions may be required to allow the release and removal of gas from the saturated zone, possibly involving the de-gassing of super saturated leachate. Otherwise, leachate recirculation may be delayed until rates of gas production have reduced.

8.6.9 Restoration, settlement and planning issues

Sites operated on the high rate flushing bioreactor principle will be more intensively active (after the initial landfilling phase has been completed) but for a shorter period of time than conventional landfills. Accelerated rates of settlement, together with an overriding requirement to operate and maintain systems to flush the waste, mean that full restoration (for example to a high quality agricultural after-use), cannot be achieved until near the end of the stabilisation period. Full restoration should not be completed until the majority of degradation, settlement and flushing has taken place and:-

1 the desired final landform has been created by re-filling areas of the site where there has been excessive or uneven settlement, with stabilised wastes (e.g. from an adjacent cell or site); and
2 there is confidence that any further settlement will be small enough not to damage the final restoration and will not alter the final landform in any significant way.

In conventional landfill sites the same amount of settlement is likely to occur as in the high rate flushing bioreactor landfill but over a much longer period of time. The consequent problems are therefore prolonged (into a timescale measured in centuries), with ongoing maintenance and the possible need to refill low areas of the site, requiring removal and replacement of the restoration. The high rate flushing bioreactor landfill shortens the period over which settlement problems occur and over which active maintenance is required. The land is therefore returned to a permanent and beneficial after-use and the full amount of potential airspace is realised in a shortened timescale.

8.6.10 Site location

Sites operated on the high rate flushing bioreactor principle will be active processing units requiring access to significant volumes of processing liquid and ultimately the ability to dispose of large volumes of treated leachates. Therefore, sites should be located in areas where there is an adequate supply of (possibly low grade) water and a receiving environment which can accept and dilute the residual inorganic ion concentrations of the treated leachate. In addition, the operation of the high rate flushing bioreactor landfill with a large saturated zone means that there would be large volumes of potentially polluting liquid (leachate) in storage, circulation or in treatment. The transfer of a significant proportion of the solid waste's polluting potential into leachate creates a greater hazard to the hydrological environment. Although high quality engineering of the basal liner could minimise the risk of pollution, it would still perhaps be unwise to place such landfills on sensitive environmental locations, such as upon unconfined aquifers. Non-sensitive locations, such as on low permeability strata near to large rivers or coastal waters would be ideal for high rate flushing bioreactor landfills.

8.6.11 Summary of overall design concept

A proposed design for a high rate flushing bioreactor landfill, which addresses many of the issues outlined above, is shown in Figure 8.44. In summary, it is proposed that the landfill is engineered as a containment site with a high quality composite liner. Different types of waste are mixed and then homogenised to create a uniform waste mass to accelerate degradation and encourage the even distribution of circulated liquids. Landfilled wastes are rapidly saturated to provide control over the bulk hydraulic conductivity of the landfill leading to more efficient flushing. Leachate collection, injection and recirculation systems are incorporated which will allow water or treated leachate to be introduced and distributed at infiltration rates equivalent to between 3 and 10 metres/annum. A total of approximately 2.7 m^3 of leachate will be flushed from the landfill per unit volume over a time-span of 30 - 50 years.

Figure 8.44 Proposed high rate flushing bioreactor design

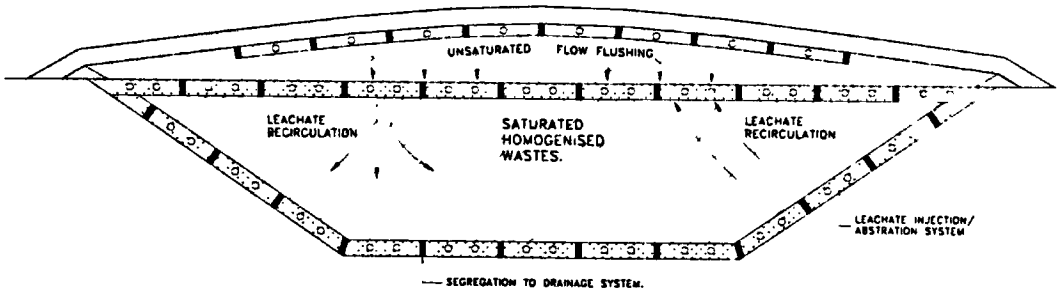

Chapter 9

Summary, conclusions and recommendations

There is a widely accepted view that sustainable development is *"development that meets the needs of the present without compromising the ability of future generations to meet their own needs"* (World Commission on Environment and Development, 1987). Given the polluting potential of waste it is important that disposal techniques are developed which take into consideration the impact that today's waste can have in the future.

Victorian concerns over public health lead to both modern day waste disposal practices and sewage treatment systems. Whilst the latter have developed progressively higher standards of treatment of effluent before its return to the environment, landfilling has progressed towards zero (or inadequate) treatment and full containment of wastes. Methods for handling and disposal of sewage are therefore considered to meet the requirements of sustainable development better than those used in the landfilling of solid wastes.

A sustainable landfill is defined as one that is in equilibrium with its surrounding environment within 30-50 years of the cessation of landfilling activities, such that no future maintenance or monitoring of the waste is required. To achieve a stable non-polluting state it has been demonstrated (elsewhere) that degradation rates must be accelerated and that soluble degradation products must be flushed from the waste. As one of the key methods for accelerating degradation rates is the addition and recirculation of water through a landfill, the hydrogeological properties of the waste have a large bearing on whether both objectives can be met within a sustainable

timescale. The geotechnical properties of waste influence its hydrogeology and must also, therefore, be taken into account.

This thesis has reported the findings of an investigation into the hydrogeological and geotechnical properties of waste using a large-scale, purpose built compression cell. A number of conclusions can be drawn in relation to the research methodology, the results and their application to the flushing of wastes within landfills. The findings make a significant contribution to the existing knowledge-base in relation to research techniques, the geotechnical and hydrogeological properties of waste, leachate control systems, the modelling of fluid flow in landfills and the flushing of wastes. The findings also add to the ongoing debate about the use of high rate flushing bioreactors as a means to achieving sustainable landfilling.

The findings reported here have important implications for the waste management industry and, in particular, for the development of sustainable landfilling. A number of recommendations are derived from the work.

9.1 Research methodology

9.1.1 The compression cell

Previous research into the hydrogeological properties of waste have either been undertaken using field scale leachate pumping tests or in relatively small-scale laboratory experiments. In the former it has not been possible to relate the results to the physical characteristics and heterogeneities of the waste; in the latter it has not been possible to test representative samples of waste. The research reported in this thesis goes some way towards bridging this gap by using a purpose-built compression cell able to accommodate large samples of waste in controlled conditions. The main design criteria for the test cell were that it should be large enough to accommodate the heterogeneous nature of the materials to be tested without the need for particle size reduction and it should be capable of simulating loads on the material being tested equivalent to a minimum 50 metre depth of landfill.

The size and dimensions of the compression cell were dictated by the physical characteristics of the household waste to be tested. The diameter of the testing cylinder, at 2 metres, was at least 10 times the average particle size of household waste. The height of the cylinder was 3 metres. Other research suggests that to overcome the effects of sidewall friction the height of the cell should be 1/4 of its diameter, or 0.5 metres in this case. However, this would not have been large enough to allow vertical hydraulic

conductivity to be measured, for which a height of at least 1 m of waste is required: prior to compression this equates to approximately 2 metres. To increase the diameter of the cell to the corresponding 8 metres was neither financially or practically viable. Consequently, innovative techniques had to be developed to compensate for the effects of sidewall friction. Although these techniques led to results within acceptable levels of error, it would have been preferable not to have had to use them. It is concluded, however, that to satisfy the above technical requirements a waste testing cylinder would need to be so large that the costs, both economically and practically, would not be justified by the benefits to be gained. It is possible, though, that a cylinder 3 metres in diameter and 2 metres high would have reduced the need for corrections and would not have cost significantly more.

9.1.2 Testing methods

There were some aspects of the equipment design that worked particularly well during the testing program, and a number of features that caused problems.

The use of a hydraulic system with pressure relief valves provided an easy and reliable way to apply a constant load over long periods of time. Having determined the initial mass of dry solids in the compression cell, calculation of the dry density from the position of the upper platen was straightforward.

The methodologies adopted for measuring the hydrogeological properties of the waste produced reliable results at relatively low applied stresses and waste densities, where the hydraulic conductivity was generally above 1×10^{-7} m/s. The insertion of piezometers into the waste at various heights provided considerable detail about vertical variations in properties within the cell.

The loading of waste into the compression cell was a difficult and time consuming process. Between 2.5 and 6.5 tonnes of waste were loaded into the compression cell for each test. This was accomplished by tilting the testing cylinder to 30° to the horizontal and using a hydraulically operated grab to load the waste into the cell. The waste tended to bank up against the lower edge of the cylinder and had to be raked level on a number of occasions. It was potentially difficult to achieve an even distribution and packing of waste. In retrospect, it would have been preferable if the design of the compression cell had allowed waste to be loaded whilst the cylinder was oriented vertically.

The use of load cells to weigh the compression cell in its entirety, and thereby to provide an indication of changes in water contents, did not provide the level of accuracy initially anticipated. Short term fluctuations in readings were partially related to temperature

changes, but the reason for a longer term drift in readings was not established and meant the data were not as reliable as had been hoped. These problems were not satisfactorily resolved within the timescale of the research and it is recommended that further attempts are made to implement a system that provides a better level of accuracy.

Earth pressure cells were installed within the waste to indicate the transmission of stress but interpretation of data from these cells proved problematical. A theoretical consideration did not lead to usable cell action (correction) factors. Direct calibration (in the laboratory) of a cell installed in a layer of gravel was more successful. The reduction in stress within the cell was finally calculated by means of an analytical solution, using the internal angle of friction of the waste and the angle of sidewall friction between the waste and the inside of the compression cylinder. The method was based on Jaky's relationship between vertical and horizontal effective stress ($\sigma_h' = (1-\sin\phi')\sigma_v'$), which is generally applied to geotechnical materials. There is a need for further research to establish whether this relationship requires modification for waste materials.

Attempts to measure differential compression at different levels within the waste using strings inserted through the piezometer ports were unsuccessful because of difficulties in anchoring and measuring the strings. The accurate measurement of differential compression is important because it could provide another means of analysing the effects of side-wall friction on the results obtained. Consequently, it is recommended that for future testing using the compression cell alternative ways of measuring differential compression are developed.

It is an established fact that any preferential peripheral flow will effect hydraulic conductivity results. A review of the literature on hydraulic conductivity testing using fixed wall test cells suggested that peripheral flow is unlikely to be a problem when relatively deformable materials are being tested. Household waste materials fall into this category. However, it is recommended that further work is undertaken in the compression cell to establish whether any peripheral flow is taking place, and conclusively eliminate any uncertainties.

9.1.3 Future research developments

The compression cell has been used to investigate the effects of increases in stress and depth of burial on various properties of household waste. There are other factors that are likely to have an impact on these hydrogeological properties. These include:-

1) rebound effects following reduction in effective stress;
2) vertical and horizontal anisotropy;

3) the effect of biodegradation; and
4) the degree of saturation, which in turn may be related to gas production.

It is recommended that further research is undertaken into these aspects. This is explained in more detail in Sections 9.2 to 9.5.

9.1.4 Timescale of testing

When planning future tests using the compression cell careful consideration needs to be paid to the length of time required. The large-scale of the equipment means that significantly longer time needs to be allocated than for similar tests using small-scale laboratory equipment. In particular, more time is needed to prepare for tests, undertake the tests, and address any problems that occur.

9.2 The geotechnical and hydrogeological properties of waste

A number of geotechnical and hydrogeological properties of waste have been explored through the research reported in this thesis. The main focus has been on the inter-relationship between the hydrogeological properties of waste, density, and effective stress.

During the research three types of waste were tested. All exhibited similar patterns of behaviour when subjected to increases in vertical effective stress. The main features were:-

1) an increase in waste density. For example, the density at field capacity of crude unprocessed household waste (DM3) increased from approximately 0.8 to 1.15 t/m^3 over a stress range of 35 to 460 kPa. The bulk density of the waste is highly dependent on its water content. Consequently, if the above waste had been kept at its original water content (WC_{dry}) of 51.5%, then the corresponding increase in density (over the same stress range) would have been 0.6 to 1.1 t/m^3.

2) a decrease in drainable or effective porosity. All wastes had a relatively large drainable porosity of at least 15% at effective stresses below 35 kPa. This reduced to less than 5% at stresses above approximately 130 kPa and to less than 2% at stresses above 250 kPa. The decrease in drainable porosity probably results from the collapse of macropores. This may change the dominant flow mechanism, from one based on flow in macropores to flow along the interfaces of touching particles, or to flow through micropores. This is a topic that requires further research.

3) a decrease in the water content at field capacity (when expressed as a dry weight water content, WC_{dry}). As an example, the water content at field capacity of crude unprocessed household waste reduced from 100% to 60% over an effective stress range of 35 to 460 kPa. However, if the water content is expressed as a volumetric water content (WC_{vol}), then there is little change in the water content at field capacity with changing effective stress. The volumetric water content of the crude unprocessed household waste was between 40% and 45% over the above effective stress range.

4) a reduction in hydraulic conductivity. Data from all the waste types followed the same general trend. 'Best fit' and 'worst case fit' lines for crude household waste (DM3) and for all wastes, gave the following relationships:-

	Best fit	Worst case fit
DM3	$K = 2.1(\sigma_v')^{-2.71}$	$K = 17(\sigma_v')^{-3.26}$
All waste	$K = 10(\sigma_v')^{-3.1}$	$K = 80(\sigma_v')^{-3.63}$

where σ_v' is in kPa and K is in m/s. Valid for 40 kPa< σ_v'<500 kPa

When samples of waste were extruded from the compression cell after being subjected to stresses of approximately 500 kPa, there was evidence of distinct layering. This could potentially cause an anisotropy in hydraulic conductivity, thereby affecting the movement of fluid through wastes. It is recommended that the effect of this layering should be investigated.

5) an increase in the dry particle density of the waste. As an example, the average dry particle density of a crude unprocessed household waste (DM3) increased from 0.88 t/m^3 to 1.3 t/m^3 over an effective stress range from 35 to 460 kPa.

6) an increase in the stiffness of the waste. The constrained modulus of all waste varied from between 3.5 to 7 times the average vertical effective stress.

These hydrogeological results were obtained from nominally saturated waste. They provide an essential baseline from which predictions can be made about the behaviour of waste within saturated landfills. However, the hydrogeological properties will vary according to the degree of saturation. These results may not, therefore, be directly applicable to landfill sites where active gas generation is likely to reduce the degree of saturation of the waste. It is recommended that further research is undertaken to

investigate the effect of unsaturated conditions on flow in landfills. This could either relate to flow through the unsaturated zone, or to flow in the nominally saturated zone.

In addition, waste degradation and its impact on both the geotechnical and hydrogeological properties requires further research. The design of leachate control and recirculation systems needs to take into account any resulting changes in the properties of waste. The data from aged waste (AG1) included in this research did not suggest that the properties were too different from that of undegraded waste, but a direct comparison cannot be made as the original properties were not known.

Much of the analysis and use of the data produced by this research has been based on the assumption that Terzaghi's equation ($\sigma_v' = \sigma_v - u$) is applicable to waste materials. A brief review of the research that originally proved the validity of the equation, for most geotechnical materials, indicated that it is also likely to be applicable to wastes. However, given that many of the principles of soil mechanics are based on an assumption of constant dry particle density, and following the finding that, for waste, the dry particle density is not constant, a more detailed study is recommended.

There is also a need to investigate further the extent to which the properties of waste are or are not reversible following reductions in effective stress. This is important because it would indicate whether landfill design needs to incorporate mechanisms to keep effective stresses low (e.g. restricting the depth of landfills or operating with a large saturated depth) and thereby hydraulic conductivities high.

The increase in effective stress with depth from self weight effects in a typical landfill was calculated using a simple finite difference analysis and a spreadsheet. Within the unsaturated zone there is a relatively rapid increase in effective stress with increasing depth. However, there is little change in effective stress with depth below the water or leachate table under hydrostatic conditions - the saturated unit weight of the wastes tested was similar to that of water. Consequently, it is feasible that landfills of significant depth with a large saturated zone could have hydrogeological properties that are similar to shallow landfill sites. This would suggest that it may be possible to flush pollutants from existing deep (as well as shallow) sites where there is a large saturated zone.

9.3 Leachate control systems

This research provides baseline data that can be used to make predictions about the hydrogeology of landfill sites requiring leachate control measures. This does not replace the need for full site investigations to produce design data, but it does allow the scale of any problems to be indicated and considered in advance.

In sites where there is a requirement to lower leachate levels the volume of leachate needing to be removed (per unit volume of waste) is related to the drainable porosity. Likely values of drainable porosity can be deduced/ inferred from factors such as depth of landfill, depth of unsaturated zone, waste compaction techniques and an effective stress history. Old, relatively shallow sites where waste was placed with minimal compaction (e.g. with bulldozers rather than compactors) are likely to have high drainable porosities and would, therefore, be expected to yield considerably more leachate than the same volume of waste in a deep landfill which had been heavily compacted. Similarly, consideration of the above factors can be used to estimate likely values of hydraulic conductivity, and hence, in the early design of leachate control systems.

A continuing problem faced by landfill operators is the control of leachate levels in old sites where leachate underdrains were not installed. The research has indicated that the use of vertical wells to maintain leachate levels in deep sites to within 1-2 metres of the base is not possible without using an inordinate number of wells - at least 100 wells per hectare in sites over 40 metres deep.

9.4 Modelling of fluid flow in landfills

The potential decrease in hydraulic conductivity with depth in a landfill means that flow rates (especially where horizontal flow is concerned) will also vary with depth and are difficult to predict. It is important to be able to simulate these variations to help make decisions about the optimum design of flushing systems. Prior to the start of this research such simulations were constrained by the inability of most groundwater flow modelling software to alter hydraulic conductivity values in relation to effective stress. A new module was, therefore, written for the USGS's 3d groundwater flow model MODFLOW to allow hydraulic conductivity of cells to vary. The module was verified against two analytical solutions of flow in a landfill.

The widespread use of this new module is restricted by MODFLOW's limitations in the way it handles changes from saturated to unsaturated conditions in a modelled cell, and because unsaturated flow is not catered for. Consequently the module has only been used to investigate flow between a grid of confined injection and abstraction wells.

There is at least one commercially available package (MODFLOW-SURFACT, by HydroGeoLogic Inc.) that replaces MODFLOW's own block centred flow package and provides a rigorous treatment of 3d flow, including unsaturated flow. It is likely that by combining such a flow package with the stress dependent hydraulic conductivity module developed through this research, more complicated flow problems could to be modelled that are more representative of full scale landfills. It is recommended that this merits further development.

Furthermore, it is possible that the aquifer compaction package that already exists for MODFLOW could be incorporated. This deals with the release of water from storage as a result of aquifer compaction (from dewatering) and could help model changes in water content that are related to effective stress and (stress related) settlement. Finally, the model could be developed further to relate the density and hydrogeological properties of the waste to the maximum stress history of the waste and to incorporate the ability to model a vertical to horizontal anisotropy in hydraulic conductivity. Use of these facilities would be subject to further research into the consequence of effective stress reduction on hydrogeological properties, and the anisotropy of wastes.

More accurate modelling of fluid flow in landfills would help achieve improvements to leachate flushing systems. The module developed through this research is a positive step in this direction.

9.5 Sustainable flushing of wastes

It is accepted that removal of the pollution load from landfills must include some flushing of wastes. Whether this can be achieved within a timescale that meets sustainability criteria - within 30 to 50 years- remains a subject of some debate. The hydrogeological and geotechnical data generated from this research contributes to that debate by allowing possible systems of flushing to be assessed.

The main conclusions are as follows:

9.5.1 Flushing volume

Two types of flushing models were considered, a continuously mixed reactor model, and a fill and drain model. The continuously mixed reactor model is based on the bed volume of a landfill. It is concluded that for recirculation through unsaturated wastes, the bed volume is approximately 40% by volume, irrespective of the density of the waste in the landfill. For saturated wastes at low densities, the bed volume can be as high as

55% (by volume), but this reduces to that associated with unsaturated waste at higher waste densities.

The volume of water required to raise the water content of a landfill to field capacity is approximately 15-20% (by volume). Flushing cannot occur until this has been achieved.

The volume of liquid that must be flushed through a unit volume of waste to remove soluble degradation products is approximately 2.7 m^3. This volume is independent of waste density or the two simple flushing models considered. However, it is based on reducing NH3-N concentrations in the leachate to below 10 mg/l and assumes that degradation and the release of nitrogen from the solid to the liquid phase has been completed before flushing starts.

It is recommended that further research is required on the applicability of flushing models to landfills. The relative merits of the various flushing models require investigation, as too do the implications of flushing reactive rather than conservative species. Work is also required on the factors controlling the dissipation of contaminants from micro to macro-pores.

9.5.2 Flushing rates

The required rate of flushing can be expressed as a specific flushing rate. This is useful as it can indicate the degree of flushing that occurs at varying distances from leachate wells. The specific flushing rate to flush 2.7 m^3 of liquid through a unit volume of waste in 30 years is 2.85×10^{-9} sec^{-1}.

A specific flushing rate of 2.85×10^{-9} sec^{-1} can also be expressed as a vertical infiltration rate, where:

$$\text{Infiltration rate (m/a)} \sim \frac{\text{Depth of landfill (m)}}{10}$$

9.5.3 Flushing scenarios

The ability to achieve this specific flushing rate through unsaturated wastes is only possible if the depth of landfill is less than 35 metres and, ideally, less than approximately 20 metres, and if the wastes have not been pre-compacted to a density in excess of 0.8 to 0.9 t/m^3.

The generally perceived need to flush through unsaturated (rather than saturated) waste relates to possible risks associated with leachate saturation. Risks are considered to be

greater if there are large leachate heads (which increase the potential for migration) and if there are large volumes of leachate (such that any leak could result in serious environmental damage). However, this research has shown that there is little difference (at effective stresses over approximately 100 kPa) between the water content of unsaturated waste at field capacity and saturated waste, because the drainable porosity of saturated waste is low. This has two main implications:-

1) the volume of freely draining leachate in saturated wastes may be relatively small and therefore the risks may not be as great as feared; and

2) during leachate recirculation through unsaturated wastes it may be difficult to stop at least part of the wastes becoming saturated (as it would involve only a small change in water content), with the consequential establishment of leachate heads.

A major benefit of operating flushing systems through saturated wastes is that higher flushing rates can be achieved. The maintenance of high pore water pressures (leachate heads) in the waste leads to low effective stresses and high hydraulic conductivities. It is concluded that a combination of engineering and operational measures can be taken to prevent these elevated leachate heads leading to a higher risk of leachate migration. A hydraulic break can be engineered into the basal liner system to prevent leachate heads being transmitted to the liner overlying the external geology, and dewatering of the basal leachate collection layer can prevent heads being transmitted on to the top of the lining system.

A further benefit of working with saturated wastes is that it provides a much wider range of options for flushing. Flushing through unsaturated waste can only be vertically downwards, with movement controlled by gravity. It is theoretically possible to operate flushing through saturated wastes in virtually any direction dependent only on the configuration of the injection and collection infrastructure. The ability to flush the same waste from a variety of directions may be advantageous, especially if there are impediments to flow (e.g. low permeability layers) in certain directions.

Finally, operating leachate recirculation through saturated wastes probably results in a more efficient flushing mechanism, with potentially higher and more uniform rates of diffusion of contaminants from micro to macropores. This, however, requires further research.

Various leachate recirculation schemes based on saturated waste were evaluated using the findings from the research. The main factor that determined whether the required flushing rates were achievable for any given scheme was the relationship between

hydraulic conductivity and stress. If the relationship between hydraulic conductivity and effective stress is reversible, then the hydrogeological properties of the waste impose very few operational restrictions to achieve the necessary flushing rates through saturated waste. If, as is more likely, the hydraulic conductivity is based on the maximum historical effective stress then there would need to be restrictions to the depth of landfill (linked to the level of saturation), pre-compaction of the waste, and mode of operation of any recirculation system. If the hydraulic conductivity is linked to a stress distribution associated with unsaturated waste, then the maximum depth of landfill at which the required flushing rate can be achieved with downward vertical flow is approximately 40 metres. In addition, waste must not be pre-compacted to a bulk density greater than between 0.9 and 1 t/m^3.

Flushing at the required rate through deeper depths of landfills may be achieved if effective stresses during landfilling have been kept low by, for example, raising the leachate level in the site as the depth of landfill increases, and/or a combination of upward and downward flow is adopted.

The presence of any horizontal layer of low permeability material in a landfill will severely affect the ability to achieve the required flushing rates. A single 0.5 metre layer with a hydraulic conductivity of $1x10^{-9}$ m/s was shown to restrict flushing rates to significantly below the required rate. Recommendations are made in Section 9.6 on possible measures that could be taken to prevent landfilling of low permeability materials.

Vertical wells have the capacity to achieve the required flushing rates if operated in wastes with a large saturated depth, and are largely unaffected by horizontal layers of low permeability. It has been demonstrated that a 20 m grid of injection and abstraction wells with a 20 metre confined saturated zone in a 30 m deep landfill, achieved the required flushing rates even when the hydraulic conductivity was based on a stress distribution associated with unsaturated wastes.

9.6 Implications for sustainable landfilling practice

The research has demonstrated that the operation of landfills as high rate flushing bioreactors to achieve sustainable landfilling is a feasible proposition. The physical and hydrogeological properties of household waste need not preclude the flushing of wastes at rates that are considered to be sustainable. However, to a large extent the success of any such landfill will be dependent on engineering and operational requirements, as discussed in Section 8.6. In summary, the major features are as follows-

9.6.1 Depth of landfill

The maximum depth of landfill that will allow flushing to occur at the required rates is mainly dependent on whether saturated or unsaturated conditions exist during operation and placement of wastes. In general, if flushing is to be through unsaturated waste the depth of landfill should ideally be restricted to below 20 metres; if flushing is to be through saturated waste, but introduction of liquid into the site is delayed until after final landfill heights have been achieved, depths should be restricted to below 40 metres; if, on the other hand, leachate levels are increased as the height of landfill is increased (or the relationship between hydraulic conductivity and effective stress is reversible) there appears to be no practical limit on landfill depth.

9.6.2 Saturation of waste

This research has shown that there are considerable advantages to flushing through saturated waste. In any landfill design these advantages would need to be weighed against the additional engineering measures required to the basal liner system and the likely regulatory and planning difficulties that this would create.

9.6.3 Liners

The liner used in a high rate flushing bioreactor can be based on existing technology and designs. If the site is to be operated with unsaturated flushing, current composite lining systems would be appropriate. If the landfill is operated with a large saturated depth, then a hydraulic break would need to be included in the design.

9.6.4 Pre-processing of waste

The evidence from this research suggests that the processing (and shredding) of household waste will not significantly alter its hydrogeological properties and will not, therefore, alter the ability to flush it. Shredding has the added advantages that it may enhance biodegradation rates and it creates a more homogenous waste mass that should aid in the even distribution of flow.

9.6.5 Waste placement densities

It has been shown that for a given situation there is a maximum waste density that must not be exceeded if flushing rates are to be met. It is difficult to be too specific about these requirements as waste density at the tipping face is very dependent on water content, which can vary considerably. In general terms, though, as placed densities should not be greater than between 0.9 and 1.1 t/m^3. A problem is experienced when these densities are related to the operation of various types of compaction plant. It is concluded that the largest available compactors (e.g. Cat^R 836) when used to their full potential, will compact waste to densities over 1.1 t/m^3 thus precluding flushing of waste at the rate required. It is recommended that further research is undertaken into the relationship between compaction plant, mode of operation and waste density in a way that allows it to be linked in with (this) research on the hydrogeological properties of waste.

9.6.6 Removing barriers to flow

The presence of low permeability layers in a landfill has been shown to restrict the ability to achieve the required flushing rates. Consequently, they should be excluded from, or segregated within the site. The use of low permeability clay or soils as daily cover material should be prohibited and alternative methods, such as foam or hessian sheets, encouraged in their place.

9.6.7 Leachate recirculation infrastructure

The need to recirculate large volumes of leachate around a landfill requires robust systems to both inject fluid into and abstract leachate from the site. The systems need to be resistant to clogging and, in the case of the upper layers, be capable of withstanding a considerable amount of waste settlement. It has been shown that vertical leachate wells can have an important role in the flushing of wastes in saturated sites. As they can be installed after landfilling has been completed they are a replacement option if the performance of the original flushing systems reduces over time.

9.6.8 Source of new water

The minimum volume of new water required to flush wastes in a landfill is that needed to bring the waste up to field capacity, approximately 0.2 m^3 per tonne of waste. The maximum volume required is approximately 2.7 m^3 per unit volume (or tonne). The actual volume required will depend on the extent to which the flushing fluid can re-use treated leachate, and how much dilution it requires from other sources. These sources do not need to be of high quality and a variety of grey water sources, including treated

sewage effluent, would be appropriate. It is noted that even if the wastes in a landfill were flushed with clean water the volumes required would only represent an increase of between 1 and 4% of existing water supplies. It is suggested that this is an efficient use of water when compared with sewage treatment processes where between 20 and 100 times more water is used to treat the same pollution load.

9.6.9 Siting of a high rate flushing bioreactor

The siting of high rate flushing bioreactor landfills is important. There must be a source of (possibly low quality) water to be used for the flushing, and adequate dilution in the receiving environment for disposal of the inorganic ion concentration of treated leachate. Although the leachate head on the basal liner can be kept small by pumping from the basal leachate drainage layer and by the incorporation of hydraulic breaks in the composite liner system, this type of landfill should not be located directly on sensitive aquifers.

9.7 Concluding remarks

For a landfill to be sustainable it must be brought to a stable non-polluting state within a timescale that does not pass pollution problems on to future generations. This requires that methods have to be adopted to remove the pollution load of the waste which, if undertaken within the landfill, will require an element of accelerated flushing. The ability to flush a waste is dependent on its hydrogeological properties. (Section 1.1).

The research reported in this thesis has contributed to the understanding of the hydrogeological properties of waste. This has been used to consider the design and operational methods needed to remove the pollution load of waste in a sustainable timescale. Application of this research brings the development and operation of a high rate flushing bioreactor one step nearer.

Bibliography

Barlaz, M.A. and Ham, R.K. (1990) *Methane production from municipal refuse: a review of enhancement techniques and microbial dynamics* Critical Reviews in Environmental Control Vol 19 (6) pp557-585.

Beaven, R.P. (1996). *Geotechnical and hydrogeological properties of wastes.* In: Engineering Geology of Waste Storage and Disposal. Bentley, S.P. (ed.) Geological Society Engineering Geology Special Publication No. 11, pp 57-65 London.

Beaven, R.P. (1996a). *A hydrogeological approach to sustainable landfill design* Paper presented at Harwell waste management symposium on 'Progress practice and landfill research' 22 May. AEA Technology, Harwell.

Beaven, R.P. and Walker, A.N (1997). *Evaluation of the total pollution load of MSW* Proc. 6th International Sardinia Landfill Symposium. S. Margherita di Pula, Cagliari, Italy. Vol I pp 57-71. October 1997.

Belevi, H. and Baccini, P. (1989) Longterm behaviour of municipal solid waste landfills. *Waste Management & Research,* Vol. 7, pp 43-56.

Benson, C.H and Othman, M.A. (1993) *Hydraulic and mechanical characterisation of a compacted municipal waste compost* Waste Management & Research. Vol 11 (2) pp 127-142.

Bevan, R.E. (1967) *Notes on the science and practice of the controlled Tipping of Refuse* The Institute of Public Cleansing, London 1967

Blakey, N. (1982). *Absorptive capacity of refuse - WRC Research.* Landfill Leachate Symposium, Harwell, UK. May

Blakey, N.; Bradshaw, K.; Reynolds, P. and Knox, K. (1997) *Bio-reactor landfill - a field trial of accelerated waste stabilisation* Proc of Sardinia 97, Sixth International Landfill Symposium. S. Margherita di Pula, Cagliari. Vol I pp375-385.

Bleiker, D.E.; McBean, E. and Farquhar, G. (1993) *Refuse sampling and permeability testing at the Brock West and Keele Valley Landfills.* Proceedings of the Sixteenth International Waste Conference - Madison USA.

Blight, G.E; Ball, J.M. and Blight, J.J. (1991) *Moisture distribution in sanitary landfills* Proc. Third International landfill Symposium. Sardinia Italy. pp813-822.

Bouwer, H. (1978) *Groundwater Hydrology* McGraw-Hill ISBN 0-07-006715-5

Brinkmann, U.; Horing, K.; Heim, M. and Ehrig, H.J. (1995) *Effect of pre-composting on the long term behaviour of MSW landfills.* Proc' of Sardinia 95, 5th International Landfill Symposium. Cagliari. Vol. I; pp 971-985.

Buivid, M.G.; Wise, D.C.; Blancket, M.J.; Remedios, E.C.; Jenkins, B.M. Boyd, W.F. and Pacey, J.G. (1981) *Fuel gas enhancement by controlled landfilling of municipal solid waste.* Resources and Conservation, Vol 6, pp3-20.

Burland, J.B. and Roscoe, K.H. (1969) *Local strains and pore pressures in a normally consolidated clay layer during one-dimensional consolidation* Geotechnique, Vol 19, No 3, pp335-356.

Burrows, M.R.; Joseph, J.B. and Mather, J.D. (1997) *The hydraulic properties of in situ landfilled waste* Proc of Sardinia 97, Sixth International Landfill Symposium. S. Margherita di Pula, Cagliari. Vol II pp 73-83.

Burton, S.A.Q. and Watson-Craik, I.A. (1997) *Ammonia production and turnover in landfilled refuse.* Proc' Sardinia 97, 6th International Landfill Symposium. Cagliari. CISA

Campbell, D. (1982). *Absorptive capacity of refuse - Harwell Research.* Landfill Leachate Symposium, Harwell, UK. May.

Campbell, D.J.V. (1997). *Enhanced landfill gas production at the Brogborough Test Cells.* Proceedings of the IBC conference on "Designing and Managing Sustainable Landfill". 26-27 February. Scientific Societies Lecture Theatre. London

Caterpillar (1995). *Cat® 816B & 826C Compaction study vs Hanomag CD 280, Bomag 601 RB.* Caterpillar Product Information Performance Report. January 1995.

Chelmsford Borough Council (c.1998) *Chelmsford 21 - Improving our environment* Meridan Design Solutions for Environmental Services, Chelmsford Borough Council. 16pp.

Chen, W.W.H.; Zimmerman, R.E. and Franklin, A.G. (1977) *Time settlement characteristics of milled urban refuse.* Proc' of Conf. on Geotech. Practice for disposal of solid waste materials. ASCE.

Chen, Ten-Hong. and Chynoweth, D.P. (1995) *Hydraulic conductivity of compacted municipal solid waste.* Bioresource Technology. vol 51 pp 205-212.

Civic Trust (c.1968) *Derelict Land - A study of Industrial dereliction and how it may be redeemed* 70pp.

Clayton, C.R.I. and Bica, A.V.D. (1993) *The design of diaphragm-type boundary total stress cells* Geotechnique Vol 43 No 4 pp523-535

Colden, D. (1990) *Modelling of the seepage flux of ground water from coastal landfills* MSc thesis. University of Rhode Island. USA.

Collins, R; Lee, K.J.; Lilly, G.P. and Westman, R.A. (1972) *Mechanics of pressure cells* Experimenal Mechanics, Vol 12, No 11, pp514-519.

Cooper, H.H. and Jacob C.E. (1946) *A generalised graphical method for evaluating formation constants and summarizing well field history.* Am. Geophys. Union Trans. Vol. 27, pp525-534.

Cossu, R. (1995) *Utilization of MSW compost in landfills: effects on leachate and biogas quality.* Proc of Sardinia 95, Fifth International Landfill Symposium. S. Margherita di Pula, Cagliari. Vol I, pp79-94.

Cossu, R.; Frongia, G.; Muntoni, A.; Nobile, A. and Raga, R. (1997) *Use of pumping tests for the assessment of leachate flow regime, waste hydraulic parameters and well efficiency.* Proc of Sardinia 97, Sixth International Landfill Symposium. S. Margherita di Pula, Cagliari. Vol II, pp53-62.

Daniel, D.E. (1994) *State-of-the-art: Laboratory hydraulic conductivity tests for saturated soils* in 'Hydraulic Conductivity and Waste Contaminant Transport in Soil' ASTM STP 1142, pp.30-78, eds. Daniel, D.E. and Trautwein, S.J. American Society for Testing and Materials, Philadelphia.

Darcy, (1856) *Les fontaines publiques de la Ville de Dijon* pp570, 590-594, V. Dalmont, Paris.

DETR (1997) *The urban waste water treatment (England and Wales) Regulations 1994 - Working note for discharges and regulators.* A guidance note issued by the Department of the Environment, Transport and the Regions and the Welsh Office. July 1997

DETR (1998) *Sustainable Development: Opportunities for Change. Consultaion Paper on a revised UK strategy.* Department of the Environment, Transport and the Regions. Sustainable Development Unit : Ref 97 EP 0277; 4 February 1998. http://www.environment.detr.gov.uk/sustainable/consult1/index.htm

DoE (1971) *Refuse Disposal*; Report of the Working Party on Refuse Disposal. HMSO, London. (chairman J. Sumner). London, HMSO 1971. ISBN 0 11 750348 7

DoE (1978) *Co-operative Programme of Research on the Behavior of Hazardous Wastes in Landfill Sites. Final Report of the policy Review Committee.* (chairman J. Sumner). HMSO, London. ISBN 0 11 7514257 5

DoE (1986) *Landfilling Wastes: A technical memorandum for the disposal of wastes on landfill sites. DoE Waste Management Paper 26* HMSO, London, 206pp. 1st pub 1986 ISBN 0 11 751891 3.

DoE (1988) *Town and Country Planning (assessment of Environmental effects) Regulations 1988.* SI 1988 No. 1199. HMSO, London, 1988.

DoE (1990) *Environmental Protection Act 1990* (c. 43) ISBN 0 10 544390 5

DoE (1991) *Water Resources Act 1991* (c. 57). HMSO, London. ISBN 0 10 545791 4

DoE (1991a) *Waste Management Paper 27, Landfill Gas* HMSO, London, 1991. ISBN 0 11 752488 3

DoE (1992) *Waste Management Paper Number 1: A review of options.* Second Edition HMSO, London, 1992.

DoE (1994) *The Waste Management Licensing Regulations 1994* SI 1994 No 1056. HMSO, London. ISBN 0 11 044056 0.

DoE (1994a) *National Household Waste Analysis Project - Phase 2 Volume 1 Report on composition and weight data* Report No CWM 082/94 produced for the Waste Technical Division of the Department of the Environment under Research Contract PECD 7/10/288 by Warren Spring Laboratory and Aspinwall & Co.

DoE (1995) *Environment Act 1995 c.25* ISBN 0-10-542595-8

DoE (1995a). *Landfill design construction and operational practice.* Waste Management Paper 26B. HMSO London 289pp.

DoE (1995b). *Making Waste Work - A strategy for sustainable waste management in England and Wales.* HMSO. London.

DoE (1995c) *National Household Waste Analysis Project - Phase 2 Volume 3 Chemical Analysis Data* Report No CWM 087/94 produced for the Waste Technical Division of the Department of the Environment under Research Contract PECD 7/10/288 by The National Environmental Technology Centre.

DoE (1996) *The Environment Agency and Sustainable Development - PART I Statutory Guidance under Section 4 of the Environment Act 1995 with respect to objectives of the Environment Agency and its contribution towards achieving Sustainable development* HMSO, November 1996

EC (1980) *Directive on Protection of Groundwater against pollution caused by certain dangerous substances (80/68/EEC)* OJ, L20, 26.01.80.

EC (1985) *Directive on the assessment of the effects of certain public and private projects on the environment* 85/337/EC OJ, L175, 5 July.

EC (1991) *The Framework Directive on Waste - Directive 75/442/EEC, as amended by 91/156/EEC* OJ L78, 26 March 1991.

EC (1993) *Towards sustainability, A European Community Programme of policy and action in relation to the Environment and Sustainable development.* OJ No C 138 17/05/1993

EC (1998) *Common position EC No 49/48 adopted by the council on 4 June 1998 with a view to adopting Council Directive 98/ /EC, of... on the landfill of waste* OJ C C333/15 (98C 333/02)

Ehrig, H.J. and Scheelhaase, T. (1993) Pollution potential and long term behaviour of sanitary landfills. *Proc' Sardinia 93, 4th International Landfill Symposium.* Cagliari. CISA pp 1203-1225

EMCON Associates (1983) *Field assessment of site closure, Boone county, Kentucky.* Report to US EPA; N.T.I.S. No: PB 83-251-629.

ENDS (1997) *Landfill faces "leap to utopia" with flushing bioreactors* hjh

ENGLAND (1842) Poor Law Commission. [1834-47.] *Report to Her Majesty's Principal Secretary of State for the Home Department, from the Poor Law Commissioners, on an inquiry into the sanitary condition of the labouring population of Great Britain; with appendices. [Compiled by E. Chadwick.]* Made at the request of Her Majesty's Principal Secretary of State for the Home Department. Pub: 4 pt. London, 1842, 43. 8o. Series: [House of Lords Sessional Papers. Session 1842. vol. 26-28; session 1843. vol. 32.]

ENGLAND (1848) *(11 and 12 Vict. c. 63.) The Public Health Act. The Act for promoting the Public Health, passed 31st of Aug. 1848. With notes.* Publisher: M. Taylor, London, [1848.] 8o.

Ettala, M. (1987) *Infiltration and hydraulic conductivity at a sanitary landfill* Aqua Fennica, Vol 17, No 2, pp231-237

Fang, H.Y. (1983) *Physical properties of Compacted disposal materials* Unpublished report (cited in Oweis & Khera, 1986).

Franzius, V., (1977) *Der SickerwasserabfluB aus Mulldeponien - Ein mathematisches Modell* - Wasserbau Mitteilungen, Nr. 16. Technische Universitat Darmstadt, Institut fur Wasserbau und Wasserwirtschaft.

Frost, J. (1997) *Sustainable landfill practices - an overview of environmental constraints* Proceedings of the IBC conference on "Designing and Managing Sustainable Landfill". 26-27 February. Scientific Societies Lecture Theatre. London

Fungaroli, A.A and Steiner, R.L (1979) *Investigation of sanitary landfill behavior.* US EPA report 600/2-79-053a.

Giardi, M. (1997) *Hydraulic behaviour of waste: observations from pumping tests* Proc of Sardinia 97, Sixth International Landfill Symposium. S. Margherita di Pula, Cagliari. Vol II, pp63-72.

Giroud, J.P. and Houlihan, M.F. (1995) *The design of leachate collection layers* Proceedings of Sardinia 95, 5th International Landfill Symposium. Cagliari. Vol. II; pp 613-640.

Giroud, J.P. and Bonaparte, R. (1989) *Leakage through liners constructed with geomembranes - Part I. Geomembrane liners* Geotextile and Geomembranes, Vol 8, No 1, pp27-67.

Giroud, J.P. and Bonaparte, R. (1989a) *Leakage through liners constructed with geomembranes - Part II. Composite liners* Geotextile and Geomembranes, Vol 8, No 2. pp71-111.

Gupta, S. (1972) *Some engineering properties of milled refuse* MSc Thesis. Dept of Civil Engineering. Northwestern University, USA.

Gronow, J. (1996). *Bioreactors and landfill research.* Proceedings of IWM annual conference - Torquay 13 June.

Hall, D.H. (1997) *Designing barrier systems for a sustainable landfill* Proceedings of the IBC conference on "Designing and Managing Sustainable Landfill". 26-27 February. Scientific Societies Lecture Theatre. London

Ham, R.K.; Reinhardt, J.J and Sevick, G.W. (1978) *Density of milled and unprocessed waste* ASCE Jour' of the Environmental Engineering Division Vol 104, pp109-125.

Hanna, A.Y.; Harlan, P.W. and Lewis, D.T. (1983) *Effect of slope on water balance under center pivot irrigation* Soil Science Society of America Vol 47, pp.760-764.

Hantush, M.S. (1962) *On the validity of the Dupuit-Forchheimer Well-discharge formula* Jour. of Geophysical Research, Vol 67, No 6, pp2417-2420

Harbaugh, A.W. and McDonald, M.G. (1996) *User's documentation for MODFLOW-96, an update to the U.S. Geological Survey modular finite difference ground water flow model:* U.S. Geological Survey Open-file report 96-485 56pp.

Harbaugh, A.W. and McDonald, M.G. (1996a) *Programmer's documentation for MODFLOW-96, an update to the U.S. Geological Survey modular finite difference ground water flow model:* U.S. Geological Survey Open-file report 96-486 220pp.

Harris, M.R.R. (1979) *Geotechnical characteristics of landfilled domestic refuse* Proc' of The Engineering behavior of Industrial and Urban Fill. Midland Geotechnical Society.

Harris, R.C.; Knox, K. and Walker, N. (1994) *A strategy for the development of sustainable landfill designs and operations* Proc of the Institute of Waste Management. Jan 1994 pp26-29.

Hassan, J. (1998) *A history of water in modern England and Wales* Manchester Universtiy Press 1998. ISBN: 0 7190 4308 5-

Heerenklage, J. and Stegmann, R. (1995) *Overview on mechanical-biologcal pretreatment of residual MSW* Proc. 5th International Sardinia Landfill Conference. S. Margherita di Pula, Cagliari, Italy. Vol I pp 913-925. October 1995.

Heyer, K.U. & Stegmann, R. (1995) The long-term behaviour and residual emission potential of landfills. *Proc' of Sardinia 95, 5th International Landfill Symposium.* Cagliari. Vol. I; pp 149-161.

Hillel, D. (1971) *Soil and Water* Academic Press, New York

Hinrichsen, D. (1987) *Our common future- a readers guide. The Brundtland report explained.* Earthscan 2nd ed. 1987 ISBN 1-85383 0100 (4th printing 1989)

Holmes, R (1980) *The water balance method of estimating leacahte production from landfill sites* Solid Waste January 1980 pp10-20.

HMSO (1956) *Clean Air Act 1956* HMSO, London

HMSO (1972) *Deposit of poisonous wastes Act 1956* HMSO, London

HMSO (1974) *Control of Pollution Act 1974* HMSO, London

HMSO (1994) *Sustainable Development - The UK Strategy.* Presented to UK Parliament, January 1994. London: HMSO Cm2426.

IWM (1999) *The role and operation of the flushing bioreactor* Report of the Institute of Wastes Management Sustainable Landfill Working Group. Pub. IWM Business Services Ltd.

Jaky, J. (1944) *The coefficient of earth pressure at rest.* J. Hungarian Soc of Architects and Civil Engineers, pp355-358.

Jessberger, H.L. and Kockel, R. (1991) *Mechanical properties of waste materials.* Ciclo di Conferenze di geotechnica di Torino. Torino, Italy.

Jones, P.T. (1997) *Sustainability strategies; their possible impacts on waste compositional flows and the implications for Waste Management paper 26B* Proceedings of the IBC conference on "Designing and Managing Sustainable Landfill". 26-27 February. Scientific Societies Lecture Theatre. London

Jones, R.J.A. and Malone, P.G. (1982) *Disposal of treated and untreated electroplating waste in a simulated municipal landfill.* Proc. Conf. EPA 8th annual research symposium, Kentucky, USA EPA-600/9-82-002 pp294-314.

Jones, B.B. and Owen, F. (1934) *Some notes on the scientific aspects of controlled tipping - an account of experimental tests carried out at Wythenshawe, Manchester 1932-33.* Henry Blacklock & Co. Ltd, Manchester, 1934.

Kabbe, G.; Roos, H.J.; Wirtz, A.; Forge, F.; Schroder, H.F. and Dohmann, M. (1995) *Long-term emission behaviour of sanitary landfills* Proc. 5th International Sardinia Landfill Conference. S. Margherita di Pula, Cagliari, Italy. Vol I, pp163-172. October 1995.

Keeling, F. (1999) *pers comm*

Kinman, R.N.; Rickabaugh, J.I.; Walsch, J.J. and Vogt, W.G. (1982) *Leachate from co-disposal of municipal and hazardous waste in landfill simulators* EPA 8th annual research symposium Land disposal of hazardous wastes. EPA-600/9-82-002, pp274-293.

Knox, K. (1990) *The relationship between leachate and gas* Proc. of the International conference on Landfill Gas: Energy and Environment. ISBN 0-7058-1628-1.

Knox, K. (1992) *A review of water balance methods and their application to landfills in the UK.* Report CWM 031/91 produced for the Waste Technical Division of the UK Department of the Environment under Research Contract PECD.

Knox, K. (1996) *A review of the Brogborough and Landfill 2000 test cells monitoring data.* Final report for the Environment Agency R&D Technical Report P231. 113pp.

Knox, K. (1996a) *Leachate recirculation and its role in sustainable development* IWM Proceedings March 1996 pp 10-15.

Knox, K. and Gronow, J. (1995) *A pilot scale study of denitrification and contaminant flushing during prolonged leachate recirculation.* Proc' of Sardinia 95, 5th International Landfill Symposium. Cagliari. Vol. I; pp 419-436

Korfiatis, G.P. and Demetracopoulos, A.C. (1984) *Moisture transport in a solid waste column* Jour. of Env. Engineering Vol 110 (4) pp780-.

Lambe, T.W. (1951) *Soil testing for Engineers* John Wiley & Sons, New York.

Landva A. and Clark J., (1986) *Geotechnical Testing of Wastefill.* Proc 39th Canadian Geotechnical Conf, pp371-385.

Landva A. and Clark J., (1990) *Geotechnics of waste fills - theory and practice* . In Geotechnics of Waste Fills. Eds Landva and Knowles. ASTM Special Publication. Baltimore.

Landva A.; Clark J.; Weisner J.R. and Burwash, W.J. (1984) *Geotechnical Engineering and refuse landfills* 6th National Conference on Waste Management in Canada, Vancouver.

Leake, S.A. and Prudic, D.E. (1991) *Documentation of a computer program to simulate aquifer system compaction using the modular finite difference ground water flow model:* U.S. Geological Survey Techniques of Water-Resource Investigations, book 6, chap. A2, 68pp.

Lloyd, J.W.; Ramanathan, C. and Pacey, N. (1979) *the use of point dilution methods in determining the permeabilities of landfill materials* Water Services. Vol 83 (100) pp843-846.

Maurer, R. W. (1993) *Landfill Tomorrow: A Paradigm shift from Storage to Bioreactors.* Proceedings of Seminar - Landfill Tomorrow, Bioreactors or Storage. Imperial College, Centre for Environmental Control & Waste Management, London.

McDonald, M.G. and Harbaugh, A.W. (1984). *A modular three-dimensional finite-difference ground-water flow model:* U.S. Geological Survey Open-File Report 83-875, 528pp.

McDonald, M.G.; Harbaugh, A.W.; Orr, B.R. and Ackerman, D.J. (1992) *A method of converting no-flow cells to variable head cells for the U.S. Geological Survey modular finite-difference ground-water flow model.* U.S. Geological Survey Open-File Report 96-486, 220pp.

McEnroe, B.M. (1989) *Hydraulics of leacahte collection and cover drainage in sanitary landfills* Proc' of Sardinia 89, 2nd International Landfill Symposium. Vol. I, ppXIII-1.

Ministry of Housing and Local Government (1961) *Pollution of Water by Tipped Refuse.* Report of the Technical Committee on the experimental disposal of House Refuse in Wet and dry Pits. (chairman: A. Key): HMSO, London 1961.

Ministry of Housing and Local Government (1970) *Disposal of Solid Toxic Wastes.* Report of the Technical Committee on the Disposal of Toxic Solid Wastes (chairman A. Key). HMSO, London 1970.

Mitchell, J. K. (1993) *Fundamentals of soil behaviour.* Wiley 2nd ed ISBN:0471856401

Morris, C. (1752) *Observations on the past growth and present state of the City of London.* London, 1752.

Newton, J.R. (1976) *Pilot-scale experiments on leaching from landfills. II Experimental procedures and comparison of overall performance of all experimental units., November 1973 - August 1975.* WLR Technical Note No 17. DoE, UK.

Noble, J.J. and Nair, G.M. (1990) *The effect of capillarity on moisture profiles in landfills* 44th Purdue Industrial Waste Conference Proceedings. Lewis Publishers, Inc., Chelsea, Michigan

NRA (1992) *Policy and Practice for the Protection of Groundwater.* National Rivers Authority, Bristol. ISBN 1 873160 37 2.

NWWDO (1988) *Guidelines on the use of landfill liners* Lancashire Waste Disposal Authority, Preston.

Oweis, I.S. and Khera, R. (1986) *Criteria for geotechnical construction on landfill sites.* In Int. symposium on Env. Geotechnology. Ed. Fang, H.Y. Vol 1 pp205-222.

Oweis, I.S. and Khera, R.P. (1990). *Geotechnology of Waste Management.* Butterworths, London.

Oweis, I.S.; Smith, D.A.; Elwood, R.B. and Greene, D.S. (1990) *Hydraulic characteristics of municipal refuse* J. Geotechnical Engineering Vol 116 No.4 pp539-553.

Parsons, H. de B. (1906) *The disposal of municipal refuse* J. Wiley & Sons, New York. 1906

Papworth, R. (1998) *pers comm.*

Peattie, R. and Sparrow, R.W. (1954) *The fundamental action of earth pressure cells* Jour. of the Mechanics and Physics of Solids, Vol. 2, pp141-155.

Pohland, F.G. (1975) *Sanitary landfill stabilization with leachate recycle and residual treatment.* EPA-600/2-75-043

Poll, A.J. (1988) *Sampling and analysis of domestic refuse - a review of procedures at Warren Spring Laboratory* Warren Spring Laboratory WSL LR 667 (MR)M ISBN 0 85624 527 5

Powrie, W. and Beaven, R.P. (1999) *The hydraulic properties of household waste and implications for landfills* Proceedings of the Institution of Civil Engineers, Geotechnical Engineering, Vol 137, Oct 1999, pp235-247.

Powrie, W.; Paksy, A.; Robinson, J. and Peeling L. (1997) *Pilot scale field trials of landfill drainage systems* Proc. 6th International Sardinia Landfill Symposium. S. Margherita di Pula, Cagliari, Italy. Vol III pp 373-382. October 1997.

Quarrie, J. (1992) *Earth Summit 1992.* Regency Press ISBN 0-9520469-0-3

Reeds, J. (1997) *Water, water, everywhere?* Surveyor 20 February 1997 pp14-16

Robinson, H.D; Barber, C. and Maris, P.J. (1981) *Generation and treatment of leachate from domestic wastes in landfills.* Water Pollution control Vol 81 (4), pp465-478.

Robinson, H.D.; Last, S.D.; Raybould, A.; Savory, D. and Walsh, T.C. (1997) *State of the art landfill leacahte treatment. Schemes in the United Kingdom* Proc. 6th

International Sardinia Landfill Symposium. S. Margherita di Pula, Cagliari, Italy. Vol II, pp191-210. October 1997.

Rowe, R.K. (1995) *Considerations in the design of hydraulic control layers* Proc. of Sardinia 95, 5th International Landfill Symposium. Cagliari. Vol. II; pp 103-114

Rowe, R.K. and Nadarajah, P. (1996) *Estimating leachate drawdown due to pumping wells in landfills.* Canadian Geotechnical Journal. Vol 33 pp1-10.

Rowe, R.K.; Fleming, I.R.; Armstrong, M.D.; Cooke, A.J.; Cullimore, D.R.; Rittmann, B.E.; Bennett, P. and Longstaffe, F.J. (1997) *Recent advances in undersatnding the clogging of leachate collection systems* Proc. 6th International Sardinia Landfill Symposium. S. Margherita di Pula, Cagliari, Italy. Vol III pp 383-390. October 1997.

Rovers, F.A. and Farquhar, G.J. (1973) *Infiltration and landfill behaviour.* ASCE J. Env. Eng. Div. October.

Royal Commission on Environmental Pollution (1993) *Incineration of Wastes.* Seventeenth Report. HMSO.

Ryan, G. (1986) *Report of the non-statutory Public Inquiry into the Gas Explosion at Loscoe, Derbyshire - 24th March 1986.* pub. Derbyshire County Council, Matlock, February 1988.

Savory, D. (1998) *The flushing bioreactor - panacea of paradigm?* Proceedings of conference on "The future of Waste Management? the landfill option." Scientific Societies lecture theatre London. IBC UK conferences Ltd.

Schevon, G.R. and Damas, G. (1986) *Using double liners in landfill design and operation* Waste Management & Research, Vol. 4, No.2, pp161-176.

Schomaker, N.B. (1972) *Construction techniques for sanitary landfill* Waste Age, March/April pp24-25 & 42-44.

Scott, M.P. (1977) *Investigation into the effects of different operating methods on initial refuse density.* Cleanaway Ltd Internal report.

Shad, H-S. (1989) *Design and performance of an experimental earth pressure cell.* Ph.D Thesis, Queen Mary and Westfield College, University of London.

Skempton, A.W. (1960) *Effective stresses in soils, concrete and rocks* Proceedings of the conference on pore water and suction in soils. Butterworths, London.

Stegmann, R., (1982). *Absorptive capacity of refuse - West German Research.* Landfill Leachate Symposium, Harwell, UK. May.

Stegmann, R. (1997) *Sustainable landfill and the German approach to waste disposal* Proceedings of the IBC conference on "Designing and Managing Sustainable Landfill". 26-27 February. Scientific Societies Lecture Theatre. London

Stephen, J. (1951) *Thomson's modern public cleansing practice - its principles and problems* The Technical Publications Co. Ltd. 3rd ed. London.

Taylor, D.W. (1947) *Pressure distribution theories, earth pressure cell investigations and pressure distribution data.* Vicksburg: US Army Engineer Waterways Experiment Station

Tory, A.C. and Sparrow, R.W. (1967) *The influence of diaphragm flexibility on the performance of an earth pressure cell* J. Sci. Intrum., Vol. 44 pp781-785.

Tchobanoglous, G.; Theisen, H. and Vigil, S. (1993) *Integrated solid waste management - Engineering principles and management issues* McGraw Hill, USA ISBN 0 07 063237 5

Terzaghi, K. (1936) *The shearing resistance of saturated soils* Proceedings of the First International Conference on Soil Mechanics, 1, pp54-56.

Townsend, T.G.; Miller, W.L. and Earle, J.F.K. (1995) *Leachate recycle infiltration ponds* Jour. of Env' Engineering. Vol 121 (6) pp465-471.

Udaloy, A.G.; Komorita, J.D. and Rowland, P.J. (1993) *Retrofitting a combined leachate and landfill gas collection system in solid waste.* Presented at the NSWMA WasteTech '93 Conference, USA.

Vaughan, P.R. (1994) *Assumption, prediction and reality in geotechnical engineering* Geotechnique, Vol 44, No4, pp573-609.

von Felde, D and Doedens, H. (1997) *Mechanical-biological pretreatment: Results of full scale plant* Proc of Sardinia 97, Sixth International Landfill Symposium. S. Margherita di Pula, Cagliari. Vol I pp 531-542.

Walker, A.N. (1993) *Landfill leachate control - A diagnosis and prognosis* Proceedings of the Institute of Waste Management. pp 3-10. January 1993.

Walker, N. (1994) *Managing landfill to minimise groundwater pollution* Paper presented at IWEM SE branch Conference 'Groundwater - managing a scarce resource' Gatwick Penta Hotel, 23 March.

White, C.; Barker, R.; Griffith, D. and Dyer, M. (1995) *The art of detection* Surveyor, 7 December 1995, Vol. 182 pp.14-16.

Winkler, P.F. and Wilson, D.C. (1973) *Size characteristics of municipal solid wastes* Compost Science. Vol 14 (5) pp6-11.

World Commission on Environment and Development (1987) *Our common future* Oxford University Press. ISBN 019282080x

WSA (1996) *Waterfacts 1996* The Water Sevices Association of England and Wales. ISBN 0 947886 39 7

Young, A. (1989) *Mathematical modelling of landfill degradation* J. Chem Tech. Biotechnol. pp189-208.

Papers based on the findings of this thesis

Beaven, R.P. (1996). *A hydrogeological approach to sustainable landfill design* Paper presented at Harwell waste management symposium on 'Progress practice and landfill research' 22 May. AEA Technology, Harwell.

Beaven, R.P. (1997). *Hydraulic and Engineering Properties of Household Waste* Proceedings of the IBC conference on "Designing and Managing Sustainable Landfill". 26-27 February. Scientific Societies Lecture Theatre. London

Beaven, R.P. (1997). *Is accelerated stabilisation achievable?* Paper presented at the IWM 1997 annual conference - Torbay 10 June.

Beaven, R.P. and Powrie, W. (1995). *Determination of the hydrogeological and geotechnical properties of refuse using a large scale compression cell.* Proc. 5th International Sardinia Landfill Conference. S. Margherita di Pula, Cagliari, Italy. Vol II pp 745-760. October 1995.

Beaven, R.P. and Powrie, W. (1996). *Determination of the Hydrogeological and Geotechnical Properties of Refuse in relation to Sustainable Landfilling.* Paper presented at the Nineteenth International Madison Waste Conference, September 25-26, 1996, Department of Engineering Professional Development, University of Wisconsin-Madison. USA.

Beaven, R.P. and Powrie, W. (1999) *Analysis of waste flushing and flow to wells using MODFLOW and an effective stress dependent hydraulic conductivity* Proceedings Sardinia 99, Seventh International Waste Management and Landfill Symposium, S. Margherita di Pula, Cagliari, Italy; 4-8 October 1999. Vol II pp 33-41.

Powrie, W. and Beaven, R.P. (1998) *Hydraulic conductivity of waste - current research and implications for leachate management* Waste Management November 1998 pp22-23.

Powrie, W. and Beaven, R.P. (1999) *The hydraulic properties of household waste and implications for landfills* Proceedings of the Institution of Civil Engineers, Geotechnical Engineering, Vol 137, Oct 1999, pp235-247.

Powrie, W.; Beaven, R.P. and Harkness. (1999). *Applicability of soil mechanics principles to household waste* Proceedings Sardinia 99, Seventh International Waste Management and Landfill Symposium, S. Margherita di Pula, Cagliari, Italy; 4-8 October 1999. Vol III, pp429-436.

Powrie, W.; Richards, D. and Beaven, R.P. (1998). *Compression of waste and implications for practice.* Proc of the Symposium on Geotechnical Engineering of landfills. pp 3-18. Held at Nottingham Trent University 24 September 1998 by the East Midlands Geotechnical Group of the ICE. Ed. Dixon, N. et al; Pub. Thomas Telford Ltd. ISBN 0 7277 2708 7.

Walker, A.N; Beaven, R.P. and Powrie, W.P. (1997). *Overcoming problems in the development of a high rate flushing bioreactor* Proc. 6th International Sardinia Landfill Symposium. S. Margherita di Pula, Cagliari, Italy. Vol I pp 397-408. October 1997.

Walker, A.N; Beaven, R.P. and Powrie, W.P. (1998). *A conceptual design for sustainable landfill* Proceedings of the 18th annual IAH groundwater seminar, Portlaoise, Ireland; April 1998. pp1-13.

Appendix A - Specifications

Fabrication of compression cell

It is not feasible to include the complete design of the compression cell in this thesis. Detailed design drawings are now held by the Department of Civil and Environmental Engineering at the University of Southampton and may be available on request.

Hydraulic and electrical circuit diagrams

A schematic of the hydraulic system is provided in Figure 3.6. Figure A1 shows the electrical circuit that controls the hydraulic solenoids within this circuit.

Figure A2 shows the master control circuit relating to the safety devices and the proximity switches.

Figure A3 shows the main electrical power circuits.

Water recirculation pump

A water recirculation pump was used to pump water or leachate into the header tanks.

Make:	Stork
Type:	Fre-Flow open impeller electrical pump
Model:	40-110 RNK /WP
Electrical rating:	415/3/50 Hz; 1.1 kW
rpm:	2900
Flow rate:	24 m^3/hr at 8 metres head
	10 m^3/hr at 14 metres head
	0 m^3/hr at 18 metres head
Supplier:	Stork Pumps Ltd
	Meadow Brook Industrial Estate
	Maxwell Way, Crawley
	West Sussex, RH10 2SA
	01293 553495

Figure A1 Hydraulic control circuit

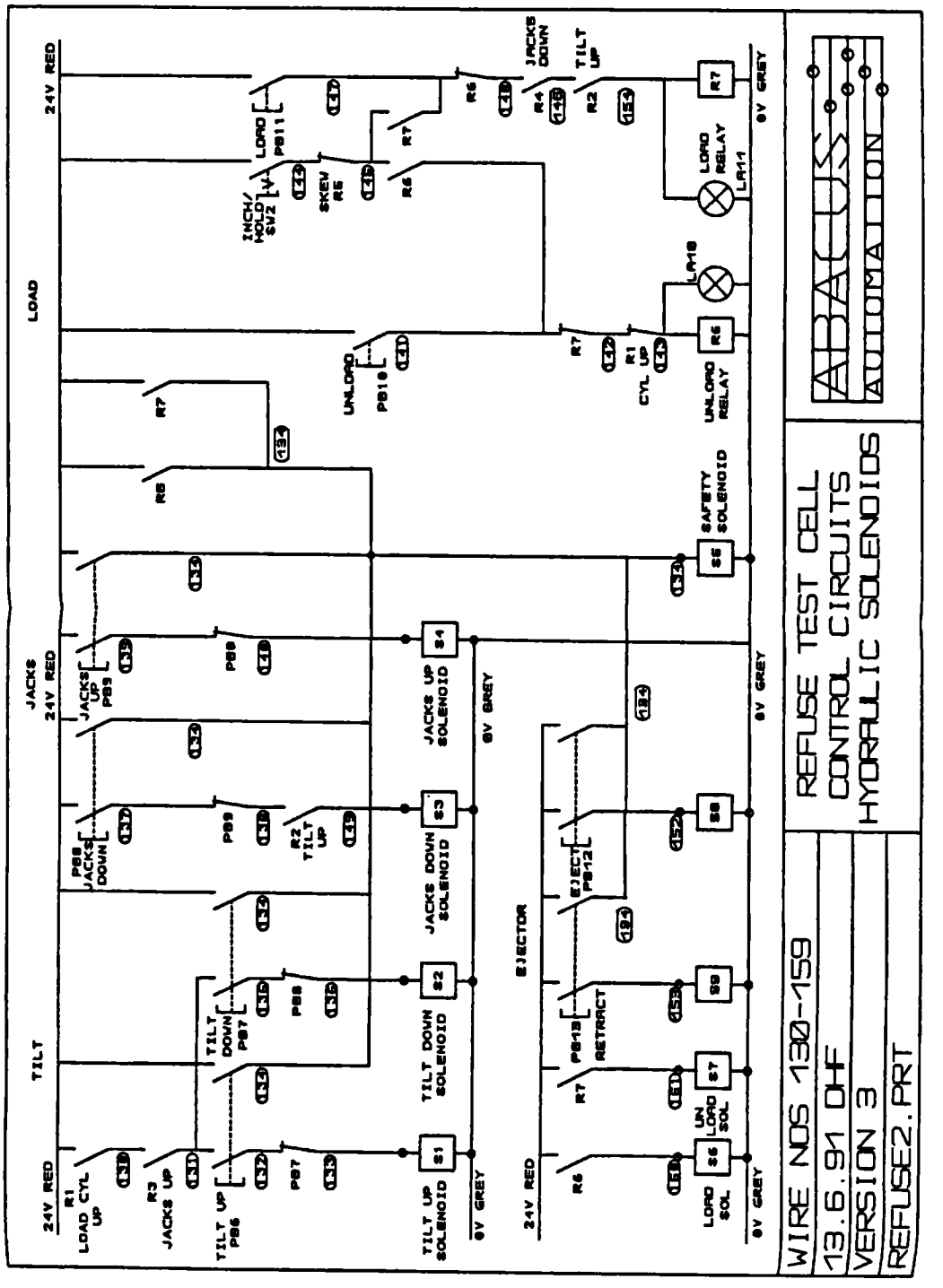

Figure A2 Master electrical circuit

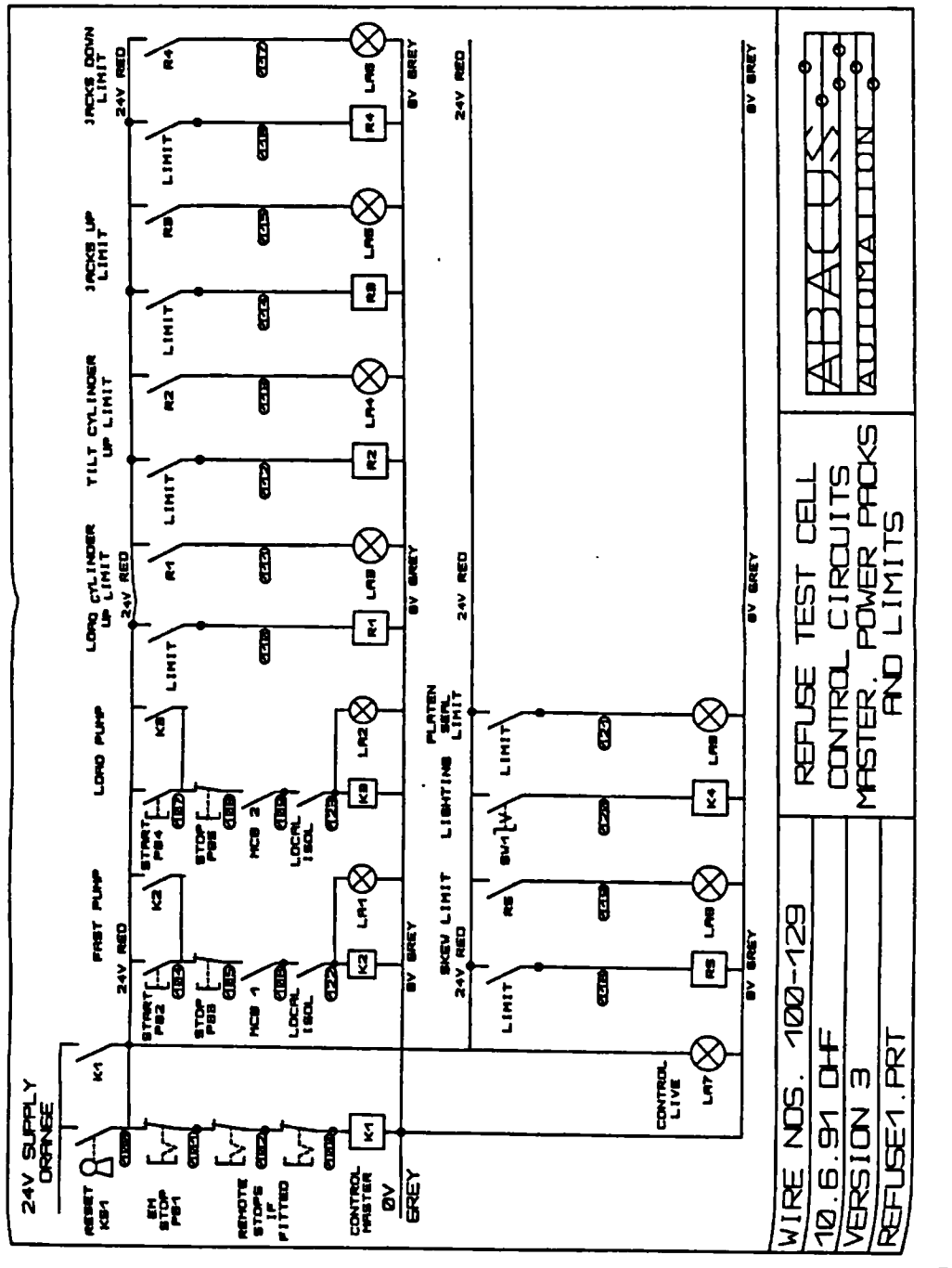

Figure A3 Power circuits

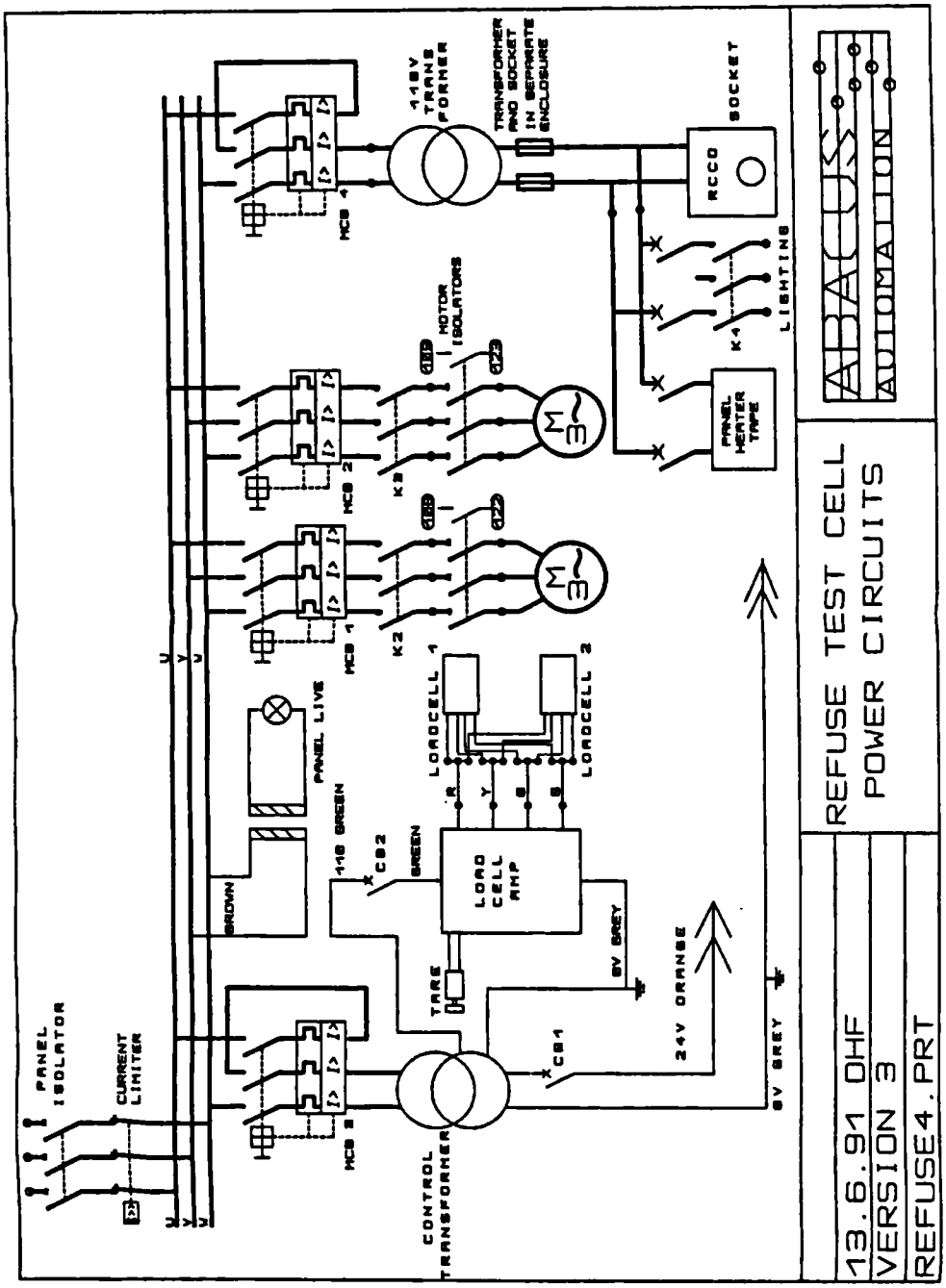

Hydraulic pumps

Two hydraulic pumps (Load and Fast) were used in the operation of the compression cell. Each pump consisted of an electrical motor connected to a hydraulic pump unit through a bell housing and a flexible shaft coupling.

Electrical motors

	Load Pump	**Fast Pump**
Make:	EFACEC	EFACEC
Model:	BF5 90L 44	BF5 132 M84
	IM1001	IM2001
	6205 2Z	6208 2Z
Power:	3~ 380-415v	3~ 380-415v
Rating	3.9 A	16.5 A
RPM	~1380	~1435
Weight	13.4 kg	45 kg
Serial No:	900700698	913050693
Supplier:	AER Ltd	AER Ltd
	Ashford	Ashford
	Kent	Kent
	01233 632777	01233 632777

Hydraulic pump units

	Load Pump	**Fast Pump**
Make:	VOITH	MARZOCCHI
Type:	Radial Piston Pump	Gear Pump
Model:	R 0.9	Series 2 D25
Flow rate	0.9 litres/min	15 l/min
	at 1380 rpm	at 1435 rpm
Max. operating pressure	>250 bar	230 bar
Supplier	Koppen & Lethen	
	Newark	
	01636 676974	

Load cells

Load cells were used to measure the total mass of the compression cell and its contents. Initially only two cells were used under two of the four mounting points. This was increased to four midway through the research.

Make:	Thames Side
Type:	Folded shear beam load cell
Model:	T90-103
Capacity:	10,000 kg
Supply voltage:	10Vdc
Rated output/ sensitivity:	2.0 mV/V
Deviation from rated output:	<±0.25% of rated output
Hysteresis and non linearity error:	<±0.05% of rated output
Repeatability	<±0.025% of rated output
Creep (max change under normal load)	<±0.03% of rated output
Temperature effect:	<±0.008% of rated output per °C
Supplier:	Thames Side Ltd
	Unit 3, Southview Park, Caversham
	Reading, Berks, RG4 0AF
	0118 9474379

Electromagnetic flow recorders

Three electromagnetic flow meters were used to monitor the flow of water in the various experiments.

Make:	Endress & Hauser
Type:	Electromagnetic flow recorder
Model:	Discomag DMI 6531
Nominal diameter:	25 mm
Lining:	PTFE
Nominal measuring range:	0-10 m^3/hr
Accuracy:	1%
Input voltage:	110v 50Hz
Current output:	4-20mA
Totaliser:	Hengstler 6 digit resetable counter
	24v DC
Supplier:	Endress & Hauser Ltd
	Ledson Rd, Manchester
	0161 9980321

Appendix B - Analysis of differential compression data

Slab Analysis for DM2

						Cell 013	Cell 014	Cell 015
Dry mass of waste below total pressure cell (kg)						0	1121	2428
Depth of cell below top platen at start of DM2COM1 (mm)						2492	1457	309
Depth of Lower gravel		150 mm						
Depth of Upper gravel		100 mm						
		SLAB NUMBER						
		1	2	3	4	5	6	7
Conditions at 10:25 18/5/92 during DM2C2COM:-								
Average wet density (approx) = 0.88 t/m3								
Average dry density = 0.426 t/m3								
Base level of slab	mm AD	2050	2200	2500	2800	3200	3500	3800
Top level of slab	mm AD	2200	2500	2800	3200	3500	3800	3990
Mid level of slab	mm AD	2125	2350	2650	3000	3350	3650	3895
Thickness of slab	mm	150	300	300	400	300	300	190
Cumulative thickness of waste	mm	150	450	750	1150	1450	1750	1940
Wet mass of waste in slab	kg	414.7	829.4	829.4	1105.8	829.4	829.4	525.3
Wet density of slab	t/m3	0.88	0.88	0.88	0.88	0.88	0.88	0.88
Dry mass of waste in slab	kg	201.0	401.9	401.9	535.9	401.9	401.9	254.5
Dry density of slab	t/m3	0.426	0.426	0.426	0.426	0.426	0.426	0.426
Total measured compression to end of DM2COM2	mm	5	30	55	100	145	210	286
Differential compression of slab	mm	5	25	25	45	45	65	76
New base level of compressed slab	mm AD	2050	2195	2470	2745	3100	3355	3590
New top level of compressed slab	mm AD	2195	2470	2745	3100	3355	3590	3704
New slab thickness	mm	145	275	275	355	255	235	114
Extrapolate compression to end of Applied stress of 87 kPa (i.e. start of DM2C3COM)								
Calculated slab thickness at start of DM3C2COM	mm	140.66	266.77	266.77	344.38	247.37	227.97	110.59
Base level of compressed slab at end of 87 kPa	mm AD	2050.0	2190.7	2457.4	2724.2	3068.6	3315.9	3543.9
Top level of compressed slab at end of 87 kPa	mm AD	2190.7	2457.4	2724.2	3068.6	3315.9	3543.9	3654.5
Mid level of slab	mm AD	2120.3	2324.0	2590.8	2896.4	3192.3	3429.9	3599.2
Dry mass in slab	kg	200.96	401.91	401.91	535.88	401.91	401.91	254.54
Cumulative mass in slabs	kg	200.96	602.87	1004.78	1540.66	1942.57	2344.48	2599.02
Recalulated dry density	t/m3	0.455	0.480	0.480	0.495	0.517	0.561	0.733
Calculated elevation of Pressure Cell 013	mm AD	1975.0						
Calculated elevation of Pressure Cell 014	mm AD				2798.9			
Calculated elevation of Pressure Cell 015	mm AD							3580.2
Depth of cell 015 below upper platen	mm							174
DM2C3COM Applied stress = 165 kPa								
Re-define slabs								
Base level of slab	mm AD	2050	2200	2500	2800	3200	3500	
Top level of slab	mm AD	2200	2500	2800	3200	3500	3653	
Mid level of slab	mm AD	2125	2350	2650	3000	3350	3576.5	
Dry mass of waste in slab	kg	215.03	451.97	455.73	631.46	512.87	328.51	
Dry density of slab	t/m3	0.456	0.480	0.484	0.503	0.544	0.683	
Compression during DM2C3COM								
Total measured compression to end of DM2C3COM	mm	5	20	40	80	113	127	
Differential compression of slab	mm	5	15	20	40	33	14	
New base level of compressed slab	mm AD	2050	2195	2480	2760	3120	3387	
New top level of compressed slab	mm AD	2195	2480	2760	3120	3387	3526	
New slab thickness	mm	145	285	280	360	267	139	
Extrapolate compression to end of Applied stress of 165 kPa (i.e. start of DM2C4COM)								
Calculated slab thickness at end of 165 kPa	mm	144.24	283.51	278.53	358.11	265.60	138.27	
Base level of compressed slab at end of 165 kPa	mm AD	2050.0	2194.2	2477.7	2756.3	3114.4	3380.0	
Top level of compressed slab at end of 165 kPa	mm AD	2194.2	2477.7	2756.3	3114.4	3380.0	3518.3	
Mid level of slab	mm AD	2122.1	2336.0	2617.0	2935.3	3247.2	3449.1	
Dry mass in slab	kg	215.03	451.97	455.73	631.46	512.87	328.51	
Cumulative mass in slabs	kg	215.03	667.00	1122.73	1754.19	2267.06	2595.58	
Recalulated dry density	t/m3	0.475	0.507	0.521	0.561	0.615	0.756	
Calculated elevation of Pressure Cell 013	mm AD	2040.0						
Calculated elevation of Pressure Cell 014	mm AD			2755.2				
Calculated elevation of Pressure Cell 015	mm AD						3447.7	
Depth of cell 015 below upper platen	mm						171	
DM2C4COM Applied stress = 322 kPa								
Re-define slabs								
Base level of slab	mm AD	2050	2200	2500	2800	3200		
Top level of slab	mm AD	2200	2500	2800	3200	3518		
Mid level of slab	mm AD	2125	2350	2650	3000	3359		
Dry mass of waste in slab	kg	224.21	479.20	496.41	719.68	675.45		
Dry density of slab	t/m3	0.476	0.508	0.527	0.573	0.676		
Compression during DM2C4COM								
Total measured compression to end of DM2C4COM	mm	14	47	89	151	207		
Differential compression of slab	mm	14	33	42	62	56		
New base level of compressed slab	mm AD	2050	2186	2453	2711	3049		
New top level of compressed slab	mm AD	2186	2453	2711	3049	3311		
New slab thickness	mm	136	267	258	338	262		

Slab Analysis for DM2

						Cell 013	Cell 014	Cell 015
Dry mass of waste below total pressure cell (kg)						0	1121	2428
Depth of cell below top platen at start of DM2COM1	(mm)					2492	1457	309
Depth of Lower gravel	150 mm							
Depth of Upper gravel	100 mm							
		SLAB NUMBER						
		1	2	3	4	5	6	7
Extrapolate compression to end of Applied stress of 322 kPa (i.e. start of DM2C5COM)								
Calculated slab thickness at start of DM2C5COM	mm	136.00	267.00	258.00	338.00	262.00		
Base level of compressed slab at end of 322 kPa	mm AD	2050.0	2186.0	2453.0	2711.0	3049.0		
Top level of compressed slab at end of 322 kPa	mm AD	2186.0	2453.0	2711.0	3049.0	3311.0		
Mid level of slab	mm AD	2118.0	2319.5	2582.0	2880.0	3180.0		
Dry mass in slab	kg	224.21	479.20	496.41	719.68	675.45		
Cumulative mass in slabs	kg	224.21	703.41	1199.82	1919.50	2594.95		
Recalulated dry density	t/m3	0.525	0.571	0.612	0.678	0.821		
Calculated elevation of Pressure Cell 013	mm AD	1975.0						
Calculated elevation of Pressure Cell 014	mm AD			2670.0				
Calculated elevation of Pressure Cell 015	mm AD					3246.2		
Depth of cell 015 below upper platen	mm					165		
DM2C5COM Applied stress = 603 kPa								
Re-define slabs								
Base level of slab	mm AD	2050	2200	2500	2800	3200		
Top level of slab	mm AD	2200	2500	2800	3200	3308		
Mid level of slab	mm AD	2125	2350	2650	3000	3254		
Dry mass of waste in slab	kg	249.34	544.51	595.48	919.46	286.16	0.00	
Dry density of slab	t/m3	0.5291	0.58	0.632	0.732	0.843		
Compression during DM2COM5								
Total measured compression to end of DM2COM5		10	30	63	122	141		
Differential compression of slab		10	20	33	59	19		
New base level of compressed slab	mm AD	2050	2190	2470	2737	3078		
New top level of compressed slab	mm AD	2190	2470	2737	3078	3167		
New slab thickness		140	280	267	341	89		
Extrapolate compression to end of Applied stress of 603 kPa (i.e. end of test)								
Calculated slab thickness at start of DM3C6COM	mm	140.00	280.00	267.00	341.00	89.00		
Base level of compressed slab at end of 322 kPa	mm AD	2050.0	2190.0	2470.0	2737.0	3078.0		
Top level of compressed slab at end of 322 kPa	mm AD	2190.0	2470.0	2737.0	3078.0	3167.0		
Mid level of slab	mm AD	2120.0	2330.0	2603.5	2907.5	3122.5		
Dry mass in slab	kg	249.34	544.51	595.48	919.46	286.16		
Cumulative mass in slabs	kg	249.34	793.84	1389.33	2308.79	2594.95		
Recalulated dry density	t/m3	0.567	0.619	0.710	0.858	1.023		
Calculated elevation of Pressure Cell 013	mm AD	1975.0						
Calculated elevation of Pressure Cell 014	mm AD			2616.7				
Calculated elevation of Pressure Cell 015	mm AD					3115.1		
Depth of cell 015 below upper platen	mm					152		
DM2C5COM Applied stress = 603 kPa								
Re-define slabs								
Base level of slab	mm AD	2050	2200	2500	2800			
Top level of slab	mm AD	2200	2500	2800	3167			
Mid level of slab	mm AD	2125	2350	2650	2983.5			
Dry mass of waste in slab	kg	268.78	591.97	698.44	1035.76		0.00	
Dry density of slab	t/m3	0.5704	0.63	0.741	0.898			

Slab Analysis for DM3

		Cell 013	Cell 014	Cell 015	Total
Dry mass of waste below total pressure cell (kg)		0	1683.66	2313.3	2671.7
Depth of cell below top platen during DM3COM1 (mm)		2483	1037	496	
Depth of Lower gravel	145 mm				
Depth of upper gravel	188 mm				

		SLAB NUMBER 1	2	3	4	5	6	7	8
Conditions at 12:01 10/2/95 during DM3COM1:-									
Average wet density = 0.58 t/m3									
Average dry density = 0.37 t/m3									
Base level of slab	mm AD	2045	2200	2500	2800	3200	3800	4100	
Top level of slab	mm AD	2200	2500	2800	3200	3800	4100	4340	
Mid level of slab	mm AD	2122.5	2350	2650	3000	3500	3950	4220	
Thickness of slab	mm	155	300	300	400	600	300	240	
Cumulative thickness of waste	mm	155	455	755	1155	1755	2055	2295	
Wet mass of waste in slab	kg	248.3	494.8	512.7	703.7	1085.7	554.2	448.6	
Wet density of slab	t/m3	0.51	0.525	0.544	0.56	0.578	0.588	0.595	
Dry mass of waste in slab	kg	163 9	326.6	338 4	464.5	716.6	365 8	296 1	
Dry density of slab	t/m3	0.337	0.347	0.359	0.370	0.380	0.388	0.393	
Total interpolated compression to end of DM3COM1	mm	2	4	6	13	40	69	111	
Differential compression of slab	mm	2	2	2	7	27	29	42	
New base level of compressed slab	mm AD	2045	2198	2496	2794	3187	3760	4031	
New top level of compressed slab	mm AD	2198	2496	2794	3187	3760	4031	4229	
New slab thickness	mm	153	298	298	393	573	271	198	
Extrapolate compression to end of Applied stress of 40 kPa (i.e. start of DM3C2COM)									
Calculated slab thickness at start of DM3C2COM	mm	150.41	292.95	292.95	386.34	563.29	266.41	194.65	
Base level of compressed slab at end of 40 kPa	mm AD	2045.0	2195.4	2488.4	2781.3	3167.7	3730.9	3997.4	
Top level of compressed slab at end of 40 kPa	mm AD	2195.4	2488.4	2781.3	3167.7	3730.9	3997.4	4192 0	
Mid level of slab	mm AD	2120.2	2341.9	2634.8	2974.5	3449.3	3864.1	4094.7	
Dry mass in slab	kg	163.91	326.57	338.39	464.45	716.58	365.76	296.09	
Cumulative mass in slabs	kg	163.91	490.47	828.86	1293 32	2009.90	2375.66	2671.75	
Recalculated dry density	t/m3	0.347	0.355	0.368	0.383	0.405	0.437	0.484	
Calculated elevation of Pressure Cell 013	mm AD	2040.0							
Calculated elevation of Pressure Cell 014	mm AD					3474.5			
Calculated elevation of Pressure Cell 015	mm AD						3951.9		
Depth of Cell 013 below upper platen	mm	2340							
Depth of Cell 014 below upper platen	mm					906			
Depth of Cell 015 below upper platen	mm						428		
DM3C2COM Applied stress = 87 kPa									
Re-define slabs									
Base level of slab	mm AD	2045	2200	2500	2800	3200	3500	3800	
Top level of slab	mm AD	2200	2500	2800	3200	3500	3800	4192	
Mid level of slab	mm AD	2122.5	2350	2650	3000	3350	3650	3996	
Dry mass of waste in slab	kg	169.03	334.90	347.41	483.14	358.37	382 62	596.30	
Dry density of slab	t/m3	0.347	0.355	0.369	0.384	0.380	0.406	0.484	
Compression during DM3C2COM									
Total measured compression to end of DM3C2COM	mm	4	14	28	50	70	93	133	
Differential compression of slab	mm	4	10	14	22	20	23	40	
New base level of compressed slab	mm AD	2045	2196	2486	2772	3150	3430	3707	
New top level of compressed slab	mm AD	2196	2486	2772	3150	3430	3707	4059	
New slab thickness	mm	151	290	286	378	280	277	352	
Extrapolate compression to end of Applied stress of 87 kPa (i.e. start of DM3C3COM)									
Calculated slab thickness at end of 87 kPa	mm	148.68	285.54	281.60	372.18	275.69	272.74	346.58	
Base level of compressed slab at end of 87 kPa	mm AD	2045.0	2193.7	2479.2	2760.8	3133.0	3408.7	3681.4	
Top level of compressed slab at end of 87 kPa	mm AD	2193.7	2479.2	2760.8	3133.0	3408.7	3681.4	4028.0	
Mid level of slab	mm AD	2119.3	2336.4	2620.0	2946.9	3270.8	3545.0	3854.7	
Dry mass in slab	kg	169 03	334.90	347.41	483.14	358.37	382.62	596.30	
Cumulative mass in slabs	kg	169 03	503.92	851.33	1334.47	1692.83	2075.45	2671.75	
Recalculated dry density	t/m3	0.362	0.373	0.393	0.413	0.414	0.447	0.548	
Calculated elevation of Pressure Cell 013	mm AD	2040.0							
Calculated elevation of Pressure Cell 014	mm AD					3401.6			
Calculated elevation of Pressure Cell 015	mm AD							3819.7	
Depth of Cell 013 below upper platen	mm	2176							
Depth of Cell 014 below upper platen	mm					814			
Depth of Cell 015 below upper platen	mm							396	
DM3C3COM Applied stress = 165 kPa									
Re-define slabs									
Base level of slab	mm AD	2045	2200	2500	2800	3200	3500	3800	
Top level of slab	mm AD	2200	2500	2800	3200	3500	3800	4028	
Mid level of slab	mm AD	2122.5	2350	2650	3000	3350	3650	3914	
Dry mass of waste in slab	kg	176.44	353.12	372.64	519.37	399 37	458 53	392.28	
Dry density of slab	t/m3	0.362	0.375	0.395	0.413	0.424	0.487	0.548	
Compression during DM3C3COM									
Total measured compression to end of DM3C3COM	mm	11	30	53	90	135	180	235	
Differential compression of slab	mm	11	19	23	37	45	45	55	
New base level of compressed slab	mm AD	2045	2189	2470	2747	3110	3365	3620	
New top level of compressed slab	mm AD	2189	2470	2747	3110	3365	3620	3793	
New slab thickness	mm	144	281	277	363	255	255	173	
Extrapolate compression to end of Applied stress of 165 kPa (i.e. start of DM3C4COM)									
Calculated slab thickness at start of DM3C4COM	mm	140.13	273.44	269.55	353.24	248.14	248.14	168.35	
Base level of compressed slab at end of 165 kPa	mm AD	2045.0	2185.1	2458.6	2728.1	3081.4	3329.5	3577.7	
Top level of compressed slab at end of 165 kPa	mm AD	2185.1	2458.6	2728.1	3081.4	3329.5	3577.7	3746.0	
Mid level of slab	mm AD	2115.1	2321.9	2593.3	2904.7	3205.4	3453.6	3661.8	
Dry mass in slab	kg	176.44	353.12	372.64	519.37	399.37	458.53	392.28	
Cumulative mass in slabs	kg	176.44	529.57	902.20	1421.57	1820.94	2279.47	2671.75	
Recalculated dry density	t/m3	0.401	0.411	0.440	0.468	0.512	0.588	0.742	
Calculated elevation of Pressure Cell 013	mm AD	2040.0							
Calculated elevation of Pressure Cell 014	mm AD					3244.2			
Calculated elevation of Pressure Cell 015	mm AD						3596.0		
Depth of Cell 013 below upper platen	mm	1894							
Depth of Cell 014 below upper platen	mm					690			
Depth of Cell 015 below upper platen	mm						338		

Slab Analysis for DM3

						Cell 013	Cell 014	Cell 015	Total
Dry mass of waste below total pressure cell (kg)						0	1683.66	2313.3	2671 7
Depth of cell below top platen during DM3COM1 (mm)						2483	1037	496	
Depth of Lower gravel	145 mm								
Depth of upper gravel	188 mm								

		SLAB NUMBER							
		1	2	3	4	5	6	7	8
DM3C4/5COM Applied stress = 244/322 kPa									
Re-define slabs									
Base level of slab	mm AD	2045	2200	2350	2500	2650	2800	3200	3500
Top level of slab	mm AD	2200	2350	2500	2650	2800	3200	3500	3748
Mid level of slab	mm AD	2122.5	2275	2425	2575	2725	3000	3350	3623
Dry mass of waste in slab	kg	195.65	193.71	197.48	207.36	213.68	604.62	523.48	535 76
Dry density of slab	t/m3	0.4018	0.41	0.419	0.440	0.453	0.481	0.555	0.693
Compression during DM3COM4&5									
Total measured compression to end of DM3COM5		8	18	34	52	75	149	210	270
Differential compression of slab		8	10	16	18	23	74	61	60
New base level of compressed slab	mm AD	2045	2192	2332	2466	2598	2725	3051	3290
New top level of compressed slab	mm AD	2192	2332	2466	2598	2725	3051	3290	3476
New slab thickness		147	140	134	132	127	326	239	186
Extrapolate compression to end of Applied stress of 322 kPa (i.e. start of DM3C6COM)									
Calculated slab thickness at start of DM3C6COM	mm	141.97	135.21	129.41	127.48	122.65	314.84	230.82	179.63
Base level of compressed slab at end of 322 kPa	mm AD	2045.0	2187.0	2322.2	2451.6	2579.1	2701 7	3016.6	3247 4
Top level of compressed slab at end of 322 kPa	mm AD	2187.0	2322.2	2451.6	2579.1	2701.7	3016.6	3247.4	3427.0
Mid level of slab	mm AD	2116.0	2254.6	2386.9	2515.3	2640.4	2859.1	3132.0	3337.2
Dry mass in slab	kg	195.65	193.71	197.48	207.36	213.68	604.62	523.48	535 76
Cumulative mass in slabs	kg	195 65	389.36	586.84	794.20	1007.88	1612.50	2135.98	2671.75
Recalulated dry density	t/m3	0 439	0 456	0.486	0.518	0.555	0.611	0.722	0.949
Calculated elevation of Pressure Cell 013	mm AD	2040.0							
Calculated elevation of Pressure Cell 014	mm AD							3047.9	
Calculated elevation of Pressure Cell 015	mm AD								3306.8
Depth of Cell 013 below upper platen	mm	1575							
Depth of Cell 014 below upper platen	mm							567	
Depth of Cell 015 below upper platen	mm								308
DM3C6COM Applied stress = 603 kPa									
Re-define slabs									
Base level of slab	mm AD	2045	2200	2350	2500	2650	2800	3200	
Top level of slab	mm AD	2200	2350	2500	2650	2800	3200	3427	
Mid level of slab	mm AD	2122.5	2275	2425	2575	2725	3000	3313.5	
Dry mass of waste in slab	kg	214.32	217.50	233.77	252.19	278.85	831.92	643.19	
Dry density of slab	t/m3	0.440	0.462	0.496	0.535	0.592	0.662	0.902	
Compression during DM3COM6									
Total measured compression to end of DM3COM5	mm	10	20	35	50	68	135	188	
Differential compression of slab	mm	10	10	15	15	18	67	53	
New base level of compressed slab	mm AD	2045	2190	2330	2465	2600	2732	3065	
New top level of compressed slab	mm AD	2190	2330	2465	2600	2732	3065	3239	
Mid level of slab	mm AD	2117.5	2260.0	2397.5	2532.5	2666.0	2898.5	3152.0	
New slab thickness	mm	145	140	135	135	132	333	174	
Dry mass in slab	kg	214.32	217.50	233.77	252.19	278.85	831.92	643.19	
Cumulative mass in slabs	kg	214.32	431.82	665.59	917.78	1196.63	2028 55	2671.75	
Recalulated dry density		0.470	0.495	0.551	0.595	0.672	0.795	1.177	
Calculated elevation of Pressure Cell 013	mm AD	2040.0							
Calculated elevation of Pressure Cell 014	mm AD						2926.9		
Calculated elevation of Pressure Cell 015	mm AD							3142.0	
Depth of Cell 013 below upper platen	mm	1387							
Depth of Cell 014 below upper platen	mm						500		
Depth of Cell 015 below upper platen	mm							285	

Slab Analysis for AG1

					Cell 013	Cell 014	Cell 015	Total
Dry mass of waste below total pressure cell (kg)					0	1168	3492	3825
Depth of cell below top platen at start (mm)					2410	1711	319	
Depth of Lower gravel		150 mm						
Depth of upper gravel		120 mm						
		SLAB NUMBER						
		1	2	3	4	5	6	7
Conditions at 10:55 25/7/95 AG1Load:-								
Average wet density = 0.91 t/m3								
Average dry density = 0.53 t/m3								
Base level of slab	mm AD	2050	2200	2500	2800	3200	3500	3800
Top level of slab	mm AD	2200	2500	2800	3200	3500	3800	4340
Mid level of slab	mm AD	2125	2350	2650	3000	3350	3650	4070
Thickness of slab	mm	150	300	300	400	300	300	540
Cumulative thickness of waste	mm	150	450	750	1150	1450	1750	2290
Wet mass of waste in slab	kg	429.0	858.1	858.1	1144.1	858.1	858 1	1544.5
Wet density of slab	t/m3	0.91	0.91	0.91	0.91	0.91	0.91	0.91
Dry mass of waste in slab	kg	250.6	501.1	501.1	668.2	501.1	501.1	902.0
Dry density of slab	t/m3	0.532	0.532	0.532	0.532	0.532	0.532	0.532
Total interpolated compression to end of AG1COM1	mm	5	14	45	85	130	180	334
Differential compression of slab	mm	5	9	31	40	45	50	154
New base level of compressed slab	mm AD	2050	2195	2486	2755	3115	3370	3620
New top level of compressed slab	mm AD	2195	2486	2755	3115	3370	3620	4006
New slab thickness	mm	145	291	269	360	255	250	386
Extrapolate compression to end of Applied stress of 40 kPa (i.e. start of AG1C2COM)								
Calculated slab thickness at start of AG1C2COM	mm	141.52	284.01	262.54	351.35	248.87	243.99	376.72
Base level of compressed slab at end of 40 kPa	mm AD	2050.0	2191.5	2475.5	2738.1	3089.4	3338.3	3582.3
Top level of compressed slab at end of 40 kPa	mm AD	2191.5	2475.5	2738.1	3089.4	3338.3	3582.3	3959.0
Mid level of slab	mm AD	2120.8	2333.5	2606.8	2913.7	3213.8	3460.3	3770.6
Dry mass in slab	kg	250.56	501.12	501.12	668.16	501.12	501.12	902.01
Cumulative mass in slabs	kg	250 56	751.68	1252.80	1920.95	2422.07	2923.19	3825.20
Recalulated dry density	t/m3	0.564	0.562	0.608	0.605	0.641	0.654	0.762
Calculated elevation of Pressure Cell 013	mm AD	2020.0						
Calculated elevation of Pressure Cell 014	mm AD				2693.5			
Calculated elevation of Pressure Cell 015	mm AD							3819.8
Depth of Cell 013 below upper platen	mm	2059						
Depth of Cell 014 below upper platen	mm				1386			
Depth of Cell 015 below upper platen	mm							259
AG1C2COM Applied stress = 87 kPa								
Re-define slabs								
Base level of slab	mm AD	2050	2200	2500	2800	3200	3500	3800
Top level of slab	mm AD	2200	2500	2800	3200	3500	3800	3959
Mid level of slab	mm AD	2125	2350	2650	3000	3350	3650	3879.5
Dry mass of waste in slab	kg	265.53	532.87	572.19	773.05	610.58	690.29	380.70
Dry density of slab	t/m3	0.563	0.565	0.607	0.615	0.648	0.732	0.762
Compression during AG1C2COM								
Total measured compression to end of AG1C2COM	mm	2	7	17	35	55	88	135
Differential compression of slab	mm	2	5	10	18	20	33	47
New base level of compressed slab	mm AD	2050	2198	2493	2783	3165	3445	3712
New top level of compressed slab	mm AD	2198	2493	2783	3165	3445	3712	3824
New slab thickness	mm	148	295	290	382	280	267	112
Extrapolate compression to end of Applied stress of 87 kPa (i.e. start of AG1C3COM)								
Calculated slab thickness at end of 87 kPa	mm	146.33	291.67	286.73	377.69	276 84	263.99	110.74
Base level of compressed slab at end of 87 kPa	mm AD	2050.0	2196.3	2488.0	2774.7	3152.4	3429 3	3693.3
Top level of compressed slab at end of 87 kPa	mm AD	2196.3	2488.0	2774.7	3152.4	3429.3	3693.3	3804.0
Mid level of slab	mm AD	2123.2	2342.2	2631.4	2963.6	3290.9	3561.3	3748.6
Dry mass in slab	kg	265 53	532.87	572.19	773.05	610.58	690 29	380 70
Cumulative mass in slabs	kg	265.53	798.40	1370.59	2143 63	2754.21	3444.50	3825 20
Recalulated dry density	t/m3	0 578	0.582	0.635	0.652	0.702	0.832	1.094
Calculated elevation of Pressure Cell 013	mm AD	2020.0						
Calculated elevation of Pressure Cell 014	mm AD			2673.2				
Calculated elevation of Pressure Cell 015	mm AD							3707.1
Depth of Cell 013 below upper platen	mm	1904						
Depth of Cell 014 below upper platen	mm			1251				
Depth of Cell 015 below upper platen	mm							217
AG1C3COM Applied stress = 165 kPa								
Re-define slabs								
Base level of slab	mm AD	2050	2200	2500	2800	3200	3500	
Top level of slab	mm AD	2200	2500	2800	3200	3500	3804	
Mid level of slab	mm AD	2125	2350	2650	3000	3350	3652	
Dry mass of waste in slab	kg	272 23	550 10	599 96	826.25	690 60	886 05	
Dry density of slab	t/m3	0.578	0 584	0.637	0.658	0.733	0.928	
Compression during AG1C3COM								
Total measured compression to end of AG1C3COM	mm	5	12	32	78	118	164	
Differential compression of slab	mm	5	7	20	46	40	46	
New base level of compressed slab	mm AD	2050	2195	2488	2768	3122	3382	
New top level of compressed slab	mm AD	2195	2488	2768	3122	3382	3640	
New slab thickness	mm	145	293	280	354	260	258	

Slab Analysis for AG1

					Cell 013	Cell 014	Cell 015	Total
Dry mass of waste below total pressure cell (kg)					0	1168	3492	3825
Depth of cell below top platen at start (mm)					2410	1711	319	
Depth of Lower gravel		150 mm						
Depth of upper gravel		120 mm						
		SLAB NUMBER						
		1	2	3	4	5	6	7
Extrapolate compression to end of Applied stress of 165 kPa (i.e. start of AG1C4COM)								
Calculated slab thickness at start of DM3C4COM	mm	144.18	291 34	278 42	352.00	258 53	256 54	
Base level of compressed slab at end of 165 kPa	mm AD	2050 0	2194.2	2485 5	2763.9	3115.9	3374 5	
Top level of compressed slab at end of 165 kPa	mm AD	2194.2	2485.5	2763.9	3115 9	3374.5	3631 0	
Mid level of slab	mm AD	2122.1	2339 9	2624 7	2939 9	3245.2	3502.7	
Dry mass in slab	kg	272.23	550 10	599.96	826.25	690.60	886.05	
Cumulative mass in slabs	kg	272.23	822.33	1422.29	2248.55	2939.15	3825.20	
Recalulated dry density	t/m3	0 601	0.601	0.686	0.747	0.850	1.099	
Calculated elevation of Pressure Cell 013	mm AD	2020.0						
Calculated elevation of Pressure Cell 014	mm AD			2645.9				
Calculated elevation of Pressure Cell 015	mm AD						3534.5	
Depth of Cell 013 below upper platen	mm	1731						
Depth of Cell 014 below upper platen	mm			1105				
Depth of Cell 015 below upper platen	mm						216	
AG1C4COM Applied stress = 322 kPa								
Re-define slabs								
Base level of slab	mm AD	2050	2200	2500	2650	2800	3200	3500
Top level of slab	mm AD	2200	2500	2650	2800	3200	3500	3631
Mid level of slab	mm AD	2125	2350	2575	2725	3000	3350	3565.5
Dry mass of waste in slab	kg	283.22	570.31	323.24	330.18	966.17	899.63	452 46
Dry density of slab	t/m3	0.6010	0.61	0.686	0.701	0.769	0.955	1.099
Compression during AG1COM4								
Total measured compression to end of AG1COM4		7	20	27	38	88	135	162
Differential compression of slab		7	13	7	11	50	47	27
New base level of compressed slab	mm AD	2050	2193	2480	2623	2762	3112	3365
New top level of compressed slab	mm AD	2193	2480	2623	2762	3112	3365	3469
New slab thickness		143	287	143	139	350	253	104
Extrapolate compression to end of Applied stress of 322 kPa (i.e. start of AG1C5COM)								
Calculated slab thickness at start of DM3C6COM	mm	141.89	284.78	141.89	137.92	347.29	251.04	103.19
Base level of compressed slab at end of 322 kPa	mm AD	2050.0	2191.9	2476 7	2618.6	2756.5	3103.8	3354.8
Top level of compressed slab at end of 322 kPa	mm AD	2191.9	2476.7	2618 6	2756.5	3103.8	3354.8	3458.0
Mid level of slab	mm AD	2120.9	2334.3	2547.6	2687.5	2930.1	3229.3	3406 4
Dry mass in slab	kg	283.22	570.31	323.24	330.18	966.17	899.63	452.46
Cumulative mass in slabs	kg	283.22	853.53	1176 77	1506.95	2473.12	3372.75	3825.20
Recalulated dry density	t/m3	0.635	0.637	0.725	0.762	0.886	1.141	1.396
Calculated elevation of Pressure Cell 013	mm AD	2020.0						
Calculated elevation of Pressure Cell 014	mm AD			2614.7				
Calculated elevation of Pressure Cell 015	mm AD							3382 0
Depth of Cell 013 below upper platen	mm	1558						
Depth of Cell 014 below upper platen	mm			963				
Depth of Cell 015 below upper platen	mm							196
AG1C5COM Applied stress = 603 kPa								
Re-define slabs								
Base level of slab	mm AD	2050	2200	2350	2500	2650	2800	3200
Top level of slab	mm AD	2200	2350	2500	2650	2800	3200	3458
Mid level of slab	mm AD	2125	2275	2425	2575	2725	3000	3329
Dry mass of waste in slab	kg	299 46	300 40	306.83	345 35	375.98	1189.96	1007 22
Dry density of slab	t/m3	0.635	0.637	0.651	0 733	0.798	0 947	1.243
Compression during AG1COM5								
Total measured compression to end of AG1COM5	mm	3	8	13	23	28	60	120
Differential compression of slab	mm	3	5	5	10	5	32	60
New base level of compressed slab	mm AD	2050	2197	2342	2487	2627	2772	3140
New top level of compressed slab	mm AD	2197	2342	2487	2627	2772	3140	3338
Mid level of slab	mm AD	2123 5	2269 5	2414.5	2557 0	2699 5	2956 0	3239 0
New slab thickness	mm	147	145	145	140	145	368	198
Dry mass in slab	kg	299 46	300 40	306 83	345 35	375 98	1189 96	1007 22
Cumulative mass in slabs	kg	299 46	599 86	906 69	1252 04	1628 02	2817 98	3825 20
Recalulated dry density		0 648	0.659	0.674	0 785	0 825	1 029	1 619
Calculated elevation of Pressure Cell 013	mm AD	2020 0						
Calculated elevation of Pressure Cell 014	mm AD				2592.9			
Calculated elevation of Pressure Cell 015	mm AD							3272 5
Depth of Cell 013 below upper platen	mm	1438						
Depth of Cell 014 below upper platen	mm				865			
Depth of Cell 015 below upper platen	mm							186

Appendix C - MODFLOW program listings

Source code for MAIN.for

```
C     ******************************************************************
C     MAIN CODE FOR U.S. GEOLOGICAL SURVEY MODULAR MODEL -- MODFLOW-96
C           BY MICHAEL G. MCDONALD AND ARLEN W. HARBAUGH
C     MODFLOW-88 documented in:
C           McDonald, M.G. and Harbaugh, A.W., 1988, A modular
C           three-dimensional finite-difference ground-water flow
C           model: U.S. Geological Survey Techniques of Water
C           Resources Investigations, Book 6, Chapter A1, 586 p.
C     MODFLOW-96 documented in:
C           Harbaugh, A.W. and McDonald, M.G., 1996, User's
C           documentation for the U.S. Geological Survey modular
C           finite-difference ground-water flow model: U.S. Geological
C           Survey Open-File Report 96-485
C-----VERSION 0950 23MAY1996 MAIN
C-----VERSION 1401 03DEC1996 -- added PCG2, STR1, IBS1, CHD1, GFD1,
C                               HFB1, TLK1, DE45, and RES1 as documented
C                               in USGS reports
C-----VERSION 2016 08APR1999 -- SDK package added
C     ******************************************************************
C
C        SPECIFICATIONS:
C     ------------------------------------------------------------------
C1------SPECIFY THE SIZE OF THE X ARRAY.  TO CHANGE THE SIZE OF THE
C1------X ARRAY, CHANGE VALUE OF LENX IN THE NEXT STATEMENT.
      PARAMETER (LENX=3000000)
      COMMON X(LENX)
      COMMON /FLWCOM/LAYCON(200)
      CHARACTER*16 VBNM(40)
      CHARACTER*80 HEADNG(2)
      DIMENSION VBVL(4,40),IUNIT(40)
      DOUBLE PRECISION DUMMY
      EQUIVALENCE (DUMMY,X(1))
      CHARACTER*20 CHEDFM,CDDNFM
      CHARACTER*80 FNAME
      LOGICAL EXISTS
      CHARACTER*4 CUNIT(40)
C ************************************************************************
C *        NEW CODE - CUNIT(28) = 'SDK'                                  ***********
C ************************************************************************
      DATA CUNIT/'BCF ','WEL ','DRN ','RIV ','EVT ','TLK ','GHB ',
     1           'RCH ','SIP ','DE4 ','SOR ','OC  ','PCG ','GFD ',
     2           '    ','HFB ','RES ','STR ','IBS ','CHD ','FHB ',
     3           '    ','    ','    ','    ','    ','    ','SDK ',
     4           '    ','    ','    ','    ','    ','    ','    ',
     5           '    ','    ','    ','    ','    '/
C     ------------------------------------------------------------------
C     set string for use if RCS ident command
      FNAME =
     &'$Id: modflw96.f,v 3.2 1998/01/09 19:19:39 rsregan Exp rsregan $'
      FNAME =
     &     '@(#)MODFLOW-96 - Modular 3-D Finite-Difference GW Flow Model'
      FNAME = '@(#)MODFLOW-96 - USGS TWRI, Book 6, Chap. A1, McDonald an
     &d Harbaugh'
      FNAME = '@(#)MODFLOW-96 - USGS OFR 96-485, Harbaugh and McDonald'
      FNAME =
     &      '@(#)MODFLOW-96 - Contact: h2osoft@usgs.gov'
      FNAME = '@(#)MODFLOW-96 - Version: 3.0 1996/12/03 includes MOC'
      FNAME =
     &      '@(#)MODFLOW-96 - Version: 3.1 1997/03/11 fixed HFB1FM call'
      FNAME = '@(#)MODFLOW-96 - Version: 3.2x 1998/01/09 includes FHB'
C     ------------------------------------------------------------------
      INUNIT=99
      IBUNIT=98
      IBOUTS=97
      IBATCH=0
      INQUIRE(FILE='modflow.bf',EXIST=EXISTS)
      IF(EXISTS) THEN
```

```
         IBATCH=1
         OPEN(UNIT=IBUNIT,FILE='modflow.bf',STATUS='OLD')
         OPEN(UNIT=IBOUTS,FILE='modbatch.rpt')
         WRITE(IBOUTS,*) ' USGS MODFLOW MODEL BATCH-MODE REPORT'
      END IF
C
C2------OPEN FILE OF FILE NAMES.
50    IF(IBATCH.GT.0) THEN
         READ(IBUNIT,'(A)',END=500) FNAME
         IF(FNAME.EQ.' ') GO TO 50
         WRITE(IBOUTS,'(1X,/1X,A)') FNAME
      ELSE
         WRITE(*,*) ' Enter the name of the NAME FILE:'
         READ(*,'(A)') FNAME
      END IF
      INQUIRE(FILE=FNAME,EXIST=EXISTS)
      IF(.NOT.EXISTS) THEN
         IF(IBATCH.GT.0) THEN
            WRITE(IBOUTS,*) ' Specified name file does not exist.'
            WRITE(IBOUTS,*) ' Processing will continue with the next ',
     1                      'name file in modflow.bf.'
         ELSE
            WRITE(*,*) ' File does not exist'
         END IF
         GO TO 50
      END IF
      OPEN(UNIT=INUNIT,FILE=FNAME,STATUS='OLD')
C
C3------DEFINE PROBLEM--ROWS,COLUMNS,LAYERS,STRESS PERIODS,PACKAGES.
      CALL BAS5DF(ISUM,HEADNG,NPER,ITMUNI,TOTIM,NCOL,NROW,NLAY,
     1        NODES,INBAS,IOUT,IUNIT,CUNIT,INUNIT,IXSEC,ICHFLG,IFREFM)
C
C4------ALLOCATE SPACE IN "X" ARRAY.
      CALL BAS5AL(ISUM,LENX,LCHNEW,LCHOLD,LCIBOU,LCCR,LCCC,LCCV,
     1              LCHCOF,LCRHS,LCDELR,LCDELC,LCSTRT,LCBUFF,LCIOFL,
     2              INBAS,ISTRT,NCOL,NROW,NLAY,IOUT,IAPART,IFREFM)
      IF(IUNIT(1).GT.0) CALL BCF5AL(ISUM,LENX,LCSC1,LCHY,
     1     LCBOT,LCTOP,LCSC2,LCTRPY,IUNIT(1),ISS,
     2     NCOL,NROW,NLAY,IOUT,IBCFCB,LCWETD,IWDFLG,LCCVWD,
     3     WETFCT,IWETIT,IHDWET,HDRY,IAPART,IFREFM)
      IF(IUNIT(2).GT.0) CALL WEL5AL(ISUM,LENX,LCWELL,MXWELL,NWELLS,
     1                 IUNIT(2),IOUT,IWELCB,NWELVL,IWELAL,IFREFM)
      IF(IUNIT(3).GT.0) CALL DRN5AL(ISUM,LENX,LCDRAI,NDRAIN,MXDRN,
     1                 IUNIT(3),IOUT,IDRNCB,NDRNVL,IDRNAL,IFREFM)
      IF(IUNIT(4).GT.0) CALL RIV5AL(ISUM,LENX,LCRIVR,MXRIVR,NRIVER,
     1            IUNIT(4),IOUT,IRIVCB,NRIVVL,IRIVAL,IFREFM)
      IF(IUNIT(5).GT.0) CALL EVT5AL(ISUM,LENX,LCIEVT,LCEVTR,LCEXDP,
     1            LCSURF,NCOL,NROW,NEVTOP,IUNIT(5),IOUT,IEVTCB,IFREFM)
      IF(IUNIT(6).GT.0) CALL TLK1AL(ISUM,LENX,NCOL,NROW,NLAY,
     1          LCRAT,LCZCB,LCA1,LCB1,LCALPH,LCBET,LCRM1,LCRM2,LCRM3,
     2          LCRM4,LCTL,LCTLK,LCSLU,LCSLD,NODES1,NM1,NM2,NUMC,
     3          NTM1,ITLKSV,ITLKRS,ITLKCB,ISS,IUNIT(6),IOUT)
      IF(IUNIT(7).GT.0) CALL GHB5AL(ISUM,LENX,LCBNDS,NBOUND,MXBND,
     1            IUNIT(7),IOUT,IGHBCB,NGHBVL,IGHBAL,IFREFM)
      IF(IUNIT(8).GT.0) CALL RCH5AL(ISUM,LENX,LCIRCH,LCRECH,NRCHOP,
     1            NCOL,NROW,IUNIT(8),IOUT,IRCHCB,IFREFM)
      IF(IUNIT(9).GT.0) CALL SIP5AL(ISUM,LENX,LCEL,LCFL,LCGL,LCV,
     1          LCHDCG,LCLRCH,LCW,MXITER,NPARM,NCOL,NROW,NLAY,
     2          IUNIT(9),IOUT,IFREFM)
      IF(IUNIT(10).GT.0) CALL DE45AL(ISUM,LENX,LCAU,LCAL,LCIUPP,
     1           LCIEQP,LCD4B,LCLRCH,LCHDCG,
     2           MXUP,MXLOW,MXEQ,MXBW,IUNIT(10),ITMX,ID4DIR,
     3           NCOL,NROW,NLAY,IOUT,ID4DIM)
      IF(IUNIT(11).GT.0) CALL SOR5AL(ISUM,LENX,LCA,LCRES,LCHDCG,LCLRCH,
     1       LCIEQP,MXITER,NCOL,NLAY,NSLICE,MBW,IUNIT(11),IOUT,IFREFM)
      IF(IUNIT(13).GT.0) CALL PCG2AL(ISUM,LENX,LCV,LCSS,LCP,LCCD,
     1       LCHCHG,LCLHCH,LCRCHG,LCLRCH,MXITER,ITER1,NCOL,NROW,NLAY,
     2       IUNIT(13),IOUT,NPCOND,LCIT1)
      IF(IUNIT(14).GT.0) CALL GFD1AL(ISUM,LENX,LCSC1,LCCDTR,LCCDTC,
     1     LCBOT,LCTOP,LCSC2,IUNIT(14),ISS,NCOL,NROW,NLAY,IOUT,IGFDCB)
      IF(IUNIT(16).GT.0) CALL HFB1AL(ISUM,LENX,LCHFBR,NHFB,IUNIT(16),       *HFB*
     1            IOUT)                                                     *HFB*
      IF(IUNIT(17).GT.0) CALL RES1AL(ISUM,LENX,LCIRES,LCIRSL,LCBRES,
     1  LCCRES,LCBBRE,LCHRES,LCHRSE,IUNIT(17),IOUT,NRES,IRESCB,
     2  NRESOP,IRESPT,NPTS,NCOL,NROW)
      IF(IUNIT(18).GT.0) CALL STR1AL(ISUM,LENX,LCSTRM,ICSTRM,MXSTRM,     STR1
```

```
     1                 NSTREM,IUNIT(18),IOUT,ISTCB1,ISTCB2,NSS,NTRIB,    STR1
     2                  NDIV,ICALC,CONST,LCTBAR,LCTRIB,LCIVAR,LCFGAR)    STR1
      IF (IUNIT(19).GT.0) CALL IBS1AL(ISUM,LENX,LCHC,LCSCE,LCSCV,         IBS
     1           LCSUB,NCOL,NROW,NLAY,IIBSCB,IIBSOC,ISS,IUNIT(19),IOUT)  IBS
      IF(IUNIT(20).GT.0) CALL CHD1AL(ISUM,LENX,LCCHDS,NCHDS,MXCHD,        CHD
     1           IUNIT(20),IOUT)                                         CHD
      IF(IUNIT(21).GT.0) CALL FHB1AL(ISUM,LENX,LCFLLC,LCBDTM,LCFLRT,
     1          LCBDFV,LCBDHV,LCHDLC,LCSBHD,NBDTIM,NFLW,NHED,IUNIT(21),
     2          IOUT,IFHBCB,NFHBX1,NFHBX2,IFHBD3,IFHBD4,IFHBD5,
     3          IFHBSS,ISS)
C
C *************************************************************************
C *      NEW CODE  -  ALLOCATE SPACE TO SDK MODULE IF CALLED              ***********
C *************************************************************************
C
      IF(IUNIT(28).GT.0) CALL SDK1AL(ISUM,LENX,LCHYOLD,LCESMID,LCPWP,
     1  LCDEN,LCISDKCF,LCUSATD,LCSATD,NCOL,NROW,NLAY,ISDKFLAG,
     2  IUNIT(28),IOUT)
C
C5------IF THE "X" ARRAY IS NOT BIG ENOUGH THEN STOP.
      IF(ISUM-1.GT.LENX) STOP
C
C6------READ AND PREPARE INFORMATION FOR ENTIRE SIMULATION.
      CALL BAS5RP(X(LCIBOU),X(LCHNEW),X(LCSTRT),X(LCHOLD),
     1        ISTRT,INBAS,HEADNG,NCOL,NROW,NLAY,VBVL,X(LCIOFL),
     2        IUNIT(12),IHEDFM,IDDNFM,IHEDUN,IDDNUN,IOUT,IPEROC,ITSOC,
     3        CHEDFM,CDDNFM,IBDOPT,IXSEC,LBHDSV,LBDDSV,IFREFM)
      IF(IUNIT(1).GT.0) CALL BCF5RP(X(LCIBOU),X(LCHNEW),X(LCSC1),
     1           X(LCHY),X(LCCR),X(LCCC),X(LCCV),X(LCDELR),
     2      X(LCDELC),X(LCBOT),X(LCTOP),X(LCSC2),X(LCTRPY),IUNIT(1),
     3      ISS,NCOL,NROW,NLAY,IOUT,X(LCWETD),IWDFLG,X(LCCVWD))
      IF(IUNIT(6).GT.0) CALL TLK1RP(X(LCRAT),X(LCZCB),X(LCA1),X(LCB1),
     1           X(LCALPH),X(LCBET),X(LCRM1),X(LCRM2),X(LCRM3),X(LCRM4),
     2           NODES1,NM1,NM2,NUMC,NTM1,ITLKRS,DELTM1,X(LCBUFF),
     3           X(LCDELC),X(LCDELR),TLKTIM,NROW,NCOL,IUNIT(6),IOUT)
      IF(IUNIT(9).GT.0) CALL SIP5RP(NPARM,MXITER,ACCL,HCLOSE,X(LCW),
     1           IUNIT(9),IPCALC,IPRSIP,IOUT,IFREFM)
      IF(IUNIT(10).GT.0) CALL DE45RP(IUNIT(10),MXITER,NITER,ITMX,
     1             ACCL,HCLOSE,IFREQ,IPRD4,IOUT,MUTD4)
      IF(IUNIT(11).GT.0) CALL SOR5RP(MXITER,ACCL,HCLOSE,IUNIT(11),
     1          IPRSOR,IOUT,IFREFM)
      IF(IUNIT(13).GT.0) CALL PCG2RP(MXITER,ITER1,HCLOSE,RCLOSE,
     1          NPCOND,NBPOL,RELAX,IPRPCG,IUNIT(13),IOUT,MUTPCG,
     2          NITER,X(LCIT1),DAMP)
      IF(IUNIT(14).GT.0) CALL GFD1RP(X(LCIBOU),X(LCHNEW),X(LCSC1),
     1           X(LCCDTR),X(LCCDTC),X(LCCR),X(LCCC),X(LCCV),X(LCDELR),
     2           X(LCDELC),X(LCBOT),X(LCTOP),X(LCSC2),
     3           IUNIT(14),ISS,NCOL,NROW,NLAY,NODES,IOUT)
      IF(IUNIT(16).GT.0) CALL HFB1RP(X(LCCR),X(LCCC),X(LCDELR),            *HFB*
     1          X(LCDELC),X(LCHFBR),IUNIT(16),NCOL,NROW,NLAY,NODES,        *HFB*
     1          NHFB,IOUT)                                                 *HFB*
      IF(IUNIT(19).GT.0) CALL IBS1RP(X(LCDELR),X(LCDELC),X(LCHNEW),      IBS
     1       X(LCHC),X(LCSCE),X(LCSCV),X(LCSUB),NCOL,NROW,NLAY,          IBS
     2       NODES,IIBSOC,ISUBFM,ICOMFM,IHCFM,ISUBUN,ICOMUN,IHCUN,       IBS
     3       IUNIT(19),IOUT)                                             IBS
      IF(IUNIT(21).GT.0) CALL FHB1RP(X(LCIBOU),NROW,NCOL,NLAY,
     &           X(LCFLLC),X(LCBDTM),NBDTIM,X(LCFLRT),NFLW,NHED,
     &           X(LCHDLC),X(LCSBHD),IUNIT(21),IOUT,
     &           NFHBX1,NFHBX2,IFHBD3,IFHBD5)
C
C *************************************************************************
C *      NEW CODE  - READ DATA INTO SDK MODULE IF CALLED                  ***********
C *************************************************************************
C                                                                          *
      IF(IUNIT(28).GT.0) CALL SDK1RP(NROW,NCOL,NLAY,VAR1,VAR2,VAR3,VAR4,
     1     VAR5,VAR6,DCFACT,TCFACT,HYCLOSE,DENW,TSSURF,X(LCISDKCF),
     2     X(LCUSATD),X(LCSATD),IUNIT(28),IOUT)
C *                                                                        *
C *************************************************************************
C
C
C7------SIMULATE EACH STRESS PERIOD.
      DO 300 KPER=1,NPER
      KKPER=KPER
C
C7A-----READ STRESS PERIOD TIMING INFORMATION.
```

```
      CALL BAS5ST(NSTP,DELT,TSMULT,PERTIM,KKPER,INBAS,IOUT,IFREFM)
C
C7B-----READ AND PREPARE INFORMATION FOR STRESS PERIOD.
      IF(IUNIT(2).GT.0) CALL WEL5RP(X(LCWELL),NWELLS,MXWELL,IUNIT(2),
     1             IOUT,NWELVL,IWELAL,IFREFM)
      IF(IUNIT(3).GT.0) CALL DRN5RP(X(LCDRAI),NDRAIN,MXDRN,IUNIT(3),
     1                  IOUT,NDRNVL,IDRNAL,IFREFM)
      IF(IUNIT(4).GT.0) CALL RIV5RP(X(LCRIVR),NRIVER,MXRIVR,IUNIT(4),
     1            IOUT,NRIVVL,IRIVAL,IFREFM)
      IF(IUNIT(5).GT.0) CALL EVT5RP(NEVTOP,X(LCIEVT),X(LCEVTR),
     1            X(LCEXDP),X(LCSURF),X(LCDELR),X(LCDELC),NCOL,NROW,
     1            IUNIT(5),IOUT,IFREFM)
      IF(IUNIT(7).GT.0) CALL GHB5RP(X(LCBNDS),NBOUND,MXBND,IUNIT(7),
     1              IOUT,NGHBVL,IGHBAL,IFREFM)
      IF(IUNIT(8).GT.0) CALL RCH5RP(NRCHOP,X(LCIRCH),X(LCRECH),
     1            X(LCDELR),X(LCDELC),NROW,NCOL,IUNIT(8),IOUT,IFREFM)
      IF(IUNIT(17).GT.0) CALL RES1RP(X(LCIRES),X(LCIRSL),X(LCBRES),
     1   X(LCCRES),X(LCBBRE),X(LCHRSE),X(LCIBOU),X(LCDELR),X(LCDELC),
     2   NRES,NRESOP,NPTS,NCOL,NROW,NLAY,PERLEN,DELT,NSTP,TSMULT,
     3   IUNIT(17),IOUT)
      IF(IUNIT(18).GT.0) CALL STR1RP(X(LCSTRM),X(ICSTRM),NSTREM,          STR1
     1                     MXSTRM,IUNIT(18),IOUT,X(LCTBAR),NDIV,NSS,     STR1
     2                     NTRIB,X(LCIVAR),ICALC,IPTFLG)                 STR1
      IF(IUNIT(20).GT.0) CALL CHD1RP(X(LCCHDS),NCHDS,MXCHD,X(LCIBOU),    CHD
     1            NCOL,NROW,NLAY,PERLEN,DELT,NSTP,TSMULT,IUNIT(20),IOUT)CHD
C
C7C-----SIMULATE EACH TIME STEP.
      DO 200 KSTP=1,NSTP
      KKSTP=KSTP
C
C ***************************************************************************
C *        NEW CODE - SET SDKFLAG TO 0 IF MODULE CALLED                      ***********
C
      IF(IUNIT(28).GT.0) ISDKFLAG=0
C                                                                            *
C ***************************************************************************
C
C7C1----CALCULATE TIME STEP LENGTH. SET HOLD=HNEW..
      CALL BAS5AD(DELT,TSMULT,TOTIM,PERTIM,X(LCHNEW),X(LCHOLD),KKSTP,
     1              NCOL,NROW,NLAY)
      IF(IUNIT(6).GT.0) CALL TLK1AD(X(LCRAT),X(LCZCB),X(LCA1),X(LCB1),
     1          X(LCALPH),X(LCBET),X(LCRM1),X(LCRM2),X(LCRM3),X(LCRM4),
     2          X(LCTL),X(LCTLK),X(LCSLU),X(LCSLD),NM1,NM2,NUMC,NTM1,
     3          DELTM1,X(LCHNEW),X(LCIBOU),X(LCTOP),
     4          NROW,NCOL,NLAY,DELT,TLKTIM,IUNIT(6),IOUT)
      IF(IUNIT(20).GT.0) CALL CHD1FM(NCHDS,MXCHD,X(LCCHDS),X(LCIBOU),    CHD
     1          X(LCHNEW),X(LCHOLD),PERLEN,PERTIM,DELT,NCOL,NROW,NLAY)   CHD
      IF(IUNIT(1).GT.0) CALL BCF5AD(X(LCIBOU),X(LCHOLD),X(LCBOT),
     1             X(LCWETD),IWDFLG,ISS,NCOL,NROW,NLAY)
      IF(IUNIT(17).GT.0) CALL RES1AD(X(LCHRES),X(LCHRSE),X(LCIRES),
     1 X(LCBRES),X(LCDELR),X(LCDELC),NRES,IRESPT,NCOL,NROW,
     1       PERLEN,PERTIM,TOTIM,KKSTP,KKPER,IOUT)
      IF(IUNIT(21).GT.0) CALL FHB1AD(X(LCHNEW),X(LCHOLD),NCOL,NROW,NLAY,
     &          ISS,TOTIM,DELT,X(LCBDTM),NBDTIM,X(LCFLRT),
     &          X(LCBDFV),X(LCBDHV),NFLW,X(LCSBHD),X(LCHDLC),NHED,
     &          NFHBX1,NFHBX2,IFHBD3,IFHBD4,IFHBD5,IFHBSS)
C
C
C ***************************************************************************
C *        NEW CODE - SET MARKER TO ALLOW HEAD ITERATION TO BE RERUN IF      ***********
C                     K HAS CHANGED                                          *
 80   CONTINUE
C                                                                            *
C ***************************************************************************

C7C2----ITERATIVELY FORMULATE AND SOLVE THE EQUATIONS.
      DO 100 KITER=1,MXITER
      KKITER=KITER
C
C7C2A---FORMULATE THE FINITE DIFFERENCE EQUATIONS.
      CALL BAS5FM(X(LCHCOF),X(LCRHS),NODES)
      IF(IUNIT(1).GT.0) CALL BCF5FM(X(LCHCOF),X(LCRHS),X(LCHOLD),
     1          X(LCSC1),X(LCHNEW),X(LCIBOU),X(LCCR),X(LCCC),X(LCCV),
     2          X(LCHY),X(LCTRPY),X(LCBOT),X(LCTOP),X(LCSC2),
     3          X(LCDELR),X(LCDELC),DELT,ISS,KKITER,KKSTP,KKPER,NCOL,
     4          NROW,NLAY,IOUT,X(LCWETD),IWDFLG,X(LCCVWD),WETFCT,
```

```
     5          IWETIT,IHDWET,HDRY,X(LCBUFF))
      IF(IUNIT(14).GT.0) CALL GFD1FM(X(LCHCOF),X(LCRHS),X(LCHOLD),
     1          X(LCSC1),X(LCHNEW),X(LCIBOU),X(LCCR),X(LCCC),X(LCCV),
     2          X(LCCDTR),X(LCCDTC),X(LCBOT),X(LCTOP),X(LCSC2),
     3          DELT,ISS,KKITER,KKSTP,KKPER,NCOL,NROW,NLAY,IOUT)
      IF(IUNIT(16).GT.0) CALL HFB1FM(X(LCHNEW),X(LCCR),X(LCCC),          *HFB*
     1          X(LCBOT),X(LCTOP),X(LCDELR),X(LCDELC),X(LCHFBR),         *HFB*
     2          NCOL,NROW,NLAY,NHFB)                                     *HFB*
      IF(IUNIT(6).GT.0) CALL TLK1FM(X(LCRAT),X(LCTL),X(LCTLK),X(LCSLU),
     1          X(LCSLD),NUMC,X(LCHNEW),X(LCIBOU),X(LCTOP),X(LCCV),
     2          X(LCHCOF),X(LCRHS),NROW,NCOL,NLAY)
      IF(IUNIT(2).GT.0) CALL WEL5FM(NWELLS,MXWELL,X(LCRHS),X(LCWELL),
     1           X(LCIBOU),NCOL,NROW,NLAY,NWELVL)
      IF(IUNIT(3).GT.0) CALL DRN5FM(NDRAIN,MXDRN,X(LCDRAI),X(LCHNEW),
     1         X(LCHCOF),X(LCRHS),X(LCIBOU),NCOL,NROW,NLAY,NDRNVL)
      IF(IUNIT(4).GT.0) CALL RIV5FM(NRIVER,MXRIVR,X(LCRIVR),X(LCHNEW),
     1           X(LCHCOF),X(LCRHS),X(LCIBOU),NCOL,NROW,NLAY,NRIVVL)
      IF(IUNIT(5).GT.0) CALL EVT5FM(NEVTOP,X(LCIEVT),X(LCEVTR),
     1           X(LCEXDP),X(LCSURF),X(LCRHS),X(LCHCOF),X(LCIBOU),
     1           X(LCHNEW),NCOL,NROW,NLAY)
      IF(IUNIT(7).GT.0) CALL GHB5FM(NBOUND,MXBND,X(LCBNDS),X(LCHCOF),
     1           X(LCRHS),X(LCIBOU),NCOL,NROW,NLAY,NGHBVL)
      IF(IUNIT(8).GT.0) CALL RCH5FM(NRCHOP,X(LCIRCH),X(LCRECH),
     1           X(LCRHS),X(LCIBOU),NCOL,NROW,NLAY)
      IF(IUNIT(17).GT.0) CALL RES1FM(X(LCIRES),X(LCIRSL),X(LCBRES),
     1   X(LCCRES),X(LCBBRE),X(LCHRES),X(LCIBOU),X(LCHNEW),X(LCHCOF),
     2   X(LCRHS),NRES,NRESOP,NCOL,NROW,NLAY)
      IF(IUNIT(18).GT.0) CALL STR1FM(NSTREM,X(LCSTRM),X(ICSTRM),         STR1
     1                     X(LCHNEW),X(LCHCOF),X(LCRHS),X(LCIBOU),       STR1
     2               MXSTRM,NCOL,NROW,NLAY,IOUT,NSS,X(LCTBAR),           STR1
     3               NTRIB,X(LCTRIB),X(LCIVAR),X(LCFGAR),ICALC,CONST)    STR1
      IF(IUNIT(19).GT.0) CALL IBS1FM(X(LCRHS),X(LCHCOF),X(LCHNEW),       IBS
     1        X(LCHOLD),X(LCHC),X(LCSCE),X(LCSCV),X(LCIBOU),             IBS
     2        NCOL,NROW,NLAY,DELT)                                       IBS
      IF(IUNIT(21).GT.0) CALL FHB1FM(X(LCRHS),X(LCIBOU),X(LCFLLC),
     1 X(LCBDFV),NFLW,NCOL,NROW,NLAY,IFHBD4)
C
C7C2B---MAKE ONE CUT AT AN APPROXIMATE SOLUTION.
      IF(IUNIT(9).GT.0) CALL SIP5AP(X(LCHNEW),X(LCIBOU),X(LCCR),X(LCCC),
     1     X(LCCV),X(LCHCOF),X(LCRHS),X(LCEL),X(LCFL),X(LCGL),X(LCV),
     2     X(LCW),X(LCHDCG),X(LCLRCH),NPARM,KKITER,HCLOSE,ACCL,ICNVG,
     3     KKSTP,KKPER,IPCALC,IPRSIP,MXITER,NSTP,NCOL,NROW,NLAY,NODES,
     4     IOUT)
      IF(IUNIT(10).GT.0) CALL DE45AP(X(LCHNEW),X(LCIBOU),X(LCAU),
     1  X(LCAL),X(LCIUPP),X(LCIEQP),X(LCD4B),MXUP,MXLOW,MXEQ,MXBW,
     2  X(LCCR),X(LCCC),X(LCCV),X(LCHCOF),X(LCRHS),ACCL,KKITER,ITMX,
     3  MXITER,NITER,HCLOSE,IPRD4,ICNVG,NCOL,NROW,NLAY,IOUT,X(LCLRCH),
     4  X(LCHDCG),IFREQ,KKSTP,KKPER,DELT,NSTP,ID4DIR,ID4DIM,MUTD4)
      IF(IUNIT(11).GT.0) CALL SOR5AP(X(LCHNEW),X(LCIBOU),X(LCCR),
     1     X(LCCC),X(LCCV),X(LCHCOF),X(LCRHS),X(LCA),X(LCRES),X(LCIEQP),
     2     X(LCHDCG),X(LCLRCH),KKITER,HCLOSE,ACCL,ICNVG,KKSTP,KKPER,
     3     IPRSOR,MXITER,NSTP,NCOL,NROW,NLAY,NSLICE,MBW,IOUT)
      IF(IUNIT(13).GT.0) CALL PCG2AP(X(LCHNEW),X(LCIBOU),X(LCCR),
     1      X(LCCC),X(LCCV),X(LCHCOF),X(LCRHS),X(LCV),X(LCSS),X(LCP),
     2      X(LCCD),X(LCHCHG),X(LCLHCH),X(LCRCHG),X(LCLRCH),KKITER,
     3      NITER,HCLOSE,RCLOSE,ICNVG,KKSTP,KKPER,IPRPCG,MXITER,ITER1,
     4      NPCOND,NBPOL,NSTP,NCOL,NROW,NLAY,NODES,RELAX,IOUT,MUTPCG,
     5      0,0,SN,SP,SR,X(LCIT1),DAMP)
C
C7C2C---IF CONVERGENCE CRITERION HAS BEEN MET STOP ITERATING.
      IF(ICNVG.EQ.1) GO TO 110
  100 CONTINUE
      KITER=MXITER
  110 CONTINUE
C
C
C ***************************************************************************
C *        NEW CODE - CALL MODULE SDKFM AND RETURN TO START OF HEAD       *
C                     ITERATION (MARKER 80) IF ISDKFLAG=0                  ***********
C
      IF(IUNIT(28).GT.0) THEN
        CALL SDK1FM(X(LCBOT),X(LCCV),X(LCCVWD),X(LCDEN),X(LCESMID),
     1    X(LCPWP),X(LCHNEW),X(LCHY),X(LCHYOLD),X(LCIBOU),X(LCTOP),
     2    X(LCISDKCF),X(LCUSATD), X(LCSATD),X(LCBUFF),X(LCDELR),
     3    X(LCDELC),NROW,NCOL,NLAY,NRCL,IWDFLG,ISDKFLAG,
     4    VAR1,VAR2,VAR3,VAR4,VAR5,VAR6,DCFACT,TCFACT,HYCLOSE,DENW,
```

```
     5   TSSURF,KSTP,KPER,IUNIT(28),IOUT)
         GOTO 120
       ELSE
         GOTO 130
       ENDIF
 120   CONTINUE
       IF(ISDKFLAG.EQ.0) GOTO 80
 130   CONTINUE
C                                                                       *
C ***********************************************************************
C
C7C3----DETERMINE WHICH OUTPUT IS NEEDED.
       CALL BAS5OC(NSTP,KKSTP,ICNVG,X(LCIOFL),NLAY,IBUDFL,ICBCFL,
     1   IHDDFL,IUNIT(12),IOUT,KKPER,IPEROC,ITSOC,IBDOPT,IXSEC,IFREFM)
C
C7C4----CALCULATE BUDGET TERMS. SAVE CELL-BY-CELL FLOW TERMS.
       MSUM=1
       IF(IUNIT(6).GT.0) CALL TLK1BD(X(LCRAT),X(LCTL),X(LCTLK),
     1           X(LCSLU),X(LCSLD),NUMC,ITLKCB,X(LCHNEW),X(LCBUFF),
     2           X(LCIBOU),X(LCTOP),X(LCCV),VBNM,VBVL,MSUM,NCOL,NROW,
     3           NLAY,DELT,KSTP,KPER,ICBCFL,IOUT)
C7C4A---THE ORIGINAL BCF BUDGET MODULE HAS BEEN REPLACED BY THREE
C7C4A---SUBMODULES: SBCF5S, SBCF5F, AND SBCF5B .
       IF(IUNIT(1).GT.0) THEN
          CALL SBCF5S(VBNM,VBVL,MSUM,X(LCHNEW),X(LCIBOU),X(LCHOLD),
     1      X(LCSC1),X(LCTOP),X(LCSC2),DELT,ISS,NCOL,NROW,NLAY,KKSTP,
     2      KKPER,IBCFCB,ICBCFL,X(LCBUFF),IOUT,PERTIM,TOTIM)
          CALL SBCF5F(VBNM,VBVL,MSUM,X(LCHNEW),X(LCIBOU),X(LCCR),
     1      X(LCCC),X(LCCV),X(LCTOP),DELT,NCOL,NROW,NLAY,KKSTP,KKPER,
     2      IBCFCB,X(LCBUFF),IOUT,ICBCFL,PERTIM,TOTIM,ICHFLG)
          IBDRET=0
          IC1=1
          IC2=NCOL
          IR1=1
          IR2=NROW
          IL1=1
          IL2=NLAY
          DO 155 IDIR=1,3
          CALL SBCF5B(X(LCHNEW),X(LCIBOU),X(LCCR),X(LCCC),X(LCCV),
     1       X(LCTOP),NCOL,NROW,NLAY,KKSTP,KKPER,IBCFCB,X(LCBUFF),
     2       IOUT,ICBCFL,DELT,PERTIM,TOTIM,IDIR,IBDRET,ICHFLG,
     3       IC1,IC2,IR1,IR2,IL1,IL2)
155       CONTINUE
       END IF
       IF(IUNIT(14).GT.0) CALL GFD1BD(VBNM,VBVL,MSUM,X(LCHNEW),
     1      X(LCIBOU),X(LCHOLD),X(LCSC1),X(LCCR),X(LCCC),X(LCCV),
     2      X(LCTOP),X(LCSC2),DELT,ISS,NCOL,NROW,NLAY,KKSTP,KKPER,
     3      IGFDCB,ICBCFL,X(LCBUFF),IOUT)
       IF(IUNIT(2).GT.0) CALL WEL5BD(NWELLS,MXWELL,VBNM,VBVL,MSUM,
     1      X(LCWELL),X(LCIBOU),DELT,NCOL,NROW,NLAY,KKSTP,KKPER,IWELCB,
     1      ICBCFL,X(LCBUFF),IOUT,PERTIM,TOTIM,NWELVL,IWELAL)
       IF(IUNIT(3).GT.0) CALL DRN5BD(NDRAIN,MXDRN,VBNM,VBVL,MSUM,
     1      X(LCDRAI),DELT,X(LCHNEW),NCOL,NROW,NLAY,X(LCIBOU),KKSTP,
     2      KKPER,IDRNCB,ICBCFL,X(LCBUFF),IOUT,PERTIM,TOTIM,NDRNVL,
     3      IDRNAL)
       IF(IUNIT(4).GT.0) CALL RIV5BD(NRIVER,MXRIVR,X(LCRIVR),X(LCIBOU),
     1      X(LCHNEW),NCOL,NROW,NLAY,DELT,VBVL,VBNM,MSUM,KKSTP,KKPER,
     2      IRIVCB,ICBCFL,X(LCBUFF),IOUT,PERTIM,TOTIM,NRIVVL,IRIVAL)
       IF(IUNIT(5).GT.0) CALL EVT5BD(NEVTOP,X(LCIEVT),X(LCEVTR),
     1      X(LCEXDP),X(LCSURF),X(LCIBOU),X(LCHNEW),NCOL,NROW,NLAY,
     2      DELT,VBVL,VBNM,MSUM,KKSTP,KKPER,IEVTCB,ICBCFL,X(LCBUFF),IOUT,
     3      PERTIM,TOTIM)
       IF(IUNIT(7).GT.0) CALL GHB5BD(NBOUND,MXBND,VBNM,VBVL,MSUM,
     1      X(LCBNDS),DELT,X(LCHNEW),NCOL,NROW,NLAY,X(LCIBOU),KKSTP,
     2      KKPER,IGHBCB,ICBCFL,X(LCBUFF),IOUT,PERTIM,TOTIM,NGHBVL,
     3      IGHBAL)
       IF(IUNIT(8).GT.0) CALL RCH5BD(NRCHOP,X(LCIRCH),X(LCRECH),
     1      X(LCIBOU),NROW,NCOL,NLAY,DELT,VBVL,VBNM,MSUM,KKSTP,KKPER,
     2      IRCHCB,ICBCFL,X(LCBUFF),IOUT,PERTIM,TOTIM)
       IF(IUNIT(17).GT.0) CALL RES1BD(X(LCIRES),X(LCIRSL),X(LCBRES),
     1       X(LCCRES),X(LCBBRE),X(LCHRES),X(LCIBOU),X(LCHNEW),
     2       X(LCBUFF),VBVL,VBNM,MSUM,KSTP,KPER,NRES,NRESOP,
     3       NCOL,NROW,NLAY,DELT,IRESCB,ICBCFL,IOUT)
       IF(IUNIT(18).GT.0) CALL STR1BD(NSTREM,X(LCSTRM),X(ICSTRM),          STR1
     1   X(LCIBOU),MXSTRM,X(LCHNEW),NCOL,NROW,NLAY,DELT,VBVL,VBNM,MSUM,  STR1
     2   KKSTP,KKPER,ISTCB1,ISTCB2,ICBCFL,X(LCBUFF),IOUT,NTRIB,NSS,      STR1
```

```
     3   X(LCTRIB),X(LCTBAR),X(LCIVAR),X(LCFGAR),ICALC,CONST,IPTFLG)     STR1
      IF(IUNIT(19).GT.0) CALL IBS1BD(X(LCIBOU),X(LCHNEW),X(LCHOLD),      IBS
     1       X(LCHC),X(LCSCE),X(LCSCV),X(LCSUB),X(LCDELR),X(LCDELC),     IBS
     2       NCOL,NROW,NLAY,DELT,VBVL,VBNM,MSUM,KSTP,KPER,IIBSCB,        IBS
     3       ICBCFL,X(LCBUFF),IOUT)                                      IBS
      IF(IUNIT(21).GT.0) CALL FHB1BD(X(LCFLLC),X(LCBDFV),NFLW,
     1      VBNM,VBVL,MSUM,X(LCIBOU),DELT,NCOL,NROW,NLAY,KKSTP,KKPER,
     2      IFHBCB,ICBCFL,X(LCBUFF),IOUT,IFHBD4)
C
C7C5---PRINT AND OR SAVE HEADS AND DRAWDOWNS. PRINT OVERALL BUDGET.
      CALL BAS5OT(X(LCHNEW),X(LCSTRT),ISTRT,X(LCBUFF),X(LCIOFL),
     1      MSUM,X(LCIBOU),VBNM,VBVL,KKSTP,KKPER,DELT,PERTIM,TOTIM,
     2      ITMUNI,NCOL,NROW,NLAY,ICNVG,IHDDFL,IBUDFL,IHEDFM,IHEDUN,
     3      IDDNFM,IDDNUN,IOUT,CHEDFM,CDDNFM,IXSEC,LBHDSV,LBDDSV)
C
C7C5A--PRINT AND OR SAVE SUBSIDENCE, COMPACTION, AND CRITICAL HEAD.
      IF(IUNIT(19).GT.0) CALL IBS1OT(NCOL,NROW,NLAY,PERTIM,TOTIM,KSTP,   IBS
     1       KPER,NSTP,X(LCBUFF),X(LCSUB),X(LCHC),IIBSOC,ISUBFM,ICOMFM,  IBS
     2       IHCFM,ISUBUN,ICOMUN,IHCUN,IUNIT(19),IOUT)                   IBS
C
C7C6----IF ITERATION FAILED TO CONVERGE THEN STOP.
      IF(ICNVG.EQ.0) STOP
  200 CONTINUE
  300 CONTINUE
C
C7C7----WRITE RESTART RECORDS
C7C7A---WRITE RESTART RECORDS FOR TRANSIENT-LEAKAGE PACKAGE
      IF(IUNIT(6).GT.0) CALL TLK1OT(X(LCRM1),X(LCRM2),
     1      X(LCRM3),X(LCRM4),NM1,NM2,ITLKSV,DELTM1,TLKTIM,IOUT)
C
C8------END OF SIMULATION
      IF(IBATCH.GT.0) THEN
         WRITE(IBOUTS,*) ' Normal termination of simulation.'
         DO 400 I=1,IBOUTS-1
            INQUIRE(UNIT=I,OPENED=EXISTS)
            IF(EXISTS) CLOSE(I)
  400    CONTINUE
         GO TO 50
      END IF
  500 STOP
C
      END
```

Source code for new SDK module

```
C*****************************************************************
C   STRESS DEPENDENT HYDRAULIC CONDUCTIVITY PACKAGE FOR MODFLOW-96
C
C
C
C-----VERSION 1440 12APR1999 SDK4.for
C
C*****************************************************************
C
      SUBROUTINE SDK1AL(ISUM,LENX,LCHYOLD,LCESMID,LCPWP,LCDEN,
     1      LCISDKCF,LCUSATD,LCSATD,NCOL,NROW,NLAY,ISDKFLAG,
     2      IN,IOUT)
C
C     ALLOCATE STORAGE FOR SDK PACKAGE
C     ******************************************************************
C
C-----VERSION 2 DEC 1998 SDK1AL
C
C     ******************************************************************
C
C        SPECIFICATIONS:
C
      WRITE(IOUT,1)IN
    1 FORMAT(1H0,'SDK1 -- STRESS DEPENDENT HYDRAULIC COND','VERSION 1,',
     1     ' November 98',' INPUT READ FROM UNIT',I3)
C2------ALLOCATE SPACE FOR THE ARRAYS HYOLD, ESMID,DEN
C2A                                  ISDKCF,USATD and SATD.
      ISOLD=ISUM
      NRCL=NROW*NCOL*NLAY
      LCHYOLD=ISUM
      ISUM=ISUM+NRCL
      LCESMID=ISUM
      ISUM=ISUM+NRCL
      LCPWP=ISUM
      ISUM=ISUM+NRCL
      LCDEN=ISUM
      ISUM=ISUM+NRCL
      LCISDKCF=ISUM
      ISUM=ISUM+NRCL
      LCUSATD=ISUM
      ISUM=ISUM+NRCL
      LCSATD=ISUM
      ISUM=ISUM+NRCL
C
C3------CALCULATE & PRINT AMOUNT OF SPACE USED BY PACKAGE.
      ISOLD=ISUM-ISOLD
      WRITE(IOUT,4)ISOLD
    4 FORMAT(1X,I8,' ELEMENTS OF X ARRAY USED FOR STRESS DEPENDENT K')
      ISUM1=ISUM-1
      WRITE(IOUT,5)ISUM1,LENX
    5 FORMAT(1X,I8,' ELEMENTS OF X ARRAY USED OUT OF',I8)
      IF(ISUM1.GT.LENX)WRITE(IOUT,6)
    6 FORMAT(1X,'   ***X ARRAY MUST BE MADE LARGER***')
C
      RETURN
      END
C
C
      SUBROUTINE SDK1RP(NROW,NCOL,NLAY,VAR1,VAR2,VAR3,VAR4,VAR5,VAR6,
     1   DCFACT,TCFACT,HYCLOSE,DENW,TSSURF,ISDKCF,USATD,SATD,IN,IOUT)
C
C     READ SDK DATA
C     ******************************************************************
C
C-----VERSION 1 SEP 1998 SDK1RP
C
C     ******************************************************************
C
C        SPECIFICATIONS:
C ---------------------------------------------------------------
C    READ IN VARIABLES FROM INPUT FILE
C *** NB ALL VARIABLES MUST BE for kPa m/s and t/m3 **
```

```
C1      VAR1 is Unsaturated zone density to stress constant
C2      VAR2 is Unsaturated zone density to stress power term
C3      VAR3 is Saturated zone density to stress constant
C4      VAR4 is Saturated zone density to stress power term
C5      VAR5 is stress to Hydraulic Conductivity constant
C6      VAR6 is Stress to Hydraulic Conductivity constant
C7      DCFACT is the conversion factor from model units to metres
C7a             ie if model units are cm then DCFACT=0.01
C8      TCFACT is the NUMBER OF seconds IN A model unit (NB diff to DCFACT)
C8a             ie if model units are days then TCFACT=864000.
C9      HYCLOSE is the max allowable percent variation in K between
C               two iterations
C10     DENW is the density of water/leachate in t/m3
C11     TSSURF is the surcharge at the surface in kPa
C
      DIMENSION ISDKCF(NCOL,NROW,NLAY), USATD(NCOL,NROW,NLAY),
     1          SATD(NCOL,NROW,NLAY)
C
C  SKIP THE FIRST LINE IN DATA FILE WHICH IS USED FOR LABEL
      READ(IN,50) VAR1,VAR2,VAR3,VAR4,VAR5,VAR6,DCFACT,TCFACT,
     1     HYCLOSE,DENW,TSSURF
   50 FORMAT(11(/,F11.4))
C
C  WRITE TO FILE FACTORS USED
      WRITE(IOUT,55)
   55 FORMAT(/,'-----------------------------------------------------',
     1  /,'SDK PACKAGE STARTED - READING IN DATA')
      WRITE(IOUT,60) VAR1,VAR2,VAR3,VAR4,VAR5,VAR6,DCFACT,TCFACT,
     1     HYCLOSE,DENW,TSSURF
   60 FORMAT('VARIABLE 1 =',F11.4,/,'VARIABLE 2 =',F11.4,
     1  /,'VARIABLE 3 =',F11.4,/,'VARIABLE 4 =',F11.4,
     2  /,'VARIABLE 5 =',F11.4,/,'VARIABLE 6 =',F11.4,
     3  /,'Number of METRES in a model unit =',F11.4,
     4  /,'Number of SECONDS in a model unit =',F11.4,
     5  /,'Percent variation for closure of K =',F11.4,
     6  /,'Density of water =',F11.4,
     7  /,'Surface surcharge in kPa =',F11.4)
C1  SET SDK CELL FLAG TO 1 FOR ALL CELLS
      DO 100 K=1,NLAY
      DO 100 I=1,NROW
      DO 100 J=1,NCOL
      ISDKCF(J,I,K)=1
  100 CONTINUE
C2  READ NUMBER OF LAYERS WHERE PACKAGE IS SWITCHED OFF
      READ(IN,120) NSDKLAY
  120 FORMAT(I5)
      IF(NSDKLAY.EQ.0) GOTO 200
      DO 150 K=1,NSDKLAY
      READ(IN,130) LAYNUM,USTD,STD
  130 FORMAT(I5,2F10.2)
      DO 140 I=1,NROW
      DO 140 J=1,NCOL
      ISDKCF(J,I,LAYNUM)=0
      USATD(J,I,LAYNUM)=USTD
      SATD(J,I,LAYNUM)=STD
  140 CONTINUE
  150 CONTINUE
  200 CONTINUE
C3  READ LOCATIONS OF INDIVIDUAL CELLS WHICH ARE ON OR OFF
      READ(IN,250) NSDKCELL
  250 FORMAT (I5)
      IF (NSDKCELL.EQ.0) GOTO 400
      DO 300 II=1,NSDKCELL
      READ(IN,260) I,J,K,IFLAG,USTD,STD
  260 FORMAT (4I5,2F10.2)
      ISDKCF(J,I,K)=IFLAG
      USATD(J,I,K)=USTD
      SATD(J,I,K)=STD
  300 CONTINUE
  400 CONTINUE
C
       RETURN
       END
C
C
C
```

```
      SUBROUTINE SDK1FM(BOT,CV,CVWD,DEN,ESMID,PWP,HNEW,HY,HYOLD,IBOUND,
     1        TOP,ISDKCF,USATD,SATD,BUFF,DELR,DELC,NROW,NCOL,NLAY,NRCL,
     2        IWDFLG,ISDKFLAG,VAR1,VAR2,VAR3,VAR4,VAR5,VAR6,DCFACT,
     3        TCFACT,HYCLOSE,DENW,TSSURF,KSTP,KPER,IN,IOUT)
C
C     ******************************************************************
C     FORMULATE NEW Ks
C     ******************************************************************
C
C-----VERSION 1 SEP 1998 SDK1FM
C
C     ******************************************************************
C
C        SPECIFICATIONS:
C ------------------------------------------------------------------
      CHARACTER*16 TEXT
      DOUBLE PRECISION HNEW
C
      DIMENSION BOT(NCOL,NROW,NLAY), CV(NCOL,NROW,NLAY),
     1    DEN(NCOL,NROW,NLAY), ESMID(NCOL,NROW,NLAY),
     2    PWP(NCOL,NROW,NLAY), BUFF(NCOL,NROW,NLAY),
     3    HNEW(NCOL,NROW,NLAY), HY(NCOL,NROW,NLAY),
     4    HYOLD(NCOL,NROW,NLAY), IBOUND(NCOL,NROW,NLAY),
     5    TOP(NCOL,NROW,NLAY), ISDKCF(NCOL,NROW,NLAY),
     6    USATD(NCOL,NROW,NLAY), SATD(NCOL,NROW,NLAY),
     7    CVWD(NCOL,NROW,NLAY), DELR(NCOL), DELC(NROW)
C
      COMMON /FLWCOM/LAYCON(200)
C
C     ------------------------------------------------------------------
      WRITE(IOUT,5)
   5  FORMAT('SDK FORMULATE PACKAGE INVOKED')
C
C       SET G = ACCELERATION DUE TO GRAVITY (in M/S^2)
      G=9.81
      E=2.71828
C
C------CHECK THAT LAYCON OF EACH LAYER = 3
      DO 10 K=1,NLAY
      IF(LAYCON(K).NE.3) THEN
      WRITE(IOUT,20)
      STOP
      ENDIF
  10  CONTINUE
  20  FORMAT('THIS SDK PACKAGE IS NOT DESIGNED TO WORK FOR LAYERS WHERE
     1   LAYCON NOT EQUAL TO 3',/'PROGRAM TERMINATED')
C
C -----CHECK THAT DEPTH OF EACH LAYER IS GT 0.0
      NERR=0
      DO 50 K=1,NLAY
      DO 50 I=1,NROW
      DO 50 J=1,NCOL
      D=TOP(J,I,K)-BOT(J,I,K)
      IF(D.LE.0.0) THEN
      NERR=NERR+1
      WRITE(IOUT,55)D,I,J,K
  55  FORMAT('Depth of ',F6.1,' at cell',I3,',',I3,',',I3,' INCORRECT',
     1 /,'Define TOP of layer in GW Vistas and make sure LAYER TYPE=3',
     2 /,'First 100 errors displayed -  PROGRAM TERMINATED')
      IF (NERR.GT.100) GOTO 60
      ENDIF
  50  CONTINUE
  60  CONTINUE
      IF(NERR.GT.0) STOP
C
C     COPY HYDRAULIC CONDUCTIVITES INTO HYOLD
      DO 100 K=1,NLAY
      DO 100 I=1,NROW
      DO 100 J=1,NCOL
      HYOLD(J,I,K)=HY(J,I,K)
      PWP(J,I,K)=0.0
C ***** next line not needed until Kx different to Ky ********
C      TRPYOLD(J,I,K)=TRPY(J,I,K)
  100 CONTINUE
C     SET VARIABLE WHICH TRACKS MAXIMUM K CHANGE DURING ITERATION
      HYBIGG=0.0
```

```
C ********************************************************
C     CALCULATE EFFECTIVE STRESS AT EACH CELL
C ********************************************************
      DO 400 I=1,NROW
      DO 400 J=1,NCOL
C1      SET TOTAL STRESS AT TOP OF LAYER 1 TO SURFACE SURCHARGE
      TSTOP=TSSURF
      DO 400 K=1,NLAY
C1a     First calculate total stress at midpoint and base of cell
C1b     DETERMINE WHETHER CELL IS SATURATED OR UNSATURATED
      IF(IBOUND(J,I,K).EQ.0) THEN
       GOTO 150
      ELSE
       GOTO 170
      ENDIF
C
C2 *****  CALCULATE TOTAL STRESS FOR UNSATURATED LAYER ********
150   CONTINUE
C2A     CALCULATE STRESS IN kPa AT MIDPOINT OF CELL USING EQUATION 7.12
C2B     DETERMINE THICKNESS OF CELL, D in metres
      D=(TOP(J,I,K)-BOT(J,I,K))*DCFACT
C2      If isdkcf=0 then density not related to stress and is constant
      IF (ISDKCF(J,I,K).EQ.0) THEN
        DEN(J,I,K)=USATD(J,I,K)
        TSBOT=TSTOP+DEN(J,I,K)*D*G
        ESMID(J,I,K)=(TSBOT+TSTOP)/2
        GOTO 190
      ELSE
        CONTINUE
      ENDIF
C2C     DETERMINE CONSTANT A
      A=VAR1*G*D/2.0
C2D     MAKE STARTING QUESS FOR MEAN TOTAL STRESS
      TSMID=TSTOP+1.4*G*D*0.5
C2E     CALCULATE ERROR ACCORDING TO EQUATION 7.13
155   CONTINUE
      TSERR=TSTOP-TSMID+(A*(TSMID)**VAR2)
c       If error is within 0.1 kPa then continue, otherwise .....
      IF(TSERR.LT.0.1) GOTO 160
      IF(TSERR.GT.-0.1) GOTO 160
C       ..... halve error and retry
      TSOLD=TSMID
      TSMID=TSOLD+0.5*TSERR
      GOTO 155
160   CONTINUE
C2F     CALCULATE AVERAGE DENSITY OF CELL (NB PWP=0 SO ESMID=TSMID)
      ESMID(J,I,K)=TSMID
      DEN(J,I,K)=VAR1*(ESMID(J,I,K)**VAR2)
C2G     CALCULATE TOTAL STRESS AT BASE OF CELL
      TSBOT=TSTOP+DEN(J,I,K)*G*D
C        JUMP TO HYDRAULIC CONDUCTIVITY PART
      GOTO 190
C
C3 ***** CALCULATE TOTAL STRESS FOR SATURATED LAYERS *****************
C
170   CONTINUE
C3A     CALCULATE STRESS AT MIDPOINT OF CELL USING EQUATION 7.12
C3B     DETERMINE THICKNESS OF CELL, D IN METRES
      D=(TOP(J,I,K)-BOT(J,I,K))*DCFACT
C3CA    CONVERT HEAD INTO POREWATER PRESSURE
      PWP(J,I,K)=(HNEW(J,I,K)-(0.5*(BOT(J,I,K)+TOP(J,I,K))))
     1           *DCFACT*G*DENW
      IF(PWP(J,I,K).LT.0.0) PWP(J,I,K)=0.0
C ********************************************************************
C3      If isdkcf=0 then density not related to stress and is constant
C ********************************************************************
      IF (ISDKCF(J,I,K).EQ.0) THEN
        DEN(J,I,K)=SATD(J,I,K)
        TSBOT=TSTOP+DEN(J,I,K)*D*G
        TSMID=(TSTOP+TSBOT)/2
C3F   CHECK THAT PWP NOT GREATER THAN STRESS
        IF (PWP(J,I,K).GT.TSMID) THEN
C          STOP SIMULATION
C          AND WRITE ERROR MESSAGE
          WRITE(IOUT,177)PWP(J,I,K),HNEW(J,I,K)*DCFACT,HNEW(J,I,K),
     1           TSMID,J,I,K
```

```
          STOP
        ENDIF
        ESMID(J,I,K)=TSMID-PWP(J,I,K)
        GOTO 190
      ELSE
        CONTINUE
      ENDIF
C *************************************************************************
C   IF ISDKCF=1 THEN CALCUALTE DENSITY AS FOLLOWS
C *************************************************************************
C3C     DETERMINE CONSTANT A
      A=VAR3*G*D/2.0
C3D     MAKE STARTING QUESS FOR MEAN TOTAL STRESS
      TSMID=TSTOP+1.4*G*D*0.5
C3E     CALCULATE ERROR ACCORDING TO EQUATION 7.17
175   CONTINUE
C3F   CHECK THAT PWP NOT GREATER THAN STRESS
      IF (PWP(J,I,K).GT.TSMID) THEN
C        STOP SIMULATION
C        AND WRITE ERROR MESSAGE
      WRITE(IOUT,177) PWP(J,I,K),HNEW(J,I,K)*DCFACT,HNEW(J,I,K),
     1                TSMID, J, I, K
  177 FORMAT(1X,'Pore water pressure of',F10.4,'kPa (',F10.4,' metres',
     1F10.4,'Model Units)',/'is greater than stress of',F10.4,
     2/'at Column', I8,/'   Row',I8,/'   Layer',I8,/'SIMULATION STOPPED'
     3)
        STOP
      ENDIF
      TSERR=TSTOP-TSMID+(A*(TSMID-PWP(J,I,K))**VAR4)
c       If error is within 0.1 kPa then continue, otherwise .....
      IF(ABS(TSERR).LT.0.1) GOTO 180
C       ..... halve error and retry
      TSOLD=TSMID
      TSMID=TSOLD+0.5*TSERR
      GOTO 175
180   CONTINUE
C2F     CALCULATE AVERAGE DENSITY OF CELL
      ESMID(J,I,K)=TSMID-PWP(J,I,K)
      DEN(J,I,K)=VAR3*(ESMID(J,I,K)**VAR4)
C2G     CALCULATE TOTAL STRESS AT BASE OF CELL
      TSBOT=TSTOP+DEN(J,I,K)*G*D
C  PRINTOUT EFF STRESS FOR AUDIT PURPOSES
C      WRITE(??,??)
C        JUMP TO HYDRAULIC CONDUCTIVITY PART
      GOTO 190
C *************************************************************************
C
190   CONTINUE
C   CALCULATE HYDRAULIC CONDUCTIVITIES IN M/S
C   IF ISDKCF=0 THEN NO CHANGE TO K
      IF (ISDKCF(J,I,K).EQ.0) GOTO 200
      HYTEMP=VAR5*(ESMID(J,I,K)**VAR6)
C  MAKE SURE H CONDUCTIVITY IS NOT GREATER THAN 1X10-4 M/S
      IF (HYTEMP.GE.0.0001) HYTEMP=0.0001
C     CONVERT HYTEMP TO MODEL UNITS AND STORE AS HY(J,I,K)
      HY(J,I,K)=HYTEMP*TCFACT/DCFACT
C  CALCULATE DIFFERENCE IN K AND STORE IF LARGEST VARIATION
      IF(HY(J,I,K)-HYOLD(J,I,K).EQ.0.0) GOTO 200
      HYDIFF=ABS((HY(J,I,K)-HYOLD(J,I,K))/HYOLD(J,I,K))
      IF (HYDIFF.GT.HYBIGG) HYBIGG=HYDIFF
 200  CONTINUE
C ** INSERT CODE TO STORE THE CELL LOCATION OF MAXIMUM K CHANGE
C
C   WRITE OUT LOCATION AND CELL ADDRESS OF MAXIMUM K CHANGE
C
C
C ** IF MAX K CHANGE IS LESS THAN CONVERGENCE CRITERIA SET FLAG TO 1
      IF(HYBIGG.LT.HYCLOSE) GOTO 350
      ISDKFLAG=0
      GOTO 360
 350  ISDKFLAG=1
 360  CONTINUE
C       SET TSTOP TO TSBOT AS MOVING ON TO NEXT LAYER IN DO LOOP
      TSTOP=TSBOT
 400  CONTINUE
C
```

```
C   CALCULATE VCONT TERMS
C   IF ONLY ONE LAYER SKIP THIS STAGE
C   CV IS VCONT: CALCULATE FOR EACH LAYER EXCLUDING THE BOTTOM LAYER
      ZERO=0.0
      K1=NLAY-1
      IF(NLAY.EQ.1) GOTO 600
      DO 550 I=1,NROW
      DO 550 J=1,NCOL
      DO 550 K=1,K1
C  CALCULATE VERTICAL K HARMONIC MEAN
      HKV=2*HY(J,I,K)*HY(J,I,K+1)/(HY(J,I,K)+HY(J,I,K+1))
C  CALCULATE VERTICAL LEAKANCE
      CV(J,I,K)=HKV/(0.5*(TOP(J,I,K)-BOT(J,I,K+1)))
C1------MULTIPLY VERTICAL LEAKANCE BY AREA TO MAKE CONDUCTANCE.
      CV(J,I,K)=CV(J,I,K)*DELR(J)*DELC(I)
  550 CONTINUE
C
C2------IF WETTING CAPABILITY IS ACTIVATED, SAVE CV IN CVWD FOR USE WHEN
C2------WETTING CELLS.
      IF(IWDFLG.EQ.0) GO TO 570
      DO 560 K=1,K1
      DO 560 I=1,NROW
      DO 560 J=1,NCOL
      CVWD(J,I,K)=CV(J,I,K)
  560 CONTINUE
C
C3------IF IBOUND=0, SET CV=0 AND CC=0 (CC DISABLED)
C4--------  NB NEW CODE WILL BE REQUIRED IF LAYCON.NE.3
  570 DO 580 K=1,NLAY
      DO 580 I=1,NROW
      DO 580 J=1,NCOL
      IF(IBOUND(J,I,K).NE.0) GO TO 580
      IF(K.NE.NLAY) CV(J,I,K)=ZERO
      IF(K.NE.1) CV(J,I,K-1)=ZERO
C     CC(J,I,K)=ZERO
  580 CONTINUE
C
 600  CONTINUE
C
C IF ISDKFLAG =1 THEN WRITE OUT DEN, ESMID, PWP, HY AND CY FOR ALL CELLS
      IF (ISDKFLAG.EQ.0) GOTO 700
C     ------------------------------------------------------------------
C0------PRINT OUT DEN
      TEXT='   DENSITY t/m3)'
C0------SET PRINT FORMAT TO 15F7.2 PER STRIP
      IHEDFM=4
C
C4------FOR EACH LAYER: CALL ULAPRW TO PRINT DEN.
        DO 610 K=1,NLAY
        KK=K
        CALL ULAPRW(DEN(1,1,K),TEXT,KSTP,KPER,
     1              NCOL,NROW,KK,IHEDFM,IOUT)
  610   CONTINUE
C     ------------------------------------------------------------------
C0------PRINT OUT EFFECTIVE STRESS
      TEXT='EFF STRESS (kPA)'
C0------SET PRINT FORMAT TO 15F7.2 PER STRIP
      IHEDFM=4
C
C4------FOR EACH LAYER: CALL ULAPRW TO PRINT DEN.
        DO 620 K=1,NLAY
        KK=K
        CALL ULAPRW(ESMID(1,1,K),TEXT,KSTP,KPER,
     1              NCOL,NROW,KK,IHEDFM,IOUT)
  620   CONTINUE
C     ------------------------------------------------------------------
C0------PRINT OUT PWP
      TEXT='       PWP (kPa)'
C0------SET PRINT FORMAT TO 15F7.2 PER STRIP
      IHEDFM=4
C
C4------FOR EACH LAYER: CALL ULAPRW TO PRINT PWP.
        DO 630 K=1,NLAY
        KK=K
        CALL ULAPRW(PWP(1,1,K),TEXT,KSTP,KPER,
     1              NCOL,NROW,KK,IHEDFM,IOUT)
```

```
  630   CONTINUE
C     -----------------------------------------------------------------
C0------PRINT OUT HYDRAULIC CONDUCTIVITY
      TEXT='K in MODEL UNITS'
C0------SET PRINT FORMAT TO 9G11.4 PER STRIP
      IHEDFM=12
C
C4------FOR EACH LAYER: CALL ULAPRW TO PRINT K.
        DO 640 K=1,NLAY
        KK=K
        CALL ULAPRW(HY(1,1,K),TEXT,KSTP,KPER,
     1              NCOL,NROW,KK,IHEDFM,IOUT)
  640   CONTINUE
C     -----------------------------------------------------------------
C0------PRINT OUT VERTICAL CONDUCTANCE
      TEXT='        CV      '
C0------SET PRINT FORMAT TO 10G10.3 PER STRIP
      IHEDFM=1
C     IF (NLAY.EQ.1) GOTO 700
C4------FOR EACH LAYER: CALL ULAPRW TO PRINT CV.
        DO 650 K=1,NLAY-1
        KK=K
        CALL ULAPRW(CV(1,1,K),TEXT,KSTP,KPER,
     1              NCOL,NROW,KK,IHEDFM,IOUT)
  650   CONTINUE
C
C
  700 CONTINUE
      WRITE(IOUT,750)
  750 FORMAT('SDK PACKAGE COMPLETED - CONTROL RETURNED TO MAIN')
      RETURN
      END
*******************************************************************************************
C   PARAMETER LIST
C
*******************************************************************************************
C       A         Local   REAL                                Constant
C       BOT       Global  DIMENSION(NCOL,NROW,NLAY)           Elevation of base of cell
C       BUFF      Global  DIMENSION(NCOL,NROW,NLAY)           Buffer used in printing variables
C       CV        Global  DIMENSION(NCOL,NROW,NLAY)           Vertical Conductance
C       CVWD              DIMENSION(NCOL,NROW,NLAY)           Spare array for CV (if wetting
C                                                             capability invoked)
C       D         LOCAL   REAL                                Depth of cell
C       DELC      GLOBAL  DIMENSION(NROW)                     Spacing of columns
C       DELR      GLOBAL  DIMENSION(NCOL)                     Spacing of rows
C       DEN       Global  DIMENSION(NCOL,NROW,NLAY)           Average wet density of cell
C       DENW      Local   REAL                                Density of water/leachate
C       DCFACT    Local   REAL                                Conversion factor from model
C                                                              units to metres
C       E         Local   REAL                                The constant E
C       ESMID     Global  DIMENSION(NCOL,NROW,NLAY)           Effective stress at midpoint
C                                                              of cell
C       G         Local   REAL                                Acceleration due to gravity
C       HKV       Local   REAL                                Vertical K harmonic mean
C       HNEW      GLOBAL  DIMENSION(NCOL,NROW,NLAY)           Head at cell
C       HY        global  DIMENSION(NCOL,NROW,NLAY)           Hydraulic conductivity at cell
C       HYBIGG    Local   REAL                                Largest recorded differnce in K

C       HYDIFF    Local   REAL                                Difference in K
C       HYOLD     Local   DIMENSION(NCOL,NROW,NLAY)           Iniital K values
C       HYTEMP    Local   REAL                                Calculated K in m/s
C       I         Local   INT                                 Counter for rows
C       IBOUND    Global  DIMENSION(NCOL,NROW,NLAY)           Flag for flow status of cell
C                             <0 - CELL CONSTANT HEAD
C                             =0 - CELL INACTIVE (DRY)
C                             >0 - CELL VARIABLE HEAD
C       ISDKCF            DIMENSION(NCOL,NROW,NLAY)           Flag for whether SDK package
C                                                             is applicable to cell
C                              =0 - K and densities DO NOT VARY
C                              =1 - K and densities (Sat & unsat') vary with Eff' stress
C       ISDKFLAG  Local   INT                                 Flag for whether hydraulic
C                                                             conductivity has converged
C                              =0 - K not converged - do another loop
C                              =1 - K converged - proceed with main programme
C       ISUM                                                  Counter for positon in X array
C       IWDFLG            INT                                 Flag for whether wetting
```

```
C                                                          capabilityis active
C       J        Local   INT                               Counter for columns
C       K        Local   INT                               Counter for layers
C       KPER     Global  INT                               Number of stress period
C       KSTP     Global  INT                               Number of time steps
C       HYCLOSE  Local   REAL                              Max allowable percent variation
C                                                          in Kbetween iterations
C       LAYNUM           INT                               Layer number where SDK package
C                                                          not applicable
C       LCBOT            INT                               Starting position in X array of
C                                                          BOT
C       LCCV             INT                               Starting position in X array of
C                                                          CV
C       LCVWD            INT                               Starting position in X array of
C                                                          CVWD
C       LCDELC           INT                               Starting position in X array of
C                                                          DELC
C       LCDELR           INT                               Starting position in X array of
C                                                          DELR
C       LCDEN            INT                               Starting position in X array of
C                                                          DEN
C       LCESMID          INT                               Starting position in X array of
C                                                          ESMID
C       LCHNEW           INT                               Starting position in X array of
C                                                          HNEW
C       LCHY             INT                               Starting position in X array of
C                                                          HY
C       LCHYOLD          INT                               Starting position in X array of
C                                                          HYOLD
C       LCIBOUND         INT                               Starting position in X array of
C                                                          IBOUND
C       LCISDKCF         INT                               Starting position in X array of
C                                                          ISDKCF
C       LCSATD           INT                               Starting position in X array of
C                                                          SATD
C       LCTOP            INT                               Starting position in X array of
C                                                          TOP
C       LCUSATD          INT                               Starting position in X array of
C                                                          USATD
C       LENX             INT                               Length of X array
C       NCOL     Global  INT                               Number of columns in grid
C       NRCL     Global  INT                               Number= rows*columns*layers
C       NROW     Global  INT                               Number of row in grid
C       NSDKLAY          INT                               Number of layers where SDK
C                                                          package not applicable
C       NLAY     Global  INT                               Number of layers in grid
C       PWP      Local   DIMENSION(NCOL,NROW,NLAY)         Pore water pressure in stress
C                                                          units
C       SATD             DIMENSION(NCOL,NROW,NLAY)         Saturated density of cells
C                                                          where ISDKCF(j,i,k)=0
C       TCFACT   Local   REAL                              Conversion factor from model
C                                                          units to SECONDS
C       TOP      Global DIMENSION(NCOL,NROW,NLAY)          Elevatton of base of cell
C       (TRPYOLD) - NOT USED AT PRESENT
C       (TRPY)    - NOT USED AT PRESENT
C       TSBOT    Local   REAL                              Total stress at bottom of cell
C       TSERR    Local   REAL                              Total stress iteration error
C       TSSURF   Local   REAL                              Surface surcharge in kPa
C       TSMID    Local   REAL                              Total stress at midpoint of cell
C       TSOLD    Local   REAL                              Old total stress at MP of cell
C       TSTOP    Local   REAL                              Total stress at top of cell
C       USATD            DIMENSION(NCOL,NROW,NLAY)         Unsaturated density of cells
C                                                          where ISDKCF(j,i,k)=0
C       VAR1     Local   REAL                              Unsaturated zone density to
C                                                          stress constant
C       VAR2     Local   REAL                              Unsaturated zone density to
C                                                          stress power term
C       VAR3     Local   REAL                              Saturated zone density to
C                                                          stress constant
C       VAR4     Local   REAL                              Saturated zone density to
C                                                          stress power term
C       VAR5     Local   REAL                              Stress to Hydraulic Conductivity
C                                                          constant
C       VAR6     Local   REAL                              Stress to Hydraulic Conductivity
C                                                          power term
C       X        Global  DIMENSION(LENX)                   Main storage array
```

Appendix D - Flushing volumes

The following is an example of the analysis used in Section 8.5.3

Dry density of waste	0.49 t/m3	% of macropores in BV	12.7
Bed volume per unit volume of waste	0.51 m3	% of micropores in BV	87.3
Releasable N	2.7 kg/dry tonne		
Releasable N	1.323 kg per unit volume of waste		
Initial NH3-N conc' in bed volume	2594.1 mg/l		

Fill/drain Cycle number	Volume of macro-pore m3	NH3-N conc in macro-pore mg/l	Mass of N in macro-pore g	Volume of micro-pore m3	NH3-N conc in micro-pores mg/l	Mass of N in micro-pores g	Total mass g	Total vol removed m3
0	0.06477	2594.117647	168.021	0.44523	2594.1	1154.979	1323	0
1	0.06477	2309.958	149.6159797	0.44523	2309.958	1028.4626	1154.979	0.06477
2	0.06477	2010.726041	130.2347257	0.44523	2010.726041	895.2355551	1005.363	0.12954
3	0.06477	1750.256589	113.3641193	0.44523	1750.256589	779.2667413	875.12829	0.19431
4	0.06477	1523.528351	98.67893128	0.44523	1523.528351	678.3205276	761.76418	0.25908
5	0.06477	1326.170488	85.89606252	0.44523	1326.170488	590.4508865	663.08524	0.32385
6	0.06477	1154.378363	74.76908658	0.44523	1154.378363	513.9638786	577.18918	0.38862
7	0.06477	1004.84019	65.08349911	0.44523	1004.84019	447.3849978	502.4201	0.45339
8	0.06477	874.6731918	56.65258263	0.44523	874.6731918	389.4307452	437.3366	0.51816
9	0.06477	761.3680265	49.31380708	0.44523	761.3680265	338.9838865	380.68401	0.58293
10	0.06477	662.7404124	42.92569651	0.44523	662.7404124	295.0719138	331.37021	0.6477
11	0.06477	576.8890194	37.36510178	0.44523	576.8890194	256.8482981	288.44451	0.71247
12	0.06477	502.1588158	32.5248265	0.44523	502.1588158	223.5761696	251.07941	0.77724
13	0.06477	437.1091628	28.31156047	0.44523	437.1091628	194.6141125	218.55458	0.84201
14	0.06477	380.4860418	24.64408093	0.44523	380.4860418	169.4038004	190.24302	0.90678
15	0.06477	331.19788	21.45168669	0.44523	331.19788	147.4592321	165.59894	0.97155
16	0.06477	288.2945066	18.67283519	0.44523	288.2945066	128.3573632	144.14725	1.03632
17	0.06477	250.9488362	16.25395612	0.44523	250.9488362	111.7299504	125.47442	1.10109
18	0.06477	218.440924	14.14841865	0.44523	218.440924	97.25645258	109.22046	1.16586
19	0.06477	190.1440867	12.31563249	0.44523	190.1440867	84.65785172	95.072043	1.23063
20	0.06477	165.5128217	10.72026546	0.44523	165.5128217	73.6912736	82.756411	1.2954
21	0.06477	144.0722908	9.331562273	0.44523	144.0722908	64.14530602	72.036145	1.36017
22	0.06477	125.4091662	8.122751697	0.44523	125.4091662	55.83592308	62.704583	1.42494
23	0.06477	109.1636628	7.070530442	0.44523	109.1636628	48.6029376	54.581831	1.48971
24	0.06477	95.02260195	6.154613928	0.44523	95.02260195	42.30691307	47.511301	1.55448
25	0.06477	82.71337409	5.35734524	0.44523	82.71337409	36.82647555	41.356687	1.61925
26	0.06477	71.99868361	4.663354738	0.44523	71.99868361	32.05597391	35.999342	1.68402
27	0.06477	62.67197414	4.059263765	0.44523	62.67197414	27.90344305	31.335987	1.74879
28	0.06477	54.55344661	3.533426737	0.44523	54.55344661	24.28883103	27.276723	1.81356
29	0.06477	47.48659314	3.075706637	0.44523	47.48659314	21.14245586	23.743297	1.87833
30	0.06477	41.33517986	2.6772796	0.44523	41.33517986	18.40366213	20.66759	1.9431
31	0.06477	35.98062066	2.3304648	0.44523	35.98062066	16.01965174	17.99031	2.00787
32	0.06477	31.31969106	2.02857639	0.44523	31.31969106	13.94446605	15.659846	2.07264
33	0.06477	27.26253828	1.765794604	0.44523	27.26253828	12.13809992	13.631269	2.13741
34	0.06477	23.73094907	1.537053571	0.44523	23.73094907	10.56573046	11.865475	2.20218
35	0.06477	20.65684193	1.337943652	0.44523	20.65684193	9.197045732	10.328421	2.26695
36	0.06477	17.98095463	1.164626431	0.44523	17.98095463	8.005660428	8.9904773	2.33172
37	0.06477	15.65170176	1.013760723	0.44523	15.65170176	6.968607176	7.8258509	2.39649
38	0.06477	13.62418032	0.882438159	0.44523	13.62418032	6.065893803	6.8120902	2.46126
39	0.06477	11.859304	0.76812712	0.44523	11.859304	5.280117919	5.929652	2.52603
40	0.06477	10.32304976	0.668623933	0.44523	10.32304976	4.596131444	5.1615249	2.5908
41	0.06477	8.985801893	0.582010389	0.44523	8.985801893	4.000748577	4.4929009	2.65557
42	0.06477	7.821781116	0.506616763	0.44523	7.821781116	3.482491606	3.9108906	2.72034
43	0.06477	6.80854759	0.440989627	0.44523	6.80854759	3.031369644	3.4042738	2.78511
44	0.06477	5.926568335	0.383863831	0.44523	5.926568335	2.63868602	2.9632842	2.84988
45	0.06477	5.158840673	0.33413811	0.44523	5.158840673	2.296870633	2.5794203	2.91465
46	0.06477	4.490564452	0.29085386	0.44523	4.490564452	1.999334011	2.2452822	2.97942
47	0.06477	3.908856733	0.253176651	0.44523	3.908856733	1.740340283	1.9544284	3.04419
48	0.06477	3.402503432	0.220380147	0.44523	3.402503432	1.514896603	1.7012517	3.10896
49	0.06477	2.961743137	0.191832103	0.44523	2.961743137	1.318656897	1.4808716	3.17373
50	0.06477	2.578078931	0.166982172	0.44523	2.578078931	1.147838083	1.2890395	3.2385
51	0.06477	2.244114587	0.145351302	0.44523	2.244114587	0.999147137	1.1220573	3.30327
52	0.06477	1.953411983	0.126522494	0.44523	1.953411983	0.869717617	0.976706	3.36804
53	0.06477	1.700366995	0.11013277	0.44523	1.700366995	0.757054397	0.8501835	3.43281
54	0.06477	1.480101454	0.095866171	0.44523	1.480101454	0.65898557	0.7400507	3.49758
55	0.06477	1.288369112	0.083447667	0.44523	1.288369112	0.57362058	0.6441846	3.56235
56	0.06477	1.121473777	0.072637857	0.44523	1.121473777	0.49931377	0.5607369	3.62712
57	0.06477	0.976198064	0.063228349	0.44523	0.976198064	0.434632664	0.488099	3.69189
58	0.06477	0.849741367	0.055037748	0.44523	0.849741367	0.378330349	0.4248707	3.75666
59	0.06477	0.73966587	0.047908158	0.44523	0.73966587	0.329321435	0.3696329	3.82143
60	0.06477	0.643849553	0.041702136	0.44523	0.643849553	0.286661137	0.3219248	3.8862
61	0.06477	0.560445282	0.036300041	0.44523	0.560445282	0.249527053	0.2802226	3.95097
62	0.06477	0.4878452	0.031597734	0.44523	0.4878452	0.217203319	0.2439226	4.01574
63	0.06477	0.424649733	0.027504563	0.44523	0.424649733	0.189066801	0.2123249	4.08051
64	0.06477	0.369640607	0.023941622	0.44523	0.369640607	0.164575087	0.1848203	4.14528
65	0.06477	0.321757362	0.020840224	0.44523	0.321757362	0.14325603	0.1608787	4.21005

Dry density of waste	0.49 t/m3	% of macropores in BV	12.7
Bed volume per unit volume of waste	0.51 m3	% of micropores in BV	87.3
Releasable N	2.7 kg/dry tonne		
Releasable N	1.323 kg per unit volume of waste		
Initial NH3-N conc' in bed volume	2594.1 mg/l		

Fill/drain Cycle number	Volume of macro-pore m3	NH3-N conc in macro-pore mg/l	Mass of N in macro-pore g	Volume of micro-pore m3	NH3-N conc in micro-pores mg/l	Mass of N in micro-pores g	Total mass g	Total vol removed m3
66	0.06477	0.280076914	0.018140582	0.44523	0.280076914	0.124698644	0.1400385	4.27482
67	0.06477	0.24379575	0.015790651	0.44523	0.24379575	0.108545182	0.1218979	4.33959
68	0.06477	0.212214449	0.01374513	0.44523	0.212214449	0.094484239	0.1061072	4.40436
69	0.06477	0.184724189	0.011964586	0.44523	0.184724189	0.082244751	0.0923621	4.46913
70	0.06477	0.160795018	0.010414693	0.44523	0.160795018	0.071590766	0.0803975	4.5339
71	0.06477	0.139965631	0.009065574	0.44523	0.139965631	0.062316898	0.0699828	4.59867
72	0.06477	0.121834483	0.007891219	0.44523	0.121834483	0.054244367	0.0609172	4.66344
73	0.06477	0.106052044	0.006868991	0.44523	0.106052044	0.047217552	0.053026	4.72821
74	0.06477	0.092314062	0.005979182	0.44523	0.092314062	0.04110099	0.046157	4.79298
75	0.06477	0.080355699	0.005204639	0.44523	0.080355699	0.035776768	0.0401778	4.85775
76	0.06477	0.069946422	0.00453043	0.44523	0.069946422	0.031142245	0.0349732	4.92252
77	0.06477	0.060885562	0.003943558	0.44523	0.060885562	0.027108079	0.0304428	4.98729
78	0.06477	0.052998446	0.003432709	0.44523	0.052998446	0.023596498	0.0264992	5.05206
79	0.06477	0.046133028	0.002988036	0.44523	0.046133028	0.020539808	0.0230665	5.11683
80	0.06477	0.040156955	0.002600966	0.44523	0.040156955	0.017879081	0.0200785	5.1816
81	0.06477	0.034955023	0.002264037	0.44523	0.034955023	0.015563025	0.0174775	5.24637
82	0.06477	0.03042695	0.001970754	0.44523	0.03042695	0.013546991	0.0152135	5.31114
83	0.06477	0.026485443	0.001715462	0.44523	0.026485443	0.011792114	0.0132427	5.37591
84	0.06477	0.023054518	0.001493241	0.44523	0.023054518	0.010264563	0.0115273	5.44068
85	0.06477	0.020068036	0.001299807	0.44523	0.020068036	0.008934892	0.010034	5.50545
86	0.06477	0.017468423	0.00113143	0.44523	0.017468423	0.007777466	0.0087342	5.57022
87	0.06477	0.015205563	0.000984864	0.44523	0.015205563	0.006769973	0.0076028	5.63499
88	0.06477	0.013235834	0.000857285	0.44523	0.013235834	0.005892991	0.0066179	5.69976
89	0.06477	0.011521264	0.000746232	0.44523	0.011521264	0.005129613	0.0057606	5.76453
90	0.06477	0.0100288	0.000649565	0.44523	0.0100288	0.004465123	0.0050144	5.8293
91	0.06477	0.008729669	0.000565421	0.44523	0.008729669	0.003886711	0.0043648	5.89407
92	0.06477	0.007598828	0.000492176	0.44523	0.007598828	0.003383226	0.0037994	5.95884
93	0.06477	0.006614476	0.00042842	0.44523	0.006614476	0.002944963	0.0033072	6.02361
94	0.06477	0.005757636	0.000372922	0.44523	0.005757636	0.002563472	0.0028788	6.08838
95	0.06477	0.005011792	0.000324614	0.44523	0.005011792	0.0022314	0.0025059	6.15315
96	0.06477	0.004362565	0.000282563	0.44523	0.004362565	0.001942345	0.0021813	6.21792
97	0.06477	0.003797438	0.00024596	0.44523	0.003797438	0.001690733	0.0018987	6.28269
98	0.06477	0.003305518	0.000214098	0.44523	0.003305518	0.001471716	0.0016528	6.34746
99	0.06477	0.002877321	0.000186364	0.44523	0.002877321	0.00128107	0.0014387	6.41223
100	0.06477	0.002504593	0.000162222	0.44523	0.002504593	0.00111512	0.0012523	6.477
101	0.06477	0.002180148	0.000141208	0.44523	0.002180148	0.000970667	0.0010901	6.54177
102	0.06477	0.001897732	0.000122916	0.44523	0.001897732	0.000844927	0.0009489	6.60654
103	0.06477	0.001651899	0.000106994	0.44523	0.001651899	0.000735475	0.000826	6.67131
104	0.06477	0.001437912	0.0000931336	0.44523	0.001437912	0.000640202	0.000719	6.73608
105	0.06477	0.001251645	0.0000810691	0.44523	0.001251645	0.00055727	0.0006258	6.80085
106	0.06477	0.001089507	0.0000705674	0.44523	0.001089507	0.000485081	0.0005448	6.86562
107	0.06477	0.000948372	0.0000614261	0.44523	0.000948372	0.000422244	0.0004742	6.93039
108	0.06477	0.00082552	0.0000534689	0.44523	0.00082552	0.000367546	0.0004128	6.99516
109	0.06477	0.000718582	0.0000465426	0.44523	0.000718582	0.000319934	0.0003593	7.05993
110	0.06477	0.000625497	0.0000405135	0.44523	0.000625497	0.00027849	0.0003127	7.1247
111	0.06477	0.00054447	0.0000352653	0.44523	0.00054447	0.000242414	0.0002722	7.18947
112	0.06477	0.00047394	0.0000306971	0.44523	0.00047394	0.000211012	0.000237	7.25424
113	0.06477	0.000412545	0.0000267206	0.44523	0.000412545	0.000183678	0.0002063	7.31901
114	0.06477	0.000359104	0.0000232592	0.44523	0.000359104	0.000159884	0.0001796	7.38378
115	0.06477	0.000312586	0.0000202462	0.44523	0.000312586	0.000139173	0.0001563	7.44855
116	0.06477	0.000272094	0.0000176235	0.44523	0.000272094	0.000121144	0.000136	7.51332
117	0.06477	0.000236847	0.0000153406	0.44523	0.000236847	0.000105451	0.0001184	7.57809
118	0.06477	0.000206165	0.0000133533	0.44523	0.000206165	0.000091791	0.0001031	7.64286
119	0.06477	0.000179459	0.0000116235	0.44523	0.000179459	0.0000799	0.0000897	7.70763
120	0.06477	0.000156212	0.0000101178	0.44523	0.000156212	0.00006955	0.0000781	7.7724